1-1-2019

Optimization Of Underbody Blast Energy-Attenuating Seat Mechanisms Using Modified Madymo Hybrid Iii And Human Body Models

Kelly Erin Bryan Bosch
Wayne State University, kebosch86@gmail.com

OPTIMIZATION OF UNDERBODY BLAST ENERGY-ATTENUATING SEAT MECHANISMS USING MODIFIED MADYMO HYBRID III AND HUMAN BODY MODELS

by

KELLY E. B. BOSCH, PE

DISSERTATION

Submitted to the Graduate School

of Wayne State University,

Detroit, Michigan

in partial fulfillment of the requirements

for the degree of

DOCTOR OF PHILOSOPHY

2019

MAJOR: BIOMEDICAL ENGINEERING

Approved By:

_____

Advisor Date

_____

Co-advisor Date

_____

_____

_____

ACKNOWLEDGEMENTS

I would like to take the opportunity to thank everyone that has supported me in my doctoral studies at Wayne State University, starting with Mrs. Risa Scherer, who inspired me to pursue my PhD while working at TARDEC. I would like to sincerely thank my advisors, Dr. John Cavanaugh and Dr. Paul Begeman for their support and invaluable feedback.

I would like to extend my appreciation to my doctoral committee, Dr. King H. Yang, Dr. Liying Zhang, and Dr. Jingwen Hu, for their time and willingness to support my research.

I would like to thank the US Government Warrior Injury Assessment (WIAMan) Program and the University of Virginia, especially Dr. Meade Spratley, Dr. Ann Bailey, and Dr. Rob Salzar, for supplying the data required for me to complete my research. My sincerest gratitude is also expressed to Mr. Nachiket Pendse and Mr. John Cooper and for their technical support in MADYMO. I am also indebted to the generosity of TASS International (Siemens) for access to a MADYMO license for completing my research. I would also like to thank the WIAMan Engineering Office (WEO) and Dr. Kathryn Loftis for their technical input.

Of course, my heartfelt appreciation is extended to my family, especially my husband, Jeff, for his unwavering support through long hours of classwork, studying, and research, and our newborn son, Carter, for being my motivation to finish.

TABLE OF CONTENTS

LIST OF TABLES

LIST OF FIGURES

CHAPTER 1 – INTRODUCTION

1.1. Statement of Problem

Underbody blast events (UBBs) caused by improvised explosive devices (IEDs) have been responsible for more than 50,000 injuries and casualties on the battlefield in modern warfare [28]. These high energy UBB events impart vertical forces to military ground vehicles, which are then transferred to the Warfighters seated inside the vehicle, often resulting in catastrophic injuries. The US Government has made large strides in improving vehicle design to mitigate the effects of the blast event, including the introduction of blast mitigation energy attenuating (EA) or energy absorbing seating systems, which are known to improve Warfighter survivability when combined with other strategies such as armor plating on the exterior of the vehicle [67].

EA seats, although not new to the market, have not been fully characterized with respect to energy attenuation capability and the resulting effects on occupant protection. The U.S. Army – Tank Automotive Research, Development and Engineering Center (TARDEC) Ground System Survivability (GSS) Interior Blast Mitigation Seat Team (IBMT) has been testing and evaluating EA seats on the drop tower located in the TARDEC Occupant Protection Laboratory (OPL) in efforts to understand how seats afford protection to occupants at varying threat level simulations. Although this testing sets the foundation for general EA seat evaluation, it does not address some of the basic questions behind the optimization of seat design [10].

EA seats utilize stroking mechanisms to absorb energy and reduce the vertical forces imparted on the occupant's pelvis and lower spine complex. Although a variety of EA seats are available on the market, the fundamental question behind how to optimize the

force and deflection rates of the EA mechanisms to effectively reduce occupant injury has not yet been answered. Using modeling and simulation techniques, this research was able to develop optimal force and deflection profiles to reduce pelvis and lower spine injuries experienced by Warfighters in underbody blast events using a generic seat model with MAthematical DYnamic MOdels (MADYMO) software (TASS International, Inc - Siemens) and modeFRONTIER optimization software. This optimized model can then be shared with EA seat manufacturers and applied to military seat development efforts for EA mechanisms for a given occupant and designated blast severity.

1.2. Background and Significance

IEDs, or improvised explosive devices, have been noted as military warfare on ships dating back to the 1500s [60]. Throughout time, IEDs have been used as a covert attack mechanism on adversaries and are becoming more prevalent in modern warfare. The Department of Defense defines an IED as a weapon that is manufactured from unconventional materials or methods that is designed to incapacitate or kill [26]. The current versions of IEDs in modern warfare are fabricated to breach armor on ground vehicles that are designated as mine-resistant. NATO states that anti-tank mines are "one of the most efficient and least expensive lethal weapons [44]."

Two of the latest US conflicts, Operation Iraqi Freedom (OIF) and Operation Enduring Freedom (OEF), have shown increasing trends in the use of explosive devices, including IEDs, as major mechanisms of injuries to Warfighters. In Afghanistan in 2011, IEDs were responsible for over half of deaths reported for US troops [60]. Since World War I, explosions have more than doubled as the cause of injuries, from 35% to 81%, warranting the shift of research and development in ground vehicles to occupant protection from

underbody blast events [11]. Approximately half of the injuries sustained during these conflicts affect the musculoskeletal system, and injuries usually span multiple body regions [8]. Explosions on the battlefield are now the leading cause of death [14] and currently account for more than 75% of casualties in OIF and OEF [8].

The Joint Trauma Analysis and Prevention of Injury in Combat (JTAPIC) partnership performed a theater injury data analysis on blast events and reported that 46% of killed-in-action (KIA) casualties and 5% of wounded-in-action (WIA) casualties were due to pelvic fractures [2]. 18% of reported injuries were in the lumbar spine, as well, demonstrating the need for improvement to occupant safety [2, 49]. This study was focused on a set of 608 casualties from recent events in theater [2]. Emphasis on the pelvic complex is important due to its importance with respect to weight-bearing for the Soldier, as well as the fact that there is the potential for high morbidity rates in conjunction with blunt pelvic injuries [4]. A more recent JTAPIC review, which included injuries from Operation New Dawn (OND) in addition to OIF and OEF, reported that spinal fractures were frequent for both WIA and KIA, with WIA experiencing lumbar spine fractures in 11% of cases and thoracic spine fractures in 8% of cases. These percentages were lower for KIA injuries, at 7% experiencing lumbar spine fractures and 6% experiencing thoracic spine fractures. Pelvic fractures were not listed in the top five most frequent injuries for WIA nor KIA in this data set [34].

Based on the most recent threats reported in theater and their appearance in the national spotlight, TARDEC has adopted a more occupant-centric approach for its vehicle design philosophy, which focuses first on protecting the soldier. This new design philosophy then works outward to the seat, restraints, vehicle structure, and beyond [21].

In addition to occupant-focused design, vehicles are being equipped with mine blast underbody hull kits and EA seats to improve occupant survivability [32]. An improved understanding of the force and deflection properties of a seat and how it affects occupant injury will lead to more efficient seat designs, and ultimately, fewer injuries due to underbody blast loading.

1.3. Specific Aims

One of the fundamental questions behind protecting Warfighters with energy absorbing (EA) seats during underbody blast events is how to optimize the force and deflection rates of the seat to prevent injury to the pelvis and lower spine region while working within the constraints of available seat stroke. This research used MADYMO, a computational computer simulation program for occupant safety, to model the human interaction with a generic EA seat interface. This then allowed the development of an optimization tool so that optimal energy absorption rates can be determined to aid in the design of EA seats with any EA mechanism to reduce pelvis and lower spine injuries. The MADYMO models are that of the 50^{th} percentile male occupant using both a Human Body Model (HBM) and Hybrid III anthropomorphic test device (ATD) in the same seat to investigate the effects of the various energy absorption profiles.

Although EA seats often feature foam for comfort and limited energy absorption properties, the model was based on a bare seat modeled as a spring and damper system, which represented the seat frame EA mechanism combined with the EA properties of foam.

As all underbody blast events are unique, TARDEC and various researchers have developed generic representative pulses that are representative of actual theater events

using data collected during live fire test events. Examples of generic idealized pulses are shown in Figure 1-1 with related velocities in Figure 1-2, which reach between 200 and 350 g with resulting velocities between 6 and 13 m/s [10]. Representative pulses from theater events were implemented in this research to evaluate how these laboratory simulated inputs affected the effectiveness of optimized EA mechanisms, which were noisier and less idealized than those shown below for reference.

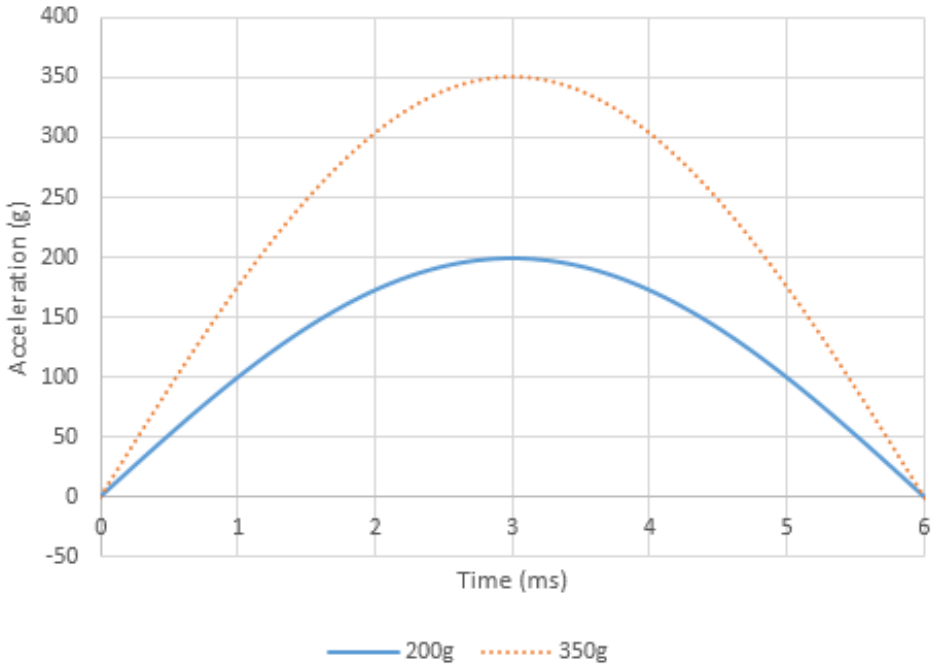

Figure 1-1. TARDEC generic underbody blast pulse floor accelerations for low severity (blue) and higher severity (red dashed) events [10]

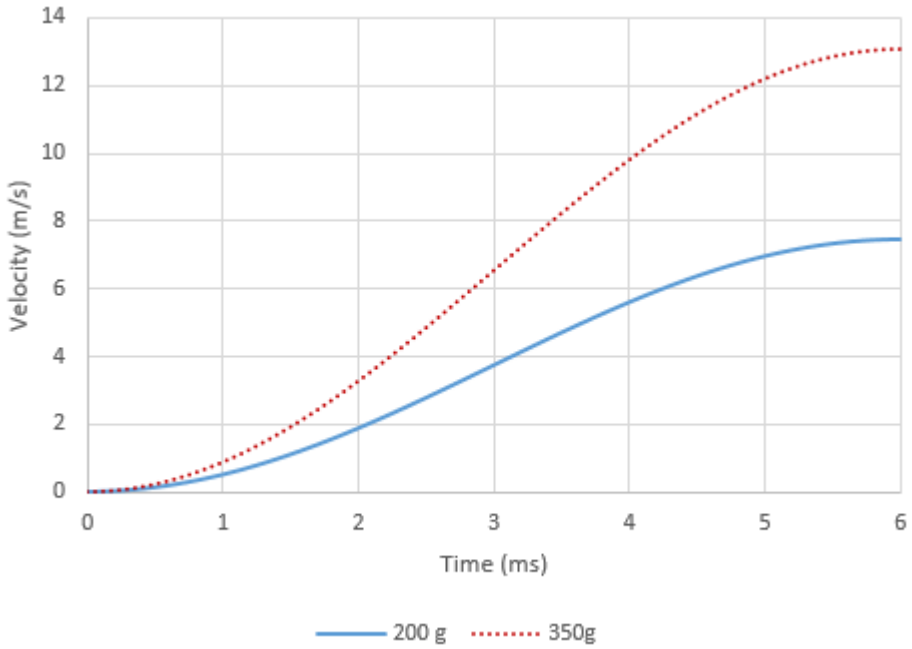

Figure 1-2. TARDEC generic underbody blast pulse floor velocities for low severity (blue) and higher severity (red dashed) events [10]

The force and deflection rates needed to be optimized within a specific design package including limited stroke distance, ranging up to a maximum of six (6) inches, which represented a more aggressive upper limit of packaging space in military vehicles according to TARDEC research of commercially available seats and publicly available literature [3, 53]. The rate of energy absorption was dictated by the pulse input, as it was critical that the seat stroked quickly enough to reduce the vertical accelerative loading transferred to the occupant.

The purpose of this study was to produce optimized force-deflection curves that were achievable within the laws of physics. The optimization study leveraged literature research and past publications for background information and a starting point for the EA optimization. These studies included the blast seat mitigation studies conducted at TARDEC [10, 11].

Success of the model was defined by evaluation of the pelvis and lower spine forces within the MADYMO occupant model. For the Human Body Model, literature research was conducted to determine vertical acceleration and loading limits to the human body at the threshold of pelvis and lower spine injury. The models were then run again with the Hybrid III ATD model to provide data on the loads and accelerations as measured by the ATD for future physical seat testing applications. The end product of this research effort was a tool that provides optimal force and deflection profiles that can be shared with manufacturers in the EA seating industry to aid in future military seat EA mechanism development efforts.

This continued research in blast energy-attenuating seats supports the TARDEC 30-year Strategy for Warfighter survivability, specifically in VS1, LoE3 – KO2 (1.3.2) Protected Mobility. This strategy requires that TARDEC develop, integrate and demonstrate force protection capability suites (i.e. technologies to mitigate/defeat the enemy's ability to detect, hit, penetrate and kill) which enable the system and its occupants to survive threats, while striving to maintain the optimal balance of mobility and protection and allow sustained operations anywhere in the world. "To accomplish this requires driving developments in new, lighter-weight protection technologies for both the system and its occupants (to ensure survival against any threat), as well as developments in innovative ground vehicle mobility and gap crossing capabilities in order to operate in any terrain, in any situation, at any vehicle weight, anywhere in the world." [67]

CHAPTER 2 – UNDERBODY BLAST AND WARFIGHTER INJURY

2.1. IED Effects

IEDs are often buried under soil roads so that they can be detonated when adversarial vehicles traverse the target location. When an IED is detonated, it causes the propagation of a shock wave to form high pressure, hot gases. These gases are formed by an exothermic chemical reaction. As the gases expand, they disrupt the soil, causing an explosive interaction as the blast wave touches the surface of the air above the soil. The hot gases are expelled through the soil, ejecting soil particles at speeds up to 2000 mph [900 m/s]. The expansion of the gas and the physical momentum from the moving soil interact with the vehicle's underbody resulting in a transfer of load during the first 5 to 10 milliseconds after detonation. The shape of the vehicle's hull can greatly impact the effects of the blast; a V-shaped hull can deflect the high pressure flow while a flat-bottom vehicle will trap the soil ejecta and pressure waves, potentially causing a breach in the hull in addition to global motion vertically. The vertical motion of the vehicle upwards is determined by the vehicle's mass, hull shape, and moment of inertia, if the loading is off-center [54]. The vertical jump of the vehicle begins 10 to 20 ms after the IED detonates, with the maximum jump height achieved about 100 to 300 ms later [44].

As the shock waves from the IED impact the vehicle, the effects on the occupant can be characterized into four categories. The primary injury, often termed "blast lung", is caused by the rapid increase in air pressure, which can affect any organ containing air. Primary injury is typically experienced by dismounted Warfighters. Wounds caused by fragments from the soil or vehicle are considered secondary blast injuries. Tertiary blast injuries, which are the focus of this research, are caused by the rapid global and local

motion of the vehicle and floor structure. The axial loading due to the rapid upward motion of the vehicle causes compression of the human skeletal structure, which is manifested in injuries to the lower leg, pelvis, and lumbar spine. The vertical acceleration of the vehicle due to the blast are then translated to the occupant, with the load path through the lower extremities from the floor and into the pelvis and spinal column via the seat interface. Excursion injuries can also result from head impacts to the interior of the vehicle [28]. Flail injuries to the arms can also occur but are much more difficult to characterize. The fourth category of blast injuries comprises thermal injuries such as burns or post-blast risks, such as drowning if the vehicle is overturned during the event [54].

The injuries caused by the global motion of the vehicle as well as the high frequency motion of the vehicle's floor due to the shock waves of the IED are the most prevalent. The severity of injury is directly related to the severity of the blast, location of the blast, and the direct surroundings of the occupant with respect to the vehicle's interior and the presence of injury mitigation structures. Other factors such as initial posture, PPE, and restraint use may also affect injury levels [44].

Blast mitigation seating systems with energy attenuating mechanisms are becoming more common in ground vehicles to absorb some of the vertical forces before they affect the pelvis and lumbar spine. The injuries to the pelvis or spine of the occupants can be debilitating, meaning the Warfighter cannot complete the mission or escape the vehicle. The loads from underbody blast reach the pelvis between 10 and 30 ms after detonation, with later loading times corresponding to seats mounted to the wall or ceiling as opposed to directly to the floor, as shown in Figure 2-1 and Figure 2-2 [44]. The body experiences a secondary impact during slam-down, when the vehicle returns to earth approximately

one second after the initial jump. Although less severe, the occupant is loaded again in a longer duration but lower accelerative event [44].

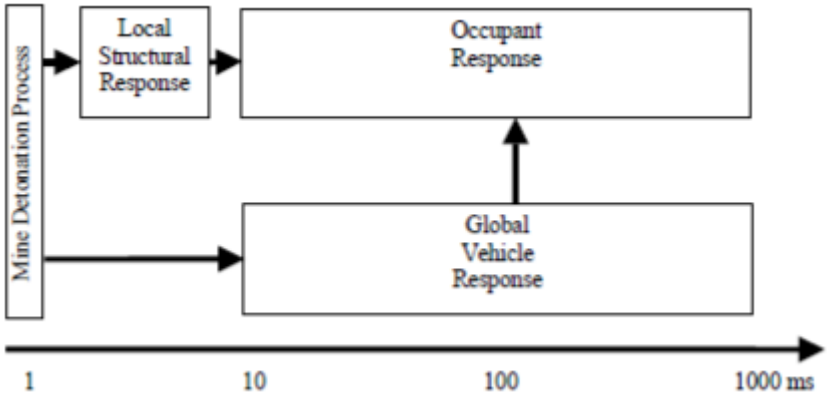

Figure 2-1. Sequence of events for vehicle and occupant in an underbody blast [44]

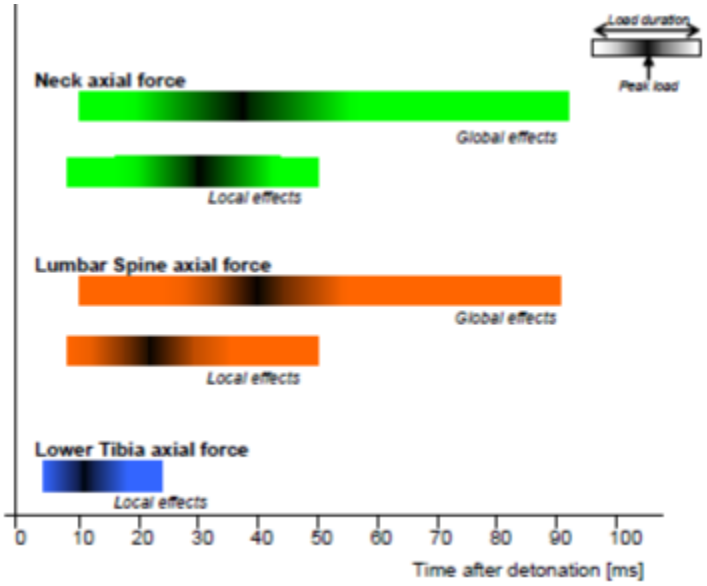

Figure 2-2. Sequence of events for tibia, lumbar spine, and neck compressive forces in an underbody blast [44]

2.2. Blast Energy Attenuating (EA) Seats

Blast EA seats are designed to absorb the energy traveling through the vehicle structure when undergoing a UBB event by isolating the occupant from the vehicle's upward global momentum. Several manufacturers have produced blast EA seats, so the design of seats vary widely as shown in Figure 2-3. Typically, seats are attached to the floor, wall, or ceiling of the vehicle, and these different mounting structures change the load path into the occupant. Integration to the vehicle is key in the design of seats, as they are considered part of the total vehicle design by manufacturers [43]. EA seats often incorporate a stroking mechanism to dissipate vertical acceleration by mechanical means before the forces are transferred to the occupant, thus reducing injuries, especially to the pelvis and lower spine. This energy absorption can be via plastic or elastic deformation [66]. Lower leg injuries are mitigated via other means, including foot rests, blast mats, or stroking floors.

Figure 2-3. Examples of currently available blast mitigation seats [26, 51, 71]

The design of the stroking mechanism of the seats is often dictated by the packaging space of the vehicle [39]. Each EA seat design employs unique mechanisms resulting in varying stroke lengths. Common EA mechanisms include shock tubes, springs, draw wires, and magneto-rheological devices, but the theory behind absorbing energy before it reaches the occupant is universally implemented across all designs. Materials such as supportive seat foam act as secondary EA solutions, as well as play a key role in Warfighter comfort. Stroke lengths often vary from a few inches to over a foot in displacement depending on the available package space in the vehicle. The key to proper EA design is optimizing the energy absorption properties of the seat while accounting for the size of the occupant and the severity of the blast. A smaller occupant may be too light to engage the active stroking mechanism, and a heavy occupant may overextend the stroking mechanism and cause it to bottom out, potentially resulting in greater injury to the occupant due to the interaction with the stops in the seat stroking mechanism. Seats must also be capable of first surviving the initial blast event and then the secondary slam-down, which imparts another vertical accelerative load to the seat and occupant [39]. Some seats incorporate resettable or reusable EA devices to survive multiple blast events. Seat designs are often tuned to a specific expected vehicle response to blast, meaning seats are marketed to different levels of severity, often characterized by “g rating”.

Standards do not currently exist to dictate the level of protection that must be afforded to the occupant during an accelerative loading event, as there is no one representative input pulse to cover the infinite range of blast events. Although EA seats are not new to the market, they have not been fully characterized with respect to energy attenuation

capability and the resulting effects on occupant protection. As a start to the characterization of the available EA seats on the market, the TARDEC Ground System Survivability Interior Blast Mitigation Seat Team tested and evaluated EA seats over a one-year period using a drop tower test method. Data from three different ATDs, or crash test dummies, was recorded on tests in twelve different seat styles that were dropped at two different heights on the drop tower. The Hybrid III ATDs represented 90 percent of the human population and are characterized as a 5th percentile female, 50th percentile male, and 95th percentile male [10]. An evaluation of the data allowed the assessment of commercially available and prototype seats to understand the performance of the seats with varying occupant weights and to evaluate the test methodology and occupant injury assessment performance criteria. The results from this data review afforded a better understanding of how seat design affects performance with varying occupant size, including weight and stature. The analysis also provided the TARDEC Seat Team with an overview of general trends and lessons learned toward developing blast seat performance specifications and standards for evaluation.

2.3. Military Helicopter Seats

The energy absorption technology utilized in the design of helicopter seats for crash events can be leveraged in the design of military blast EA seats. Similar to the blast seat application, helicopter seats are designed to limit the loads imparted parallel to the occupant's spine during a crash event by controlling the stroke of the seat and have been in use since the 1970s [33]. A review of the available seat technology by Desjardins in 2003 determined that several types of EA mechanisms were being employed in seats, all with the common goal of maximizing the efficiency of energy absorption. The most

common types of successful mechanisms included inversion tubes, wire and strap benders, tube and die, and metal cutters [19]. It is important to note that although the theory behind these designs is the same as that for blast seats, the magnitude and timing of helicopter crashes compared to blast events are significantly different. Desjardins states that the loading profile of a helicopter crash can be approximated by a triangular acceleration pulse with a peak of approximately 50 g and duration of more than 50 ms as shown in Figure 2-4. A blast event often results in a peak floor acceleration more than six times that of a helicopter crash with durations less than a factor of ten, which greatly affects the approach to EA mechanisms and the speed at which they must react to absorb energy as shown in Figure 2-5 [19].

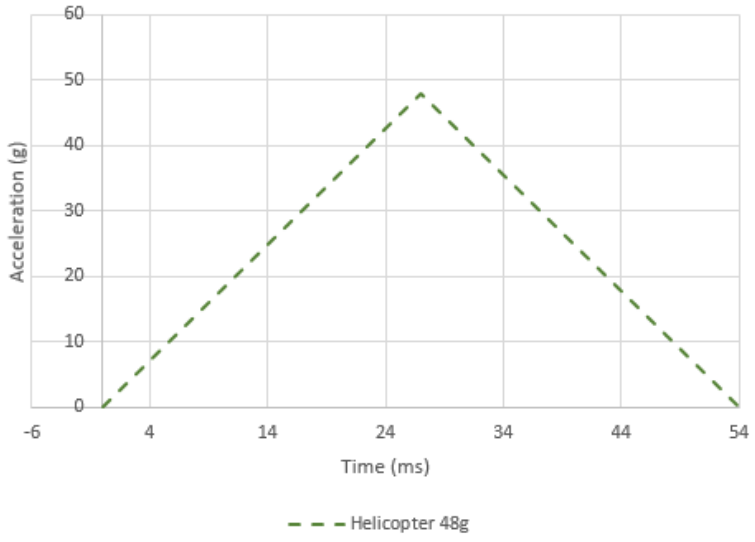

Figure 2-4. Representative accelerative loading profile during helicopter crash event [19]

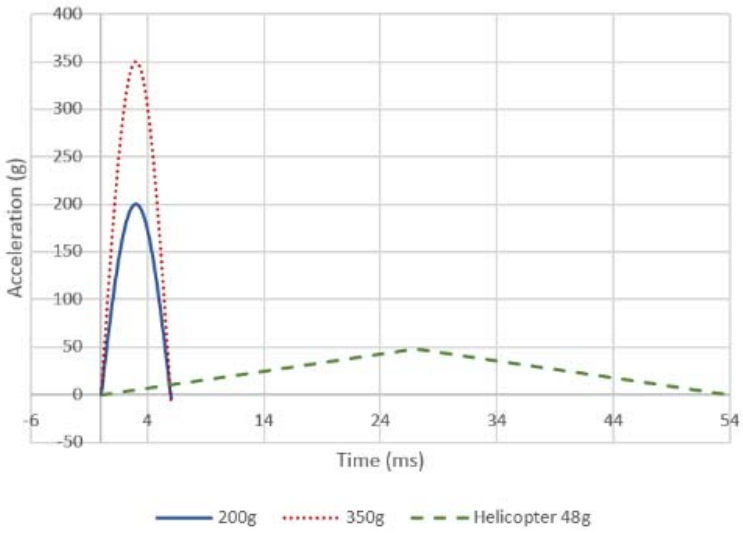

Figure 2-5. Helicopter crash event pulse compared to blast pulses show large differences in order of magnitude and timing

Several different approaches for helicopter EA mechanisms exist, including Fixed Load Energy Absorbers (FLEA), Variable Load Energy Absorbers (VLEA), Fixed Profile Energy Absorbers (FPEA), and Variable Profile Energy Absorbers (VPEA). Each approach has its own advantages and disadvantages, and knowledge of these can be leveraged for blast seat design. The FLEA was designed to optimize only for the 50th percentile occupant, which exposed lighter occupants to a higher deceleration while potentially bottoming out the stroke for the heavier occupant, although the deceleration was reduced. The VLEA involves a manually adjustable system to adjust the limiting load on the seat to compensate for the weight of each occupant to afford the same level of protection. FPEA systems produce a constant profile load-displacement independent of occupant weight. VPEA combines the theory of the other approaches and limits the loads based on the weights of the occupant. The ultimate design would create a system that develops unique nonlinear load-deflection profiles for each occupant while taking weight into consideration [19].

Civil helicopter standards state that the limit for lumbar spine loading in an occupant as measured by a 50th percentile male ATD is 1500 lbs [6672 N] [19]. Labun et al suggested limiting the seat acceleration to 14.5 g, however, this is based on Dynamic Response Index, which, as explained later, will not be used in this study [33].

Helicopter seat designs target either constant loading profiles or profiles that sync with the human body's natural dynamic spring rates to improve efficiency while reducing overshoot [19, 33]. Helicopter seat design also focuses on maximizing the amount of work done by the EA mechanism before the lumbar spine load peaks, thus reducing injury potential [33]. Labun et al suggested implementing a design that varies the force of the EA mechanism dynamically as the seat strokes to improve efficiency [33]. The seats installed in the U.S. Army Black Hawk helicopter claim to provide protection with crashes up to 18.3 m/s [19], but it is important to reiterate that the loading profile of a helicopter crash is vastly different to that of an underbody blast event. Common with the view point of TARDEC and the U.S. Army, a more biofidelic ATD for vertical loading should be employed during future helicopter seat assessments, as the Hybrid III ATD was not designed for vertical blast events and lacks biofidelity under these accelerative conditions.

2.4. Personal Protective Equipment

Personal protective equipment (PPE), which includes the Army Combat Uniform (ACU), Improved Outer Tactical Vest (IOTV) with associated gear, and boots, is traditionally worn in theater by Warfighters and has been shown to have an effect on injury outcomes during blast events as measured by the small occupant Hybrid III ATD [11]. The addition of PPE, although more realistic to the condition of the Warfighters' encumbrance during an underbody blast event, adds a layer of complexity with

evaluation, especially in modeling due to the interaction of the PPE with the body, and due to the fact that every Warfighter has a unique gear configuration. Studies are limited on the effects of PPE on injury thresholds, as well. The specific details of PPE is not public release, further complicating its use in evaluation. For the purposes of this research, only a simplified approximation of PPE was used.

2.5. Underbody Blast Evaluation Methods

To protect Warfighters from underbody blast events, a better understanding of the interaction between the occupant and the vehicle is needed, as well as knowledge of occupant kinematics and kinetics. Actual vehicle acceleration data from theater is not accessible, so alternative methods to obtain vehicle blast data have been devised, such as live fire blast testing. Military vehicles or generic hulls are subjected to controlled blasts with representative charges buried in soil prepared similar to that of theater conditions, and Hybrid III ATDs collect data during the event. Floor acceleration data is recorded at the base of seats within these vehicles, and those pulses can then be replicated on a smaller scale for use on drop towers or vertical accelerative loading fixtures to study the load profile effects on the seating system. Both ATDs and post-mortem human surrogates (PMHS), or cadavers, are tested in similar input conditions to closer study the effects of loading and the effectiveness of mitigation strategies. Programs such as TARDEC's Ground System Survivability Interior Blast Mitigation and the Warrior Injury Assessment Manikin (WIAMan) are leveraging this range of test data to improve Warfighter safety by focusing on short duration vertical acceleration pulses with high magnitudes and high input loading rates [2]. Data from the WIAMan program including input conditions and occupant kinetics were utilized in this research effort.

CHAPTER 3 – ANATOMY AND INJURY ASSESSMENT

3.1. Pelvis

The critical load path from the EA seat to the upper body during a vertical accelerative loading event is first through the pelvis and then transmitted superiorly through the lumbar and into the remainder of the spine. As the pelvis and lower spine complex are the first to receive the force transfer, these two structures often experience fractures that are more severe than those sustained in the rest of the load path from the EA seat [4]. An understanding of the anatomy of the pelvis and lumbar spine complex and the resulting injuries due to underbody blast is important in developing fracture mitigation strategies.

3.1.1. Pelvis Anatomy

The pelvis, or pelvic girdle, as shown in Figure 3-1, is a bony structure consisting of right and left innominantes or hip bones, as well as the sacrum (Figure 3-2). Each innominate is formed during the fusion of three separate bones during puberty: the ilium, ischium, and pubis. The most inferior protuberance of the pelvic girdle is the ischial tuberosity; the left and right ischial tuberosities function as two of the three contact points of the pelvic girdle for load transmission from the seat pan.

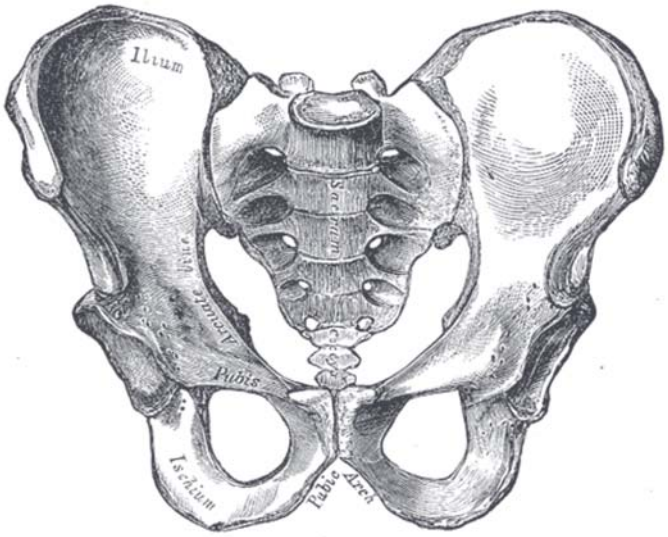

Figure 3-1. Pelvic girdle [22]

The ring shape of the pelvic girdle's outlet is defined by the medial surfaces of the iliac wings. It is bounded in the posterior aspect by the sacrum and the anterior aspect by the pubic symphysis, a joint formed by the left and right pubic rami. The acetabulum, which houses the femoral head, is a cup-shaped depression formed into the ilium.

The third load contact point for vertical loading is the coccyx, which is connected to the sacrum. The sacrum is a bony structure formed by the fusion of five vertebrae which is connected to the right and left ilium via sacroiliac joints consisting of flexible ligaments. The coccyx is connected to the inferior portion of the sacrum by sacrococcygeal ligaments, allowing some flexibility in the joint. The sacrum features several pairs of foramen, or channels through the bone, for the sacral plexus nerves to pass through [41].

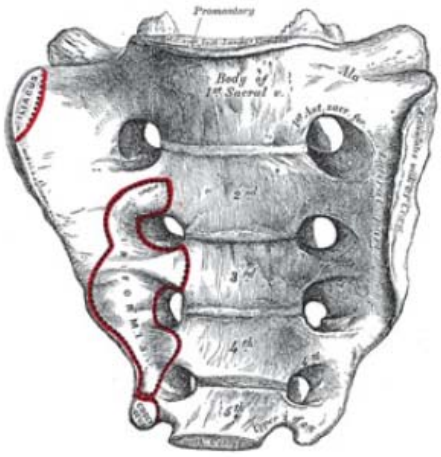

Figure 3-2. Sacrum [22]

3.1.2. Pelvis Injury Classifications

There are several ways to classify the types of pelvic fractures, including the Tile classification of Type A, B, and C. Type A fractures are rotationally stable [18], meaning the posterior arch is intact. Type A fractures include avulsion injuries, iliac-wing or anterior-arch fractures, or transverse sacrococcygeal fractures. Type B fractures are partially stable, which means that there is an incomplete disruption of the posterior arch of the pelvis. Type B fractures are further classified as open-book injuries with external rotation, lateral-compression injuries with internal rotation, or bilateral fractures. Unstable fractures with complete disruption of the posterior arch are considered Type C fractures. This most severe category of lesions includes unstable unilateral fractures of the iliac and sacrum or sacroiliac fracture-dislocation and unstable bilateral fractures [70]. Examples of Type B and C fractures are shown in Figure 3-3.

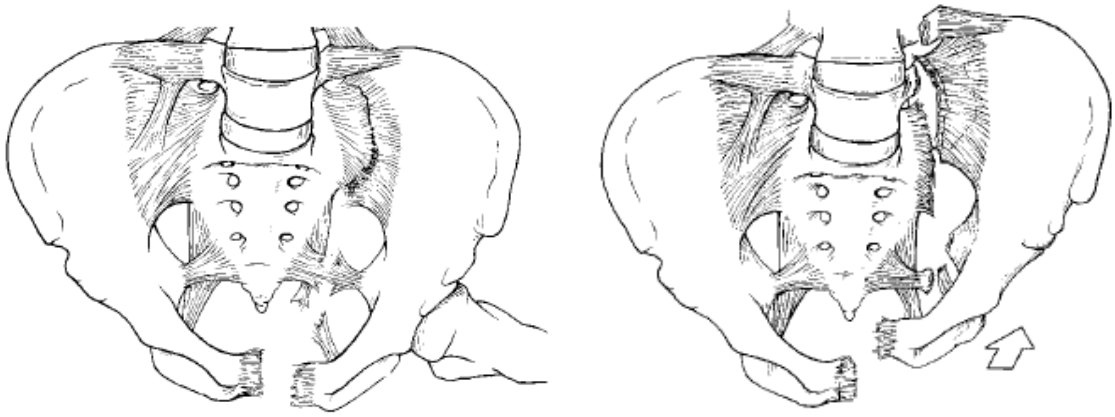

Figure 3-3. Examples of Tile Type B (open book) (left) and Type C (right) fractures [70]

3.1.3. Common Underbody Blast Pelvis Injuries and Injury Thresholds

Most studies focusing on fracture loading for the pelvis and lumbar spine concentrate on frontal or lateral loading, which corresponds to automotive vehicle crashes for velocity, duration, and directionality. The focus on understanding of injury thresholds for vertical loading in an underbody blast event is an emerging field, and data is currently limited but rapidly being published. The Abbreviated Injury Scale (AIS) is often referenced with respect to assessing the severity of injury, and the latest update to this scale has incorporated military injuries, but it does not properly account for long-term functional challenges that accompany underbody blast injuries [2, 34].

Numerous studies of theater data provide details on the most common injuries reported by occupants involved in underbody blast events. For the purposes of this study, only skeletal injuries will be discussed. The global motion of the body, previously described as tertiary blast effects, result in blunt and crush injuries, often with traumatic brain injuries [28]. Arepally et al describes one of the main injury mechanisms in underbody blast as the tension and compression of the body during loading, with injury being caused during the exceedance of elastic tolerances [3]. Injury mechanisms are

also based on the time duration-dependent aspect of accelerations, forces, and moments applied to the body [3, 15]. Comparison studies to previous pelvic injury research demonstrate a distinct difference in resulting injury due to direction of impact, with well-known injury patterns due to lateral pelvic structures vastly different than those seen in vertical loading situations [5]. There is also emerging data to support that the rate of loading can affect the injury patterns and locations within the pelvis and lumbar vertebrae due to mass recruitment effects [5].

A study by Davis et al [18] determined that more than 26% of the fatalities in OIF/OEF during 2008 involved combat-related pelvic fractures, with these fracture patterns classified as much higher severity and lethality than pelvic fractures common to civilian studies. Pelvic fractures due to underbody blast are characterized as blunt trauma events and often include concomitant injuries throughout the body. Davis et al found that the mortality rate for Warfighters sustaining combat-related pelvic fractures was more than 90% based on their specific data set [18]. Type A fractures, or stable fractures, were more common in the survivor data set, while Type C fractures had the highest mortality rate. Due to the large number of major blood vessels concentrated in the pelvic girdle, fractures can lead to hemorrhaging, which is often the cause of death with severe pelvic fractures [18].

Current underbody blast injury prediction methods are most often based on automotive injury assessment reference values, which does not fully represent the order of magnitude for the acceleration and duration of loading for underbody blast [72]. The WIAMan program, sponsored by the U.S. Department of Defense (DoD) was developed to produce a new biofidelic ATD for use in underbody blast and to provide updated injury

criteria using post-mortem human surrogate (PMHS) testing in vertical accelerative loading conditions [72]. The development of this data will be key to fully understanding how the body reacts to vertical blast loading, building on the currently available ejection seat injury thresholds. However, data from this program has not yet been fully released, so injury probability must be based on currently available literature and the emerging PMHS research from this effort.

According to the WIAMan program, typical underbody blast pelvic injuries, as determined from an interpretation of tomography reconstructions, include fractures of the pubic rami, ischium, sacral alar, acetabulum, and sacroiliac joint [68]. These fractures, except for the pubic rami, are considered partially stable or unstable using the Orthopedic Trauma Association definition [72]. Weaver et al postulated that the high mortality (46% of KIA from JTAPIC) related to pelvic fractures may be associated with the severity of the threat causing additional injuries or the inability to bear weight and safely evacuate from the vehicle to receive medical attention or avoid additional threats [72].

A recent in-depth review of JTAPIC data by Danelson et al determined that unstable pelvis fractures were the most common pelvic injury in recent theater events. This review also differentiated pelvic injuries between standard seats and “extended time with decreased magnitude (ETDM)” seats, which would be representative of a stroking blast seat. ETDM seats were much less likely to be involved when severe pelvic fractures were identified [17].

The latest JTAPIC review by Loftis et al did not list pelvis fractures in the top five most common injuries for WIA or KIA for OIF, OEF, and OND [34], but this may be due to the protection provided by blast seats as described by Danelson et al [17].

Studies have been performed in attempts to understand the best indicator of injury in underbody blast. Kulkarni et al (2013) stated that the Survivability design community often relies on the change of velocity (Δv) to define the severity of the pulse, however, more information is needed, as a specific Δv can be achieved by several combinations of acceleration and duration. Kulkarni (2013) concluded from a modeling and simulation analysis using MADYMO that Δv is the best indicator to use when estimating injury probability [31]. Benesch also stated that Δv, and additionally, displacement, correlates well to pelvis injuries measured by an ATD [9].

The University of Virginia (UVA) has released several publications highlighting the preliminary work on their underbody blast research efforts. UVA has performed several PMHS tests at underbody blast input conditions on their horizontal sled system and have released thresholds for injury as measured at the seat and pelvis. For their test series, the seat pan accelerations ranged from 291 to 738 g for 3 ms durations, which aligns with other published underbody blast seat acceleration ranges. This acceleration results in seat velocities of 5.2 to 10.2 m/s [5].

Bailey et al from UVA lists pelvic ring fractures and ischium fractures as common underbody blast injuries. These fractures should be considered high priority to address, as the pelvis is key in weight-bearing and ambulation [6]. Bailey et al performed whole body PMHS testing to simulate underbody blast loading to determine the thresholds of pelvic fracture as measured at the seat pan and listed the following locations as suffering fractures due to vertical loading: sacral alar, acetabulum, superior and inferior pubic ramus, and ischial tuberosity, which demonstrates the variation in pelvic injury due to underbody blast events [6]. Accelerometers located on the sacrum of these PMHS

recorded peak accelerations ranging from 100 to 381 g, or velocities from 1.7 to 6.0 m/s [5]. Although the study was limited to five PMHS, Bailey et al determined that the vertical injury threshold is approximately a delta velocity of 6.5 m/s over a 5 ms duration at the seat pan, with a 300 g acceleration peak [6]. A second publication by Bailey et al listed the injury threshold to be approximately 6.65 to 7.63 m/s at the seat pan [5]. Using a Weibull Regression analysis, Bailey et al also calculated a 50% pelvis injury probability to occur at a seat acceleration of approximately 290 g or a sacrum acceleration of about 190 g (resulting in a sacrum velocity of 2.8 m/s) [5].

Danelson et al [16] recently conducted vertical accelerative loading tests on a blast buck with PMHS and Hybrid III to compare responses in the underbody blast environment. Blast tests were conducted at a mild and enhanced charge level in efforts to replicate injuries reported in theater. Danelson et al reported that the Hybrid III has a stiffer response than the PMHS and cannot accurately replicate lower extremity kinematics, which is part of the motivation for the WIAMan program. PMHS experienced fractures to the ischial tuberosities, inferior and superior pubic rami, ilium, and acetabulum, as shown in Figure 3-4, but these injuries were more severe than those reported in more recent reviews of theater injuries [34]. Additionally, many specimen had separations of the sacroiliac joints and pubic symphysis. Fractures occurred between 8 and 14 ms after the initiation of the blast event. PMHS pelvis fractures were recorded when accelerations measured at the sacrum were above approximately 175 g, which corresponds to a pelvis velocity of 4 m/s. Danelson et al reported that some of the pelvic fractures may have been due to a horizontal load input from the pelvis contacting the back of the seat, specifically fractures to the sacroiliac joint and iliac crest. Pelvic injuries in

this series seemed to be associated with higher energy events, meaning higher magnitude and shorter duration accelerations, resulting in high velocities.

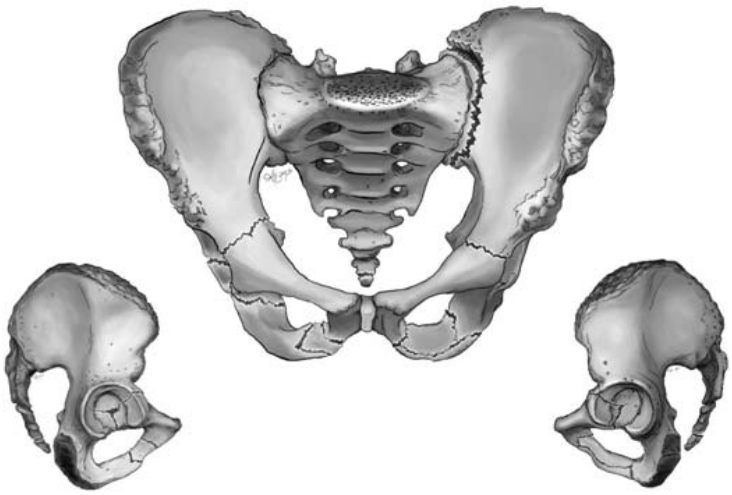

Figure 3-4. Pelvis fracture patterns experienced during simulated underbody blast loading [16]

Yoganandan et al performed a series of underbody blast simulations with PMHS with varying input pulses ranging from 2.8 to 12.5 m/s with multiple pulse shapes including triangle and sigmoid. Normalized measured sacrum accelerations ranged from 10 to approximately 204 g, and spine accelerations were reported from about 12 to 85 g, demonstrating the energy absorbing properties of the body as the acceleration moves superiorly. Seat pan forces at injurious levels were as low as approximately 7500 N. Resultant spine accelerations at injury were as low as approximately 30 g, and resultant sacrum accelerations for injury were around 30 g [75].

Using the pelvis accelerometer within the Hybrid III, the US Army Aberdeen Test Center has set the injury threshold for pelvis acceleration at 15 g for low injury risk, 18 g for medium risk, and 23 g for high risk over a 7 ms interval [66].

In the Condition A testing for the WIAMan program with 4 m/s in 5 ms input at the floor and seat interface, the PMHS tested did not sustain injuries with resultant accelerations at the pelvis up to approximately 70 g and at the T12 location in the z-axis up to approximately 90 g [49].

Injury thresholds reported in the literature include seat load, velocity and acceleration and spine and pelvis acceleration, as summarized in Table 3-1. Variations are partially due to the differences in setup, test fixtures, and instrumentation used for each study. Additionally, all of these studies had small PMHS sample sizes. For the purposes of this research, “threshold” refers to the lowest reported force causing fracture from the literature references. When a range of values was provided, the lowest value of that range with a pertinent fracture was selected and rounded to the nearest 100. As additional research emerges, these values should be updated.

Table 3-1. Pelvis injury threshold summary

Injury Threshold	Occupant	Study
6.5 m/s, 5 ms duration, 300 g peak at the seat**	PMHS	Bailey [6]
6.65-7.63 m/s at seat pan**	PMHS	Bailey [5]
8-14 ms (timing of fracture)	PMHS	Danelson [16]
175 g, 4 m/s at pelvis accel**	PMHS	Danelson [16]
7500 N at seat, 30 g at spine, 30 g at sacrum**	PMHS	Yoganandan [75]
15 g low, 18 g medium, 23 g high risk at Hybrid III pelvis accel (7 ms interval)	Hybrid III	Tabiei [66]

**Denotes pertinent threshold for UBB loading

3.2. Lumbar

The lumbar vertebrae are the next anatomical structure to absorb vertical loading after the pelvis and sacrum complex.

3.2.1. Lumbar Anatomy

The five vertebrae of the lumbar region form the base of the spine, or vertebral column. Each vertebrae is separated by a semi-rigid intervertebral disc. The lumbar vertebrae are numbered from one to five starting with the most superior vertebra and are adjacent to the twelfth thoracic vertebra superiorly and the sacrum inferiorly. As shown in Figure 3-5, the vertebral column comprises lumbar, thoracic, and cervical vertebrae. The lumbar and cervical segments have a lordotic curve, which arches inward, and the thoracic segment has a kyphotic curve, which arches outward.

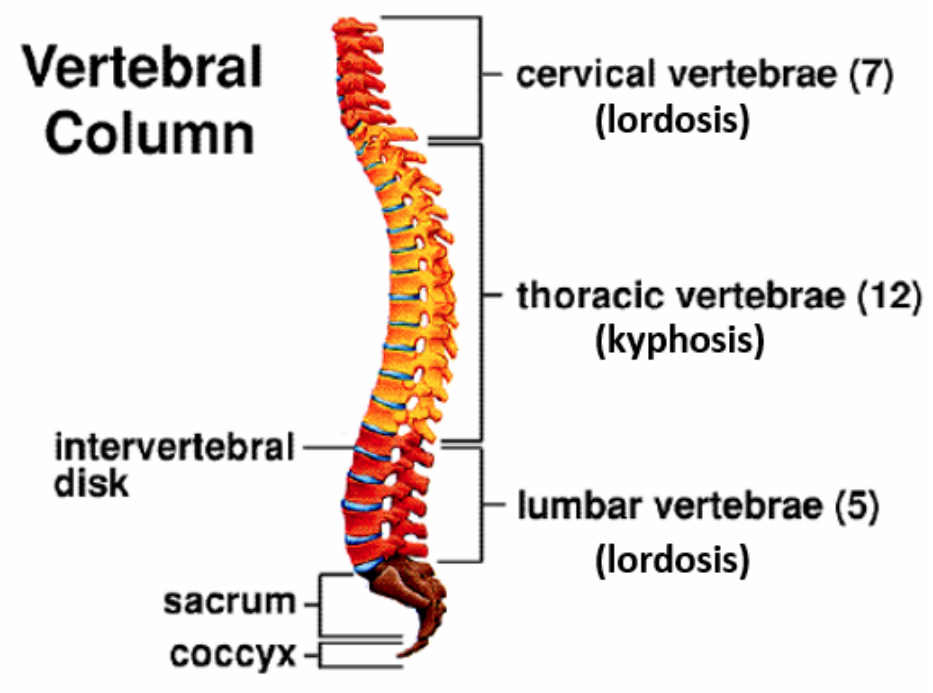

Figure 3-5. Vertebral column showing cervical, thoracic, and lumbar segments with lordotic and kyphotic curvatures [44]

Each vertebrae features a vertebral body, vertebral arch, and seven bony processes (Figure 3-6). The vertebral body provides support to the spinal column and carries the force of the body weight. The arch houses and provides protection to the spinal cord.

The articular processes (superior and inferior) feature surfaces that restrict movement from one vertebra to the next. The two transverse processes and single spinous process of each vertebra provide bony surfaces for muscle attachment and movement of the spinal column [41].

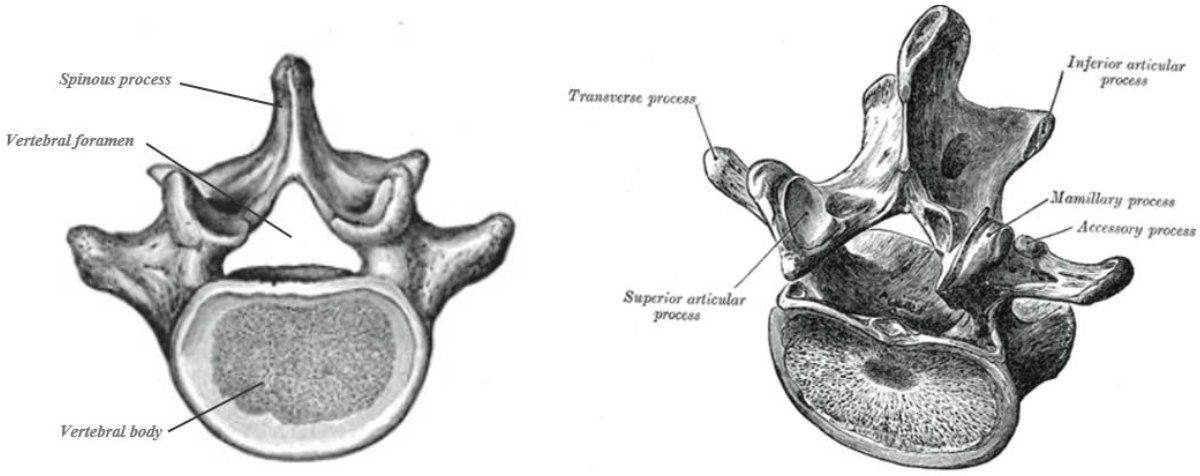

Figure 3-6. Anatomy of lumbar vertebra [22]

Individual vertebrae are connected by a series of ligaments which are critical for stability and mobility. Ligaments exist between vertebral bodies, vertebral processes, and facet joints. The various ligaments are shown in Figure 3-7.

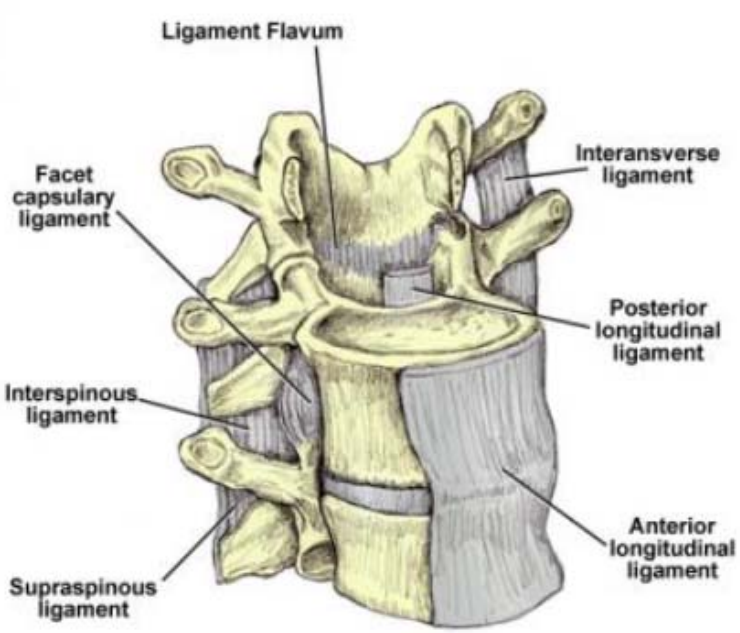

Figure 3-7. Ligaments in the spinal column connect the features of the vertebrae to provide stability and mobility [61]

3.2.2. Lumbar Injury Classifications

Fractures of the vertebral body can often be classified based on the directionality of the loading and resulting fracture patterns of the vertebral body. The major classifications include anterior wedge fractures, burst fractures, dislocations, Chance fractures, hyperextension injuries, and rotational injuries [30].

Anterior compression or wedge fractures are the most common thoracolumbar injury and can be caused by underbody blast events or by interaction with three-point restraints in motor vehicles. Research by King et al proposed that these injuries are due to a compression and bending mechanism, as the center of gravity of the torso is anterior to the spine. Along with facet dislocations, anterior wedge fractures can occur during ejection and severe vertical accelerative events [29, 30]. Anterior wedge fractures are

characterized by a buckle in the anterior cortex along with a loss of height of the anterior section of the vertebral body [24, 30].

Burst fractures are a result of high compressive loads on the spine. They are common during falls when there is a direct impact to the buttocks. Burst fractures can cause retropulsion of vertebral bone into the spinal canal, which can cause paraplegia [29]. Several examples of burst fracture patterns are shown in Figure 3-8.

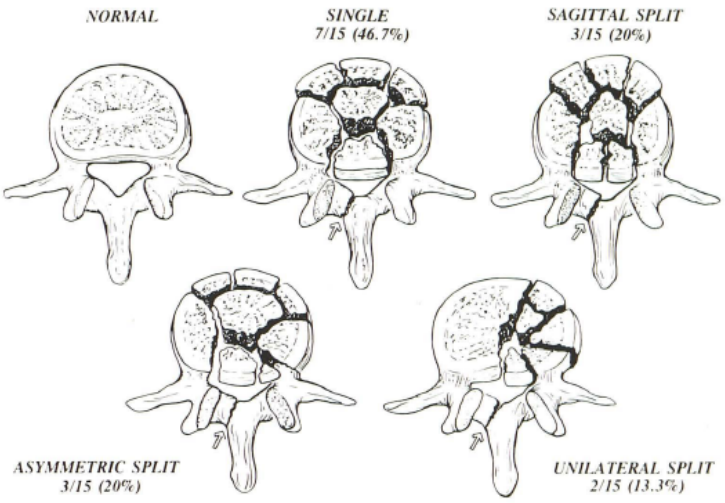

Figure 3-8. Various burst fractures showing the four basic patterns of the fracture and retropulsed fragment in the Atlas et al case study [4]

Chance fractures are flexion-distraction injuries characterized by horizontal fracture lines through the pedicles without anterior vertebral compression as shown in Figure 3-9. Ragel et al describes the cause of these fractures as a “hyperflexion of the spine over a fulcrum located anterior to the vertebral body,” but the exact mechanism of injury due to an underbody blast has not been determined [51].

Figure 3-9. Chance fractures sustained by Warfighters in OEF – asterisks denote fracture locations; arrow denotes anterior vertebral loss of body height [52]

Hyperextension injuries have been noted during aircraft ejection events and are characterized by an opening of the disc space with resulting damage to the bone [30]. Rotational injuries to the lumbar vertebrae are uncommon, but they are often a combination of compression and twisting, resulting in a diagonal shearing of the vertebral complex as shown in Figure 3-10 [30, 38].

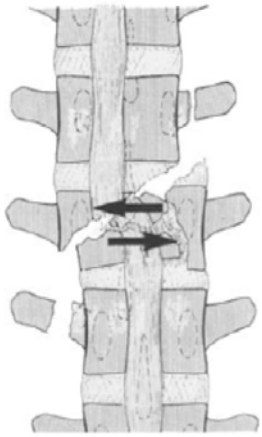

Figure 3-10. Fracture due to rotational injury with dislocation [30, 38]

3.2.3. Common Underbody Blast Lumbar Injuries and Injury Thresholds

The wide range of blast event severities makes it difficult to define the most likely injury patterns for lumbar vertebrae, but several studies have been published with medical records listing common fractures due to underbody blast. According to NATO research, occupants involved in underbody blast events experience spinal bony, ligamentous, and muscle injuries. Common vertebral fractures include wedge and compression fractures, as well as spinous and transverse process fractures. Kang et al reported that spine injury patterns due to high-energy blasts include Chance fractures, low lumbar spine burst fractures, and lumbosacral dissociation injuries [28]. A study of thoracolumbar fractures from OEF reported that Chance fractures and burst fractures were prevalent injuries [51]. The human spine is known to be sensitive to the rate of loading, so understanding the different injury mechanisms for high rate vertical accelerative loading is key to injury prevention [73].

Early studies on vertical loading injuries to the thoracolumbar spine were developed to investigate the injuries suffered by jet aircraft pilots during ejection maneuvers. These pilots primarily sustained anterior wedge fractures between T10 and

L2 due to the flexion-compression motion of the spine (Figure 3-11). These studies provided an injury tolerance threshold of approximately 20 g at the thoracolumbar region for younger occupants under short duration vertical loading [22, 30].

Figure 3-11. Wedge fracture of lumbar vertebra [29].

Stemper et al conducted testing on PMHS lumbar spine segments to replicate helicopter pilot ejections and helicopter crash vertical loading. Although the loading peak accelerations are lower than expected in a blast environment at 20-22 g for the ejection testing and 44-65 g for the crash simulations, the fractures reported from this testing are representative of vertical loading injuries (Figure 3-12). Both sets of tests resulted in burst and anterior compression fractures, an inferior migration of injury from L1 to L5 with higher loading tests [65].

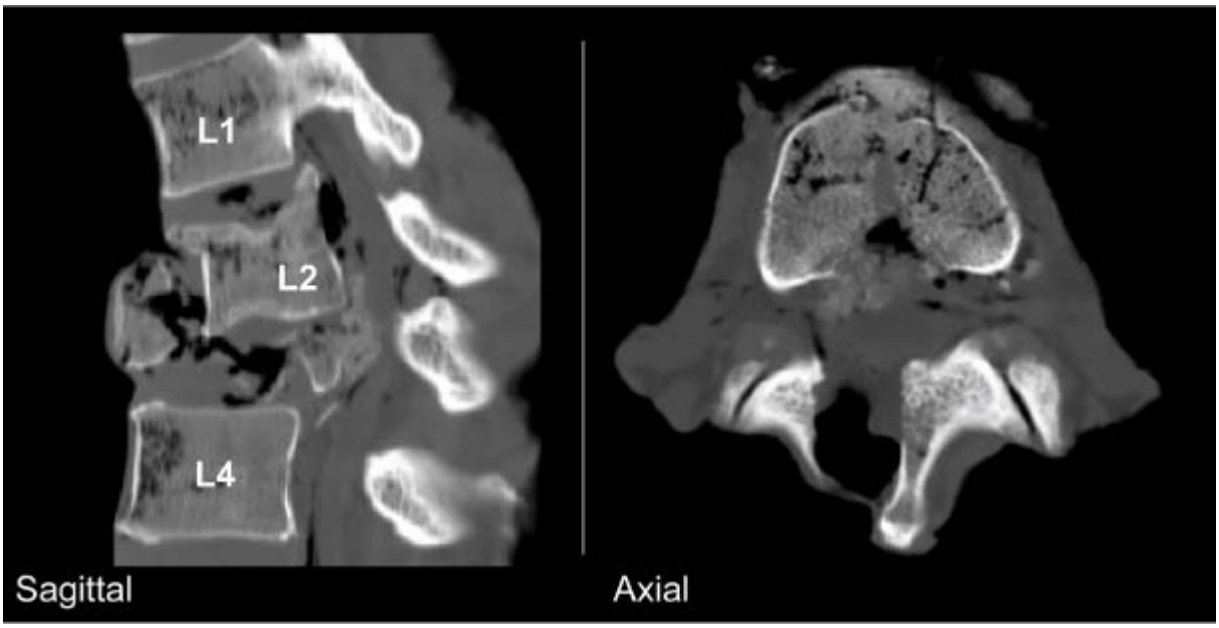

Figure 3-12. Burst fracture of L3 sustained during Stemper et al helicopter load simulation testing [65]

Burst fractures are caused by high rate compressive loading on the spine, which are often accompanied by wedging. Studies by Denis (1983) determined that L1 was the most likely to be fractured [19, 30]. Willen et al proposed an injury threshold of 8000 N for tolerance of the thoracolumbar spine to burst fractures [30, 73]. Tests conducted by Yoganandan et al to replicate ejection seat conditions with lumbar spine fractures resulted in peak axial forces of 4800 to 7200 N, respectively [74], with peak accelerations of approximately 14 to 40 g. A separate study by Oxland in 1992 reported that burst fractures of segments of the lumbar spine occurred at an average of approximately 6000 N, which corresponds to an acceleration of approximately 13 g at fracture [47].

Myklebust et al completed axial compressive loading studies on thoracolumbar spines and determined that the average failure loading for segmented spines was 2056 ± 1468 N, and the average failure loading decreased to 1787 ± 693 N when tested in an

intact cadaver. This loading often resulted in wedge compression fractures. It should be noted that these tests were completed at low rates with unique interface conditions, but provide relevant tolerance data points [42].

Yoganandan et al (2015) determined that peak axial force limits for injury in the lumbar spine ranged from 5200 N to 7200 N under loading designed to simulate helicopter crashes [75]. These injuries included compression fractures and bilateral facet dislocations and registered peak accelerations up to 56 g in the z-axis [75]. This test series indicated that lumbar spine injuries increase as the vertical acceleration imparted to them increase, and that the injuries tend to shift inferiorly toward L5 as severity increase [75].

The recent vertical blast studies carried out by Danelson et al reported mainly minor or inconsequential damage to the spine due to axial loading, but one PMHS did have a compression fracture of L4 [16]. This research found that accelerations above 100 g as measured at the lumbar spine in the z-direction were indicative of at least sustaining minor damage such as fracture of the lateral processes. Danelson et al stated that the lumbar spine is expected to fracture before the pelvis based on prior research findings, but the use of a rigid seat in this study may have affected the fracture locations, as there were limited major lumbar spine fractures in this study. According to this test series, lumbar spine injury seems to be dependent on high accelerations and resulting high velocities [16].

As there has been limited studies of the effects of vertical loading on the pelvis and lumbar spine complex, there are still unknowns on how these two structures interact, but Danelson et al stated that there is a relationship between fractures in the lumbar spine

and pelvis regions, which are most likely due to the duration of contact and input energy. Danielson et al postulated that pelvis fractures seem to be more likely when a PMHS is tested on a rigid seat with short duration and high energy events [16], which leads one to believe that the introduction of an energy absorption mechanism to a seat that elongates the contact duration may cause a migration of injury superior in the body toward the lumbar spine region.

The recent JTAPIC study by Danelson et al identified compression as the most common mechanism of injury for fractures of the spine. The spine region was the second most frequent region of the body to be damaged in this data set. 29% of the reviewed population experienced lumbar spine injuries. As with the pelvis, the use of an ETDM, or stroking seat, was less likely to cause spinal injury [17].

Using the lumbar spine load cell within the Hybrid III, the US Army Aberdeen Test Center has set the injury threshold for lumbar spine axial compression force at 6672 N (1500 lbs), but according to Chandler, this was determined based on the results of the Part 572 dummy, or the Hybrid II ATD [15]. They have also specified that the compression load cannot exceed 3800 N over a 30 ms period [66].

NATO suggests using Dynamic Response Index (DRI) to assess lumbar spine fracture [44], but numerous studies have determined that DRI is an antiquated approximation of human injury. DRI is a mechanical model that uses a simple lumped mass parameter model to simulate the response of the pelvis and spine with a single spring-mass-damper system. DRI uses spring and damper coefficients that were measured from Air Force pilots more than 50 years ago and then related these coefficients to risk of spinal injury using seat acceleration as an input to the model. With

the advent of the Hybrid III anthropomorphic test device (ATD), a direct measurement of lumbar spine compressive force can be measured, which takes into account the energy absorption properties of the seat foam and human body, and this is a much improved representation of lumbar spine response. DRI cannot be measured from the pelvis accelerometer of the ATD, as this leads to unrealistic responses, as it was designed for seat pan acceleration [15]. DRI also assumes that the occupant is in a perfect upright posture, which is often not representative [15]. While ATD lumbar spine load is a real-time response of the body, DRI can be affected by late data beyond the initial compression duration and also assumes linear human response, which is unrealistic [69]. For the purposes of this research, DRI will not be used.

Table 3-2 contains a summary of the PMHS and Hybrid III injury thresholds reviewed in this chapter. Many of the studies conducted were at lower loading rates than experienced during underbody blast or at load ranges above injury tolerance, but these studies provide a general overview of the range of loading tolerated by the spine. For the purposes of this research, “threshold” refers to the lowest reported force causing fracture from the literature references. When a range of values was provided, the lowest value of that range with a pertinent fracture was selected. As additional research emerges, these values should be updated.

Table 3-2. Lumbar spine injury threshold summary

Injury Threshold	Occupant	Study
8000 N (burst fx)	PMHS	Willen [73]
20-22 g, 44-65 g	PMHS	Stemper [65]
20 g at thoracolumbar region	PMHS	Evans [22]
6000 N, 13 g	PMHS	Oxland [47]
5200-7200 N, 56 g**	PMHS	Yoganandan [75]
100 g**	PMHS	Danelson [16]
2056 N	PMHS segmented lumbar	Myklebust [42]
1787 N	PMHS	Myklebust [42]
6672 N peak measured at lumbar load cell, 3800 N over 30 ms period	Hybrid III	Tabiei [66]

**Denotes pertinent threshold for UBB loading

CHAPTER 4 – RESEARCH PROPOSAL

4.1. Research Proposal

Although there are several EA blast seats commercially available, the effort to determine optimal force and deflection profiles based on common blast pulses has not yet been undertaken. This research utilized MADYMO to perform a sensitivity study on the loading profiles of generic EA devices with varying pulses that can be implemented within the laws of physics.

The University of Virginia (UVA) has been involved in the WIAMan program and has conducted multiple test case conditions with both the 50th percentile Hybrid III ATD and PMHS on their horizontal sled system to replicate underbody blast loading. The WIAMan program developed several specific sub-injurious test conditions designed to replicate underbody blast in a laboratory setting using the UVA sled with a rigid seat. The pulses described in Figure 4-1 (floor), Figure 4-2 (seat), and Table 4-1 represent Condition A from the WIAMan program and Condition B from the Bailey et al studies, both tested at UVA [5, 49]. The velocity traces are shown in Figure 4-3 and Figure 4-4. Both floor and seat accelerations were applied to the model, as there was a slight offset in the pulses, and exact pulse data was required for validation.

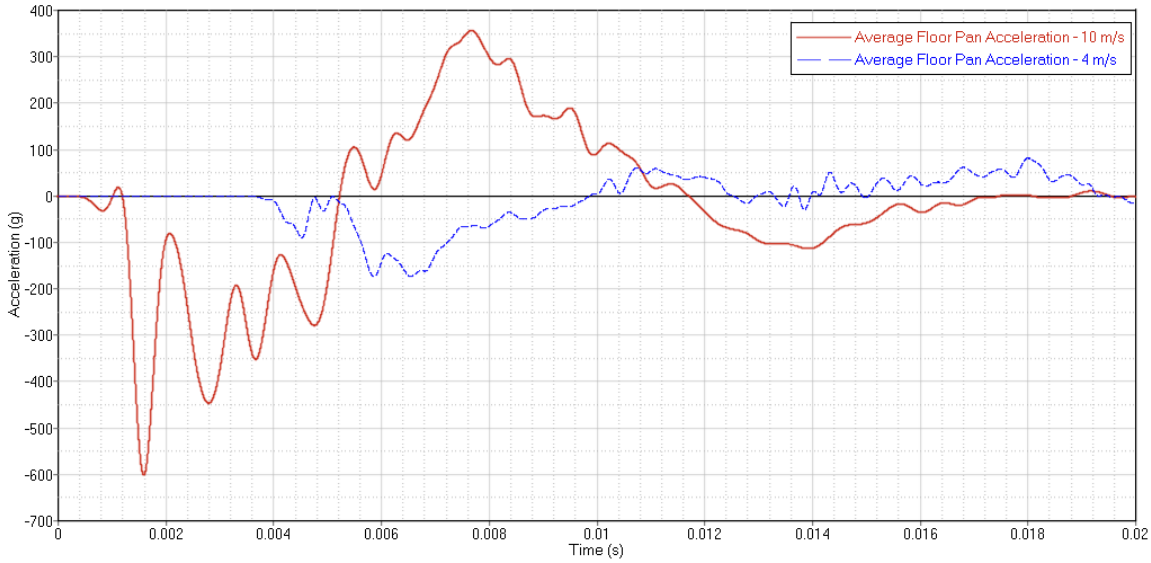

Figure 4-1. Input acceleration pulse for sub-injurious Condition A (blue) and injurious Condition B (red) at the floor as measured on the UVA sled

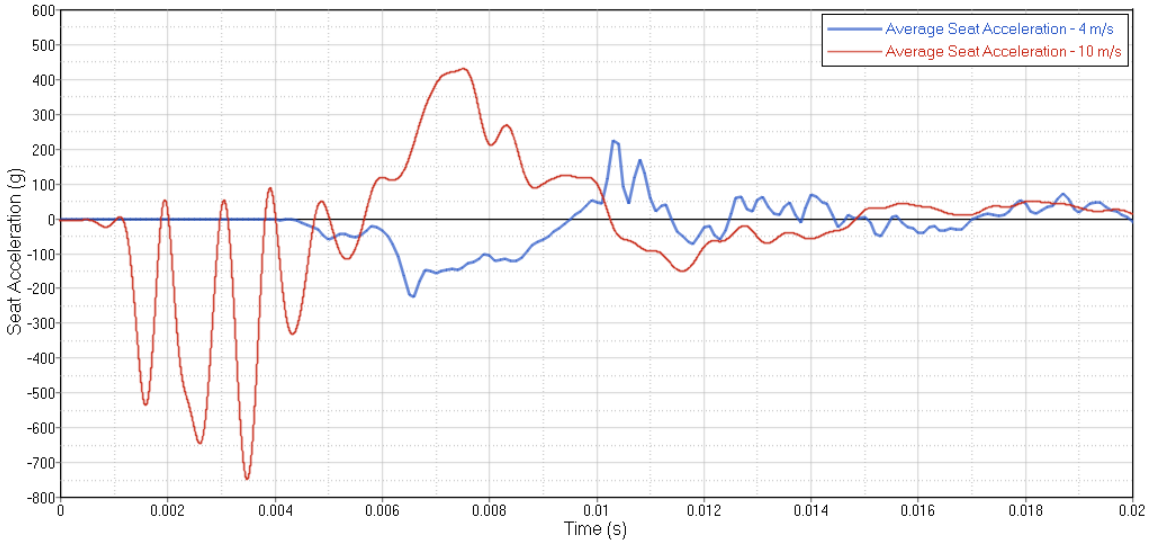

Figure 4-2. Input acceleration pulse for sub-injurious Condition A (blue) and injurious Condition B (red) at the seat as measured on the UVA sled

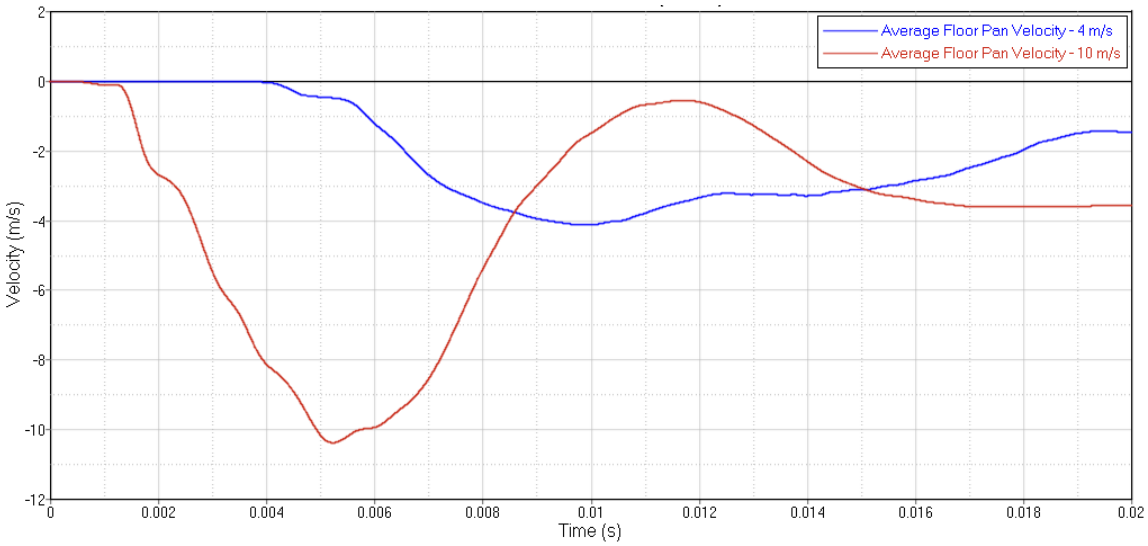

Figure 4-3. Input velocity pulse for sub-injurious Condition A (blue) and injurious Condition B (red) at the floor as measured on the UVA sled

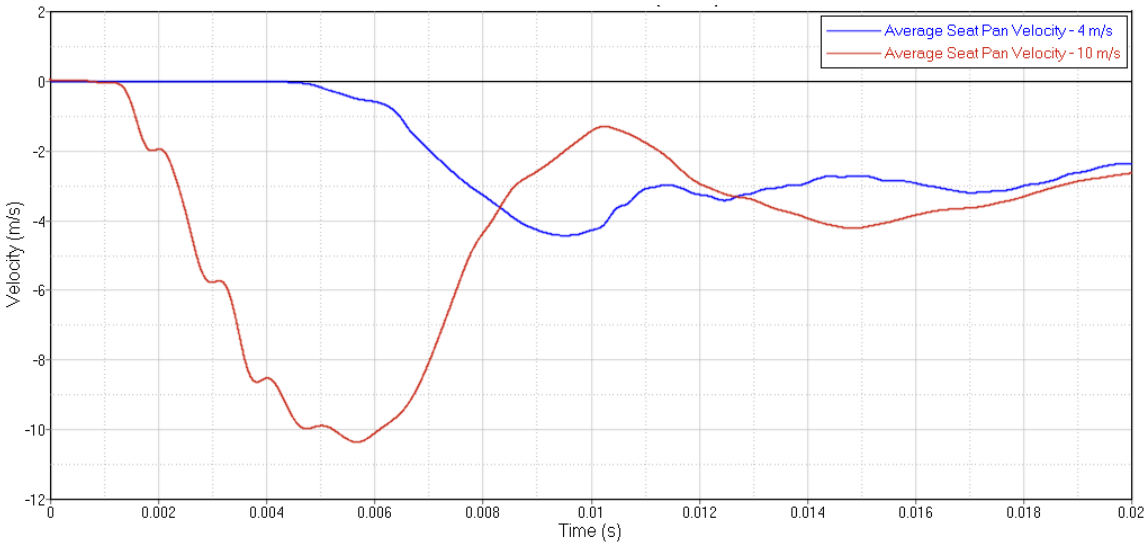

Figure 4-4. Input velocity pulse for sub-injurious Condition A (blue) and injurious Condition B (red) at the seat as measured on the UVA sled

Table 4-1. Sled input velocity conditions [49]

Condition	Floor Velocity	Floor Velocity Time-to-Peak (ms)	Seat Velocity (m/s)	Seat Velocity Time-to-Peak (ms)	Injury Condition
A	4	5	4	5	Sub-injurious
B	10.4	4.6	10	5.7	Injurious

Condition A is a rigid seat condition with the occupant seated in a “90/90/90” posture, meaning that the ankle, knee, and hip joints are all at 90 degrees to each other as shown in Figure 4-5. UVA conducted four PMHS tests in this configuration. The input velocity is 4 m/s with a 5 ms time-to-peak, resulting in no recorded injuries to the PMHS tested in the pelvis, lumbar spine, thoracic spine, or lower extremities, or an AIS of 0. Condition B is similar, but with a 10 m/s input velocity with a 5 ms time-to-peak. Three PMHS were tested in this configuration. In PMHS testing at this input, injuries included rami, sacral, acetabular, and ischial tuberosity fractures, as well as an L5 transverse process fracture. Lower extremity injuries included calcaneus, metatarsal, and tibia plafond fractures [5], confirming the higher input configuration.

Figure 4-5. Lateral view of underbody blast simulator sled at UVA [49]

This research was divided into four specific aims which will be further described in the next section:

1. **Hybrid III Rigid Seat Validation:** Validate Hybrid III ATD model response in rigid seat replicating UVA's underbody blast simulation sled testing for sub-injurious Condition A. For the purposes of this research, validation refers to a Correlation and Analysis (CORA) score of Good or Excellent as further explained in Chapter 5.
2. **Human Body Model Rigid Seat Validation**
    a. **Condition A:** Validate Human Body Model (HBM) response in rigid seat replicating UVA's underbody blast simulation sled testing with PMHS for sub-injurious Condition A.
    b. **Condition B:** Validate HBM response with injurious Condition B in rigid seat.
3. **Seat Optimization with Human Body Model:** Vary force and deflection properties of energy absorbing seat and run parametric sensitivity study with HBM to reduce acceleration and forces in pelvis and lower spine region for injurious Condition B. Optimization study will utilize software to alter properties of translational joint between floor and seat within 6" stroke limitation with the goal of reducing pelvis and lower spine response to below injurious thresholds per literature research.
4. **Hybrid III Output from Optimized Seat:** Verify Hybrid III response with injurious Condition B in rigid seat, then apply optimal force and deflection properties of energy absorbing seat and determine acceleration in pelvis and lower spine forces for Hybrid III ATD model for Condition B input data. As most seat manufacturers leverage the Hybrid III ATD as a surrogate for a PMHS in seat evaluations, the

resulting Hybrid III ATD lumbar spine force and pelvis acceleration values that represent minimal injuries in the human body model will provide industrial EA seat manufacturers with target Hybrid III injury criteria to optimize current and future EA mechanisms to reduce Warfighter injury during underbody blast events.

4.2. Specific Aim Details

The following sections provide a detailed description of the specific aims of this research.

4.2.1. Hybrid III Rigid Seat Validation

The first phase of this project was the validation of the Hybrid III 50th percentile male ATD model within MADYMO in a rigid seat model. The acceleration pulses from the UVA sled testing in Condition A as measured at the floor and seat were used as the input to the model, and the time-history data from the Hybrid III ATD instrumentation was compared between the MADYMO model and experimental results to validate positioning and ATD kinetics of the occupant.

Figure 4-6 shows the Hybrid III model installed in the horizontal sled simulation within MADYMO. Separate floor and seat acceleration pulses were required as inputs to the model due to an offset and slight difference in the UVA seat and floor loading profiles.

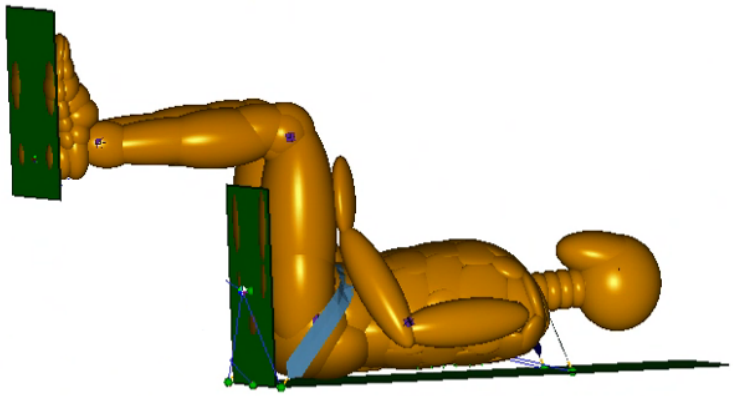

Figure 4-6. MADYMO model of Hybrid III in rigid seat

4.2.2. Human Body Model Rigid Seat Validation

After the rigid seat model was validated with the Hybrid III ATD, the HBM was positioned in the rigid seat model according to the UVA and WIAMan positioning procedure as described in a later section. The same Condition A input was modeled, and the time-history data from the accelerometers in the PMHS was compared to the data output at the same locations in the MADYMO model (Specific Aim 2a).

The floor and seat accelerations from Condition A were then replaced with the injurious pulses from Condition B, and the HBM was validated against the PMHS response (Specific Aim 2b).

4.2.3. Seat Optimization with Human Body Model

Once the rigid seat model was validated with the HBM with the input from injurious Condition B, the rigid attachment between the seat and floor models was replaced with a translational joint with varying spring and damper properties. These properties were altered in a parametric sensitivity study to minimize the accelerations and forces as measured in the pelvis and lower spine, thus reducing the probability of injury with injurious Condition B inputs. The minimized accelerations and forces were compared to

current literature on the fracture limits of the pelvis and lumbar vertebrae as previously described. Optimization software was used for the parametric study.

4.2.4. Hybrid III Output from Optimized Seat

As most seat manufacturers leverage the Hybrid III ATD as a surrogate for a PMHS in seat evaluations, the optimized force and deflection properties determined in the sensitivity study were applied to the translational joint and the model was executed again with the Hybrid III ATD to provide expected pelvis acceleration and lumbar spine compressive forces that equated to the least injurious measurements from the HBM. These values provided industrial EA seat manufacturers with target injury criteria to optimize current and future EA mechanisms to reduce Warfighter injury during underbody blast events.

4.3. Simulation Details

The simulation for this research revolved around a simplified model of a generic seat on a floor plane connected with a translational joint constraint to evaluate the optimal force and deflection properties based on several vertical accelerative loading inputs using MADYMO.

4.4.1. Software

MADYMO was utilized in conjunction with modeFRONTIER, an optimization software, in this research to optimize the force and deflection properties in EA seats using occupant models. MADYMO is a software package from TASS International, Inc., that is commonly used in the automotive industry to analyze occupant safety and is known for being quick and accurate for assessment of injury risk [53]. More recently, MADYMO has been used by the Army Research Laboratories and TARDEC for military applications [59].

This software can utilize human body or anthropomorphic test device models to measure response data to a seat interface during a blast event. It allowed for the analysis of a high number of iterative simulations to optimize the modeled spring-damper system while reporting out lumbar spine compressive load and pelvis acceleration, which was then interpreted against PMHS data [35].

The MADYMO software package includes solvers and workspaces that can combine various analyses of the models and simulations to produce animations, videos, and time history data traces [59]. MADYMO combines lumped parameter, rigid body, and finite element analysis into one computational model and leverages Newton-Euler equations of motion for its evaluations [3]. One of the important features of MADYMO that was critical for this research is the ability to implement specific characteristics of the joint restraints to control the seat EA response, which included elastic loading, friction coefficients, and damping characteristics. Hysteresis, initial strains, and dynamic amplifications could also be added [59]. MADYMO can also provide acceleration and position time history data, as well as record forces throughout the modeled system at prescribed nodes, which was important in this analysis to evaluate the effectiveness of the EA features as measured by the seat and occupant [59]. MADYMO also features a post-processor, Objective Rating, which was initially employed to compare peaks, timing, and other metrics to assess the effectiveness of each EA iteration using Correlation and Analysis (CORA) techniques [59].

Alternate software packages such as LS-DYNA can also be used in underbody blast modeling, however, a comparative study by Kulkarni et al (2013) demonstrated that there were no significant differences in outcome between MADYMO and LS-DYNA

models for underbody blast modeling with a Hybrid III model. They also found that the MADYMO run times were significantly less than that of LS-DYNA, allowing more simulations to be conducted in a shorter time period [31]. Similarly, Shukla compared MADYMO to the Articulated Total Body Model used by the US Army Research Laboratory's Survivability/Lethality Analysis Directorate (ARL/SLAD) and also found that MADYMO was superior for blast modeling for occupant analysis [59]. Given that this research is interested in a sensitivity study to evaluate the decrease in pelvis and lower spine loading, it was determined that the lumped parameter occupant models were sufficient in providing comparative results.

4.4.2. Seat Model

This analysis was conducted on a rigid seat in a generic sled model with a representative floor pan to receive the initial blast loading input as shown in Figure 4-7. The MADYMO model was developed using rigid bodies representing the sled rail, the sled system, and the rigid seat. The surfaces of the seat and floor were non-deformable, while linked with a rigid or translational joint. The seat and floor were modeled as simple planes, as this research was not focused on floor or seat deformations, and all laboratory testing that was referenced for injury thresholds used non-deformable rigid seat pans. Based on the original experimental setup, the sled system was set to 77 kg, the moving seat mass was 27.2 kg, and the moving floor platen was 27.9 kg which is representative of the UVA sled system. The floor plate and seat plates were on independent rail systems from the main sled system. The seat back was independent of the moving seat platen, but was connected to the seat pan in the model to provide a surface for the occupant's back to react against, as the full sled system was not modeled. General dimensions

including seat pan width, depth, and height above the floor as well as the seat back height and restraint anchorage positions were replicated. The seat pan and back were in a 90 degree configuration to match the original PMHS test setups [49].

Translational joints were implemented to connect the floor to the sled rigid body, and a second translational joint was placed between the rigid seat and the floor. This second joint could be locked to represent a solid connection between the floor and seat, and the joint was created to allow for altering its force and deflection properties for later portions of the research. Due to an offset in timing between the floor and seat inputs, this joint was left unlocked and separate floor and seat input accelerations were applied to the node. Contacts were established between the Hybrid III model and the seat pan, seat back, and floor, and a gravitational force was applied to the system to ensure the occupant model experienced the same initial conditions as the physical testing.

For Specific Aims 3 and 4, the constraints of the translational joint between the floor and seat represented an EA mechanism with force and deflection coefficients. The force and deflection coefficients were tuned to limit motion of the seat to no more than six (6) inches, which was representative of allowable stroke distances in military vehicles and has been used in previous blast mitigation seat studies as a limiting factor [3, 53].

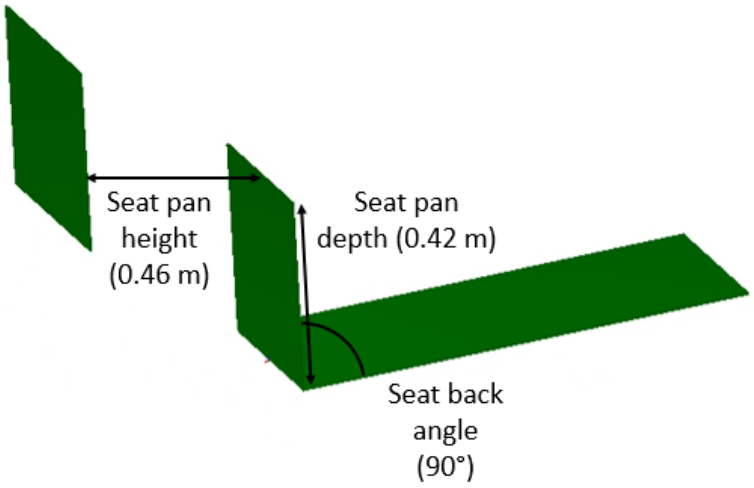

Figure 4-7. Basic seat and floor setup in MADYMO using planes [59]

Five-point restraints were included in this model, but they did not affect the resulting injury prediction as the effectiveness of restraints was not realized until after the initial compressive loading was complete and during the slam-down phase when the vehicle returns to earth. The upward movement of the vehicle and resulting downward movement of the occupant was not affected by restraints, and as typical blast events last about 20 ms [31], injuries will have occurred due to the force transmission before the restraints would engage the occupant, however, an artificial “slingshot” effect was noted later in the data trace from the seat being pulled toward the occupant rapidly as the occupant is moving away from the seat. This was an unrealistic artifact of the MADYMO model and was not considered as a valid response. Restraints were adjusted about the occupant model using the belt fit wizard integrated in the MADYMO software [59].

Several simulation studies have been conducted involving basic EA systems in generic seats, providing baseline estimates that were leveraged in determining a start point for this research. Kulkarni et al (2013) used two EA profiles, a stiffer and softer step function pulse at 15 kN and 7.5 kN limits [31]. Arepally et al used an EA profile that was

limited to 254 mm of deflection and was actuated at 4 kN with a gradual increase with loading [3]. Optimization software was used to vary the spring and damper properties to minimize lumbar spine and pelvis force. The translational joint only allowed movement in the axial direction.

Within the six inch displacement limitation, a sensitivity study was conducted by varying the spring and damper properties within the translational joint between the seat and floor planes. The optimization process included varying the force limit to engage stroking and the overall limiting stroke distance within a linear profile. Example load displacement characteristics from the Desjardins helicopter study are shown in Figure 4-8. Helicopter seat design tends toward concepts that display the most constant load-displacement characteristics, which may be similar to the needs of blast seats [20]. The EA mechanism must also account for occupant weight and seat weight, as this can affect the final characteristics.

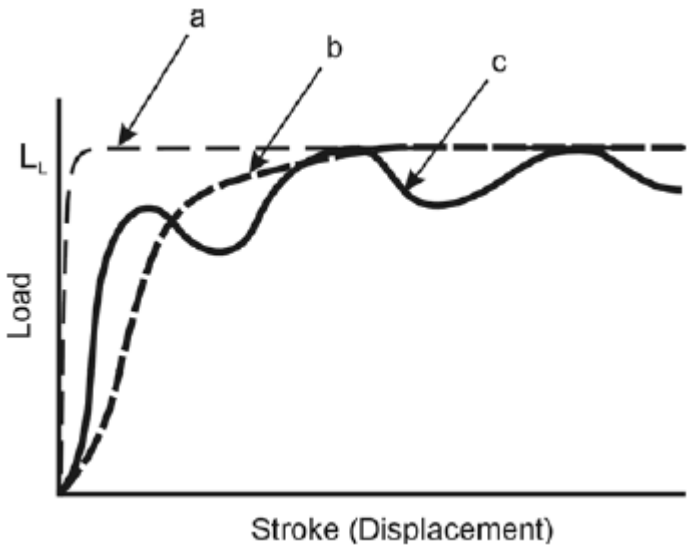

Figure 4-8. Varying load displacement curves from crashworthy helicopter seats [20]

4.4.3. Occupant Models

The simulations were conducted with both the 50th percentile active HBM and Hybrid III 50th percentile ATD ellipsoid model that are native to MADYMO. The MADYMO active HBM had all muscles deactivated to simulate the PMHS response.

4.4.3.1. Hybrid III

The Hybrid III model comprised a number of rigid-body elements represented as ellipsoids, hyper-ellipsoids, or planes (Figure 4-9). The model contained 211 bodies; 50 bodies were used for the jacket, and 6 bodies were required for each shoe. Some of the bodies were linked together as groups when multiple bodies are required to form a component, such as the jacket. The spinebox comprised three bodies to represent the spine, upper load cell, and lower load cell to replicate the actual Hybrid III geometry. The lumbar spine was constructed of seven bodies, where five comprised the spine and two bodies represent the load cells. The pelvis contained three bodies and three joints to represent the physical ATD pelvis. Each rigid element had a center of gravity, mass, and associated mass moment of inertia. The elements were connected by various joints, including bracket, hinge, and ball-and-socket joints to represent the actual Hybrid III ATD. Each joint had specific damping and friction properties assigned, as well [59]. Additional details on the model construction are available in the MADYMO dummy model manual [36]. The Hybrid III model was capable of measuring accelerations, forces, and moments in the major body segments including lumbar spine and pelvis [3]. MADYMO automatically filtered each ATD channel with its associated CFC filter according to the SAE J211 standard [58]. Accelerations were compared between the Hybrid III and the HBM in similar locations, such as the S1 on the pelvis, which was also a location used in

PMHS testing [72]. The specific channels compared for the Hybrid III validation are listed in Table 4-2.

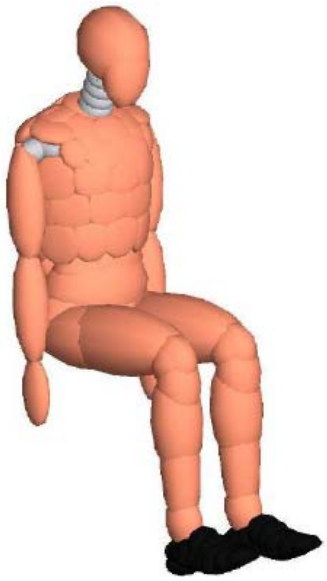

Figure 4-9. Hybrid III model in MADYMO [37]

Table 4-2. Validation channels used for Hybrid III model

Hybrid III and Rig Channels – Legs	**Hybrid III and Rig Channels – Upper Body**
Tibia Ax	Pelvis Ax
Tibia Az	Pelvis Az
Lower Tibia Fx	Lumbar Fx
Lower Tibia Fz	Lumbar Fz
Lower Tibia My	Lumbar My
Upper Tibia Fx	Seat Load Cell
Upper Tibia Fz	
Upper Tibia My	
Floor Load Cell	

One of the issues with using the Hybrid III model was that it was designed for frontal impacts in commercial vehicles, not high rate vertical accelerative loading in military applications. Additionally, blast pulses are often up to ten times larger in magnitude and one-fifth the duration of a frontal impact [32], and injury mechanisms at

these high rates are not fully understood. However, as a vertical blast ATD has not yet been released for use, the Hybrid III is the current tool used to assess underbody blast occupant injuries in physical testing, so determining the forces, moments, and accelerations of the Hybrid III model will allow a correlation to the HBM with the potential for future physical validation testing.

4.4.3.2. Human Body Model

The MADYMO facet active HBM was used for comparison to PMHS (Figure 4-10a). The HBM featured separate vertebrae as rigid bodies connected with kinematic joints, and the pelvis bone was deformable. The skin was a deformable feature, as well, to properly mimic that of a real human [21]. This model uses facet surfaces as the outside geometry to interact with environmental structures, such as the seat surface. The model comprised 186 bodies, of which 178 were rigid and 8 were flexible. These bodies were connected by joints and contacts with varying properties to represent human muscles and ligaments. The facet model was composed of branches that connected the trunk and limbs together.

The spine was representative of the human spine, with ellipsoid rigid bodies for each separate cervical, thoracic, and lumbar vertebra (Figure 4-10b and c). In addition to the single vertebral body ellipsoid, the cervical vertebrae also contained ellipsoids to represent the transverse and spinous processes. Each vertebral body ellipsoid was connected by free joints with a lumped joint restraint providing resistance to represent the actual human biofidelic response of the intervertebral discs, ligaments, and muscles. Initially, the spine was positioned to represent the curvature of an erect standing person.

The rotational position of each vertebral body could be set by the user to alter the posture of the model as needed.

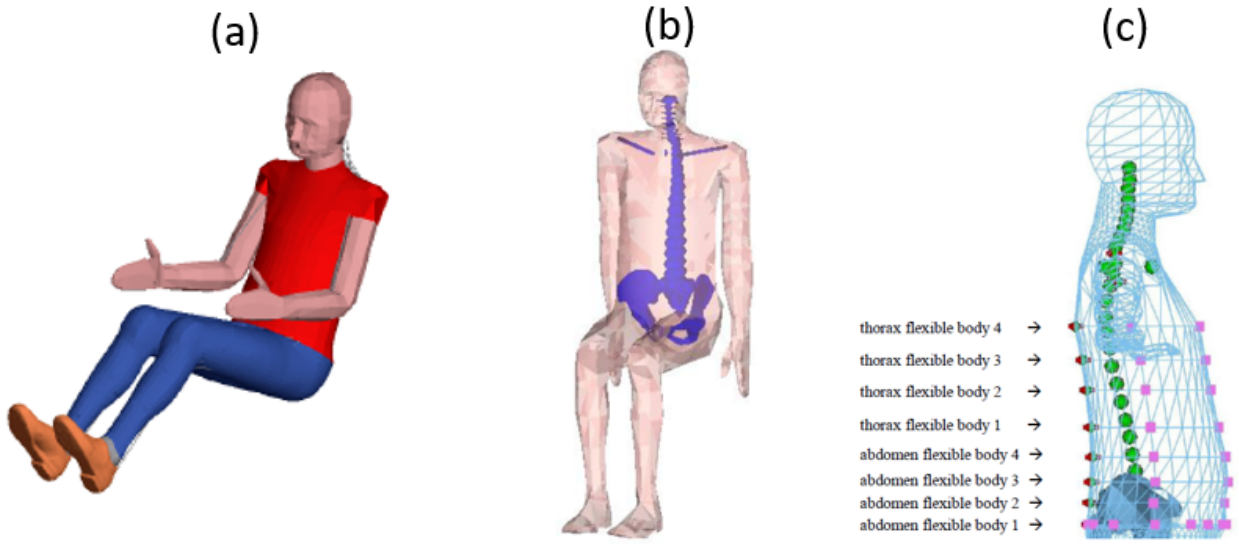

Figure 4-10. MADYMO active HBM (a), HBM spine and pelvis model (b), and spine flexible body details (c) [35]

Instrumentation used during the PMHS testing is shown in Figure 4-11 [49], which included accelerometers and strain gages. The validation of the HBM was conducted using the channels listed in Table 4-3. Strain gage data was not used in the HBM validation.

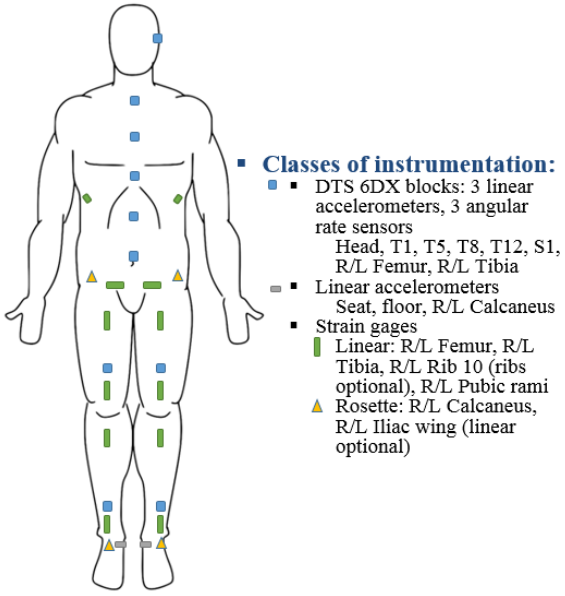

Figure 4-11. PMHS Instrumentation included accelerometers at T12 and S1 [49]

Table 4-3. Validation channels used for human body model

PMHS and Rig Channels – Legs	PMHS and Rig Channels – Upper Body
Foot Az	Pelvis Ax
Distal Tibia Ax	Pelvis Az
Distal Tibia Az	T12 Ax
Distal Femur Ax	T12 Az
	T8 Ax
	T8 Az
	T5 Ax
	T5 Az
	T1 Ax
	T1 Az

4.4.3.3. Positioning

Proper positioning was used to reflect the “90/90/90” posture, which represents 90 degree angles at the ankles, knees, and pelvis to torso, which is similar to that used in PMHS and Hybrid III laboratory testing [49]. The positions for PMHS were based off of the Seated Soldier Study performed at the University of Michigan Transportation

Research Institute which determined the relative locations of anatomical landmarks that represent the 90/90/90 posture of the US Warfighter population [49]. The Hybrid III was positioned according to Pietsch et al [49]. The starting locations of the ankles, knees, and femurs were set to 90 degree angles, and the pelvis was oriented such that it achieved a tilt angle of approximately 45 degrees. The head was rotated to match the head orientation of the physical test. The final orientations of the joints were slightly different due to the joint position variation conducted during the validation process.

The seating posture of the two models was slightly different because of the geometric variations between their external surfaces [21]. Previous studies employing both Hybrid III and HBMs in MADYMO have noted differences in the models, including differences in flesh deformation around the waist and thigh regions, which has been confirmed in laboratory testing as well, and with difficulties with the setting the Hybrid III back against the seat and achieving a horizontal Frankfort plane [16]. The curvature of the spines are different, as well, with the ATD spine being more curved, especially in the lumbar spine region while in the seated posture [21]. The Hybrid III ATD and model do not have the same spine segmentation as the HBM. In the Dooge et al study, the ATD spine model had a lower stiffness and did not represent the human kinematics well. The lower stiffness of the spine provided less acceleration transmission to the head in these models, as well. The pelvis of the ATD model, however, was much stiffer than that of the human model due to material property differences. This manifested in faster pelvis acceleration responses and higher peak values [21]. Bailey et al performed matched pair testing with PMHS and Hybrid III ATDs in underbody blast simulation events. Comparison of the pelvis acceleration data demonstrates the stiffness of the Hybrid III pelvis compared

to the PMHS, with a sharp rise to peak in the acceleration data. The Hybrid III pelvis design is overall less compliant than human bone, and there is a lack of flesh under the ischial tuberosities, both of which alter pelvic response [6]. Although testing of the Hybrid III in a separate study at the University of Virginia showed consistent responses, the overall ATD response was stiffer than the PMHS and was considered to over-predict injury in a vertical accelerative loading condition [62]. Danelson et al reported that the Hybrid III pelvis had a lower acceleration but higher time to peak, as well as higher velocity as measured at the pelvis when compared to the PMHS in matched pair testing [16]. Sources of variation between Hybrid III and PMHS response may also have been due to the phasing and mass recruitment of the body under loading [61], but as previously mentioned, the Hybrid III is the only tool currently publicly available to assess injury in underbody blast.

Based on existing simulations and PMHS testing, the HBM was positioned in the seat to represent a pelvis angle between 35º and 45º as measured on the plane from the anterior superior iliac spines (ASIS) to the center of the pubic symphysis as shown in Figure 4-12 [72, 61]. The Hybrid III was likewise positioned to maximize similarities in posture. The angles between the vertebral bodies in the HBM were adjusted to represent the seated posture in the rigid seat.

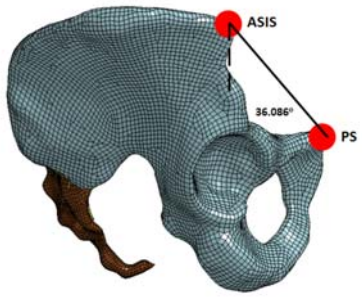

Figure 4-12. Pelvis angle plane measured on PMHS [72]

4.4.4. Accelerative Pulse

Blast events are completely unique due to the variation in charge type, burial depth, vehicle design, and vehicle stand-off, so it was deemed necessary to develop representative pulses that could be employed for modeling and physical sled testing to ensure consistency when evaluating human tolerance and response to high rate loading. The resources required to model a blast event in a simulation program and the variability introduced in the modeling from the phenomena that are present in an actual blast add complexity that would convolute the focus of this study, including the need to account for soil mechanics, shock physics, and structural dynamics, hence the decision to model the seat as a stand-alone system using pulses already developed to represent actual live fire events [21]. Many experienced modelers state that it is common practice to sacrifice simulation accuracy for efficiency when developing unique and complex blast models [21]. Furthermore, it is difficult to use actual blast data, either from theater or live fire testing, as it is of a sensitive nature and often classified and not available for public domain forums, along with the lack of human or Hybrid III data in these events for validation purposes [21].

During live fire testing, accelerations are measured at a rigid location such as a structural floor beam, pillar, or roof joint within the vehicle [32]. Due to the infinite combinations of vehicles and threat sizes, there is no standardized blast pulse, although there are several publications listing typical attributes of blast pulses. Kulkarni et al (2014) stated that blast pulses are typically triangular in shape [32]. Laboratory investigations at the University of Virginia (UVA) using PMHS to investigate injuries from underbody blast events report using 4 m/s pulses with 5 ms and 20 ms times to peak on a horizontal sled

apparatus [61]. The associated accelerations measured at the seat were 135 g and 54 g [61]. In these tests, reported lumbar spine peak compressive forces were 9.1 kN and 6.4 kN, respectively, with pelvis accelerations of 156 g and 58 g [61]. Arepally et al provided a range of pulses that are common, from 20 g with a 30 ms duration to 350 g with a 5 ms duration in a half sine shape (Figure 4-13) [3]. Tabiei et al used a 171 g pulse with a 5 ms duration in a primarily triangular shape in his investigation of EA mechanisms [66]. Alem et al performed live fire testing of an undisclosed military truck and reported a floor velocity of 19.4 m/s but a peak acceleration of 119 g [68]. The wide variation of blast pulses was also attributed to the types of filters applied to the data and what kind of accelerometers that were used during testing, as some provided mechanical dampening and filtering, thus changing the signal.

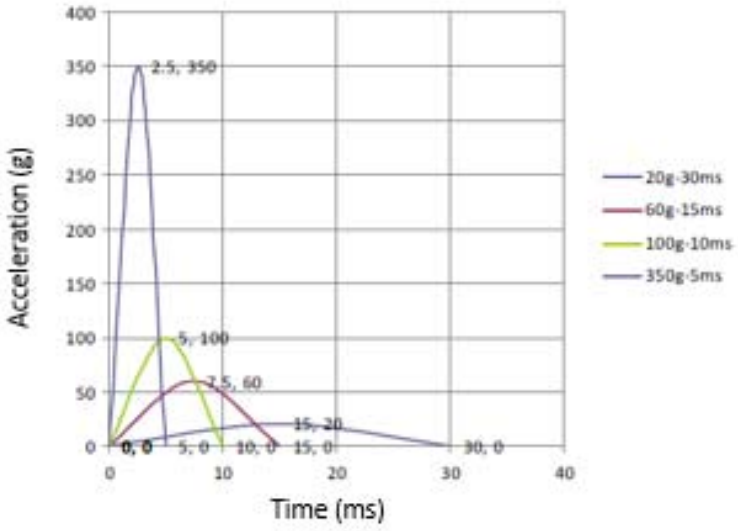

Figure 4-13. Generic mine blast pulse examples from literature [3]

Based on representative live fire blast data collected, the WIAMan program developed target accelerative load profiles to use in biomechanical research to investigate the role of high energy loading into PMHS. The WIAMan program developed

several specific pulses based on exploratory testing that determined the threshold seat input delta velocity to cause injury in PMHS pelvis and lower spine complexes, which were the basis behind Condition A. Condition A was a considered sub-injurious pulse, as the majority of PMHS tested at this conditions did not experience skeletal injury, which allowed for a better understanding of biofidelic response to loading without interrupting the load path by skeletal fracture. Condition B was collected in a separate study at UVA to investigate underbody blast injuries and was considered an injurious pulse. Condition A and Condition B floor pulses are shown below in Figure 4-14.

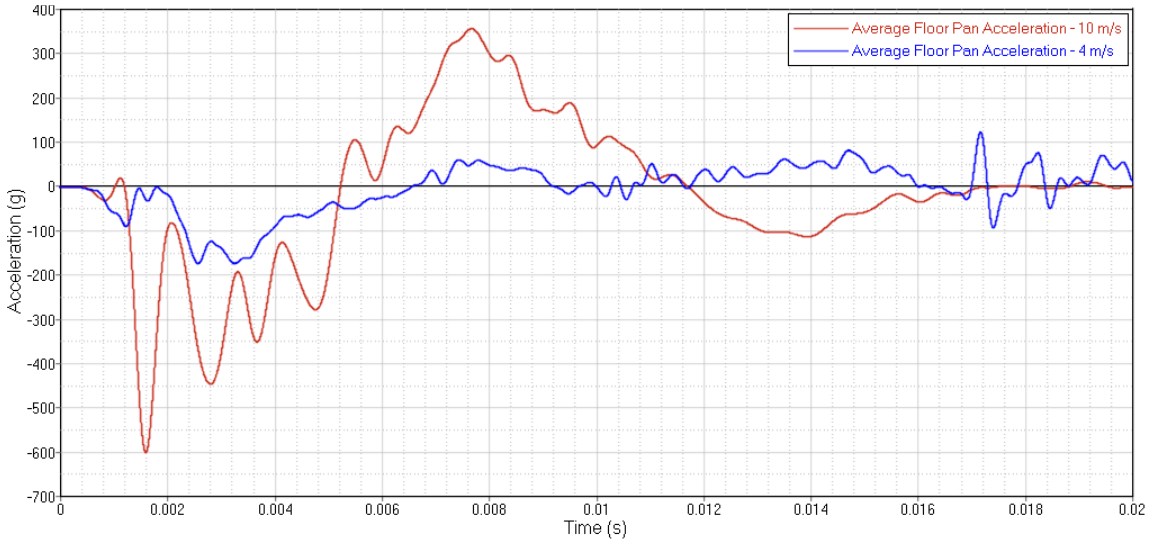

Figure 4-14. Condition A (blue) and Condition B (red) input pulses for floor

Similar to existing simulations, the blast pulse was input as a base excitation to the floor and seat base via the planar floor model in the global x-direction, which locally represented a z-direction loading to the horizontal sled system [31].

4.4.5. Rationale and Expected Outcomes

The goal of this research was to produce a tool that could determine optimal combinations of force and deflection properties using the rigid seat model by varying translational joint properties for an injurious input floor acceleration pulse. As there are

limited EA seat design guidelines for occupant protection, this research hopes to start a foundation for a better understanding of how EA mechanism design directly affects the vertical forces and accelerations imparted to the pelvis and lower spine.

Success of the force/deflection profiles was determined via the acceleration and force outputs reported by the HBM at the pelvis and lower spine complex, which were compared to the injury limits of current PMHS testing. These force and deflection properties were then simulated with the Hybrid III model to determine an approximate pelvis acceleration and lumbar spine compressive force that corresponded to the minimized injury risk in the HBM.

It is the researcher's hope that this tool to develop force and deflection profiles can be leveraged for the design of real EA mechanisms produced by EA seat manufacturers. It is important that the manufacturer understands that the addition of cushion, flexible seat pans, and seat adjustment mechanisms can all change the predicted performance of the EA mechanism, and that an occupant's use of arm rests can artificially circumvent the effectiveness of an EA mechanism by unloading the pelvis through the diversion of force to the occupant's elbows [15].

CHAPTER 5 – SPECIFIC AIM 1 – INITIAL HYBRID III VALIDATION

5.1. Specific Aim 1 – Hybrid III Rigid Seat Validation – Model Conditions

As previously explained, the initial sled setup in MADYMO required validation prior to altering the properties of the translational joint between the floor and seat. The Hybrid III testing was used for this validation, as the Hybrid III is a recognized test measurement device with multiple sensors throughout the ATD to compare to actual test data.

To achieve model correlation with the standard Hybrid III ATD model offered by MADYMO, contact characteristics were altered between the floor and shoe and between the pelvis and seat. The original Hybrid III model was stiffer in response for the lower leg and delayed in loading for the lumbar spine when compared to the experimental testing response. The internal joint properties of the Hybrid III model could not be altered in MADYMO, as the model is encrypted. The standard shoe does not have the same energy absorption properties as that of the desert style military combat boot used in the physical testing, so a stress-strain curve for the boots was provided by UVA and imported to the model as a force-deflection property to allow the use of an MB-MB (multibody) relationship between the shoes and floor. This stress-strain relationship was derived from testing at impact velocities representing underbody blast at UVA. At the time of this research, the boot properties had not been published but has been presented at conferences [62, 64]. Slight variations in scale were employed to improve model correlation by applying constant multipliers to the force and deflection axes to compensate for the existing MADYMO shoe properties that were encrypted within the model. The input force-deflection curve is shown in Figure 5-1.

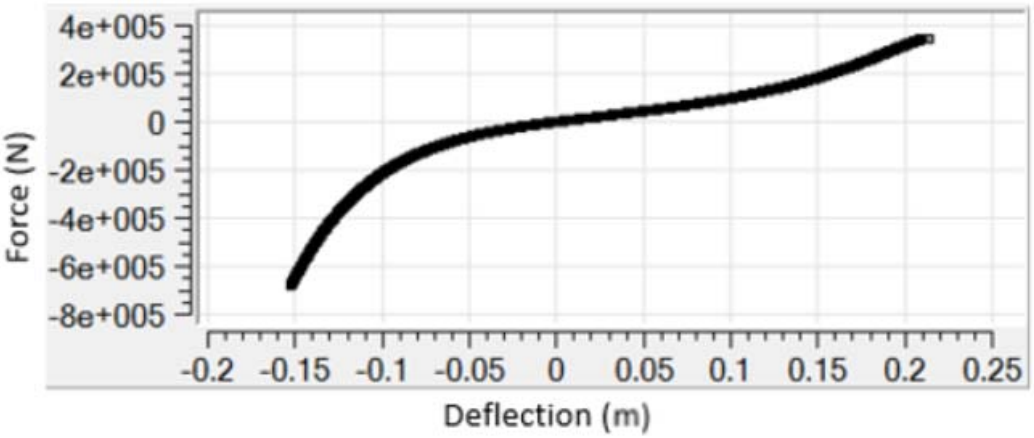

Figure 5-1. Force (N) deflection (m) properties from MADYMO for boot/floor contact

Similarly, new external contact characteristics between the ATD pelvis and rigid seat bottom were created. As the MADYMO ATD model was created for frontal impacts, there was limited model correlation to the interaction between the pelvis and the seat, and the correlation that was conducted was not at blast-representative velocities. Data from a measurement system validation test of the Hybrid III pelvis in TARDEC's Component Impact Simulator (CIS) (Figure 5-2) was used to create a force-deflection curve for the contact characteristic as shown in Figure 5-3. This testing was conducted at sub-injurious blast loading velocity (2 m/s in 10 ms) to prevent pelvis punch-through. The loading function was derived directly from the CIS testing, and the unloading function is a scaled version of the loading function. Hysteresis was incorporated in the function and altered to match the Hybrid III loading and unloading curves from the UVA test. A damping coefficient was also introduced to improve model correlation.

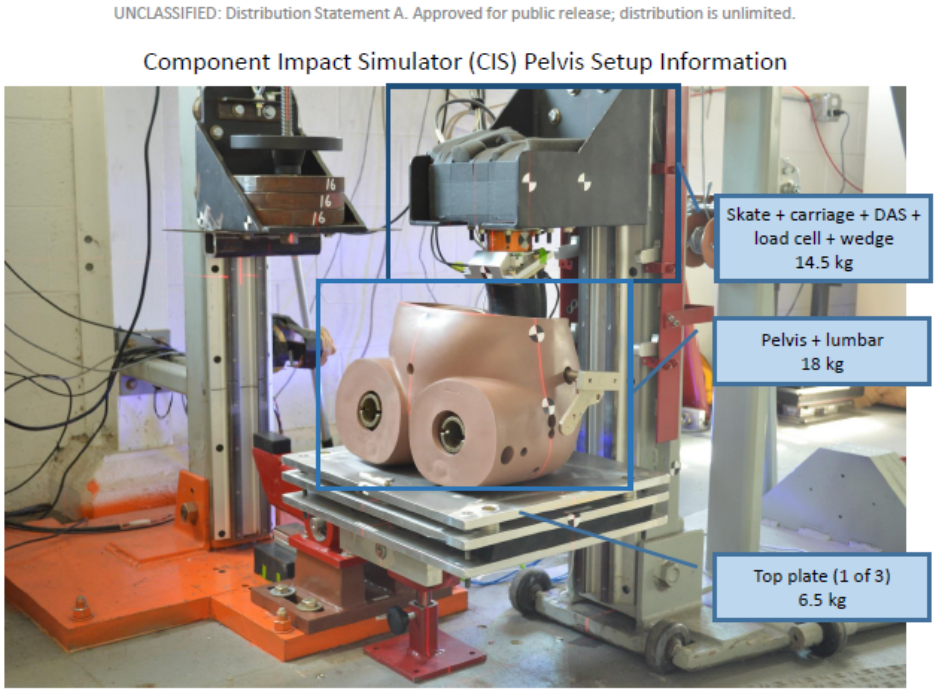

Figure 5-2. TARDEC's Component Impact Simulator

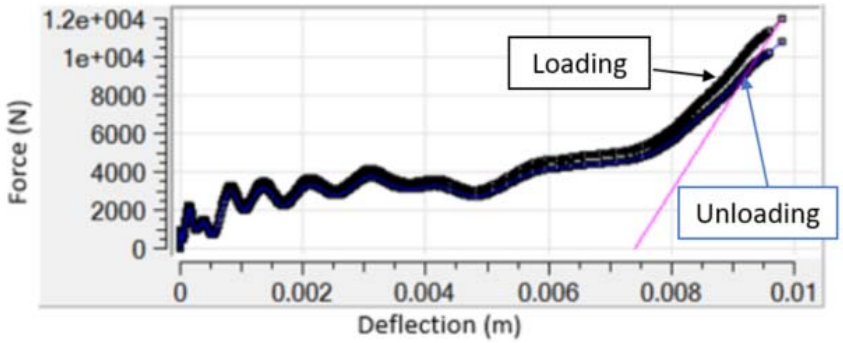

Figure 5-3. Force (N) deflection (m) properties for pelvis/seat contact

Exact ATD positioning was not available, as joint location coordinate data was not recorded, so the model was positioned based on video of the test and data analysis. Several parameters were varied to achieve correlation, such as hip, knee, and ankle angles, and these parameters were varied to improve model correlation.

5.2. Specific Aim 1 – Hybrid III Rigid Seat Validation – Objective Rating

The Objective Rating software within the MADYMO software suite was utilized to judge the overall fit of the simulation output to the UVA test results described in Chapter 4 as only one experimental curve was available. Within Objective Rating, the overall CORA score along with Corridor and Cross Correlation scores are reported as shown in Figure 5-4. CORA evaluates the fit of the curve on a point-by-point basis. The Corridor portion judges how well the simulation curve matches the reference curve within a two standard deviation window, with a score of 1 for a perfect fit and a 0 if the simulation curve is not within the corridor. The Cross Correlation portion combines scores from how well the simulation curve matches the reference curve from phasing, size, and shape [49].

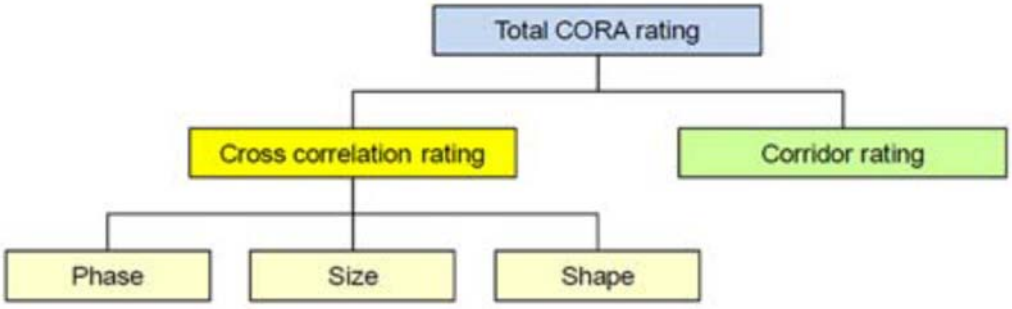

Figure 5-4. CORA rating breakdown [49]

The rating of each channel follows that of the WIAMan program, which is derived from ISO 9790, the biofidelity assessment of the WorldSID ATD (Table 5-1) [49]. As the focus of this model was to evaluate z-axis biofidelity, the target CORA score for z-axis channels was 65% or above, or a Good rating. X-axis motion was of minor importance to monitor for overall kinematics and is thus presented. The key channels evaluated included floor contact force, lower and upper tibia forces, tibia acceleration, pelvis acceleration, lumbar

spine forces, and seat contact force. Y-axis motion was only reported for moments for the tibia and lumbar spine.

Table 5-1. Biofidelity rating scheme [49]

Biofidelity Rating	CORA Score
Excellent	85% ≤ Score ≤ 100%
Good	65% ≤ Score < 85%
Fair	44% ≤ Score < 65%
Marginal	26% ≤ Score < 44%
Unacceptable	0% ≤ Score < 26%

The settings for CORA are listed in Table 5-2. The default settings were used for this evaluation, and the time period of rating was set to 50 ms.

Table 5-2. MADYMO Objective Rating CORA settings.

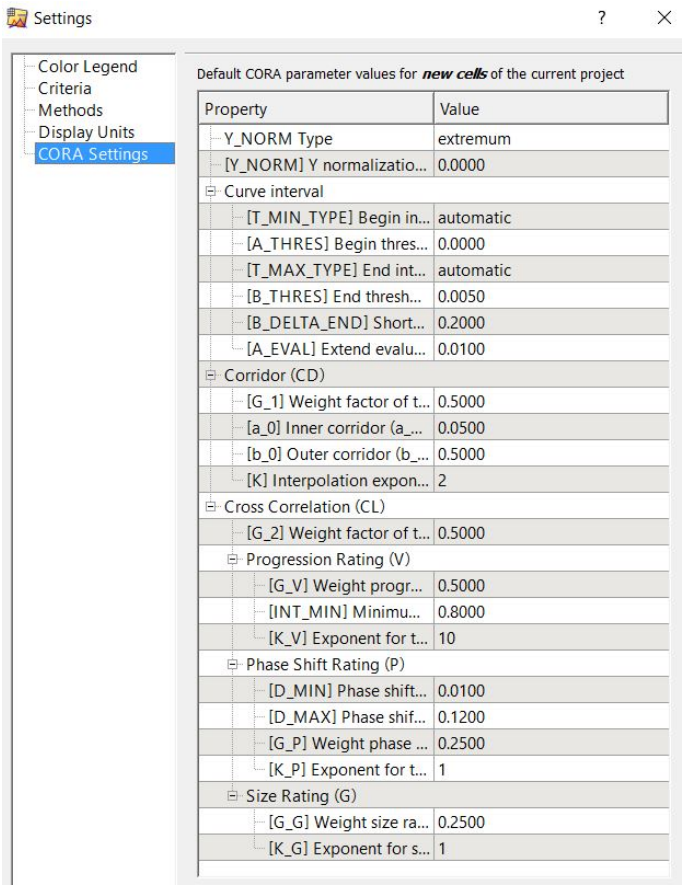

The Objective Ratings for the Condition A Hybrid III validation are displayed in Table 5-3. The z-axis channels for tibia force and acceleration and lumbar spine force were all in the Good category. The seat load cell rated as Excellent. The pelvis acceleration and lumbar spine force were in general inversely related – as one improved, the other degraded in score, due to pelvis punch-through, where the metal pelvis penetrates through the pelvis flesh, causing metal-to-metal contact with the seat. The pelvis Az channel had high spikes from the metal-to-metal contact, but the pelvis Fz force did not demonstrate the same sensitivity and high spikes. Efforts to increase the pelvis Az in the simulation resulted in overshoot in the peak for lumbar Fz. Similarly, lower and upper tibia forces were often inversely related – an improvement in upper tibia Fz lowered the score for lower tibia Fz. This is likely due to the construction of the tibia tube, which was angled, as well as the slight inherent rotation of the floor platen during the loading period. The focus was on lower tibia Fz since it was closer to the loading, but the angle of the tibia tube and rotation of the floor platen caused a difference in force distribution between the Fx and Fz axes of the upper tibia.

Table 5-3. CORA scores for Condition A Hybrid III validation

	Combined Scores	Tibia Acceleration	Pelvis	Tibia Lower F/M	Lumbar	Upper Tibia F/M	Floor F	Seat F
Combined Scores	**Matrix score = 54.99%** **CORA = 54.99%** **CORA-CD = 61.48%** **CORA-CL = 48.50%**	**Column score = 65.69%** **CORA = 65.69%** **CORA-CD = 74.98%** **CORA-CL = 56.39%**	**Column score = 47.56%** **CORA = 47.56%** **CORA-CD = 67.63%** **CORA-CL = 27.49%**	**Column score = 55.68%** **CORA = 55.68%** **CORA-CD = 57.77%** **CORA-CL = 53.59%**	**Column score = 46.28%** **CORA = 46.28%** **CORA-CD = 37.34%** **CORA-CL = 55.22%**	**Column score = 49.53%** **CORA = 49.53%** **CORA-CD = 60.25%** **CORA-CL = 38.81%**	**Column score = 70.28%** **CORA = 70.28%** **CORA-CD = 76.10%** **CORA-CL = 64.45%**	**Column score = 87.65%** **CORA = 87.65%** **CORA-CD = 89.78%** **CORA-CL = 85.52%**
X	**Row score = 38.50%** **CORA = 38.50%** **CORA-CD = 53.21%** **CORA-CL = 23.78%**	Cell score = 48.39% CORA = 48.39% CORA-CD = 69.31% CORA-CL = 27.47%	Cell score = 38.69% CORA = 38.69% CORA-CD = 68.73% CORA-CL = 8.64%	Cell score = 33.25% CORA = 33.25% CORA-CD = 37.23% CORA-CL = 29.27%	Cell score = 41.20% CORA = 41.20% CORA-CD = 33.88% CORA-CL = 48.51%	Cell score = 30.97% CORA = 30.97% CORA-CD = 56.92% CORA-CL = 5.02%		
Z	**Row score = 70.70%** **CORA = 70.70%** **CORA-CD = 73.51%** **CORA-CL = 67.89%**	Cell score = 70.88% CORA = 70.88% CORA-CD = 77.64% CORA-CL = 64.13%	Cell score = 46.74% CORA = 46.74% CORA-CD = 55.32% CORA-CL = 38.17%	Cell score = 82.48% CORA = 82.48% CORA-CD = 80.41% CORA-CL = 84.55%	Cell score = 68.33% CORA = 68.33% CORA-CD = 64.95% CORA-CL = 71.72%	Cell score = 68.54% CORA = 68.54% CORA-CD = 70.40% CORA-CL = 66.68%	Cell score = 70.28% CORA = 70.28% CORA-CD = 76.10% CORA-CL = 64.45%	Cell score = 87.65% CORA = 87.65% CORA-CD = 89.78% CORA-CL = 85.52%
MY	**Row score = 43.24%** **CORA = 43.24%** **CORA-CD = 40.77%** **CORA-CL = 45.71%**			Cell score = 51.32% CORA = 51.32% CORA-CD = 55.69% CORA-CL = 46.95%	Cell score = 29.31% CORA = 29.31% CORA-CD = 13.20% CORA-CL = 45.43%	Cell score = 49.09% CORA = 49.09% CORA-CD = 53.44% CORA-CL = 44.73%		
Resultant	**Row score = 67.52%** **CORA = 67.52%** **CORA-CD = 78.42%** **CORA-CL = 56.61%**	Cell score = 77.79% CORA = 77.79% CORA-CD = 78.01% CORA-CL = 77.57%	Cell score = 57.24% CORA = 57.24% CORA-CD = 78.84% CORA-CL = 35.65%					

The plots comparing the actual Hybrid III data from the UVA testing against the simulation Hybrid III data for Condition A are contained in Figure 5-5 through Figure 5-21. In general, phasing and peaks are aligned between the actual and simulation data in the z-direction.

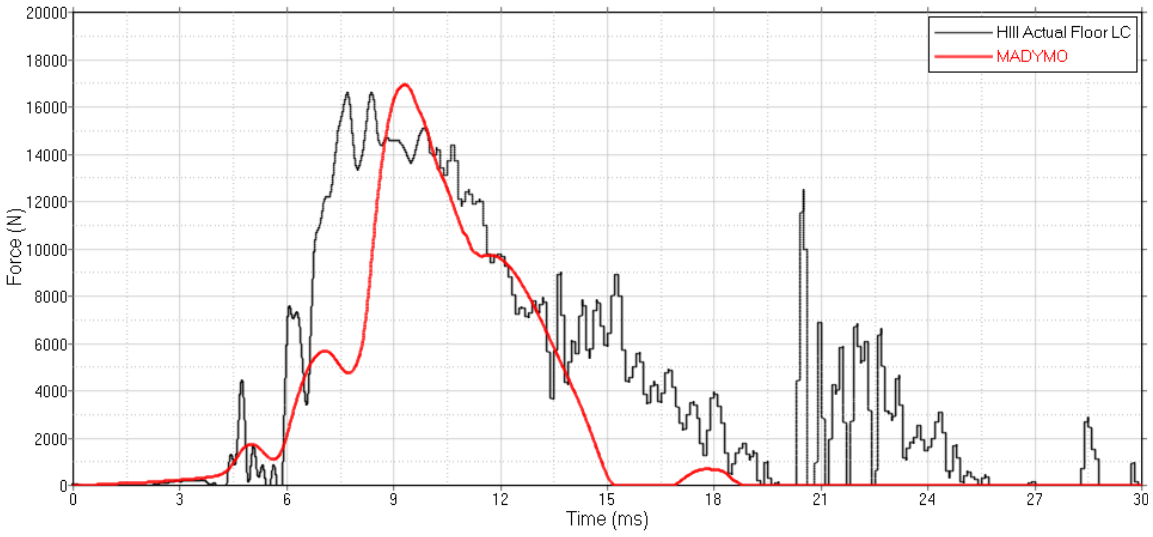

Figure 5-5. Floor load cell comparing actual Hybrid III (black) against the MADYMO simulation (red)

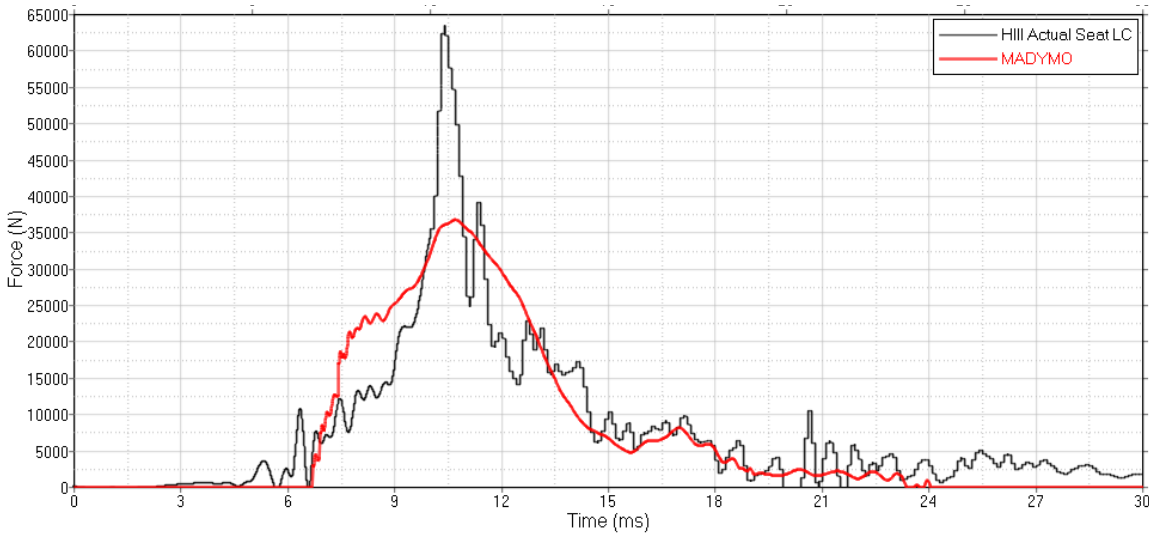

Figure 5-6. Seat load cell comparing actual Hybrid III (black) against the MADYMO simulation (red)

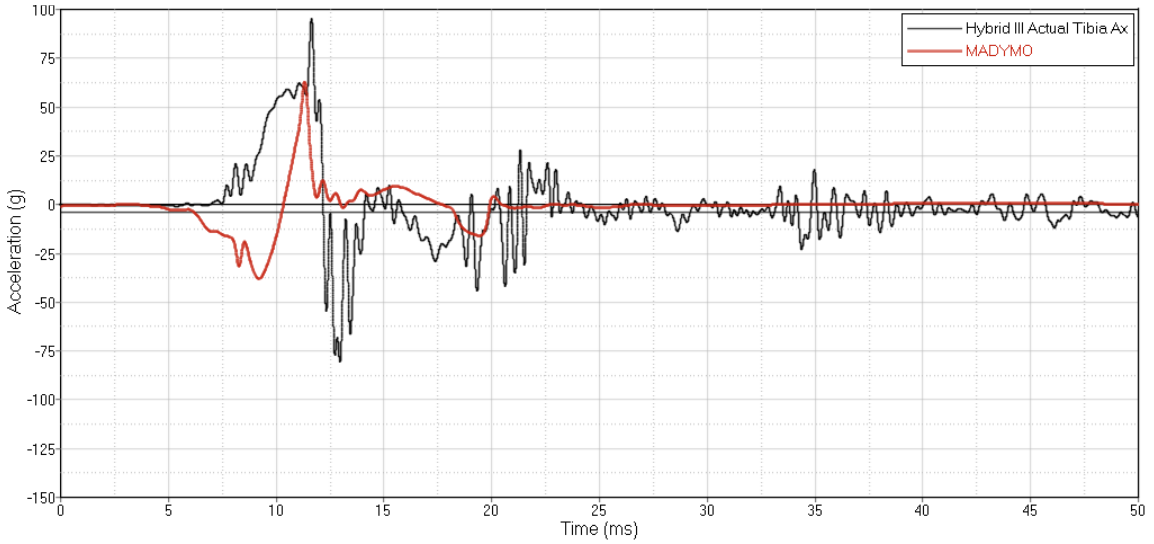

Figure 5-7. Tibia Ax comparing actual Hybrid III (black) against the MADYMO simulation (red)

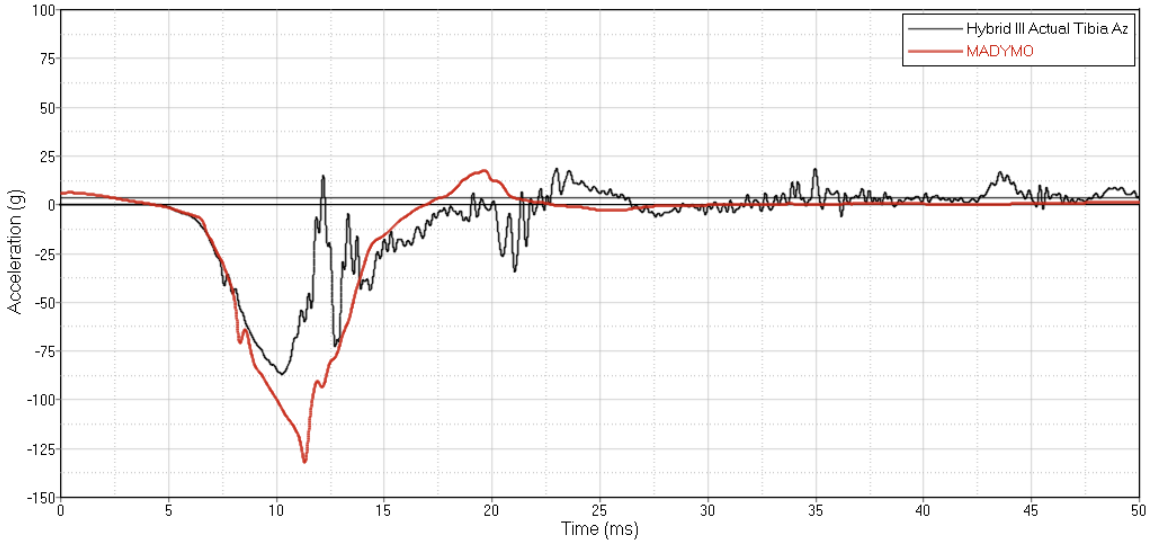

Figure 5-8. Tibia Az comparing actual Hybrid III (black) against the MADYMO simulation (red)

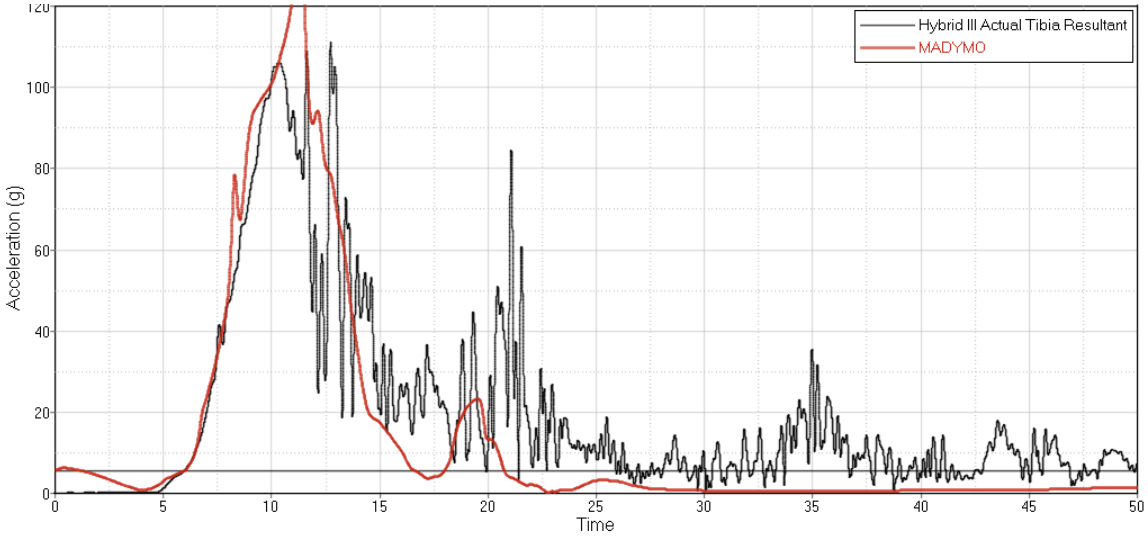

Figure 5-9. Tibia Resultant Acceleration comparing actual Hybrid III (black) against the MADYMO simulation (red)

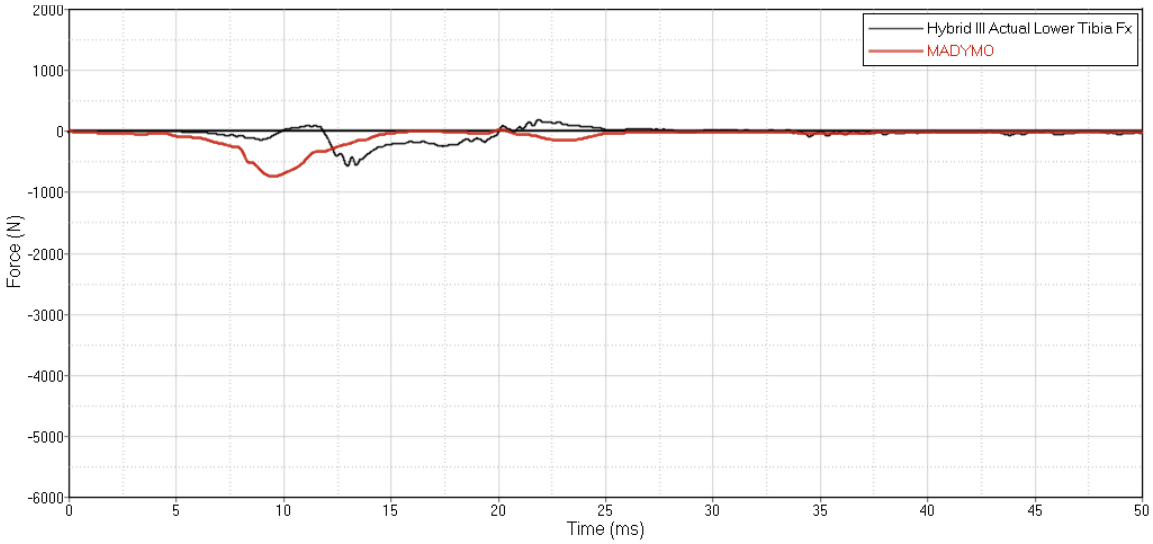

Figure 5-10. Lower Tibia Fx comparing actual Hybrid III (black) against the MADYMO simulation (red)

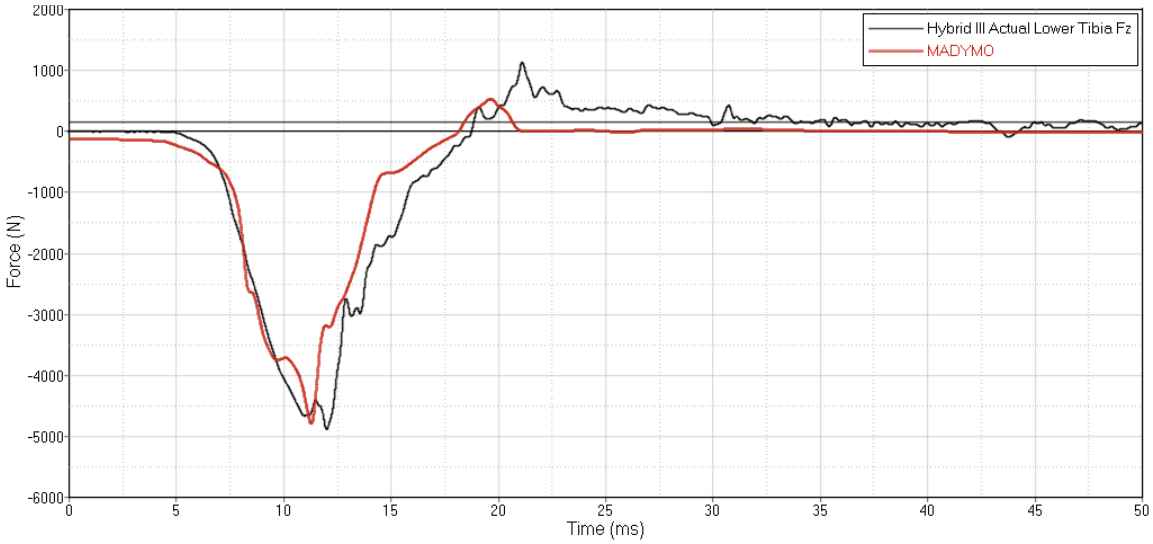

Figure 5-11. Lower Tibia Fz comparing actual Hybrid III (black) against the MADYMO simulation (red)

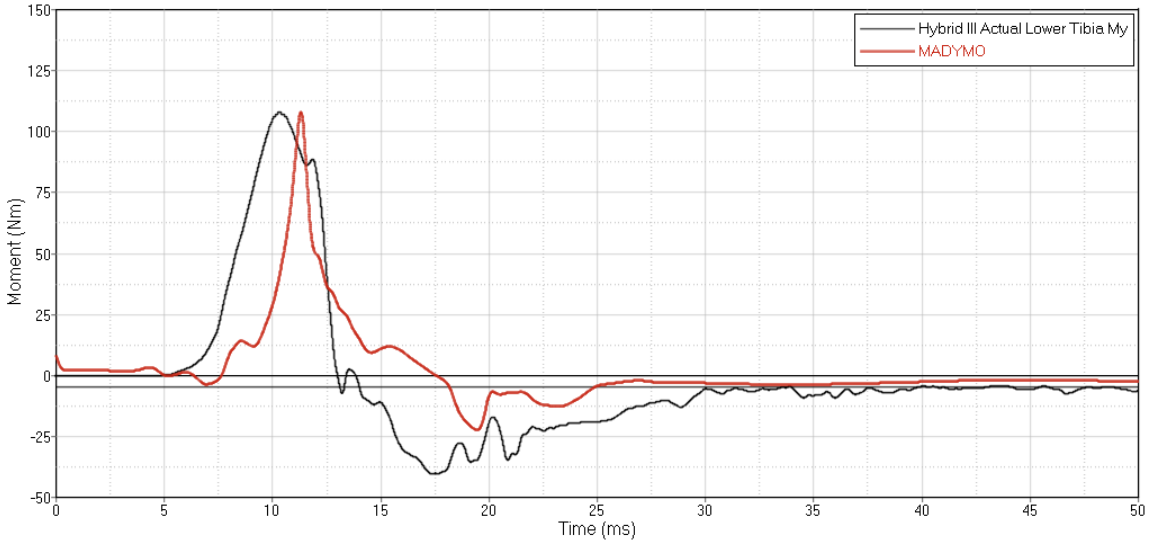

Figure 5-12. Lower Tibia My comparing actual Hybrid III (black) against the MADYMO simulation (red)

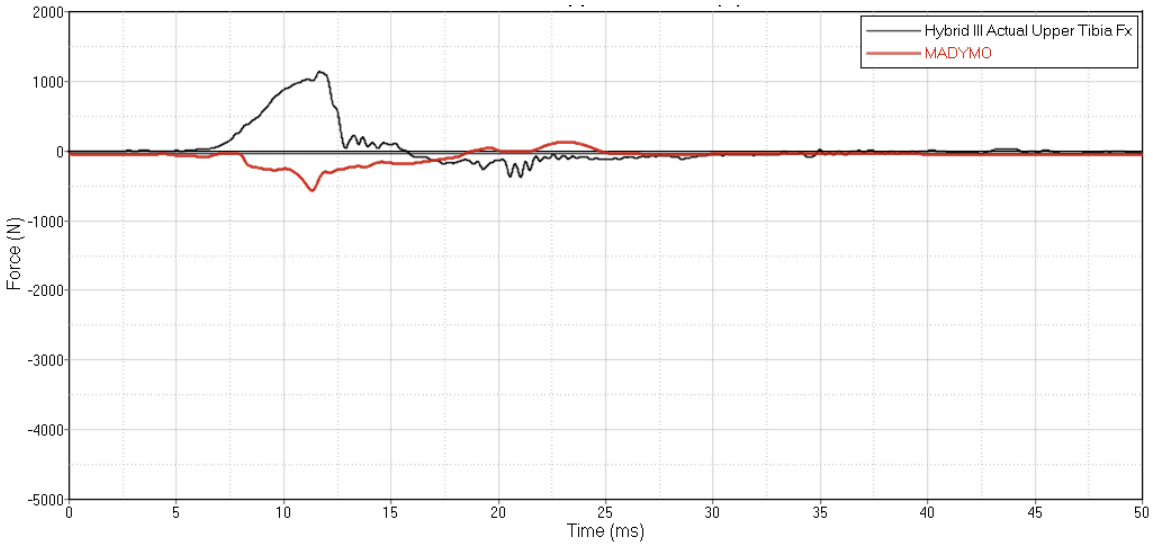

Figure 5-13. Upper Tibia Fx comparing actual Hybrid III (black) against the MADYMO simulation (red)

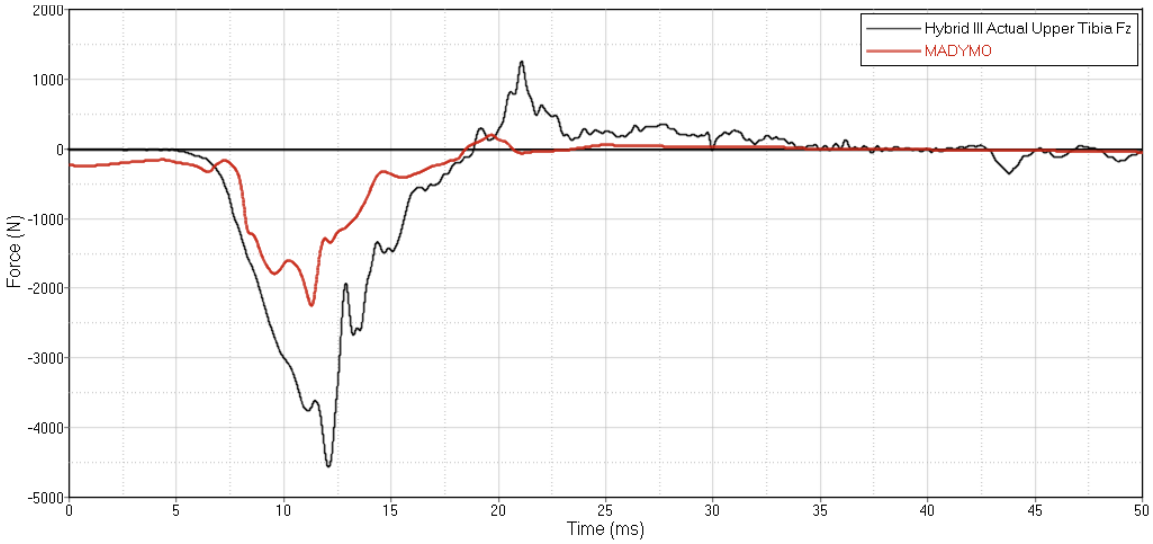

Figure 5-14. Upper Tibia Fz comparing actual Hybrid III (black) against the MADYMO simulation (red)

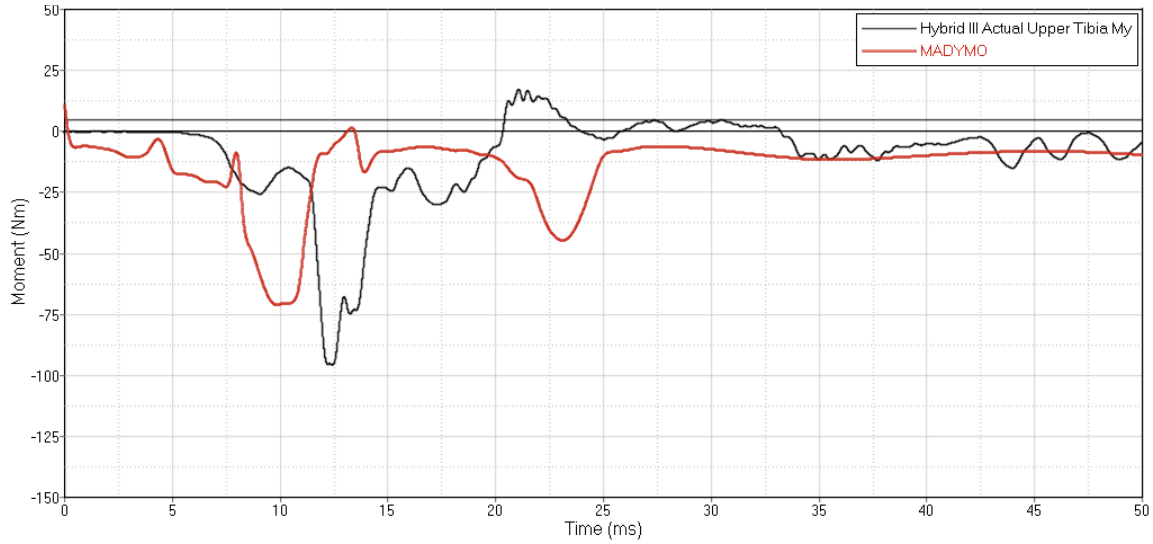

Figure 5-15. Upper Tibia My comparing actual Hybrid III (black) against the MADYMO simulation (red)

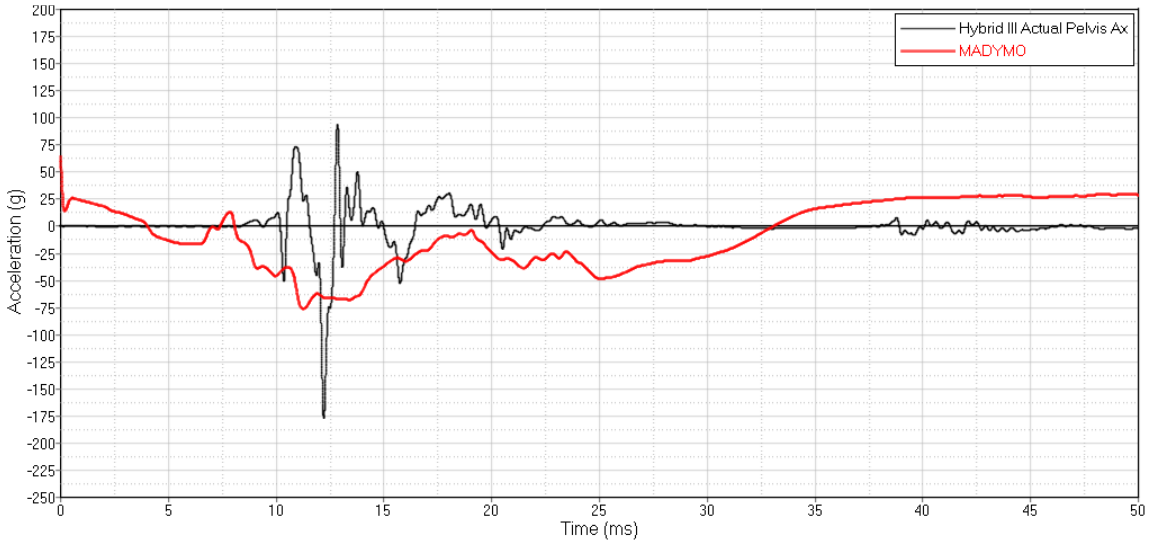

Figure 5-16. Pelvis Ax comparing actual Hybrid III (black) against the MADYMO simulation (red)

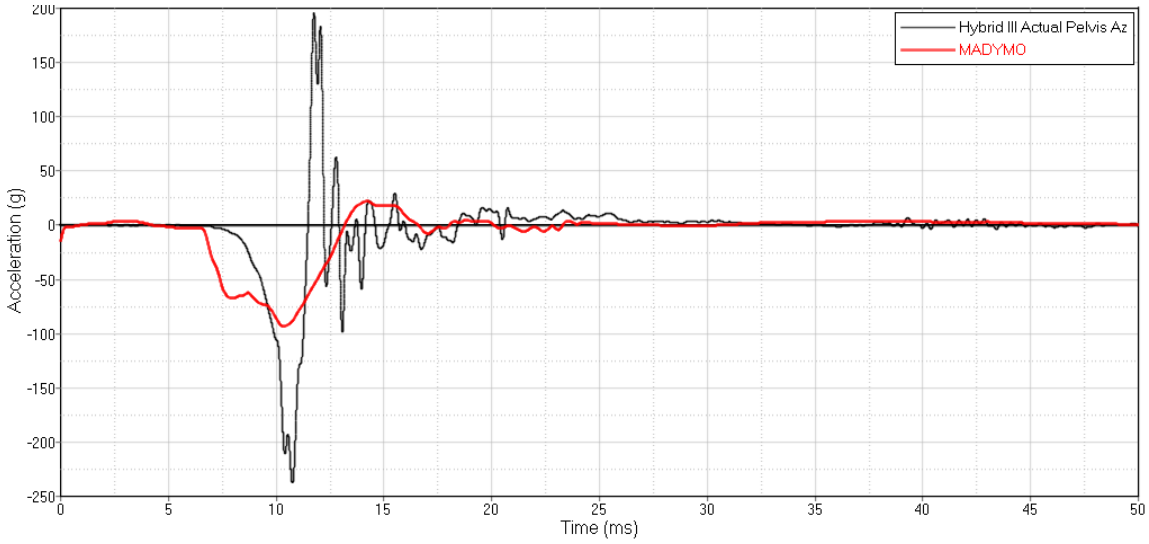

Figure 5-17. Pelvis Az comparing actual Hybrid III (black) against the MADYMO simulation (red)

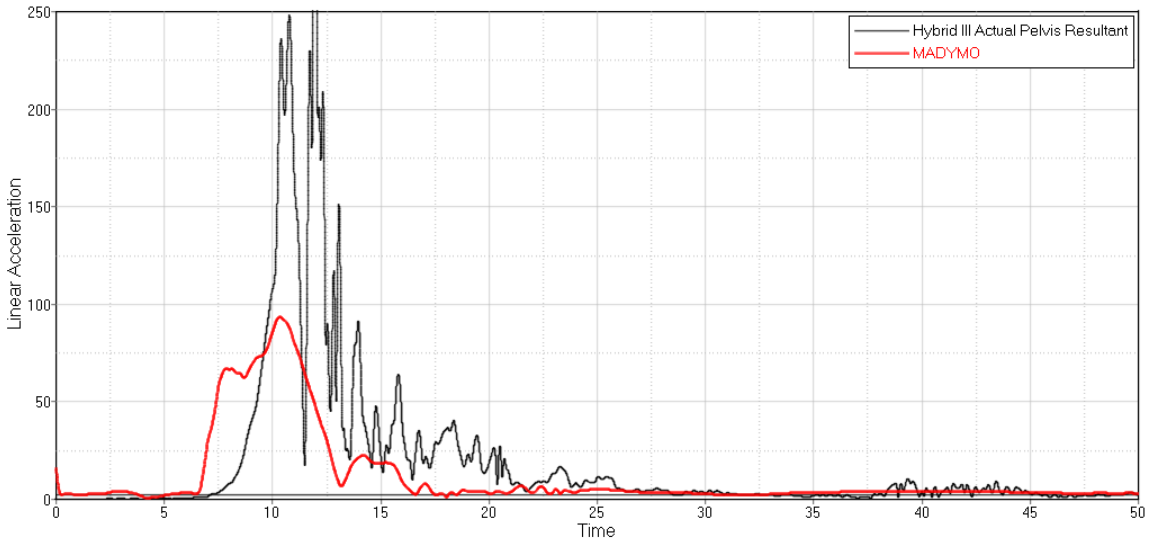

Figure 5-18. Pelvis Resultant Acceleration comparing actual Hybrid III (black) against the MADYMO simulation (red)

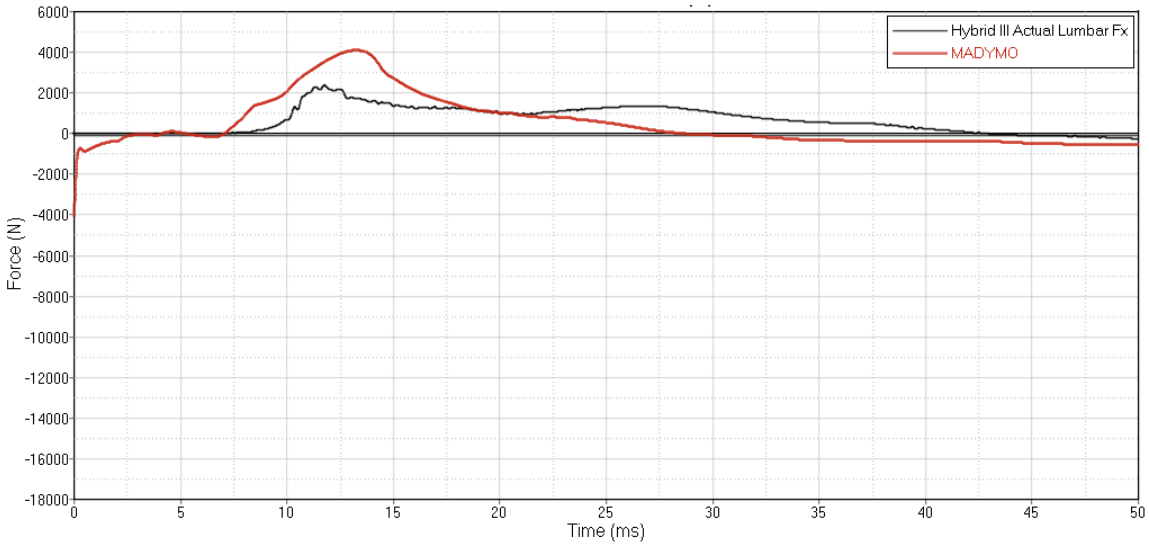

Figure 5-19. Lumbar Fx comparing actual Hybrid III (black) against the MADYMO simulation (red)

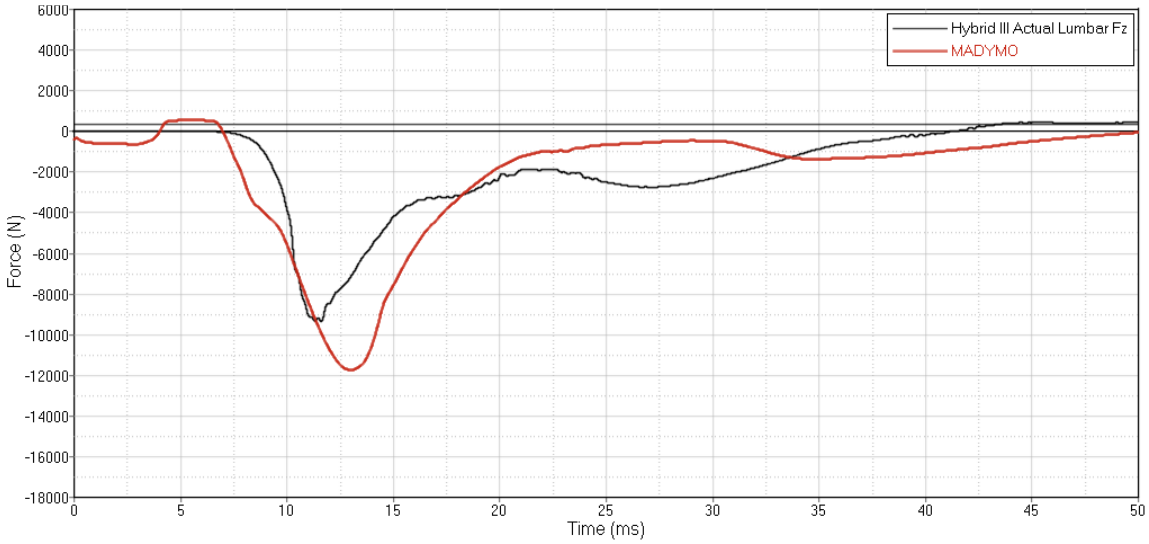

Figure 5-20. Lumbar Fz comparing actual Hybrid III (black) against the MADYMO simulation (red)

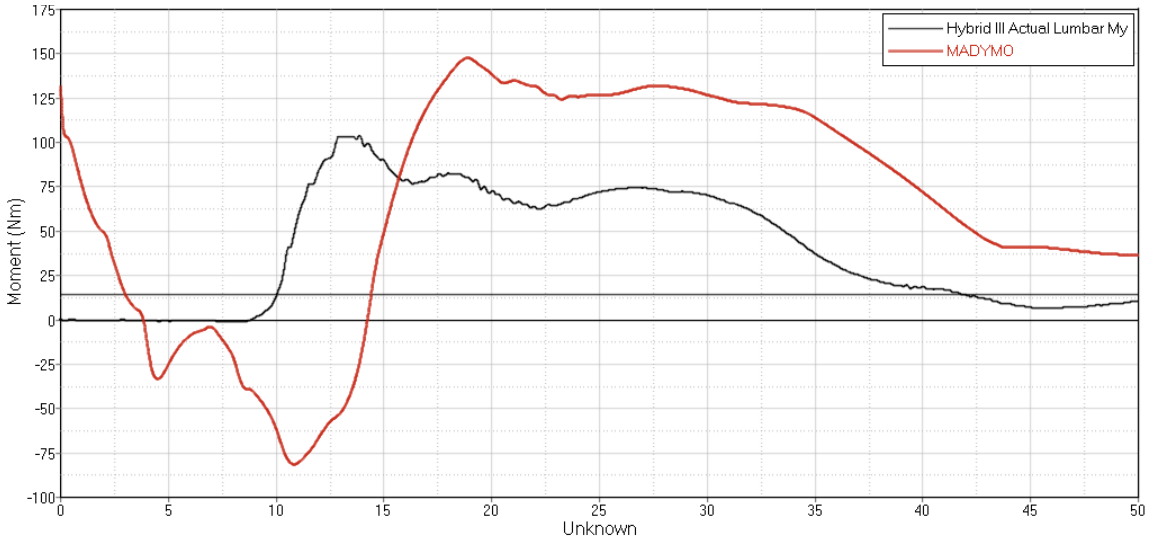

Figure 5-21. Lumbar My comparing actual Hybrid III (black) against the MADYMO simulation (red)

A screen shot showing the comparative kinematics between the model and actual test at 25 ms is shown in Figure 5-22. Limited overall motion occurs in the first 30 ms, and some differences in tibia angle were noted at 50 ms. The general approach was a focus on ATD kinetics while verifying that kinematics were representative of actual ATD motion.

A rotational joint was put into place to represent the motion of the foot plate, and foot plate lift off occurs at similar time between the model and actual test. The pelvis was obscured by the test rig.

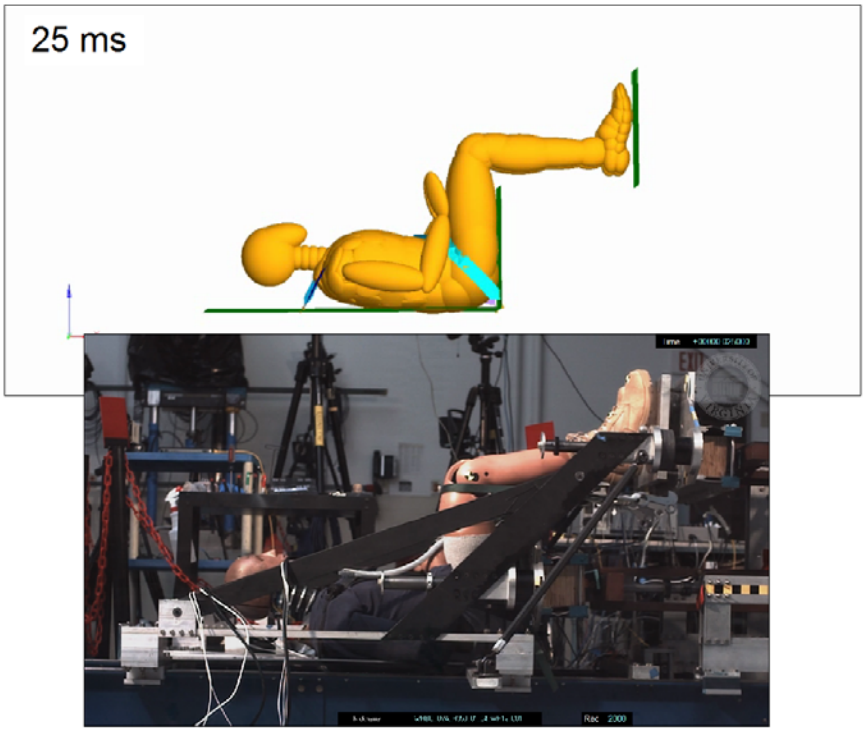

Figure 5-22. Kinematic comparison of MADYMO and actual test at 25 ms

5.3. Specific Aim 1 – Hybrid III Rigid Seat Validation – Limitations

There were some limitations in the fidelity of the simulations which prevent scoring excellent across all key rankings. The initial position of the Hybrid III was not recorded during the Condition A testing, so positioning was set based on video images and tuning to achieve better performance against the actual test data. The quality of the Hybrid III was unknown with respect to pelvis punch-through, where the metal pelvis penetrates through the foam and vinyl toward the seat. Pelvis punch-through causes high accelerative spikes from metal-to-metal contact with the seat which accounts for the mismatch between Pelvis Az and Lumbar Fz. The material properties for the contact

between the pelvis and the seat were based off of a Hybrid III pelvis tested at TARDEC, not the original pelvis used at UVA, which also introduces some variation. The joint friction within the Hybrid III and actual foot plate motion is unknown beyond the z-axis acceleration, which accounts for some of the differences in resulting tibia angle and x-axis motion.

The focus of tuning the simulations was more on the load cells than the accelerometers, as the load cells provide cleaner signals. There was also an inverse relationship between pelvis acceleration and lumbar spine force – as the score for one improved, it degraded in the other. Best efforts were made to maximize the scores of both while maintaining a good rating for Lumbar Fz.

The sled setup in Condition A with the Hybrid III model was considered validated to an acceptable level. The next phase of the research was to replace the Hybrid III model with the HBM and repeat the validation process.

CHAPTER 6 – SPECIFIC AIM 2 – PMHS MODEL VALIDATION

6.1. Specific Aim 2a – PMHS Rigid Seat Validation – Condition A – Model Conditions

The Hybrid III ATD was replaced with the MADYMO Human Body Model (HBM) with the same sled rig configurations including the five-point restraint system as shown in Figure 6-1. The muscles were deactivated to represent the PMHS with no muscle contribution during the event. The model included accelerometer outputs as standard at T12 and T1. Accelerometers were added to the calcaneus, tibias, femurs, pelvis, T8, and T5 vertebra to represent those in the PMHS (Figure 6-2). Vertebral accelerometers were located at the center of the vertebral ellipsoid body. Table 6-1 lists the channels assessed for Condition A with the HBM. The target was to achieve at least a rating of Good for each channel using the CORA scoring methodology previously described.

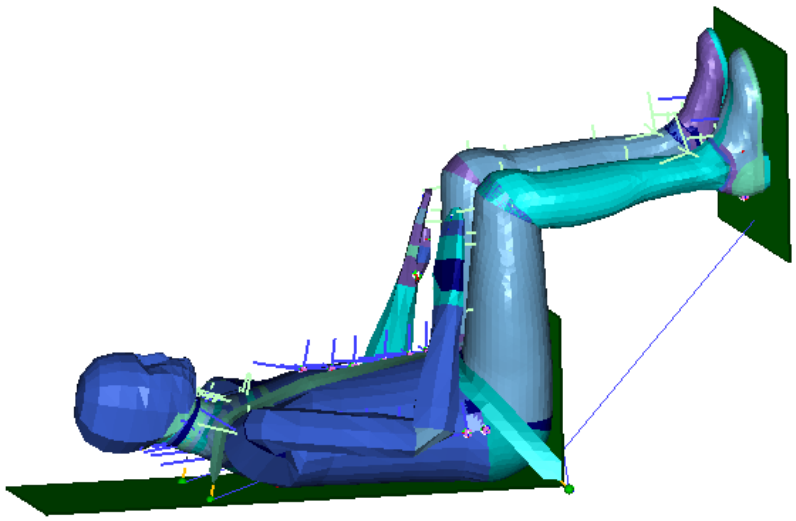

Figure 6-1. HBM in test position.

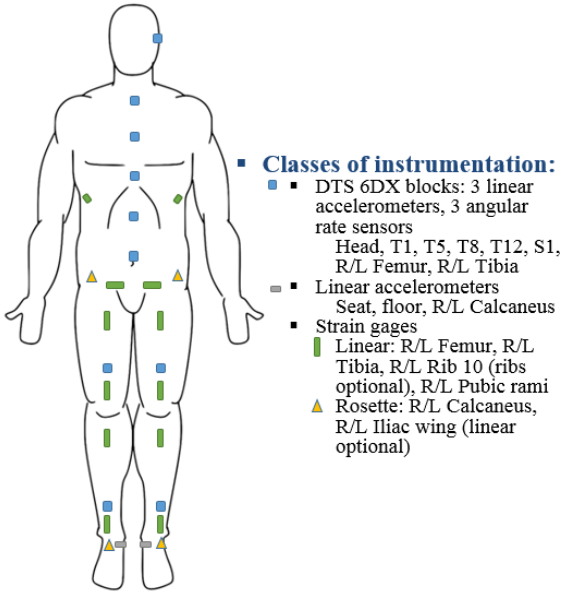

Figure 6-2. PMHS Instrumentation includes accelerometers at T12 and S1 [49]

Table 6-1. Validation channels used for human body model

PMHS and Rig Channels – Legs	PMHS and Rig Channels – Upper Body
Foot Az	Pelvis Ax
Distal Tibia Ax	Pelvis Az
Distal Tibia Az	T12 Ax
Distal Femur Ax	T12 Az
	T8 Ax
	T8 Az
	T5 Ax
	T5 Az
	T1 Ax
	T1 Az

The HBM was positioned to replicate the PMHS positioning procedure, which included setting the distance between the feet at 295 ± 10 mm, maintaining a 90-90-90 degree posture for the ankles, knees, and hips, and ensuring the C7 spinous process (cervicale landmark) was 90 ± 10 mm in front of the ASIS. The spine curvature was

adjusted by changing the angles between the vertebral bodies to adjust to the contour of the seat.

The same pulse used in a series of four Condition A tests was used as input to the floor and seat in the model. The HBM positioning of the legs and spine were adjusted as required to match pre-test images of the PMHS positioning and were altered slightly as needed during the validation process to improve correlation. The rotation of the accelerometers was tuned to balance the distribution of acceleration between the x- and z-axes. As with the Hybrid III, contact properties were altered between the floor and feet to represent the boots and between the seat and pelvis to tune the upper body response. The unaltered HBM was stiffer in response for the lower leg and delayed in loading for the pelvis and spine when compared to the PMHS testing response. When assessed against the PMHS data, the HBM had a CORA score of 0.599, or Fair. The boot contact properties were the same as those used for the Hybrid III, but scaled as needed to match the actual PMHS lower leg response by applying a separate constant multiplying factor to each of the displacement and force axes to elongate or shorten the loading and unloading profile. An unloading curve was also added to improve correlation, as shown in Figure 6-3. The contact properties for the pelvis (Figure 6-4) were derived from component testing conducted at UVA [48]. As with the boot properties, these were also scaled in the same manner by applying a separate constant multiplying factor to the displacement and force to achieve an optimal correlation.

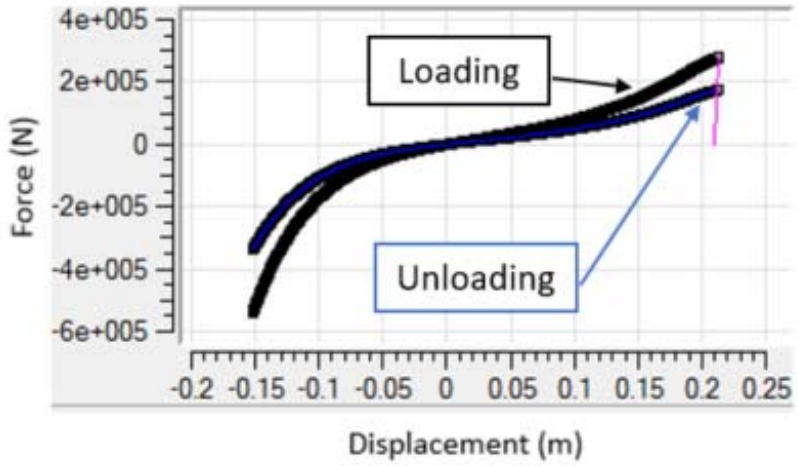

Figure 6-3. Force (N) deflection (m) properties from MADYMO for boot/floor contact

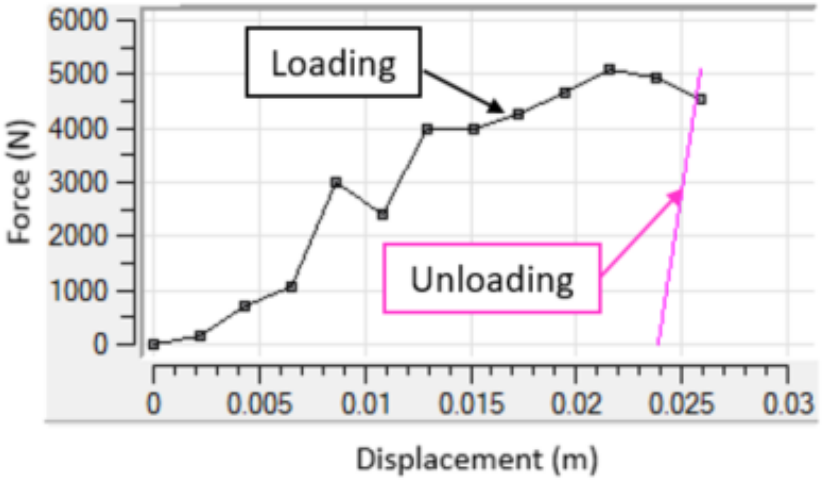

Figure 6-4. Force (N) deflection (m) properties from MADYMO for pelvis/seat contact [48]

After the kinetics for the lower leg and pelvis were optimized, the accelerometers in the thoracic spine segments were noticeably lagging in phase. After confirming with TASS that the joint and material properties of the HBM, including the spine, were encrypted and not alterable by the user, external Kelvin restraints were added to the spine. According to TASS, the only way to tune the spine model response to improve phasing and peaks to match the PMHS data at the same spinal levels was to add these

restraints between the vertebral bodies in the model to stiffen the response, as the model had its own inherent stiffness between vertebrae, but this stiffness was not sufficient to represent a response from underbody blast. Table 6-2 contains the details for the four Kelvin restraint segments, including the locations of each of the connections (Point Object 1 and 2) and hysteresis slope. A parallel spring and damper comprised the MADYMO Kelvin restraint. All restraints used active damping with the MADYMO default setting, and initial strain was 0.0. The restraint properties for the spine segments were derived from the work conducted by Yoganandan et al [76]. The Yoganandan research produced load and deflection curves from axial compressive tests of PMHS intervertebral joints. These curves were then scaled and had an offset, or delay in loading, introduced for use in the model's Kelvin restraints. The scaling and offset were required because the HBM already had stiffness properties for the intervertebral disks included, so the Kelvin restraints provided complimentary stiffness. As this testing was conducted on segments of the spine, scaling was also required to represent the compilation of spinal segments in the model. The final scaled force and deflection curves for the four Kelvin restraints in the model are shown in Figure 6-5 through Figure 6-8. The restraints were attached between the sacrum and the various spinal segments (L5, T12, T8, T5, and T1) to achieve the desired output to match the PMHS data at the same spinal levels (Figure 6-9). For the optimization process, the final T12 z-axis force was the sum of the T12 joint output force and the forces from the Kelvin restraints at L5/T12, sacrum/T8, and sacrum/T5 locations. The Kelvin restraint force data needed to be filtered at CFC 60 to remove noise in the data due to the interaction of the restraints, as the restraints consisted of overlapping springs and dampers that caused a vibration effect. The x-scale and y-scale for the

loading and unloading curves, as well as the offset to the start of loading, were the most influential factors in tuning spinal response for each of the restraint segments.

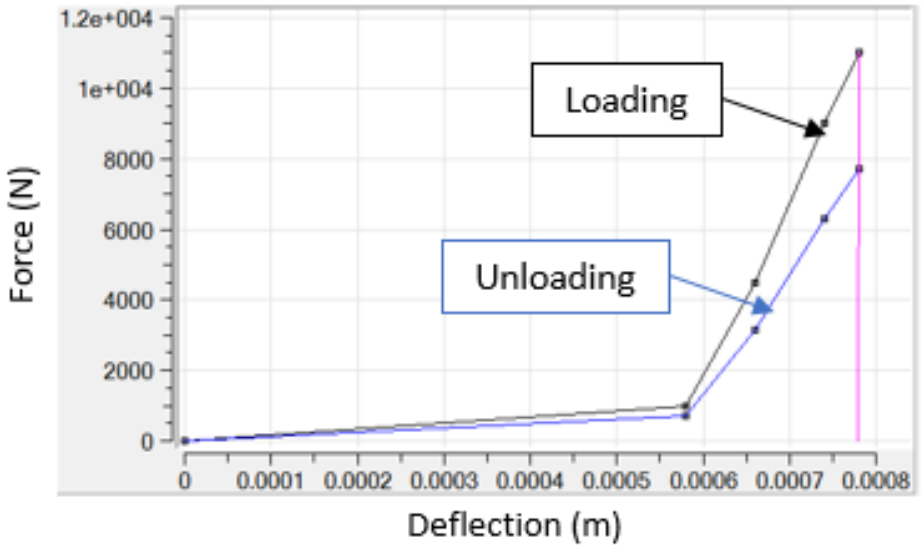

Figure 6-5. Final scaled force (N) deflection (m) properties from MADYMO for spinal restraint between L5 and T12

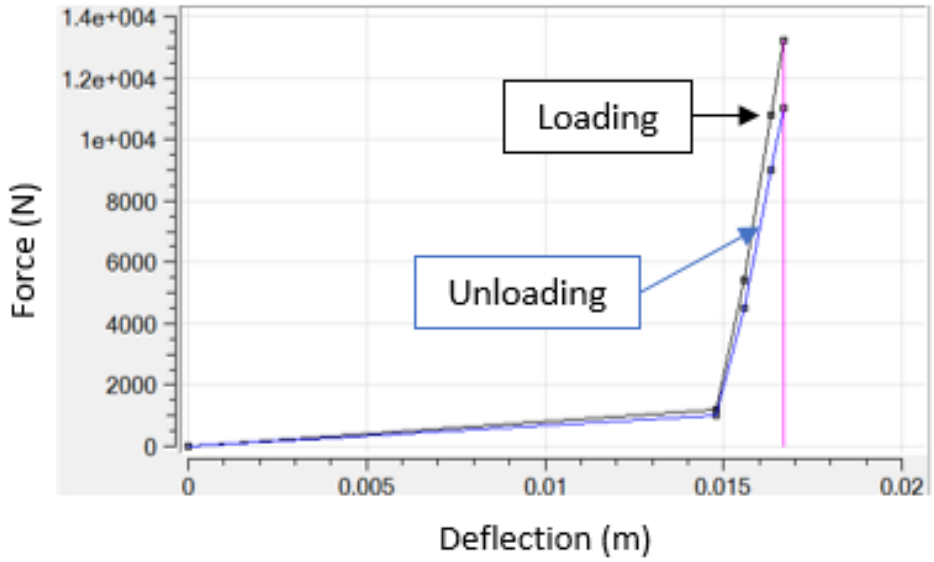

Figure 6-6. Final scaled force (N) deflection (m) properties from MADYMO for spinal restraint between sacrum and T8

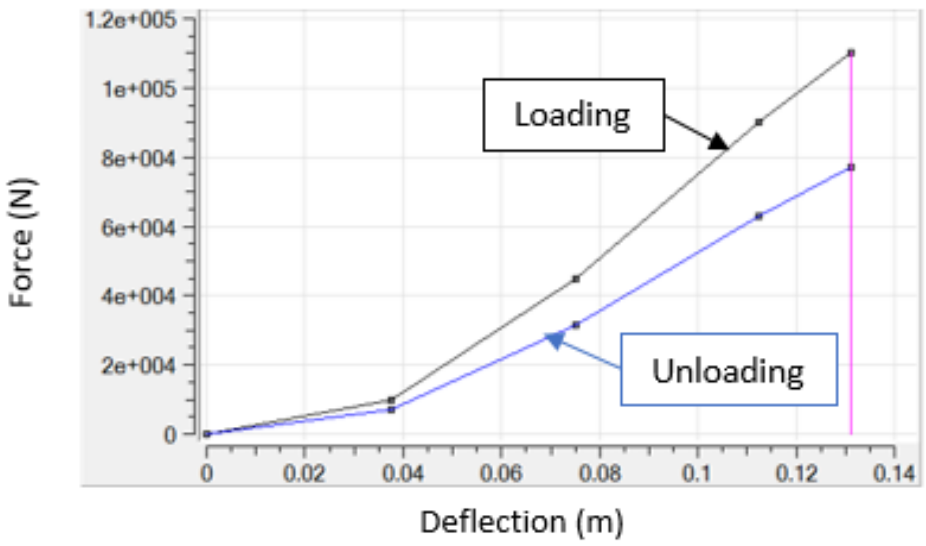

Figure 6-7. Final scaled force (N) deflection (m) properties from MADYMO for spinal restraint between sacrum and T5

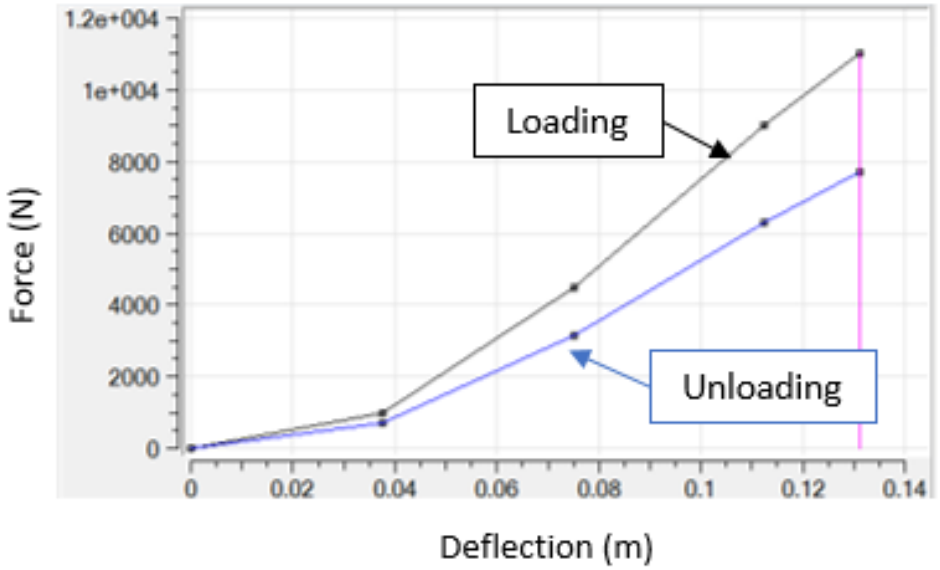

Figure 6-8. Final scaled force (N) deflection (m) properties from MADYMO for spinal restraint between T5 and T1

Table 6-2. Spinal restraint connection details

Point Object 1	Point Object 2	Hysteresis Slope	Loading Curve		Unloading Curve	
			Displacement (m)	Force (N)	Displacement (m)	Force (N)
L5	T12	7.00E+10	0	0	0	0
			0.00058	1000	0.00058	700
			0.00066	4500	0.00066	3150
			0.00074	9000	0.00074	6300
			0.00078	11000	0.00078	7700
Sacrum	T8	1.00E+09	0	0	0	0
			0.0148125	1200	0.0148125	1000
			0.0155625	5400	0.0155625	4500
			0.0163125	10800	0.0163125	9000
			0.0166875	13200	0.0166875	11000
Sacrum	T5	5.00E+11	0	0	0	0
			0.0375	10000	0.0375	7000
			0.075	45000	0.075	31500
			0.1125	90000	0.1125	63000
			0.13125	110000	0.13125	77000
T5	T1	1.00E+10	0	0	0	0
			0.0375	1000	0.0375	700
			0.075	4500	0.075	3150
			0.1125	9000	0.1125	6300
			0.13125	11000	0.13125	7700

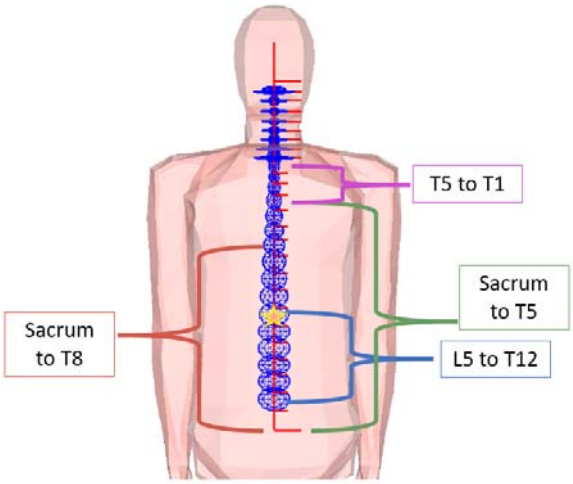

Figure 6-9. Spinal restraint connections

For all tunable parameters including the scaling factors described above, trial and error was used to determine a reasonable optimal range for each parameter based on the overall peak and phasing of the affected channel compared to the PMHS channel, and then these ranges were systematically evaluated to determine the final value for the validation as described in the following section. For the Kelvin restraints, this trial and error process included evaluating if offsets were needed for the onset of the displacement, as well as separate scaling factors for the displacement and force values. The unloading curves were the same as the final loading curves, but with a constant multiplying factor less than 1 applied to the force value for a hysteresis effect.

6.2. Specific Aim 2a – PMHS Rigid Seat Validation – Condition A – CORA Rating

Four PMHS were tested at UVA as part of the WIAMan program for Condition A. Biofidelity Response Corridors were created from this data, which represents the average response of a 50th percentile male, as published in the work from Pietsch el al [49]. The BRCs and average response curves were provided by UVA to the author. Pre-processing of the data included filtering the data using a 3000 Hz cutoff, then transforming the acceleration traces. The transformation resulted in a shift in the data trace to an anatomical point other than the location it was recorded, for example, from the spinous process of a vertebra to the center of the vertebra. The data was then normalized to represent a 50^{th} percentile male based on scaling techniques outlined in Pietsch et al [49]. The data was then aligned and an average response curve was created. Inner and outer corridors were created based on one and two standard deviations around the average, respectively, as shown below in Figure 6-10. To prevent pinch points, a minimum corridor

width of 5% of the maximum standard deviation was used where the curves converged. The CORA 3.6.1 software was utilized to score the Condition A PMHS simulation goodness of fit using the same CORA parameters as the WIAMan program. The input CORA file is provided in Appendix A. The remainder of the BRCs used in the correlation are provided in Appendix B as well as in Figure 6-11 through Figure 6-24, although only the inner corridor is shown in these figures. The CORA scoring table is shown in Table 6-3 again for reference.

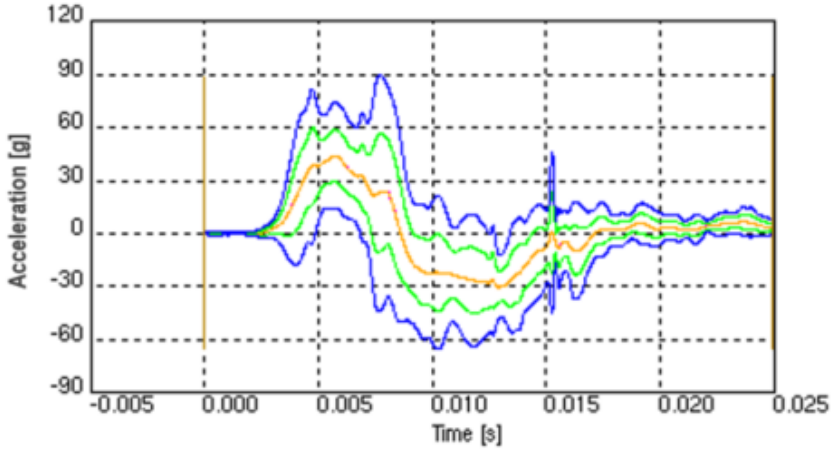

Figure 6-10. Example BRC from UVA Condition A data with reference curve (orange), inner one standard deviation curve (green), and outer two standard deviation curve (blue)

Table 6-3. Biofidelity rating scheme [49]

Biofidelity Rating	CORA Score
Excellent	85% ≤ Score ≤ 100%
Good	65% ≤ Score < 85%
Fair	44% ≤ Score < 65%
Marginal	26% ≤ Score < 44%
Unacceptable	0% ≤ Score < 26%

Once the major tunable parameters were identified, a series of DOEs, or Design of Experiments, were carried out to optimize the CORA scores of the pelvis and thoracic vertebrae. A DOE allows an assessment of the design space for the parametric study to understand the effects of the variables [40]. As the lower legs were already in the Good/Excellent category from trial and error tuning, the final series of DOEs were run on the pelvis, T12, T8, T5, and T1 vertebrae. Each DOE consisted of varying three key influential parameters ±25% around the best run from the previous series in a full factorial structure. The main contributing factors included scaling factors of contact properties and restraints and the angle of the accelerometers around the y-axis. The focus of the DOE was to maintain a Good rating of all channels and achieve Excellent ratings for Pelvis Az and T12 Az, which were the main focus of the force/deflection optimization in Specific Aim 3. The results of the DOEs are shown below in Table 6-4 through Table 6-8. The final CORA score for the optimized model is 0.796 as a composite score, in the Good category, with Pelvis Az and T12 Az both as Excellent, at 0.900 and 0.903 respectively. The best run from each DOE is in the thick border box in Table 6-4 through Table 6-8, and this run was used as the starting point for the next superior vertebrae DOE.

Table 6-4. Pelvis DOE results

RUN	PMHS_A_ Foot_Az	PMHS_A_ Tibia_Ax	PMHS_A_ Tibia_Az	PMHS_A_ Femur_Ax	PMHS_A_ Pelvis_Ax	PMHS_A_ Pelvis_Az	PMHS_A_ T12_Ax	PMHS_A_ T12_Az	PMHS_A_ T8_Ax	PMHS_A_ T8_Az	PMHS_A_ T5_Ax	PMHS_A_ T5_Az	PMHS_A_ T1_Ax	PMHS_A_ T1_Az	CORA TOTAL
1	0.908	0.793	0.795	0.760	0.803	0.854	0.772	0.850	0.785	0.771	0.776	0.826	0.796	0.730	0.801
2	0.907	0.794	0.788	0.772	0.786	0.892	0.790	0.879	0.772	0.785	0.758	0.817	0.792	0.711	0.803
3	0.905	0.795	0.782	0.780	0.776	0.887	0.800	0.899	0.765	0.797	0.739	0.816	0.789	0.699	0.802
4	0.911	0.793	0.797	0.767	0.781	0.883	0.764	0.847	0.774	0.755	0.759	0.794	0.807	0.701	0.795
5	0.909	0.794	0.790	0.778	0.775	0.893	0.781	0.879	0.761	0.766	0.738	0.784	0.805	0.683	0.795
6	0.907	0.795	0.782	0.786	0.772	0.898	0.795	0.900	0.750	0.774	0.720	0.780	0.802	0.672	0.795
7	0.913	0.792	0.797	0.774	0.779	0.871	0.757	0.847	0.759	0.737	0.740	0.762	0.821	0.677	0.788
8	0.912	0.794	0.789	0.784	0.774	0.877	0.772	0.875	0.745	0.745	0.718	0.750	0.818	0.659	0.787
9	0.910	0.796	0.782	0.794	0.771	0.879	0.785	0.888	0.734	0.747	0.706	0.746	0.814	0.644	0.785
10	0.908	0.793	0.795	0.760	0.804	0.868	0.772	0.850	0.785	0.771	0.776	0.826	0.796	0.730	0.802
11	0.907	0.794	0.788	0.772	0.788	0.880	0.790	0.879	0.772	0.785	0.758	0.817	0.792	0.711	0.802
12	0.905	0.795	0.782	0.780	0.777	0.876	0.800	0.899	0.765	0.797	0.739	0.816	0.789	0.699	0.801
13	0.911	0.793	0.797	0.767	0.782	0.897	0.764	0.847	0.774	0.755	0.759	0.794	0.807	0.701	0.796
14	0.909	0.794	0.790	0.778	0.776	0.895	0.781	0.879	0.761	0.766	0.738	0.784	0.805	0.683	0.796
15	0.907	0.795	0.782	0.786	0.773	0.885	0.795	0.900	0.750	0.774	0.720	0.780	0.802	0.672	0.794
16	0.913	0.792	0.797	0.774	0.779	0.884	0.757	0.847	0.759	0.737	0.740	0.762	0.821	0.677	0.789
17	0.912	0.794	0.789	0.784	0.775	0.890	0.772	0.875	0.745	0.745	0.718	0.750	0.818	0.659	0.788
18	0.910	0.796	0.782	0.794	0.772	0.884	0.785	0.888	0.734	0.747	0.706	0.746	0.814	0.644	0.786
19	0.908	0.793	0.795	0.760	0.805	0.856	0.772	0.850	0.785	0.771	0.776	0.826	0.796	0.730	0.802
20	0.907	0.794	0.788	0.772	0.789	0.868	0.790	0.879	0.772	0.785	0.758	0.817	0.792	0.711	0.802
21	0.905	0.795	0.782	0.780	0.778	0.864	0.800	0.899	0.765	0.797	0.739	0.816	0.789	0.699	0.801
22	0.911	0.793	0.797	0.767	0.783	0.892	0.764	0.847	0.774	0.755	0.759	0.794	0.807	0.701	0.796
23	0.909	0.794	0.790	0.778	0.777	0.882	0.781	0.879	0.761	0.766	0.738	0.784	0.805	0.683	0.795
24	0.907	0.795	0.782	0.786	0.773	0.872	0.795	0.900	0.750	0.774	0.720	0.780	0.802	0.672	0.793
25	0.913	0.792	0.797	0.774	0.780	0.898	0.757	0.847	0.759	0.737	0.740	0.762	0.821	0.677	0.790
26	0.912	0.794	0.789	0.784	0.775	0.885	0.772	0.875	0.745	0.745	0.718	0.750	0.818	0.659	0.787
27	0.910	0.796	0.782	0.794	0.772	0.871	0.785	0.888	0.734	0.747	0.706	0.746	0.814	0.644	0.785

Table 6-5. T12 DOE results

RUN	PMHS_A_ Foot_Az	PMHS_A_ Tibia_Ax	PMHS_A_ Tibia_Az	PMHS_A_ Femur_Ax	PMHS_A_ Pelvis_Ax	PMHS_A_ Pelvis_Az	PMHS_A_ T12_Ax	PMHS_A_ T12_Az	PMHS_A_ T8_Ax	PMHS_A_ T8_Az	PMHS_A_ T5_Ax	PMHS_A_ T5_Az	PMHS_A_ T1_Ax	PMHS_A_ T1_Az	CORA TOTAL
1	0.906	0.796	0.780	0.792	0.768	0.891	0.736	0.893	0.756	0.793	0.722	0.796	0.805	0.674	0.793
2	0.906	0.796	0.780	0.792	0.768	0.891	0.776	0.885	0.756	0.793	0.722	0.796	0.805	0.674	0.796
3	0.906	0.796	0.780	0.792	0.768	0.891	0.772	0.879	0.756	0.793	0.722	0.796	0.805	0.674	0.795
4	0.907	0.795	0.781	0.789	0.769	0.893	0.741	0.900	0.753	0.785	0.721	0.790	0.804	0.673	0.793
5	0.907	0.795	0.781	0.789	0.769	0.893	0.782	0.894	0.753	0.785	0.721	0.790	0.804	0.673	0.795
6	0.907	0.795	0.781	0.789	0.769	0.893	0.780	0.889	0.753	0.785	0.721	0.790	0.804	0.673	0.795
7	0.907	0.795	0.782	0.787	0.771	0.896	0.748	0.904	0.751	0.778	0.720	0.783	0.802	0.672	0.793
8	0.907	0.795	0.782	0.787	0.771	0.896	0.790	0.899	0.751	0.778	0.720	0.783	0.802	0.672	0.795
9	0.907	0.795	0.782	0.787	0.771	0.896	0.788	0.894	0.751	0.778	0.720	0.783	0.802	0.672	0.795
10	0.907	0.795	0.781	0.789	0.770	0.894	0.743	0.901	0.753	0.783	0.721	0.788	0.803	0.673	0.793
11	0.907	0.795	0.781	0.789	0.770	0.894	0.784	0.895	0.753	0.783	0.721	0.788	0.803	0.673	0.795
12	0.907	0.795	0.781	0.789	0.770	0.894	0.782	0.891	0.753	0.783	0.721	0.788	0.803	0.673	0.795
13	0.907	0.795	0.782	0.786	0.772	0.898	0.752	0.904	0.750	0.774	0.720	0.780	0.802	0.672	0.792
14	0.907	0.795	0.782	0.786	0.772	0.898	0.795	0.900	0.750	0.774	0.720	0.780	0.802	0.672	0.795
15	0.907	0.795	0.782	0.786	0.772	0.898	0.793	0.895	0.750	0.774	0.720	0.780	0.802	0.672	0.795
16	0.908	0.795	0.783	0.784	0.774	0.900	0.762	0.901	0.749	0.766	0.718	0.770	0.800	0.671	0.792
17	0.908	0.795	0.783	0.784	0.774	0.900	0.805	0.896	0.749	0.766	0.718	0.770	0.800	0.671	0.794
18	0.908	0.795	0.783	0.784	0.774	0.900	0.804	0.892	0.749	0.766	0.718	0.770	0.800	0.671	0.794
19	0.907	0.795	0.782	0.786	0.772	0.897	0.752	0.905	0.751	0.774	0.720	0.780	0.802	0.672	0.793
20	0.907	0.795	0.782	0.786	0.772	0.897	0.794	0.900	0.751	0.774	0.720	0.780	0.802	0.672	0.795
21	0.907	0.795	0.782	0.786	0.772	0.897	0.793	0.895	0.751	0.774	0.720	0.780	0.802	0.672	0.795
22	0.908	0.795	0.783	0.783	0.774	0.900	0.764	0.900	0.748	0.765	0.718	0.769	0.800	0.671	0.791
23	0.908	0.795	0.783	0.783	0.774	0.900	0.807	0.894	0.748	0.765	0.718	0.769	0.800	0.671	0.794
24	0.908	0.795	0.783	0.783	0.774	0.900	0.806	0.891	0.748	0.765	0.718	0.769	0.800	0.671	0.794
25	0.908	0.795	0.784	0.781	0.775	0.900	0.772	0.892	0.746	0.758	0.716	0.759	0.798	0.671	0.790
26	0.908	0.795	0.784	0.781	0.775	0.900	0.816	0.887	0.746	0.758	0.716	0.759	0.798	0.671	0.792
27	0.908	0.795	0.784	0.781	0.775	0.900	0.815	0.883	0.746	0.758	0.716	0.759	0.798	0.671	0.792

Table 6-6. T8 DOE results

RUN	PMHS_A_ Foot_Az	PMHS_A_ Tibia_Ax	PMHS_A_ Tibia_Az	PMHS_A_ Femur_Ax	PMHS_A_ Pelvis_Ax	PMHS_A_ Pelvis_Az	PMHS_A_ T12_Ax	PMHS_A_ T12_Az	PMHS_A_ T8_Ax	PMHS_A_ T8_Az	PMHS_A_ T5_Ax	PMHS_A_ T5_Az	PMHS_A_ T1_Ax	PMHS_A_ T1_Az	CORA TOTAL
1	0.907	0.794	0.785	0.784	0.774	0.898	0.755	0.900	0.746	0.786	0.729	0.773	0.809	0.676	0.794
2	0.907	0.794	0.785	0.784	0.774	0.898	0.755	0.900	0.763	0.773	0.729	0.773	0.809	0.676	0.794
3	0.907	0.794	0.785	0.784	0.774	0.898	0.755	0.900	0.787	0.763	0.729	0.773	0.809	0.676	0.795
4	0.908	0.795	0.784	0.784	0.774	0.899	0.759	0.900	0.740	0.783	0.723	0.771	0.804	0.673	0.793
5	0.908	0.795	0.784	0.784	0.774	0.899	0.759	0.900	0.756	0.769	0.723	0.771	0.804	0.673	0.793
6	0.908	0.795	0.784	0.784	0.774	0.899	0.759	0.900	0.780	0.758	0.723	0.771	0.804	0.673	0.794
7	0.908	0.795	0.783	0.784	0.774	0.900	0.761	0.901	0.735	0.781	0.720	0.771	0.801	0.672	0.792
8	0.908	0.795	0.783	0.784	0.774	0.900	0.761	0.901	0.750	0.767	0.720	0.771	0.801	0.672	0.792
9	0.908	0.795	0.783	0.784	0.774	0.900	0.761	0.901	0.775	0.756	0.720	0.771	0.801	0.672	0.793
10	0.908	0.795	0.784	0.784	0.774	0.899	0.759	0.900	0.739	0.783	0.723	0.771	0.804	0.673	0.793
11	0.908	0.795	0.784	0.784	0.774	0.899	0.759	0.900	0.755	0.769	0.723	0.771	0.804	0.673	0.793
12	0.908	0.795	0.784	0.784	0.774	0.899	0.759	0.900	0.780	0.758	0.723	0.771	0.804	0.673	0.794
13	0.908	0.795	0.783	0.784	0.774	0.900	0.762	0.901	0.733	0.780	0.718	0.770	0.800	0.671	0.791
14	0.908	0.795	0.783	0.784	0.774	0.900	0.762	0.901	0.749	0.766	0.718	0.770	0.800	0.671	0.792
15	0.908	0.795	0.783	0.784	0.774	0.900	0.762	0.901	0.773	0.756	0.718	0.770	0.800	0.671	0.793
16	0.908	0.795	0.783	0.784	0.773	0.900	0.764	0.901	0.728	0.779	0.717	0.771	0.798	0.670	0.791
17	0.908	0.795	0.783	0.784	0.773	0.900	0.764	0.901	0.744	0.765	0.717	0.771	0.798	0.670	0.791
18	0.908	0.795	0.783	0.784	0.773	0.900	0.764	0.901	0.768	0.755	0.717	0.771	0.798	0.670	0.792
19	0.908	0.795	0.783	0.784	0.774	0.900	0.762	0.901	0.734	0.780	0.719	0.771	0.800	0.672	0.792
20	0.908	0.795	0.783	0.784	0.774	0.900	0.762	0.901	0.750	0.766	0.719	0.771	0.800	0.672	0.792
21	0.908	0.795	0.783	0.784	0.774	0.900	0.762	0.901	0.774	0.756	0.719	0.771	0.800	0.672	0.793
22	0.908	0.795	0.783	0.784	0.773	0.900	0.764	0.901	0.728	0.779	0.717	0.771	0.797	0.670	0.791
23	0.908	0.795	0.783	0.784	0.773	0.900	0.764	0.901	0.744	0.765	0.717	0.771	0.797	0.670	0.791
24	0.908	0.795	0.783	0.784	0.773	0.900	0.764	0.901	0.768	0.755	0.717	0.771	0.797	0.670	0.792
25	0.908	0.795	0.782	0.784	0.773	0.900	0.765	0.901	0.724	0.778	0.716	0.772	0.796	0.668	0.790
26	0.908	0.795	0.782	0.784	0.773	0.900	0.765	0.901	0.739	0.764	0.716	0.772	0.796	0.668	0.790
27	0.908	0.795	0.782	0.784	0.773	0.900	0.765	0.901	0.764	0.754	0.716	0.772	0.796	0.668	0.791

Table 6-7. T5 DOE results

RUN	PMHS_A_ Foot_Az	PMHS_A_ Tibia_Ax	PMHS_A_ Tibia_Az	PMHS_A_ Femur_Ax	PMHS_A_ Pelvis_Ax	PMHS_A_ Pelvis_Az	PMHS_A_ T12_Ax	PMHS_A_ T12_Az	PMHS_A_ T8_Ax	PMHS_A_ T8_Az	PMHS_A_ T5_Ax	PMHS_A_ T5_Az	PMHS_A_ T1_Ax	PMHS_A_ T1_Az	CORA TOTAL
1	0.907	0.794	0.786	0.784	0.775	0.899	0.757	0.903	0.742	0.784	0.684	0.784	0.802	0.682	0.792
2	0.907	0.794	0.786	0.784	0.775	0.899	0.757	0.903	0.742	0.784	0.710	0.774	0.802	0.682	0.793
3	0.907	0.794	0.786	0.784	0.775	0.899	0.757	0.903	0.742	0.784	0.737	0.766	0.802	0.682	0.794
4	0.909	0.798	0.777	0.790	0.770	0.894	0.769	0.889	0.717	0.795	0.665	0.753	0.778	0.651	0.783
5	0.909	0.798	0.777	0.790	0.770	0.894	0.769	0.889	0.717	0.795	0.676	0.747	0.778	0.651	0.783
6	0.909	0.798	0.777	0.790	0.770	0.894	0.769	0.889	0.717	0.795	0.694	0.743	0.778	0.651	0.784
7	0.909	0.799	0.776	0.793	0.770	0.889	0.767	0.885	0.712	0.799	0.641	0.748	0.773	0.647	0.779
8	0.909	0.799	0.776	0.793	0.770	0.889	0.767	0.885	0.712	0.799	0.652	0.741	0.773	0.647	0.779
9	0.909	0.799	0.776	0.793	0.770	0.889	0.767	0.885	0.712	0.799	0.669	0.734	0.773	0.647	0.780
10	0.908	0.795	0.783	0.784	0.774	0.900	0.761	0.901	0.735	0.781	0.702	0.779	0.801	0.672	0.791
11	0.908	0.795	0.783	0.784	0.774	0.900	0.761	0.901	0.735	0.781	0.720	0.771	0.801	0.672	0.792
12	0.908	0.795	0.783	0.784	0.774	0.900	0.761	0.901	0.735	0.781	0.738	0.764	0.801	0.672	0.793
13	0.909	0.798	0.776	0.792	0.770	0.892	0.768	0.886	0.715	0.798	0.652	0.748	0.776	0.649	0.781
14	0.909	0.798	0.776	0.792	0.770	0.892	0.768	0.886	0.715	0.798	0.662	0.742	0.776	0.649	0.781
15	0.909	0.798	0.776	0.792	0.770	0.892	0.768	0.886	0.715	0.798	0.680	0.737	0.776	0.649	0.782
16	0.909	0.799	0.776	0.794	0.769	0.888	0.767	0.884	0.710	0.801	0.635	0.749	0.772	0.646	0.779
17	0.909	0.799	0.776	0.794	0.769	0.888	0.767	0.884	0.710	0.801	0.646	0.741	0.772	0.646	0.779
18	0.909	0.799	0.776	0.794	0.769	0.888	0.767	0.884	0.710	0.801	0.663	0.734	0.772	0.646	0.779
19	0.908	0.796	0.782	0.784	0.772	0.898	0.764	0.899	0.728	0.782	0.702	0.778	0.797	0.666	0.790
20	0.908	0.796	0.782	0.784	0.772	0.898	0.764	0.899	0.728	0.782	0.716	0.770	0.797	0.666	0.790
21	0.908	0.796	0.782	0.784	0.772	0.898	0.764	0.899	0.728	0.782	0.734	0.765	0.797	0.666	0.791
22	0.909	0.799	0.776	0.793	0.770	0.890	0.767	0.885	0.713	0.799	0.644	0.748	0.774	0.647	0.780
23	0.909	0.799	0.776	0.793	0.770	0.890	0.767	0.885	0.713	0.799	0.654	0.741	0.774	0.647	0.780
24	0.909	0.799	0.776	0.793	0.770	0.890	0.767	0.885	0.713	0.799	0.672	0.735	0.774	0.647	0.781
25	0.909	0.799	0.776	0.794	0.769	0.886	0.766	0.883	0.708	0.802	0.632	0.750	0.771	0.645	0.778
26	0.909	0.799	0.776	0.794	0.769	0.886	0.766	0.883	0.708	0.802	0.643	0.742	0.771	0.645	0.778
27	0.909	0.799	0.776	0.794	0.769	0.886	0.766	0.883	0.708	0.802	0.660	0.734	0.771	0.645	0.779

Table 6-8. T1 DOE results

RUN	PMHS_A_ Foot_Az	PMHS_A_ Tibia_Ax	PMHS_A_ Tibia_Az	PMHS_A_ Femur_Ax	PMHS_A_ Pelvis_Ax	PMHS_A_ Pelvis_Az	PMHS_A_ T12_Ax	PMHS_A_ T12_Az	PMHS_A_ T8_Ax	PMHS_A_ T8_Az	PMHS_A_ T5_Ax	PMHS_A_ T5_Az	PMHS_A_ T1_Ax	PMHS_A_ T1_Az	CORA TOTAL
1	0.907	0.794	0.786	0.784	0.775	0.900	0.756	0.903	0.742	0.785	0.683	0.786	0.738	0.671	0.786
2	0.907	0.794	0.786	0.784	0.775	0.900	0.756	0.903	0.742	0.785	0.683	0.786	0.803	0.683	0.792
3	0.907	0.794	0.786	0.784	0.775	0.900	0.756	0.903	0.742	0.785	0.683	0.786	0.862	0.705	0.798
4	0.907	0.794	0.786	0.784	0.776	0.898	0.760	0.903	0.742	0.783	0.687	0.778	0.734	0.667	0.786
5	0.907	0.794	0.786	0.784	0.776	0.898	0.760	0.903	0.742	0.783	0.687	0.778	0.797	0.680	0.791
6	0.907	0.794	0.786	0.784	0.776	0.898	0.760	0.903	0.742	0.783	0.687	0.778	0.863	0.701	0.797
7	0.907	0.794	0.786	0.784	0.776	0.898	0.760	0.903	0.742	0.783	0.687	0.777	0.733	0.667	0.786
8	0.907	0.794	0.786	0.784	0.776	0.898	0.760	0.903	0.742	0.783	0.687	0.777	0.797	0.679	0.791
9	0.907	0.794	0.786	0.784	0.776	0.898	0.760	0.903	0.742	0.783	0.687	0.777	0.863	0.701	0.797
10	0.907	0.794	0.786	0.784	0.775	0.899	0.757	0.903	0.742	0.784	0.684	0.784	0.737	0.670	0.786
11	0.907	0.794	0.786	0.784	0.775	0.899	0.757	0.903	0.742	0.784	0.684	0.784	0.802	0.682	0.792
12	0.907	0.794	0.786	0.784	0.775	0.899	0.757	0.903	0.742	0.784	0.684	0.784	0.862	0.704	0.798
13	0.907	0.794	0.786	0.784	0.776	0.898	0.760	0.903	0.742	0.783	0.687	0.777	0.733	0.667	0.786
14	0.907	0.794	0.786	0.784	0.776	0.898	0.760	0.903	0.742	0.783	0.687	0.777	0.797	0.679	0.791
15	0.907	0.794	0.786	0.784	0.776	0.898	0.760	0.903	0.742	0.783	0.687	0.777	0.863	0.701	0.797
16	0.907	0.794	0.786	0.784	0.776	0.898	0.760	0.903	0.742	0.783	0.687	0.777	0.733	0.667	0.786
17	0.907	0.794	0.786	0.784	0.776	0.898	0.760	0.903	0.742	0.783	0.687	0.777	0.797	0.679	0.791
18	0.907	0.794	0.786	0.784	0.776	0.898	0.760	0.903	0.742	0.783	0.687	0.777	0.863	0.701	0.797
19	0.907	0.794	0.786	0.784	0.776	0.899	0.758	0.903	0.742	0.784	0.684	0.782	0.736	0.669	0.786
20	0.907	0.794	0.786	0.784	0.776	0.899	0.758	0.903	0.742	0.784	0.684	0.782	0.800	0.681	0.791
21	0.907	0.794	0.786	0.784	0.776	0.899	0.758	0.903	0.742	0.784	0.684	0.782	0.863	0.703	0.798
22	0.907	0.794	0.786	0.784	0.776	0.898	0.760	0.903	0.742	0.783	0.687	0.777	0.733	0.667	0.786
23	0.907	0.794	0.786	0.784	0.776	0.898	0.760	0.903	0.742	0.783	0.687	0.777	0.797	0.679	0.791
24	0.907	0.794	0.786	0.784	0.776	0.898	0.760	0.903	0.742	0.783	0.687	0.777	0.863	0.701	0.797
25	0.907	0.794	0.786	0.784	0.777	0.898	0.760	0.903	0.742	0.783	0.687	0.777	0.733	0.666	0.786
26	0.907	0.794	0.786	0.784	0.777	0.898	0.760	0.903	0.742	0.783	0.687	0.777	0.797	0.679	0.791
27	0.907	0.794	0.786	0.784	0.777	0.898	0.760	0.903	0.742	0.783	0.687	0.777	0.863	0.701	0.797

Table 6-9. Final PMHS Condition A CORA score

Foot_Az	Tibia_Ax	Tibia_Az	Femur_Ax	Pelvis_Ax	Pelvis_Az	T12_Ax	T12_Az	T8_Ax	T8_Az	T5_Ax	T5_Az	T1_Ax	T1_Az	CORA TOTAL
0.907	0.794	0.786	0.784	0.775	0.900	0.756	0.903	0.742	0.785	0.683	0.786	0.862	0.705	**0.798**

The composite CORA score comprises an average of the corridor and correlation score. As shown in Table 6-10, the Correlation score, which factors in size, shape, and phase, is overall higher than that of the corridor. In this condition, the Correlation score is 8% higher than the Corridor score.

Table 6-10. Final PMHS Condition A CORA score with corridor and correlation scores

4 m/s	Corridor	Correlation		Overall CORA
Foot_Az	0.932	0.883		0.907
Tibia_Ax	0.636	0.953		0.794
Tibia_Az	0.668	0.904		0.786
Femur_Ax	0.660	0.907		0.784
Pelvis_Ax	0.885	0.665		0.775
Pelvis_Az	0.846	0.953		0.900
T12_Ax	0.688	0.825		0.756
T12_Az	0.899	0.907		0.903
T8_Ax	0.698	0.787		0.742
T8_Az	0.814	0.756		0.785
T5_Ax	0.621	0.744		0.683
T5_Az	0.763	0.810		0.786
T1_Ax	0.832	0.892		0.862
T1_Az	0.646	0.763		0.705
CORA TOTAL	**0.756**	**0.839**		**0.798**

The final overlays of the validated model are shown in Figure 6-11 through Figure 6-24, where the thick black line is the average PMHS response from the Condition A testing at UVA, the thin grey lines are the one standard deviation curves, and the green line is the MADYMO model response.

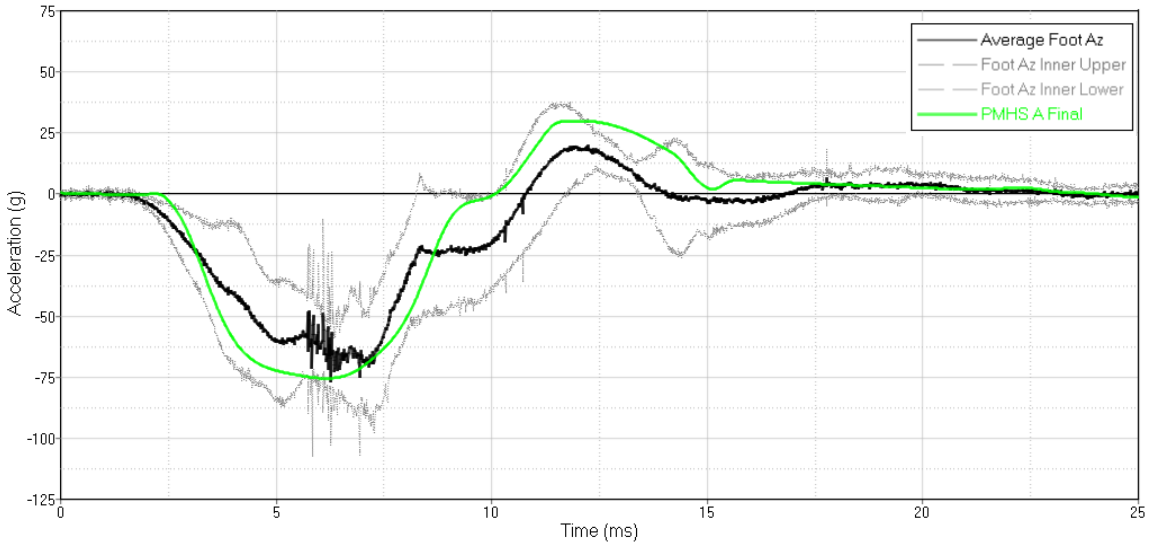

Figure 6-11. Foot Az comparing actual PMHS (black with grey inner corridor) against the MADYMO simulation (green)

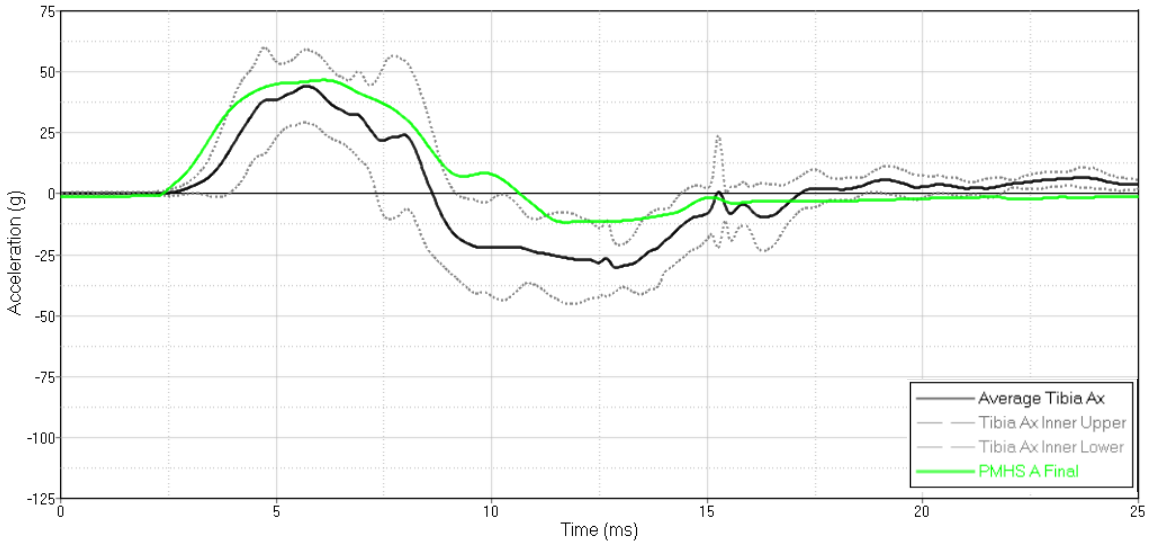

Figure 6-12. Tibia Ax comparing actual PMHS (black with grey inner corridor) against the MADYMO simulation (green)

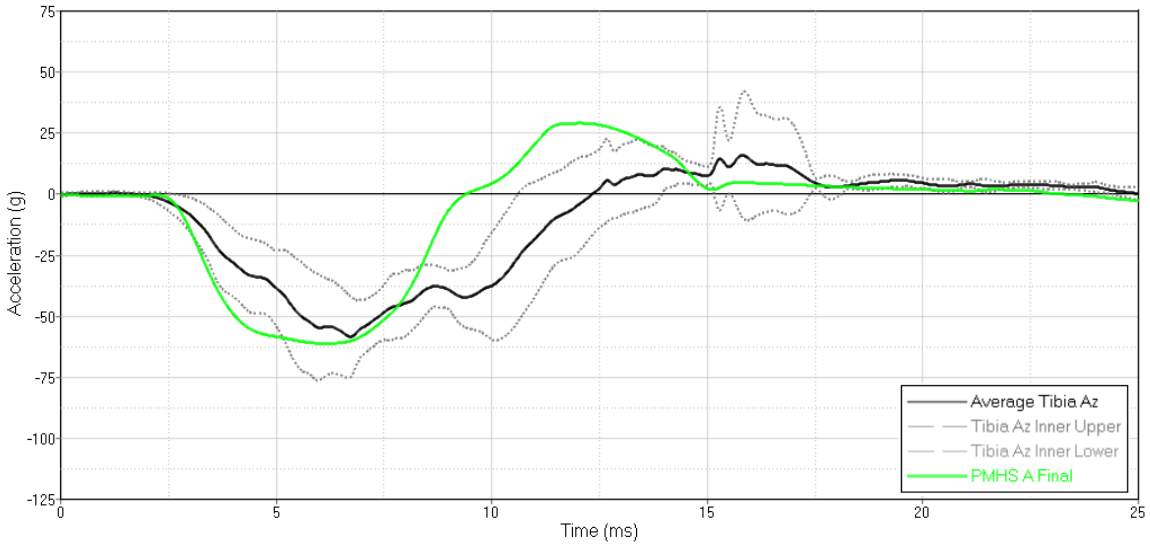

Figure 6-13. Tibia Az comparing actual PMHS (black with grey inner corridor) against the MADYMO simulation (green)

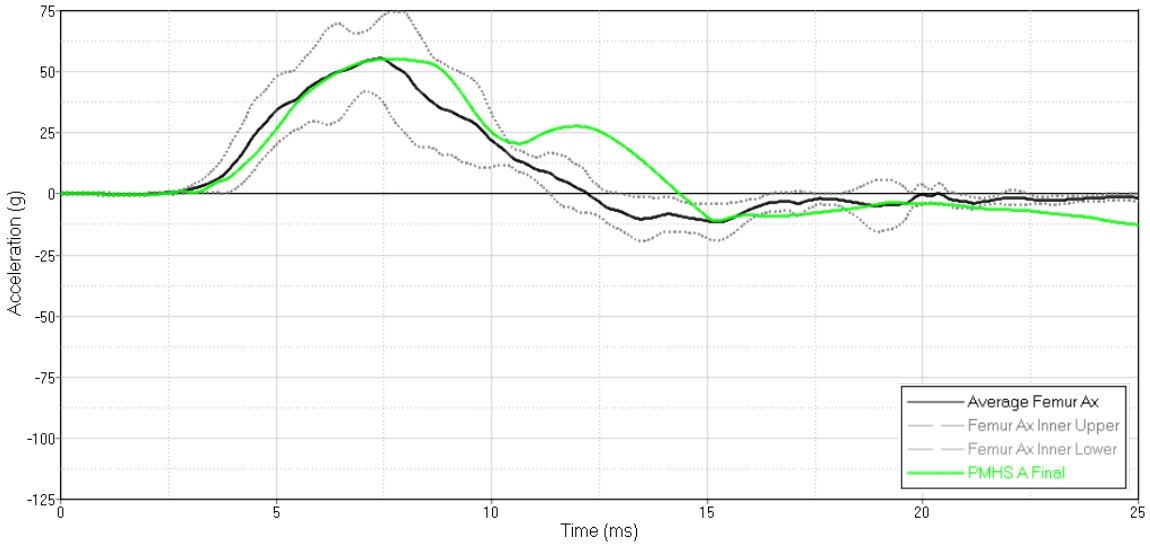

Figure 6-14. Femur Ax comparing actual PMHS (black with grey inner corridor) against the MADYMO simulation (green)

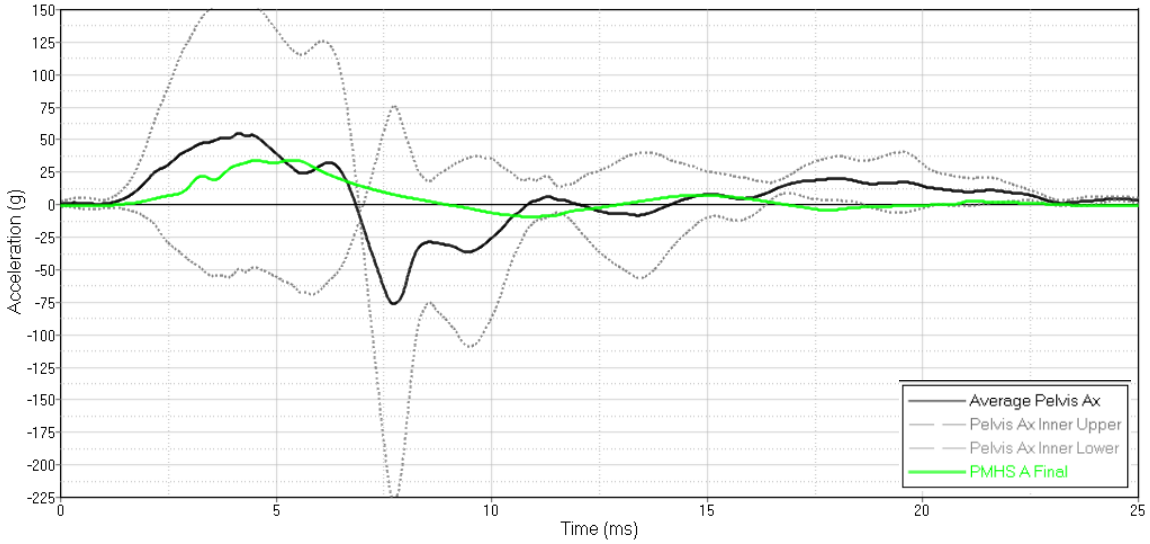

Figure 6-15. Pelvis Ax comparing actual PMHS (black with grey inner corridor) against the MADYMO simulation (green)

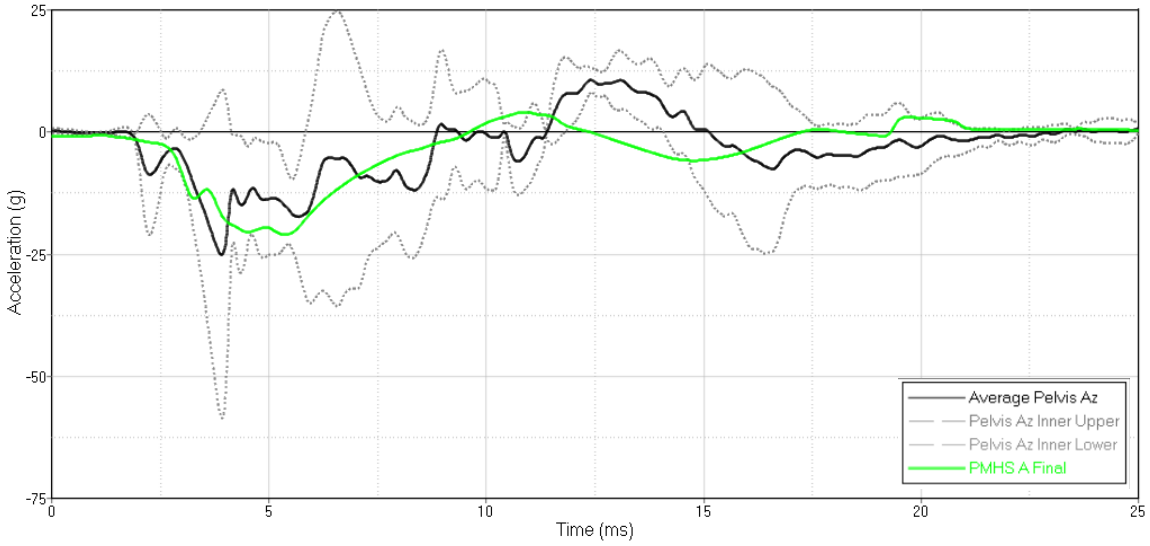

Figure 6-16. Pelvis Az comparing actual PMHS (black with grey inner corridor) against the MADYMO simulation (green)

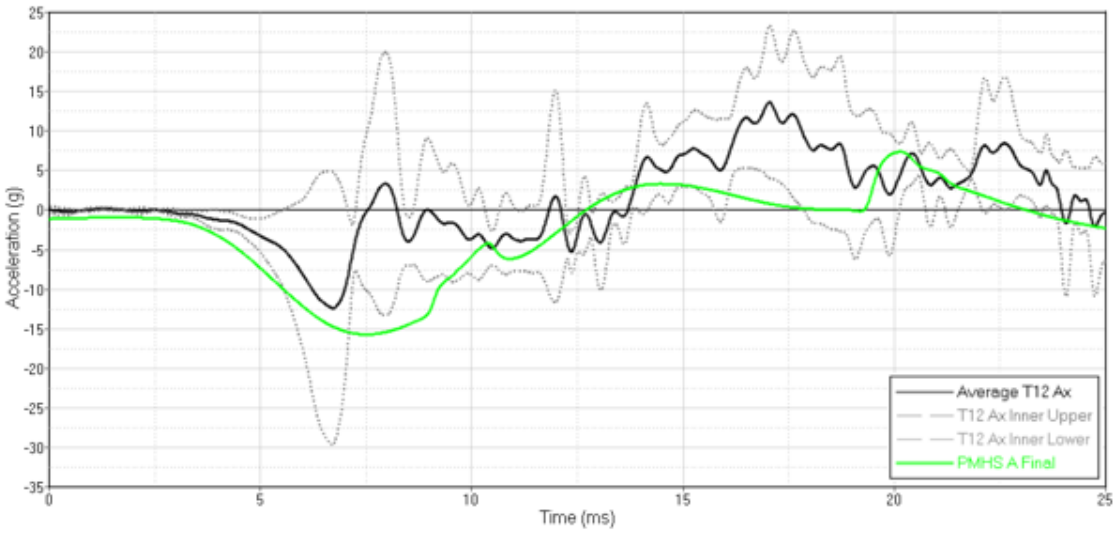

Figure 6-17. T12 Ax comparing actual PMHS (black with grey inner corridor) against the MADYMO simulation (green)

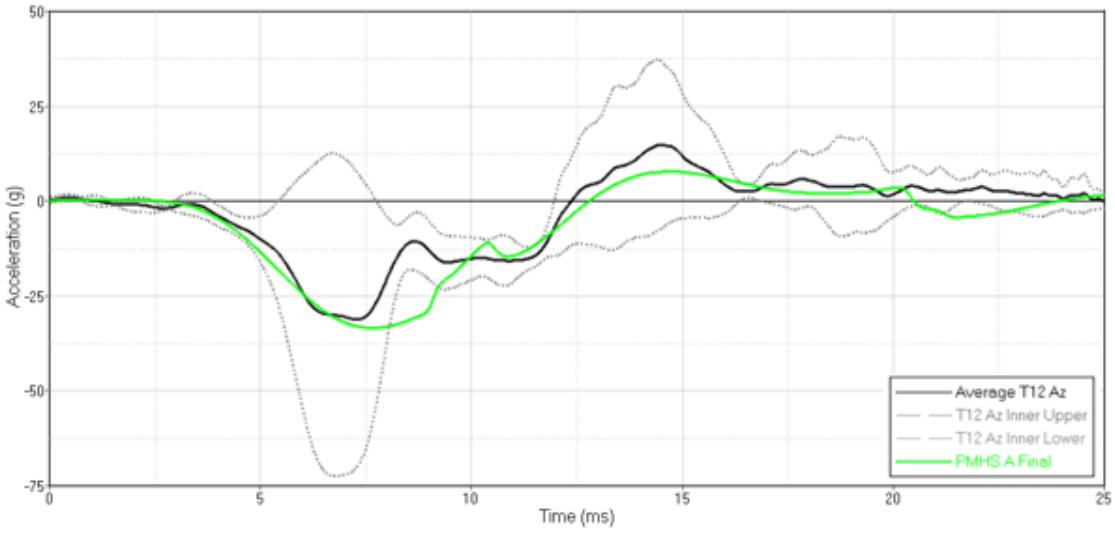

Figure 6-18. T12 Az comparing actual PMHS (black with grey inner corridor) against the MADYMO simulation (green)

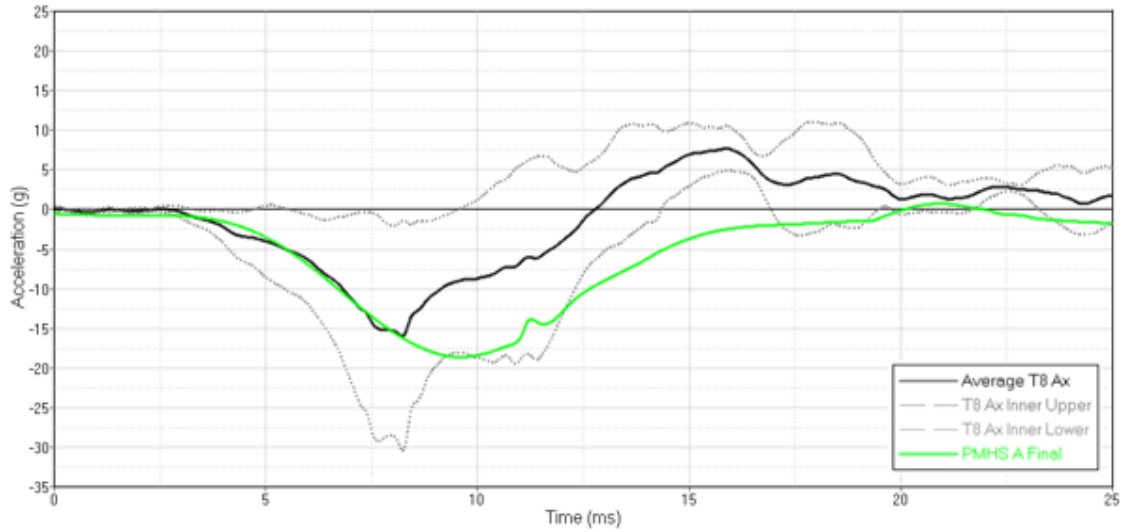

Figure 6-19. T8 Ax comparing actual PMHS (black with grey inner corridor) against the MADYMO simulation (green)

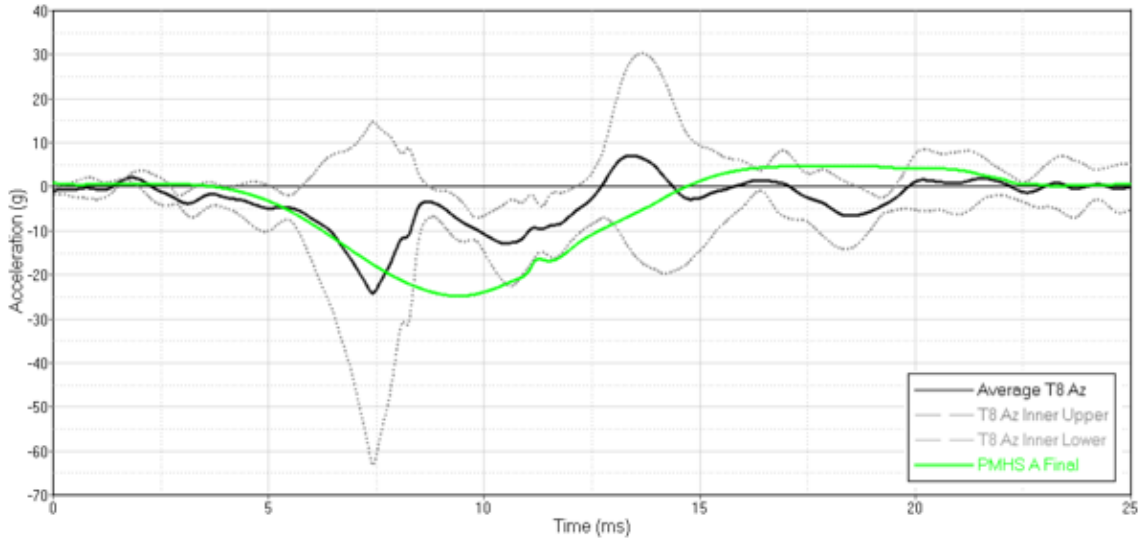

Figure 6-20. T8 Az comparing actual PMHS (black with grey inner corridor) against the MADYMO simulation (green)

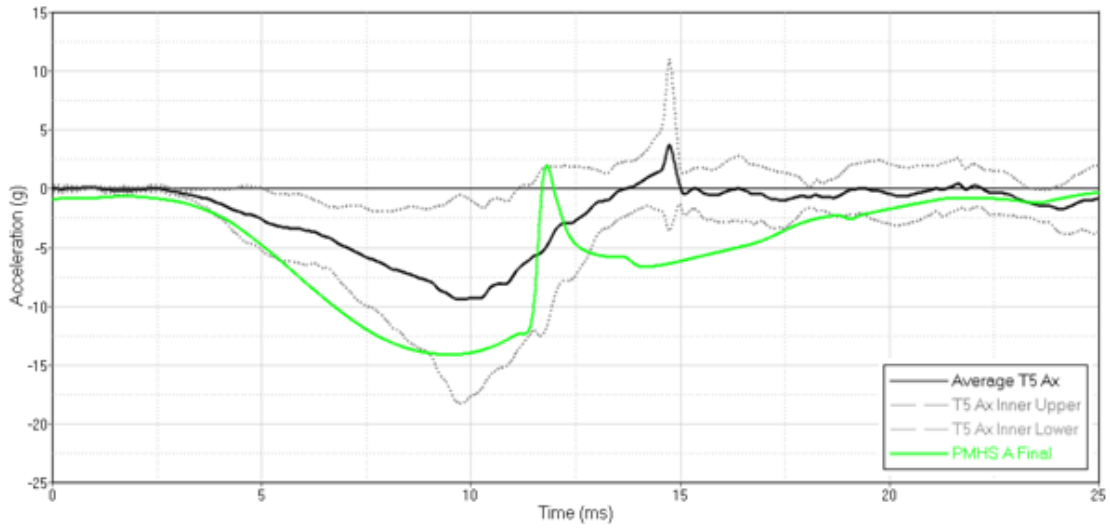

Figure 6-21. T5 Ax comparing actual PMHS (black with grey inner corridor) against the MADYMO simulation (green)

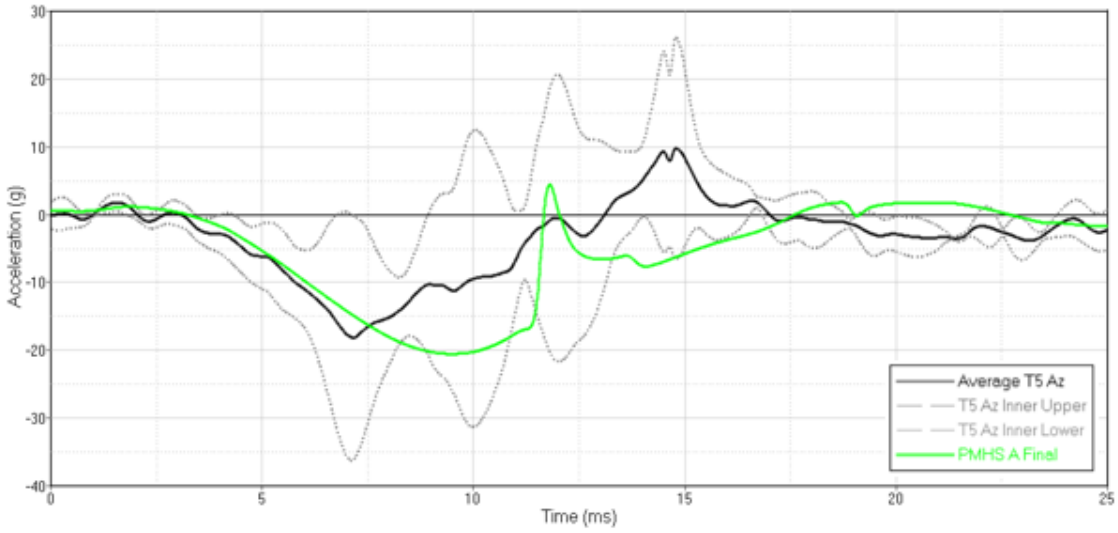

Figure 6-22. T5 Az comparing actual PMHS (black with grey inner corridor) against the MADYMO simulation (green)

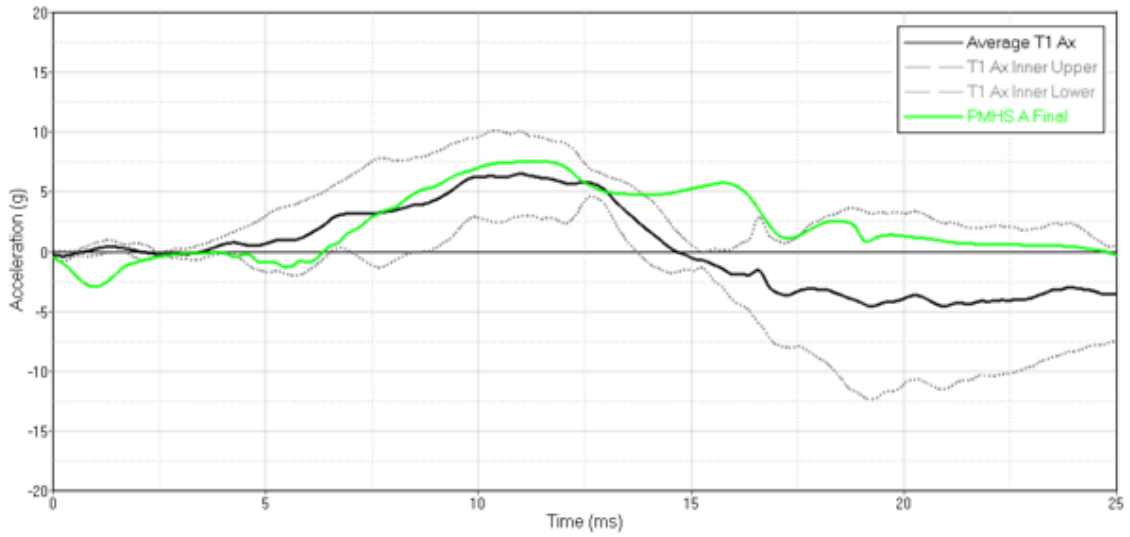

Figure 6-23. T1 Ax comparing actual PMHS (black with grey inner corridor) against the MADYMO simulation (green)

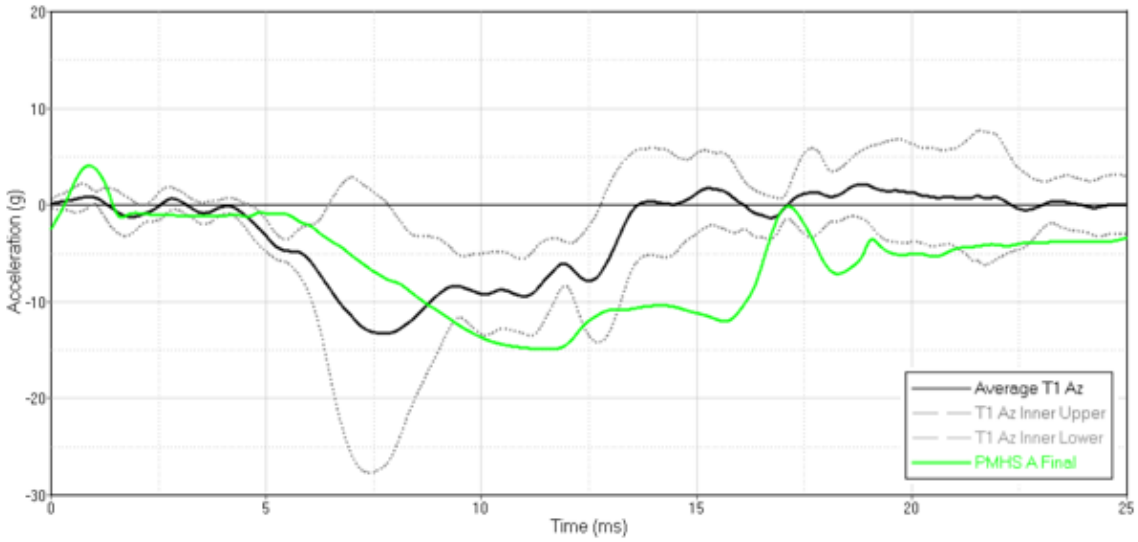

Figure 6-24. T1 Az comparing actual PMHS (black with grey inner corridor) against the MADYMO simulation (green)

The final CORA output file is attached in Appendix B. The HBM was considered validated for the Condition A output.

6.3. Specific Aim 2a – PMHS Rigid Seat Validation – Condition A – Limitations

Validation of the HBM included some limitations that prevented a higher level of correlation. The main issue with the HBM is that the model was encrypted, which prevented any changes to the characteristics of the joints or material properties inside the body, which limited the user's ability to fine-tune performance to exterior influences like contact forces and external restraints. The mass recruitment effect noted in literature may not be present in this model due to the use of the external Kelvin restraints in the spine.

6.4. Specific Aim 2b – PMHS Rigid Seat Validation – Condition B – Model Conditions

To validate the model at a higher blast condition, the seat and floor accelerations were replaced with those from the testing conducted by Bailey et al [6] on the UVA sled from a test series designed to investigate high velocity underbody blast injuries. General model conditions remained the same, including accelerometer locations (Table 6-11), the five-point restraint system, and HBM muscle activation set to off. Accelerometers were not present in the PMHS at T12, T8, or T5, but they were monitored for loading patterns. The instrumentation from Bailey's work is shown in Figure 6-25. Runs 1.1, 1.2, and 1.10 were utilized, as they all had similar loading conditions as listed in Table 6-12.

The target was to achieve at least a rating of Good for each channel using the CORA scoring methodology previously described.

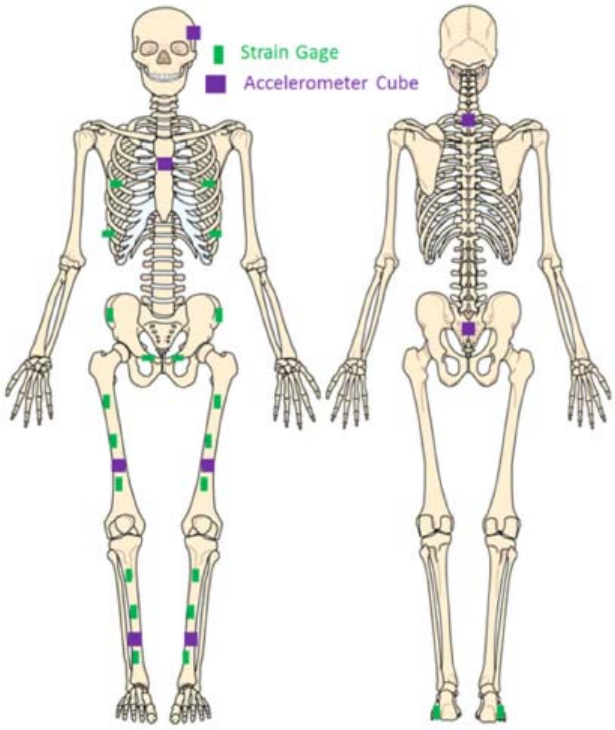

Fig. 3 Diagram of PMHS instrumentation locations

Figure 6-25. PMHS Instrumentation includes accelerometers at T12 and S1 [6]

Table 6-11. Validation channels used for human body model

PMHS and Rig Channels – Legs	PMHS and Rig Channels – Upper Body
Foot Az	Pelvis Ax
Distal Tibia Ax	Pelvis Az
Distal Tibia Az	T1 Ax
Distal Femur Ax	T1 Az

Table 6-12. Floor and seat accelerations and velocities for Condition B

Test ID	Peak floor velocity (m/s) in (ms)	Peak seat velocity (m/s) in (ms)	Peak floor acceleration (g) in (ms)	Peak seat acceleration (g) in (ms)
1.1	10.5 in 4.1	10.2 in 4.8	615 in 1.1	738 in 3.0
1.2	10.3 in 4.5	10.2 in 4.8	585 in 1.3	735 in 3.0
1.10	10.4 in 5.2	9.7 in 7.5	472 in 1.4	241 in 4.0

The HBM was positioned to replicate the positioning of the PMHS in the videos provided by UVA and then adjusted as needed to match kinetics and measured accelerations (Figure 6-26). A block below the heels and head support were added based on the original test setup description and video review [6]. The rotation of the accelerometers was tuned around the y-axis to balance the distribution of acceleration between the x- and z-axes, which was slightly different than that of the HBM in Condition A, as these test series were completed at different times. The accelerometer tuning was conducted by varying the angle of rotation about the y-axis and evaluating the resulting x- and z-accelerations for pulse matching and CORA score.

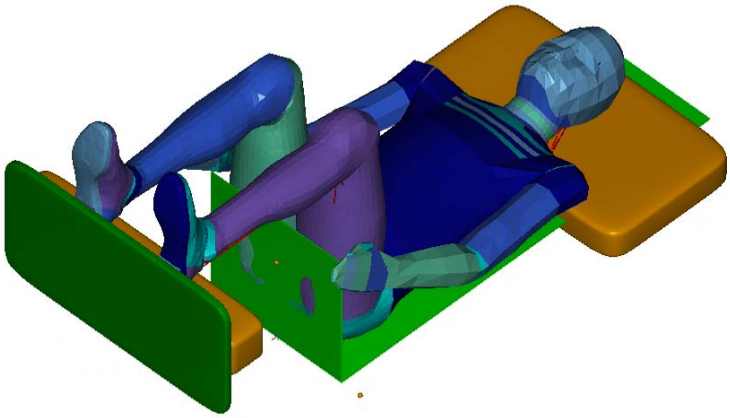

Figure 6-26. HBM in test position for Condition B with additional foot and head supports (orange) based on the original test setup.

As with Condition A, external contact properties were altered between the floor and feet to represent the boots and between the seat and pelvis to tune the upper body response. The boot contact properties were the same as those used for Condition A, but scaled using separate constant multiplying factors along the force and deflection axes as needed to match the actual lower leg response (Figure 6-3). This tuning was required due to the rate dependency of the boot. The contact properties for the pelvis (Figure 6-4)

were also scaled in the same manner as those of the boot as needed to match the high input response.

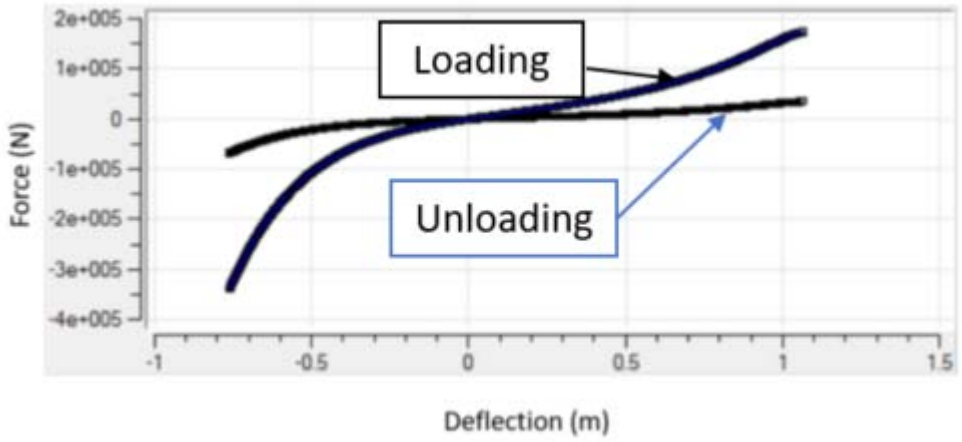

Figure 6-27. Force (N) deflection (m) properties from MADYMO for boot/floor contact

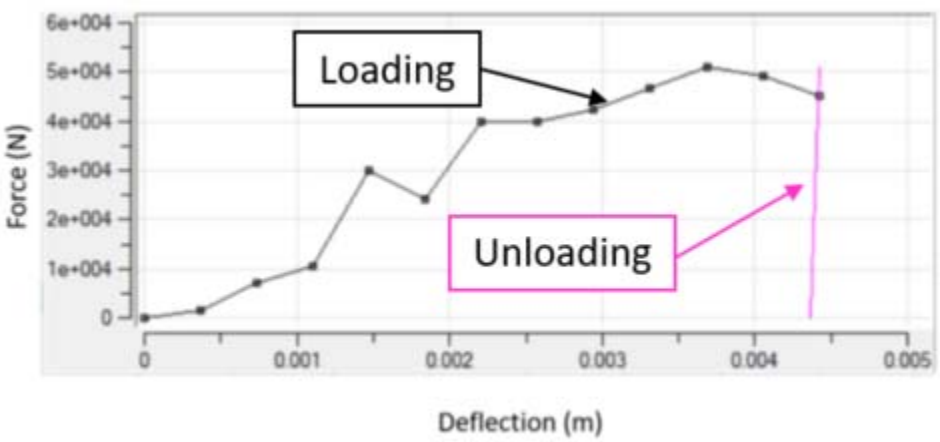

Figure 6-28. Force (N) deflection (m) properties from MADYMO for pelvis/seat contact

Since the PMHS in this test series did not have multiple accelerometers throughout the thoracic spine, the performance could not be monitored at T12, T8, and T5. In Condition A, external Kelvin restraints were added at each of the monitored vertebrae as previously described, and these four Kelvin restraints were individually and separately scaled to improve phasing and peak values at T12, T8, T5, and T1. Due to the absence of data for comparison, Kelvin restraints with the same properties were applied to each

lumbar and thoracic vertebrae and tuned to optimize response at T1 as shown in Figure 6-29 for the Condition B model. These individual restraints were added between successive vertebra from L5 up to T1 (L5 to L4, L4 to L3, etc). The force/deflection base data is the same as that used in Condition A, and the x-scale, y-scale, and loading offset were adjusted as required to improve correlation. The final scaled force and deflection loading and unloading curve was applied to every connection, and the coordinates of these curves are listed in Table 6-13. All restraints used active damping with the MADYMO default setting, and initial strain was 0.0. The resultant acceleration at T12, T8, T5, and T1 showed a logical progression of accelerative loading, with a delay in loading as expected moving superiorly in the spine.

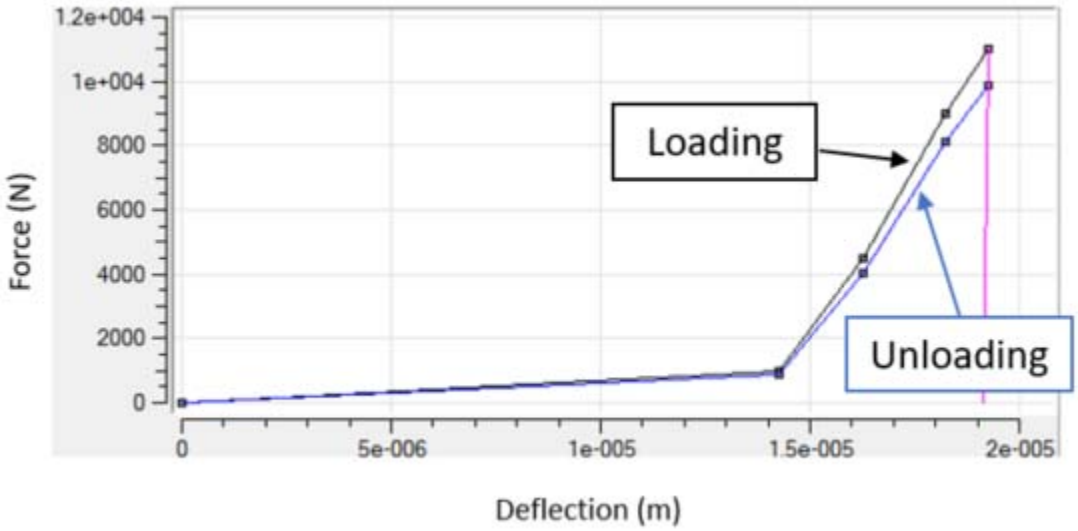

Figure 6-29. Final scaled force (N) deflection (m) properties from MADYMO for spinal restraints applied to each spinal segment

Table 6-13. Coordinates of loading and unloading curves for spinal Kelvin restraints for Condition B model

Loading Curve		Unloading Curve	
Displacement (m)	**Force (N)**	**Displacement (m)**	**Force (N)**
0.000000	0	0.000000	0
0.000014	1000	0.000014	900
0.000016	4500	0.000016	4050
0.000018	9000	0.000018	8100
0.000019	11000	0.000019	9900

The HBM was developed for longitudinal and lateral loading, so some issues were encountered with the introduction of the extreme vertical loading, including the onset of loading for the spine as described above, the need for additional contact properties between the pelvis and seat to represent the stiffness of the flesh under high rate vertical loading, as well as boundary issues at the interface between the foot and ankle and between the tibia and femur. Initially, the model showed a local collapse of the joints at the foot/ankle and tibia/femur, where the solid bodies contacted and moved through each other, which was an unrealistic contact condition. Based on discussions with TASS, it was suggested that external restraints (Kelvin and Point) be added to provide resistance to the loading, which prevented the unrealistic contact. TASS provided the initial loading profiles (Figure 6-30 and Figure 6-31), which were then scaled as needed to improve correlation using separate constant multiplying factors for the force and displacement. The Kelvin restraints for the ankle were set to active damping and a 0.0 initial strain, with a 7E10 hysteresis slope with the 3A hysteresis model. A Point restraint was used for the knee joint, using hysteresis model 2 and a slope of 1E8. The Point restraint uses three perpendicular parallel springs and dampers to connect two bodies.

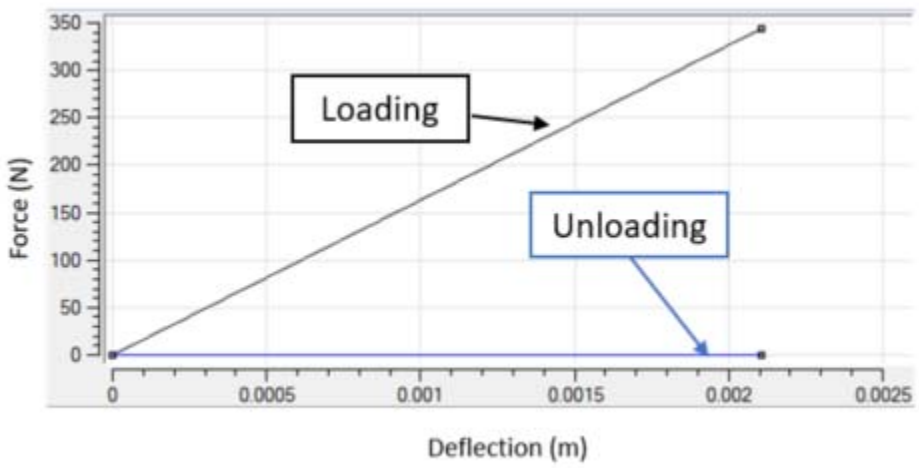

Figure 6-30. Force (N) deflection (m) properties from MADYMO for ankle restraint

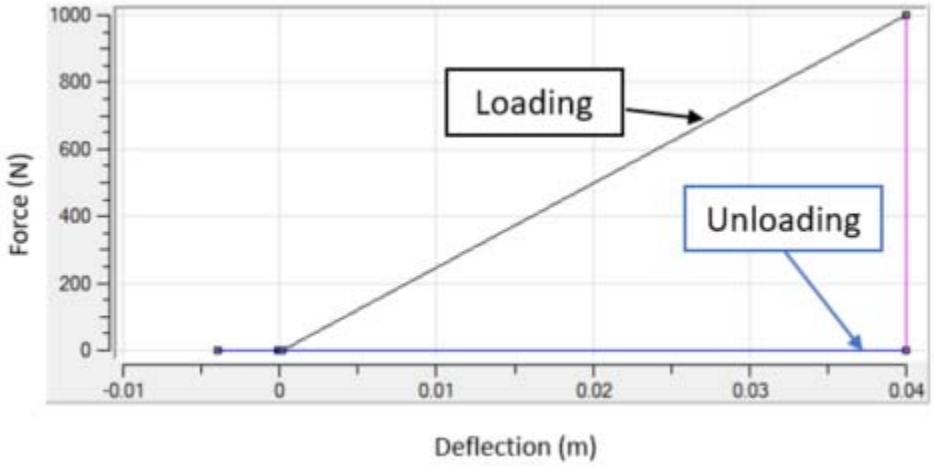

Figure 6-31. Force (N) deflection (m) properties from MADYMO for knee restraint

A log showing the progression of the validation is provided in Appendix C. This log shows the trial and error process of determining the most influential parameters and their associated reasonable ranges that led into the final CORA evaluation DOEs.

6.5. Specific Aim 2b – PMHS Rigid Seat Validation – Condition B – CORA Rating

Three PMHS were tested at UVA as part of the Bailey et al research for Condition B, which were a subset of a larger study with multiple seat and floor accelerative inputs.

Data processing included filtering the data with a CFC 1000 filter in accordance with the SAE-J211 standards (CFC 1000) [6] and aligning the data traces. Biofidelity Response Corridors were created from these three runs, which were scaled to a 50th percentile male using the scaling properties as listed below in Equations (1) through (3) [49]. The scaled data for each channel was averaged to create a reference curve, and then one and two standard deviation curves were developed for the CORA inner and outer corridors. To avoid pinch points where the curves converged, the corridors were set up so that the width was no smaller than 5% of the maximum standard deviation. As with the Condition A data, the CORA 3.6.1 software was used to score the PMHS data. The transformations of the data traces including to the center of the vertebra were not conducted on this data set, but this was deemed to have a limited effect for the T1 correlation, as the accelerometers in the model were rotated about the y-axis to capture the effect of any angularity of the accelerometer in the physical testing.

$$\lambda_m = \frac{m_{50th\ percentile}}{m_{subject}} \tag{1}$$

$$t_{scaled} = \lambda_m^{\frac{1}{3}} t_{subject} \tag{2}$$

$$a_{scaled} = \lambda_m^{-\frac{1}{3}} a_{subject} \tag{3}$$

The parameters with the highest influence on accelerative responses were identified using a series of DOEs with ±25% ranges and then input into modeFRONTIER (2017R5), which is a multidisciplinary design optimization software that can quickly integrate multiple software programs to conduct DOE and optimization. Figure 6-32 shows the schematic of the information flow in modeFRONTIER. The software automates the process to run

multiple MADYMO simulations by allowing the user to select variables from MADYMO to create a DOE to assess the interaction of the various parameters. The software offers several DOE options including full factorial and Uniform Latin Hypercube to evaluate the influence of each parameter. ModeFRONTIER then pulls the acceleration (.lac) file from MADYMO and creates a .dat file using MATLAB for each run. The .dat file, which is a simple text file with all key BRCs, is then passed into the CORA software via a DOS node, and CORA files are produced for each run. Finally, modeFRONTIER provides tables and graphs showing the Overall CORA scores. The modeFRONTIER DOE files are provided in Appendix D.

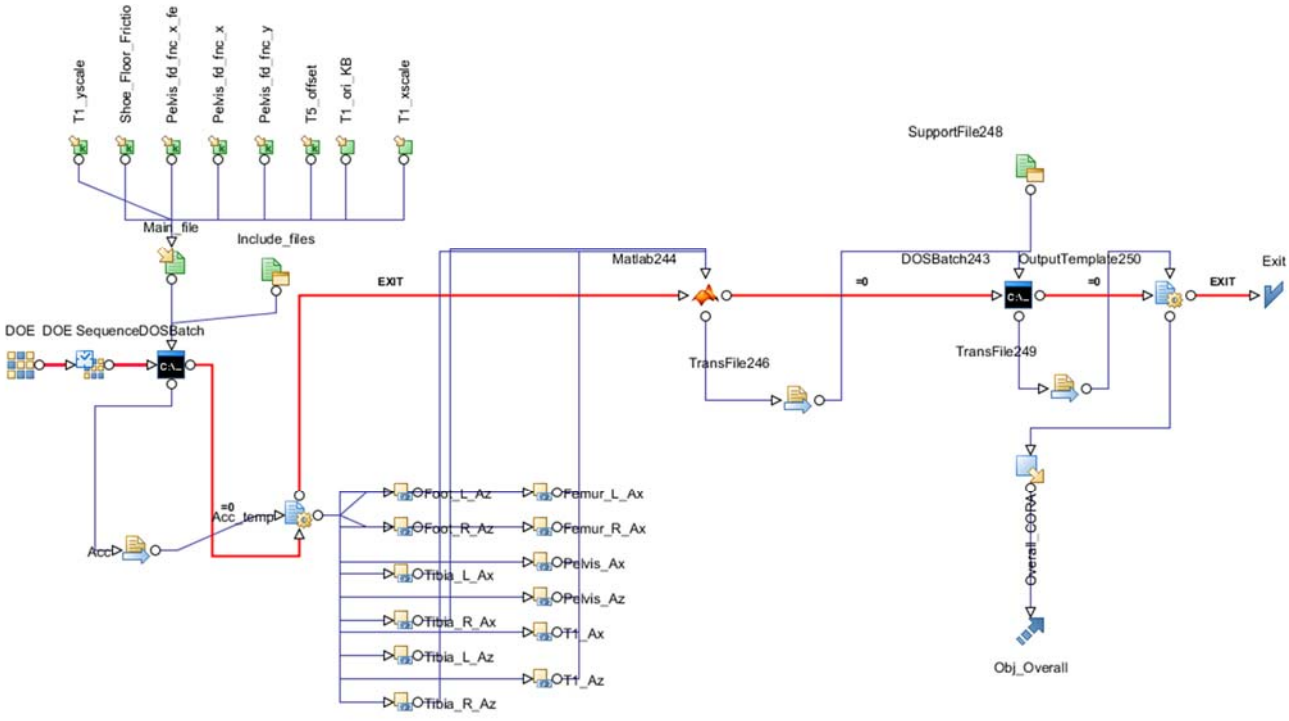

Figure 6-32. modeFRONTIER schematic

For Condition B, the scaling factors for the spinal Kelvin restraints, floor friction, and pelvis contact force were evaluated for their effect on Overall CORA score. A series of three Full Factorials (20-27 runs each) and one Uniform Latin Hypercube (100

randomized runs with seven parameters at 3 levels) were used to determine the best correlation. Although the final simulation selected did not have the highest score, engineering judgement was used to select a configuration with the best match for peak Pelvis Az and T1 Az, which will be used in Specific Aim 3 to optimize the seat parameters to reduce pelvis and spine acceleration. The final CORA scores are shown in Table 6-14, with the Overall CORA score of 0.760. All criteria except T1 Ax are Good or Excellent, as the priority for correlation was T1 Az, and an improvement in Az caused a degradation in Ax. As Table 6-14 shows, the Correlation score (0.845) is almost 17% higher than the Corridor score (0.676). The Corridors in this data set were extremely narrow, especially for T1 Ax, which caused a reduction in overall score. Engineering judgment was used to maximize the Correlation over matching the Corridors. All Correlation scores are in the Good and Excellent category. The CORA score was evaluated over 25 ms to match that of Condition A.

Table 6-14. Final PMHS Condition B CORA score

10 m/s	Corridor	Correlation		Overall CORA
Foot_Az	0.669	0.759		0.714
Tibia_Ax	0.872	0.675		0.773
Tibia_Az	0.949	0.902		0.925
Femur_Ax	0.640	0.897		0.769
Pelvis_Ax	0.619	0.808		0.714
Pelvis_Az	0.706	0.939		0.823
T1_Ax	0.435	0.854		0.644
T1_Az	0.519	0.922		0.720
CORA TOTAL	**0.676**	**0.845**		**0.760**

The final overlays of the validated model are shown in Figure 6-33 through Figure 6-40, where the thick black line is the average PMHS response from the UVA Condition

B testing, the thin grey lines are the one standard deviation curves, and the blue line is the MADYMO model response.

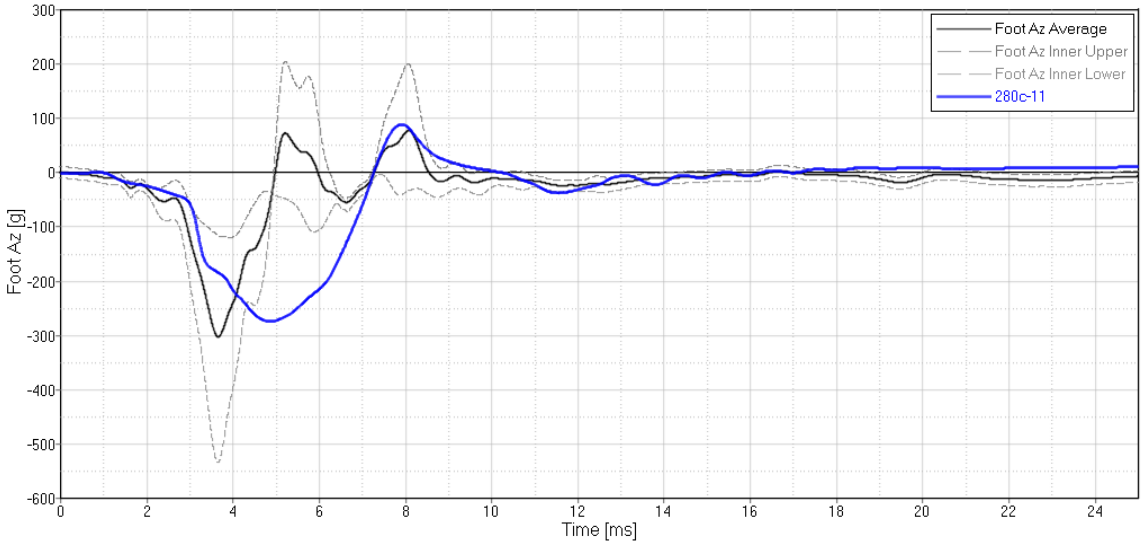

Figure 6-33. Foot Az comparing actual PMHS (black with grey inner corridor) against the MADYMO simulation (blue)

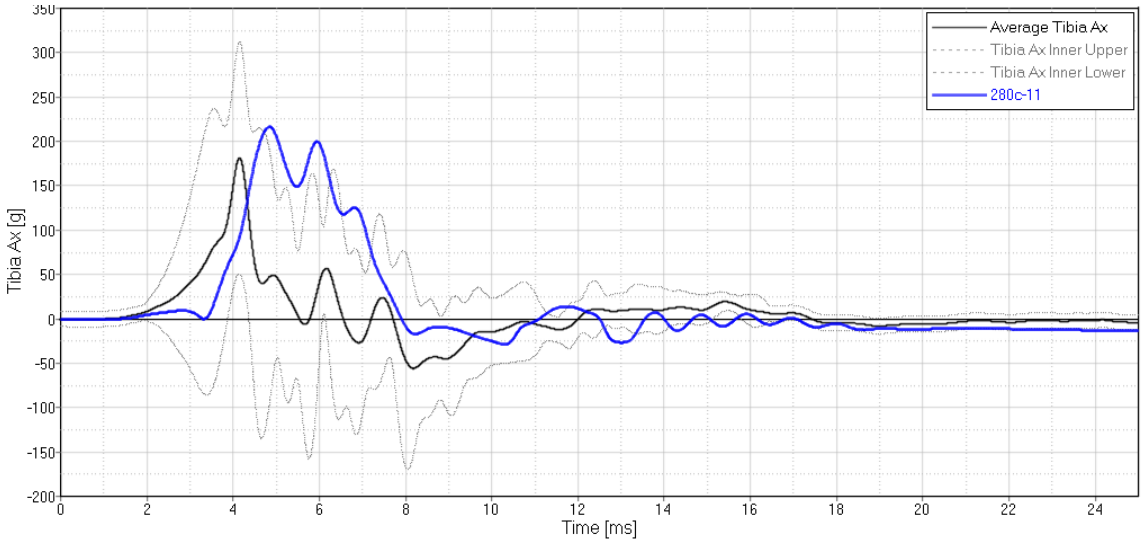

Figure 6-34. Tibia Ax comparing actual PMHS (black with grey inner corridor) against the MADYMO simulation (blue)

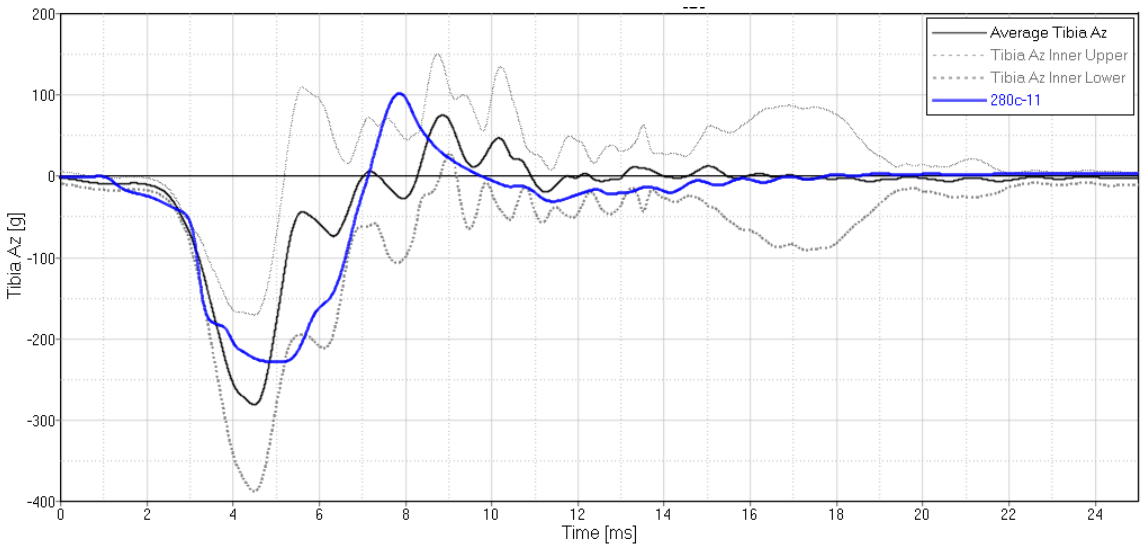

Figure 6-35. Tibia Az comparing actual PMHS (black with grey inner corridor) against the MADYMO simulation (blue)

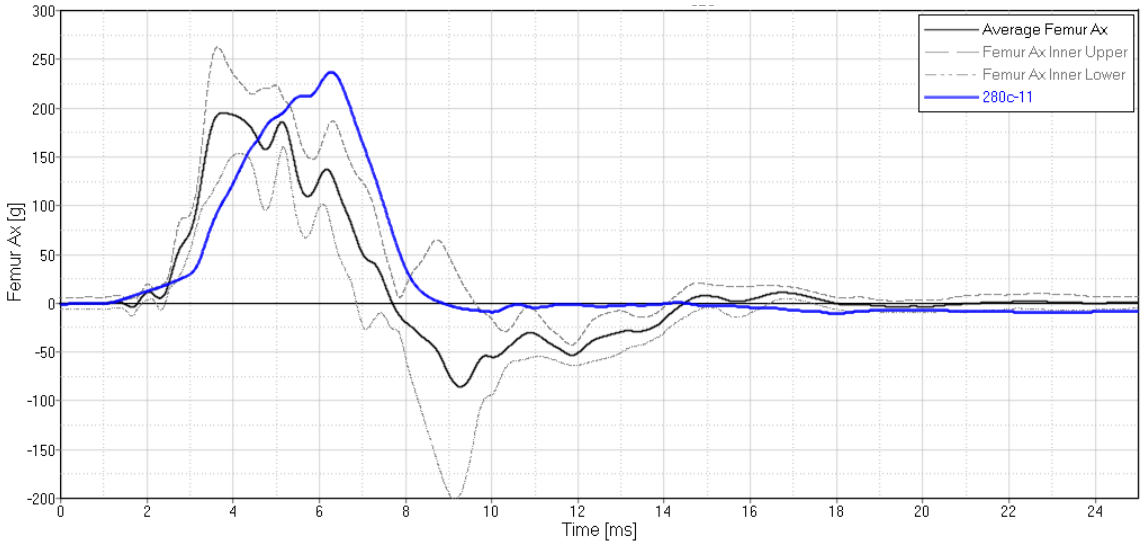

Figure 6-36. Femur Ax comparing actual PMHS (black with grey inner corridor) against the MADYMO simulation (blue)

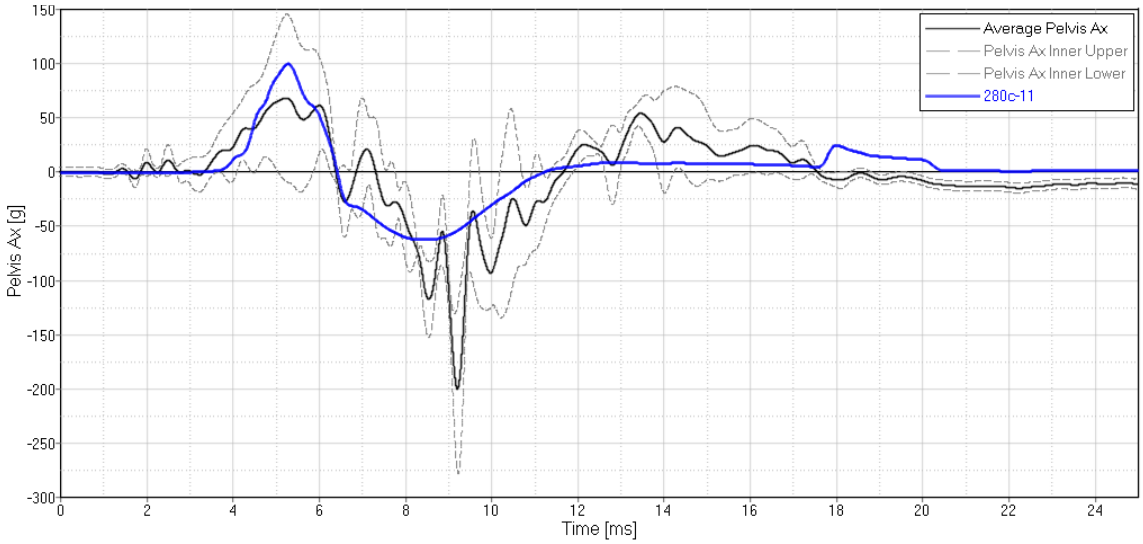

Figure 6-37. Pelvis Ax comparing actual PMHS (black with grey inner corridor) against the MADYMO simulation (blue)

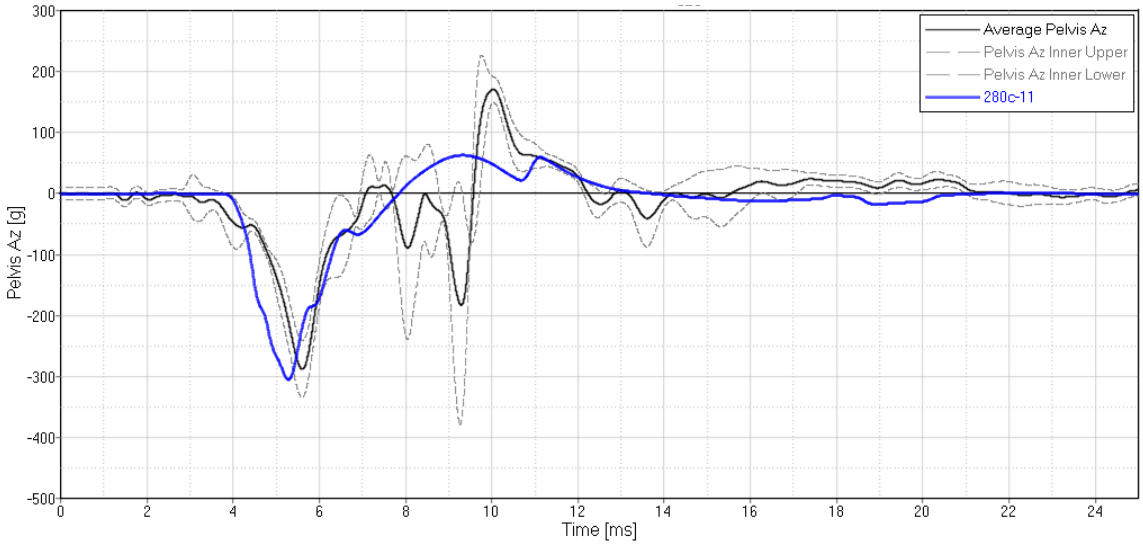

Figure 6-38. Pelvis Az comparing actual PMHS (black with grey inner corridor) against the MADYMO simulation (blue)

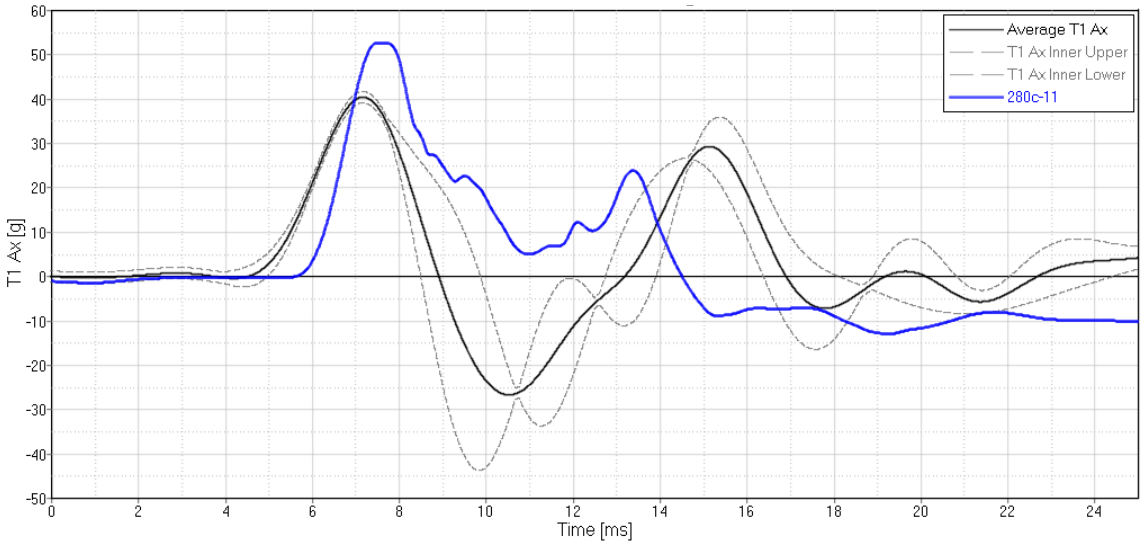

Figure 6-39. T1 Ax comparing actual PMHS (black with grey inner corridor) against the MADYMO simulation (blue)

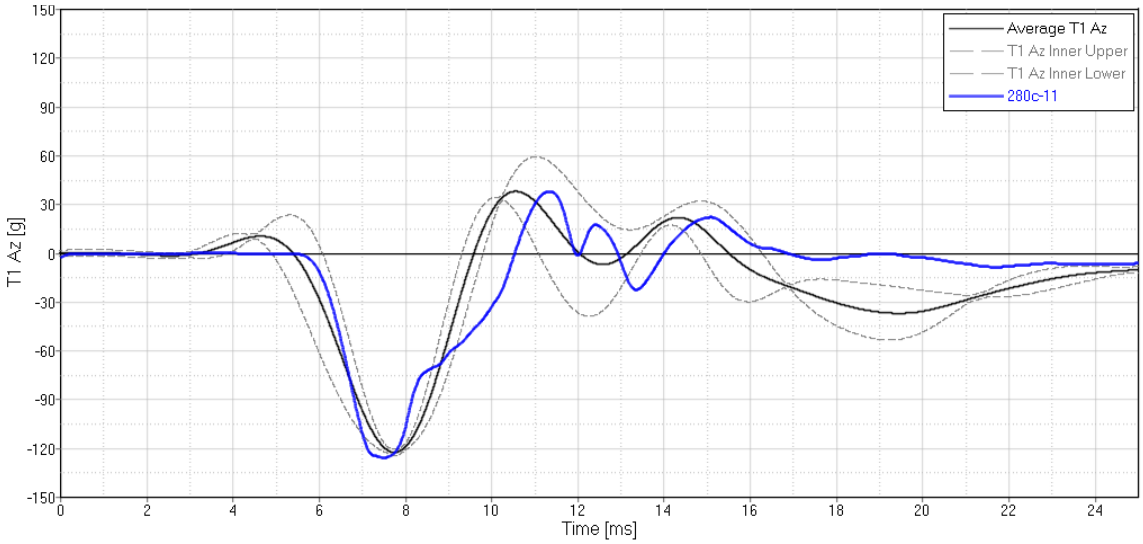

Figure 6-40. T1 Az comparing actual PMHS (black with grey inner corridor) against the MADYMO simulation (blue)

The final CORA output file is attached in Appendix E. The HBM was considered validated for the Condition B output.

6.6. Specific Aim 2b – PMHS Rigid Seat Validation – Condition B – Limitations

Data from the WIAMan program was not available at injurious conditions from UVA in a rigid seat condition without padding at the time of this research, so data from Bailey et al was leveraged [6]. Since the Bailey data was collected several years before the WIAMan program research, the amount of data collected was limited. Only one PMHS had accelerometers on the calcaneus, so the left and right accelerometers were averaged, providing a corridor created from only two curves. The input pulses were slightly different between the three tests, but as the BRCs demonstrate, the slight differences in pulses did not create widely varying PMHS response.

These PMHS also experienced a range of injuries, but overall, the injuries did not appear to have a significant influence on the corridors, as the three different tests provided similar responses. The pelvis fracture in one of the tests, however, resulted in the inability to use the data from test 1.1 for pelvis response. The injuries for this test series are listed in Table 6-15.

Table 6-15. PMHS injury summary table from Bailey et al [6]

PMHS injury summary

Test ID	Lower extremity injuries	Pelvic injuries	Other injuries
1.1	R tibia plafond Fx, L calcaneus Fx, L 4th metatarsal Fx, R 4th metatarsal Fx	Bilateral upper sacral alar Fx, Bilateral medial acetabulum Fx, R superior and inferior pubic ramus Fx, bilateral ischial tuberosity Fx	R clavicle, R scapula, R 5th–7th ribs (*suggestion of mid and upper T-spine anterior compression Fxs)
1.2	None	R sacral alar Fx, saggital Fx in mid to lower sacrum, nondisplaced Fx anterior/medial R. Acetabulum and lateral L. superior pubic ramus/ acetabulum	Bilateral clavicle Fx, compression Fx at T6, possible compression Fx at T5, anterior wedge Fx at C7–T4, R. 3rd rib
1.10	None	Bilateral sacral alar Fx, S2 Fx, nondisplaced bilateral anterior pubic rami Fx	Bilateral L5 transverse process Fx

6.7. Specific Aim 2b – PMHS Rigid Seat Validation – Comparison of Condition A and Condition B Models

Initially, it was thought that the validation for Condition A would yield acceptable results when used with the Condition B loading inputs. Due to the rate dependency of the contact properties of the boots, pelvis, and external spine restraints, the CORA scores for the Condition A model with the Condition B input was 0.57, or Fair. The Condition B model over-predicted peak accelerations with the Condition A model accelerative input. As the MADYMO HBM is encrypted, the internal contact properties within the model could not be directly influenced.

The Condition B model needed to be stiffened at the feet, pelvis, and spine to adequately reflect the increased loading rate at the internal sensors compared to the Condition A model. As previously explained, the Kelvin restraint construction in the spine was different between the two models, as well. Since the Condition A PMHS had accelerometers at T12, T8, T5, and T1, a set of four unique Kelvin restraints (sacrum to T8, sacrum to T5, L5 to T12, and T5 to T1) were used to provide proper phasing and peaks at the recorded vertebrae. For the Condition B model, PMHS data was only available at T1, so the same Kelvin restraint was applied between successive vertebrae between L5 and T1 (L5 to L4, L4 to L3, etc).

External restraints were also necessary between the tibias and the femurs to prevent a local collapse of the joint due to the high rate accelerative input, as well as between the shoe and tibia at the ankle.

As the optimization process results in a non-injurious condition, the Condition A model with the four unique Kelvin restraints, which was validated at a seat velocity

closest to the expected optimized seat velocity, was deemed as the most appropriate validated model choice to minimize force transmission to the occupant in the stroking seat condition.

CHAPTER 7 – SPECIFIC AIM 3 SEAT OPTIMIZATION

7.1. Specific Aim 3 – Seat Optimization Model Setup

After the HBM model was validated in Condition A, the model was altered such that the floor and seat no longer experienced separate blast inputs as in the experimental setup, but were connected with a translational joint. This joint allowed a single floor blast pulse to be input to the seating system through the floor. The Condition B seat acceleration pulse (Figure 4-2) was used for this portion of the study to allow a direct comparison to the rigid seat models. The translational joint was set up with a characteristic function that provided the force-deflection properties that were tuned to reduce pelvis and spine injuries using modeFRONTIER. No EA mechanism or mitigation strategy was present at the interface with the feet; it should be noted that the high accelerative input to the feet may influence the overall acceleration at the pelvis, and the introduction of a blast mat or similar mitigation device may affect the final outcome [12].

It was decided based on industry experience and literature review that a linear force-deflection approach would be most realistic and achievable for adoption by EA seat manufacturers. Most seats employ something similar to a “shear pin” design, where the seat will not begin to stroke by the EA device until a certain loading threshold is reached, which was a key tunable parameter. If the shear pin force is too low, the seat could stroke under normal operating use, which is not preferable. The lower shear pin force range, set as 2 kN to 5 kN, was determined based on review of blast seat patents [13], helicopter seat specifications [20, 57], lumbar spine injury criteria [45], prior experience, and analysis of the sensitivity of the parameters in the optimization process. The total stroke, or upper displacement, was limited to 6 inches (0.1524 m), which is an aggressive limit based on

industry experience and literature research [3, 53], as well as initial optimization analysis to verify that the optimization would produce non-injurious results. The ability of the model to reach a solution with the aggressive 6 inch (0.1524 m) upper joint limit would mean that a larger displacement limit should also reach a non-injurious optimized solution. The lower shear pin activation displacement range was set between 0 and 0.025 m (0 and 1 inch), and the active upper stroke distance was set between 0.0762 and 0.152 m (3 and 6 inches). The maximum allowable load was set between 5 kN and 20 kN based on literature research for loading limits [20] and analysis of the parameter sensitivity. The variables within the loading profile were defined as shown in Table 7-1 and included lower and upper force and deflection limits.

Table 7-1. Force-deflection joint tuning parameters

Parameter Name	Description	Range
Opt_joint_lower	Shear pin force	2 kN – 5 kN
Opt_joint_lower_disp	Shear pin activation displacement	0.0 – 0.0254 m (0 – 1 inch)
Opt_joint_upper	EA device maximum load	5 kN – 20 kN
Opt_joint_upper_disp	EA device maximum displacement	0.0762 – 0.1524 m (3 – 6 inches)

Figure 7-1 shows the full initial loading profile within MADYMO, which includes a high force at the end of the loading profile to represent the bottoming out of the EA device when it reaches full stroke of 6 inches. Figure 7-2 is zoomed in to show the shear pin force and EA maximum force over the allowable displacement limits.

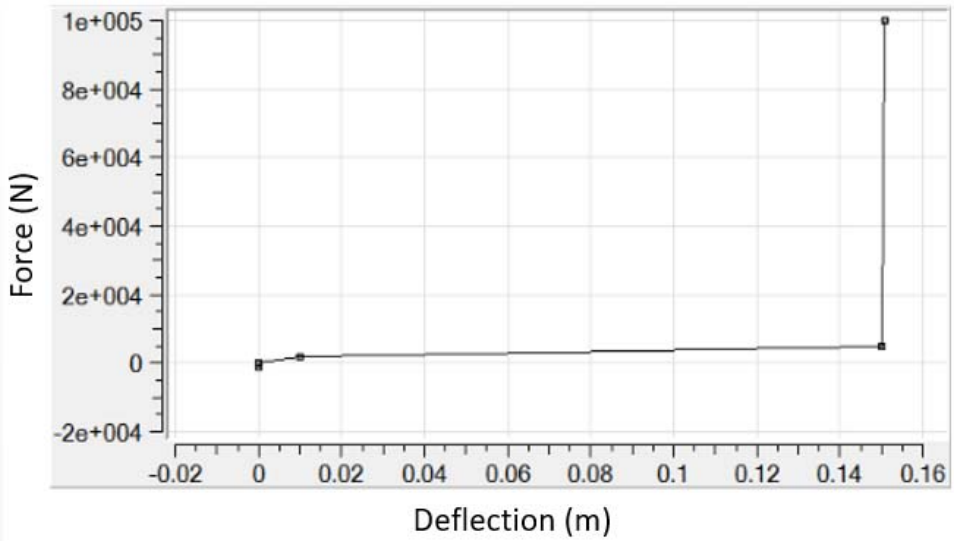

Figure 7-1. Initial profile of force-deflection properties for seat joint optimization

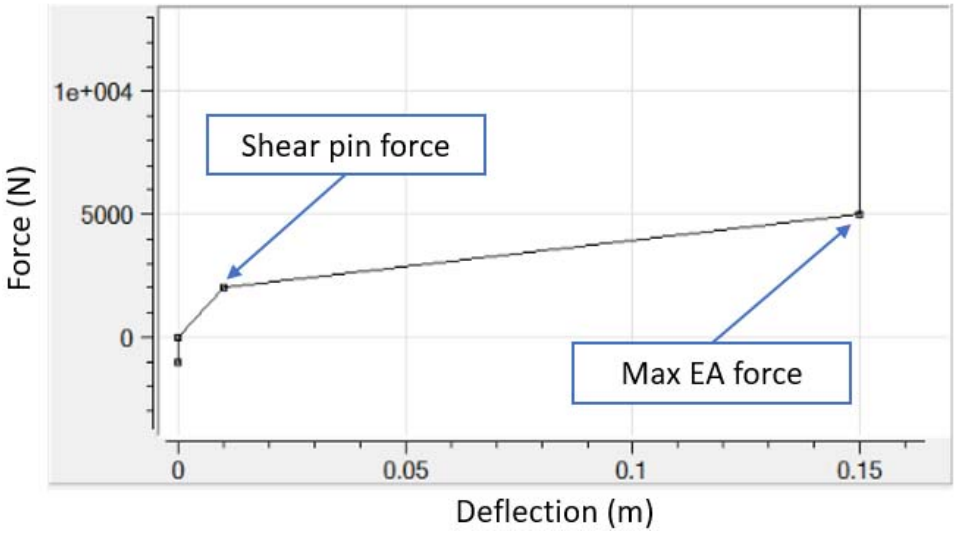

Figure 7-2. Initial profile of force-deflection properties for seat joint optimization – zoomed into loading profile

Once the MADYMO file was updated with the translational joint properties, modeFRONTIER was employed to first analyze the sensitivity of the variables, and then to determine the optimal combination of parameters to minimize injury. As shown in Figure 7-3, the four characteristics of the joint previously described were parametrized, and then the HBM response was monitored. Z-axis accelerations at the pelvis and T12

and X-axis and Z-axis forces at the pelvis and T12 were extracted from each MADYMO run, and each value was normalized based on literature research presented in Chapter 3 according to Equation 1. For the purposes of this research, the injury thresholds were the lowest reported force or acceleration values associated with fracture from pertinent vertical loading PMHS testing, which provides a more conservative approach for the optimization. The force values were rounded to the nearest 100 (Table 7-2). The normalization technique was used as blast injury research is limited and usually does not contain injury risk curves. The threshold values listed in Table 7-2 are the normalization values used in the denominator of the mathematical terms in Equation 1. The numerator in Equation 1 is the output value for the channel from the MADYMO model. Once the values were normalized such that a value of 1.0 represented injury, constraints were placed on each normalized value so that optimized solutions could not include normalized parameters over a value of 1.0, therefore restricting solutions to only those that are non-injurious. A combined score metric was created to use as a minimizing function, which summed the normalized value of each injury criteria as shown in Equation 2. The results of this study are presented in the next section.

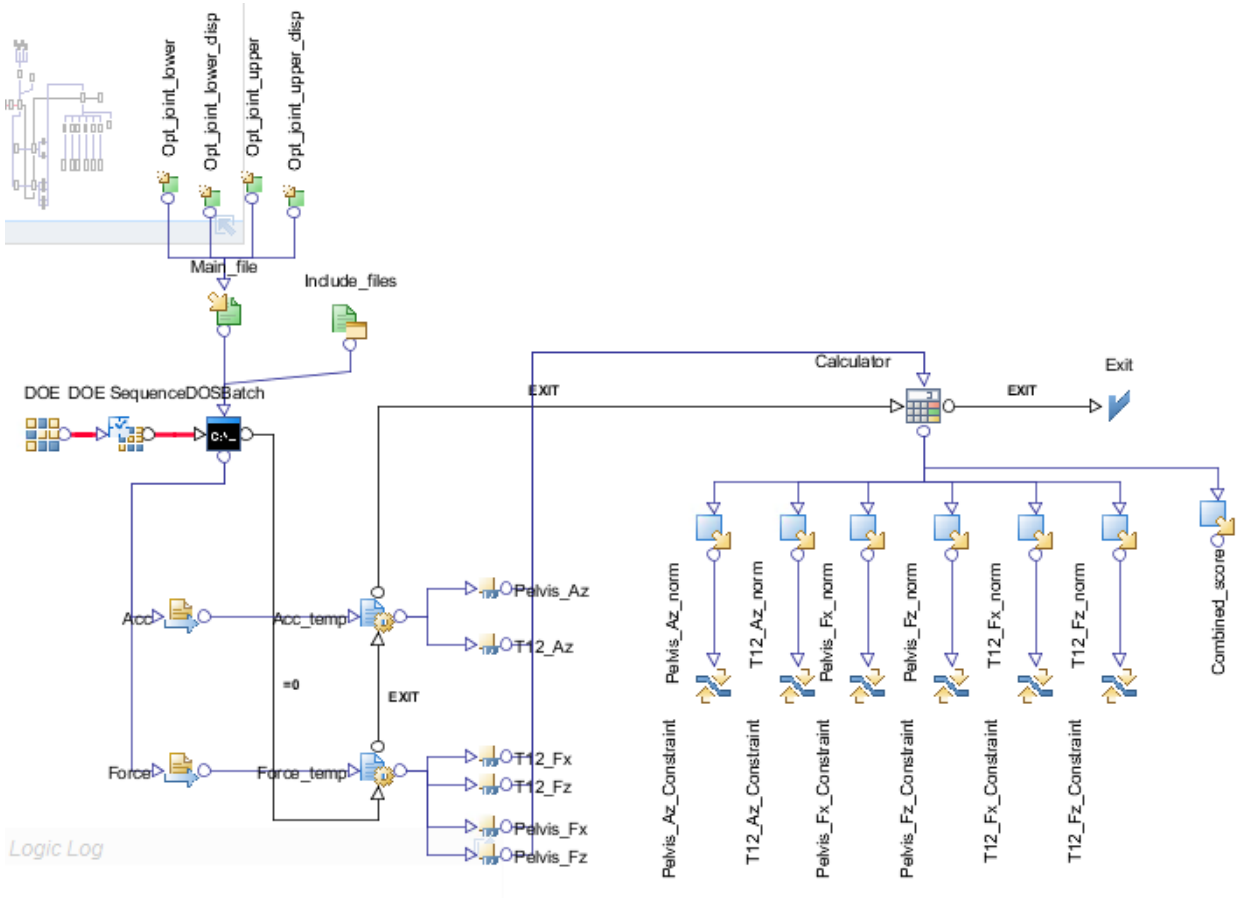

Figure 7-3. modeFRONTIER schematic for optimization of EA translational joint properties

$$Normalized\ value = \frac{MADYMO\ peak\ output\ value}{\text{Table 7-2}\ injury\ threshold\ value} \qquad \text{(Equation 1)}$$

Table 7-2. Injury metrics and thresholds used in optimization

Injury Metric	Injury Threshold	Injury Description
Pelvis Az	175 g [16]	Pelvis fractures
T12 Az	56 g [75]	Compression/unstable fractures
Pelvis Fx	6000 N [56]	50% probability of pelvis fracture or dislocation
Pelvis Fz	7500 N [75]	Pelvis fractures (AIS 3)
T12 Fx	1200 N [7]	Anterior lumbar failure
T12 Fz	5200 N [47, 75]	Compression/unstable fractures

$$Combined\ score = (Pelvis\ Az)_{norm} + (T12\ Az)_{norm} + (Pelvis\ Fx)_{norm} + (Pelvis\ Fz)_{norm} + (T12\ Fx)_{norm} + (T12\ Fz)_{norm}$$

(Equation 2)

The combined score serves as a single value for the optimization software to minimize; for the purposes of this research, it does not have weighting factors for the different metrics, so each metric is viewed as equally important. The injury threshold for each metric is the dictating element for the overall final effect on the combined score. For example, although the channels in the x-direction are not the primary load path, the injury threshold is lower, so the overall effect on the combined score may be greater for a particular x-direction channel.

7.2. Specific Aim 3 – Seat Optimization Results – Nominal Posture

Once the optimization model was set up, a sensitivity analysis was conducted to understand the role of the four input parameters and their effect on the output parameters, with the primary focus on the combined score. The input parameters were varied between 2 kN and 20 kN to understand appropriate boundaries for the lower and upper forces and adjusted to the final configuration in Table 7-1. A Uniform Latin Hypercube DOE with 100 simulations was used for this analysis with undefined steps, allowing a random distribution of configurations.

The sensitivity study included an assessment of the feasibility of designs with respect to the constraints limits and a Student's T test analysis to determine the size of the effect of the four parameters. The resulting statistical significance ($p < 0.05$) on the overall injury parameters and whether it was a direct or inverse effect was also assessed. The effect size was determined as the difference between the means calculated for the upper and

lower part of the input variable domains and represents the strength of the relationship between the input and output parameter. If the size effect was close to zero, it meant that there was a limited relationship between the input and output parameter. As Table 7-3 and Figure 7-4 show, the most statistically significant parameters were the upper joint force limit and upper joint displacement. As expected, as the upper joint displacement increased, the injury metrics decreased, as more of the stroke was used. As the upper joint force was reduced, so were the resulting injury metrics. The lower joint, or shear pin, force limit was only significant in a few injury thresholds, and overall, the activation displacement of the lower joint was not a major contributing factor. The full data analysis and output parameter table is contained in Appendix F.

Table 7-3. Summary of parameter effects on injury thresholds for nominal posture showing whether each parameter was statistically significant or insignificant for each injury criteria

	Opt_joint_lower	Opt_joint_lower_disp	Opt_joint_upper	Opt_joint_upper_disp
Pelvis Az	Direct effect - insignificant	Inverse effect - insignificant	Direct effect - significant	Inverse effect - significant
Pelvis Fx	Direct effect - significant	Inverse effect - significant	Direct effect - significant	Inverse effect - insignificant
Pelvis Fz	Direct effect - insignificant	Direct effect - insignificant	Direct effect - significant	Inverse effect - significant
T12 Az	Direct effect - insignificant	Inverse effect - insignificant	Direct effect - significant	Inverse effect - significant
T12 Fx	Direct effect - insignificant	Direct effect - insignificant	Direct effect - significant	Inverse effect - significant
T12 Fz	Inverse effect - insignificant	Direct effect - insignificant	Direct effect - significant	Inverse effect - significant
Combined	Direct effect - insignificant	Direct effect - insignificant	Direct effect - significant	Inverse effect - significant

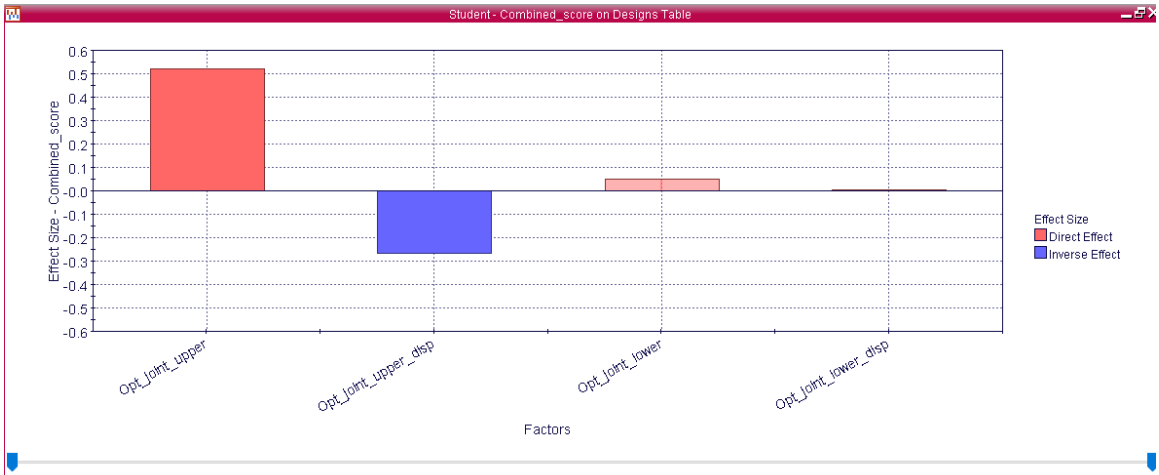

Factors	Effect Size	Significance	t-Student	critical t (sig. = 0.10)	critical t (sig. = 0.05)	critical t (sig. = 0.01)
Opt_joint_upper	5.1995E-1	0.000	9.9250E0	1.2991E0	1.6766E0	2.4049E0
Opt_joint_upper_disp	-2.6750E-1	0.000	3.8719E0	1.2991E0	1.6766E0	2.4049E0
Opt_joint_lower	5.0348E-2	0.249	6.8030E-1	1.2902E0	1.6606E0	2.3650E0
Opt_joint_lower_disp	4.5430E-3	0.476	6.1242E-2	1.2902E0	1.6606E0	2.3650E0

Figure 7-4. Sensitivity analysis output from modeFRONTIER for nominal posture combined score

Using the SIMPLEX method [50], the optimization process was conducted with the same input parameters listed in Table 7-1. The goal of this optimization was to find the minimum combined score, which represents the lowest possible combination of normalized injury thresholds for the pelvis and lower spine. The optimization converged to a solution after approximately 120 runs as shown in Figure 7-5.

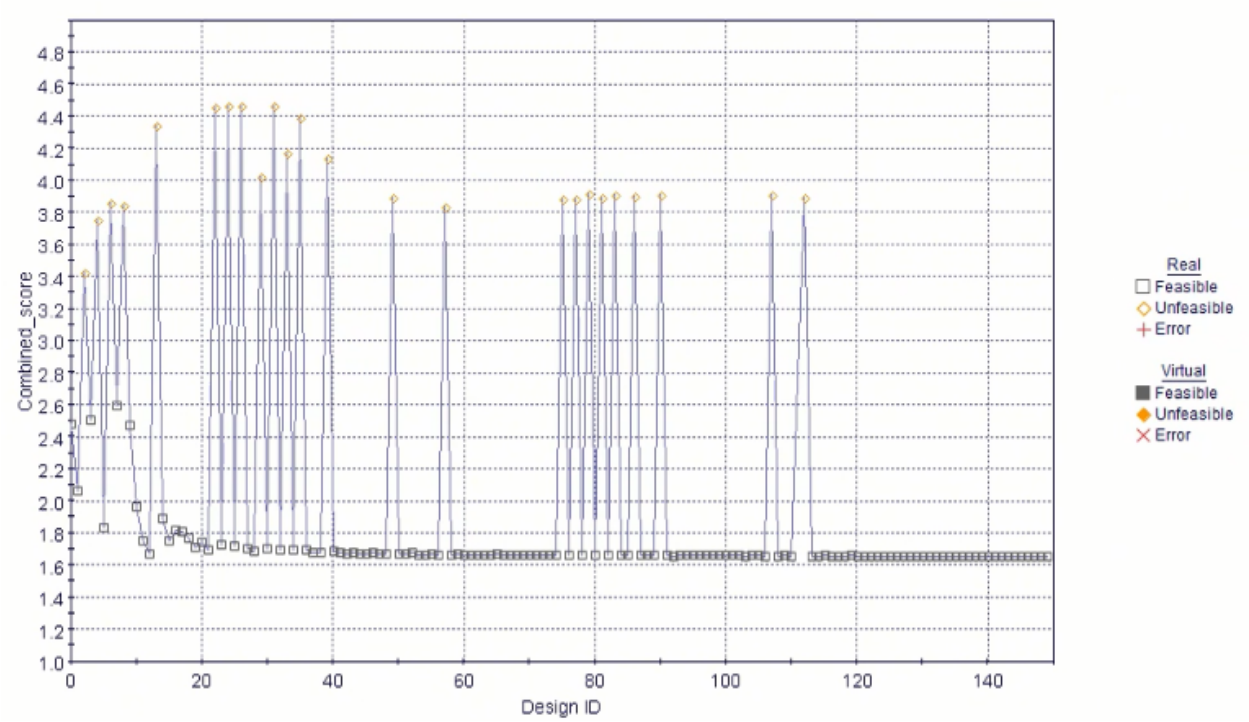

Figure 7-5. Optimization process with minimizing combined score shows convergence on a solution

The optimal solution for Condition A within the parameter ranges defined is listed in Table 7-4. As expected, the optimal combination was at the lower end of the ranges for activation forces and at the higher end of the allowable maximum displacement. Table 7-5 contains the normalized values for each injury criteria and the combined score for the optimal condition. Pelvis Fz and T12 Fz were the largest contributors to the overall score. The pelvis is designed to absorb the initial energy input, and then the forces are directly

transmitted up the spine into T12. A combined score above 1.0 does not indicate injury; the combined score was simply used as a minimizing value for the optimization.

Table 7-4. Optimization combination for PMHS Condition B

Parameter Name	Description	Optimized value
Opt_joint_lower	Shear pin force	2.004 kN
Opt_joint_lower_disp	Shear pin activation displacement	0.017 m (0.70 inch)
Opt_joint_upper	EA device maximum load	5.000 kN
Opt_joint_upper_disp	EA device maximum displacement	0.151 m (5.94 inches)

Table 7-5. Normalized injury values for optimal combination

	Pelvis Az	Pelvis Fx	Pelvis Fz	T12 Az	T12 Fx	T12 Fz	Combined Score
Normalized value	0.046 [8 g]	0.184 [1106 N]	0.445 [3339 N]	0.276 [15 g]	0.268 [322 N]	0.438 [2279 N]	1.658

The seat velocity of the optimized combination was also calculated to compare to known injurious ranges. For the optimal combination, the seat velocity was approximately 2.6 m/s (Figure 7-6), which is well below the 4 m/s from Condition A, which is accepted as a non-injurious seat velocity. This seat velocity was measured relative to the non-moving global coordinate system. The seatbelt imparted a slingshot effect in the model after 75 ms, which caused a rapid increase in seat velocity as the seat was artificially pulled toward the occupant for the optimized position. The seat velocity had relatively leveled off and reached its maximum around this point. The same slingshot effect occurred after 60 ms in the non-optimized condition. The comparison of the injury criteria between the optimized and non-optimized conditions are shown in Figure 7-7 through Figure 7-12. As expected, the peak value for each criteria is significantly reduced, and the length of the force or acceleration response is elongated, as the seat absorbs energy

through the event. The forces and accelerations do not always return to zero because the simulation was truncated after the peaks occurred but before the slingshot effect.

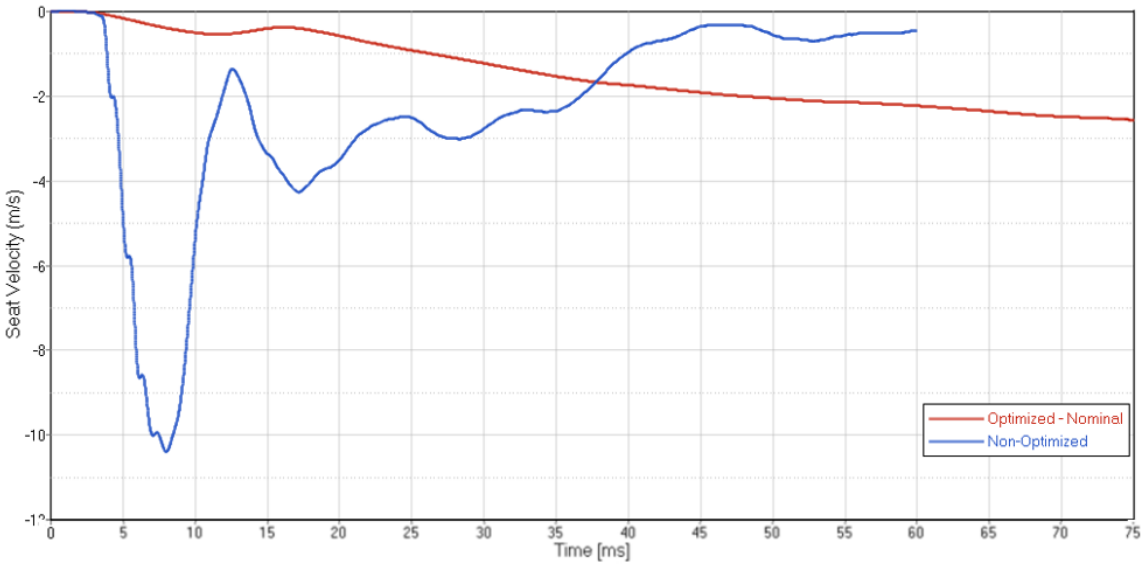

Figure 7-6. Seat velocity of optimal EA mechanism combination (red) compared to non-optimized combination (blue)

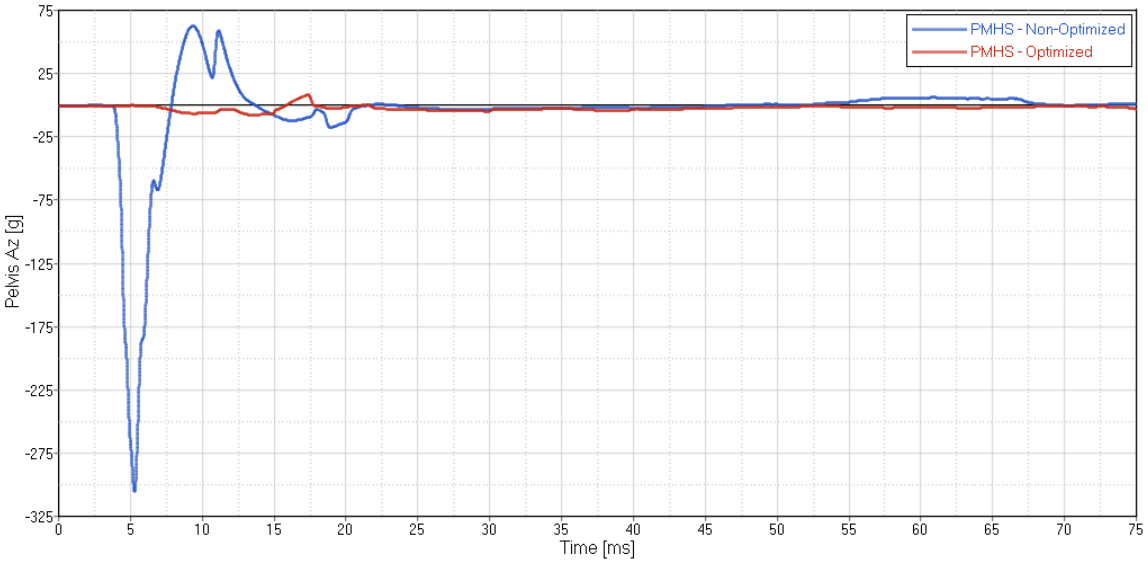

Figure 7-7. Pelvis Az of optimal EA mechanism combination (red) compared to non-optimized combination (blue)

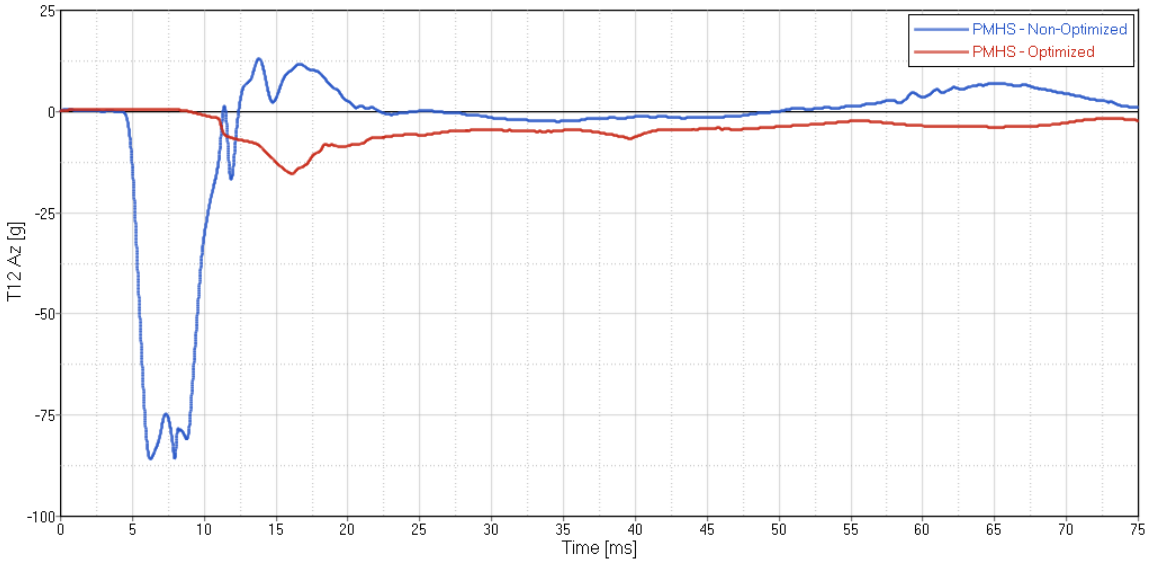

Figure 7-8. T12 Az of optimal EA mechanism combination (red) compared to non-optimized combination (blue)

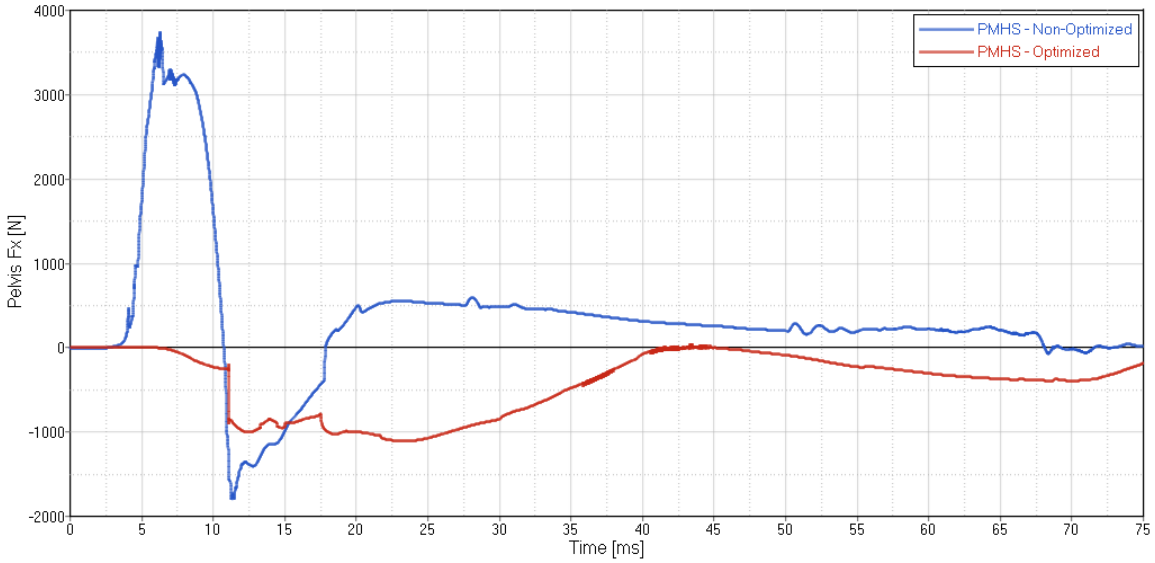

Figure 7-9. Pelvis Fx of optimal EA mechanism combination (red) compared to non-optimized combination (blue)

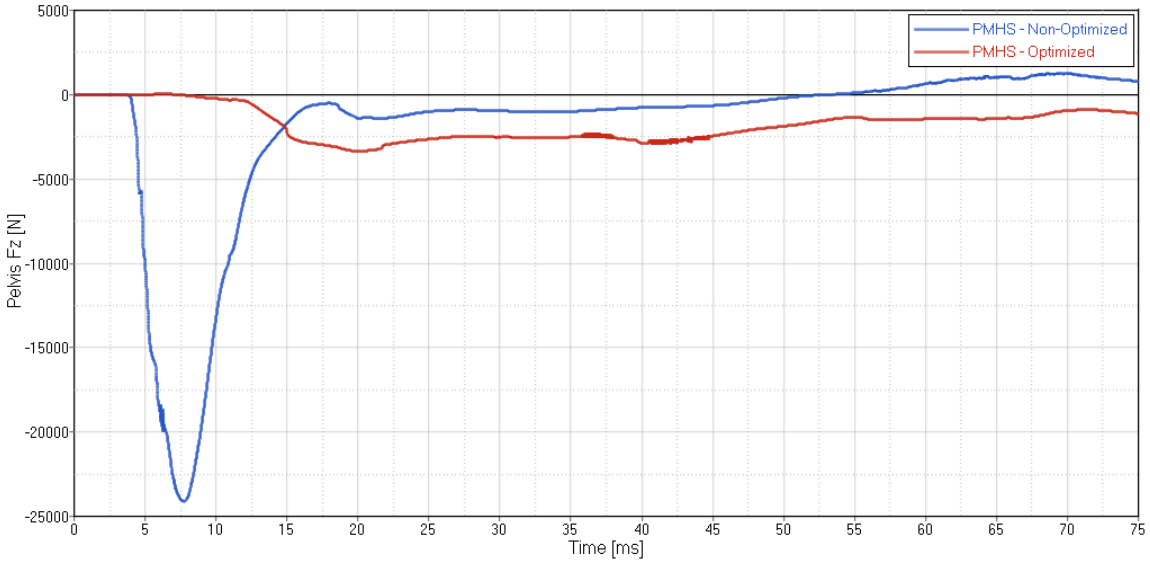

Figure 7-10. Pelvis Fz of optimal EA mechanism combination (red) compared to non-optimized combination (blue)

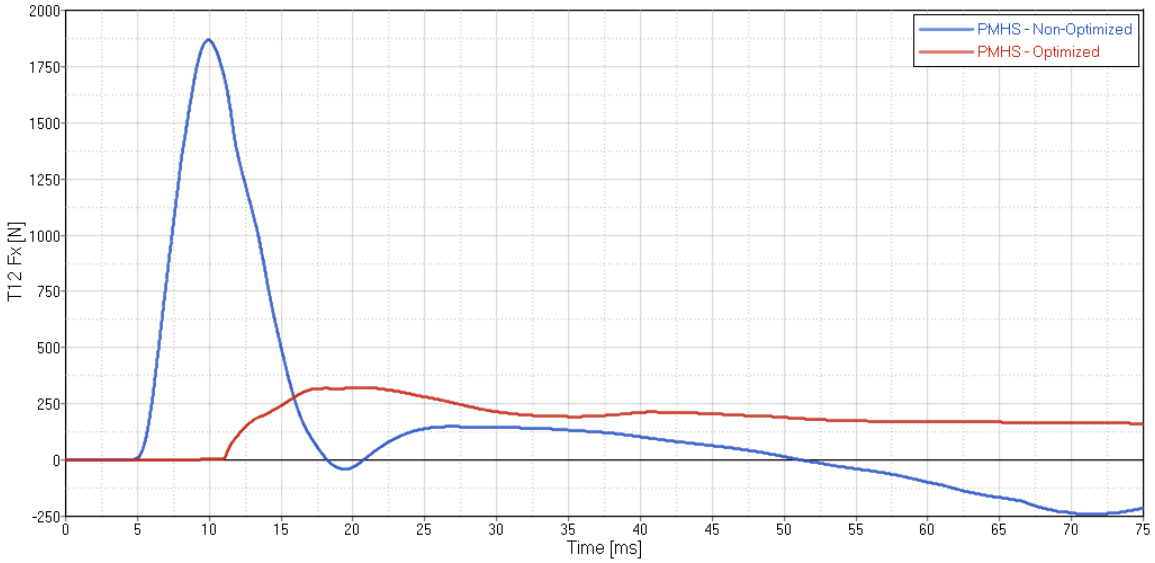

Figure 7-11. T12 Fx of optimal EA mechanism combination (red) compared to non-optimized combination (blue)

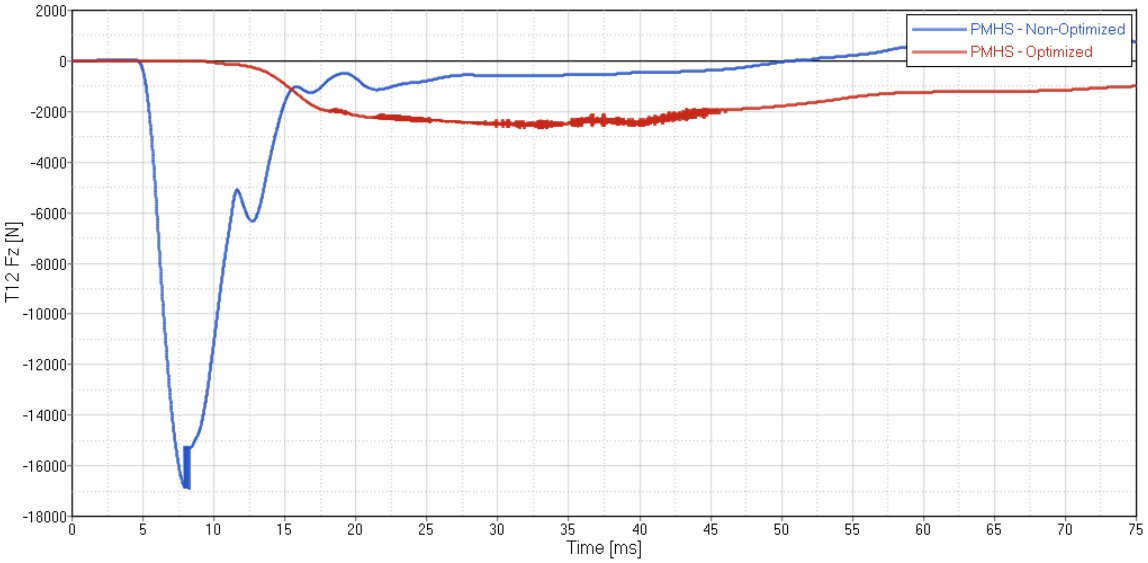

Figure 7-12. T12 Fz of optimal EA mechanism combination (red) compared to non-optimized combination (blue). Data was filtered at CFC 60 Hz to remove noise due to the interaction between Kelvin restraints.

To verify that the EA mechanism completed the full stroke as expected, the relative displacement between the floor platen and seat platen were plotted (Figure 7-13).

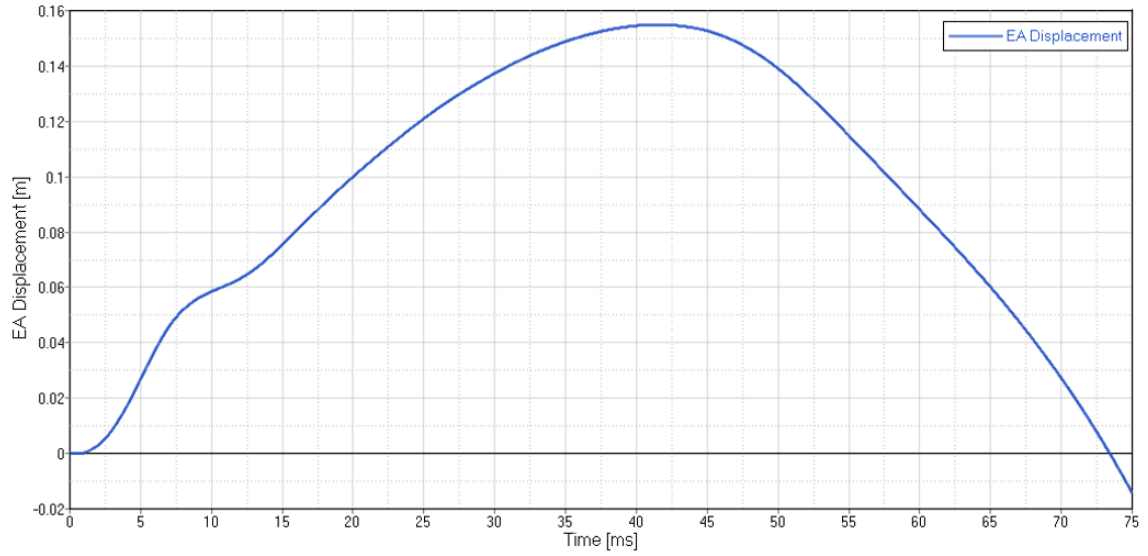

Figure 7-13. Dynamic displacement of EA mechanism shows full 6 inch stroke

The model was also assessed in the nominal posture using a square wave input instead of the linear EA mechanism to evaluate the influence of an EA pulse shape change. The EA lower shear pin and upper maximum joint were both set to 3.5 kN with the same displacement values as listed in the optimal configuration in Table 7-4, as this maintains the same energy absorption for comparison. The square wave input resulted in a large relative increase to peak Pelvis Az and T12 Az, but a small effect to overall combined score, as these parameters were less influential to the combined score based on their relative nominal value compared to their injury threshold. The change in EA mechanism shape created a difference in the shape of the acceleration and force curves, where the acceleration ramped up quicker in the square wave and had a higher peak but lower acceleration after the peak, and the force also ramped up quicker in the square wave but had essentially the same peak value with a longer sustained force duration during the initial loading.

Table 7-6. Normalized injury values for linear EA and square wave EA in nominal posture

	Pelvis Az	**Pelvis Fx**	**Pelvis Fz**	**T12 Az**	**T12 Fx**	**T12 Fz**	**Combined Score**
Normalized value – Linear EA	0.046	0.184	0.445	0.276	0.268	0.438	1.658
Normalize value – Square EA	0.093	0.189	0.434	0.355	0.268	0.453	1.793

The optimization process was repeated using only Pelvis Fz and only T12 Fz as the minimizing functions instead of the combined score to determine if the tool would converge on a different solution. The optimization outcome was very similar between the three methods (minimizing combined score, Pelvis Fz, or T12 Fz), as shown in Table 7-7.

Depending on the focus of the end user, the minimizing function could be updated to any of these channel options.

Table 7-7. Comparison of EA joint and key injury outcomes for alternate minimizing options

	Opt_joint_lower	Opt_joint_lower_disp	Opt_joint_upper	Opt_joint_upper_disp	**Pelvis Fz**	**T12 Fz**	**Combined Score**
Combined Score	2.000 kN	0.017 m	5.000 kN	0.151 m	0.445	0.438	1.658
Pelvis Fz Only	2.049 kN	0.000 m	5.056 kN	0.151 m	0.417	0.434	1.668
T12 Fz Only	2.079 kN	0.010 m	5.000 kN	0.151 m	0.440	0.436	1.669

7.3. Specific Aim 3 – Seat Optimization – Reclined Seatback Angle

To assess the sensitivity of the optimized EA force and deflection properties with respect to posture, the same parameters were used to determine the optimal combination with the seat and HBM reclined 15 degrees. The seatback was rotated about the seat bight, and the HBM was adjusted only in the spine to conform to the seatback with adjustments focused on the angle between the vertebrae from L5 to T3 (Figure 7-14). The occipital condyle joint and C1 vertebral angle were also adjusted to achieve a horizontal Frankfort Plane. Table 7-8 lists the vertebral angles for the nominal and reclined posture.

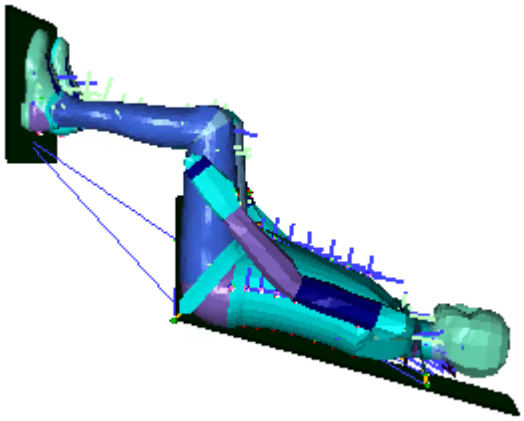

Figure 7-14. HBM in reclined posture

Table 7-8. Vertebral angles for nominal and reclined posture

Vertebra	Nominal Posture Vertebral Angle (deg)	Reclined Posture Vertebral Angle (deg)
C1	-4.2	0.0
C2	-1.8	-1.8
C3	0.0	0.0
C4	0.0	0.0
C5	0.0	0.0
C6	0.0	0.0
C7	0.0	0.0
T1	0.0	0.0
T2	0.8	0.8
T3	0.6	0.0
T4	1.1	0.0
T5	0.1	0.0
T6	1.1	0.0
T7	0.1	0.0
T8	2.0	0.0
T9	2.0	0.0
T10	2.0	0.0
T11	2.0	0.0
T12	0.3	0.0
L1	2.0	0.0
L2	2.0	0.0
L3	2.0	0.0
L4	4.7	0.0
L5	3.4	-1.5

Using the same upper and lower force and deflection limits, the sensitivity study was repeated. As shown in Table 7-9, the upper joint force limit and displacement have the greatest influence, while the lower shear pin has limited influence. Only the upper force limit and displacement has a significant effect on the overall combined score (Figure 7-15).

Table 7-9. Summary of parameter effects on injury thresholds for reclined posture showing whether each parameter was statistically significant or insignificant for each injury criteria

	Opt_joint_lower	Opt_joint_lower_disp	Opt_joint_upper	Opt_joint_upper_disp
Pelvis Az	Inverse effect - insignificant	Direct effect - significant	Direct effect - significant	Inverse effect - insignificant
Pelvis Fx	Direct effect - insignificant	Direct effect - insignificant	Direct effect - significant	Inverse effect - significant
Pelvis Fz	Inverse effect - insignificant	Direct effect - insignificant	Direct effect - significant	Inverse effect - significant
T12 Az	Inverse effect - insignificant	Inverse effect - insignificant	Direct effect - significant	Inverse effect - insignificant
T12 Fx	Inverse effect - insignificant	Direct effect - insignificant	Direct effect - significant	Inverse effect - significant
T12 Fz	Direct effect - insignificant	Direct effect - insignificant	Direct effect - significant	Inverse effect - significant
Combined	Inverse effect - insignificant	Direct effect - insignificant	Direct effect - significant	Inverse effect - significant

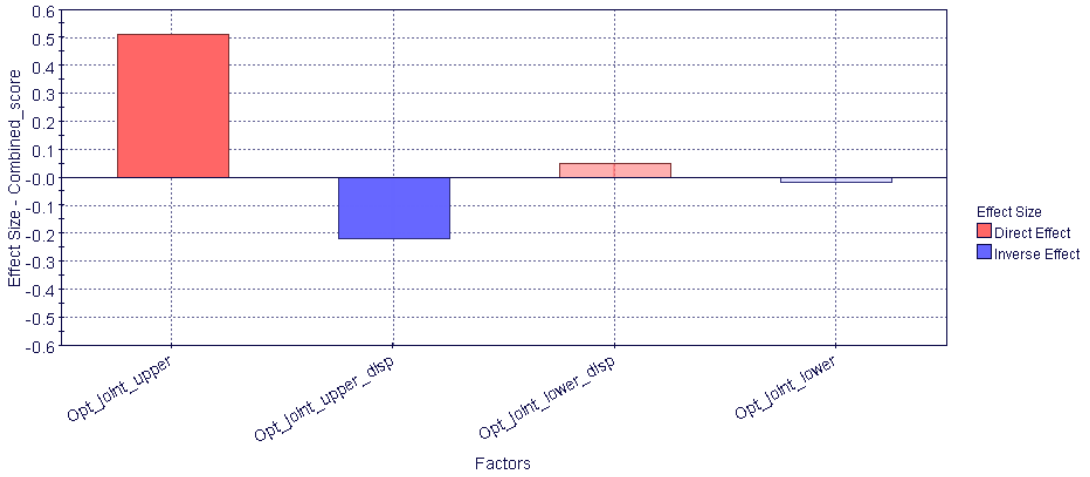

Factors	Effect Size	Significance	t-Student	critical t (sig. = 0.10)	critical t (sig. = 0.05)	critical t (sig. = 0.01)
Opt_joint_upper	5.1220E-1	0.000	9.8933E0	1.2902E0	1.6606E0	2.3650E0
Opt_joint_upper_disp	-2.1941E-1	0.001	3.1454E0	1.2902E0	1.6606E0	2.3650E0
Opt_joint_lower_disp	5.1775E-2	0.240	7.0918E-1	1.2902E0	1.6606E0	2.3650E0
Opt_joint_lower	-1.8500E-2	0.401	2.5283E-1	1.2991E0	1.6766E0	2.4049E0

Figure 7-15. Sensitivity analysis output from modeFRONTIER for combined score for reclined posture

As with the nominal optimization, the SIMPLEX method [50] was used with the same input parameters listed in Table 7-1 for the optimization of the reclined posture setup. The minimized combined injury score was determined within about 60 runs as shown in Figure 7-16. This figure shows the iterative process by which modeFRONTIER uses the SIMPLEX method to converge on an EA mechanism configuration that results in the lowest combined injury score.

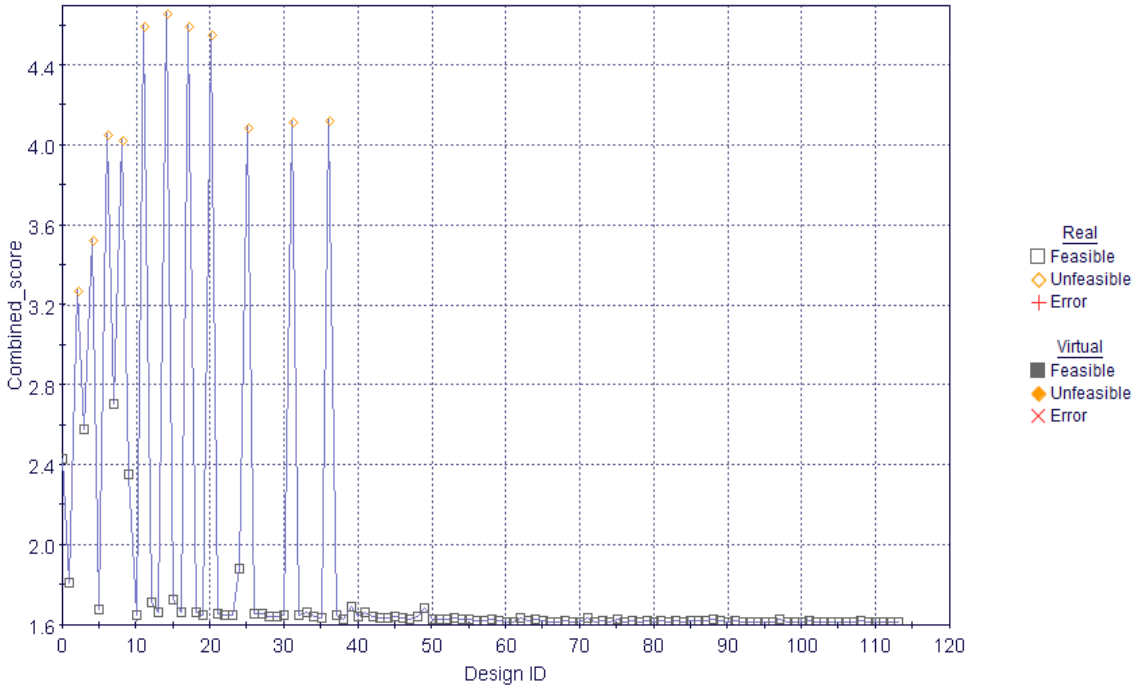

Figure 7-16. Optimization process with minimizing combined score shows convergence on a solution for reclined posture

The optimal solution for the reclined posture is listed in Table 7-10. The upper joint maximum load was about 19% higher than that of the nominal configuration. The lower shear pin force was 25% higher than the nominal configuration, but the lower EA joint effects are generally considered statistically insignificant to the final injury outcomes based on the sensitivity analysis. The overall combined injury score was very similar to

that of nominal posture, with a slight difference in distribution in the body segments, mainly in Pelvis Fx and Pelvis Az, due to the change in spine posture and force transmission. The pelvis and T12 z-direction forces had the highest influence on the overall combined score (Table 7-11). The details of the sensitivity and optimization analysis are contained in Appendix G.

Table 7-10. Optimization combination for reclined seat posture

Parameter Name	Description	Optimized value
Opt_joint_lower	Shear pin force	2.593 kN
Opt_joint_lower_disp	Shear pin activation displacement	0.011 m (0.43 inch)
Opt_joint_upper	EA device maximum load	6.056 kN
Opt_joint_upper_disp	EA device maximum displacement	0.146 m (5.75 inches)

Table 7-11. Normalized injury values for optimal combination for reclined seat

	Pelvis Az	Pelvis Fx	Pelvis Fz	T12 Az	T12 Fx	T12 Fz	Combined Score
Normalized value	0.096	0.045	0.466	0.227	0.281	0.498	1.614

The seat velocity for the optimal reclined posture configuration was higher than that of nominal posture at approximately 3.2 m/s (Figure 7-17). This is likely due to the higher limit on the upper joint force. Figure 7-18 through Figure 7-23 contain the comparison of the injury criteria between the optimized reclined posture and non-optimized conditions to show the relative improvement for the key injury parameters. As with the optimized nominal posture, the injury values are reduced and elongated as the occupant is able to ride down the pulse in a controlled manner. Data was truncated at 70 ms due to the slingshot effect previously discussed.

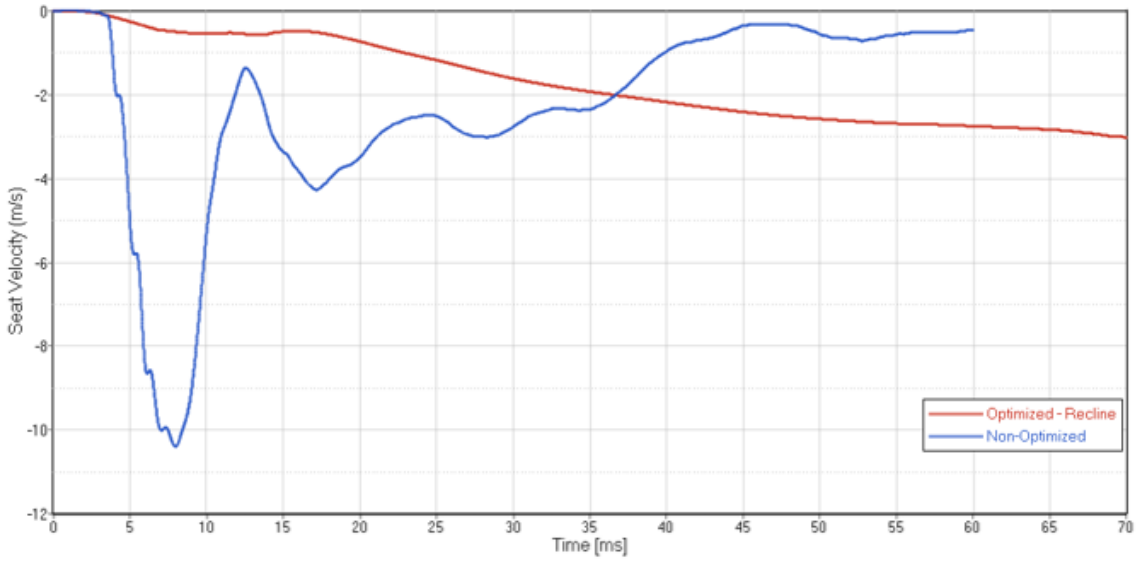

Figure 7-17. Seat velocity of optimal EA mechanism combination (red) compared to non-optimized combination (blue) for reclined posture

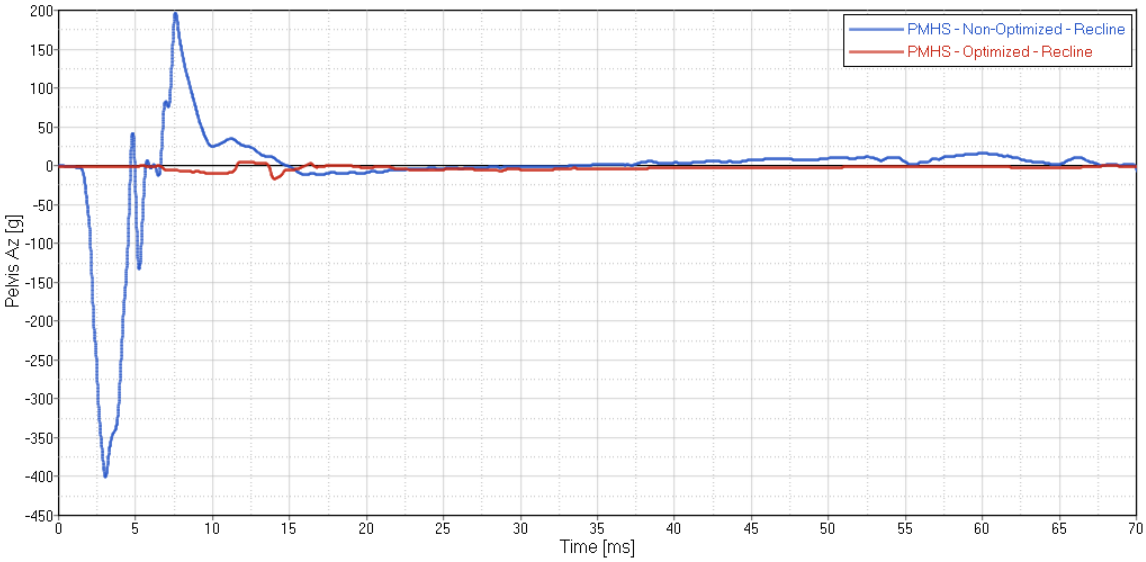

Figure 7-18. Pelvis Az of optimal EA mechanism combination (red) compared to non-optimized combination (blue) for reclined posture

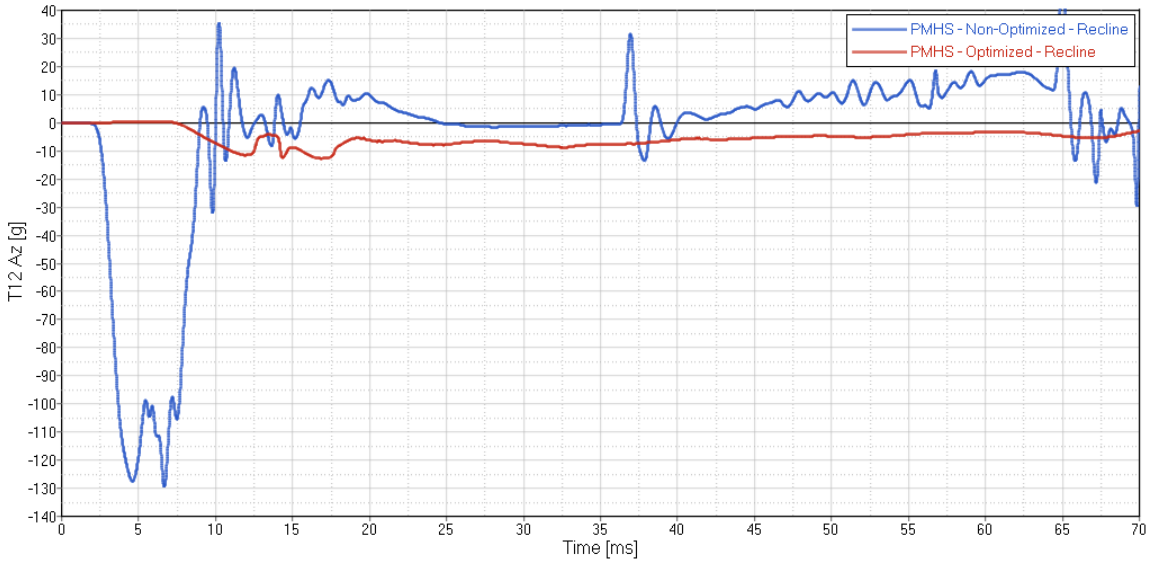

Figure 7-19. T12 Az of optimal EA mechanism combination (red) compared to non-optimized combination (blue) for reclined posture

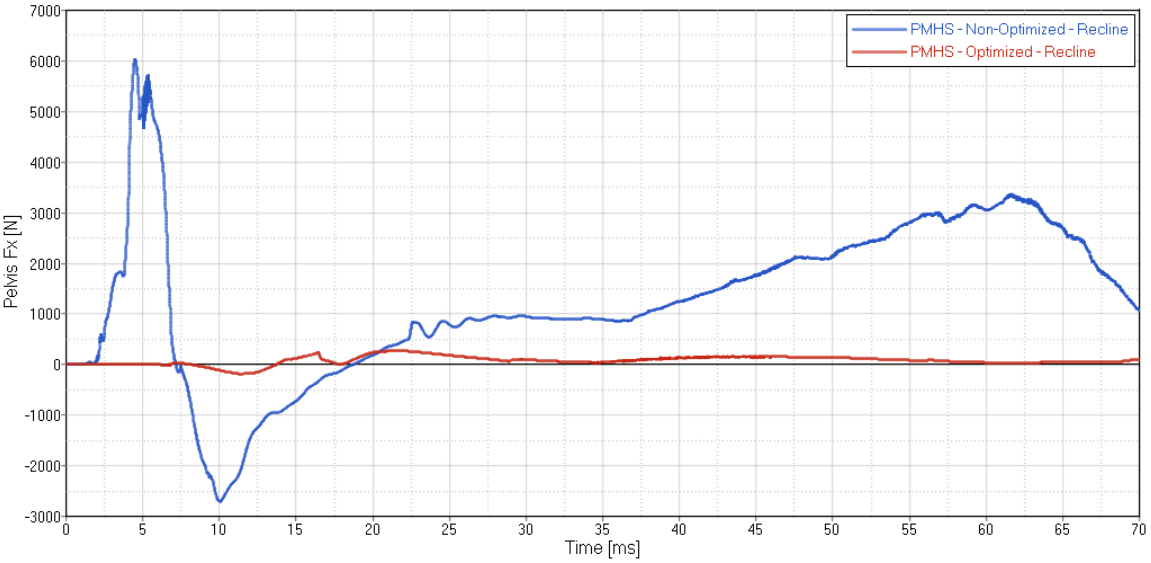

Figure 7-20. Pelvis Fx of optimal EA mechanism combination (red) compared to non-optimized combination (blue) for reclined posture

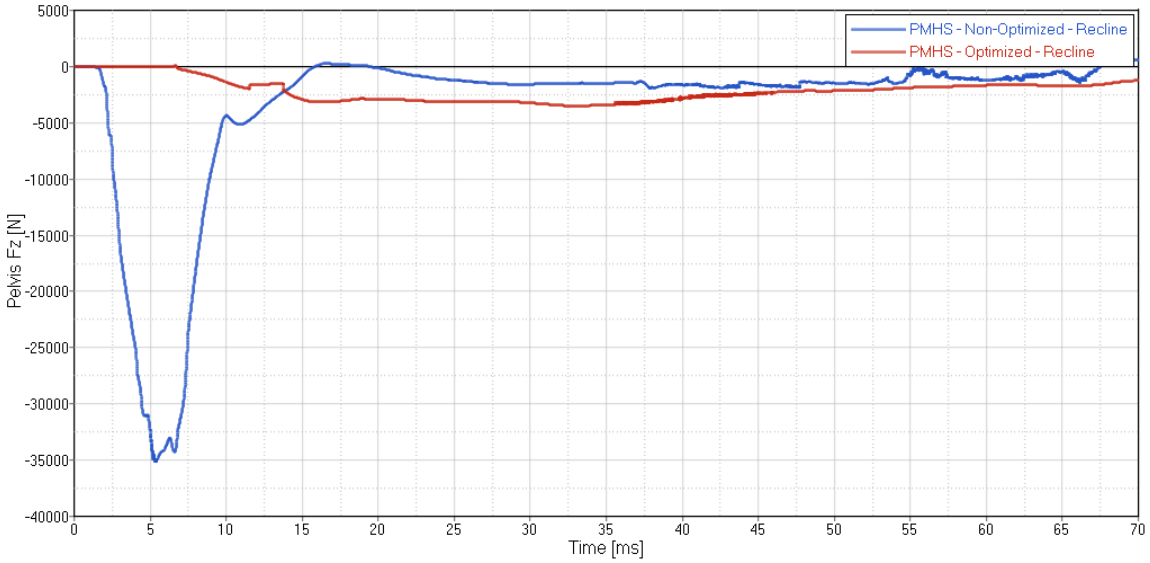

Figure 7-21. Pelvis Fz of optimal EA mechanism combination (red) compared to non-optimized combination (blue) for reclined posture

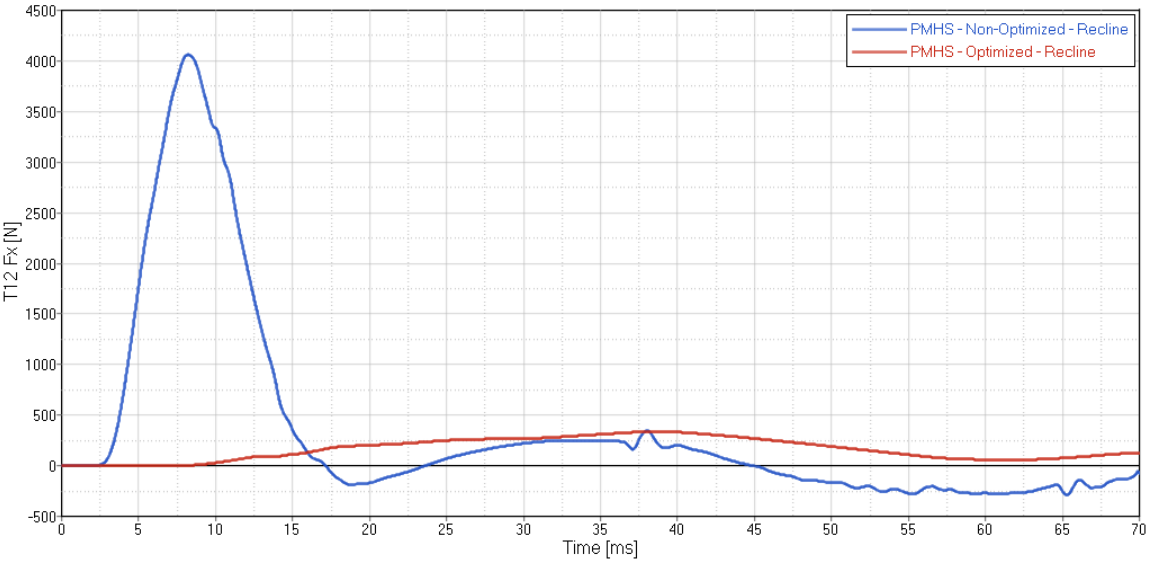

Figure 7-22. T12 Fx of optimal EA mechanism combination (red) compared to non-optimized combination (blue) for reclined posture

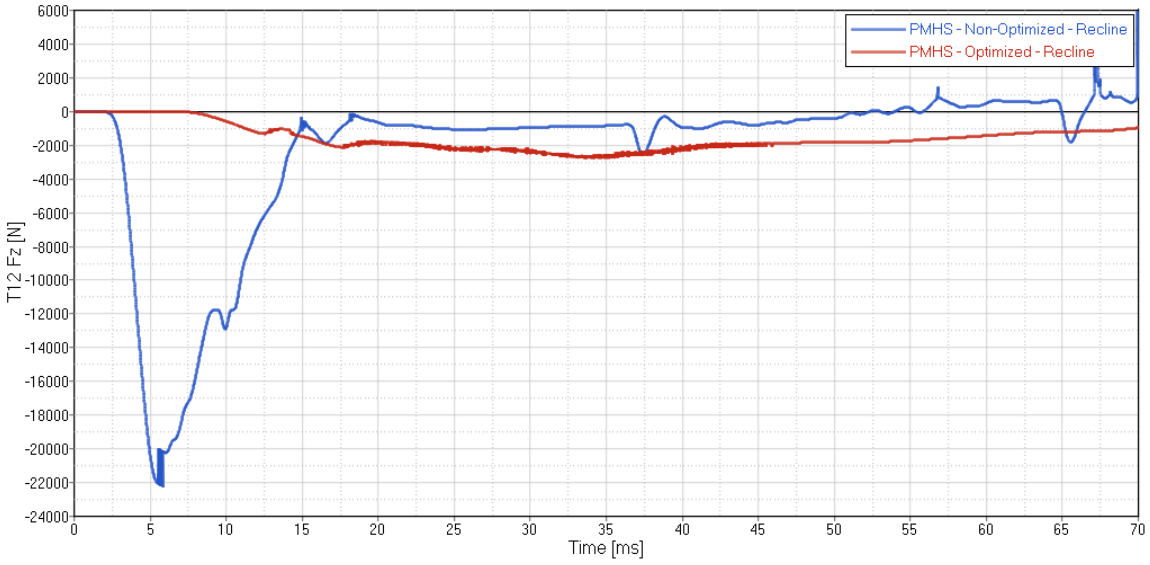

Figure 7-23. T12 Fz of optimal EA mechanism combination (red) compared to non-optimized combination (blue) for reclined posture. Data was filtered at CFC 60 Hz to remove noise due to the interaction between Kelvin restraints.

A secondary set of optimization runs were conducted with a limit on the lower EA joint of 2-3 kN to investigate if modeFRONTIER had converged on a local minimum, which resulted in higher injury values from the differences in the EA force limits. As shown in Table 7-12, the updated optimization converged on joint parameters that were much more aligned with that of the nominal posture. The overall combined injury score reduced from 1.614 to 1.442 as forces and accelerations measured in the pelvis and at T12 reduced (Table 7-13). This second optimization evaluation demonstrates that there can be multiple solutions with local minima to achieve reduced injury within EA joint parameters, which can provide more flexibility to EA mechanism designs.

Table 7-12. Optimization combination for reclined seat posture

Parameter Name	Description	Optimized value
Opt_joint_lower	Shear pin force	2.067 kN
Opt_joint_lower_disp	Shear pin activation displacement	0.004 m (0.15 inch)
Opt_joint_upper	EA device maximum load	5.003 kN
Opt_joint_upper_disp	EA device maximum displacement	0.151 m (5.94 inches)

Table 7-13. Normalized injury values for optimal combination for reclined seat

	Pelvis Az	Pelvis Fx	Pelvis Fz	T12 Az	T12 Fx	T12 Fz	Combined Score
Normalized value	0.081	0.049	0.419	0.200	0.249	0.444	1.442

The difference in EA parameters from the reduced range evaluation for the reclined posture resulted in a decrease in seat velocity, from 3.2 to 2.8 m/s (Figure 7-24), as expected, as the maximum allowable load on the upper EA joint was reduced from the original optimization at the local minimum.

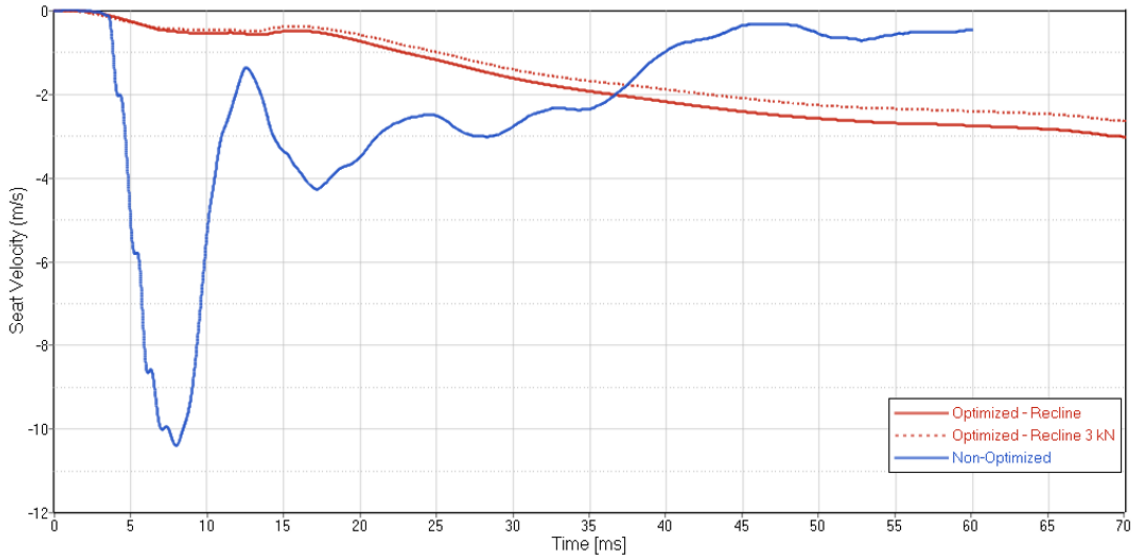

Figure 7-24. Seat velocity of optimal EA mechanism combination (red) compared to reduced range combination (red dashed) and non-optimized combination (blue) for reclined posture

7.4. Specific Aim 3 – Seat Optimization – PPE

As most Warfighters use PPE in theater, the optimization study was repeated with an increase in occupant mass to represent the addition of 27 kg (60 lbs) of PPE [10] in the nominal posture orientation. The mass was distributed around the torso to simulate the addition of an Improved Outer Tactical Vest (IOTV). The design and actual mass distribution of IOTVs are proprietary, but a best estimate of the distribution was used for the purposes of this investigation, which included increasing the mass of each of the 24 thorax and abdominal ellipsoid bodies comprising the front, left, and right sides of the HBM by approximately 1.14 kg per body. This approach may overestimate the energy increase from the added mass, as the mass was directly coupled to the occupant model instead of separated as a detached vest mass. Figure 7-25 shows the difference in loading due to the added vest mass to the pelvis z-axis force in the higher loading

Condition B, which included a quicker loading time but similar peak, with a slight increase in impulse.

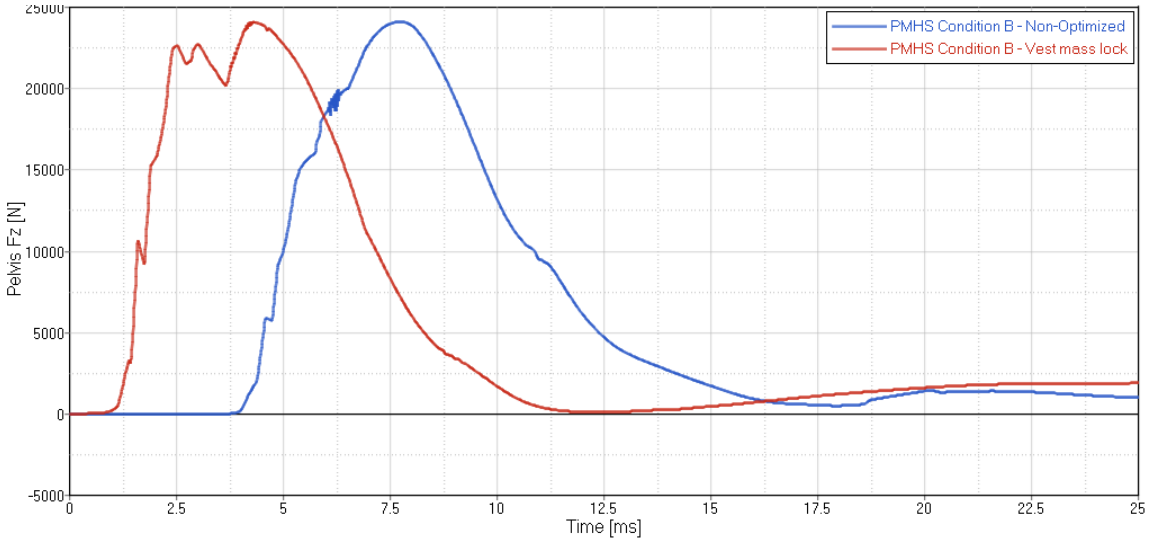

Figure 7-25. Difference in Pelvis Fz between nominal (blue) and with added vest mass (red)

The added mass from the vest led to similar trends as the nominal posture sensitivity study (Table 7-14 and Figure 7-26) with respect to the role of the significance of the upper joint maximum force and maximum displacement. The lower joint shear pin force was only significant for Pelvis z-axis acceleration and shear force with the added vest mass.

Table 7-14. Summary of parameter effects on injury thresholds with vest showing whether each parameter was statistically significant or insignificant for each injury criteria

	Opt_joint_lower	Opt_joint_lower_disp	Opt_joint_upper	Opt_joint_upper_disp
Pelvis Az	Direct effect - significant	Inverse effect - insignificant	Direct effect - significant	Inverse effect - insignificant
Pelvis Fx	Inverse effect - significant	Direct effect - significant	Inverse effect - significant	Inverse effect - insignificant
Pelvis Fz	Direct effect - insignificant	Direct effect - insignificant	Direct effect - significant	Inverse effect - significant
T12 Az	Direct effect - insignificant	Direct effect - insignificant	Direct effect - significant	Inverse effect - significant
T12 Fx	Inverse effect - insignificant	Direct effect - insignificant	Direct effect - significant	Inverse effect - significant
T12 Fz	Direct effect - insignificant	Inverse effect - insignificant	Direct effect - significant	Inverse effect - significant
Combined	Direct effect - insignificant	Direct effect - insignificant	Direct effect - significant	Inverse effect - significant

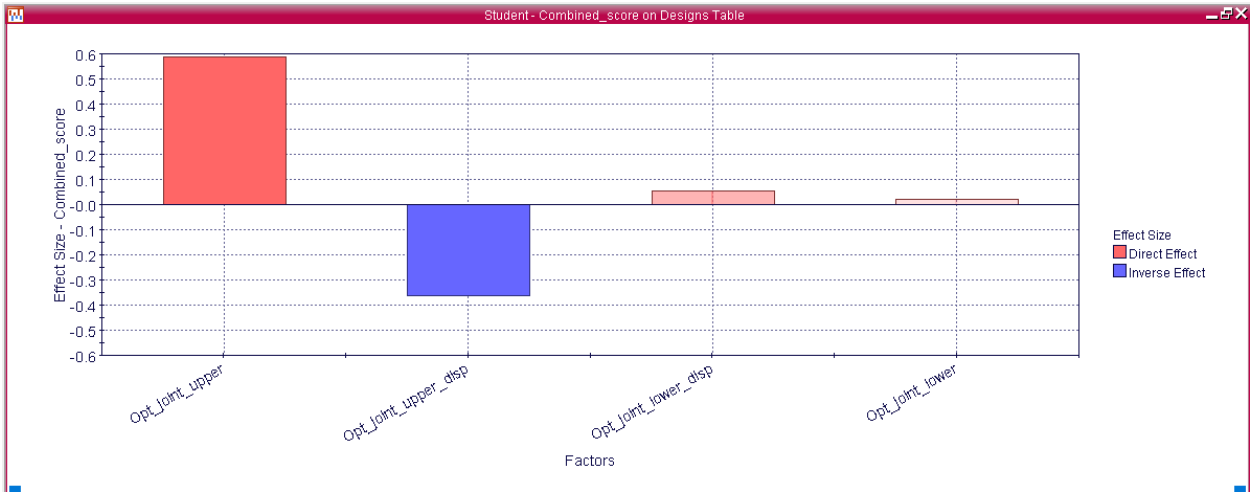

Factors	Effect Size	Significance	t-Student	critical t (sig. = 0.10)	critical t (sig. = 0.05)	critical t (sig. = 0.01)
Opt_joint_upper	5.8816E-1	0.000	1.0172E1	1.2902E0	1.6606E0	2.3650E0
Opt_joint_upper_disp	-3.6328E-1	0.000	4.8867E0	1.2991E0	1.6766E0	2.4049E0
Opt_joint_lower_disp	5.4147E-2	0.257	6.5454E-1	1.2902E0	1.6606E0	2.3650E0
Opt_joint_lower	2.0440E-2	0.403	2.4663E-1	1.2902E0	1.6606E0	2.3650E0

Figure 7-26. Sensitivity analysis output from modeFRONTIER for combined score for nominal posture with vest

The same optimization process was completed using the added vest mass, and as shown in Figure 7-27, the optimal combination was found within approximately 140 runs. The details of the sensitivity and optimization analysis are contained in Appendix H.

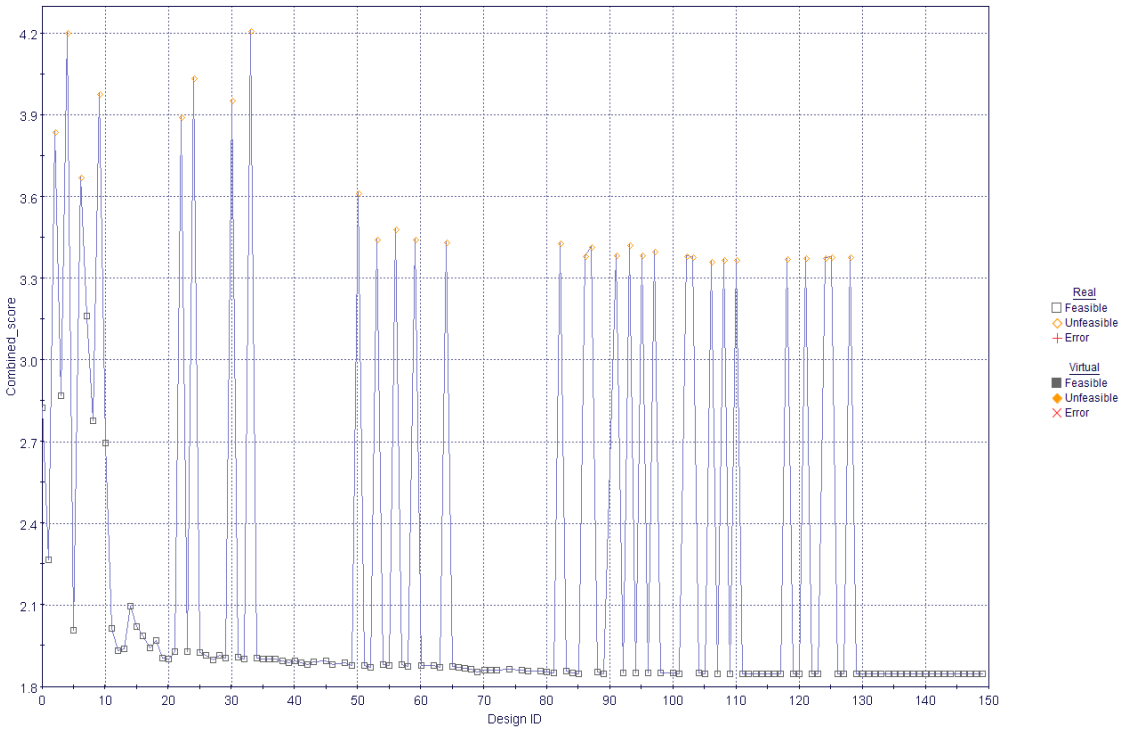

Figure 7-27. Optimization process with minimizing combined score shows convergence on a solution for nominal posture with vest

The optimal solution for the vest mass within the parameter ranges defined is listed in Table 7-15. As expected, the optimal combination was at the lower end of the ranges for activation forces and at the higher end of the allowable maximum displacement. The displacement of the lower shear pin and of the maximum upper joint were the same as that of the nominal posture.

Table 7-16 contains the normalized values for each injury criteria and the combined score for the optimal condition. Pelvis Fz and T12 Fz were the largest contributors to the overall score. The T12 Fx shear force was also influential due to the added mass in front

of the HBM center of gravity in the x-direction, which increased the shear forces at the spine exerted during the event by 41% over the nominal configuration. The combined score was 11% higher than the nominal posture configuration with the addition of the extra mass, from 1.658 to 1.847.

Table 7-15. Optimization combination with vest

Parameter Name	Description	Optimized value
Opt_joint_lower	Shear pin force	2.004 kN
Opt_joint_lower_disp	Shear pin activation displacement	0.0004 m (0.02 inch)
Opt_joint_upper	EA device maximum load	5.000 kN
Opt_joint_upper_disp	EA device maximum displacement	0.151 m (5.94 inches)

Table 7-16. Normalized injury values for optimal combination with vest

	Pelvis Az	Pelvis Fx	Pelvis Fz	T12 Az	T12 Fx	T12 Fz	Combined Score
Normalized value	0.062	0.170	0.524	0.219	0.405	0.467	1.847

The seat velocity of the optimized combination for the added vest mass was lower than that of the nominal posture, around 2.1 m/s (Figure 7-28). The improvement in injury criteria against the non-optimized Condition B configurations are contained in Figure 7-29 through Figure 7-34. The pelvis and T12 force and acceleration outputs follow the same trends as those for the optimized nominal posture configuration with a reduction in peak and elongation of pulse duration.

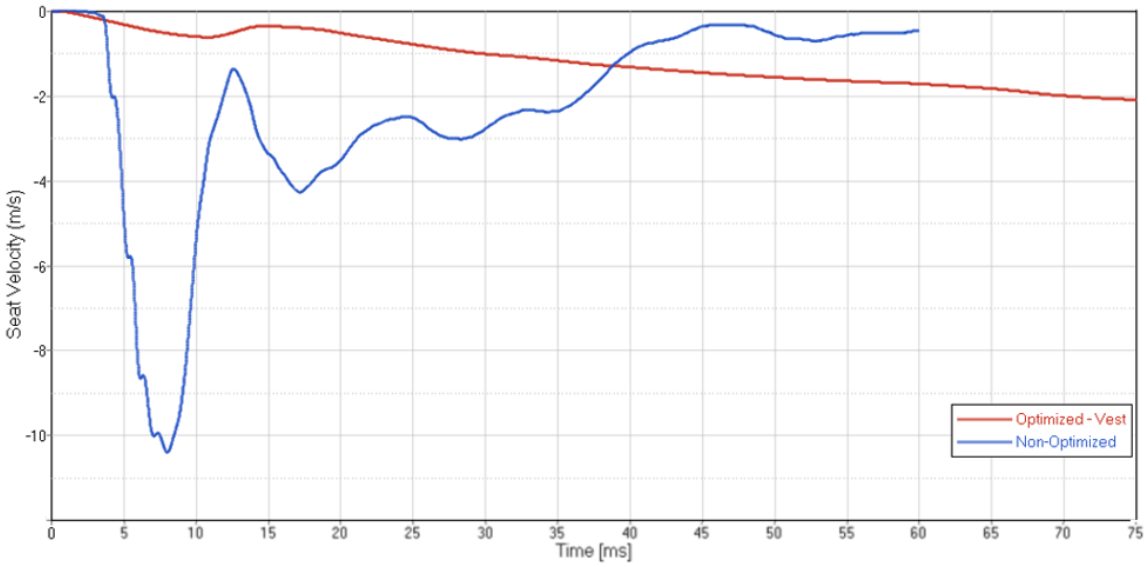

Figure 7-28. Seat velocity of optimal EA mechanism combination (red) for vest configuration compared to non-optimized combination (blue)

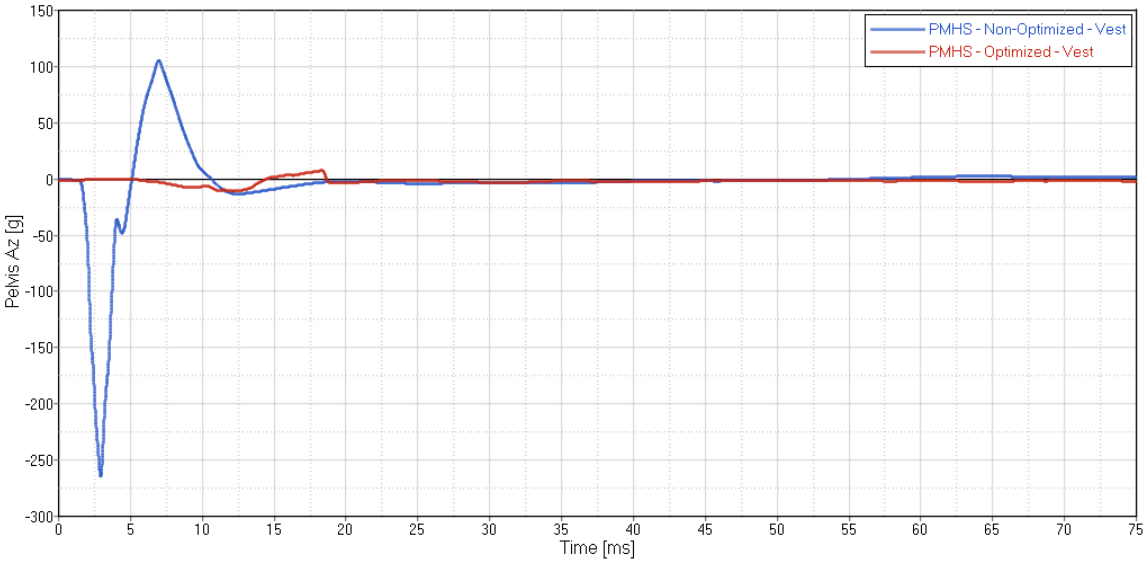

Figure 7-29. Pelvis Az of optimal EA mechanism combination (red) compared to non-optimized combination (blue) for added vest mass

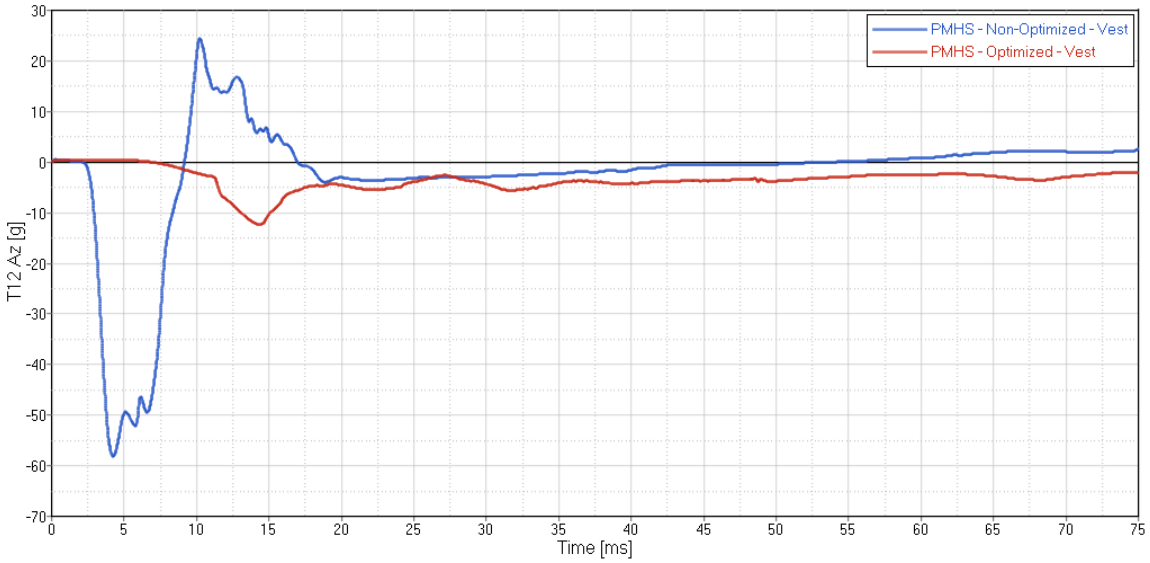

Figure 7-30. T12 Az of optimal EA mechanism combination (red) compared to non-optimized combination (blue) for added vest mass

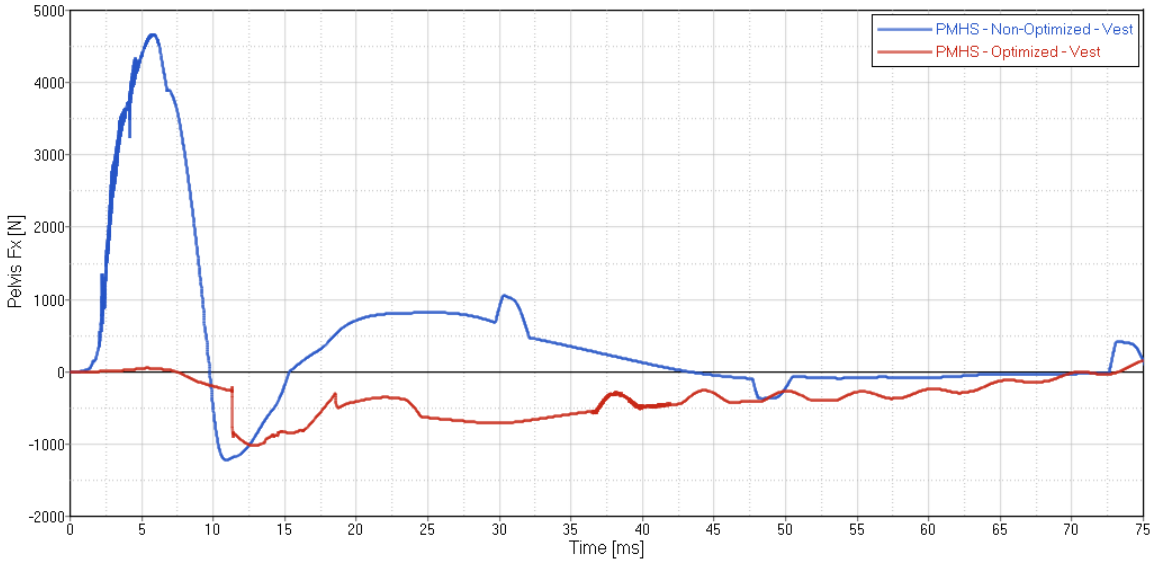

Figure 7-31. Pelvis Fx of optimal EA mechanism combination (red) compared to non-optimized combination (blue) for added vest mass

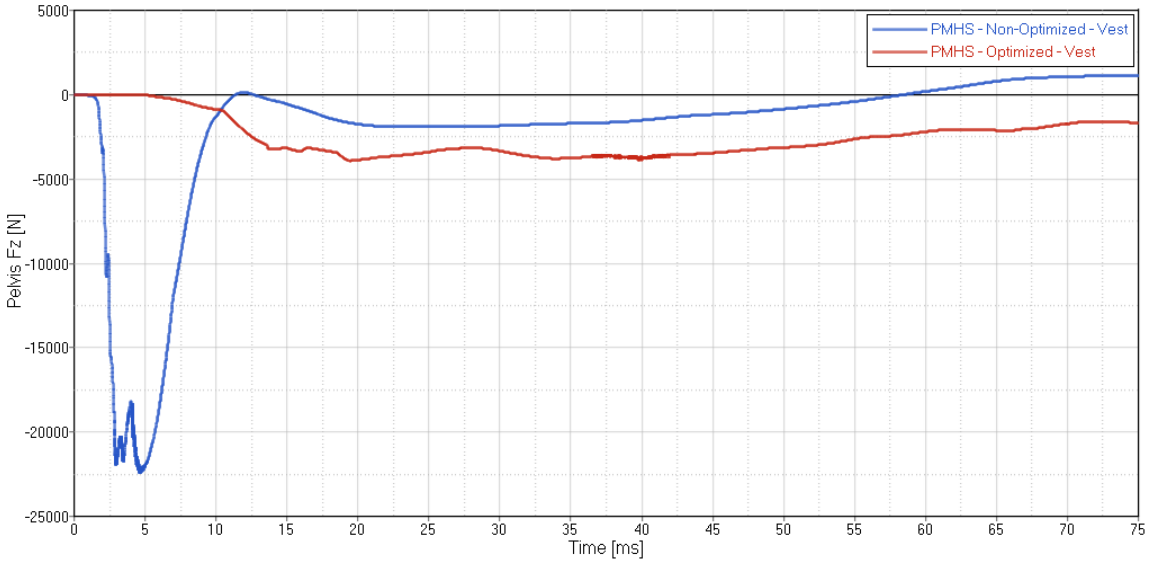

Figure 7-32. Pelvis Fz of optimal EA mechanism combination (red) compared to non-optimized combination (blue) for added vest mass

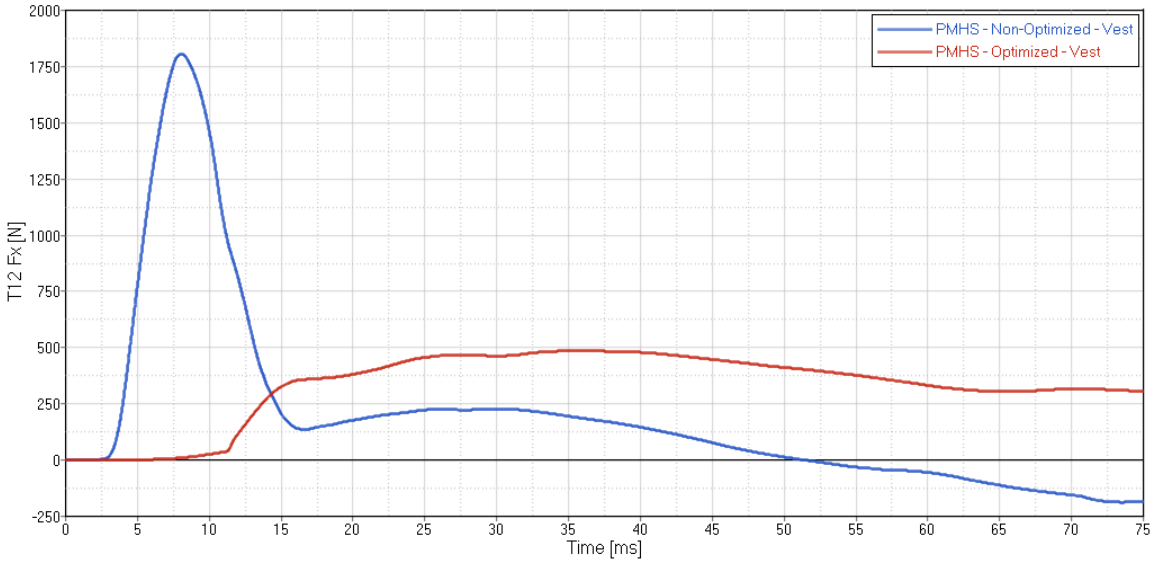

Figure 7-33. T12 Fx of optimal EA mechanism combination (red) compared to non-optimized combination (blue) for added vest mass

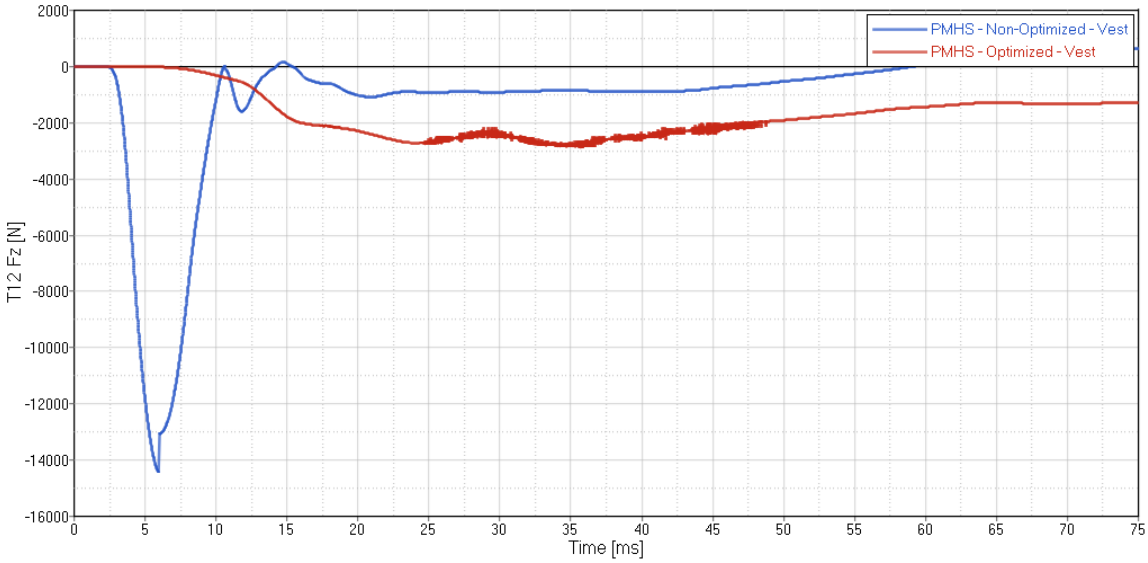

Figure 7-34. T12 Fz of optimal EA mechanism combination (red) compared to non-optimized combination (blue) for added vest mass. Data was filtered at CFC 60 Hz to remove noise due to the interaction between Kelvin restraints.

7.5. Specific Aim 3 – Seat Optimization – Reclined Seatback Angle with PPE

An investigation of the compounding effects of the added vest mass with a 15 degree reclined seatback angle was completed in accordance with the procedure outlined above. Table 7-17 and Figure 7-35 contain the results from the sensitivity analysis, which exhibit similar trends to those of the added vest mass and reclined seatback angle with 3 kN lower EA joint force limit separately; the most influential parameters continue to be the force limit and displacement limit of the upper joint.

Table 7-17. Summary of parameter effects on injury thresholds for reclined posture with vest showing whether each parameter was statistically significant or insignificant for each injury criteria

	Opt_joint_lower	Opt_joint_lower_disp	Opt_joint_upper	Opt_joint_upper_disp
Pelvis Az	Direct effect - insignificant	Direct effect - insignificant	Direct effect - significant	Inverse effect - insignificant
Pelvis Fx	Inverse effect - significant	Direct effect - insignificant	Inverse effect - insignificant	Direct effect - insignificant
Pelvis Fz	Inverse effect - insignificant	Direct effect - insignificant	Direct effect - significant	Inverse effect - significant
T12 Az	Direct effect - insignificant	Direct effect - insignificant	Direct effect - significant	Inverse effect - significant
T12 Fx	Inverse effect - insignificant	Direct effect - insignificant	Direct effect - significant	Inverse effect - significant
T12 Fz	Direct effect - insignificant	Inverse effect - insignificant	Direct effect - significant	Inverse effect - significant
Combined	Inverse effect - insignificant	Direct effect - insignificant	Direct effect - significant	Inverse effect - significant

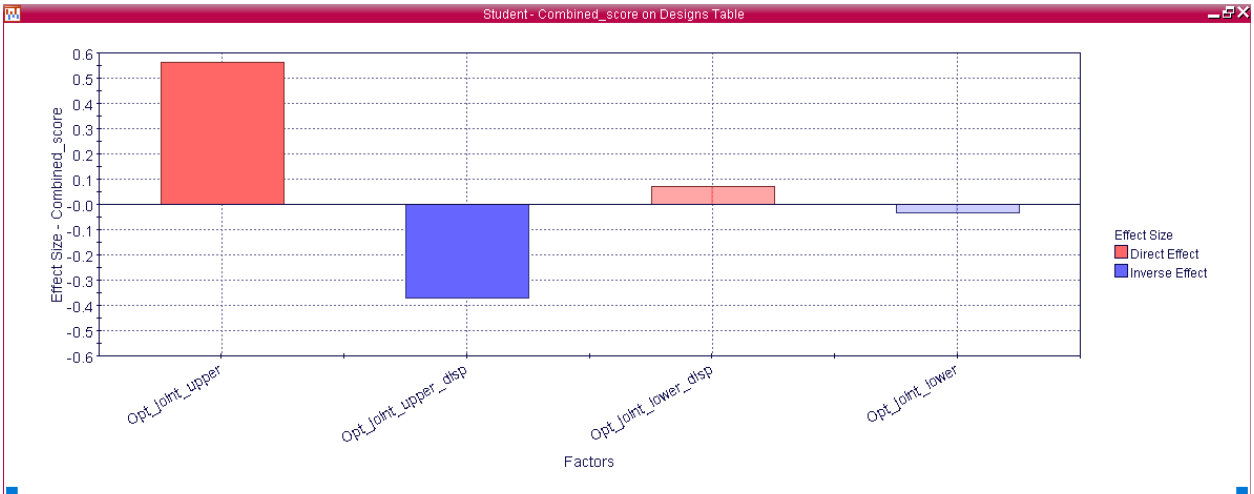

Factors	Effect Size	Significance	t-Student	critical t (sig. = 0.10)	critical t (sig. = 0.05)	critical t (sig. = 0.01)
Opt_joint_upper	5.6308E-1	0.000	8.8485E0	1.2902E0	1.6606E0	2.3650E0
Opt_joint_upper_disp	-3.6989E-1	0.000	4.8202E0	1.2902E0	1.6606E0	2.3650E0
Opt_joint_lower_disp	6.8875E-2	0.210	8.0965E-1	1.2902E0	1.6606E0	2.3650E0
Opt_joint_lower	-3.4394E-2	0.344	4.0330E-1	1.2902E0	1.6606E0	2.3650E0

Figure 7-35. Sensitivity analysis output from modeFRONTIER for combined score for reclined posture with vest

Figure 7-36 shows the convergence of the optimization process to a stable solution after approximately 100 runs.

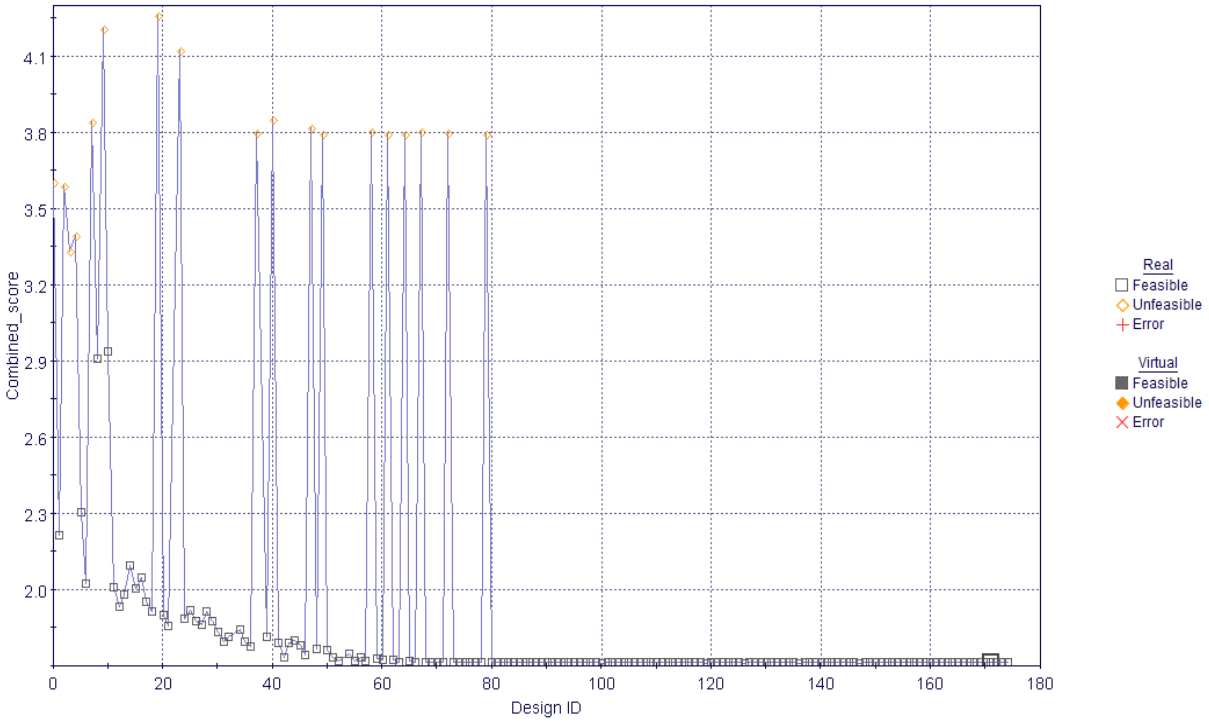

Figure 7-36. Optimization process with minimizing combined score shows convergence on a solution for reclined posture with vest

Table 7-18 contains the optimized values for each parameter. The values in general are similar to those of the other configurations, with the upper joint displacement nearly at the 0.152 m (6 inch) displacement maximum. Table 7-19 lists the individual injury criteria normalized values. The increase to Pelvis Fz and T12 Fx demonstrate the added complexity of the heavier vest mass coupled with the increased shear forces due to the reclined posture. The details of the sensitivity and optimization analysis are contained in Appendix I.

Table 7-18. Optimization combination for PMHS Condition B for reclined seat with vest

Parameter Name	Description	Optimized value
Opt_joint_lower	Shear pin force	2.075 kN
Opt_joint_lower_disp	Shear pin activation displacement	0.001 m (0.04 inch)
Opt_joint_upper	EA device maximum load	5.125 kN
Opt_joint_upper_disp	EA device maximum displacement	0.151 m (5.94 inches)

Table 7-19. Normalized injury values for optimal combination for reclined seat with vest

	Pelvis Az	Pelvis Fx	Pelvis Fz	T12 Az	T12 Fx	T12 Fz	Combined Score
Normalized value	0.050	0.146	0.527	0.137	0.404	0.451	1.714

As with the added vest mass, the final seat velocity of the optimized solution was close to 2.2 m/s (Figure 7-37). The final reduction in pelvis and T12 forces and accelerations compared to the non-optimized configuration are shown in Figure 7-38 through Figure 7-43.

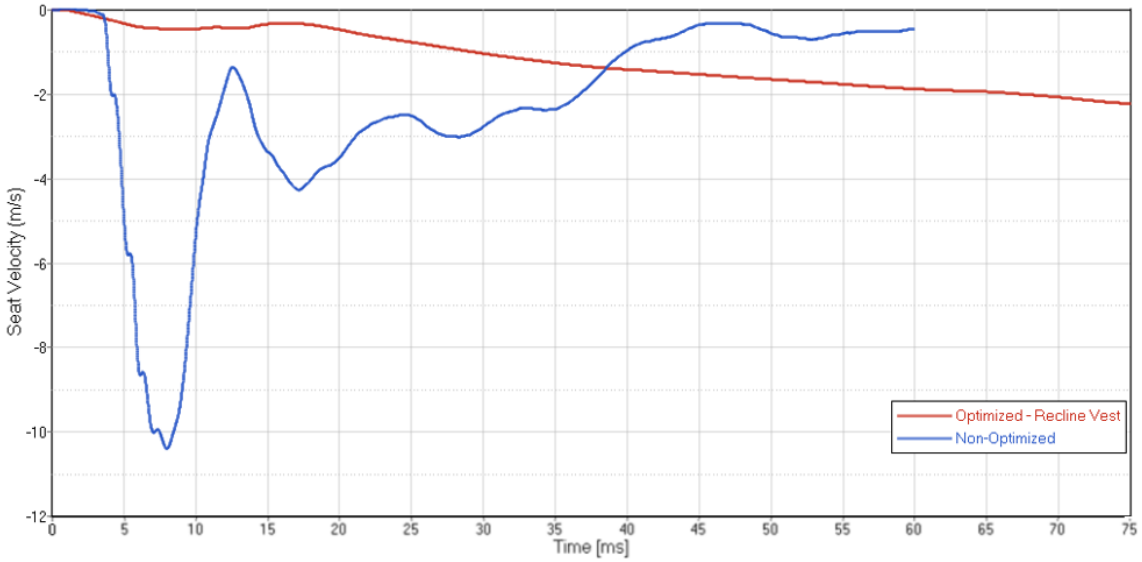

Figure 7-37. Seat velocity of optimal EA mechanism combination (red) compared to non-optimized combination (blue) for reclined posture with added vest mass

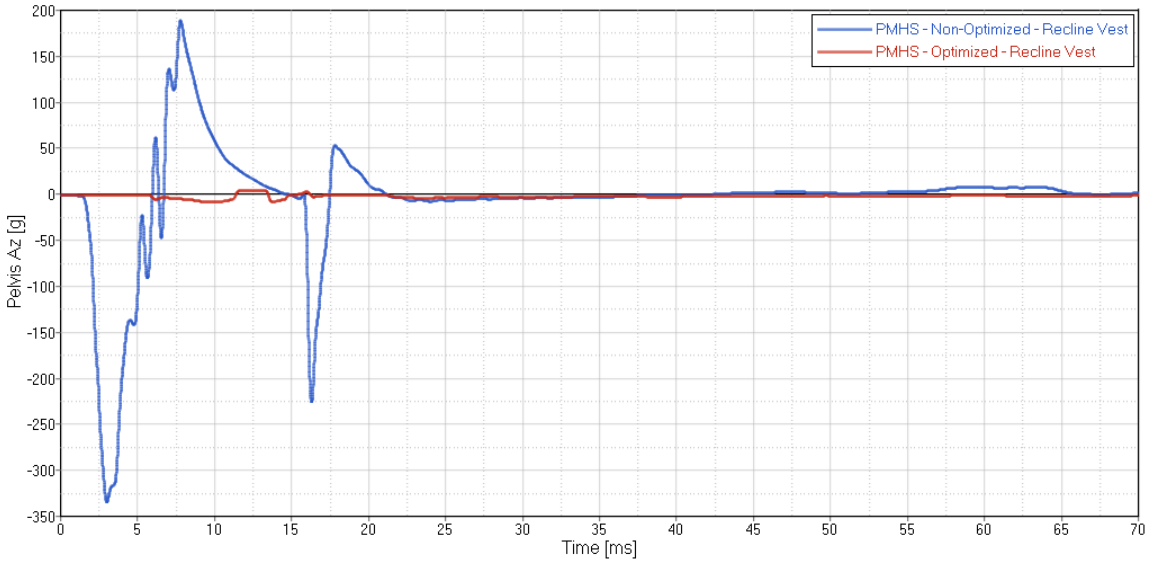

Figure 7-38. Pelvis Az of optimal EA mechanism combination (red) compared to non-optimized combination (blue) for reclined posture with added vest mass

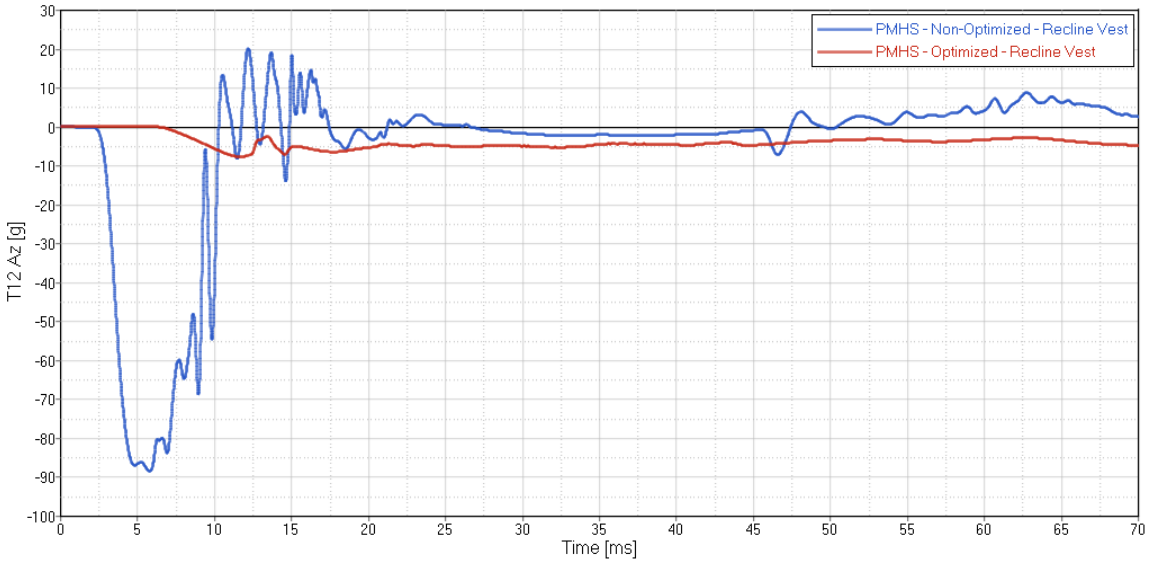

Figure 7-39. T12 Az of optimal EA mechanism combination (red) compared to non-optimized combination (blue) for reclined posture with added vest mass

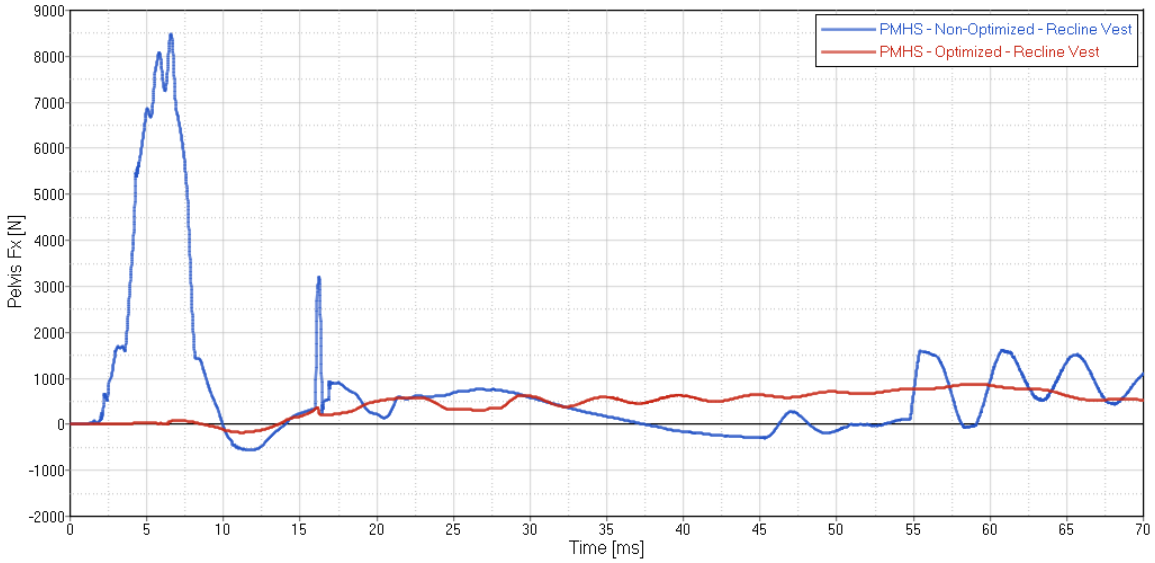

Figure 7-40. Pelvis Fx of optimal EA mechanism combination (red) compared to non-optimized combination (blue) for reclined posture with added vest mass

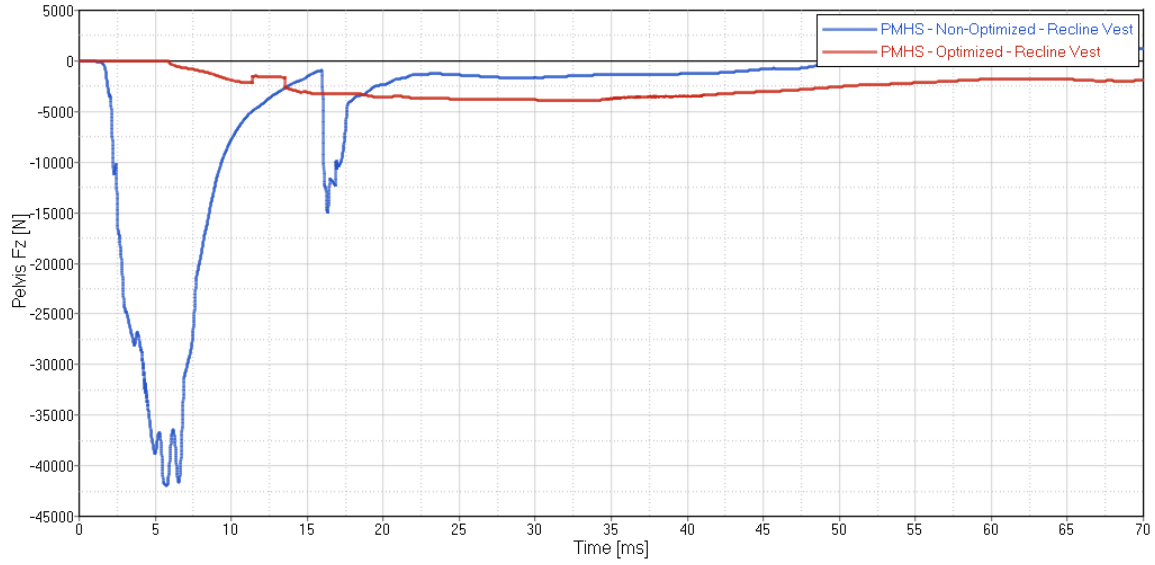

Figure 7-41. Pelvis Fz of optimal EA mechanism combination (red) compared to non-optimized combination (blue) for reclined posture with added vest mass

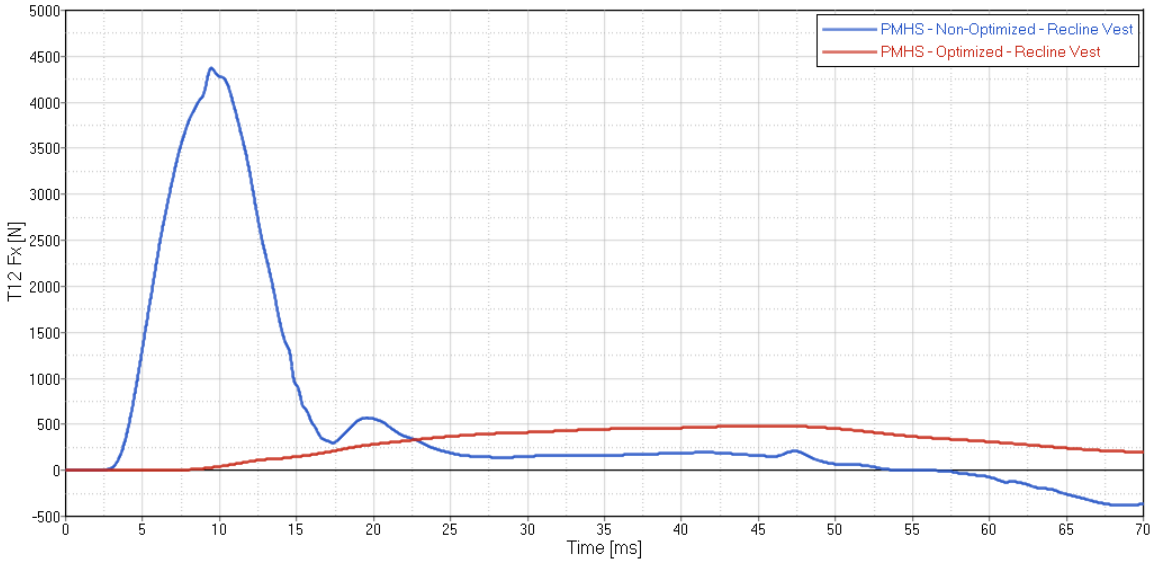

Figure 7-42. T12 Fx of optimal EA mechanism combination (red) compared to non-optimized combination (blue) for reclined posture with added vest mass

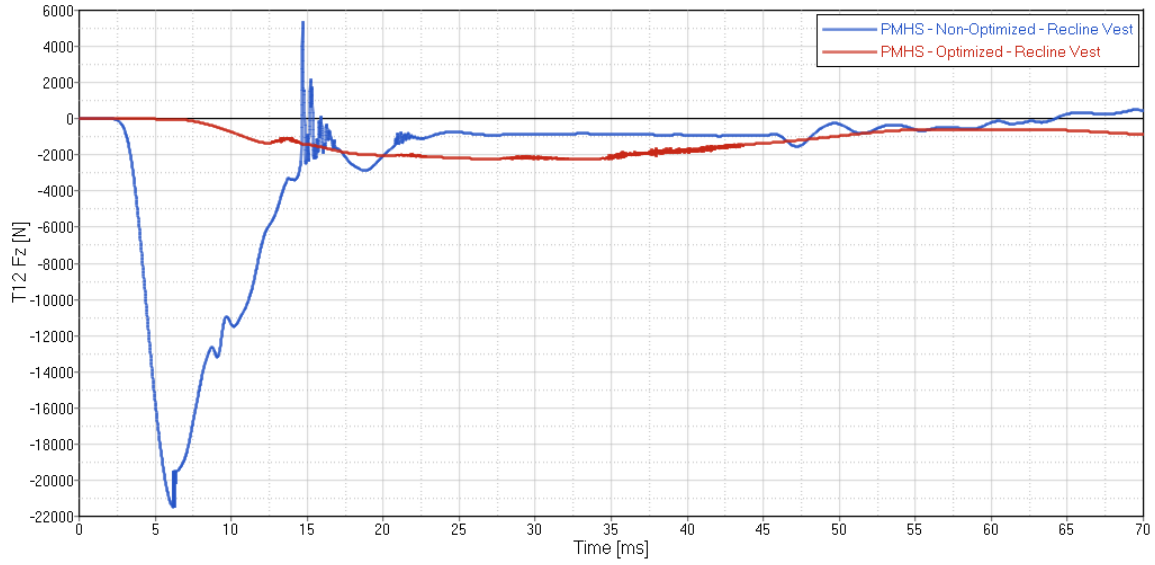

Figure 7-43. T12 Fz of optimal EA mechanism combination (red) compared to non-optimized combination (blue) for reclined posture with added vest mass. Data was filtered at CFC 60 Hz to remove noise due to the interaction between Kelvin restraints.

7.6. Specific Aim 3 – Seat Optimization – Summary

Overall, the sensitivity analysis and optimization process for all four configurations (nominal posture, reclined posture, added vest mass, and reclined posture with added vest mass) produced similar results. The upper joint displacement and limiting force were almost always significant across all configurations. In general, the upper joint displacement tended toward the upper limit around 0.152 m (6 inches), as expected. The upper joint force was usually at the lower end of the bound, around 5 kN, which is below the expected injury range and produced non-injurious results. The lower joint, although not listed as a statistically significant contributor to the final injury values, tended to be optimal when the shear pin displacement was less than 0.017 m (0.67 inch) and close to the lower limit of 2 kN. The optimization process also demonstrated that local minima may be found as in the case with the recline posture, but with the constraint that no injury value could exceed its respective IARV, any solution should prevent pelvic or lower spine fracture based on known injury criteria limits.

Table 7-20 contains the injury metric results and combined score for each configuration. Pelvis Fz and T12 Fz were the most influential parameters for dictating the overall combined injury score, as the pelvis received the force first during loading, which was then transmitted up the spine. In the model, the forces are transmitted directly from vertebra to vertebra, as well as through the Kelvin restraints as shown in Figure 6-9, as these provide a significant parallel load path. The forces reaching T12 were attenuated by the lumbar spine segment and sacroiliac joint. T12 Fx was also influential, as the spine generally had lower force and acceleration injury limits than the pelvis. In general, the addition of the vest mass increased the combined score, and the reclined posture had a

slight reduction in overall combined score due to the redistribution of loading. All optimized force and deflection configurations resulted in seat velocities below the known non-injurious limit of 4 m/s (Figure 7-44).

Table 7-20. Summary of injury results for each configuration; actual values are listed for the normalized posture

	Pelvis Az	Pelvis Fx	Pelvis Fz	T12 Az	T12 Fx	T12 Fz	Combined Score
Nominal Posture Normalized Value [Actual Value]	0.046 [8 g]	0.184 [1106 N]	0.445 [3339 N]	0.276 [15 g]	0.268 [322 N]	0.438 [2279 N]	1.658
Reclined Posture Normalized Value	0.096	0.045	0.466	0.227	0.281	0.498	1.614
Reclined Posture (3kN lower joint limit) Optimized Value	0.081	0.049	0.419	0.200	0.249	0.444	1.442
Added Vest Mass Normalized Value	0.062	0.170	0.524	0.219	0.405	0.467	1.847
Reclined Posture with Added Vest Mass Normalized Value	0.050	0.146	0.527	0.137	0.404	0.451	1.714

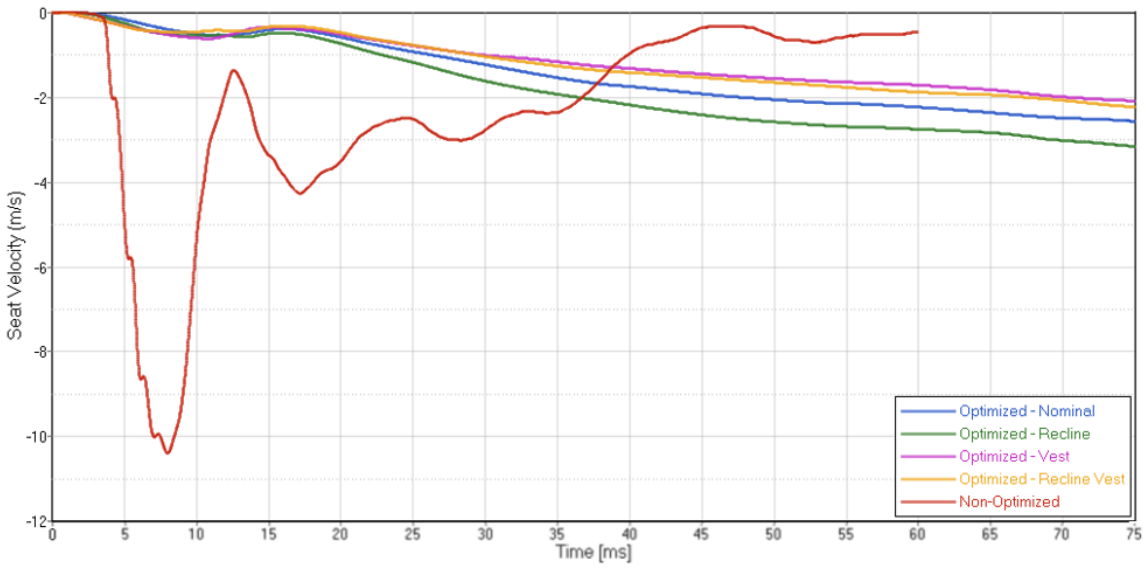

Figure 7-44. Seat velocity of optimal EA mechanism combination for all four configurations compared to non-optimized combination (blue)

This study demonstrates that the optimization tool for determining force and deflection properties for lower shear pin and upper load limiter can successfully produce a stable solution with the goal of reducing injury to the pelvis and lower spine within set parameters; however, more validation would be required to utilize this tool with a significantly different input pulse to ensure the HBM is tuned before optimization is conducted. This tool can also be used to assess the predicted injury outcomes with a prescribed EA mechanism configuration with defined upper and lower joint parameters.

7.7. Specific Aim 3 – Seat Optimization – Limitations

There are several limitations of note within the optimization portion of this study. There is limited research on underbody blast injury thresholds; as such, the latest and most pertinent injury values were used when setting up the normalized injury value. The selection of the lowest reported fracture force and acceleration values provides a more conservative approach to the optimization study. As all of the normalized injury values

were below 0.53, updating the injury thresholds as more data becomes available is not expected to drastically change the optimization outcome. When injury risk curves are available, this research can be updated with improved injury criteria. It should also be noted that future injury thresholds should take into account the longer duration of loading introduced by an EA seat, which has been shown to cause a superior migration of injuries [75]. Additionally, weighting factors can be added into the combined injury score to place greater emphasis on channels considered to be more influential for future studies.

There is limited public data available for shear pin parameters including release force. The optimization parameters for the lower shear pin were based on limited patent data and the author's work experience. As more information is made available, the shear pin parameters can be tuned based on individual seat durability requirements.

This research focused on a simple linear EA profile based on known stroke profiles from helicopter seats and so as to provide basic profiles for EA manufacturers to replicate. This study can be repeated with more complex profiles if required based on the selection of EA device for a particular seat.

Validation was not possible for the reclined posture or added vest mass in Condition B, as tests with PMHS in these scenarios have not yet been conducted. The vest is considered an approximation of an IOTV, but this study shows that the additional mass has an effect on final optimal parameters. This information can be expanded upon when considering designing a seat for the full occupant range including the 5th percentile female up to the 95th percentile male.

CHAPTER 8 – SPECIFIC AIM 4 – HYBRID III SEAT OPTIMIZATION

8.1. Specific Aim 4 – Hybrid III Rigid Seat Validation – Condition B – Model Conditions

As most EA seat manufacturers do not currently have access to PMHS or WIAMan for their testing, the Hybrid III is the most common tool to assess EA seat performance. Condition B seat and floor acceleration pulses were input to the Hybrid III model, and the model validation process was repeated. As with the HBM, it was rate sensitive, meaning that the major parameters required different scaling factors than those in Condition A.

Three tests at the Condition B configuration were available to create the Hybrid III BRCs (Table 8-1). The same pelvis was used for all three tests, which was known to have pelvis punch-through, where the metal ischial tuberosities pierce the pelvis flesh. The Hybrid III did not have lumbar spine load cells, as the forces imparted to the lumbar spine during this high acceleration condition were beyond the limitations of the instrumentation. In addition to the lower leg load cells and accelerometers and pelvis accelerometers, a T1 accelerometer was added for this analysis (Table 8-2).

Table 8-1. Floor and seat accelerations and velocities for Condition B

Test ID	Peak floor velocity (m/s) in (ms)	Peak seat velocity (m/s) in (ms)	Peak floor acceleration (g) in (ms)	Peak seat acceleration (g) in (ms)
2.1	10.2 in 4.8	10.8 in 2.9	517 in 1.3	919 in 1.9
2.2	9.8 in 4.8	8.8 in 4.5	565 in 1.2	701 in 3.2
2.5	8.0 in 5.5	9.7 in 4.8	530 in 1.4	421 in 2.8

Table 8-2. Validation channels used for Hybrid III Condition B model

Hybrid III Channels – Legs	Hybrid III Channels – Upper Body
Lower Tibia Fx	Pelvis Ax
Lower Tibia Fz	Pelvis Az
Upper Tibia Fx	T1 Ax
Upper Tibia Fz	T1 Az
Tibia Ax	
Tibia Az	

As with the transition from Condition A to Condition B for HBM, the characteristics for the boot and between the pelvis and seat were altered to achieve correlation, with the final characteristics shown in Figure 8-1 and Figure 8-2. External Kelvin restraints were added to each lower leg between the shoe and tibia to reduce a collapsing issue between the segments which was not realistic (final characteristics shown in Figure 8-3). Additionally, an external Kelvin restraint was added between the pelvis and spine box to stiffen the lumbar spine to improve the phasing of the T1 accelerometer (final characteristics shown in Figure 8-4). The Hybrid III was positioned according to videos of the setup, which was at the nominal 90-90-90 posture for ankles, knees, and pelvis. The joint positions were adjusted as needed to achieve correlation.

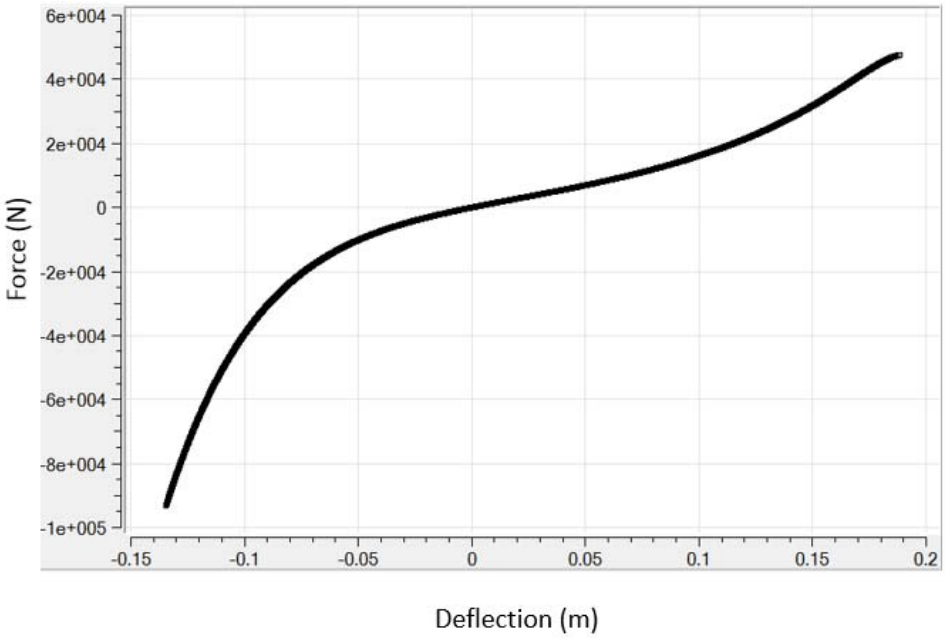

Figure 8-1. Final force (N) deflection (m) properties for boot/floor contact

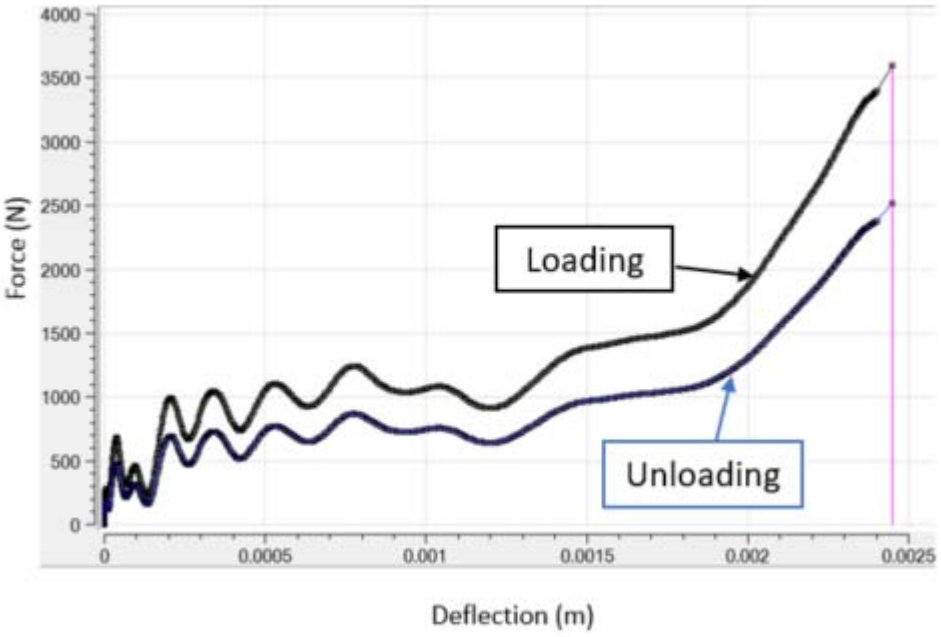

Figure 8-2. Final force (N) deflection (m) properties for pelvis/seat contact

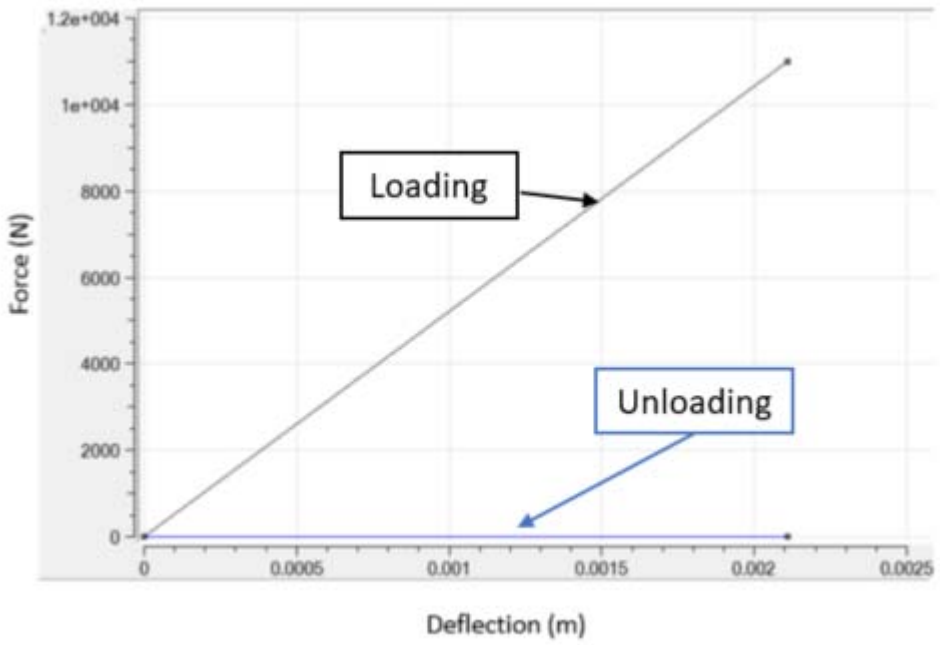

Figure 8-3. Final force (N) deflection (m) properties for Kelvin restraint between shoe and tibia

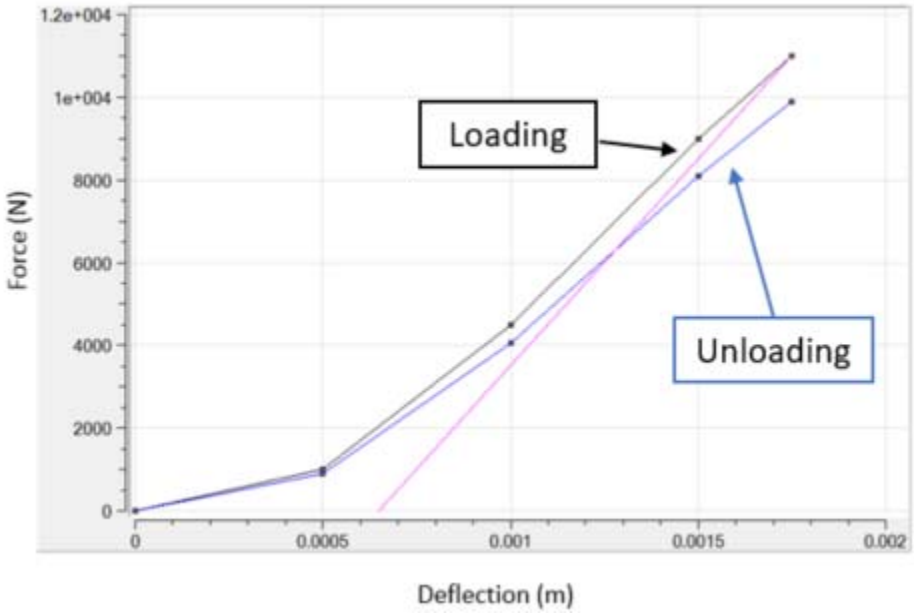

Figure 8-4. Final force (N) deflection (m) properties for Kelvin restraint between spine box and pelvis

8.2. Specific Aim 4 – Hybrid III Rigid Seat Validation – Condition B – CORA Rating

BRCs were created for each lower leg and lower body channel in the same manner as the PMHS corridors. A series of approximately 85 investigative runs and a series of eight DOEs using Random Latin Hypercube for 100 runs each to maximize the correlation CORA score for the simulation. These DOEs were focused by body region (lower legs, pelvis, and T1), and included sweeps of boot and pelvis contact property scaling, damping coefficients, lower leg joint positioning, scaling properties of the T1 Kelvin restraint, and accelerometer orientation. Engineering judgement was used to review the top CORA scores and select the best run from each DOE to start the next DOE based on the best match for peak and overall shape. The final CORA scores are shown in Table 8-3. The Overall CORA score is 0.711, with more than half of the channels in the Good category. The Correlation score was used as the primary assessment score, which was 0.818 (Good), with half of the channels scoring Excellent. The corridors for this data set were often narrow, so emphasis was placed on the Correlation score over the Corridor score when assessing the final validation model configuration. The final CORA output files are contained in Appendix J.

Table 8-3. Final CORA score for Hybrid III Condition B

10 m/s	Corridor	Correlation		Overall CORA
Lower Tibia Fx	0.579	0.892		0.780
Lower Tibia Fz	0.450	0.940		0.765
Lower Tibia My	0.507	0.924		0.775
Upper Tibia Fz	0.373	0.736		0.606
Upper Tibia Ax	0.844	0.733		0.773
Upper Tibia Az	0.578	0.941		0.811
Pelvis Ax	0.446	0.694		0.606
Pelvis Az	0.337	0.813		0.643
T1 Ax	0.482	0.887		0.742
T1 Az	0.577	0.622		0.606
CORA TOTAL	**0.517**	**0.818**		**0.711**

The final overlays for the Condition B Hybrid III runs from UVA testing compared with the MADYMO simulations are contained in Figure 8-5 through Figure 8-14. In accordance with the CORA score, the general shape and peak for each channel was maintained, but the corridors on most channels are small, which demonstrates the repeatability of the Hybrid III, even at high input velocities and pelvis punch through.

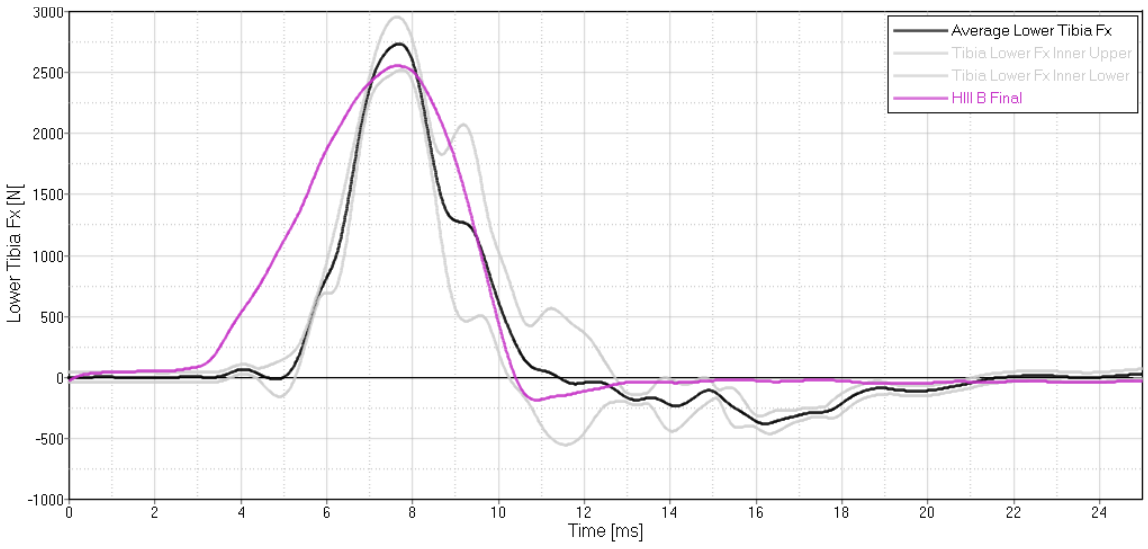

Figure 8-5. Lower Tibia Fx comparing actual Hybrid III (black with grey inner corridor) against the MADYMO simulation (purple)

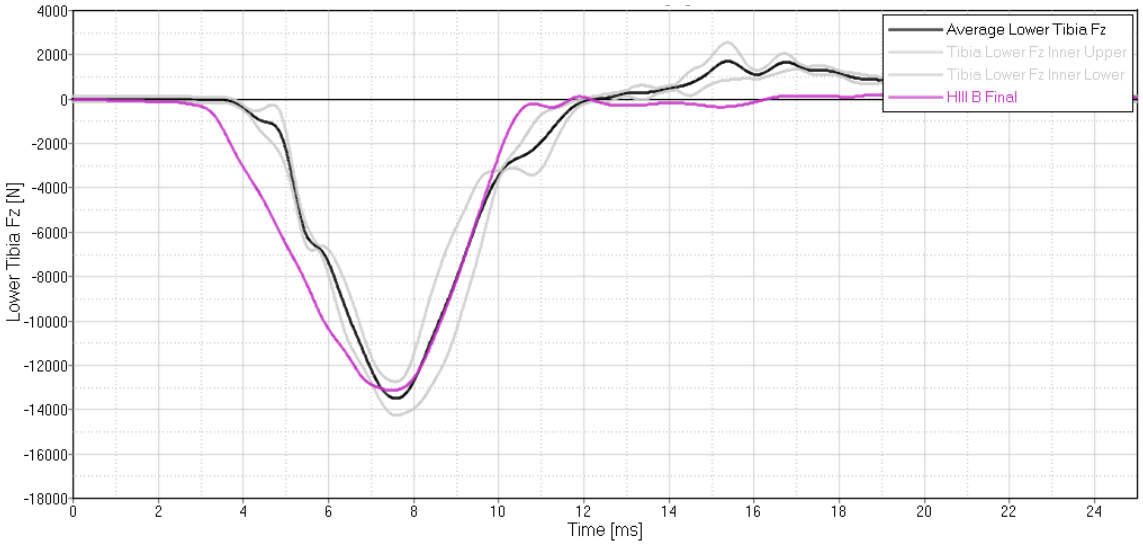

Figure 8-6. Lower Tibia Fz comparing actual Hybrid III (black with grey inner corridor) against the MADYMO simulation (purple)

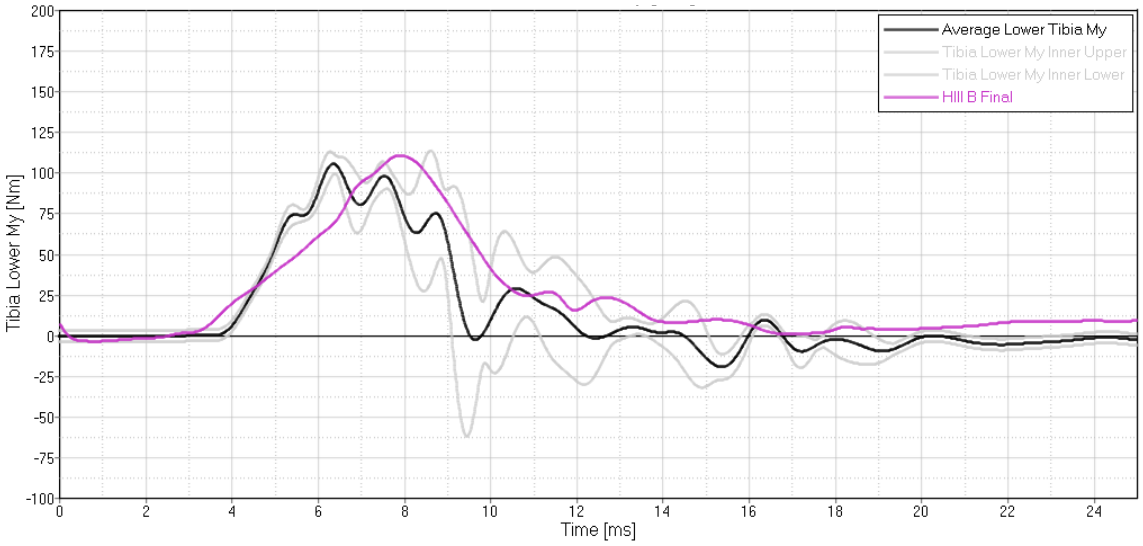

Figure 8-7. Lower Tibia My comparing actual Hybrid III (black with grey inner corridor) against the MADYMO simulation (purple)

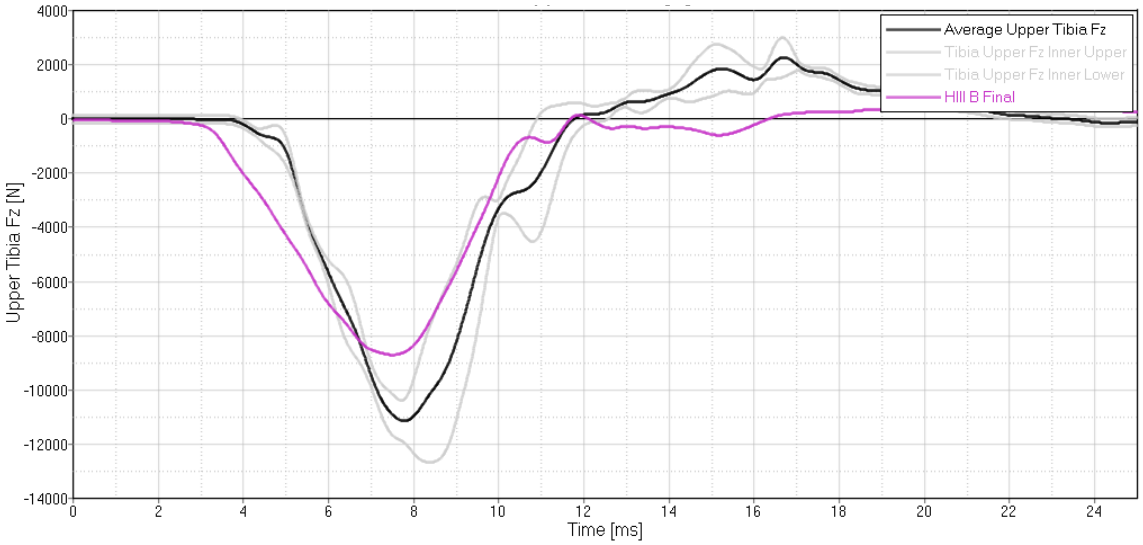

Figure 8-8. Upper Tibia Fz comparing actual Hybrid III (black with grey inner corridor) against the MADYMO simulation (purple)

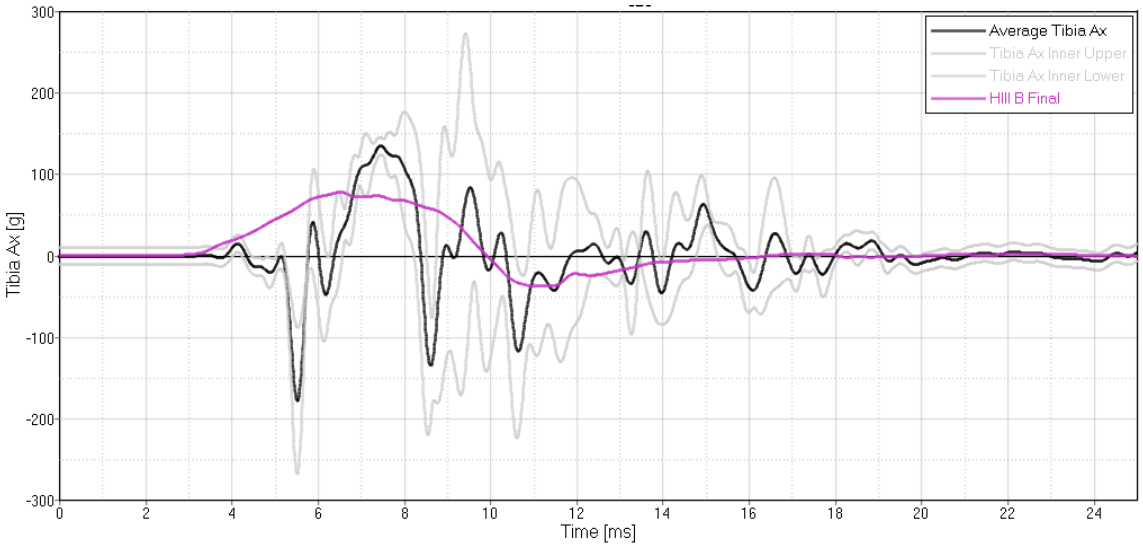

Figure 8-9. Tibia Ax comparing actual Hybrid III (black with grey inner corridor) against the MADYMO simulation (purple)

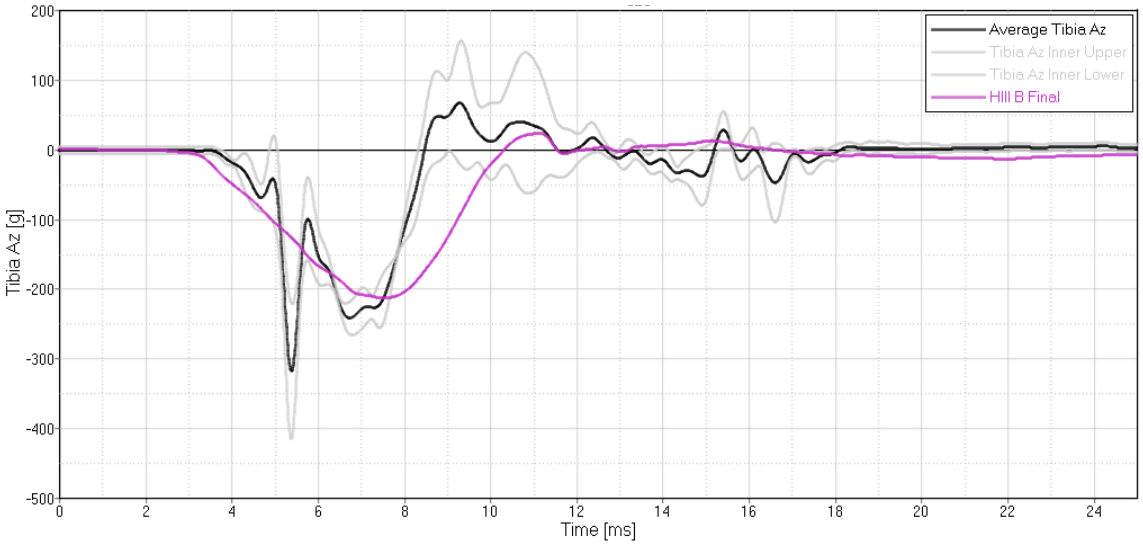

Figure 8-10. Tibia Az comparing actual Hybrid III (black with grey inner corridor) against the MADYMO simulation (purple)

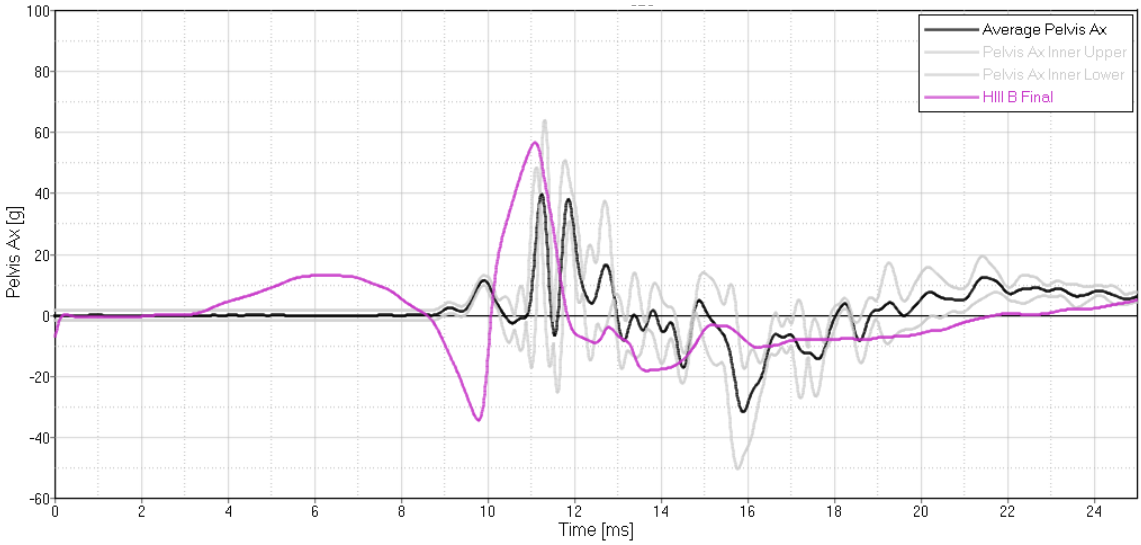

Figure 8-11. Pelvis Ax comparing actual Hybrid III (black with grey inner corridor) against the MADYMO simulation (purple)

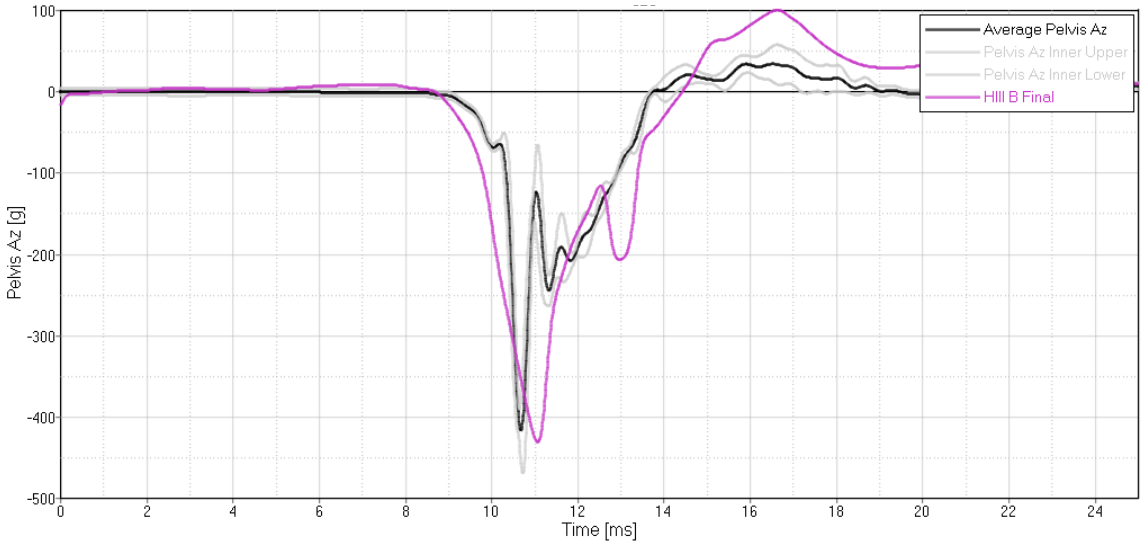

Figure 8-12. Pelvis Az comparing actual Hybrid III (black with grey inner corridor) against the MADYMO simulation (purple)

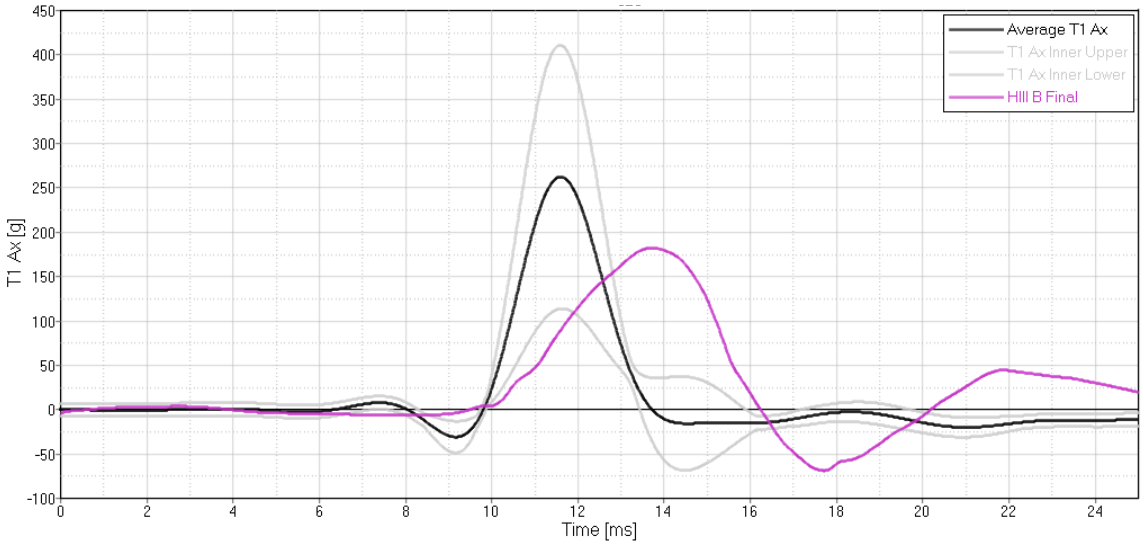

Figure 8-13. T1 Ax comparing actual Hybrid III (black with grey inner corridor) against the MADYMO simulation (purple)

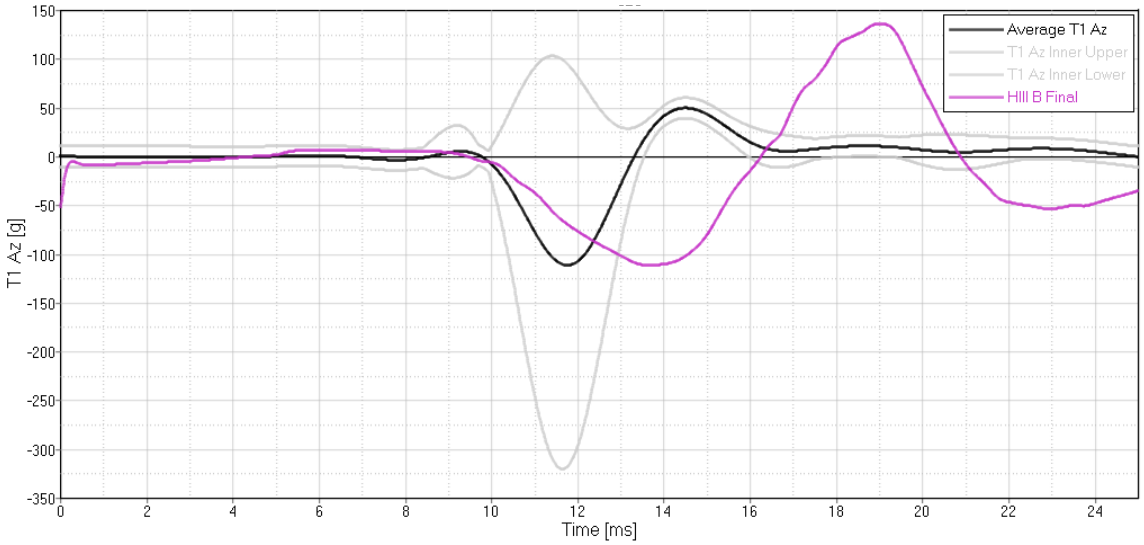

Figure 8-14. T1 Az comparing actual Hybrid III (black with grey inner corridor) against the MADYMO simulation (purple)

8.3. Specific Aim 4 – Hybrid III Rigid Seat Validation – Comparison of Condition A and Condition B and Limitations

Due to the rate dependency of the contact properties of the boot and pelvis, as well as the fidelity of the original MADYMO model, the validation for Condition A was not optimal for Condition B. The collapse of the foot into the tibia is an example of the limitations of the original Hybrid III model when exposed to very high vertical accelerative loads.

Condition B had three tests from which to create BRCs, while Condition A was based on a single test; the repeat tests allowed for corridors showing the variation in testing, compared to the single test performed in Condition A. Condition A testing was able to use a lumbar spine load cell, where Condition B relied only on pelvis and T1 acceleration, as the lumbar spine load cell would have exceeded its limit under the 10 m/s seat velocity. The Condition A validation was limited by balancing the difference

between pelvis acceleration and lumbar spine loading, where this was not a conflict in the Condition B validation.

Based on the acceleration traces, discussions with the UVA test engineers, and prior testing knowledge for high speed vertical loading to the pelvis, the pelvis was damaged during both Condition A and Condition B testing, which is the cause of the large spikes in the Pelvis Az channels. The same pelvis was used for all three Condition B tests and had pelvis punch through, so the metal pelvis was able to contact the metal seat through the pelvis flesh.

The Condition B Hybrid III videos showed some minor inconsistencies in positioning between runs (Figure 8-15), especially in the legs, but the consistency of the data shows that the Hybrid III is relatively insensitive to the differences in positioning. One of the legs was the standard Hybrid III leg, and the other was a MIL-Lx leg, which differs from the Condition A configuration.

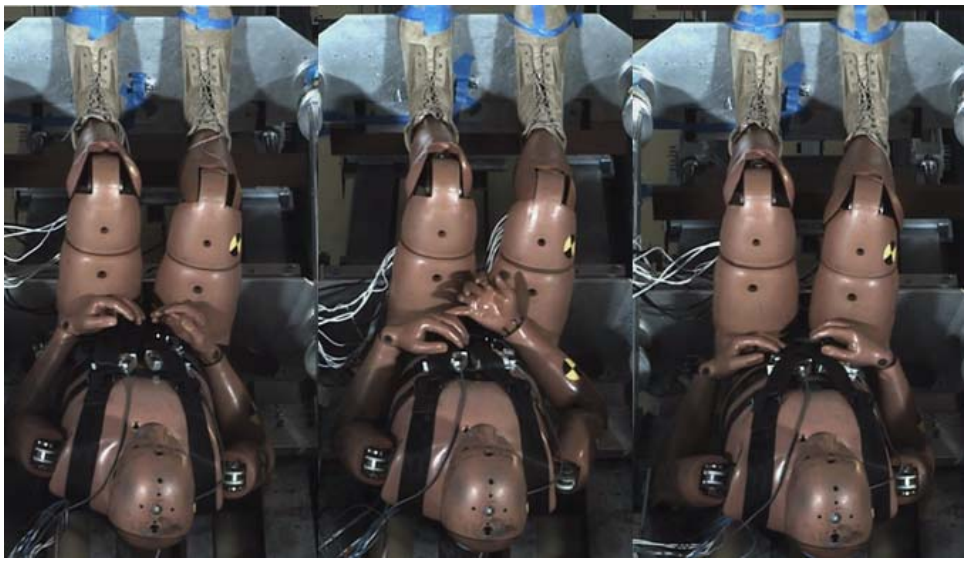

Figure 8-15. Positioning of the Hybrid III in Condition B tests from the videos provided by UVA [6].

8.4. Specific Aim 4 – Hybrid III Rigid Seat Validation – Optimization

Since PMHS are not readily obtainable for testing by EA seat manufacturers, they must rely on the next closest human surrogate, which is currently the Hybrid III until the WIAMan replacement ATD is accessible. There is limited data that connects the performance of a MADYMO HBM to that of the Hybrid III for a seat manufacturer to understand if a non-injurious result for Hybrid III results in a non-injurious condition for a Solider. The final specific aim for this research was to determine if the optimal seat EA mechanism parameters that lead to a non-injurious seat velocity for the HBM would also reflect a non-injury condition for Hybrid III using available Injury Assessment Reference Values (IARVs) as referenced in Chapter 3.

As with the HBM, the rigid seat model for the Hybrid III for both Condition A and Condition B were updated with the translational joint between the seat and floor to represent an EA mechanism (Figure 8-16). The upper and lower joints were set to the same parameters as the optimized HBM in the nominal position (Table 8-4), and the 10 m/s seat acceleration pulse from the HBM was set as the input to the floor. Both the Condition A and Condition B Hybrid III models were used to understand how the validation affects the final outcome; the Condition A model was validated at seat velocities closer to the final optimized seat velocity, but the validation was only based on one test. The Condition B model was also assessed because of its improved correlation based on BRCs from three tests. The pelvis was likely already damaged in both Condition A and Condition B validations.

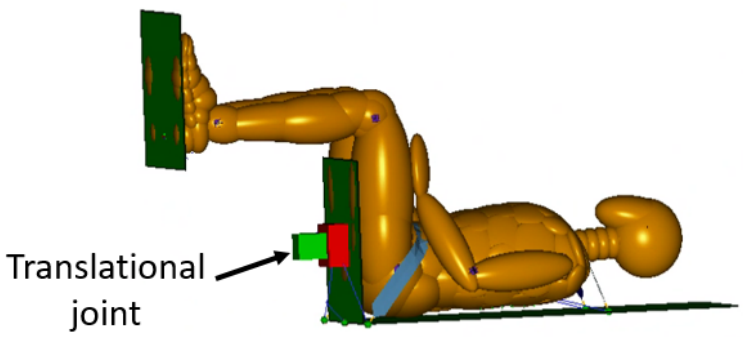

Figure 8-16. Hybrid III MADYMO model showing location of enlarged translational joint connecting center of seat to center of floor platen for stroking mechanism. Translational joint only allows motion along the local z-axis (from feet to head)

Table 8-4. Optimization combination for PMHS Condition B

Parameter Name	Description	Optimized value
Opt_joint_lower	Shear pin force	2.001 kN
Opt_joint_lower_disp	Shear pin activation displacement	0.015 m (0.72 inch)
Opt_joint_upper	EA device maximum load	5.000 kN
Opt_joint_upper_disp	EA device maximum displacement	0.145 m (5.71 inches)

The Hybrid III has limited IARVs for underbody blast, so the shear and compressive forces as well as the pelvis z-axis acceleration were extracted for both Condition A and Condition B validated models. As shown in Table 8-5, the two injury criteria for the lumbar spine were not exceeded. The lumbar spine shear (Fx) force for both Condition A and Condition B models were very close, as the model was not specifically tuned differently in this area. The compressive (Fz) force for the lumbar spine shows a larger difference between Condition A and Condition B due to the scaling of the contact force between the pelvis and the seat. Lumbar Fz was also over-predicting the peak during validation by approximately 20% in order to balance the Pelvis

Az channel. The combination of the over-prediction and the contact force scaling would account for the higher Lumbar Fz prediction in the Combination A Hybrid III model. The 7 ms clip was determined for each Hybrid III, and both exceeded the limit significantly. This is likely due to the fact that the pelvis in the validation models experienced metal-to-metal contact with the seat, so the acceleration in the pelvis is much higher than that of an undamaged pelvis. Lumbar spine axial force (Fz) was a much more reliable measure of injury criteria in the vertical loading direction.

Table 8-5. Comparison of Condition A and Condition B Hybrid III IARVs for optimized EA joint

	Lumbar Fx		**Lumbar Fz**		**Pelvis Az**	
IARV Limit	6000 N		6672 N		23 g for 7 ms interval	
Hybrid III A	4070 N	67%	4267 N	64%	172 g	748%
Hybrid III B	3764 N	63%	3764 N	56%	83 g	361%

The seat velocity for Condition A and Condition B compared to the Condition B rigid seat with the 10 m/s pulse are shown in Figure 8-17. The peak optimized seat velocity for Condition A was 4.3 m/s, and 3.7 m/s for the Condition B simulation. Due to the stiffness of the Hybrid III pelvis, the ATD bounced out of the seat and had a noisy interaction with the seatbelts after approximately 75 ms; the peak seat velocity was selected for each curve before the bouncing slingshot phase. The Hybrid III seat velocity was higher than that of the HBM because the Hybrid III's legs are stiffer and unload the thighs, and the pelvis bounces out of the seat due to the stiffness of the pelvis and lumbar spine, so the seat is effectively unloaded earlier, allowing it to attain higher

velocities. The Condition A model has a higher peak seat velocity because the feet move vertically quicker than that of the Condition B model due to the rate dependency of the contact between the boots and floor, so the upper legs are unloaded from the seat at a quicker rate.

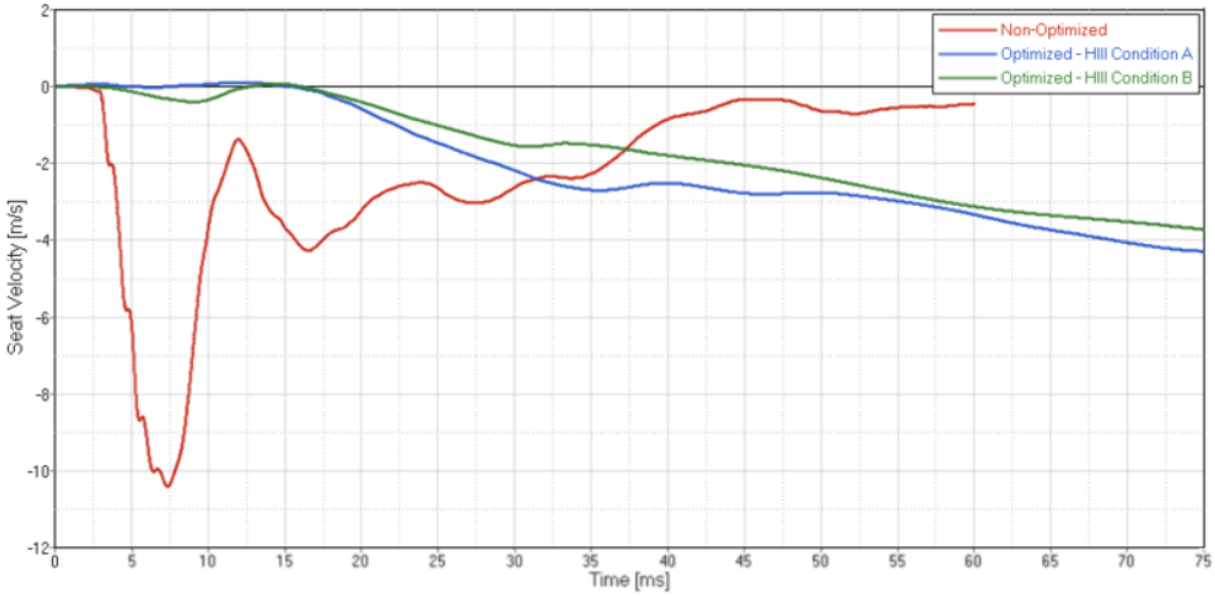

Figure 8-17. Seat velocity of optimal EA mechanism combination (red) compared to non-optimized combination (blue) for reclined posture

The curves comparing Condition A and Condition B for Lumbar Fx, Lumbar Fz, and Pelvis Az are contained in Figure 8-18 through Figure 8-20.

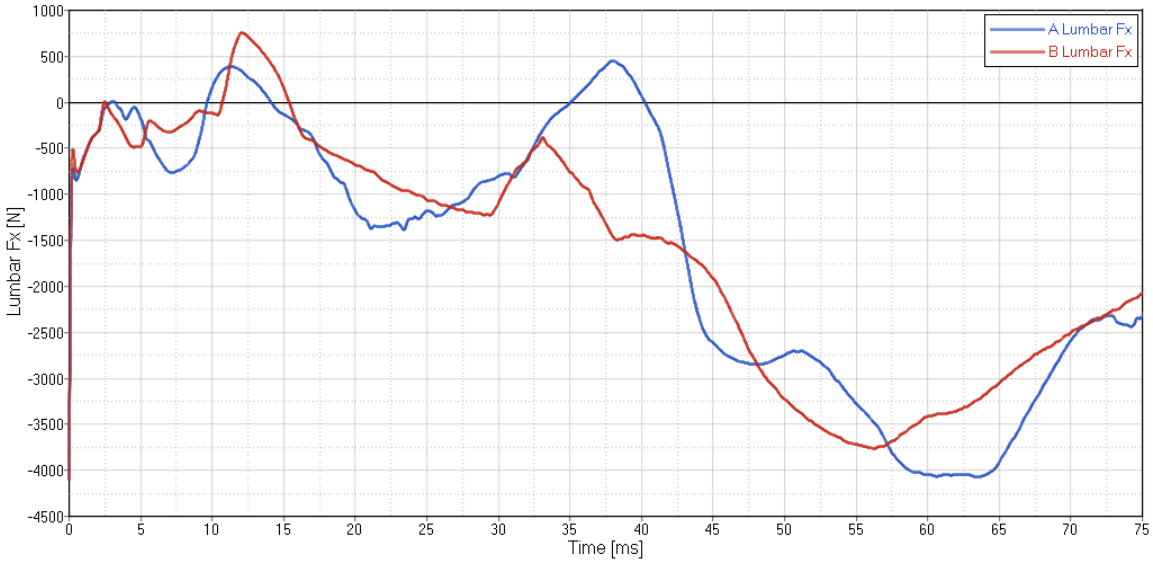

Figure 8-18. Lumbar Fx comparison between Condition A (red) and Condition B (blue) Hybrid III in optimized seat

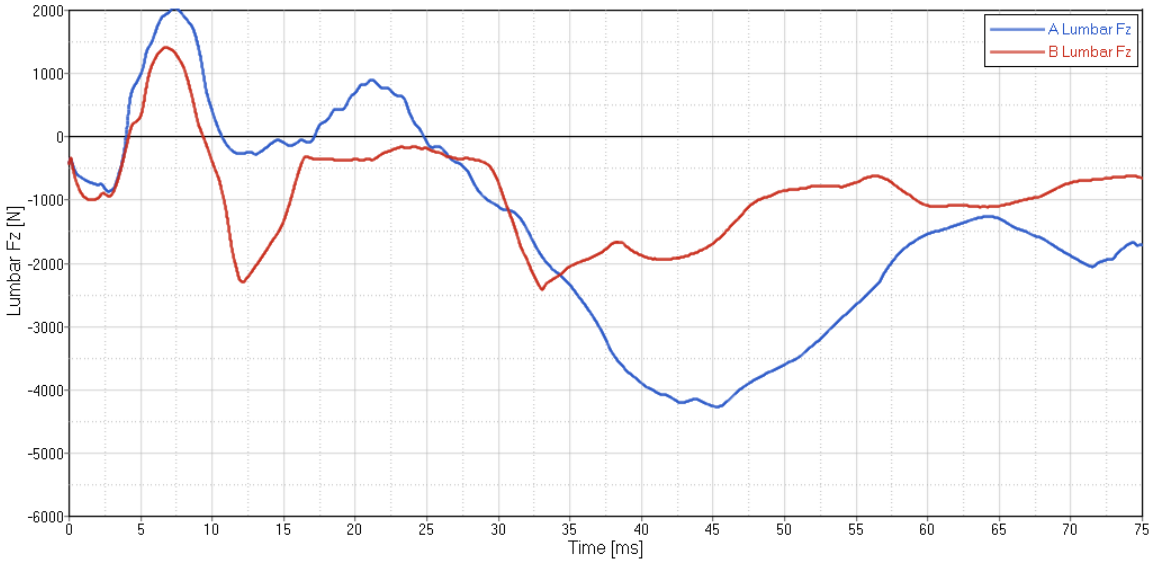

Figure 8-19. Lumbar Fz comparison between Condition A (red) and Condition B (blue) Hybrid III in optimized seat

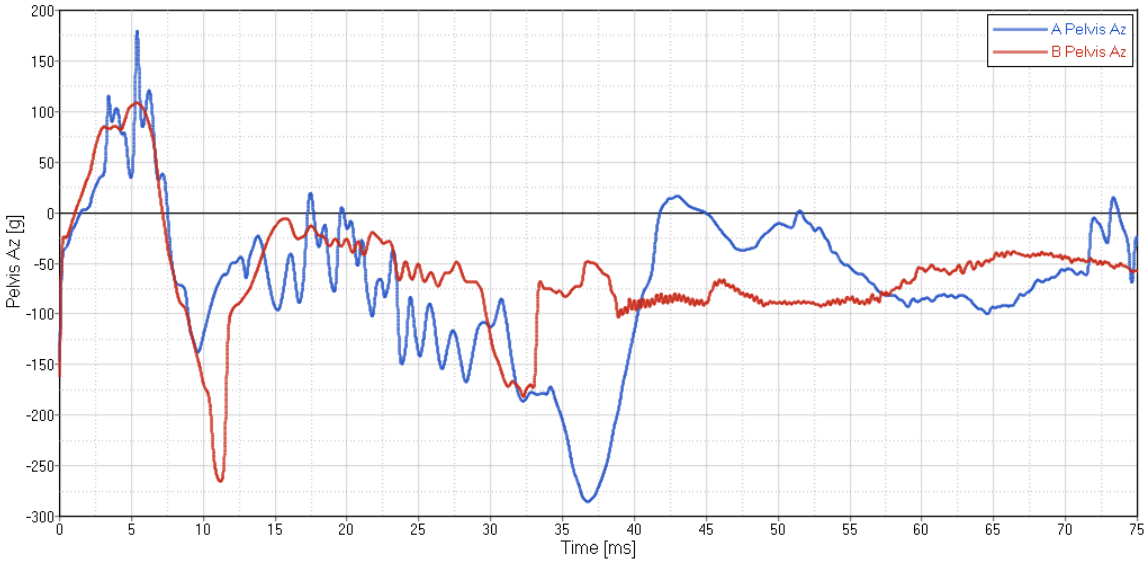

Figure 8-20. Pelvis Az comparison between Condition A (red) and Condition B (blue) Hybrid III in optimized seat

Although the two validated models provide different final seat velocities and lumbar spine forces, they still demonstrate that a non-injurious condition for the Hybrid III results from the optimal seat condition for the HBM. Pelvis Az is obviously over-predicted because of the pelvis punch through condition in the original Hybrid III ATDs used for validation with the metal-to-metal contact between the seat and metal pelvis. Shear forces in the lumbar spine/pelvis complex were over-predicted by approximately 20% with the Hybrid III over the HBM, and compression in this area was over-predicted by 37% by the Hybrid III Condition A model and under-predicted by 29% by the Hybrid III Condition B model, but in general, the Hybrid III is able to confirm via lumbar spine channels if a seat configuration in this velocity input range is able to produce a non-injurious outcome for the HBM.

CHAPTER 9 – CONCLUSIONS

This research aimed to validate the HBM and Hybrid IIII MADYMO models in two underbody blast conditions: Condition A with a 4 m/s seat and floor velocity, which is considered non-injurious, and Condition B with a 10 m/s seat and floor velocity, which is known to produce lower body injury. These models were then used to evaluate an optimization tool developed to guide the design of an underbody blast seat EA mechanism to reduce pelvis and lower spine injury.

9.1. Human Body Model Rigid Seat Validation (Specific Aim 2a and 2b)

The HBM was validated in the Condition A and Condition B model using MADYMO to replicate the PMHS testing conducted on the UVA sled. BRCs were developed from the pertinent instrumentation available on the PMHS for each series. Contact characteristics for the boot and pelvis were added and external Kelvin restraints were implemented in the spine to improve correlation. Using CORA, each BRC was evaluated, and an Overall rating was produced as a combination of Corridor and Correlation score. Both the Condition A and Condition B Overall CORA scores were in the Good rating (0.798 for Condition A and 0.760 for Condition B). As expected, the Corridor scores were lower than the Correlation scores for both conditions, as the Corridors were often narrow and could be noisy, while the Correlation score assessed the peak and shape of the MADYMO curves compared to the BRCs. The Correlation score for Condition A was 0.839, and the Correlation score for Condition B was 0.845. Both validations had about half of the Correlations scores in the Excellent category, including Pelvis Az.

The MADYMO HBM characteristics for the Condition A were applied to the Condition B input model, but due to the rate sensitivity of the contact properties, the Condition A

model characteristics resulted in a Fair CORA score. The contact and restraint properties between the boot and floor, the pelvis and seat, and between spinal segments needed to be scaled to improve the Condition B correlation. The MADYMO HBM internal properties are encrypted, so changes were limited to external restraints to validate the model. Future improvements to the encrypted HBM internal characteristics may allow for a wider range of input velocities to be used with the same model for vertical blast loading.

9.2. Hybrid III Model Rigid Seat Validation (Specific Aim 1 and 4)

The Hybrid III MADYMO model was also validated in the Condition A and Condition B input velocities. The Condition A model was limited to a single experimental test case for comparison, so BRCs could not be created in the same manner as the Hybrid III Condition B and PMHS testing, but CORA was still calculated from the constant corridors created around the single response curve. The Condition A Hybrid III Overall CORA score was Fair (0.507) due to the limitations of having a single file for comparison, although the Overall CORA score for the z-direction channels was 0.674, which was Good. The Condition B correlation was much improved, with an Overall CORA score of 0.711 with a Correlation score of 0.818, which are both in the Good category. As with the HBM, the Hybrid III models required external contact characteristics between the boots and floor and between the pelvis and seat to improve correlation.

The rigid seat validation for the Hybrid III resulted in a similar outcome as that of the HBM. The model from the Condition A did not perform well in the Condition B input velocity, so scaling was required for the boot and pelvis contacts. Additionally, the Hybrid III model was not equipped for the high rate vertical loading, so it was necessary to add Kelvin restraints between the foot and tibia tube to prevent component collapse. A Kelvin

restraint was also added between the pelvis and spine box to improve T1 acceleration response. Future improvements to the encrypted Hybrid III model could address these higher rate loading issues and allow a single set of parameters to apply to a wider range of vertical loading.

9.3. Human Body Model Seat Optimization (Specific Aim 3)

An optimization tool was developed using modeFRONTIER and MADYMO together to guide EA seat mechanism design. This tool concentrated on optimizing the force and deflection limits for the upper and lower bounds of a linear EA mechanism design. The HBM from the Condition A validation was used to produce a seat configuration that reduces the propensity for injury in the pelvis and lower spine.

After the completion of the optimization in the nominal posture, the role of a reclined seat back and added mass from an IOTV were also assessed. The optimization tool shows sensitivity in the outcome, mainly in the lower spine shear force and pelvis axial Fz force. The combined scores ranged from 1.614 for the reclined posture to a maximum of 1.847 for the added vest mass configuration. A combined score above 1.0 does not indicate injury. The purpose of the combined score was not to provide a combined injury probability score, such as that of Nij (Normalized Neck Injury Criterion) or the US New Car Assessment Program (NCAP) scoring, where each injury metric is reported as a probability. The combined score solely functioned as a method for the optimizing software to focus on a single value to minimize, and it can be replaced with single injury thresholds if requested. The lowest combined score was 1.442 for the 3 kN lower EA force limit reclined posture optimization. The reclined posture generally reduced the overall combined score while the added vest mass increased the combined score. Pelvis

Fz and T12 Fz were the greatest contributors to overall combined injury score. Pelvis Az and Fx were the least influential parameters to overall score. The use of the threshold values currently available in literature provided a more conservative approach, as these were based on small sample sets and represented fractures in these tests as opposed to injury probability curves, which had not yet been developed. It is expected that the outcomes would not greatly change as injury probability curves for underbody blast are developed used in future optimization analyses.

For the four configurations assessed, the optimal displacement and force for the upper and lower joints were very similar. The lower joint was generally statistically insignificant to the pelvis and lower spine overall injury criteria, but the shear pin force and displacement were generally at the lower end of the limits (2 kN and less than 0.017 m (0.67 inch)). Although the lower shear pin was not statistically significant to the final injury outcome in this analysis, it could become important when assessing occupants with a wider range of sizes or to ensure that the seat does not inadvertently stroke while operating under normal road conditions.

The upper joint force and displacement was significant for all configurations. As expected, the optimal upper joint force was near the lower limit of 5 kN, and the upper joint displacement was near the upper limit of 0.152 m (6 inches). To reduce injury through a reduction in seat velocity, it was necessary to use the majority of the full 0.152 m of travel distance while reducing the force to a survivable limit.

Currently, this modeFRONTIER optimization setup is only considered valid for the 10 m/s input blast pulse with the HBM validated at 4 m/s. This tool can be updated to assess various blast pulses, alternate profiles for EA mechanisms, different masses, and various

postures. This tool can also be used to assess injury outcomes with a prescribed EA mechanism by modifying the EA joint profile within the MADYMO file. An improved HBM validation model can be introduced when available. The author suggests enhancements to the injury criteria as new data is released.

9.4. Hybrid III Seat Optimization (Specific Aim 4)

The Hybrid III demonstrates the ability to recognize a non-injurious optimized seat configuration for the HBM for the lumbar spine complex. With the Hybrid III data provided for this research, the accelerations measured at the pelvis over-predict injury due to pelvis punch through causing metal-to-metal contact between the Hybrid III pelvis and seat. Future work could include a validation with a pristine Hybrid III pelvis tested in a vertical loading condition that does not result in pelvis punch through to assess the difference in pelvis acceleration. This improved validation could then be used to assess the Hybrid III in the HBM optimized seat configuration to be more representative for the comparison between a new Hybrid III and the HBM.

APPENDIX A – CONDITION A PMHS CORA CPS FILE

```
#########################################################################
#########
#
#   CORA v3.6 - revised parameters (June 2012)
#
#########################################################################
#########
#
#########################################################################
#########
#
#   Global Parameters
#
#########################################################################
#########
BEGIN GLOBAL_PARAMETERS
DES_MOD            WIAMan BRC Evaluation        ; Header of the evaluation
DES_GLO            Biomedical Response Corridors    ; Sub-header of the evaluation
#
# Global settings to define the interval of evaluation
A_THRES            0.03             ; Threshold to set the start of the interval of evaluation
[0,...,1]
B_THRES            0.075             ; Threshold to set the end of the interval of evaluation
[0,...,1]
A_EVAL             0.01             ; Extension of the interval of evaluation [0,...,1]
B_DELTA_END        0.2         ; Additional parameter to shorten the interval of
evaluation (width of the corridor: A_DELTA_END*Y_NORM) 0 = disabled
T_MIN/T_MAX        automatic automatic    ; Manually defined start (time) and end
(time) of the interval of evaluation (automatic = calculated for each channel)
T_UNIT             s                  ; Unit of T_MIN, T_MAX, t_min and t_max

#
# Global settings of the corridor method
K                  1                  ; Transition between ratings of 1 and 0 of the corridor
method [-] (1 = linear, 2 = quadratic ...)
G_1                0.5                ; Weighting factor of the corridor method [-]
a_0/b_0            0.05     0.5       ; Width of the inner and outer corridor [-]
a_sigma/b_sigma     0 0    ; Multiples of the standard deviation to widen the inner and
outer corridor [-]
# Global settings of the cross correlation method
D_MIN              0.010              ; delta_min as share of the interval of evaluation
[0,...,1]
```

```
D_MAX              0.120                ; delta_max as share of the interval of evaluation
[0,...,1]
INT_MIN            0.8              ; Minimum overlap of the interval [0,...,1]
K_V                1                ; Transition between ratings of 1 and 0 of the progression
rating [-] (1 = linear, 2 = quadratic ...)
K_G                1                ; Transition between ratings of 1 and 0 of the size rating [-]
(1 = linear, 2 = quadratic ...)
K_P                1                ; Transition between ratings of 1 and 0 of the phase shift
rating [-] (1 = linear, 2 = quadratic ...)
G_V                0.33333                ; Weighting factors of the progression rating [-]
G_G                0.33333                ; Weighting factors of the size rating [-]
G_P                0.33333                ; Weighting factors of the phase shift rating [-]
G_2                0.5                ; Weighting factors of the cross correlation method [-]
# Normalisation of the the weighting factors
WF_NORM            YES                ; Normalisation of the weighting factors [YES/NO]?
# Signal settings
ISONAME_1-2/11-12   YES YES              ; Consideration of the position 1/2 (test
object, seating position) and 11/12 (fine location 3 - dummy) of the ISO code [YES/NO]
MIN_NORM           0.00                ; Threshold (as fraction of the global absolute
maximum amplitude) to start special treatment of secondary axis [0,...,1]
Y_NORM             extremum             ; Type of calculation of Y_NORM (extremum or
value)
#
# Format settings of the html report
OUTPUT_FORMAT      Hypergraph           ; Export format (LSPOST, PAMVIEW or
Hypergraph)
# Layout of the html report
FONT_SMALL         12                ; Size of the small font
FONT_LARGE         14                ; Size of the large font
PreT_LC/PostT_LC    1  1              ; Expansion of the plotted interval of the curves (-
1: complete curve)
END GLOBAL_PARAMETERS
#
#
#
#
#########################################################################
#########
#
#  Loadcase
#  x = use global settings
#
#########################################################################
#########
#BEGIN LOADCASE
#NAM_LC             WIAMan BRC                    ; Header of the loadcase
```

```
#DES_LC          Loadcase                  ; Sub-header of the loadcase
#WF_LC           1                         ; Weighting factor of the loadcase
#
# Layout of the html report
#PreT_LC         x                         ; Expansion of the plotted interval of the curves
(pre)
#PostT_LC        x                         ; Expansion of the plotted interval of the curves
(post)
#
#
#
#########################################################################
#########



BEGIN LOADCASE
  NAM_LC          Bosch PMHS A-1                                    ; Header of
the loadcase
  DES_LC          Subloadcase               ; Sub-header of the loadcase
  WF_LC           1                         ; Weighting factor of the loadcase
#
# Layout of the html report
  PreT_LC         x                         ; Expansion of the plotted interval of the
curves (pre)
  PostT_LC        x                         ; Expansion of the plotted interval of the
curves (post)
  MinOrd_LC       1.0                       ; Scale factor of the plotted ymin
  MaxOrd_LC       1.0                       ; Scale factor of the plotted ymax
#
  BEGIN SUBLOADCASE
    NAM_SLC       PMHS_A_Foot_Az                  ; Header of the loadcase
    DES_SLC       Foot Az                   ; Sub-header of the loadcase
    WF_SLC        1                         ; Weighting factor of the loadcase
    METHOD        cora
#
BEGIN DATAFILES
#     Name                          unit    g   timeshift
#     Ref
C:/Users/kbosch/Desktop/CORA_MADYMO/PMHS_A/Exp/Foot_Az_RC.dat
m-kg-s  NO  0.0
#     Sim
C:/Users/kbosch/Desktop/CORA_MADYMO/PMHS_A/Sim/9.dat              m-kg-s  NO
0.0

END DATAFILES
```

```
   BEGIN SIGNALS
#    Channels
#    Name           WF  Y_norm   t_min  t_max  g_V  g_G  g_P  g1  g2  a_0  b_0   a_t
a_sigma  b_sigma  D_min  D_max  Filter
     11FOOTLE00H3ACZC     1 x      0      0.025 x    x    x   x   x   x    x
C:/Users/kbosch/Desktop/CORA_MADYMO/PMHS_A/Exp/Foot_Az_Corridor.dat      x
x      x      x      0
   END SIGNALS
  END SUBLOADCASE

####################
  BEGIN SUBLOADCASE
    NAM_SLC         PMHS_A_Tibia_Ax                         ; Header of the loadcase
    DES_SLC         Tibia Ax                        ; Sub-header of the loadcase
    WF_SLC          1                       ; Weighting factor of the loadcase
    METHOD          cora
#

BEGIN DATAFILES
#    Name                           unit    g   timeshift
#    Ref
C:/Users/kbosch/Desktop/CORA_MADYMO/PMHS_A/Exp/Tibia_Ax_RC.dat
m-kg-s  NO  0.0
#    Sim
C:/Users/kbosch/Desktop/CORA_MADYMO/PMHS_A/Sim/9.dat                m-kg-s  NO
0.0

END DATAFILES


   BEGIN SIGNALS
#    Channels
#    Name           WF  Y_norm   t_min  t_max  g_V  g_G  g_P  g1  g2  a_0  b_0   a_t
a_sigma  b_sigma  D_min  D_max  Filter
     11TIBIRILOH3ACXC     1 x      0      0.025 x    x    x   x   x   x    x
C:/Users/kbosch/Desktop/CORA_MADYMO/PMHS_A/Exp/Tibia_Ax_Corridor.dat      x
x      x      x      0
   END SIGNALS
  END SUBLOADCASE

####################
  BEGIN SUBLOADCASE
```

```
   NAM_SLC        PMHS_A_Tibia_Az                    ; Header of the loadcase
   DES_SLC        Tibia Az                  ; Sub-header of the loadcase
   WF_SLC         1                         ; Weighting factor of the loadcase
   METHOD         cora
#

BEGIN DATAFILES
#    Name                          unit   g   timeshift
#    Ref
C:/Users/kbosch/Desktop/CORA_MADYMO/PMHS_A/Exp/Tibia_Az_RC.dat
m-kg-s  NO  0.0
#    Sim
C:/Users/kbosch/Desktop/CORA_MADYMO/PMHS_A/Sim/9.dat              m-kg-s  NO
0.0

END DATAFILES


   BEGIN SIGNALS
#    Channels
#    Name          WF  Y_norm   t_min  t_max  g_V  g_G  g_P  g1  g2  a_0  b_0   a_t
a_sigma  b_sigma  D_min  D_max  Filter
     11TIBIRILOH3ACZC    1 x      0     0.025 x   x   x  x  x   x   x
C:/Users/kbosch/Desktop/CORA_MADYMO/PMHS_A/Exp/Tibia_Az_Corridor.dat     x
x      x      x      0
   END SIGNALS
  END SUBLOADCASE


####################
  BEGIN SUBLOADCASE
   NAM_SLC        PMHS_A_Femur_Ax                    ; Header of the loadcase
   DES_SLC        Femur Ax                  ; Sub-header of the loadcase
   WF_SLC         1                         ; Weighting factor of the loadcase
   METHOD         cora
#

BEGIN DATAFILES
#    Name                          unit   g   timeshift
#    Ref
C:/Users/kbosch/Desktop/CORA_MADYMO/PMHS_A/Exp/Femur_Ax_RC.dat
m-kg-s  NO  0.0
#    Sim
C:/Users/kbosch/Desktop/CORA_MADYMO/PMHS_A/Sim/9.dat              m-kg-s  NO
0.0
```

```
END DATAFILES


   BEGIN SIGNALS
#    Channels
#    Name           WF  Y_norm   t_min  t_max  g_V  g_G  g_P  g1  g2  a_0  b_0   a_t
a_sigma  b_sigma  D_min  D_max  Filter
     11FEMRLE00H3ACXC     1 x      0      0.025 x    x    x  x  x    x    x
C:/Users/kbosch/Desktop/CORA_MADYMO/PMHS_A/Exp/Femur_Ax_Corridor.dat      x
x      x      x      0
   END SIGNALS
  END SUBLOADCASE


####################
  BEGIN SUBLOADCASE
   NAM_SLC         PMHS_A_Pelvis_Ax                        ; Header of the loadcase
   DES_SLC         Pelvis Ax                          ; Sub-header of the loadcase
   WF_SLC          1                           ; Weighting factor of the loadcase
   METHOD          cora
#

BEGIN DATAFILES
#    Name                          unit    g   timeshift
#    Ref
C:/Users/kbosch/Desktop/CORA_MADYMO/PMHS_A/Exp/Pelvis_Ax_RC.dat
m-kg-s  NO  0.0
#    Sim
C:/Users/kbosch/Desktop/CORA_MADYMO/PMHS_A/Sim/9.dat                m-kg-s  NO
0.0

END DATAFILES


   BEGIN SIGNALS
#    Channels
#    Name           WF  Y_norm   t_min  t_max  g_V  g_G  g_P  g1  g2  a_0  b_0   a_t
a_sigma  b_sigma  D_min  D_max  Filter
     11PELV0000H3VAXC     1 x      0      0.025 x    x    x  x  x    x    x
C:/Users/kbosch/Desktop/CORA_MADYMO/PMHS_A/Exp/Pelvis_Ax_Corridor.dat      x
x      x      x      0
   END SIGNALS
  END SUBLOADCASE

####################
  BEGIN SUBLOADCASE
```

```
   NAM_SLC         PMHS_A_Pelvis_Az                    ; Header of the loadcase
   DES_SLC         Pelvis_Az                  ; Sub-header of the loadcase
   WF_SLC          1                   ; Weighting factor of the loadcase
   METHOD          cora
#

BEGIN DATAFILES
#    Name                          unit    g   timeshift
#    Ref
C:/Users/kbosch/Desktop/CORA_MADYMO/PMHS_A/Exp/Pelvis_Az_RC.dat
m-kg-s  NO  0.0
#    Sim
C:/Users/kbosch/Desktop/CORA_MADYMO/PMHS_A/Sim/9.dat              m-kg-s  NO
0.0

END DATAFILES


   BEGIN SIGNALS
#    Channels
#    Name           WF  Y_norm   t_min  t_max  g_V  g_G  g_P  g1  g2  a_0  b_0   a_t
a_sigma  b_sigma  D_min  D_max  Filter
     11PELV0000H3VAZC    1 x      0      0.025 x    x    x  x  x    x    x
C:/Users/kbosch/Desktop/CORA_MADYMO/PMHS_A/Exp/Pelvis_Az_Corridor.dat     x
x      x      x      0
   END SIGNALS
  END SUBLOADCASE


####################
#  BEGIN SUBLOADCASE
#    NAM_SLC         PMHS_A_Pelvis_AR                    ; Header of the loadcase
#    DES_SLC         Pelvis_AR                  ; Sub-header of the loadcase
#    WF_SLC          1                   ; Weighting factor of the loadcase
#    METHOD          cora
#

#BEGIN DATAFILES
#    Name                          unit    g   timeshift
#    Ref
#C:/Users/kbosch/Desktop/CORA_MADYMO/PMHS_A/Exp/Pelvis_AR_RC.dat
m-kg-s  NO  0.0
#    Sim
#C:/Users/kbosch/Desktop/CORA_MADYMO/PMHS_A/Sim/Pelvis_AR_Sim.dat
m-kg-s  NO  0.0
#
```

```
#END DATAFILES


#   BEGIN SIGNALS
#    Channels
#    Name           WF  Y_norm   t_min  t_max  g_V  g_G  g_P  g1  g2  a_0  b_0   a_t
a_sigma  b_sigma  D_min  D_max  Filter
#     11PELVRD00H3ACXA    1 x      0     0.025 x   x   x  x  x   x   x
C:/Users/kbosch/Desktop/CORA_MADYMO/PMHS_A/Exp/Pelvis_AR_Corridor.dat      x
x      x      x      0
#   END SIGNALS
#  END SUBLOADCASE


####################
  BEGIN SUBLOADCASE
    NAM_SLC         PMHS_A_T12_Ax                        ; Header of the loadcase
    DES_SLC         T12_Ax                        ; Sub-header of the loadcase
    WF_SLC          1                          ; Weighting factor of the loadcase
    METHOD          cora
#

BEGIN DATAFILES
#    Name                          unit    g   timeshift
#    Ref
C:/Users/kbosch/Desktop/CORA_MADYMO/PMHS_A/Exp/T12_Ax_RC.dat
m-kg-s  NO  0.0
#    Sim
C:/Users/kbosch/Desktop/CORA_MADYMO/PMHS_A/Sim/9.dat                m-kg-s  NO
0.0

END DATAFILES


   BEGIN SIGNALS
#    Channels
#    Name           WF  Y_norm   t_min  t_max  g_V  g_G  g_P  g1  g2  a_0  b_0   a_t
a_sigma  b_sigma  D_min  D_max  Filter
     11TS120000H3ACXA    1 x      0     0.025 x   x   x  x  x   x   x
C:/Users/kbosch/Desktop/CORA_MADYMO/PMHS_A/Exp/T12_Ax_Corridor.dat      x
x      x      x      0
   END SIGNALS
  END SUBLOADCASE

####################
  BEGIN SUBLOADCASE
```

```
   NAM_SLC        PMHS_A_T12_Az                    ; Header of the loadcase
   DES_SLC        T12_Az                  ; Sub-header of the loadcase
   WF_SLC         1                       ; Weighting factor of the loadcase
   METHOD         cora
#

BEGIN DATAFILES
#    Name                          unit   g   timeshift
#    Ref
C:/Users/kbosch/Desktop/CORA_MADYMO/PMHS_A/Exp/T12_Az_RC.dat
m-kg-s  NO  0.0
#    Sim
C:/Users/kbosch/Desktop/CORA_MADYMO/PMHS_A/Sim/9.dat              m-kg-s  NO
0.0

END DATAFILES


   BEGIN SIGNALS
#    Channels
#    Name          WF  Y_norm   t_min  t_max  g_V  g_G  g_P  g1  g2  a_0  b_0   a_t
a_sigma  b_sigma  D_min  D_max  Filter
     11TS120000H3ACZA    1 x      0      0.025 x    x    x  x  x    x    x
C:/Users/kbosch/Desktop/CORA_MADYMO/PMHS_A/Exp/T12_Az_Corridor.dat     x
x      x      x      0
   END SIGNALS
  END SUBLOADCASE


####################
  BEGIN SUBLOADCASE
   NAM_SLC        PMHS_A_T8_Ax                     ; Header of the loadcase
   DES_SLC        T8_Ax                   ; Sub-header of the loadcase
   WF_SLC         1                       ; Weighting factor of the loadcase
   METHOD         cora
#

BEGIN DATAFILES
#    Name                          unit   g   timeshift
#    Ref
C:/Users/kbosch/Desktop/CORA_MADYMO/PMHS_A/Exp/T8_Ax_RC.dat              m-
kg-s  NO  0.0
#    Sim
C:/Users/kbosch/Desktop/CORA_MADYMO/PMHS_A/Sim/9.dat              m-kg-s  NO
0.0
```

```
END DATAFILES


   BEGIN SIGNALS
#    Channels
#    Name           WF  Y_norm   t_min  t_max  g_V  g_G  g_P  g1  g2  a_0  b_0   a_t
a_sigma  b_sigma  D_min  D_max  Filter
     11TS080000H3ACXA     1 x      0      0.025 x    x    x  x  x    x    x
C:/Users/kbosch/Desktop/CORA_MADYMO/PMHS_A/Exp/T8_Ax_Corridor.dat      x
x      x      x      0
   END SIGNALS
  END SUBLOADCASE

####################
  BEGIN SUBLOADCASE
    NAM_SLC         PMHS_A_T8_Az                        ; Header of the loadcase
    DES_SLC         T8_Az                          ; Sub-header of the loadcase
    WF_SLC          1                           ; Weighting factor of the loadcase
    METHOD          cora
#

BEGIN DATAFILES
#    Name                          unit    g   timeshift
#    Ref
C:/Users/kbosch/Desktop/CORA_MADYMO/PMHS_A/Exp/T8_Az_RC.dat              m-
kg-s  NO  0.0
#    Sim
C:/Users/kbosch/Desktop/CORA_MADYMO/PMHS_A/Sim/9.dat                m-kg-s  NO
0.0

END DATAFILES


   BEGIN SIGNALS
#    Channels
#    Name           WF  Y_norm   t_min  t_max  g_V  g_G  g_P  g1  g2  a_0  b_0   a_t
a_sigma  b_sigma  D_min  D_max  Filter
     11TS080000H3ACZA     1 x      0      0.025 x    x    x  x  x    x    x
C:/Users/kbosch/Desktop/CORA_MADYMO/PMHS_A/Exp/T8_Az_Corridor.dat      x
x      x      x      0
   END SIGNALS
  END SUBLOADCASE


####################
  BEGIN SUBLOADCASE
```

```
   NAM_SLC        PMHS_A_T5_Ax                    ; Header of the loadcase
   DES_SLC        T5_Ax                  ; Sub-header of the loadcase
   WF_SLC         1                      ; Weighting factor of the loadcase
   METHOD         cora
#

BEGIN DATAFILES
#    Name                          unit   g   timeshift
#    Ref
C:/Users/kbosch/Desktop/CORA_MADYMO/PMHS_A/Exp/T5_Ax_RC.dat          m-
kg-s  NO  0.0
#    Sim
C:/Users/kbosch/Desktop/CORA_MADYMO/PMHS_A/Sim/9.dat          m-kg-s  NO
0.0

END DATAFILES


   BEGIN SIGNALS
#    Channels
#    Name          WF  Y_norm   t_min  t_max  g_V  g_G  g_P  g1  g2  a_0  b_0   a_t
a_sigma  b_sigma  D_min  D_max  Filter
     11TS050000H3ACXA    1 x      0      0.025 x    x    x  x   x    x    x
C:/Users/kbosch/Desktop/CORA_MADYMO/PMHS_A/Exp/T5_Ax_Corridor.dat     x
x      x      x      0
   END SIGNALS
  END SUBLOADCASE


####################
  BEGIN SUBLOADCASE
   NAM_SLC        PMHS_A_T5_Az                    ; Header of the loadcase
   DES_SLC        T5_Az                  ; Sub-header of the loadcase
   WF_SLC         1                      ; Weighting factor of the loadcase
   METHOD         cora
#

BEGIN DATAFILES
#    Name                          unit   g   timeshift
#    Ref
C:/Users/kbosch/Desktop/CORA_MADYMO/PMHS_A/Exp/T5_Az_RC.dat          m-
kg-s  NO  0.0
#    Sim
C:/Users/kbosch/Desktop/CORA_MADYMO/PMHS_A/Sim/9.dat          m-kg-s  NO
0.0
```

```
END DATAFILES


   BEGIN SIGNALS
#    Channels
#    Name           WF  Y_norm   t_min  t_max  g_V  g_G  g_P  g1  g2  a_0  b_0   a_t
a_sigma  b_sigma  D_min  D_max  Filter
     11TS050000H3ACZA    1 x      0      0.025 x    x    x  x  x    x    x
C:/Users/kbosch/Desktop/CORA_MADYMO/PMHS_A/Exp/T5_Az_Corridor.dat      x
x      x      x      0
   END SIGNALS
  END SUBLOADCASE


####################
  BEGIN SUBLOADCASE
   NAM_SLC         PMHS_A_T1_Ax                        ; Header of the loadcase
   DES_SLC         T1_Ax                          ; Sub-header of the loadcase
   WF_SLC          1                             ; Weighting factor of the loadcase
   METHOD          cora
#

BEGIN DATAFILES
#    Name                          unit    g   timeshift
#    Ref
C:/Users/kbosch/Desktop/CORA_MADYMO/PMHS_A/Exp/T1_Ax_RC.dat              m-
kg-s  NO  0.0
#    Sim
C:/Users/kbosch/Desktop/CORA_MADYMO/PMHS_A/Sim/9.dat                 m-kg-s  NO
0.0

END DATAFILES


   BEGIN SIGNALS
#    Channels
#    Name           WF  Y_norm   t_min  t_max  g_V  g_G  g_P  g1  g2  a_0  b_0   a_t
a_sigma  b_sigma  D_min  D_max  Filter
     11TS010000H3ACXA    1 x      0      0.025 x    x    x  x  x    x    x
C:/Users/kbosch/Desktop/CORA_MADYMO/PMHS_A/Exp/T1_Ax_Corridor.dat      x
x      x      x      0
   END SIGNALS
  END SUBLOADCASE


####################
```

```
  BEGIN SUBLOADCASE
    NAM_SLC         PMHS_A_T1_Az                    ; Header of the loadcase
    DES_SLC         T1_Az                  ; Sub-header of the loadcase
    WF_SLC          1                      ; Weighting factor of the loadcase
    METHOD          cora
#

BEGIN DATAFILES
#     Name                          unit    g   timeshift
#     Ref
C:/Users/kbosch/Desktop/CORA_MADYMO/PMHS_A/Exp/T1_Az_RC.dat             m-
kg-s  NO  0.0
#     Sim
C:/Users/kbosch/Desktop/CORA_MADYMO/PMHS_A/Sim/9.dat             m-kg-s  NO
0.0

END DATAFILES


    BEGIN SIGNALS
#     Channels
#     Name            WF  Y_norm   t_min  t_max  g_V  g_G  g_P  g1  g2  a_0  b_0   a_t
a_sigma  b_sigma  D_min  D_max  Filter
      11TS010000H3ACZA     1  x      0      0.025  x    x    x   x   x    x    x
C:/Users/kbosch/Desktop/CORA_MADYMO/PMHS_A/Exp/T1_Az_Corridor.dat      x
x       x      x       0
    END SIGNALS
  END SUBLOADCASE
END LOADCASE
```

APPENDIX B – CONDITION A PMHS CORA OUTPUT FILE

Summary Report Date: Sep 17 2018

Rating of: WIAMan BRC Evaluation

Description: Biomedical Response Corridors

Rating:

No.	Load Case	Rating	Weight
1	Bosch PMHS A-1	0.798	1.0
	Total rating	**0.798**	1.0

Load Case Report Date: Sep 17 2018

Rating of: Bosch PMHS A-1

Description: Subloadcase

Rating:

No.	Experiment	Rating	Weight
1	PMHS_A_Foot_Az	0.907	0.071
2	PMHS_A_Tibia_Ax	0.794	0.071
3	PMHS_A_Tibia_Az	0.786	0.071
4	PMHS_A_Femur_Ax	0.784	0.071
5	PMHS_A_Pelvis_Ax	0.775	0.071
6	PMHS_A_Pelvis_Az	0.90	0.071
7	PMHS_A_T12_Ax	0.756	0.071
8	PMHS_A_T12_Az	0.903	0.071
9	PMHS_A_T8_Ax	0.742	0.071
10	PMHS_A_T8_Az	0.785	0.071
11	PMHS_A_T5_Ax	0.683	0.071
12	PMHS_A_T5_Az	0.786	0.071
13	PMHS_A_T1_Ax	0.862	0.071
14	PMHS_A_T1_Az	0.705	0.071

Total rating of load case 1:	**0.798**	1.0

Experiment Report Date: Sep 17 2018

Report of Experiment: PMHS_A_Foot_Az

Description: Foot Az

Rating:

No.	Signal	Rating	Weight
1	11FOOTLE00H3ACZC	0.907	1.0
	Total rating of experiment 1:	**0.907**	1.0

Signal Report Date: Sep 17 2018

Rating of: PMHS_A_Foot_Az

Report of Signal 1 of Experiment 1: 11FOOTLE00H3ACZC

Overall Rating: 0.907

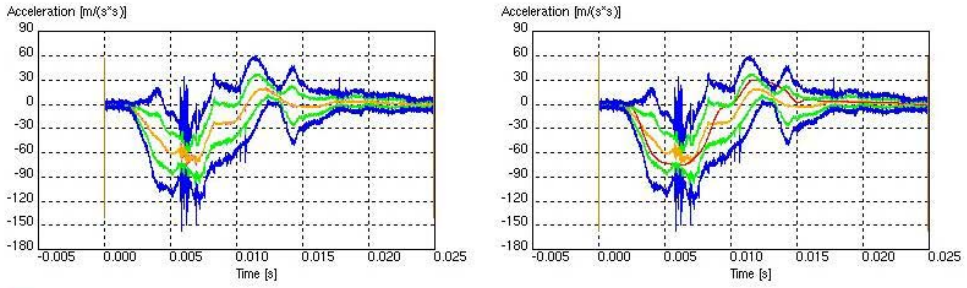

Foot_Az_RC

Average of experiments
cross-correlation reference
172_3
Limits Outer corridor
Limits inner corridor

Method	Name				Rating	Weight
1	Corridor Method				0.932	0.50
2	Correlation Method				0.883	0.50
		Value	Rating	Weight		
	Cross correlation function	0.959	0.979	0.333		
	Size	0.669	0.669	0.333		
	Phase shift	0.0000	1.0	0.333		
3	Combination of 1 and 2				**0.907**	-

Parameters:	Evaluation Intervall:	0.0000 - 0.0250
Method 1:	Max. half width of inner corridor:	-
	Max. half width of outer corridor:	-
	Corridor curve file:	Foot_Az_Corridor
	Reference value:	73.272
	Transition exponent:	1
Method 2:	Limits for phase shift:	0.0002 - 0.0030
	Rating exponents (shape, size, phase):	1, 1, 1

Experiment Report Date: Sep 17 2018

Report of Experiment: PMHS_A_Tibia_Ax

Description: Tibia Ax

Rating:

No.	Signal	Rating	Weight
1	11TIBIRILOH3ACXC	0.794	1.0
	Total rating of experiment 2:	**0.794**	1.0

Signal Report Date: Sep 17 2018

Rating of: PMHS_A_Tibia_Ax

Report of Signal 1 of Experiment 2: 11TIBIRILOH3ACXC

Overall Rating: 0.794

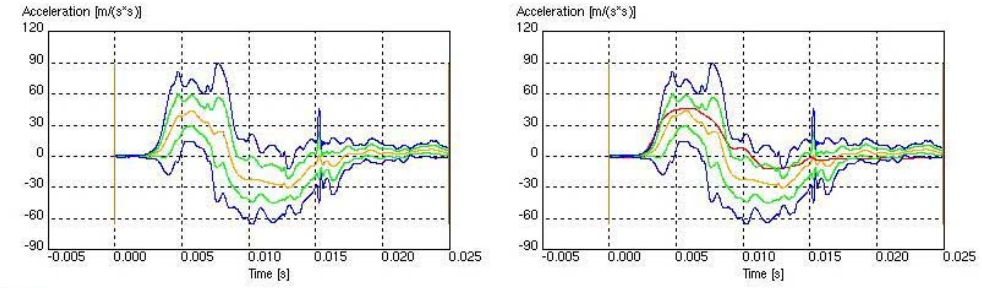

Tibia_Ax_RC

Average of experiments
cross-correlation reference
172_3
Limits Outer corridor
Limits inner corridor

Method	Name	Rating	Weight
1	Corridor Method	0.636	0.50
2	Correlation Method	0.953	0.50
3	Combination of 1 and 2	**0.794**	-

Correlation Method

	Value	Rating	Weight
Cross correlation function	0.804	0.902	0.333
Size	0.957	0.957	0.333
Phase shift	0.0000	1.0	0.333

Parameters:	Evaluation Intervall:	0.0000 - 0.0250
Method 1:	Max. half width of inner corridor:	-
	Max. half width of outer corridor:	-
	Corridor curve file:	Tibia_Ax_Corridor
	Reference value:	44.173
	Transition exponent:	1
Method 2:	Limits for phase shift:	0.0002 - 0.0030
	Rating exponents (shape, size, phase):	1, 1, 1

Experiment Report Date: Sep 17 2018

Report of Experiment: PMHS_A_Tibia_Az

Description: Tibia Az

Rating:

No.	Signal	Rating	Weight
1	11TIBIRILOH3ACZC	0.786	1.0
	Total rating of experiment 3:	**0.786**	1.0

Signal Report Date: Sep 17 2018

Rating of: PMHS_A_Tibia_Az

Report of Signal 1 of Experiment 3: 11TIBIRILOH3ACZC

Overall Rating: 0.786

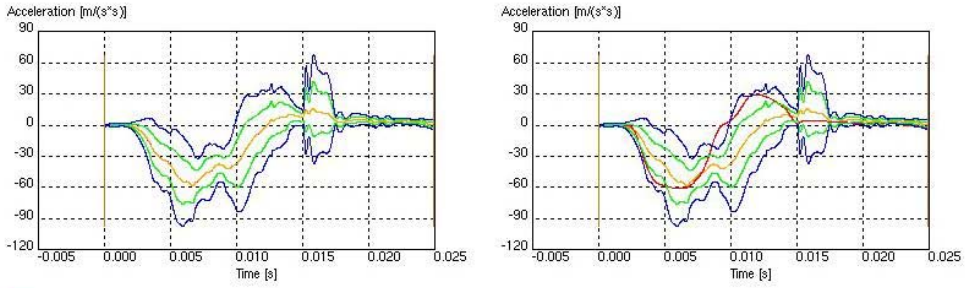

Tibia_Az_RC

Average of experiments
cross-correlation reference
172_3
Limits Outer corridor
Limits inner corridor

Method	Name				Rating	Weight
1	Corridor Method				0.668	0.50
2	Correlation Method				0.904	0.50
		Value	Rating	Weight		
	Cross correlation function	0.779	0.890	0.333		
	Size	0.822	0.822	0.333		
	Phase shift	0.0000	1.0	0.333		
3	Combination of 1 and 2				**0.786**	-

Parameters:	Evaluation Intervall:	0.0000 - 0.0250
Method 1:	Max. half width of inner corridor:	-
	Max. half width of outer corridor:	-
	Corridor curve file:	Tibia_Az_Corridor
	Reference value:	58.388
	Transition exponent:	1
Method 2:	Limits for phase shift:	0.0002 - 0.0030
	Rating exponents (shape, size, phase):	1, 1, 1

Experiment Report Date: Sep 17 2018

Report of Experiment: PMHS_A_Femur_Ax

Description: Femur Ax

Rating:

No.	Signal	Rating	Weight
1	11FEMRLE00H3ACXC	0.784	1.0
	Total rating of experiment 4:	**0.784**	1.0

Signal Report Date: Sep 17 2018

Rating of: PMHS_A_Femur_Ax

Report of Signal 1 of Experiment 4: 11FEMRLE00H3ACXC

Overall Rating: 0.784

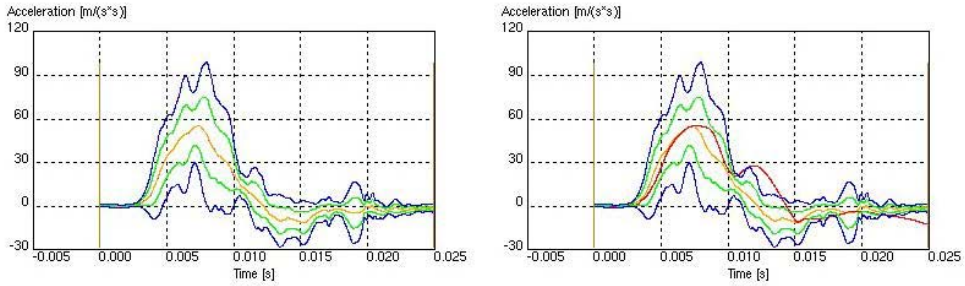

Femur_Ax_RC

Average of experiments
cross-correlation reference
172_3
Limits Outer corridor
Limits inner corridor

Method	Name				Rating	Weight
1	Corridor Method				0.660	0.50
2	Correlation Method				0.907	0.50
		Value	Rating	Weight		
	Cross correlation function	0.911	0.955	0.333		
	Size	0.767	0.767	0.333		
	Phase shift	0.0000	1.0	0.333		
3	Combination of 1 and 2				**0.784**	-

Parameters:	Evaluation Intervall:	0.0000 - 0.0250
Method 1:	Max. half width of inner corridor:	-
	Max. half width of outer corridor:	-
	Corridor curve file:	Femur_Ax_Corridor
	Reference value:	55.509
	Transition exponent:	1
Method 2:	Limits for phase shift:	0.0002 - 0.0030
	Rating exponents (shape, size, phase):	1, 1, 1

Experiment Report Date: Sep 17 2018

Report of Experiment: PMHS_A_Pelvis_Ax

Description: Pelvis Ax

Rating:

No.	Signal	Rating	Weight
1	11PELV0000H3VAXC	0.775	1.0
	Total rating of experiment 5:	**0.775**	1.0

Signal Report Date: Sep 17 2018

Rating of: PMHS_A_Pelvis_Ax

Report of Signal 1 of Experiment 5: 11PELV0000H3VAXC

Overall Rating: 0.775

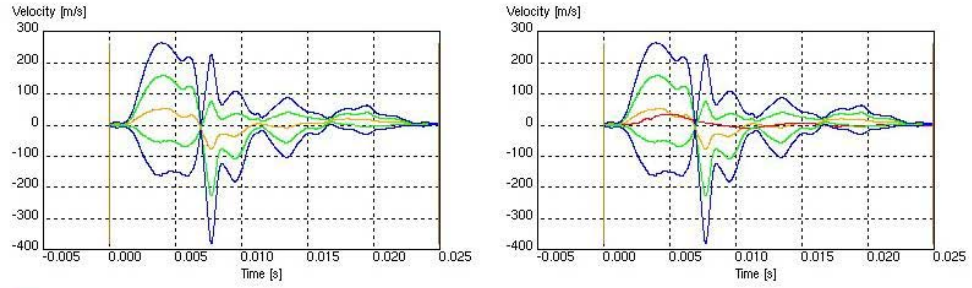

Pelvis_Ax_RC

Average of experiments
cross-correlation reference
172_3
Limits Outer corridor
Limits inner corridor

Method	Name				Rating	Weight
1	Corridor Method				0.885	0.50
2	Correlation Method				0.665	0.50
		Value	Rating	Weight		
	Cross correlation function	0.532	0.766	0.333		
	Size	0.228	0.228	0.333		
	Phase shift	0.0000	1.0	0.333		
3	Combination of 1 and 2				**0.775**	-

Parameters:	Evaluation Intervall:	0.0000 - 0.0250
Method 1:	Max. half width of inner corridor:	-
	Max. half width of outer corridor:	-
	Corridor curve file:	Pelvis_Ax_Corridor
	Reference value:	76.098
	Transition exponent:	1
Method 2:	Limits for phase shift:	0.0002 - 0.0030
	Rating exponents (shape, size, phase):	1, 1, 1

Experiment Report Date: Sep 17 2018

Report of Experiment: PMHS_A_Pelvis_Az

Description: Pelvis_Az

Rating:

No.	Signal	Rating	Weight
1	11PELV0000H3VAZC	0.90	1.0
	Total rating of experiment 6:	**0.90**	1.0

Signal Report Date: Sep 17 2018

Rating of: PMHS_A_Pelvis_Az

Report of Signal 1 of Experiment 6: 11PELV0000H3VAZC

Overall Rating: 0.90

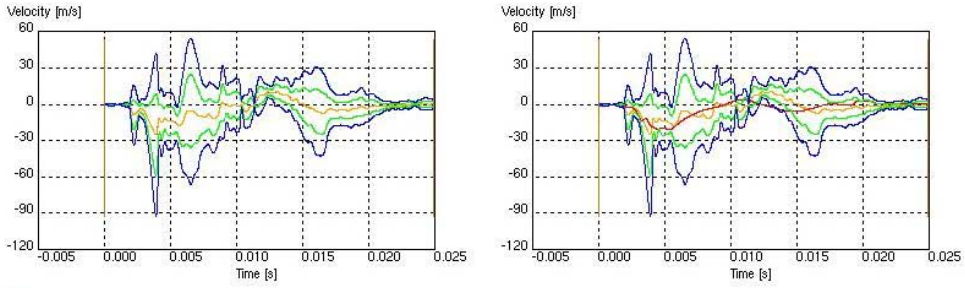

Pelvis_Az_RC

Average of experiments
cross-correlation reference
172_3
Limits Outer corridor
Limits inner corridor

Method	Name				Rating	Weight
1	Corridor Method				0.846	0.50
2	Correlation Method				0.953	0.50
		Value	Rating	Weight		
	Cross correlation function	0.734	0.867	0.333		
	Size	0.993	0.993	0.333		
	Phase shift	0.0000	1.0	0.333		
3	Combination of 1 and 2				**0.90**	-

Parameters:	Evaluation Intervall:	0.0000 - 0.0250
Method 1:	Max. half width of inner corridor:	-
	Max. half width of outer corridor:	-
	Corridor curve file:	Pelvis_Az_Corridor
	Reference value:	25.104
	Transition exponent:	1
Method 2:	Limits for phase shift:	0.0002 - 0.0030
	Rating exponents (shape, size, phase):	1, 1, 1

Experiment Report Date: Sep 17 2018

Report of Experiment: PMHS_A_T12_Ax

Description: T12_Ax

Rating:

No.	Signal	Rating	Weight
1	11TS120000H3ACXA	0.756	1.0
	Total rating of experiment 7:	**0.756**	1.0

Signal Report Date: Sep 17 2018

Rating of: PMHS_A_T12_Ax

Report of Signal 1 of Experiment 7: 11TS120000H3ACXA

Overall Rating: 0.756

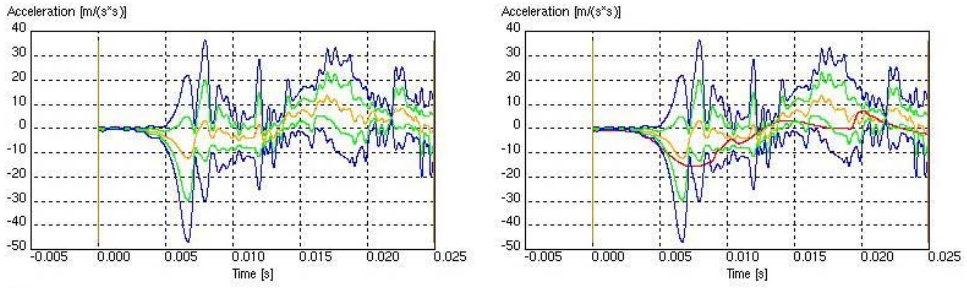

Method	Name				Rating	Weight
1	Corridor Method				0.688	0.50
2	Correlation Method				0.825	0.50
		Value	Rating	Weight		
	Cross correlation function	0.488	0.744	0.333		
	Size	0.730	0.730	0.333		
	Phase shift	0.0000	1.0	0.333		
3	Combination of 1 and 2				**0.756**	-

Parameters:	Evaluation Intervall:	0.0000 - 0.0250
Method 1:	Max. half width of inner corridor:	-
	Max. half width of outer corridor:	-
	Corridor curve file:	T12_Ax_Corridor
	Reference value:	13.646
	Transition exponent:	1
Method 2:	Limits for phase shift:	0.0002 - 0.0030
	Rating exponents (shape, size, phase):	1, 1, 1

Experiment Report Date: Sep 17 2018

Report of Experiment: PMHS_A_T12_Az

Description: T12_Az

Rating:

No.	Signal	Rating	Weight
1	11TS120000H3ACZA	0.903	1.0
	Total rating of experiment 8:	**0.903**	1.0

Signal Report Date: Sep 17 2018

Rating of: PMHS_A_T12_Az

Report of Signal 1 of Experiment 8: 11TS120000H3ACZA

Overall Rating: 0.903

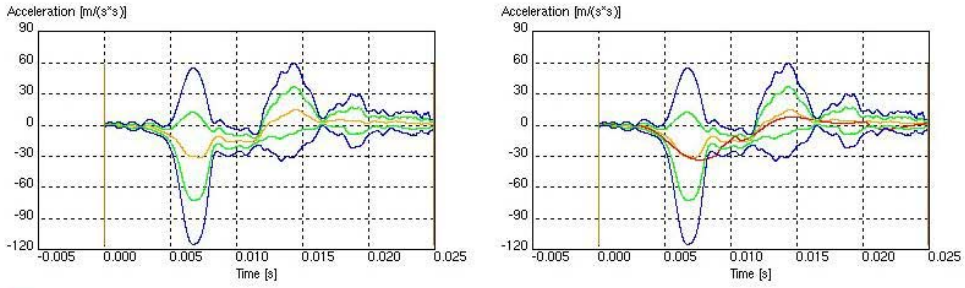

T12_Az_RC

Average of experiments
cross-correlation reference
172_3
Limits Outer corridor
Limits inner corridor

Method	Name				Rating	Weight
1	Corridor Method				0.899	0.50
2	Correlation Method				0.907	0.50
		Value	Rating	Weight		
	Cross correlation function	0.926	0.963	0.333		
	Size	0.759	0.759	0.333		
	Phase shift	0.0000	1.0	0.333		
3	Combination of 1 and 2				**0.903**	-

Parameters:	Evaluation Intervall:	0.0000 - 0.0250
Method 1:	Max. half width of inner corridor:	-
	Max. half width of outer corridor:	-
	Corridor curve file:	T12_Az_Corridor
	Reference value:	31.105
	Transition exponent:	1
Method 2:	Limits for phase shift:	0.0002 - 0.0030
	Rating exponents (shape, size, phase):	1, 1, 1

Signal Report Date: Sep 17 2018

Rating of PMHS_A_T8_Ax

Report of Signal 1 of Experiment 9: 11TS080000H3ACXA

Overall Rating: 0.742

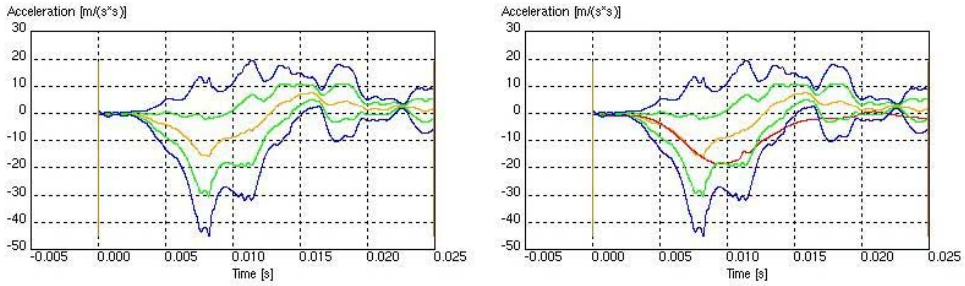

T8_Ax_RC

Average of experiments
cross-correlation reference
172_3
Limits Outer corridor
Limits inner corridor

Method	Name	Rating	Weight
1	Corridor Method	0.698	0.50
2	Correlation Method	0.787	0.50

	Value	Rating	Weight
Cross correlation function	0.694	0.847	0.333
Size	0.514	0.514	0.333
Phase shift	0.0000	1.0	0.333

3	Combination of 1 and 2	**0.742**	-

Parameters:	Evaluation Intervall:	0.0000 - 0.0250
Method 1:	Max. half width of inner corridor:	-
	Max. half width of outer corridor:	-
	Corridor curve file:	T8_Ax_Corridor
	Reference value:	15.963
	Transition exponent:	1
Method 2:	Limits for phase shift:	0.0002 - 0.0030
	Rating exponents (shape, size, phase):	1, 1, 1

Experiment Report Date: Sep 17 2018

Report of Experiment: PMHS_A_T8_Az

Description: T8_Az

Rating:

No.	Signal	Rating	Weight
1	11TS080000H3ACZA	0.785	1.0
	Total rating of experiment 10:	**0.785**	1.0

Signal Report Date: Sep 17 2018

Rating of: PMHS_A_T8_Az

Report of Signal 1 of Experiment 10: 11TS080000H3ACZA

Overall Rating: 0.785

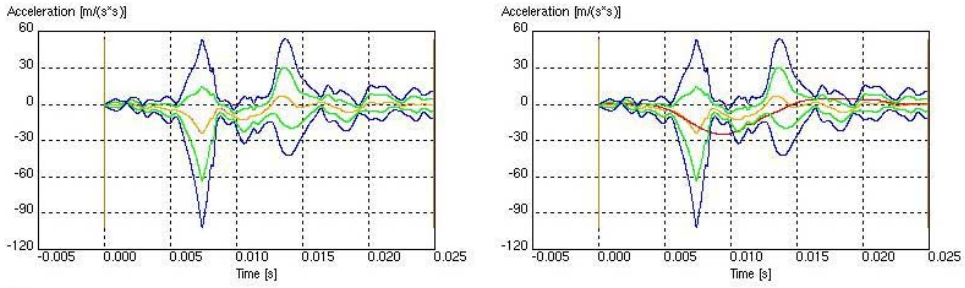

T8_Az_RC

Average of experiments
cross-correlation reference
172_3
Limits Outer corridor
Limits inner corridor

Method	Name	Rating	Weight
1	Corridor Method	0.814	0.50
2	Correlation Method	0.756	0.50
3	Combination of 1 and 2	**0.785**	-

Correlation Method

	Value	Rating	Weight
Cross correlation function	0.731	0.866	0.333
Size	0.402	0.402	0.333
Phase shift	0.0000	1.0	0.333

Parameters:	Evaluation Intervall:	0.0000 - 0.0250
Method 1:	Max. half width of inner corridor:	-
	Max. half width of outer corridor:	-
	Corridor curve file:	T8_Az_Corridor
	Reference value:	24.158
	Transition exponent:	1
Method 2:	Limits for phase shift:	0.0002 - 0.0030
	Rating exponents (shape, size, phase):	1, 1, 1

Experiment Report Date: Sep 17 2018

Report of Experiment: PMHS_A_T5_Ax

Description: T5_Ax

Rating:

No.	Signal	Rating	Weight
1	11TS050000H3ACXA	0.683	1.0
	Total rating of experiment 11:	**0.683**	1.0

Signal Report Date: Sep 17 2018

Rating of: PMHS_A_T5_Ax

Report of Signal 1 of Experiment 11: 11TS050000H3ACXA

Overall Rating: 0.683

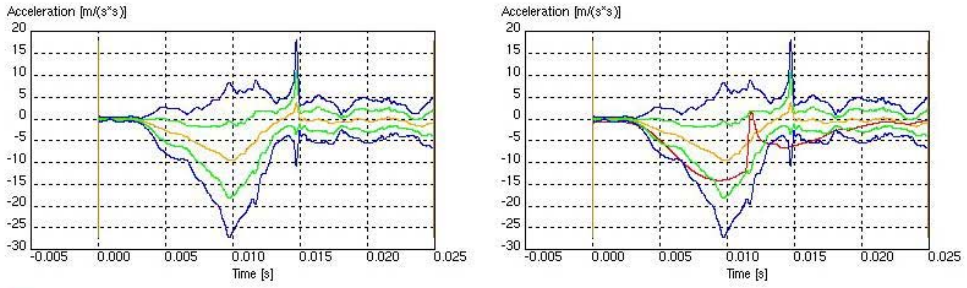

Method	Name				Rating	Weight
1	Corridor Method				0.621	0.50
2	Correlation Method				0.744	0.50
		Value	Rating	Weight		
	Cross correlation function	0.888	0.944	0.333		
	Size	0.289	0.289	0.333		
	Phase shift	0.0000	1.0	0.333		
3	Combination of 1 and 2				**0.683**	-

Parameters:	Evaluation Intervall:	0.0000 - 0.0250
Method 1:	Max. half width of inner corridor:	-
	Max. half width of outer corridor:	-
	Corridor curve file:	T5_Ax_Corridor
	Reference value:	9.419
	Transition exponent:	1
Method 2:	Limits for phase shift:	0.0002 - 0.0030
	Rating exponents (shape, size, phase):	1, 1, 1

Experiment Report Date: Sep 17 2018

Report of Experiment: PMHS_A_T5_Az

Description: T5_Az

Rating:

No.	Signal	Rating	Weight
1	11TS050000H3ACZA	0.786	1.0
	Total rating of experiment 12:	**0.786**	1.0

Signal Report Date: Sep 17 2018

Rating of: PMHS_A_T5_Az

Report of Signal 1 of Experiment 12: 11TS050000H3ACZA

Overall Rating: 0.786

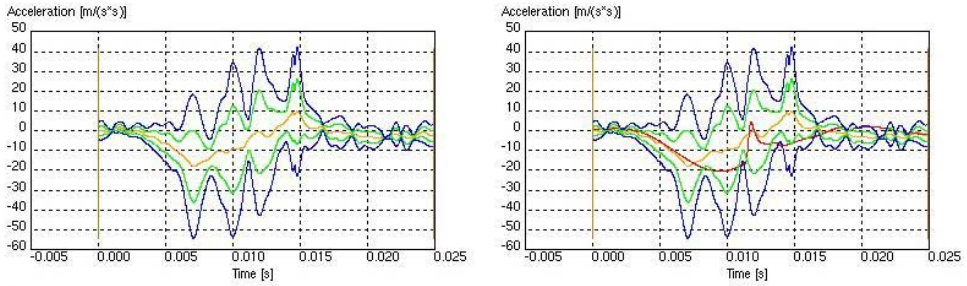

Method	Name				Rating	Weight
1	Corridor Method				0.763	0.50
2	Correlation Method				0.810	0.50
		Value	Rating	Weight		
	Cross correlation function	0.749	0.875	0.333		
	Size	0.556	0.556	0.333		
	Phase shift	0.0000	1.0	0.333		
3	Combination of 1 and 2				**0.786**	-

Parameters:	Evaluation Intervall:	0.0000 - 0.0250
Method 1:	Max. half width of inner corridor:	-
	Max. half width of outer corridor:	-
	Corridor curve file:	T5_Az_Corridor
	Reference value:	18.142
	Transition exponent:	1
Method 2:	Limits for phase shift:	0.0002 - 0.0030
	Rating exponents (shape, size, phase):	1, 1, 1

Experiment Report Date: Sep 17 2018

Report of Experiment: PMHS_A_T1_Ax

Description: T1_Ax

Rating:

No.	Signal	Rating	Weight
1	11TS010000H3ACXA	0.862	1.0
	Total rating of experiment 13:	**0.862**	1.0

Signal Report Date: Sep 17 2018

Rating of PMHS_A_T1_Ax

Report of Signal 1 of Experiment 13: 11TS010000H3ACXA

Overall Rating: 0.862

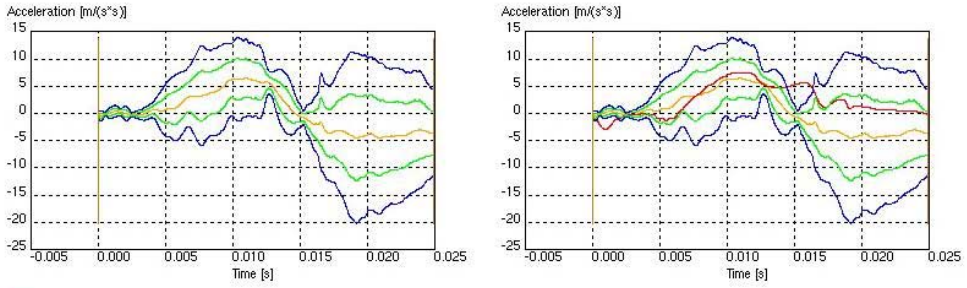

Method	Name				Rating	Weight
1	Corridor Method				0.832	0.50
2	Correlation Method				0.892	0.50
		Value	Rating	Weight		
	Cross correlation function	0.503	0.752	0.333		
	Size	0.925	0.925	0.333		
	Phase shift	0.0000	1.0	0.333		
3	Combination of 1 and 2				**0.862**	-

Parameters:	Evaluation Intervall:	0.0000 - 0.0250
Method 1:	Max. half width of inner corridor:	-
	Max. half width of outer corridor:	-
	Corridor curve file:	T1_Ax_Corridor
	Reference value:	6.507
	Transition exponent:	1
Method 2:	Limits for phase shift:	0.0002 - 0.0030
	Rating exponents (shape, size, phase):	1, 1, 1

Experiment Report Date: Sep 17 2018

Report of Experiment: PMHS_A_T1_Az

Description: T1_Az

Rating:

No.	Signal	Rating	Weight
1	11TS010000H3ACZA	0.705	1.0
	Total rating of experiment 14:	**0.705**	1.0

Signal Report Date: Sep 17 2018

Rating of: PMHS_A_T1_Az

Report of Signal 1 of Experiment 14: 11TS010000H3ACZA

Overall Rating: 0.705

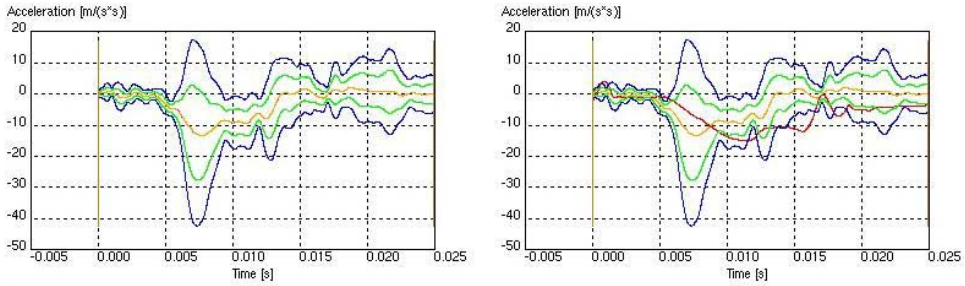

T1_Az_RC

Average of experiments
cross-correlation reference
172_3
Limits Outer corridor
Limits inner corridor

Method	Name				Rating	Weight
1	Corridor Method				0.646	0.50
2	Correlation Method				0.763	0.50
		Value	Rating	Weight		
	Cross correlation function	0.646	0.823	0.333		
	Size	0.466	0.466	0.333		
	Phase shift	0.0000	1.0	0.333		
3	Combination of 1 and 2				**0.705**	-

Parameters:	Evaluation Intervall:	0.0000 - 0.0250
Method 1:	Max. half width of inner corridor:	-
	Max. half width of outer corridor:	-
	Corridor curve file:	T1_Az_Corridor
	Reference value:	13.257
	Transition exponent:	1
Method 2:	Limits for phase shift:	0.0002 - 0.0030
	Rating exponents (shape, size, phase):	1, 1, 1

APPENDIX C – CONDITION B PMHS VALIDATION LOG

Run	ID No.	Floor Time (ms)	Seat Time (ms)	Back_M_F rx_x	Back_M_F rx_z	Back_M_F rx_LS	Shoe_floor contact_damp	Tibia Accel Angle	Floor friction	Hip IR	Knee IR	Ankle IR	PMHS Body Restraint	Femur/Tibia Load Profile	Femur/Tibia Load Profile	Knee/Tibia Interaction	Pelvis_M_fric x_femur	Pelvis_M_fric y_femur	Pelvis_Seat_contact_damp_HR M_femur	Pelvis_M_fric x_t	Pelvis_M_fric z_t	Pelvis Kin	Pelvis Vers	T12 x accle	T1 x accle	T1 y accle	T1 y accle	T1 Kin	T1 Offset	Head Angle	T1 vers	Shoe Tibia force decrease Damping	Shoe Tibia force decrease T Scale	Shoe Tibia force decrease T Scale	Notes
1	0870	0	0.036814	1	0.8	0.5	1000	0.4	0.7	-76.4668	87.4	0	-0.103	N/A	N/A	N/A	1.2	1.55	0	11	9	250k+09	0.85	N/A	375	1	0.7	1.00E+10	0	-240	0.65	N/A	N/A	N/A	Same setup pos PMHS_A_17.2.7 but new pelvis with more flesh 2.204 mm from floor based on run 1.1. Footrest accidentally +9 (+0.9) - pelvis fix correct magnitude, initial loading spike in T1
2	INC	0	0.036814	10	0.8	0.5	1000	0.4	0.7	-76.4668	87.4	0	-0.103	N/A	N/A	N/A	1.2	1.55	0	11	9	250k+09	0.85	N/A	375	1	0.7	1.00E+10	0	-240	0.65	N/A	N/A	N/A	Pelvis fix+ first, tibia reduced by factor of 2 - correct direction - limited to ages to pelvis, T1
3	INC	0	0.036814	30	0.8	0.5	1000	0.4	0.7	-76.4668	87.4	0	-0.103	N/A	N/A	N/A	1.2	1.55	0	11	9	250k+09	0.85	N/A	375	1	0.7	1.00E+10	0	-240	0.65	N/A	N/A	N/A	Slight reduction in first, tibia - not dramatic as now 1 to 2
4	INC	0	0.036814	30	0.08	0.5	1000	0.4	0.7	-76.4668	87.4	0	-0.103	N/A	N/A	N/A	1.2	1.55	0	11	9	250k+09	0.85	N/A	375	1	0.7	1.00E+10	0	-240	0.65	N/A	N/A	N/A	Way tight reduction
5	INC	0	0.036814	300	0.08	0.5	1000	0.4	0.7	-76.4668	87.4	0	-0.103	N/A	N/A	N/A	1.2	1.55	0	11	9	250k+09	0.85	N/A	375	1	0.7	1.00E+10	0	-240	0.65	N/A	N/A	N/A	Minimal reduction
6	INC	0	0.036814	300	0.08	0.5	10000	0.4	0.7	-76.4668	87.4	0	-0.103	N/A	N/A	N/A	1.2	1.55	0	11	9	250k+09	0.85	N/A	375	1	0.7	1.00E+10	0	-240	0.65	N/A	N/A	N/A	Way too high
7	INC	0	0.036814	300	0.08	0.5	0	0.4	0.7	-76.4668	87.4	0	-0.103	N/A	N/A	N/A	1.2	1.55	0	11	9	250k+09	0.85	N/A	375	1	0.7	1.00E+10	0	-240	0.65	N/A	N/A	N/A	Zero damping - maybe a fly/bees pulse?
8	INC	0	0.036814	300	0.08	0.5	100	0.4	0.7	-76.4668	87.4	0	-0.103	N/A	N/A	N/A	1.2	1.55	0	11	9	250k+09	0.85	N/A	375	1	0.7	1.00E+10	0	-240	0.65	N/A	N/A	N/A	Much better
9	INC	0	0.036814	1	0.8	0.5	100	0.4	0.7	-76.4668	87.4	0	-0.103	N/A	N/A	N/A	1.2	1.55	0	11	9	250k+09	0.85	N/A	375	1	0.7	1.00E+10	0	-240	0.65	N/A	N/A	N/A	Too high
10	INC	0	0.036814	100	0.8	0.5	100	0.4	0.7	-76.4668	87.4	0	-0.103	N/A	N/A	N/A	1.2	1.55	0	11	9	250k+09	0.85	N/A	375	1	0.7	1.00E+10	0	-240	0.65	N/A	N/A	N/A	Too low
11	INC	0	0.036814	10	0.8	0.5	100	0.4	0.7	-76.4668	87.4	0	-0.103	N/A	N/A	N/A	1.2	1.55	0	11	9	250k+09	0.85	N/A	375	1	0.7	1.00E+10	0	-240	0.65	N/A	N/A	N/A	A little low, need to shorten pulse
12	INC	0	0.036814	5	0.8	0.5	100	0.4	0.7	-76.4668	87.4	0	-0.103	N/A	N/A	N/A	1.2	1.55	0	11	9	250k+09	0.85	N/A	375	1	0.7	1.00E+10	0	-240	0.65	N/A	N/A	N/A	Higher, pulse is still too long, but shorter than 11
13	INC	0	0.036814	5	0.8	0.5	10	0.4	0.7	-76.4668	87.4	0	-0.103	N/A	N/A	N/A	1.2	1.55	0	11	9	250k+09	0.85	N/A	375	1	0.7	1.00E+10	0	-240	0.65	N/A	N/A	N/A	Delayed with slightly lower peak than 12
14	INC	0	0.036814	5	80	0.5	10	0.4	0.7	-76.4668	87.4	0	-0.103	N/A	N/A	N/A	1.2	1.55	0	11	9	250k+09	0.85	N/A	375	1	0.7	1.00E+10	0	-240	0.65	N/A	N/A	N/A	Way too high - need to match closer with HQ
15	INC	0	0.036814	5	80	0.5	100	0.4	0.7	-76.4668	87.4	0	-0.102	N/A	N/A	N/A	1.2	1.55	0	11	9	250k+09	0.85	N/A	375	1	0.7	1.00E+10	0	-240	0.65	N/A	N/A	N/A	-0.1 was too aggressive, 0.102 a bit too aggressive
16	INC	0	0.036814	5	0.8	0.5	100	0.4	0.7	-76.4668	87.4	0	-0.104	N/A	N/A	N/A	1.2	1.55	0	11	9	250k+09	0.85	N/A	375	1	0.7	1.00E+10	0	-240	0.65	N/A	N/A	N/A	Timing was right, but peak was too high
17	INC	0	0.036814	5	0.8	0.5		0.4	0.7	-76.4668	87.4	0		N/A	N/A	N/A	1.2	1.55	0	11	9	250k+09	0.85	N/A	375	1	0.7	1.00E+10	0	-240	0.65	N/A	N/A	N/A	
18	INC	0	0.036814	1	0.8	0.5	1000	0.4	0.7	-76.4668	87.4	0	-0.103	N/A	N/A	N/A	1.2	1.55	0	11	9	250k+09	0.85	N/A	375	1	0.7	1.00E+10	0	-240	0.65	N/A	N/A	N/A	Reset to 1 - changed load pulse (shifted 05 ms rig), changed floor plate to ellipsoid to prevent boundary condition at edge (+ re-fix pelvis fix file by data)
19	INC	0	0.036814	1	0.8	0.5	1000	0.4	0.7	-76.4668	87.4	0	-0.103	10000	None	Added joint restraint to tibia and femur - lowered peak slightly	1	1.2	1.55	0	11	9	250k+09	0.85	N/A	375	1	0.7	1.00E+10	0	-240	0.65	N/A	N/A	N/A	Added joint restraint to tibia and femur - lowered peak slightly
20	INC	0	0.036814	1	0.8	0.5	1000	0.4	0.7	-76.4668	87.4	0	-0.103	10000	1000		1	1.2	1.55	0	11	9	250k+09	0.85	N/A	375	1	0.7	1.00E+10	0	-240	0.65	N/A	N/A	N/A	Small improvement
21	INC	0	0.036814	1	0.8	0.5	1000	0.4	0.7	-76.4668	87.4	0	-0.103	10000	1000	Changed 0.0 05 to 0.00 0 for tend of unloading	1	1.2	1.55	0	11	9	250k+09	0.85	N/A	375	1	0.7	1.00E+10	0	-240	0.65	N/A	N/A	N/A	
22	INC	0	0.036814	1	0.8	0.5	1000	0.4	0.7	-76.4668	87.4	0	-0.105	10005	1000	Changed unloading curve to 100000 on unloading 1	1	1.2	1.55	0	11	9	250k+09	0.85	N/A	375	1	0.7	1.00E+10	0	-240	0.65	N/A	N/A	N/A	Too much extension, was extra data
23	INC	0	0.036814	1	0.8	0.5	1000	0.4	0.7	-76.4668	87.4	0	-0.103	10000	1000	Changed unloading profile to extend 2	1	1.2	1.55	0	11	9	250k+09	0.85	N/A	375	1	0.7	1.00E+10	0	-240	0.65	N/A	N/A	N/A	
24	INC	0	0.036814	1	0.8	0.5	1000	0.4	0.7	-76.4668	87.4	0	-0.103	10000	1000	Changed unloading profile to start at 0	1	1.2	1.55	0	11	9	250k+09	0.85	N/A	375	1	0.7	1.00E+10	0	-240	0.65	N/A	N/A	N/A	Fixed preloading
25	INC	0	0.036814	1	0.8	0.5	1000	0.4	0.7	-76.4668	87.4	0	-0.103	10000	10		1	1.2	1.55	0	11	9	250k+09	0.85	N/A	375	1	0.7	1.00E+10	0	-240	0.65	N/A	N/A	N/A	
26	INC	0	0.036814	1	0.8	0.5	1000	0.4	0.7	-76.4668	87.4	0	-0.103	10000	10000		1	1.2	1.55	0	11	9	250k+09	0.85	N/A	375	1	0.7	1.00E+10	0	-240	0.65	N/A	N/A	N/A	
27	INC	0	0.036814	1	0.8	0.5	1000	0.4	0.7	-76.4668	87.4	0	-0.103	10000	100000		1	1.2	1.55	0	11	9	250k+09	0.85	N/A	375	1	0.7	1.00E+10	0	-240	0.65	N/A	N/A	N/A	Minimal improvement
28	INC	0	0.036814	1	0.8	0.5	1000	0.4	0.7	-76.4668	87.4	0	-0.103	10000	10000		1	1.2	1.55	0	11	9	250k+09	0.85	N/A	375	1	0.7	1.00E+10	0	-240	0.65	N/A	N/A	N/A	
29	INC	0	0.036814	1	0.8	0.5	1000	0.4	0.7	-76.4668	87.4	0	-0.103	10000	10000	Unloading curve increased to 100000	1	1.2	1.55	0	11	9	250k+09	0.85	N/A	375	1	0.7	1.00E+10	0	-240	0.65	N/A	N/A	N/A	Rise increased
30	INC	0	0.036814			0.5		0.4	0.7	-76.4668	87.4	0	-0.103			Unloading curve decreased to 1000	1	1.2	1.55	0	11	9	250k+09	0.85	N/A	375	1	0.7	1.00E+10	0	-240	0.65	N/A	N/A	N/A	Same as run 28
31	INC	0	0.036814			0.5		0.4	0.7	-76.4668	87.4	0	-0.103			Timing of unloading curve changed to 0.04	1	1.2	1.55	0	11	9	250k+09	0.85	N/A	375	1	0.7	1.00E+10	0	-240	0.65	N/A	N/A	N/A	Same as run 28
32	INC	0	0.036814	1		0.5		0.4	0.7	-76.4668	87.4	0	-0.103			Timing of unloading curve changed to 0.4	1	1.2	1.55	0	11	9	250k+09	0.85	N/A	375	1	0.7	1.00E+10	0	-240	0.65	N/A	N/A	N/A	Same as run 28
Fixed order	INC	0	0.036814			0.5		0.4	0.7	-76.4668	87.4	0	-0.103				1	1.2	1.55	0	11	9	250k+09	0.85	N/A	375	1	0.7	1.00E+10	0	-240	0.65	N/A	N/A	N/A	
33	INC	0	0.036814	0.1		0.5	100	0.4	0.7	-76.4668	87.4	0	-0.103	1000	10000	Same as previous	1	1.2	1.55	0	11	9	250k+09	0.85	N/A	375	1	0.7	1.00E+10	0	-240	0.65	N/A	N/A	N/A	
34	INC	0	0.036814	0.01		0.5	100	0.4	0.7	-76.4668	87.4	0	-0.103	1000	10000	Same as previous	1	1.2	1.55	0	11	9	250k+09	0.85	N/A	375	1	0.7	1.00E+10	0	-240	0.65	N/A	N/A	N/A	Added x-axis fix to unloading curve
35	INC	0	0.036814	0.001		0.5	100	0.4	0.7	-76.4668	87.4	0	-0.103	1000	10000	Same as previous	1	1.2	1.55	0	11	9	250k+09	0.85	N/A	375	1	0.7	1.00E+10	0	-240	0.65	N/A	N/A	N/A	No change
36	INC	-0.5	0.036814	0.01	0.8	0.5	100	0.4	0.7	-76.4668	87.4	0	-0.103	1000	10000	Same as previous	1	1.2	1.55	0	11	9	250k+09	0.85	N/A	375	1	0.7	1.00E+10	0	-240	0.65	N/A	N/A	N/A	No change
37	INC	0	0.036814	0.01	0.8	0.5	1	0.4	0.7	-76.4668	87.4	0	-0.104	1000	10000	Same as previous	1	1.2	1.55	0	11	9	250k+09	0.85	N/A	375	1	0.7	1.00E+10	0	-240	0.65	N/A	N/A	N/A	No change
38	INC	0	0.036814	1	0.8	0.5	1	0.4	0.7	-76.4668	87.4	0		1000	10000	Same as previous	1	1.2	1.55	0	11	9	250k+09	0.85	N/A	375	1	0.7	1.00E+10	0	-240	0.65	N/A	N/A	N/A	
39	INC	0	0.036814	1	0.8	0.5		0.4	0.7	-76.4668	87.4	0		1000	10000	Same as previous	1	1.2	1.55	0	11	9	250k+09	0.85	N/A	375	1	0.7	1.00E+10	0	-240	0.65	N/A	N/A	N/A	
40	INC	0	0.036814	1	0.8	0.5	1	0.4	0.7	-76.4668	87.4	0	-0.103	1000	10000	Same as previous	1	1.2	1.55	0	11	9	250k+09	0.85	N/A	375	1	0.7	1.00E+10	0	-240	0.65	N/A	N/A	N/A	Clip ripped cannot to scale fix+ first as start, slightly lower peak, slightly faster pickup
41	INC		0.036814	1	0.8	0.5		0.4	0.7	-76.4668	87.4	0		1000	10000	Same as previous	1	1.2	1.55	0			250k+09		N/A	375	1	0.7	1.00E+10	0	-240	0.65	N/A	N/A	N/A	
42	INC	0	0.036814	1	0.8	0.5	1	0.4	0.7	-76.4668	87.4	0	-0.103	1000	10000	Same as previous	1	1.2	1.55	0	11	90	250k+09	0.85	N/A	375	1	0.7	1.00E+10	0	-240	0.65	N/A	N/A	N/A	Much higher in pelvis + need to balance with +
43	INC	0	0.036814	1	0.8	0.5	1	0.4	0.7	-76.4668	87.4	0	-0.103	1000	10000	Same as previous	1	1.2	1.55	0	5	90	250k+09	0	N/A	375	1	0.7	1.00E+10	0	-240	0.65	N/A	N/A	N/A	Much better balance pelvis x and z. Need to shorten pulse
44	INC	0	0.036814	1	0.8	0.5	1	0.4	0.7	-76.4668	87.4	0	-0.103	1000	10000	Same as previous	1	1.2	1.55	0	5	90	1.00E+09	0	N/A	375	1	0.7	1.00E+10	0	-240	0.65	N/A	N/A	N/A	Pelvis rate only quite after 10 ms - minor change
45	INC	0	0.036814	1	0.8	0.5	1	0.4	0.7	-76.4668	87.4	0	-0.103	1000	10000	Same as previous	1	1.2	1.55	0	5	45	1.00E+09	0	N/A	375	1	0.7	1.00E+10	0	-240	0.65	N/A	N/A	N/A	50% pelvis + 50% peak
46	INC	0	0.036814	1	0.8	0.5	1	0.4	0.7	-76.4668	87.4	0	-0.103	1000	10000	Same as previous	1	1.2	1.55	0	0	0	1.00E+09	0	N/A	375	1	0.7	1.00E+10	0	-240	0.65	N/A	N/A	N/A	Shifted ribs pos + in right direction, too low magnitude
47	INC	0	0.036814	1	0.8	0.5	1	0.4	0.7	-76.4668	87.4	0	-0.103	1000	10000	Same as previous	1	1.2	1.55	0	0	90	1.00E+09	0	N/A	375	1	0.7	1.00E+10	0	-240	0.65	N/A	N/A	N/A	Good pos for pelvis but at ds, initial pos too wide
48	INC	0	0.036814	1	0.8	0.5	1	0.4	0.7	-76.4668	87.4	0	-0.103	Disable	Disable	Disable	N/A	1.2	1.55	0	0	90	1.00E+09	0	N/A	375	1	0.7	1.00E+10	0	-240	0.65	N/A	N/A	N/A	Disabled
49	INC	0.2	0.036814	1	0.8	0.5	1	0.4	0.7	-76.4668	87.4	0	-0.104	Disable	Disable	Disable	N/A	1.2	1.55	0	0	90	1.00E+09	0	N/A	375	1	0.7	1.00E+10	0	-240	0.65	N/A	N/A	N/A	Pelvis fix+ first, tibia reduced by factor of 2 - correct direction - limited to ages to pelvis, T1
50	INC	-1	0.036814	1	0.8	0.5	1	0.4	0.7	-76.4668	87.4	0	-0.105	Disable	Disable	Disable	N/A	1.2	1.55	0	0	90	1.00E+09	0	N/A	375	1	0.7	1.00E+10	0	-240	0.65	N/A	N/A	N/A	Fixed leg positions to new in PMHS (moved hips 2 mm, knees to match in X) + added fix for sub x,z,θ
51	INC	-1	0.036814	0.5	0.8	0.5	1	0.4	0.7	-76.4668	87.4	0	-0.103	Disable	Disable	Disable	N/A	1.2	1.55	0	0	90	1.00E+09	0	N/A	375	1	0.7	1.00E+10	0	-240	0.65	N/A	N/A	N/A	Lower number, slightly lower, not shorter in pulse, but not significant enough
52	INC	-1	0.036814	0.5	0.8	0.5	0.5	0.4	0.7	-76.4668	87.4	0	-0.103	Disable	Disable	Disable	N/A	1.2	1.55	0	0	90	1.00E+09	0	N/A	375	1	0.7	1.00E+10	0	-240	0.65	N/A	N/A	N/A	No change
53	INC	-1	0.036814	0.5	0.8	0.5	1	0.4	0.7	-76.4668	87.4	0	-0.103	1000	10000	Same as previous	1	1.2	1.55	0	0	90	1.00E+09	0	N/A	375	1	0.7	1.00E+10	0	-240	0.65	N/A	N/A	N/A	Reset to x-axis
54	INC	-1	0.036814	0.5	0.8	0.5	1	0.4	0.7	-76.4668	87.4	0	-0.103	1000	10000	Same as previous	05	1.2	1.55	0	0	90	1.00E+09	0	N/A	375	1	0.7	1.00E+10	0	-240	0.65	N/A	N/A	N/A	Added x-axis fix to pelvis rotation - No change
55	INC	-1	0.036814	0.5	0.8	0.5	1	0.4	0.7	-76.4668	87.4	0	-0.103	1000	100	Same as previous	05	1.2	1.55	0	0	90	1.00E+09	0	N/A	375	1	0.7	1.00E+10	0	-240	0.65	N/A	N/A	N/A	Matches run 52
56	INC	-1	0.036814	0.5	0.8	0.5	1	0.4	0.7	-76.4668	87.4	0	-0.103	1000	10	Same as previous	05	1.2	1.55	0	0	90	1.00E+09	0	N/A	375	1	0.7	1.00E+10	0	-240	0.65	N/A	N/A	N/A	Moving Leluque from 05 ms up in femur fix
57	INC	-1	0.036814	0.5	0.8	0.5	1	0.4	0.7	-76.4668	87.4	0	-0.103	1000	10	Same as previous	05	1.2	1.55	0	0	90	1.00E+09	0	N/A	375	1	0.7	1.00E+10	0	-240	0.65	N/A	N/A	N/A	Moving Leluque longer
58	INC	-1	0.036814	0.5	0.08	0.01	1	0.4	0.7	-76.4668	87.4	0	-0.103	1000	10	Same as previous	05	1.2	1.55	0	0	90	1.00E+09	0	N/A	375	1	0.7	1.00E+10	0	-240	0.65	N/A	N/A	N/A	Large improvement to fit peak width for foot, but tibia fix is tricky
59	INC	-1	0.036814	0.5	0.04	0.01	1	0.4	0.7	-76.4668	87.4	0	-0.103	1000	10	Same as previous	05	1.2	1.55	0	0	90	1.00E+09	0	N/A	375	1	0.7	1.00E+10	0	-240	0.65	N/A	N/A	N/A	Lower peak but earlier, still tricky Tibia fix
60	INC	-1	0.036814	0.5	0.04	0.01	1	0.4	0.7	-76.4668	87.4	4	-0.103	1000	10	Same as previous	05	1.2	1.55	0	0	90	1.00E+09	0	N/A	375	1	0.7	1.00E+10	0	-240	0.65	N/A	N/A	N/A	Minor adjustments to tibia
61	INC	-1	0.036814	0.5	0.04	0.01	1	0.4	0.7	-76.4668	87.4	-3	-0.103	1000	10	Same as previous	05	1.2	1.55	0	0	90	1.00E+09	0	N/A	375	1	0.7	1.00E+10	0	-240	0.65	N/A	N/A	N/A	Better fix+ first, worse fix+ first, still no by Tibia fix
62	INC	-1	0.036814	0.5	0.04	0.01	1	0.4	0.7	-76.4668	88	-3	-0.103	1000	10	Same as previous	05	1.2	1.55	0	0	90	1.00E+09	0	N/A	375	1	0.7	1.00E+10	0	-240	0.65	N/A	N/A	N/A	Better fix+ tibia, worse fix+ first, still no by Tibia fix
63	INC	-1	0.036814	0.5	0.2	0.05	1	0.4	0.7	-76.4668	88	-3	-0.103	1000	10	Same as previous	05	1.2	1.55	0	0	90	1.00E+09	0	N/A	375	1	0.7	1.00E+10	0	-240	0.65	N/A	N/A	N/A	Removed wider from Tibia fix (which is too high) - Tibia fix is good, fix+ is late (too high, too wide)
64	INC	-1	0.036814	0.5	0.2	0.05	1	0.4	0.7	-77	88	-3	-0.103	1000	10	Same as previous	05	1.2	1.55	0	0	90	1.00E+09	0	N/A	375	1	0.7	1.00E+10	0	-240	0.65	N/A	N/A	N/A	Moved hips to increase pk-top on femur fix, had to shift floor and back knee + major issue with lower legs
65	INC	-1	0.036814	0.5	0.2	0.05	1	0.4	0.7	-78	86	-3	-0.104	1000	10	Same as previous	05	1.2	1.55	0	0	90	1.00E+09	0	N/A	375	1	0.7	1.00E+10	0	-240	0.65	N/A	N/A	N/A	Still major issue with lower legs
66	INC	-1	0.036814	0.5	0.2	0.05	1	0.4	0.7	-78	87	-3	-0.104	1000	10	Same as previous	05	1.2	1.55	0	0	90	1.00E+09	0	N/A	375	1	0.7	1.00E+10	0	-240	0.65	N/A	N/A	N/A	
67	INC	-1	0.036814	0.5	0.2	0.05	1	0.4	0.7	-78	88	0	-0.104	1000	10	Same as previous	05	1.2	1.55	0	0	90	1.00E+09	0	N/A	375	1	0.7	1.00E+10	0	-240	0.65	N/A	N/A	N/A	
68	INC	-1	0.036814	0.5	0.8	0.5	1	0.4	0.7	-76.4668	87.4	0	-0.103	1000	100	Same as previous	05	1.2	1.55	0	0	90	1.00E+09	0	N/A	375	1	0.7	1.00E+10	0	-240	0.65	N/A	N/A	N/A	Reset to 05, shifted peak by 1 ms - too much
69	INC	-1	0.036814	0.5	0.8	0.5	1	0.4	0.7	-76.4668	87.4	0	-0.103	1000	100	Same as previous	05	1.2	1.55	0	0	90	1.00E+09	0	N/A	375	1	0.7	1.00E+10	0	-240	0.65	N/A	N/A	N/A	Shifted rear by 0.5 ms - worse
70	INC	-1	0.036814	0.5	0.8	0.5	1	0.4	0.7	-76.4668	87.4	0	-0.103	1000	100	Same as previous	05	1.2	1.55	0	0	90	1.00E+09	0	N/A	75	1	0.7	1.00E+10	0	-240	0.65	N/A	N/A	N/A	No change from T1 x-scale
71	INC	-1	0.036814	0.5	0.8	0.5	1	0.4	0.7	-76.4668	87.4	0	-0.103	1000	100	Same as previous	05	1.2	1.55	0	0	90	1.00E+09	0	N/A	5	1	0.7	1.00E+10	0	-240	0.65	N/A	N/A	N/A	Directionality correct - too jagged, lower fix+ T1 x
72	INC	-1	0.036814	0.5	0.8	0.5	1	0.4	0.7	-76.4668	87.4	0	-0.103	1000	100	Same as previous	05	1.2	1.55	0	0	90	1.00E+09	0	N/A	5	1	0.7	1.00E+10	0	-240	0.65	N/A	N/A	N/A	Directionality correct - too jagged, lower fix+ T1 x
73	INC	-1	0.036814	0.5	0.8	0.5	1	0.4	0.7	-76.4668	87.4	0	-0.103	1000	100	Same as previous	05	1.2	1.55	0	0	90	1.00E+09	0	N/A	0.2	1	0.7	1.00E+10	0	-240	0.65	N/A	N/A	N/A	Switched peak to fix+ T1 x, also moved pulse and moved earlier (directionality correct)
74	INC	-1	0.036814	0.5	0.8	0.5	1	0.4	0.7	-76.4668	87.4	0	-0.103	1000	100	Same as previous	05	1.2	1.55	0	0	90	1.00E+09	0	N/A	0.2	1	0.7	1.00E+10	0	-240	0.65	N/A	N/A	N/A	Moved T1 y scale - no difference
75	INC	-1	0.036814	0.5	0.8	0.5	1	0.4	0.7	-76.4668	87.4	0	-0.103	1000	100	Same as previous	05	1.2	1.55	0	0	90	1.00E+09	0	N/A	0.2	1	0.7	1.00E+10	0	-240	0.65	N/A	N/A	N/A	Combined T1 to T12 scales of 0 - now is improved in timing
76	INC	-1	0.036814	0.5	0.8	0.5	1	0.4	0.7	-76.4668	87.4	0	-0.103	1000	100	Same as previous	05	0.5	1.55	0	0	90	1.00E+09	0	N/A	0.2	1	0.7	1.00E+10	0	-240	0.65	N/A	N/A	N/A	Opposite effect as started to flatten but only flattened loading, which is too late
77	INC	-1	0.036814	0.5	0.8	0.5	1	0.4	0.7	-76.4668	87.4	0	-0.103	1000	100	Same as previous	05	1.2	1	0	0	90	1.00E+09	0	N/A	0.2	1	0.7

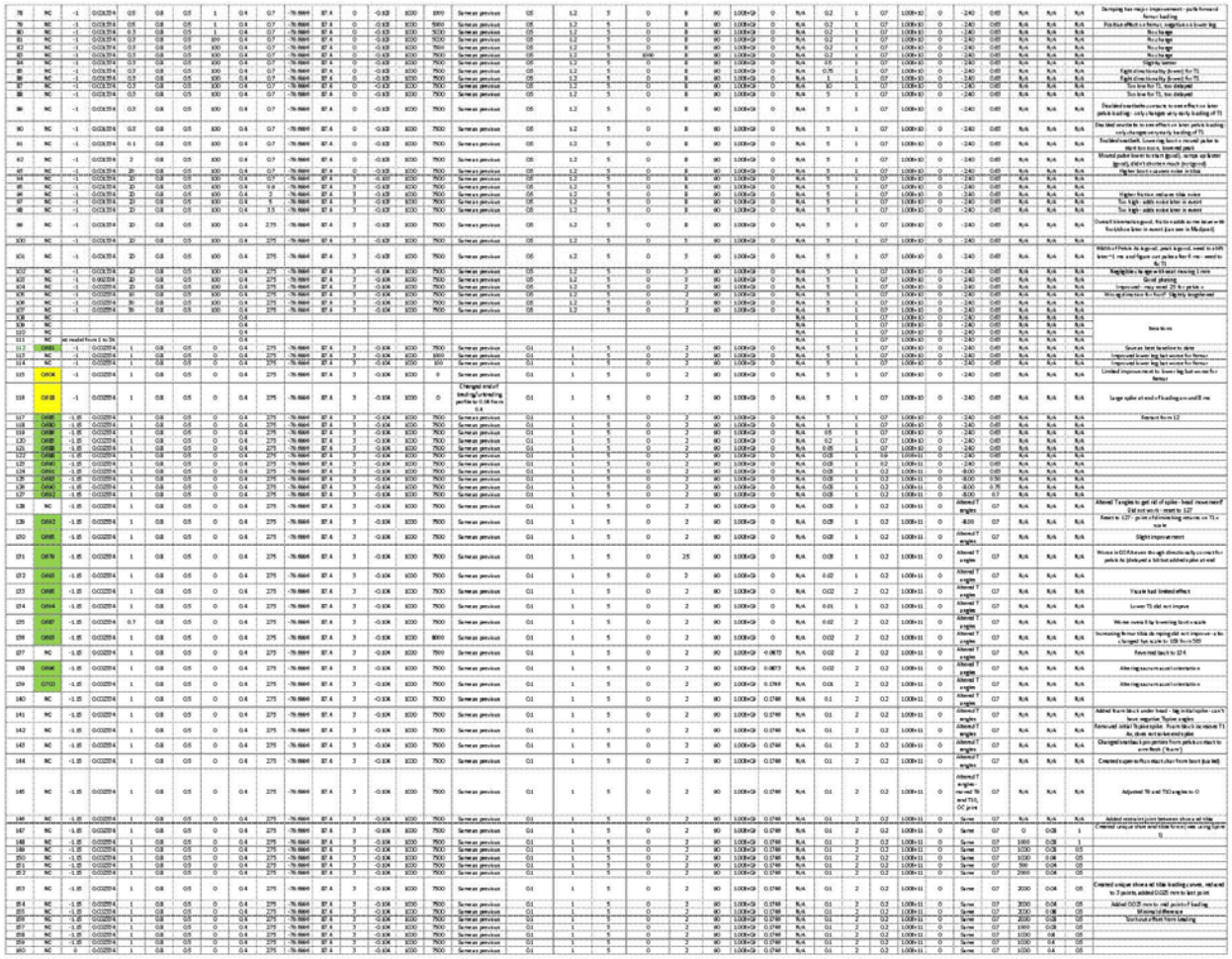

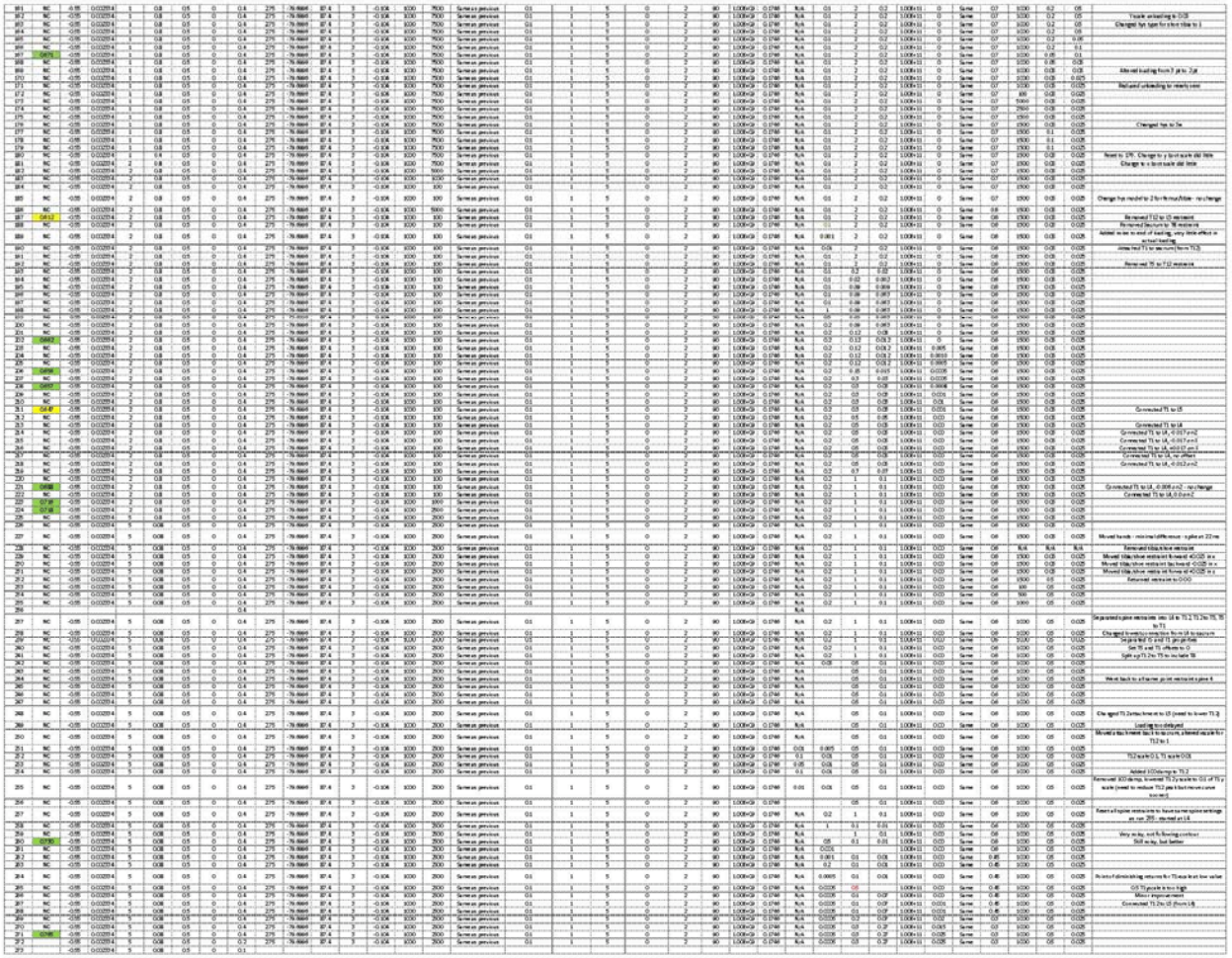

APPENDIX D – CONDITION B PMHS MODEFRONTIER DOE DATA

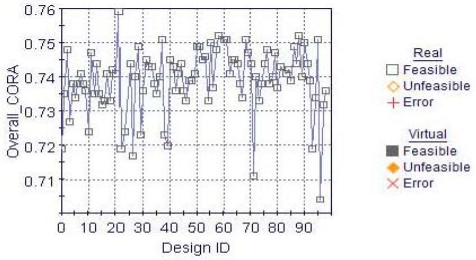


```
#--- Frontier Design DB File Info ------------
#modeFRONTIER - (c) ESTECO S.p.A.
#Design DB Table
#---------------------------------------------
#modeFRONTIER Version: modeFRONTIER 2017R5 5.7.1 b20171017
#Date: Wed Jun 20 14:05:54 EDT 2018
#Project Name: PMHS B Validation 2018-06-18_280.prj
#Operating System: Windows 10 10.0 amd64
#Java (SDK/JRE) Version: 1.8.0_60
#Java Vendor: Oracle Corporation
#Java Vendor URL: http://java.oracle.com/
#User Name: KBosch
#---------------------------------------------
#Categories
<CATEGORIES clusterPrefix="CLUSTER_" useTableNamePrefix="false">
  <CATEGORY enabled="true" label="" name="SOBOL" symbolc="SQUARE,NONE,11,,0"/>
  <CATEGORY enabled="true" label="" name="USRDOE" symbolc="SQUARE,NONE,11,,0"/>
  <CATEGORY enabled="true" label="" name="NSGA2" symbolc="SQUARE,NONE,11,,0"/>
  <CATEGORY enabled="true" label="" name="TOA" symbolc="SQUARE,NONE,11,,0"/>
  <CATEGORY enabled="true" label="" name="DOE_APPROX" symbolc="SQUARE,NONE,11,,0"/>
  <CATEGORY enabled="true" label="" name="SIMPLEX" symbolc="SQUARE,NONE,11,,0"/>
  <CATEGORY enabled="true" label="" name="ULH" symbolc="SQUARE,NONE,11,,0"/>
  <CATEGORY enabled="true" label="" name="FULLF" symbolc="SQUARE,NONE,11,#DC3912,1,#DC3912"/>
</CATEGORIES>

#---------------------------------------------
```

<ID>	Pelvis_fd_fnc_x	Pelvis_fd_fnc_x_femur	Pelvis_fd_fnc_y	Shoe_Floor_Friction_Scale	T1_ori_KB	T1_yscale	T5_offset	Overall_CORA	Obj_Overall	<ERROR>	<VIRTUAL>	<FEASIBLE>	<IMARKED>	<CATEGORY>
0	3.13E+00	1.20E+00	1.13E+02	6.00E+00	2.81E-01	1.00E+00	6.13E-03	7.19E-01	7.19E-01	false	false	true	false	ULH
1	1.88E+00	1.20E+00	6.75E+01	6.00E+00	2.81E-01	5.00E-01	6.13E-03	7.35E-01	7.35E-01	false	false	true	false	ULH
2	1.88E+00	1.05E+00	1.13E+02	6.00E+00	3.75E-01	7.50E-01	3.75E-03	7.48E-01	7.48E-01	false	false	true	false	ULH
3	2.50E+00	9.00E-01	1.13E+02	6.00E+00	4.69E-01	5.00E-01	6.13E-03	7.27E-01	7.27E-01	false	false	true	false	ULH
4	3.13E+00	9.00E-01	9.00E+01	3.00E+00	4.69E-01	5.00E-01	3.75E-03	7.38E-01	7.38E-01	false	false	true	false	ULH
5	1.88E+00	1.20E+00	1.13E+02	3.00E+00	4.69E-01	7.50E-01	3.75E-03	7.34E-01	7.34E-01	false	false	true	false	ULH
6	1.88E+00	1.05E+00	6.75E+01	6.00E+00	2.81E-01	1.00E+00	6.13E-03	7.38E-01	7.38E-01	false	false	true	false	ULH
7	2.50E+00	1.20E+00	6.75E+01	3.00E+00	2.81E-01	5.00E-01	4.94E-03	7.41E-01	7.41E-01	false	false	true	false	ULH
8	3.13E+00	9.00E-01	9.00E+01	3.00E+00	3.75E-01	5.00E-01	4.94E-03	7.38E-01	7.38E-01	false	false	true	false	ULH
9	3.13E+00	1.20E+00	9.00E+01	4.50E+00	4.69E-01	7.50E-01	3.75E-03	7.36E-01	7.36E-01	false	false	true	false	ULH
10	3.13E+00	1.20E+00	1.13E+02	6.00E+00	3.75E-01	1.00E+00	4.94E-03	7.24E-01	7.24E-01	false	false	true	false	ULH
11	1.88E+00	9.00E-01	1.13E+02	6.00E+00	2.81E-01	1.00E+00	3.75E-03	7.47E-01	7.47E-01	false	false	true	false	ULH
12	2.50E+00	1.20E+00	1.13E+02	4.50E+00	3.75E-01	1.00E+00	3.75E-03	7.35E-01	7.35E-01	false	false	true	false	ULH
13	1.88E+00	1.20E+00	6.75E+01	3.00E+00	4.69E-01	1.00E+00	4.94E-03	7.44E-01	7.44E-01	false	false	true	false	ULH
14	2.50E+00	1.05E+00	1.13E+02	4.50E+00	2.81E-01	7.50E-01	6.13E-03	7.35E-01	7.35E-01	false	false	true	false	ULH
15	2.50E+00	1.05E+00	1.13E+02	4.50E+00	4.69E-01	7.50E-01	6.13E-03	7.32E-01	7.32E-01	false	false	true	false	ULH
16	2.50E+00	1.05E+00	1.13E+02	4.50E+00	2.81E-01	5.00E-01	4.94E-03	7.33E-01	7.33E-01	false	false	true	false	ULH
17	1.88E+00	1.05E+00	1.13E+02	4.50E+00	4.69E-01	5.00E-01	3.75E-03	7.41E-01	7.41E-01	false	false	true	false	ULH
18	2.50E+00	1.20E+00	1.13E+02	4.50E+00	2.81E-01	5.00E-01	4.94E-03	7.33E-01	7.33E-01	false	false	true	false	ULH
19	2.50E+00	1.20E+00	9.00E+01	6.00E+00	4.69E-01	7.50E-01	6.13E-03	7.42E-01	7.42E-01	false	false	true	false	ULH
20	1.88E+00	1.05E+00	9.00E+01	4.50E+00	2.81E-01	1.00E+00	6.13E-03	7.41E-01	7.41E-01	false	false	true	false	ULH
21	1.88E+00	1.20E+00	9.00E+01	3.00E+00	4.69E-01	7.50E-01	4.94E-03	7.59E-01	7.59E-01	false	false	true	false	ULH
22	3.13E+00	9.00E-01	1.13E+02	4.50E+00	4.69E-01	1.00E+00	6.13E-03	7.19E-01	7.19E-01	false	false	true	false	ULH
23	2.50E+00	1.20E+00	1.13E+02	3.00E+00	3.75E-01	5.00E-01	6.13E-03	7.24E-01	7.24E-01	false	false	true	false	ULH
24	2.50E+00	1.05E+00	6.75E+01	6.00E+00	3.75E-01	1.00E+00	3.75E-03	NaN	NaN	true	false	true	false	ULH
25	3.13E+00	1.05E+00	9.00E+01	6.00E+00	3.75E-01	1.00E+00	4.94E-03	7.44E-01	7.44E-01	false	false	true	false	ULH
26	3.13E+00	9.00E-01	1.13E+02	6.00E+00	3.75E-01	1.00E+00	4.94E-03	7.17E-01	7.17E-01	false	false	true	false	ULH
27	1.88E+00	9.00E-01	1.13E+02	4.50E+00	4.69E-01	1.00E+00	3.75E-03	7.40E-01	7.40E-01	false	false	true	false	ULH
28	1.88E+00	9.00E-01	9.00E+01	3.00E+00	3.75E-01	5.00E-01	4.94E-03	7.49E-01	7.49E-01	false	false	true	false	ULH
29	3.13E+00	1.20E+00	1.13E+02	6.00E+00	3.75E-01	7.50E-01	3.75E-03	7.23E-01	7.23E-01	false	false	true	false	ULH
30	1.88E+00	1.20E+00	1.13E+02	6.00E+00	4.69E-01	5.00E-01	3.75E-03	7.36E-01	7.36E-01	false	false	true	false	ULH
31	2.50E+00	1.05E+00	9.00E+01	3.00E+00	4.69E-01	7.50E-01	4.94E-03	7.45E-01	7.45E-01	false	false	true	false	ULH
32	1.88E+00	1.20E+00	1.13E+02	3.00E+00	2.81E-01	7.50E-01	3.75E-03	7.43E-01	7.43E-01	false	false	true	false	ULH
33	2.50E+00	9.00E-01	9.00E+01	3.00E+00	4.69E-01	7.50E-01	6.13E-03	7.43E-01	7.43E-01	false	false	true	false	ULH
34	1.88E+00	1.05E+00	1.13E+02	3.00E+00	4.69E-01	5.00E-01	6.13E-03	7.38E-01	7.38E-01	false	false	true	false	ULH
35	2.50E+00	1.05E+00	1.13E+02	6.00E+00	2.81E-01	5.00E-01	3.75E-03	7.35E-01	7.35E-01	false	false	true	false	ULH
36	2.50E+00	1.05E+00	6.75E+01	4.50E+00	2.81E-01	1.00E+00	3.75E-03	7.40E-01	7.40E-01	false	false	true	false	ULH
37	1.88E+00	1.05E+00	6.75E+01	3.00E+00	4.69E-01	7.50E-01	6.13E-03	7.51E-01	7.51E-01	false	false	true	false	ULH
38	3.13E+00	1.20E+00	1.13E+02	4.50E+00	3.75E-01	7.50E-01	3.75E-03	7.23E-01	7.23E-01	false	false	true	false	ULH
39	3.13E+00	1.20E+00	1.13E+02	3.00E+00	3.75E-01	1.00E+00	6.13E-03	7.20E-01	7.20E-01	false	false	true	false	ULH
40	3.13E+00	1.05E+00	6.75E+01	3.00E+00	3.75E-01	7.50E-01	6.13E-03	7.45E-01	7.45E-01	false	false	true	false	ULH
41	1.88E+00	1.05E+00	6.75E+01	4.50E+00	3.75E-01	1.00E+00	6.13E-03	7.43E-01	7.43E-01	false	false	true	false	ULH
42	2.50E+00	9.00E-01	6.75E+01	3.00E+00	2.81E-01	7.50E-01	3.75E-03	7.36E-01	7.36E-01	false	false	true	false	ULH
43	3.13E+00	9.00E-01	9.00E+01	4.50E+00	2.81E-01	1.00E+00	4.94E-03	7.41E-01	7.41E-01	false	false	true	false	ULH
44	3.13E+00	1.05E+00	6.75E+01	4.50E+00	3.75E-01	7.50E-01	6.13E-03	7.44E-01	7.44E-01	false	false	true	false	ULH
45	2.50E+00	9.00E-01	6.75E+01	4.50E+00	2.81E-01	7.50E-01	4.94E-03	7.36E-01	7.36E-01	false	false	true	false	ULH
46	1.88E+00	1.20E+00	6.75E+01	4.50E+00	2.81E-01	5.00E-01	4.94E-03	7.33E-01	7.33E-01	false	false	true	false	ULH
47	3.13E+00	1.20E+00	9.00E+01	4.50E+00	3.75E-01	7.50E-01	4.94E-03	7.39E-01	7.39E-01	false	false	true	false	ULH
48	1.88E+00	9.00E-01	6.75E+01	6.00E+00	2.81E-01	7.50E-01	4.94E-03	7.39E-01	7.39E-01	false	false	true	false	ULH
49	3.13E+00	1.20E+00	6.75E+01	4.50E+00	2.81E-01	5.00E-01	4.94E-03	7.41E-01	7.41E-01	false	false	true	false	ULH
50	1.88E+00	1.20E+00	9.00E+01	3.00E+00	2.81E-01	5.00E-01	4.94E-03	7.49E-01	7.49E-01	false	false	true	false	ULH
51	1.88E+00	1.20E+00	9.00E+01	4.50E+00	2.81E-01	5.00E-01	4.94E-03	7.49E-01	7.49E-01	false	false	true	false	ULH
52	3.13E+00	1.20E+00	6.75E+01	4.50E+00	3.75E-01	1.00E+00	4.94E-03	7.45E-01	7.45E-01	false	false	true	false	ULH

53	2.50E+00	1.05E+00	9.00E+01	6.00E+00	4.69E-01	1.00E+00	4.94E-03	7.46E-01	7.46E-01	false	false	true	false	ULH
54	1.88E+00	1.20E+00	6.75E+01	6.00E+00	2.81E-01	1.00E+00	4.94E-03	7.33E-01	7.33E-01	false	false	true	false	ULH
55	1.88E+00	1.05E+00	1.13E+02	6.00E+00	2.81E-01	7.50E-01	6.13E-03	7.50E-01	7.50E-01	false	false	true	false	ULH
56	3.13E+00	1.05E+00	9.00E+01	6.00E+00	4.69E-01	5.00E-01	4.94E-03	7.37E-01	7.37E-01	false	false	true	false	ULH
57	2.50E+00	1.05E+00	6.75E+01	3.00E+00	3.75E-01	1.00E+00	3.75E-03	7.48E-01	7.48E-01	false	false	true	false	ULH
58	1.88E+00	1.05E+00	6.75E+01	6.00E+00	4.69E-01	5.00E-01	6.13E-03	7.52E-01	7.52E-01	false	false	true	false	ULH
60	1.88E+00	9.00E-01	6.75E+01	3.00E+00	4.69E-01	1.00E+00	3.75E-03	7.51E-01	7.51E-01	false	false	true	false	ULH
61	3.13E+00	1.05E+00	6.75E+01	3.00E+00	4.69E-01	1.00E+00	6.13E-03	7.51E-01	7.51E-01	false	false	true	false	ULH
62	2.50E+00	9.00E-01	9.00E+01	6.00E+00	2.81E-01	5.00E-01	6.13E-03	7.41E-01	7.41E-01	false	false	true	false	ULH
63	3.13E+00	9.00E-01	6.75E+01	6.00E+00	3.75E-01	5.00E-01	4.94E-03	7.45E-01	7.45E-01	false	false	true	false	ULH
64	3.13E+00	1.20E+00	9.00E+01	4.50E+00	2.81E-01	7.50E-01	6.13E-03	7.45E-01	7.45E-01	false	false	true	false	ULH
65	1.88E+00	1.05E+00	6.75E+01	4.50E+00	3.75E-01	5.00E-01	6.13E-03	7.44E-01	7.44E-01	false	false	true	false	ULH
66	1.88E+00	1.05E+00	6.75E+01	3.00E+00	2.81E-01	7.50E-01	6.13E-03	7.38E-01	7.38E-01	false	false	true	false	ULH
67	1.88E+00	1.20E+00	1.13E+02	3.00E+00	4.69E-01	1.00E+00	6.13E-03	7.34E-01	7.34E-01	false	false	true	false	ULH
68	1.88E+00	1.05E+00	9.00E+01	6.00E+00	3.75E-01	5.00E-01	3.75E-03	7.51E-01	7.51E-01	false	false	true	false	ULH
69	2.50E+00	9.00E-01	9.00E+01	6.00E+00	3.75E-01	7.50E-01	4.94E-03	7.47E-01	7.47E-01	false	false	true	false	ULH
70	2.50E+00	9.00E-01	9.00E+01	6.00E+00	4.69E-01	1.00E+00	4.94E-03	7.44E-01	7.44E-01	false	false	true	false	ULH
71	3.13E+00	1.05E+00	1.13E+02	4.50E+00	4.69E-01	5.00E-01	6.13E-03	7.11E-01	7.11E-01	false	false	true	false	ULH
72	3.13E+00	1.20E+00	9.00E+01	4.50E+00	3.75E-01	7.50E-01	3.75E-03	7.40E-01	7.40E-01	false	false	true	false	ULH
73	2.50E+00	1.05E+00	1.13E+02	6.00E+00	4.69E-01	5.00E-01	3.75E-03	7.33E-01	7.33E-01	false	false	true	false	ULH
74	2.50E+00	9.00E-01	1.13E+02	3.00E+00	3.75E-01	1.00E+00	3.75E-03	7.38E-01	7.38E-01	false	false	true	false	ULH
75	2.50E+00	1.20E+00	9.00E+01	6.00E+00	4.69E-01	1.00E+00	4.94E-03	7.44E-01	7.44E-01	false	false	true	false	ULH
76	1.88E+00	9.00E-01	6.75E+01	3.00E+00	3.75E-01	5.00E-01	3.75E-03	7.48E-01	7.48E-01	false	false	true	false	ULH
77	2.50E+00	9.00E-01	9.00E+01	4.50E+00	2.81E-01	7.50E-01	4.94E-03	7.38E-01	7.38E-01	false	false	true	false	ULH
78	3.13E+00	1.20E+00	9.00E+01	3.00E+00	3.75E-01	7.50E-01	3.75E-03	7.40E-01	7.40E-01	false	false	true	false	ULH
79	3.13E+00	1.20E+00	6.75E+01	6.00E+00	3.75E-01	5.00E-01	3.75E-03	7.47E-01	7.47E-01	false	false	true	false	ULH
80	2.50E+00	9.00E-01	9.00E+01	3.00E+00	2.81E-01	1.00E+00	3.75E-03	7.37E-01	7.37E-01	false	false	true	false	ULH
81	2.50E+00	9.00E-01	9.00E+01	3.00E+00	4.69E-01	5.00E-01	3.75E-03	7.43E-01	7.43E-01	false	false	true	false	ULH
83	2.50E+00	1.05E+00	6.75E+01	3.00E+00	2.81E-01	1.00E+00	3.75E-03	7.41E-01	7.41E-01	false	false	true	false	ULH
84	3.13E+00	1.05E+00	9.00E+01	3.00E+00	3.75E-01	5.00E-01	3.75E-03	7.42E-01	7.42E-01	false	false	true	false	ULH
85	3.13E+00	9.00E-01	9.00E+01	4.50E+00	4.69E-01	1.00E+00	6.13E-03	7.39E-01	7.39E-01	false	false	true	false	ULH
86	1.88E+00	9.00E-01	1.13E+02	4.50E+00	2.81E-01	1.00E+00	6.13E-03	7.49E-01	7.49E-01	false	false	true	false	ULH
87	1.88E+00	1.20E+00	6.75E+01	4.50E+00	4.69E-01	7.50E-01	3.75E-03	7.44E-01	7.44E-01	false	false	true	false	ULH
88	2.50E+00	9.00E-01	6.75E+01	6.00E+00	4.69E-01	5.00E-01	4.94E-03	7.52E-01	7.52E-01	false	false	true	false	ULH
89	1.88E+00	9.00E-01	6.75E+01	4.50E+00	2.81E-01	5.00E-01	4.94E-03	7.40E-01	7.40E-01	false	false	true	false	ULH
90	3.13E+00	9.00E-01	6.75E+01	6.00E+00	4.69E-01	1.00E+00	3.75E-03	7.50E-01	7.50E-01	false	false	true	false	ULH
91	2.50E+00	1.20E+00	9.00E+01	3.00E+00	2.81E-01	5.00E-01	4.94E-03	7.44E-01	7.44E-01	false	false	true	false	ULH
92	1.88E+00	9.00E-01	9.00E+01	6.00E+00	2.81E-01	7.50E-01	3.75E-03	7.39E-01	7.39E-01	false	false	true	false	ULH
93	3.13E+00	9.00E-01	1.13E+02	3.00E+00	4.69E-01	7.50E-01	3.75E-03	7.19E-01	7.19E-01	false	false	true	false	ULH
94	3.13E+00	1.20E+00	9.00E+01	3.00E+00	4.69E-01	1.00E+00	6.13E-03	7.34E-01	7.34E-01	false	false	true	false	ULH
95	1.88E+00	9.00E-01	9.00E+01	6.00E+00	4.69E-01	1.00E+00	4.94E-03	7.51E-01	7.51E-01	false	false	true	false	ULH
96	3.13E+00	9.00E-01	1.13E+02	3.00E+00	3.75E-01	5.00E-01	6.13E-03	7.04E-01	7.04E-01	false	false	true	false	ULH
97	2.50E+00	1.05E+00	1.13E+02	4.50E+00	3.75E-01	7.50E-01	6.13E-03	7.32E-01	7.32E-01	false	false	true	false	ULH
98	2.50E+00	9.00E-01	1.13E+02	6.00E+00	3.75E-01	7.50E-01	4.94E-03	7.36E-01	7.36E-01	false	false	true	false	ULH

APPENDIX E – CONDITION B PMHS CORA OUTPUT FILE

Summary Report Date: Jun 19 2018

Rating of: WIAMan BRC Evaluation

Description: Biomedical Response Corridors

Rating:

No.	Load Case	Rating	Weight
1	Bosch PMHS B-1	0.760	1.0
	Total rating	**0.760**	1.0

Load Case Report Date: Jun 19 2018

Rating of: Bosch PMHS B-1

Description: Subloadcase

Rating:

No.	Experiment	Rating	Weight
1	PMHS_B_Foot_Az	0.714	0.125
2	PMHS_B_Tibia_Ax	0.773	0.125
3	PMHS_B_Tibia_Az	0.925	0.125
4	PMHS_B_Femur_Ax	0.769	0.125
5	PMHS_B_Pelvis_Ax	0.714	0.125
6	PMHS_B_Pelvis_Az	0.823	0.125
7	PMHS_B_T1_Ax	0.644	0.125
8	PMHS_B_T1_Az	0.720	0.125

Total rating of load case 1:	**0.760**	1.0

Experiment Report Date: Jun 19 2018

Report of Experiment: PMHS_B_Foot_Az

Description: Foot Az

Rating:

No.	Signal	Rating	Weight
1	11FOOTLE00H3ACZC	0.714	1.0
	Total rating of experiment 1:	**0.714**	1.0

Signal Report Date: Jun 19 2018

Rating of: PMHS_B_Foot_Az

Report of Signal 1 of Experiment 1: 11FOOTLE00H3ACZC

Overall Rating: 0.714

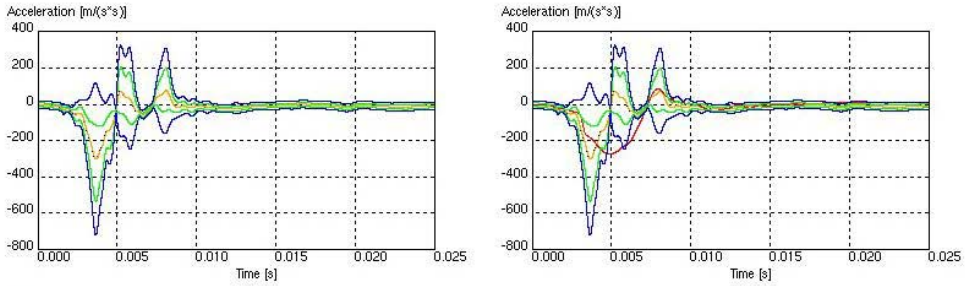

Method	Name	Rating	Weight
1	Corridor Method	0.669	0.50
2	Correlation Method	0.759	0.50

	Value	Rating	Weight
Cross correlation function	0.563	0.782	0.333
Size	0.496	0.496	0.333
Phase shift	-0.0000	1.0	0.333

3	Combination of 1 and 2	**0.714**	-

Parameters:	Evaluation Intervall:	0.0000 - 0.0250
Method 1:	Max. half width of inner corridor:	-
	Max. half width of outer corridor:	-
	Corridor curve file:	Foot_Az_Corridor
	Reference value:	302.172
	Transition exponent:	1
Method 2:	Limits for phase shift:	0.0002 - 0.0030
	Rating exponents (shape, size, phase):	1, 1, 1

Experiment Report Date: Jun 19 2018

Report of Experiment: PMHS_B_Tibia_Ax

Description: Tibia Ax

Rating:

No.	Signal	Rating	Weight
1	11TIBIRILOH3ACXC	0.773	1.0
	Total rating of experiment 2:	**0.773**	1.0

Signal Report Date: Jun 19 2018

Rating of: PMHS_B_Tibia_Ax

Report of Signal 1 of Experiment 2: 11TIBIRILOH3ACXC

Overall Rating: 0.773

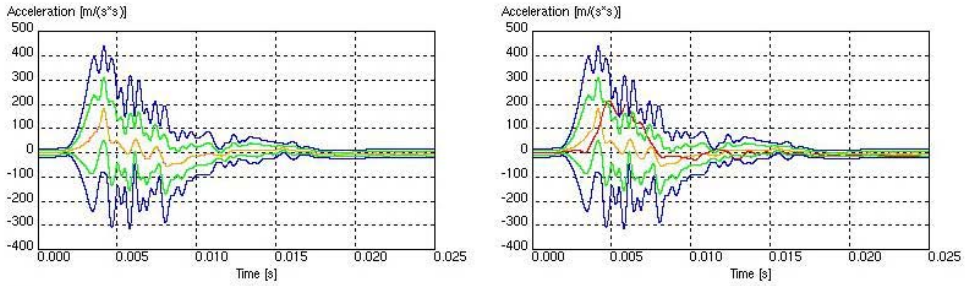

Tibia_Ax_RC

Average of experiments
cross-correlation reference
PMHS_B_output
Limits Outer corridor
Limits inner corridor

Method	Name				Rating	Weight
1	Corridor Method				0.872	0.50
2	Correlation Method				0.675	0.50
		Value	Rating	Weight		
	Cross correlation function	0.472	0.736	0.333		
	Size	0.288	0.288	0.333		
	Phase shift	0.0000	1.0	0.333		
3	Combination of 1 and 2				**0.773**	-

Parameters:	Evaluation Intervall:	0.0000 - 0.0250
Method 1:	Max. half width of inner corridor:	-
	Max. half width of outer corridor:	-
	Corridor curve file:	Tibia_Ax_Corridor
	Reference value:	181.086
	Transition exponent:	1
Method 2:	Limits for phase shift:	0.0003 - 0.0030
	Rating exponents (shape, size, phase):	1, 1, 1

Experiment Report Date: Jun 19 2018

Report of Experiment: PMHS_B_Tibia_Az

Description: Tibia Az

Rating:

No.	Signal	Rating	Weight
1	11TIBIRILOH3ACZC	0.925	1.0
	Total rating of experiment 3:	**0.925**	1.0

Signal Report Date: Jun 19 2018

Rating of: PMHS_B_Tibia_Az

Report of Signal 1 of Experiment 3: 11TIBIRILOH3ACZC

Overall Rating: 0.925

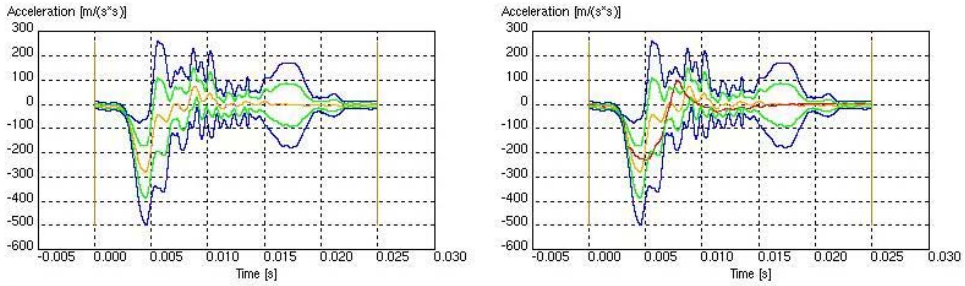

Tibia_Az_RC

Average of experiments
cross-correlation reference
PMHS_B_output
Limits Outer corridor
Limits inner corridor

Method	Name				Rating	Weight
1	Corridor Method				0.949	0.50
2	Correlation Method				0.902	0.50
		Value	Rating	Weight		
	Cross correlation function	0.850	0.925	0.333		
	Size	0.781	0.781	0.333		
	Phase shift	0.0000	1.0	0.333		
3	Combination of 1 and 2				**0.925**	-

Parameters:	Evaluation Intervall:	0.0000 - 0.0250
Method 1:	Max. half width of inner corridor:	-
	Max. half width of outer corridor:	-
	Corridor curve file:	Tibia_Az_Corridor
	Reference value:	279.213
	Transition exponent:	1
Method 2:	Limits for phase shift:	0.0003 - 0.0030
	Rating exponents (shape, size, phase):	1, 1, 1

Experiment Report Date: Jun 19 2018

Report of Experiment: PMHS_B_Femur_Ax

Description: Femur Ax

Rating:

No.	Signal	Rating	Weight
1	11FEMRLE00H3ACXC	0.769	1.0
	Total rating of experiment 4:	**0.769**	1.0

Signal Report Date: Jun 19 2018

Rating of: PMHS_B_Femur_Ax

Report of Signal 1 of Experiment 4: 11FEMRLE00H3ACXC

Overall Rating: 0.769

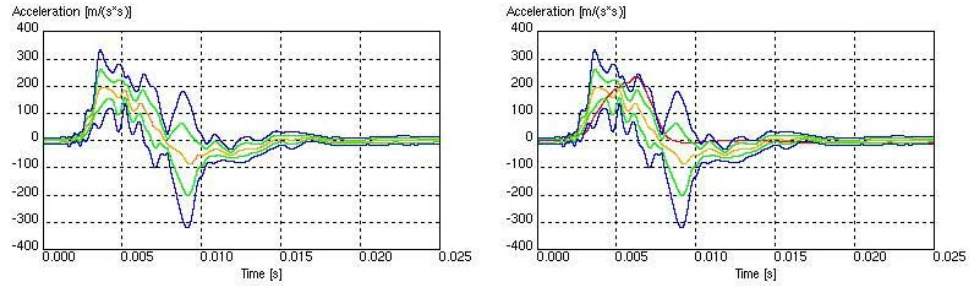

Femur_Ax_RC

Average of experiments
cross-correlation reference
PMHS_B_output
Limits Outer corridor
Limits inner corridor

Method	Name				Rating	Weight
1	Corridor Method				0.640	0.50
2	Correlation Method				0.897	0.50
		Value	Rating	Weight		
	Cross correlation function	0.818	0.909	0.333		
	Size	0.782	0.782	0.333		
	Phase shift	0.0000	1.0	0.333		
3	Combination of 1 and 2				**0.769**	-

Parameters:	Evaluation Intervall:	0.0000 - 0.0250
Method 1:	Max. half width of inner corridor:	-
	Max. half width of outer corridor:	-
	Corridor curve file:	Femur_Ax_Corridor
	Reference value:	195.128
	Transition exponent:	1
Method 2:	Limits for phase shift:	0.0003 - 0.0030
	Rating exponents (shape, size, phase):	1, 1, 1

Experiment Report Date: Jun 19 2018

Report of Experiment: PMHS_B_Pelvis_Ax

Description: Pelvis Ax

Rating:

No.	Signal	Rating	Weight
1	11PELV0000H3VAXC	0.714	1.0
	Total rating of experiment 5:	**0.714**	1.0

Signal Report Date: Jun 19 2018

Rating of: PMHS_B_Pelvis_Ax

Report of Signal 1 of Experiment 5: 11PELV0000H3VAXC

Overall Rating: 0.714

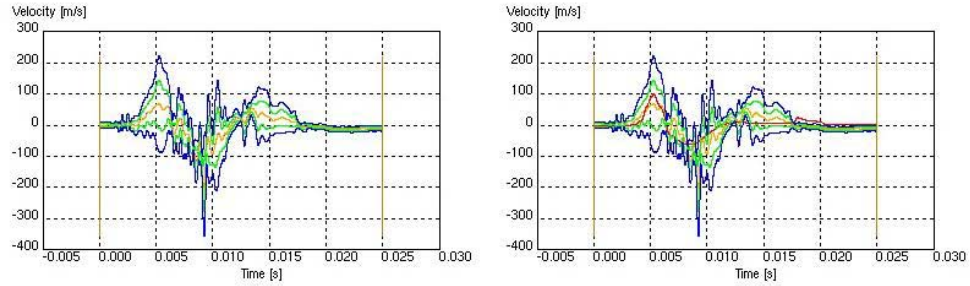

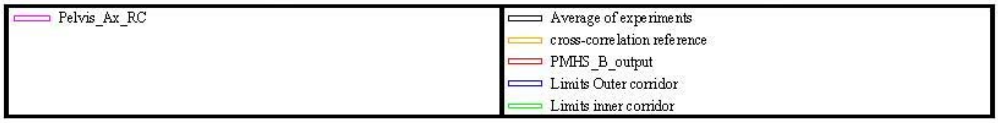

Method	Name	Rating	Weight
1	Corridor Method	0.619	0.50
2	Correlation Method	0.808	0.50
3	Combination of 1 and 2	**0.714**	-

Correlation Method

	Value	Rating	Weight
Cross correlation function	0.759	0.879	0.333
Size	0.545	0.545	0.333
Phase shift	0.0000	1.0	0.333

Parameters:	Evaluation Intervall:	0.0000 - 0.0250
Method 1:	Max. half width of inner corridor:	-
	Max. half width of outer corridor:	-
	Corridor curve file:	Pelvis_Ax_Corridor
	Reference value:	199.826
	Transition exponent:	1
Method 2:	Limits for phase shift:	0.0003 - 0.0030
	Rating exponents (shape, size, phase):	1, 1, 1

Experiment Report Date: Jun 19 2018

Report of Experiment: PMHS_B_Pelvis_Az

Description: Pelvis_Az

Rating:

No.	Signal	Rating	Weight
1	11PELV0000H3VAZC	0.823	1.0
	Total rating of experiment 6:	**0.823**	1.0

Signal Report Date: Jun 19 2018

Rating of: PMHS_B_Pelvis_Az

Report of Signal 1 of Experiment 6: 11PELV0000H3VAZC

Overall Rating: 0.823

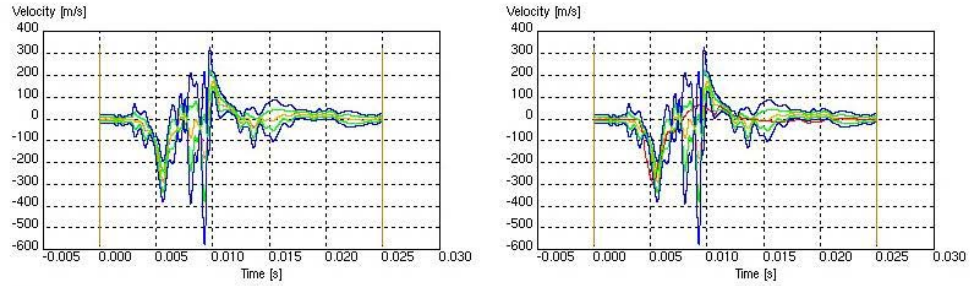

Pelvis_Az_RC

Average of experiments
cross-correlation reference
PMHS_B_output
Limits Outer corridor
Limits inner corridor

Method	Name				Rating	Weight
1	Corridor Method				0.706	0.50
2	Correlation Method				0.939	0.50
		Value	Rating	Weight		
	Cross correlation function	0.710	0.855	0.333		
	Size	0.961	0.961	0.333		
	Phase shift	0.0000	1.0	0.333		
3	Combination of 1 and 2				**0.823**	-

Parameters:	Evaluation Intervall:	0.0000 - 0.0250
Method 1:	Max. half width of inner corridor:	-
	Max. half width of outer corridor:	-
	Corridor curve file:	Pelvis_Az_Corridor
	Reference value:	288.058
	Transition exponent:	1
Method 2:	Limits for phase shift:	0.0003 - 0.0030
	Rating exponents (shape, size, phase):	1, 1, 1

Experiment Report Date: Jun 19 2018

Report of Experiment: PMHS_B_T1_Ax

Description: T1_Ax

Rating:

No.	Signal	Rating	Weight
1	11TS010000H3ACXA	0.644	1.0
	Total rating of experiment 7:	**0.644**	1.0

Signal Report Date: Jun 19 2018

Rating of: PMHS_B_T1_Ax

Report of Signal 1 of Experiment 7: 11TS010000H3ACXA

Overall Rating: 0.644

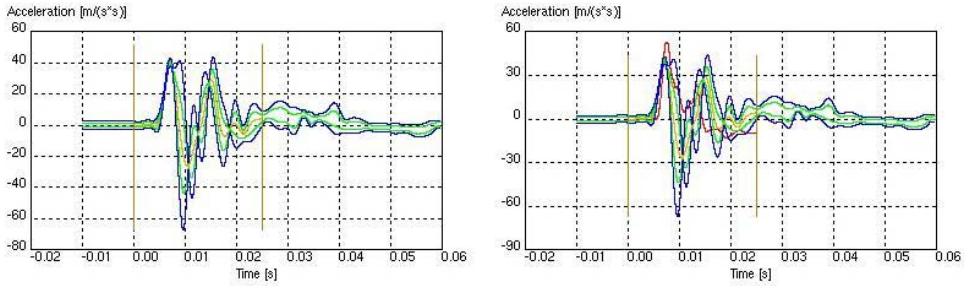

T1_Ax_RC

Average of experiments
cross-correlation reference
PMHS_B_output
Limits Outer corridor
Limits inner corridor

Method	Name				Rating	Weight
1	Corridor Method				0.435	0.50
2	Correlation Method				0.854	0.50
		Value	Rating	Weight		
	Cross correlation function	0.364	0.682	0.333		
	Size	0.881	0.881	0.333		
	Phase shift	0.0000	1.0	0.333		
3	Combination of 1 and 2				**0.644**	-

Parameters:	Evaluation Intervall:	0.0000 - 0.0250
Method 1:	Max. half width of inner corridor:	-
	Max. half width of outer corridor:	-
	Corridor curve file:	T1_Ax_Corridor
	Reference value:	40.461
	Transition exponent:	1
Method 2:	Limits for phase shift:	0.0003 - 0.0030
	Rating exponents (shape, size, phase):	1, 1, 1

Experiment Report Date: Jun 19 2018

Report of Experiment: PMHS_B_T1_Az

Description: T1_Az

Rating:

No.	Signal	Rating	Weight
1	11TS010000H3ACZA	0.720	1.0
	Total rating of experiment 8:	**0.720**	1.0

Signal Report Date: Jun 19 2018

Rating of: PMHS_B_T1_Az

Report of Signal 1 of Experiment 8: 11TS010000H3ACZA

Overall Rating: 0.720

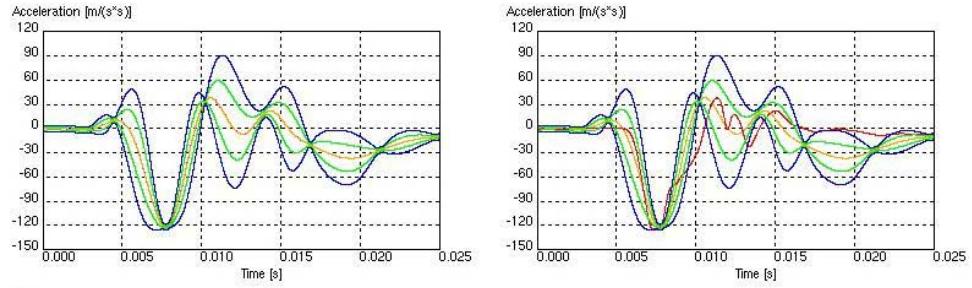

Method	Name	Rating	Weight
1	Corridor Method	0.519	0.50
2	Correlation Method	0.922	0.50
3	Combination of 1 and 2	**0.720**	-

Correlation Method

	Value	Rating	Weight
Cross correlation function	0.847	0.923	0.333
Size	0.843	0.843	0.333
Phase shift	0.0000	1.0	0.333

Parameters:	Evaluation Intervall:	0.0000 - 0.0250
Method 1:	Max. half width of inner corridor:	-
	Max. half width of outer corridor:	-
	Corridor curve file:	T1_Az_Corridor
	Reference value:	122.334
	Transition exponent:	1
Method 2:	Limits for phase shift:	0.0003 - 0.0030
	Rating exponents (shape, size, phase):	1, 1, 1

APPENDIX F – PMHS MODEFRONTIER OPTIMIZATION

```
#--- Frontier Design DB File Info ---------------
#modeFRONTIER  - (c) ESTECO S.p.A.
#Design DB Table
#-------------------------------------------------
#modeFRONTIER Version: modeFRONTIER 2017R5 5.7.1 b20171017
#Date: Thu Jan 24 12:06:05 EST 2019
#Project Name: PMHS A Opt 2019-01-22 - sensitivity complete.prj
#Operating System: Windows 10 10.0 amd64
#Java (SDK/JRE) Version: 1.8.0_60
#Java Vendor: Oracle Corporation
#Java Vendor URL: http://java.oracle.com/
#User Name: kbosch
#-------------------------------------------------
#Categories
<CATEGORIES clusterPrefix="CLUSTER_" useTableNamePrefix="false">
  <CATEGORY enabled="true" label="" name="SOSO1" symbol="SQUARE,NONE,11,,0"/>
  <CATEGORY enabled="true" label="" name="USRDOE" symbol="SQUARE,NONE,11,,0"/>
  <CATEGORY enabled="true" label="" name="NSGA2" symbol="SQUARE,NONE,11,,0"/>
  <CATEGORY enabled="true" label="" name="TOA" symbol="SQUARE,NONE,11,,0"/>
  <CATEGORY enabled="true" label="" name="DOE_APPROX" symbol="SQUARE,NONE,11,,0"/>
  <CATEGORY enabled="true" label="" name="SIMPLEX" symbol="SQUARE,NONE,11,,0"/>
  <CATEGORY enabled="true" label="" name="ULH" symbol="SQUARE,NONE,11,,0"/>
  <CATEGORY enabled="true" label="" name="FULL" symbol="SQUARE,NONE,11,#DC3912,1,#DC3912"/>
  <CATEGORY enabled="true" label="" name="SIMPLEX_DOE" symbol="SQUARE,NONE,11,#3366CC,1,#3366CC"/>
</CATEGORIES>

#-------------------------------------------------
```

<ID>	Opt joint	Opt joint	Opt joint	Opt joint	Opt joint	Combined	Pelvis Ax	Pelvis Fx	Pelvis Fz	T12 Ax	T12 Fx	T12 Fz	no Constraint	Constraint	Constraint	Constraint	Constraint	Constraint	<ERROR>	<VIRTUAL>	<FEASIBLE>	<MARKED>	<CATEGORY>
0	4392.01	0.02	19985.14	0.15	2.29	0.13	0.23	0.91	0.57	0.42	0.04	0.13	0.57	0.23	0.91	0.42	0.04	false	false	true	false	ULH
1	2743.12	0.02	6736.98	0.14	1.47	0.09	0.18	0.49	0.35	0.29	0.05	0.09	0.36	0.18	0.49	0.29	0.05	false	false	true	false	ULH
2	2800.88	0.01	18518.53	0.13	2.22	0.13	0.22	0.89	0.53	0.41	0.05	0.13	0.53	0.22	0.89	0.41	0.05	false	false	true	false	ULH
3	3488.84	0.00	15733.56	0.15	2.13	0.12	0.24	0.84	0.51	0.40	0.03	0.12	0.51	0.24	0.84	0.40	0.03	false	false	true	false	ULH
4	4234.29	0.01	11374.93	0.09	2.24	0.13	0.24	0.88	0.55	0.41	0.04	0.13	0.55	0.24	0.88	0.41	0.04	false	false	true	false	ULH
5	2755.79	0.02	17701.08	0.09	2.39	0.14	0.21	1.08	0.64	0.47	0.05	0.14	0.54	0.21	1.08	0.47	0.05	false	false	false	false	ULH
6	2048.34	0.02	5848.94	0.15	1.40	0.07	0.21	0.48	0.32	0.28	0.05	0.07	0.32	0.21	0.49	0.28	0.05	false	false	true	false	ULH
7	3702.04	0.02	5114.39	0.09	1.71	0.12	0.19	0.63	0.44	0.30	0.05	0.12	0.44	0.19	0.63	0.30	0.05	false	false	true	false	ULH
8	4999.03	0.01	14305.69	0.09	2.61	0.14	0.23	1.06	0.64	0.48	0.06	0.14	0.54	0.23	1.06	0.48	0.06	false	false	false	false	ULH
9	4019.91	0.02	12029.39	0.12	1.86	0.13	0.20	0.70	0.44	0.35	0.03	0.13	0.44	0.20	0.70	0.36	0.03	false	false	true	false	ULH
10	4487.77	0.02	15903.96	0.13	2.16	0.13	0.23	0.85	0.50	0.40	0.05	0.13	0.50	0.23	0.85	0.40	0.05	false	false	true	false	ULH
11	2221.73	0.00	15508.78	0.13	2.10	0.13	0.22	0.84	0.48	0.40	0.04	0.13	0.48	0.22	0.84	0.40	0.04	false	false	true	false	ULH
12	3644.64	0.02	17864.14	0.10	2.48	0.14	0.21	1.02	0.62	0.45	0.05	0.14	0.52	0.21	1.02	0.45	0.05	false	false	false	false	ULH
13	2259.11	0.02	5829.19	0.08	2.18	0.09	0.17	1.05	0.41	0.39	0.06	0.09	0.41	0.17	1.05	0.39	0.06	false	false	false	false	ULH
14	3238.76	0.02	15537.90	0.12	2.10	0.13	0.20	0.85	0.47	0.40	0.05	0.13	0.47	0.20	0.85	0.40	0.05	false	false	true	false	ULH
15	3371.67	0.01	19469.15	0.11	2.60	0.14	0.22	1.07	0.65	0.47	0.05	0.14	0.55	0.22	1.07	0.47	0.05	false	false	false	false	ULH
16	3796.53	0.02	19729.27	0.11	2.30	0.14	0.21	1.03	0.62	0.45	0.05	0.14	0.52	0.21	1.03	0.45	0.05	false	false	false	false	ULH
17	2969.26	0.01	17172.55	0.11	2.45	0.14	0.22	1.00	0.61	0.44	0.04	0.14	0.51	0.22	1.00	0.44	0.04	false	false	false	false	ULH
18	3158.53	0.02	19085.91	0.10	2.46	0.14	0.20	1.01	0.62	0.45	0.04	0.14	0.52	0.20	1.01	0.45	0.04	false	false	false	false	ULH
19	3943.16	0.02	14815.23	0.15	1.83	0.13	0.18	0.69	0.44	0.35	0.03	0.13	0.44	0.18	0.69	0.35	0.03	false	false	true	false	ULH
20	2624.97	0.01	10537.94	0.11	1.79	0.13	0.20	0.65	0.45	0.33	0.03	0.13	0.45	0.20	0.65	0.33	0.03	false	false	true	false	ULH
21	2452.16	0.02	15308.73	0.08	2.49	0.14	0.19	1.03	0.63	0.45	0.05	0.14	0.53	0.19	1.03	0.45	0.05	false	false	false	false	ULH
22	4195.70	0.01	15149.22	0.13	2.28	0.13	0.24	0.90	0.55	0.41	0.04	0.13	0.56	0.24	0.90	0.41	0.04	false	false	true	false	ULH
23	3064.55	0.02	17978.06	0.09	2.51	0.14	0.20	1.04	0.63	0.45	0.05	0.14	0.53	0.20	1.04	0.45	0.05	false	false	false	false	ULH
24	3579.53	0.01	9070.95	0.14	1.75	0.13	0.21	0.61	0.45	0.32	0.03	0.13	0.45	0.21	0.61	0.32	0.03	false	false	true	false	ULH
25	4458.41	0.01	11072.05	0.13	1.84	0.13	0.21	0.68	0.44	0.35	0.03	0.13	0.44	0.21	0.68	0.35	0.03	false	false	true	false	ULH
26	4251.81	0.00	18391.91	0.14	2.45	0.13	0.24	0.99	0.61	0.44	0.04	0.13	0.51	0.24	0.99	0.44	0.04	false	false	true	false	ULH
27	2180.55	0.00	18793.48	0.10	2.59	0.14	0.22	1.07	0.64	0.47	0.05	0.14	0.54	0.22	1.07	0.47	0.05	false	false	false	false	ULH
28	2942.49	0.01	14708.13	0.09	2.42	0.14	0.22	0.98	0.60	0.44	0.04	0.14	0.50	0.22	0.98	0.44	0.04	false	false	true	false	ULH
29	4088.91	0.02	17333.48	0.15	2.11	0.13	0.23	0.84	0.49	0.40	0.03	0.13	0.49	0.23	0.84	0.40	0.03	false	false	true	false	ULH
30	2001.62	0.02	19220.73	0.14	1.84	0.13	0.16	0.77	0.47	0.37	0.03	0.13	0.47	0.16	0.77	0.37	0.03	false	false	true	false	ULH
31	3659.41	0.01	15411.14	0.09	2.32	0.14	0.22	1.03	0.63	0.45	0.05	0.14	0.53	0.22	1.03	0.45	0.05	false	false	false	false	ULH
32	2893.26	0.02	19975.54	0.08	2.69	0.15	0.20	1.13	0.67	0.49	0.06	0.15	0.57	0.20	1.13	0.49	0.06	false	false	false	false	ULH
33	3716.66	0.00	15008.24	0.10	2.44	0.13	0.23	0.98	0.61	0.44	0.04	0.13	0.51	0.23	0.98	0.44	0.04	false	false	true	false	ULH
34	2578.77	0.02	16176.97	0.08	2.65	0.14	0.21	1.11	0.66	0.48	0.05	0.14	0.56	0.21	1.11	0.48	0.05	false	false	false	false	ULH
35	3559.11	0.01	14162.49	0.13	1.93	0.13	0.21	0.76	0.43	0.37	0.03	0.13	0.43	0.21	0.76	0.37	0.03	false	false	true	false	ULH
36	3270.23	0.01	5679.25	0.12	1.56	0.11	0.19	0.51	0.42	0.29	0.04	0.11	0.42	0.19	0.51	0.29	0.04	false	false	true	false	ULH
37	2500.52	0.01	9684.84	0.10	1.79	0.13	0.20	0.65	0.44	0.34	0.03	0.13	0.44	0.20	0.65	0.34	0.03	false	false	true	false	ULH
38	4285.53	0.02	18826.82	0.11	2.32	0.14	0.22	1.04	0.63	0.45	0.04	0.14	0.53	0.22	1.04	0.45	0.04	false	false	false	false	ULH
39	4605.33	0.02	17522.59	0.10	2.55	0.14	0.22	1.05	0.63	0.46	0.05	0.14	0.53	0.22	1.05	0.46	0.05	false	false	false	false	ULH
40	4856.40	0.01	8577.87	0.08	1.97	0.12	0.26	0.74	0.44	0.37	0.03	0.12	0.44	0.26	0.74	0.37	0.03	false	false	true	false	ULH
41	2110.41	0.01	9433.44	0.11	1.73	0.12	0.18	0.62	0.45	0.32	0.04	0.12	0.45	0.18	0.62	0.32	0.04	false	false	true	false	ULH
42	3813.51	0.00	7097.24	0.09	1.74	0.12	0.22	0.59	0.44	0.33	0.03	0.12	0.44	0.22	0.59	0.33	0.03	false	false	true	false	ULH
43	4924.33	0.01	12356.12	0.11	2.30	0.13	0.24	0.91	0.57	0.41	0.04	0.13	0.57	0.24	0.91	0.41	0.04	false	false	true	false	ULH
44	4840.54	0.01	8890.30	0.13	1.80	0.12	0.21	0.65	0.44	0.34	0.03	0.12	0.44	0.21	0.65	0.34	0.03	false	false	true	false	ULH
45	3380.12	0.00	7232.37	0.12	1.71	0.12	0.21	0.59	0.45	0.31	0.03	0.12	0.45	0.21	0.59	0.31	0.03	false	false	true	false	ULH
46	2537.13	0.02	7265.06	0.12	1.55	0.09	0.17	0.56	0.38	0.30	0.05	0.09	0.38	0.17	0.56	0.30	0.05	false	false	true	false	ULH
47	4401.24	0.02	10427.48	0.12	1.82	0.13	0.20	0.67	0.44	0.34	0.03	0.13	0.44	0.20	0.67	0.34	0.03	false	false	true	false	ULH
48	2856.11	0.00	7776.22	0.13	1.66	0.12	0.20	0.56	0.45	0.30	0.03	0.12	0.45	0.20	0.56	0.30	0.03	false	false	true	false	ULH
49	4129.29	0.02	8922.38	0.12	1.78	0.13	0.21	0.64	0.44	0.33	0.03	0.13	0.44	0.21	0.64	0.33	0.03	false	false	true	false	ULH
50	2177.46	0.02	13820.54	0.08	2.31	0.14	0.19	0.95	0.56	0.43	0.04	0.14	0.56	0.19	0.95	0.43	0.04	false	false	true	false	ULH
51	2088.43	0.02	11228.67	0.11	1.83	0.12	0.17	0.69	0.48	0.34	0.04	0.12	0.48	0.17	0.69	0.34	0.04	false	false	true	false	ULH
52	4685.90	0.03	5864.15	0.12	1.77	0.13	0.22	0.62	0.45	0.32	0.03	0.13	0.45	0.22	0.62	0.32	0.03	false	false	true	false	ULH
53	3115.41	0.01	12157.30	0.13	1.80	0.13	0.20	0.66	0.44	0.34	0.03	0.13	0.44	0.20	0.66	0.34	0.03	false	false	true	false	ULH
54	2120.93	0.02	8440.71	0.14	1.55	0.09	0.17	0.56	0.38	0.30	0.05	0.09	0.38	0.17	0.56	0.30	0.05	false	false	true	false	ULH
55	2559.50	0.01	15036.18	0.15	2.77	0.17	0.18	1.02	0.82	0.52	0.05	0.17	0.82	0.18	1.02	0.52	0.05	false	false	false	false	ULH
56	4181.81	0.01	13536.03	0.13	2.00	0.13	0.24	0.77	0.45	0.38	0.03	0.13	0.45	0.24	0.77	0.38	0.03	false	false	true	false	ULH
57	3889.66	0.01	7668.46	0.09	1.77	0.12	0.21	0.62	0.44	0.34	0.03	0.12	0.44	0.21	0.62	0.34	0.03	false	false	true	false	ULH
58	2906.18	0.01	9524.02	0.15	2.72	0.17	0.17	0.99	0.81	0.52	0.06	0.17	0.81	0.17	0.99	0.52	0.06	false	false	true	false	ULH
59	4516.99	0.01	5499.96	0.11	1.76	0.12	0.23	0.60	0.45	0.32	0.03	0.12	0.45	0.23	0.60	0.32	0.03	false	false	true	false	ULH
60	2315.43	0.00	5237.90	0.09	1.64	0.12	0.19	0.56	0.44	0.30	0.04	0.12	0.44	0.19	0.56	0.30	0.04	false	false	true	false	ULH
61	4317.56	0.01	5947.73	0.10	1.75	0.12	0.23	0.60	0.45	0.32	0.03	0.12	0.45	0.23	0.60	0.32	0.03	false	false	true	false	ULH
62	3008.60	0.00	10255.64	0.14	1.73	0.12	0.21	0.59	0.45	0.33	0.03	0.12	0.45	0.21	0.59	0.33	0.03	false	false	true	false	ULH
63	4696.77	0.00	6193.37	0.15	1.72	0.12	0.25	0.58	0.44	0.31	0.03	0.12	0.44	0.25	0.58	0.31	0.03	false	false	true	false	ULH
64	4797.02	0.02	11573.32	0.12	1.80	0.13	0.20	0.72	0.43	0.35	0.03	0.13	0.43	0.20	0.72	0.36	0.03	false	false	true	false	ULH
65	2653.74	0.01	8280.63	0.12	1.66	0.12	0.19	0.56	0.45	0.30	0.04	0.12	0.45	0.19	0.56	0.30	0.04	false	false	true	false	ULH
66	2691.65	0.02	7441.54	0.10	1.68	0.12	0.18	0.58	0.45	0.31	0.04	0.12	0.45	0.18	0.58	0.31	0.04	false	false	true	false	ULH
67	2299.17	0.02	15372.95	0.11	2.15	0.14	0.19	0.88	0.49	0.41	0.04	0.14	0.49	0.19	0.88	0.41	0.04	false	false	true	false	ULH
68	2657.59	0.02	17599.96	0.13	1.80	0.13	0.20	0.67	0.44	0.34	0.03	0.13	0.44	0.20	0.67	0.34	0.03	false	false	true	false	ULH
69	3750.91	0.01	10726.59	0.14	1.77	0.12	0.21	0.63	0.44	0.34	0.03	0.12	0.44	0.21	0.63	0.34	0.03	false	false	true	false	ULH
70	3981.84	0.00	12920.59	0.15	1.93	0.12	0.24	0.71	0.45	0.35	0.03	0.12	0.46	0.24	0.71	0.36	0.03	false	false	true	false	ULH
71	4357.18	0.01	19560.56	0.12	2.56	0.14	0.23	1.05	0.64	0.45	0.05	0.14	0.54	0.23	1.05	0.46	0.05	false	false	false	false	ULH
72	4881.21	0.02	10090.12	0.11	1.90	0.13	0.22	0.71	0.45	0.35	0.03	0.13	0.46	0.22	0.71	0.36	0.03	false	false	true	false	ULH
73	3415.44	0.01	15748.32	0.14	1.96	0.13	0.23	0.77	0.43	0.38	0.03	0.13	0.43	0.23	0.77	0.38	0.03	false	false	true	false	ULH
74	3613.56	0.00	18236.11	0.09	2.74	0.14	0.21	1.13	0.67	0.51	0.07	0.14	0.57	0.21	1.13	0.51	0.07	false	false	false	false	ULH
75	3504.99	0.02	11719.44	0.14	1.79	0.12	0.21	0.65	0.44	0.33	0.03	0.12	0.44	0.21	0.65	0.33	0.03	false	false	true	false	ULH
76	2412.33	0.01	8682.44	0.09	1.77	0.13	0.21	0.63	0.44	0.33	0.03	0.13	0.44	0.21	0.63	0.33	0.03	false	false	true	false	ULH
77	3450.78	0.01	11835.92	0.11	1.92	0.13	0.22	0.74	0.43	0.37	0.03	0.13	0.43	0.22	0.74	0.37	0.03	false	false	true	false	ULH
78	4558.51	0.02	13322.09	0.10	2.22	0.13	0.23	0.88	0.54	0.41	0.04	0.13	0.54	0.23	0.88	0.41	0.04	false	false	true	false	ULH
79	4135.85	0.02	5494.85	0.15	1.65	0.12	0.20	0.56	0.44	0.30	0.03	0.12	0.44	0.20	0.56	0.30	0.03	false	false	true	false	ULH
80	3726.16	0.00	9946.28	0.08	2.10	0.12	0.24	0.82	0.50	0.39	0.03	0.12	0.50	0.24	0.82	0.39	0.03	false	false	true	false	ULH
81	3046.41	0.00	12234.20	0.08	2.41	0.13	0.23	0.97	0.59	0.43	0.04	0.13	0.59	0.23	0.97	0.43	0.04	false	false	true	false	ULH
82	4714.68	0.02	10934.92	0.12	1.85	0.13	0.20	0.70	0.44	0.35	0.03	0.13	0.44	0.20	0.70	0.35	0.03	false	false	true	false	ULH
83	3327.71	0.01	5391.85	0.09	1.61	0.12	0.19	0.54	0.44	0.30	0.03	0.12	0.44	0.19	0.54	0.30	0.03	false	false	true	false	ULH
84	4878.29	0.01	13549.11	0.08	2.54	0.13	0.24	1.03	0.63	0.46	0.05	0.13	0.63	0.24	1.03	0.46	0.05	false	false	false	false	ULH
85	4773.20	0.00	14013.78	0.14	2.25	0.13	0.24	0.89	0.55	0.41	0.04	0.13	0.55	0.24	0.89	0.41	0.04	false	false	true	false	ULH
85	2438.96	0.01	14588.22	0.11	2.10	0.13	0.21	0.84	0.48	0.40	0.04	0.13	0.48	0.21	0.84	0.40	0.04	false	false	true	false	ULH

87	3083.53	0.02	5165.87	0.10	1.47	0.10	0.19	0.48	0.39	0.29	0.04	0.10	0.39	0.19	0.48	0.29	0.04	false	false	true	false	ULH
88	3893.60	0.01	8064.79	0.14	1.75	0.12	0.22	0.60	0.45	0.32	0.03	0.12	0.45	0.22	0.60	0.32	0.03	false	false	true	false	ULH
89	2838.19	0.00	9227.31	0.10	1.76	0.12	0.20	0.62	0.44	0.33	0.03	0.12	0.44	0.20	0.62	0.33	0.03	false	false	true	false	ULH
90	4547.85	0.00	10127.30	0.13	1.88	0.12	0.26	0.69	0.42	0.36	0.03	0.12	0.42	0.26	0.69	0.36	0.03	false	false	true	false	ULH
91	3853.12	0.02	12681.59	0.09	2.05	0.13	0.19	0.83	0.45	0.39	0.04	0.13	0.45	0.19	0.83	0.39	0.04	false	false	true	false	ULH
92	2383.32	0.00	12983.00	0.13	1.80	0.12	0.18	0.67	0.44	0.34	0.03	0.12	0.44	0.18	0.67	0.34	0.03	false	false	true	false	ULH
93	4620.64	0.01	18067.32	0.08	2.89	0.15	0.19	1.22	0.70	0.55	0.08	0.15	0.70	0.19	1.22	0.55	0.08	false	false	false	false	ULH
94	4751.21	0.02	13909.43	0.08	2.55	0.14	0.23	1.04	0.63	0.46	0.05	0.14	0.63	0.23	1.04	0.46	0.05	false	false	false	false	ULH
95	2303.43	0.01	13131.31	0.14	1.79	0.13	0.20	0.65	0.44	0.34	0.03	0.13	0.44	0.20	0.65	0.34	0.03	false	false	true	false	ULH
96	4053.67	0.00	17080.77	0.10	2.66	0.14	0.23	1.09	0.65	0.49	0.06	0.14	0.65	0.23	1.09	0.49	0.06	false	false	false	false	ULH
97	3208.95	0.02	16541.34	0.12	2.21	0.13	0.22	0.88	0.53	0.41	0.04	0.13	0.53	0.22	0.88	0.41	0.04	false	false	true	false	ULH
98	3194.51	0.01	19288.25	0.14	2.38	0.13	0.23	0.96	0.59	0.43	0.04	0.13	0.59	0.23	0.96	0.43	0.04	false	false	true	false	ULH
99	3959.58	0.01	7856.99	0.10	1.78	0.13	0.21	0.62	0.45	0.33	0.03	0.13	0.45	0.21	0.62	0.33	0.03	false	false	true	false	ULH

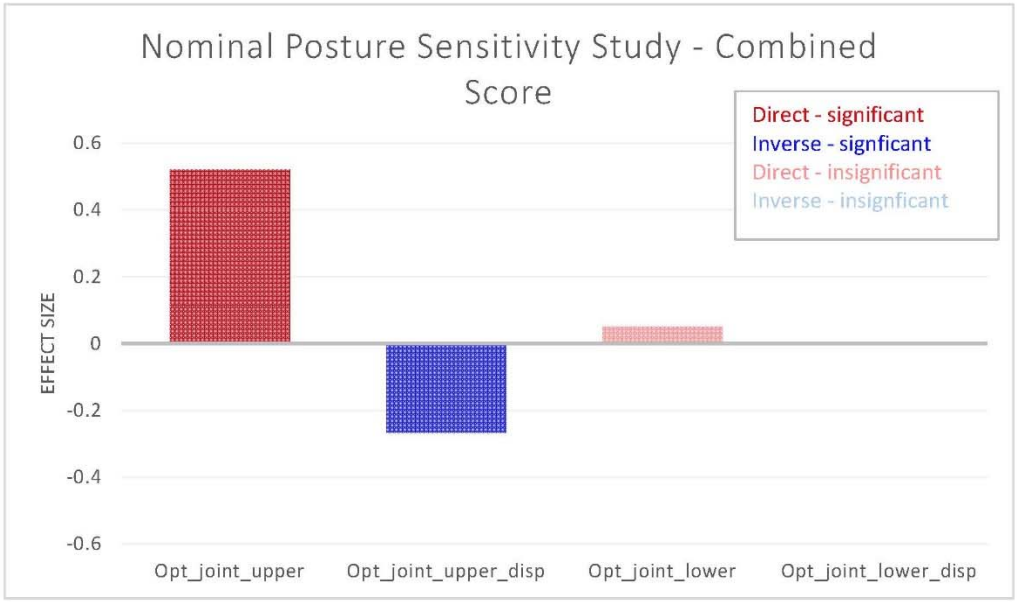
Nominal Posture Sensitivity Study - Combined Score
Direct - significant
Inverse - signficant
Direct - insignificant
Inverse - insignficant
EFFECT SIZE
0.6
0.4
0.2
0
-0.2
-0.4
-0.6
Opt_joint_upper
Opt_joint_upper_disp
Opt_joint_lower
Opt_joint_lower_disp

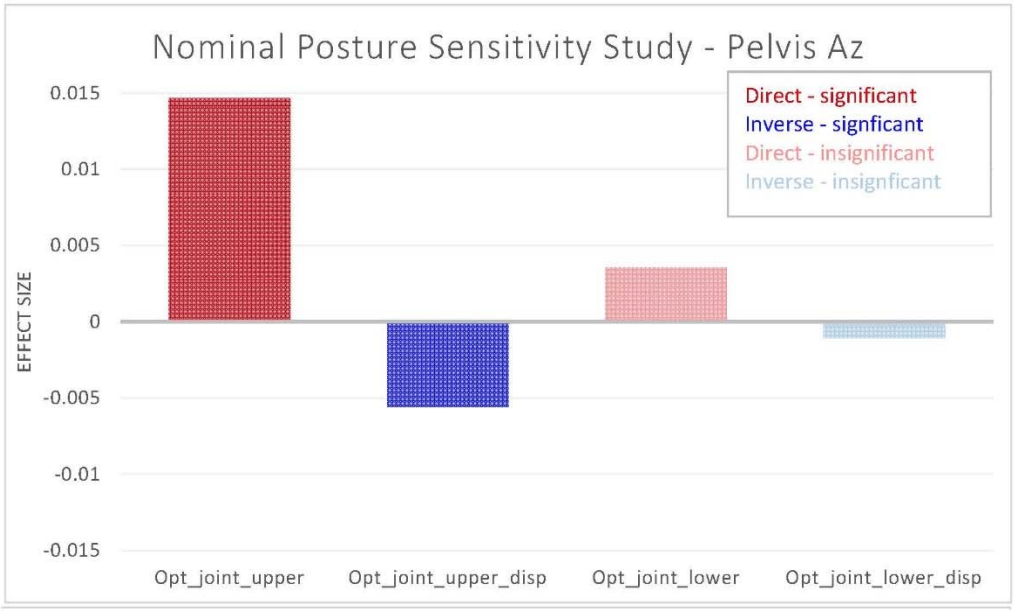
Nominal Posture Sensitivity Study - Pelvis Az
Direct - significant
Inverse - signficant
Direct - insignificant
Inverse - insignficant
EFFECT SIZE
0.015
0.01
0.005
0
-0.005
-0.01
-0.015
Opt_joint_upper
Opt_joint_upper_disp
Opt_joint_lower
Opt_joint_lower_disp

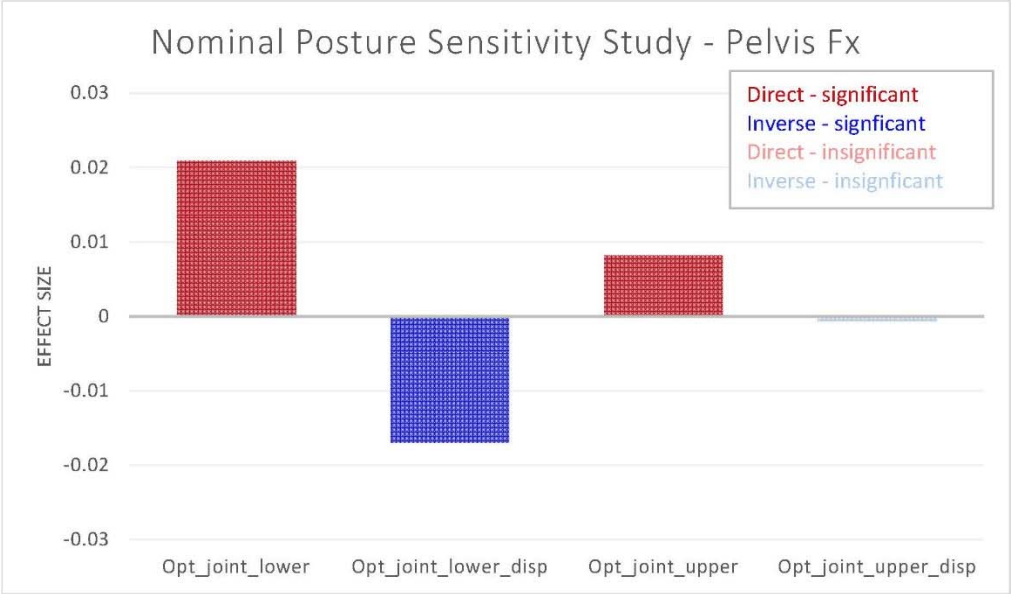
Nominal Posture Sensitivity Study - Pelvis Fx
Direct - significant
Inverse - signficant
Direct - insignificant
Inverse - insignficant
EFFECT SIZE
0.03
0.02
0.01
0
-0.01
-0.02
-0.03
Opt_joint_lower
Opt_joint_lower_disp
Opt_joint_upper
Opt_joint_upper_disp

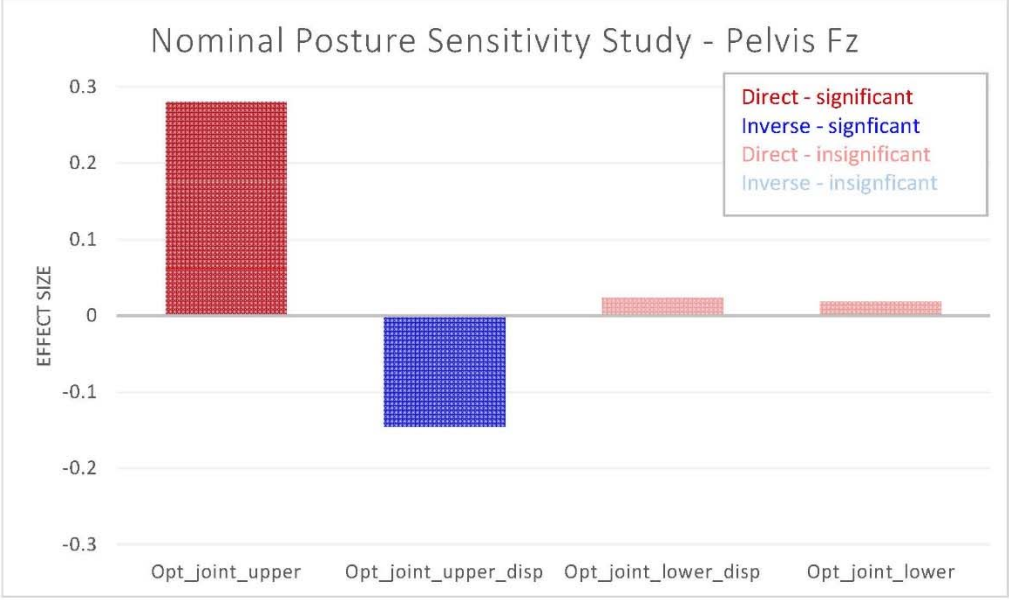
Nominal Posture Sensitivity Study - Pelvis Fz
Direct - significant
Inverse - signficant
Direct - insignificant
Inverse - insignficant
EFFECT SIZE
0.3
0.2
0.1
0
-0.1
-0.2
-0.3
Opt_joint_upper
Opt_joint_upper_disp
Opt_joint_lower_disp
Opt_joint_lower

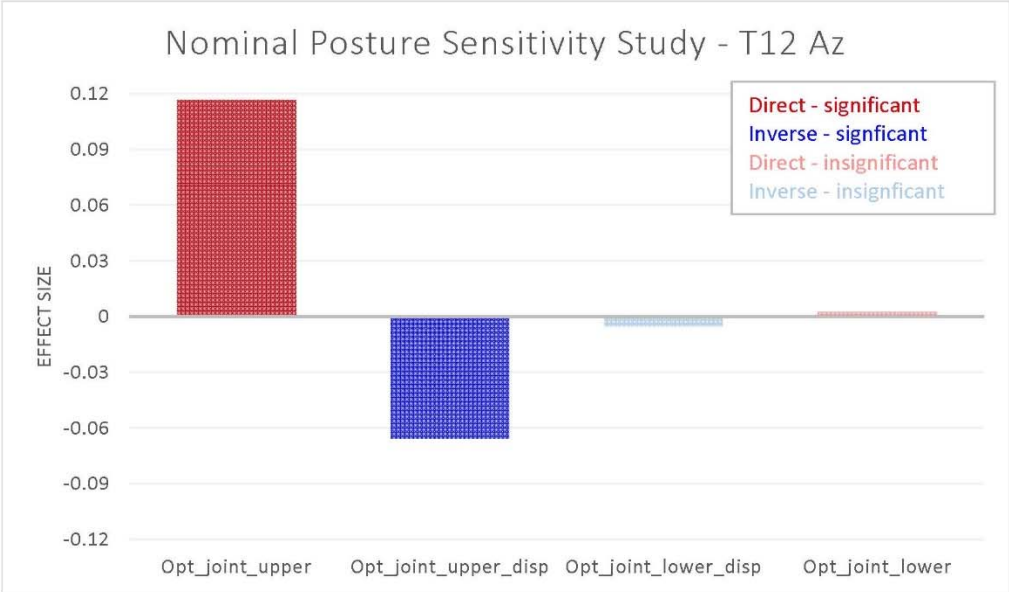
Nominal Posture Sensitivity Study - T12 Az
Direct - significant
Inverse - signficant
Direct - insignificant
Inverse - insignficant
EFFECT SIZE
0.12
0.09
0.06
0.03
0
-0.03
-0.06
-0.09
-0.12
Opt_joint_upper
Opt_joint_upper_disp
Opt_joint_lower_disp
Opt_joint_lower

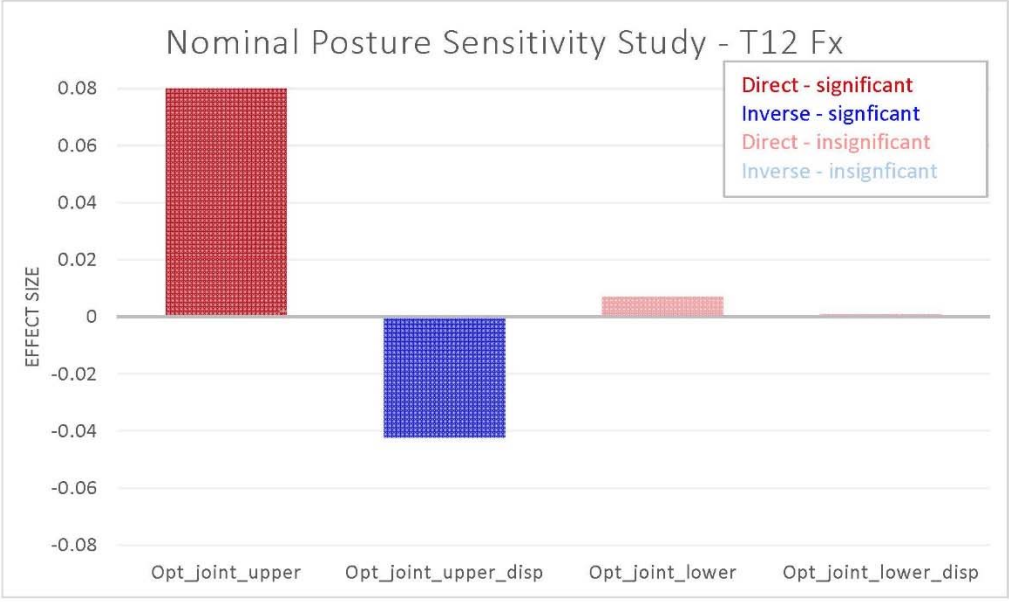
Nominal Posture Sensitivity Study - T12 Fx
Direct - significant
Inverse - signficant
Direct - insignificant
Inverse - insignficant
EFFECT SIZE
0.08
0.06
0.04
0.02
0
-0.02
-0.04
-0.06
-0.08
Opt_joint_upper
Opt_joint_upper_disp
Opt_joint_lower
Opt_joint_lower_disp

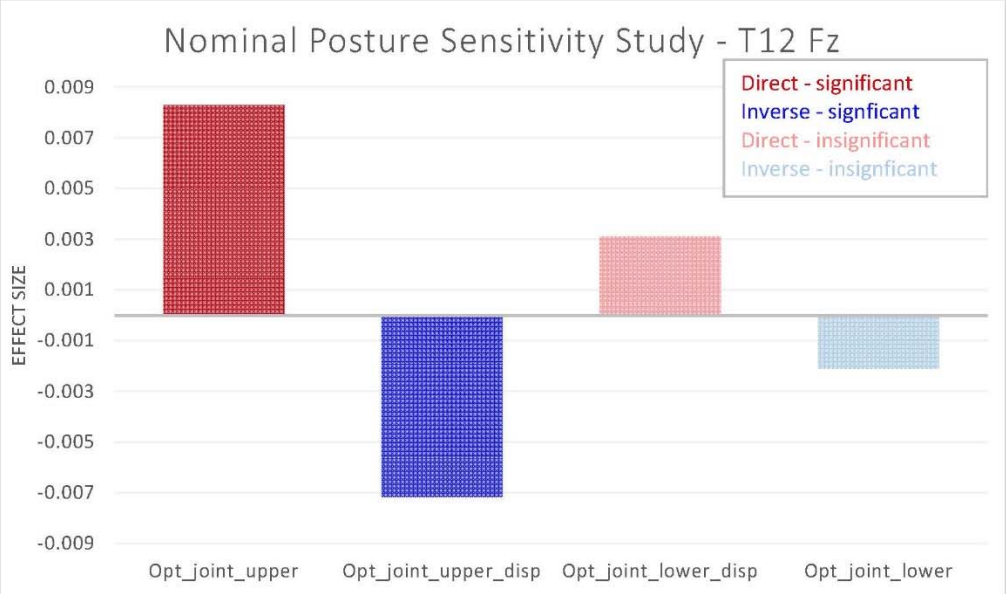
Nominal Posture Sensitivity Study - T12 Fz
Direct - significant
Inverse - signficant
Direct - insignificant
Inverse - insignficant
EFFECT SIZE
0.009
0.007
0.005
0.003
0.001
-0.001
-0.003
-0.005
-0.007
-0.009
Opt_joint_upper
Opt_joint_upper_disp
Opt_joint_lower_disp
Opt_joint_lower

```
#-- Frontier Design DB File Info ----------
#modeFRONTIER - (c) ESTECO S.p.A.
#Design 23 Table
#-----------------------------------------
#modeFRONTIER Version: modeFRONTIER 2017R5 5.7.1 b20171017
#Date: Fri Jan 25 14:07:53 EST 2019
#Project Name: PMHS A Opt 2019-01-24 - opt 200 - complete.prj
#Operating System: Windows 10 10.0 amd64
#Java (SDK/JRE) Version: 1.8.0_60
#Java Vendor: Oracle Corporation
#Java Vendor URL: http://java.oracle.com/
#User Name: RBosch
#-----------------------------------------
#Categories
<CATEGORIES classPrefix="CLUSTER " useTableNamePrefix="false">
  <CATEGORY enabled="true" label="" name="SOBOL" symbol="SQUARE_NONE_11_0" />
  <CATEGORY enabled="true" label="" name="USRDOE" symbol="SQUARE_NONE_11_0" />
  <CATEGORY enabled="true" label="" name="MS6A2" symbol="SQUARE_NONE_11_0" />
  <CATEGORY enabled="true" label="" name="TDA" symbol="SQUARE_NONE_11_0" />
  <CATEGORY enabled="true" label="" name="DOE_APPROX" symbol="SQUARE_NONE_11_0" />
  <CATEGORY enabled="true" label="" name="SIMPLEX" symbol="SQUARE_NONE_11_0" />
  <CATEGORY enabled="true" label="" name="UU-P" symbol="SQUARE_NONE_11_0" />
  <CATEGORY enabled="true" label="" name="TILLU" symbol="SQUARE_NONE_11_#3DC3912_1#3DC3912" />
  <CATEGORY enabled="true" label="" name="SIMPLEX_DOE" symbol="SQUARE_NONE_11_#3366CC_1_#3366CC" />
  <CATEGORY enabled="true" label="" name="DOE_RANDOM" symbol="SQUARE_NONE_11_#F9900_1_#F9900" />
</CATEGORIES>
#-----------------------------------------
```

<ID>	Opt_joint_	Opt_joint_	Opt_joint_	Opt_joint_	Opt_joint_	Combined_	Pelvis_Ax_	Pelvis_Tx_	Pelvis_Ty_	T13_Ax_rc	T12_Tx_rc	T12_Ty_rc	Objective3	Constraint1	Constraint2	Constraint3	Constraint4	<ERROR>	<VIRTUAL>	<FEASIBLE>	<MARKED>	<CATEGORY>
0	4330.06	0.02	11001.62	0.15	1.81	0.13	0.21	0.66	0.44	0.34	0.03	1.81	0.13	0.44	0.21	0.66	0.34	0.03	false	false	true	false	SIMPLEX_DOE
1	2014.75	0.01	6946.71	0.13	1.53	0.10	0.18	0.55	0.37	0.29	0.05	1.53	0.10	0.37	0.18	0.55	0.29	0.05	false	true	false	false	SIMPLEX_DOE
2	3947.04	0.02	14420.00	0.09	2.48	0.14	0.22	1.02	0.62	0.44	0.05	2.48	0.14	0.62	0.22	1.02	0.44	0.05	false	false	false	false	SIMPLEX_DOE
3	3014.11	0.01	10835.41	0.12	1.79	0.13	0.20	0.65	0.44	0.34	0.03	1.79	0.13	0.44	0.20	0.65	0.34	0.03	false	true	false	false	SIMPLEX_DOE
4	3771.81	0.00	10335.38	0.10	2.71	0.14	0.22	1.12	0.55	0.33	0.07	2.71	0.14	0.66	0.22	1.12	0.51	0.07	false	false	false	false	SIMPLEX_DOE
5	2981.18	0.03	5000.00	0.14	1.39	0.08	0.20	0.46	0.34	0.28	0.04	1.39	0.08	0.34	0.20	0.46	0.28	0.04	false	false	true	false	SIMPLEX
6	2373.03	0.02	5000.00	0.15	2.81	0.17	0.18	1.05	0.83	0.53	0.05	2.81	0.17	0.83	0.18	1.05	0.53	0.05	false	false	true	false	SIMPLEX
7	3341.03	0.02	11432.97	0.11	1.83	0.13	0.19	0.60	0.44	0.35	0.03	1.83	0.13	0.44	0.19	0.60	0.35	0.03	false	false	true	false	SIMPLEX
8	2779.03	0.02	5458.90	0.15	2.80	0.17	0.18	1.04	0.83	0.53	0.05	2.80	0.17	0.83	0.18	1.04	0.53	0.05	false	false	true	false	SIMPLEX
9	3338.03	0.02	9816.45	0.12	1.78	0.13	0.21	0.64	0.44	0.33	0.03	1.78	0.13	0.44	0.21	0.64	0.33	0.03	false	false	true	false	SIMPLEX
10	2000.00	0.01	5350.17	0.10	1.43	0.08	0.18	0.50	0.34	0.28	0.05	1.43	0.08	0.34	0.18	0.50	0.28	0.05	false	false	true	false	SIMPLEX
11	2152.88	0.02	5000.00	0.13	1.32	0.06	0.21	0.45	0.29	0.27	0.04	1.32	0.06	0.29	0.21	0.45	0.27	0.04	false	false	true	false	SIMPLEX
12	2000.00	0.01	5000.00	0.13	1.31	0.06	0.20	0.45	0.29	0.27	0.04	1.31	0.06	0.29	0.20	0.45	0.27	0.04	false	false	true	false	SIMPLEX
13	2252.27	0.02	5000.00	0.12	1.35	0.06	0.21	0.46	0.31	0.28	0.04	1.36	0.06	0.31	0.21	0.46	0.28	0.04	false	false	true	false	SIMPLEX
14	2250.79	0.01	5179.58	0.12	1.38	0.07	0.21	0.47	0.32	0.28	0.04	1.38	0.07	0.32	0.21	0.47	0.28	0.04	false	false	true	false	SIMPLEX
15	2000.00	0.01	5089.79	0.11	1.39	0.07	0.20	0.48	0.32	0.27	0.04	1.39	0.07	0.32	0.20	0.48	0.27	0.04	false	false	true	false	SIMPLEX
16	2457.97	0.03	5000.00	0.14	1.33	0.06	0.20	0.45	0.30	0.27	0.04	1.33	0.06	0.30	0.20	0.45	0.27	0.04	false	false	true	false	SIMPLEX
17	2370.77	0.03	5000.00	0.14	1.32	0.05	0.20	0.45	0.30	0.27	0.04	1.32	0.05	0.30	0.20	0.45	0.27	0.04	false	false	true	false	SIMPLEX
18	2000.00	0.01	5000.00	0.15	1.28	0.05	0.20	0.45	0.28	0.27	0.04	1.28	0.05	0.28	0.20	0.45	0.27	0.04	false	false	true	false	SIMPLEX
19	2185.38	0.02	5000.00	0.14	1.30	0.05	0.20	0.45	0.29	0.27	0.04	1.30	0.05	0.29	0.20	0.45	0.27	0.04	false	false	true	false	SIMPLEX
20	2000.00	0.01	5000.00	0.14	1.30	0.05	0.20	0.45	0.28	0.27	0.04	1.30	0.05	0.28	0.20	0.45	0.27	0.04	false	false	true	false	SIMPLEX
21	2070.44	0.02	5000.00	0.14	1.30	0.05	0.20	0.45	0.28	0.27	0.04	1.30	0.05	0.28	0.20	0.45	0.27	0.04	false	false	true	false	SIMPLEX
22	2228.98	0.02	5000.00	0.14	1.30	0.05	0.20	0.45	0.29	0.27	0.04	1.30	0.05	0.29	0.20	0.45	0.27	0.04	false	false	true	false	SIMPLEX
23	2092.69	0.02	5000.00	0.14	1.29	0.05	0.20	0.45	0.28	0.27	0.04	1.29	0.05	0.28	0.20	0.45	0.27	0.04	false	false	true	false	SIMPLEX
24	2000.00	0.01	5000.00	0.14	1.29	0.05	0.20	0.45	0.28	0.27	0.04	1.29	0.05	0.28	0.20	0.45	0.27	0.04	false	false	true	false	SIMPLEX
25	2038.22	0.02	5000.00	0.14	1.29	0.05	0.20	0.45	0.28	0.27	0.04	1.29	0.05	0.28	0.20	0.45	0.27	0.04	false	false	true	false	SIMPLEX
26	2134.49	0.02	5000.00	0.14	1.29	0.05	0.20	0.45	0.28	0.27	0.04	1.29	0.05	0.28	0.20	0.45	0.27	0.04	false	false	true	false	SIMPLEX
27	2046.35	0.02	5000.00	0.15	1.29	0.05	0.20	0.45	0.28	0.27	0.04	1.29	0.05	0.28	0.20	0.45	0.27	0.04	false	false	true	false	SIMPLEX
28	2000.00	0.01	5000.00	0.14	1.29	0.05	0.20	0.45	0.28	0.27	0.04	1.29	0.05	0.28	0.20	0.45	0.27	0.04	false	false	true	false	SIMPLEX
29	2019.11	0.02	5000.00	0.14	1.29	0.05	0.20	0.45	0.28	0.27	0.04	1.29	0.05	0.28	0.20	0.45	0.27	0.04	false	false	true	false	SIMPLEX
30	2057.25	0.02	5000.00	0.14	1.29	0.05	0.20	0.45	0.28	0.27	0.04	1.29	0.05	0.28	0.20	0.45	0.27	0.04	false	false	true	false	SIMPLEX
31	2023.17	0.02	5000.00	0.15	1.28	0.05	0.20	0.45	0.28	0.27	0.04	1.28	0.05	0.28	0.20	0.45	0.27	0.04	false	false	true	false	SIMPLEX
32	2000.00	0.01	5000.00	0.14	1.28	0.05	0.20	0.45	0.28	0.27	0.04	1.28	0.05	0.28	0.20	0.45	0.27	0.04	false	false	true	false	SIMPLEX
33	2009.55	0.02	5000.00	0.14	1.28	0.05	0.20	0.45	0.28	0.27	0.04	1.28	0.05	0.28	0.20	0.45	0.27	0.04	false	false	true	false	SIMPLEX
34	2028.61	0.02	5000.00	0.15	1.28	0.05	0.20	0.45	0.28	0.27	0.04	1.28	0.05	0.28	0.20	0.45	0.27	0.04	false	false	true	false	SIMPLEX
35	2031.59	0.02	5000.00	0.15	1.28	0.05	0.20	0.45	0.28	0.27	0.04	1.28	0.05	0.28	0.20	0.45	0.27	0.04	false	false	true	false	SIMPLEX
36	2000.00	0.01	5000.00	0.14	1.28	0.05	0.20	0.45	0.28	0.27	0.04	1.28	0.05	0.28	0.20	0.45	0.27	0.04	false	false	true	false	SIMPLEX
37	2004.78	0.02	5000.00	0.14	1.28	0.05	0.20	0.45	0.28	0.27	0.04	1.28	0.05	0.28	0.20	0.45	0.27	0.04	false	false	true	false	SIMPLEX
38	2014.31	0.02	5000.00	0.15	1.28	0.05	0.20	0.45	0.28	0.27	0.04	1.28	0.05	0.28	0.20	0.45	0.27	0.04	false	false	true	false	SIMPLEX
39	2005.79	0.02	5000.00	0.15	1.28	0.05	0.20	0.45	0.28	0.27	0.04	1.28	0.05	0.28	0.20	0.45	0.27	0.04	false	false	true	false	SIMPLEX
40	2000.00	0.01	5000.00	0.15	1.28	0.05	0.20	0.45	0.28	0.27	0.04	1.28	0.05	0.28	0.20	0.45	0.27	0.04	false	false	true	false	SIMPLEX
41	2002.39	0.02	5000.00	0.15	1.28	0.05	0.20	0.45	0.28	0.27	0.04	1.28	0.05	0.28	0.20	0.45	0.27	0.04	false	false	true	false	SIMPLEX
42	2007.16	0.02	5000.00	0.15	1.28	0.05	0.20	0.45	0.28	0.27	0.04	1.28	0.05	0.28	0.20	0.45	0.27	0.04	false	false	true	false	SIMPLEX
43	2002.00	0.02	5000.00	0.15	1.28	0.05	0.20	0.45	0.28	0.27	0.04	1.28	0.05	0.28	0.20	0.45	0.27	0.04	false	false	true	false	SIMPLEX
44	2000.00	0.01	5000.00	0.15	1.28	0.05	0.20	0.45	0.28	0.27	0.04	1.28	0.05	0.28	0.20	0.45	0.27	0.04	false	false	true	false	SIMPLEX
45	2001.19	0.02	5000.00	0.15	1.28	0.05	0.20	0.45	0.28	0.27	0.04	1.28	0.05	0.28	0.20	0.45	0.27	0.04	false	false	true	false	SIMPLEX
46	2003.58	0.02	5000.00	0.15	1.28	0.05	0.20	0.45	0.28	0.27	0.04	1.28	0.05	0.28	0.20	0.45	0.27	0.04	false	false	true	false	SIMPLEX
47	2001.45	0.02	5000.00	0.15	1.28	0.05	0.20	0.45	0.28	0.27	0.04	1.28	0.05	0.28	0.20	0.45	0.27	0.04	false	false	true	false	SIMPLEX
48	2000.00	0.01	5000.00	0.15	1.28	0.05	0.20	0.45	0.28	0.27	0.04	1.28	0.05	0.28	0.20	0.45	0.27	0.04	false	false	true	false	SIMPLEX
49	2000.60	0.02	5000.00	0.15	1.28	0.05	0.20	0.45	0.28	0.27	0.04	1.28	0.05	0.28	0.20	0.45	0.27	0.04	false	false	true	false	SIMPLEX
50	2001.79	0.02	5000.00	0.15	1.28	0.05	0.20	0.45	0.28	0.27	0.04	1.28	0.05	0.28	0.20	0.45	0.27	0.04	false	false	true	false	SIMPLEX
51	2000.72	0.02	5000.00	0.15	1.28	0.05	0.20	0.45	0.28	0.27	0.04	1.28	0.05	0.28	0.20	0.45	0.27	0.04	false	false	true	false	SIMPLEX
52	2000.00	0.01	5000.00	0.15	1.28	0.05	0.20	0.45	0.28	0.27	0.04	1.28	0.05	0.28	0.20	0.45	0.27	0.04	false	false	true	false	SIMPLEX
53	2000.30	0.01	5000.00	0.15	1.28	0.05	0.20	0.45	0.28	0.27	0.04	1.28	0.05	0.28	0.20	0.45	0.27	0.04	false	false	true	false	SIMPLEX
54	2000.89	0.02	5000.00	0.15	1.28	0.05	0.20	0.45	0.28	0.27	0.04	1.28	0.05	0.28	0.20	0.45	0.27	0.04	false	false	true	false	SIMPLEX
55	2000.36	0.02	5000.00	0.15	1.28	0.05	0.20	0.45	0.28	0.27	0.04	1.28	0.05	0.28	0.20	0.45	0.27	0.04	false	false	true	false	SIMPLEX
56	2000.00	0.01	5000.00	0.15	1.28	0.05	0.20	0.45	0.28	0.27	0.04	1.28	0.05	0.28	0.20	0.45	0.27	0.04	false	false	true	false	SIMPLEX
57	2000.15	0.01	5000.00	0.15	1.28	0.05	0.20	0.45	0.28	0.27	0.04	1.28	0.05	0.28	0.20	0.45	0.27	0.04	false	false	true	false	SIMPLEX
58	2000.45	0.02	5000.00	0.15	1.28	0.05	0.20	0.45	0.28	0.27	0.04	1.28	0.05	0.28	0.20	0.45	0.27	0.04	false	false	true	false	SIMPLEX
59	2000.18	0.01	5000.00	0.15	1.28	0.05	0.20	0.45	0.28	0.27	0.04	1.28	0.05	0.28	0.20	0.45	0.27	0.04	false	false	true	false	SIMPLEX
60	2000.00	0.01	5000.00	0.15	1.28	0.05	0.20	0.45	0.28	0.27	0.04	1.28	0.05	0.28	0.20	0.45	0.27	0.04	false	false	true	false	SIMPLEX
61	2000.07	0.01	5000.00	0.15	1.28	0.05	0.20	0.45	0.28	0.27	0.04	1.28	0.05	0.28	0.20	0.45	0.27	0.04	false	false	true	false	SIMPLEX
62	2000.22	0.01	5000.00	0.15	1.28	0.05	0.20	0.45	0.28	0.27	0.04	1.28	0.05	0.28	0.20	0.45	0.27	0.04	false	false	true	false	SIMPLEX
63	2000.09	0.01	5000.00	0.15	1.28	0.05	0.20	0.45	0.28	0.27	0.04	1.28	0.05	0.28	0.20	0.45	0.27	0.04	false	false	true	false	SIMPLEX
64	2000.00	0.01	5000.00	0.15	1.28	0.05	0.20	0.45	0.28	0.27	0.04	1.28	0.05	0.28	0.20	0.45	0.27	0.04	false	false	true	false	SIMPLEX
65	2000.04	0.01	5000.00	0.15	1.28	0.05	0.20	0.45	0.28	0.27	0.04	1.28	0.05	0.28	0.20	0.45	0.27	0.04	false	false	true	false	SIMPLEX
66	2000.11	0.01	5000.00	0.15	1.28	0.05	0.20	0.45	0.28	0.27	0.04	1.28	0.05	0.28	0.20	0.45	0.27	0.04	false	false	true	false	SIMPLEX
67	2000.05	0.01	5000.00	0.15	1.28	0.05	0.20	0.45	0.28	0.27	0.04	1.28	0.05	0.28	0.20	0.45	0.27	0.04	false	false	true	false	SIMPLEX
68	2000.00	0.01	5000.00	0.15	1.28	0.05	0.20	0.45	0.28	0.27	0.04	1.28	0.05	0.28	0.20	0.45	0.27	0.04	false	false	true	false	SIMPLEX
69	2000.02	0.01	5000.00	0.15	1.28	0.05	0.20	0.45	0.28	0.27	0.04	1.28	0.05	0.28	0.20	0.45	0.27	0.04	false	false	true	false	SIMPLEX
70	2000.06	0.01	5000.00	0.15	1.28	0.05	0.20	0.45	0.28	0.27	0.04	1.28	0.05	0.28	0.20	0.45	0.27	0.04	false	false	true	false	SIMPLEX
71	2000.03	0.01	5000.00	0.15	1.28	0.05	0.20	0.45	0.28	0.27	0.04	1.28	0.05	0.28	0.20	0.45	0.27	0.04	false	false	true	false	SIMPLEX
72	2000.00	0.01	5000.00	0.15	1.28	0.05	0.20	0.45	0.28	0.27	0.04	1.28	0.05	0.28	0.20	0.45	0.27	0.04	false	false	true	false	SIMPLEX
73	2000.01	0.01	5000.00	0.15	1.28	0.05	0.20	0.45	0.28	0.27	0.04	1.28	0.05	0.28	0.20	0.45	0.27	0.04	false	false	true	false	SIMPLEX
74	2000.03	0.01	5000.00	0.15	1.28	0.05	0.20	0.45	0.28	0.27	0.04	1.28	0.05	0.28	0.20	0.45	0.27	0.04	false	false	true	false	SIMPLEX
75	2000.02	0.01	5000.00	0.15	1.28	0.05	0.20	0.45	0.28	0.27	0.04	1.28	0.05	0.28	0.20	0.45	0.27	0.04	false	false	true	false	SIMPLEX
76	2000.00	0.01	5000.00	0.15	1.28	0.05	0.20	0.45	0.28	0.27	0.04	1.28	0.05	0.28	0.20	0.45	0.27	0.04	false	false	true	false	SIMPLEX
77	2000.00	0.01	5000.00	0.15	1.28	0.05	0.20	0.45	0.28	0.27	0.04	1.28	0.05	0.28	0.20	0.45	0.27	0.04	false	false	true	false	SIMPLEX
78	2000.01	0.01	5000.00	0.15	1.28	0.05	0.20	0.45	0.28	0.27	0.04	1.28	0.05	0.28	0.20	0.45	0.27	0.04	false	false	true	false	SIMPLEX
79	2000.01	0.01	5000.00	0.15	1.28	0.05	0.20	0.45	0.28	0.27	0.04	1.28	0.05	0.28	0.20	0.45	0.27	0.04	false	false	true	false	SIMPLEX
80	2000.01	0.01	5000.00	0.15	1.28	0.05	0.20	0.45	0.28	0.27	0.04	1.28	0.05	0.28	0.20	0.45	0.27	0.04	false	false	true	false	SIMPLEX
81	2000.01	0.01	5000.00	0.15	1.28	0.05	0.20	0.45	0.28	0.27	0.04	1.28	0.05	0.28	0.20	0.45	0.27	0.04	false	false	true	false	SIMPLEX
82	2000.00	0.0150	5000.00	0.145	1.281	0.050	0.195	0.446	0.275	0.269	0.043	1.28	0.05	0.28	0.20	0.45	0.27	0.04	false	false	true	false	SIMPLEX
83	4130.29	0.02	17750.75	0.14	1.83	0.13	0.19	0.69	0.44	0.35	0.03	1.83	0.13	0.44	0.19	0.69	0.35	0.03	false	false	true	false	DOE_RANDOM
84	4569.86	0.00	7689.95	0.11	1.73	0.12	0.22	0.60	0.43	0.33	0.03	1.73	0.12	0.43	0.22	0.60	0.33	0.03	false	false	true	false	DOE_RANDOM
85	4178.21	0.02	16284.48	0.08	2.61	0.14	0.21	1.00	0.65	0.47	0.05	2.61	0.14	0.65	0.21	1.00	0.47	0.05	false	false	false	false	DOE_RANDOM
86	3511.17	0.02	7650.63	0.14	1.69	0.12	0.20	0.58	0.45	0.31	0.03	1.69	0.12	0.45	0.20	0.58	0.31	0.03	false	false	true	false	DOE_RANDOM
87	3339.49	0.01	17245.34	0.11	2.43	0.14	0.22	0.99	0.61	0.44	0.04	2.43	0.14	0.61	0.22	0.99	0.44	0.04	false	false	true	false	DOE_RANDOM
88	3697.16	0.00	6383.85	0.15	2.48	0.13	0.19	0.96	0.60	0.42	0.08	2.48	0.13	0.60	0.19	0.96	0.42	0.08	false	false	true	false	SIMPLEX
89	4178.21	0.02	16284.48	0.10	2.38	0.13	0.21	0.96	0.60	0.43	0.04	2.38	0.13	0.60	0.21	0.96	0.43	0.04	false	false	true	false	SIMPLEX
90	4655.25	0.02	5000.00	0.13	1.74	0.13	0.22	0.59	0.45	0.31	0.03	1.74	0.13	0.45	0.22	0.59	0.31	0.03	false	false	true	false	SIMPLEX
91	4255.05	0.00	5000.00	0.15	2.57	0.16	0.20	0.96	0.70	0.47	0.07	2.57	0.16	0.70	0.20	0.96	0.47	0.07	false	false	true	false	SIMPLEX
92	4197.47	0.02	17278.65	0.11	1.93	0.13	0.21	0.75	0.51	0.37	0.03	1.93	0.13	0.51	0.21	0.75	0.37	0.03	false	false	true	false	SIMPLEX
93	4235.84	0.01	5000.00	0.15	1.65	0.12	0.21	0.57	0.45	0.30	0.03	1.68	0.12	0.45	0.21	0.57	0.30	0.03	false	false	true	false	SIMPLEX
94	4355.75	0.00	5000.00	0.13	1.80	0.12	0.22	0.58	0.45	0.30	0.03	1.80	0.12	0.45	0.22	0.58	0.30	0.03	false	false	true	false	SIMPLEX
95	3681.03	0.00	7670.29	0.13	NaN	NaN	NaN	NaN	NaN	NaN	NaN	NaN	NaN	NaN	NaN	NaN	NaN	NaN	true	false	false	false	SIMPLEX
96	4411.70	0.01	9867.57	0.13	1.74	0.13	0.22	0.59	0.45	0.31	0.03	1.74	0.13	0.45	0.22	0.59	0.31	0.03	false	false	true	false	SIMPLEX
97	4295.79	0.01	5000.00	0.14	1.69	0.12	0.22	0.57	0.45	0.30	0.03	1.69	0.12	0.45	0.22	0.57	0.30	0.03	false	false	true	false	SIMPLEX
98	4402.85	0.01	6344.97	0.13	1.74	0.12	0.23	0.59	0.45	0.31	0.03	1.74	0.12	0.45	0.23	0.59	0.31	0.03	false	false	true	false	SIMPLEX

99	3873.48	0.01	6375.32	0.14	1.69	0.12	0.21	0.57	0.45	0.30	0.03	1.69	0.12	0.45	0.21	0.57	0.30	0.03	false	false	true	false	SIMPLEX
100	4445.54	0.01	5000.00	0.14	1.71	0.13	0.22	0.58	0.45	0.30	0.03	1.71	0.13	0.45	0.22	0.58	0.30	0.03	false	false	true	false	SIMPLEX
101	4022.48	0.01	5000.00	0.15	1.62	0.12	0.20	0.54	0.44	0.29	0.03	1.62	0.12	0.44	0.20	0.54	0.29	0.03	false	false	true	false	SIMPLEX
102	3768.25	0.01	5662.65	0.15	1.64	0.12	0.20	0.55	0.44	0.29	0.03	1.64	0.12	0.44	0.20	0.55	0.29	0.03	false	false	true	false	SIMPLEX
103	3954.23	0.02	3992.99	0.15	2.77	0.17	0.18	1.02	0.82	0.52	0.05	2.77	0.17	0.82	0.18	1.02	0.52	0.05	false	false	false	false	SIMPLEX
104	4135.40	0.01	5248.50	0.14	1.68	0.12	0.21	0.57	0.45	0.30	0.03	1.68	0.12	0.45	0.21	0.57	0.30	0.03	false	false	true	false	SIMPLEX
105	4207.50	0.01	5000.00	0.15	2.67	0.16	0.18	0.98	0.77	0.52	0.05	2.67	0.16	0.77	0.18	0.98	0.52	0.05	false	false	true	false	SIMPLEX
106	3956.98	0.01	5776.55	0.14	1.67	0.12	0.21	0.57	0.45	0.30	0.03	1.67	0.12	0.45	0.21	0.57	0.30	0.03	false	false	true	false	SIMPLEX
107	3855.37	0.01	5471.11	0.15	2.72	0.17	0.17	0.99	0.81	0.52	0.05	2.72	0.17	0.81	0.17	0.99	0.52	0.05	false	false	true	false	SIMPLEX
108	4065.64	0.01	5304.15	0.14	1.67	0.12	0.21	0.56	0.45	0.30	0.03	1.67	0.12	0.45	0.21	0.56	0.30	0.03	false	false	true	false	SIMPLEX
109	3670.84	0.01	5871.68	0.15	1.61	0.12	0.20	0.53	0.44	0.29	0.03	1.61	0.12	0.44	0.20	0.53	0.29	0.03	false	false	true	false	SIMPLEX
110	3388.34	0.01	6307.52	0.15	1.57	0.11	0.19	0.52	0.42	0.29	0.04	1.57	0.11	0.42	0.19	0.52	0.29	0.04	false	false	true	false	SIMPLEX
111	3605.57	0.01	5860.61	0.15	1.57	0.11	0.19	0.52	0.43	0.29	0.03	1.57	0.11	0.43	0.19	0.52	0.29	0.03	false	false	true	false	SIMPLEX
112	3358.57	0.01	5861.24	0.15	2.77	0.17	0.18	1.02	0.82	0.52	0.05	2.77	0.17	0.82	0.18	1.02	0.52	0.05	false	false	false	false	SIMPLEX
113	3888.38	0.01	5443.42	0.15	1.64	0.12	0.20	0.55	0.44	0.29	0.03	1.64	0.12	0.44	0.20	0.55	0.29	0.03	false	false	true	false	SIMPLEX
114	3714.03	0.02	5393.12	0.15	1.56	0.11	0.19	0.51	0.42	0.29	0.03	1.56	0.11	0.42	0.19	0.51	0.29	0.03	false	false	true	false	SIMPLEX
115	3685.03	0.02	5258.35	0.15	1.51	0.10	0.19	0.49	0.40	0.29	0.04	1.51	0.10	0.40	0.19	0.49	0.29	0.04	false	false	true	false	SIMPLEX
116	3493.18	0.02	5519.82	0.15	2.91	0.16	0.20	1.12	0.83	0.55	0.05	2.91	0.16	0.83	0.20	1.12	0.55	0.05	false	false	true	false	SIMPLEX
117	3789.58	0.01	5462.52	0.15	1.60	0.12	0.20	0.53	0.43	0.29	0.03	1.60	0.12	0.43	0.20	0.53	0.29	0.03	false	false	true	false	SIMPLEX
118	3242.63	0.02	5194.50	0.15	1.51	0.10	0.19	0.49	0.40	0.29	0.04	1.51	0.10	0.40	0.19	0.49	0.29	0.04	false	false	true	false	SIMPLEX
119	2852.70	0.02	5791.75	0.15	1.49	0.09	0.18	0.50	0.38	0.29	0.05	1.49	0.09	0.38	0.18	0.50	0.29	0.05	false	false	true	false	SIMPLEX
120	3007.09	0.02	5396.60	0.15	1.45	0.09	0.18	0.47	0.38	0.29	0.04	1.45	0.09	0.38	0.18	0.47	0.29	0.04	false	false	true	false	SIMPLEX
121	2615.85	0.03	6862.63	0.15	1.46	0.08	0.20	0.50	0.35	0.29	0.05	1.46	0.08	0.35	0.20	0.50	0.29	0.05	false	false	true	false	SIMPLEX
122	2802.15	0.03	7018.50	0.15	1.48	0.08	0.18	0.50	0.37	0.29	0.05	1.48	0.08	0.37	0.18	0.50	0.29	0.05	false	false	true	false	SIMPLEX
123	2786.10	0.03	6424.08	0.15	1.44	0.08	0.19	0.49	0.35	0.29	0.04	1.44	0.08	0.35	0.19	0.49	0.29	0.04	false	false	true	false	SIMPLEX
124	2637.11	0.02	6856.11	0.14	1.52	0.07	0.19	0.55	0.35	0.30	0.05	1.52	0.07	0.35	0.19	0.55	0.30	0.05	false	false	true	false	SIMPLEX
125	3274.47	0.02	5957.79	0.15	1.46	0.10	0.18	0.47	0.39	0.29	0.04	1.46	0.10	0.39	0.18	0.47	0.29	0.04	false	false	true	false	SIMPLEX
126	3082.21	0.03	6105.73	0.15	1.43	0.09	0.18	0.47	0.37	0.29	0.04	1.43	0.09	0.37	0.18	0.47	0.29	0.04	false	false	true	false	SIMPLEX
127	3272.76	0.02	5425.60	0.15	2.94	0.16	0.21	1.14	0.83	0.55	0.05	2.94	0.16	0.83	0.21	1.14	0.55	0.05	false	false	false	false	SIMPLEX
128	2939.82	0.02	6618.77	0.15	1.46	0.09	0.18	0.49	0.37	0.29	0.05	1.46	0.09	0.37	0.18	0.49	0.29	0.05	false	false	true	false	SIMPLEX
129	2623.14	0.02	6814.80	0.15	1.46	0.08	0.19	0.50	0.35	0.29	0.05	1.46	0.08	0.35	0.19	0.50	0.29	0.05	false	false	true	false	SIMPLEX
130	2829.46	0.02	6251.83	0.15	1.43	0.08	0.19	0.48	0.35	0.29	0.04	1.43	0.08	0.35	0.19	0.48	0.29	0.04	false	false	true	false	SIMPLEX
131	2784.28	0.02	6008.35	0.15	3.02	0.16	0.21	1.17	0.84	0.56	0.06	3.02	0.16	0.84	0.21	1.17	0.56	0.06	false	false	false	false	SIMPLEX
132	3229.29	0.02	5774.32	0.15	1.44	0.09	0.18	0.46	0.38	0.29	0.04	1.44	0.09	0.38	0.18	0.46	0.29	0.04	false	false	true	false	SIMPLEX
133	2955.44	0.03	5881.38	0.15	1.41	0.08	0.19	0.46	0.35	0.29	0.04	1.41	0.08	0.35	0.19	0.46	0.29	0.04	false	false	true	false	SIMPLEX
134	3267.60	0.02	5582.55	0.15	3.00	0.16	0.22	1.16	0.84	0.56	0.06	3.00	0.16	0.84	0.22	1.16	0.56	0.06	false	false	true	false	SIMPLEX
135	2905.23	0.02	6213.70	0.15	1.43	0.08	0.19	0.48	0.36	0.29	0.04	1.43	0.08	0.36	0.19	0.48	0.29	0.04	false	false	true	false	SIMPLEX
136	2857.37	0.03	6452.00	0.15	1.43	0.07	0.20	0.49	0.34	0.29	0.04	1.43	0.07	0.34	0.20	0.49	0.29	0.04	false	false	true	false	SIMPLEX
137	2597.04	0.02	6293.77	0.15	1.41	0.07	0.20	0.48	0.33	0.28	0.04	1.41	0.07	0.33	0.20	0.48	0.28	0.04	false	false	true	false	SIMPLEX
138	2340.95	0.02	6387.77	0.15	3.08	0.16	0.24	1.20	0.84	0.57	0.07	3.08	0.16	0.84	0.24	1.20	0.57	0.07	false	false	false	false	SIMPLEX
139	2612.43	0.02	6225.77	0.15	3.10	0.16	0.24	1.21	0.84	0.57	0.07	3.10	0.16	0.84	0.24	1.21	0.57	0.07	false	false	false	false	SIMPLEX
140	2837.03	0.02	6216.71	0.15	1.43	0.08	0.19	0.48	0.35	0.29	0.04	1.43	0.08	0.35	0.19	0.48	0.29	0.04	false	false	true	false	SIMPLEX
141	2689.48	0.03	6170.08	0.15	1.41	0.07	0.20	0.47	0.33	0.28	0.04	1.41	0.07	0.33	0.20	0.47	0.28	0.04	false	false	true	false	SIMPLEX
142	2615.84	0.03	6181.88	0.15	1.40	0.07	0.21	0.47	0.33	0.28	0.04	1.40	0.07	0.33	0.21	0.47	0.28	0.04	false	false	true	false	SIMPLEX
143	2769.43	0.02	5811.53	0.15	3.11	0.16	0.25	1.21	0.84	0.57	0.07	3.11	0.16	0.84	0.25	1.21	0.57	0.07	false	false	false	false	SIMPLEX
144	2685.39	0.03	6291.88	0.15	1.42	0.07	0.20	0.48	0.34	0.28	0.04	1.42	0.07	0.34	0.20	0.48	0.28	0.04	false	false	true	false	SIMPLEX
145	2741.41	0.03	5971.65	0.15	3.12	0.16	0.25	1.22	0.85	0.57	0.07	3.12	0.16	0.85	0.25	1.22	0.57	0.07	false	false	false	false	SIMPLEX
146	2696.39	0.03	6291.87	0.15	1.41	0.07	0.20	0.48	0.34	0.28	0.04	1.41	0.07	0.34	0.20	0.48	0.28	0.04	false	false	true	false	SIMPLEX
147	2341.84	0.02	6547.37	0.15	1.41	0.06	0.21	0.48	0.32	0.28	0.05	1.41	0.06	0.32	0.21	0.48	0.28	0.05	false	false	true	false	SIMPLEX
148	2420.11	0.02	6384.70	0.15	1.40	0.07	0.21	0.48	0.32	0.28	0.04	1.40	0.07	0.32	0.21	0.48	0.28	0.04	false	false	true	false	SIMPLEX
149	2815.80	0.03	5967.82	0.15	1.41	0.08	0.20	0.47	0.34	0.28	0.04	1.41	0.08	0.34	0.20	0.47	0.28	0.04	false	false	true	false	SIMPLEX
150	2678.97	0.03	6058.52	0.15	1.40	0.07	0.20	0.47	0.33	0.28	0.04	1.40	0.07	0.33	0.20	0.47	0.28	0.04	false	false	true	false	SIMPLEX
151	2575.28	0.02	6126.38	0.15	3.13	0.16	0.25	1.22	0.85	0.57	0.07	3.13	0.16	0.85	0.25	1.22	0.57	0.07	false	false	false	false	SIMPLEX
152	2661.18	0.03	6159.15	0.15	1.40	0.07	0.20	0.47	0.33	0.28	0.04	1.40	0.07	0.33	0.20	0.47	0.28	0.04	false	false	true	false	SIMPLEX
153	2371.15	0.03	6474.30	0.15	1.40	0.06	0.21	0.48	0.32	0.28	0.04	1.40	0.06	0.32	0.21	0.48	0.28	0.04	false	false	true	false	SIMPLEX
154	2743.37	0.03	6027.22	0.15	1.40	0.07	0.20	0.47	0.34	0.28	0.04	1.40	0.07	0.34	0.20	0.47	0.28	0.04	false	false	true	false	SIMPLEX
155	2543.39	0.03	6186.81	0.15	1.40	0.07	0.21	0.47	0.33	0.28	0.04	1.40	0.07	0.33	0.21	0.47	0.28	0.04	false	false	true	false	SIMPLEX
156	2508.25	0.03	6268.95	0.15	1.40	0.07	0.21	0.47	0.33	0.28	0.04	1.40	0.07	0.33	0.21	0.47	0.28	0.04	false	false	true	false	SIMPLEX
157	2621.35	0.03	6088.87	0.15	1.40	0.07	0.21	0.47	0.33	0.28	0.04	1.40	0.07	0.33	0.21	0.47	0.28	0.04	false	false	true	false	SIMPLEX
158	2624.20	0.03	6042.37	0.15	1.40	0.07	0.21	0.47	0.33	0.28	0.04	1.40	0.07	0.33	0.21	0.47	0.28	0.04	false	false	true	false	SIMPLEX
159	2786.72	0.03	5888.51	0.15	1.40	0.08	0.20	0.46	0.34	0.28	0.04	1.40	0.08	0.34	0.20	0.46	0.28	0.04	false	false	true	false	SIMPLEX
160	2573.27	0.03	6060.88	0.15	1.39	0.07	0.21	0.47	0.32	0.28	0.04	1.39	0.07	0.32	0.21	0.47	0.28	0.04	false	false	true	false	SIMPLEX
161	2488.22	0.03	6077.70	0.15	1.38	0.07	0.21	0.47	0.32	0.28	0.04	1.38	0.07	0.32	0.21	0.47	0.28	0.04	false	false	true	false	SIMPLEX
162	2542.29	0.03	6039.13	0.15	1.39	0.07	0.21	0.46	0.32	0.28	0.04	1.39	0.07	0.32	0.21	0.46	0.28	0.04	false	false	true	false	SIMPLEX
163	2312.34	0.03	6284.53	0.15	1.38	0.06	0.21	0.47	0.32	0.28	0.04	1.38	0.06	0.32	0.21	0.47	0.28	0.04	false	false	true	false	SIMPLEX
164	2075.15	0.03	6482.54	0.15	1.37	0.05	0.20	0.47	0.32	0.28	0.05	1.37	0.05	0.32	0.20	0.47	0.28	0.05	false	false	true	false	SIMPLEX
165	2321.54	0.03	6134.09	0.15	1.37	0.06	0.21	0.46	0.32	0.28	0.04	1.37	0.06	0.32	0.21	0.46	0.28	0.04	false	false	true	false	SIMPLEX
166	2080.40	0.03	6324.38	0.15	1.35	0.05	0.20	0.46	0.31	0.28	0.04	1.35	0.05	0.31	0.20	0.46	0.28	0.04	false	false	true	false	SIMPLEX
167	2000.00	0.03	6455.38	0.15	1.37	0.05	0.20	0.47	0.32	0.28	0.05	1.37	0.05	0.32	0.20	0.47	0.28	0.05	false	false	true	false	SIMPLEX
168	2000.00	0.03	6470.18	0.15	1.37	0.05	0.20	0.47	0.32	0.28	0.05	1.37	0.05	0.32	0.20	0.47	0.28	0.05	false	false	true	false	SIMPLEX
169	2000.00	0.03	6627.80	0.15	1.38	0.05	0.20	0.48	0.32	0.28	0.05	1.38	0.05	0.32	0.20	0.48	0.28	0.05	false	false	true	false	SIMPLEX
170	2243.05	0.03	6077.70	0.15	1.36	0.06	0.21	0.46	0.31	0.28	0.04	1.36	0.06	0.31	0.21	0.46	0.28	0.04	false	false	true	false	SIMPLEX
171	2000.00	0.03	6543.31	0.15	1.37	0.05	0.20	0.47	0.32	0.28	0.05	1.37	0.05	0.32	0.20	0.47	0.28	0.05	false	false	true	false	SIMPLEX
172	2288.80	0.03	6114.09	0.15	1.36	0.05	0.21	0.46	0.31	0.28	0.04	1.36	0.05	0.31	0.21	0.46	0.28	0.04	false	false	true	false	SIMPLEX
173	2199.98	0.03	6000.64	0.15	1.35	0.05	0.21	0.46	0.31	0.28	0.04	1.35	0.05	0.31	0.21	0.46	0.28	0.04	false	false	true	false	SIMPLEX
174	2251.89	0.03	5789.69	0.15	1.35	0.05	0.21	0.46	0.31	0.28	0.04	1.35	0.05	0.31	0.21	0.46	0.28	0.04	false	false	true	false	SIMPLEX
175	2394.07	0.03	5692.75	0.15	1.35	0.06	0.21	0.46	0.31	0.28	0.04	1.35	0.06	0.31	0.21	0.46	0.28	0.04	false	false	true	false	SIMPLEX
176	2285.41	0.03	5808.17	0.15	1.35	0.05	0.21	0.46	0.31	0.28	0.04	1.35	0.05	0.31	0.21	0.46	0.28	0.04	false	false	true	false	SIMPLEX
177	2267.34	0.03	5729.80	0.15	1.34	0.05	0.21	0.46	0.31	0.28	0.04	1.34	0.05	0.31	0.21	0.46	0.28	0.04	false	false	true	false	SIMPLEX
178	2279.48	0.03	5555.84	0.15	1.34	0.05	0.20	0.46	0.30	0.28	0.04	1.34	0.05	0.30	0.20	0.46	0.28	0.04	false	false	true	false	SIMPLEX
179	2315.60	0.03	5598.85	0.15	1.33	0.05	0.20	0.45	0.30	0.27	0.04	1.33	0.05	0.30	0.20	0.45	0.27	0.04	false	false	true	false	SIMPLEX
180	2729.33	0.03	5000.00	0.15	1.35	0.07	0.21	0.45	0.31	0.27	0.04	1.35	0.07	0.31	0.21	0.45	0.27	0.04	false	false	true	false	SIMPLEX
181	2272.31	0.03	5433.53	0.15	1.32	0.05	0.20	0.45	0.30	0.28	0.04	1.32	0.05	0.30	0.20	0.45	0.28	0.04	false	false	true	false	SIMPLEX
182	2211.47	0.03	5303.91	0.15	1.31	0.05	0.19	0.45	0.30	0.27	0.04	1.31	0.05	0.30	0.19	0.45	0.27	0.04	false	false	true	false	SIMPLEX
183	2344.03	0.03	5005.97	0.15	1.31	0.05	0.20	0.45	0.30	0.27	0.04	1.31	0.05	0.30	0.20	0.45	0.27	0.04	false	false	true	false	SIMPLEX
184	2423.60	0.03	5000.00	0.15	1.32	0.05	0.20	0.45	0.30	0.27	0.04	1.32	0.05	0.30	0.20	0.45	0.27	0.04	false	false	true	false	SIMPLEX
185	2468.08	0.03	5000.00	0.15	1.32	0.06	0.20	0.45	0.30	0.27	0.04	1.32	0.06	0.30	0.20	0.45	0.27	0.04	false	false	true	false	SIMPLEX
186	2207.56	0.03	5086.08	0.14	1.30	0.05	0.19	0.45	0.29	0.27	0.04	1.30	0.05	0.29	0.19	0.45	0.27	0.04	false	false	true	false	SIMPLEX
187	2053.34	0.03	5070.71	0.14	1.30	0.05	0.18	0.46	0.29	0.27	0.04	1.30	0.05	0.29	0.18	0.46	0.27	0.04	false	false	true	false	SIMPLEX
188	2048.14	0.03	5074.80	0.14	1.30	0.05	0.18	0.46	0.30	0.27	0.04	1.30	0.05	0.30	0.18	0.46	0.27	0.04	false	false	true	false	SIMPLEX
189	2000.00	0.03	5387.19	0.14	1.31	0.05	0.18	0.46	0.30	0.27	0.04	1.31	0.05	0.30	0.18	0.46	0.27	0.04	false	false	true	false	SIMPLEX
190	2000.00	0.03	5406.83	0.14	1.31	0.05	0.18	0.46	0.30	0.28	0.04	1.31	0.05	0.30	0.18	0.46	0.28	0.04	false	false	true	false	SIMPLEX
191	2211.13	0.03	5151.19	0.14	1.30	0.05	0.19	0.45	0.30	0.27	0.04	1.30	0.05	0.30	0.19	0.45	0.27	0.04	false	false	true	false	SIMPLEX
192	2262.04	0.03	5042.61	0.15	1.30	0.05	0.19	0.45	0.29	0.27	0.04	1.30	0.05	0.29	0.19	0.45	0.27	0.04	false	false	true	false	SIMPLEX
193	2203.05	0.03	5000.00	0.15	1.32	0.05	0.20	0.45	0.30	0.27	0.04	1.32	0.05	0.30	0.20	0.45	0.27	0.04	false	false	true	false	SIMPLEX
194	2075.85	0.03	5000.00	0.14	1.29	0.05	0.18	0.46	0.29	0.27	0.04	1.29	0.05	0.29	0.18	0.46	0.27	0.04	false	false	true	false	SIMPLEX
195	2253.04	0.03	5000.00	0.14	1.30	0.05	0.19	0.45	0.29	0.27	0.04	1.30	0.05	0.29	0.19	0.45	0.27	0.04	false	false	true	false	SIMPLEX
196	2111.00	0.03	5000.00	0.14	1.30	0.05	0.18	0.46	0.29	0.27	0.04	1.30	0.05	0.29	0.18	0.46	0.27	0.04	false	false	true	false	SIMPLEX
197	2297.63	0.03	5000.00	0.14	1.30	0.05	0.19	0.45	0.30	0.27	0.04	1.30	0.05	0.30	0.19	0.45	0.27	0.04	false	false	true	false	SIMPLEX
198	2154.41	0.03	5045.18	0.14	1.30	0.05	0.18	0.46	0.29	0.27	0.04	1.30	0.05	0.29	0.18	0.46	0.27	0.04	false	false	true	false	SIMPLEX
199	2235.56	0.03	5000.00	0.14	1.29	0.05	0.19	0.45	0.29	0.27	0.04	1.29	0.05	0.29	0.19	0.45	0.27	0.04	false	false	true	false	SIMPLEX

APPENDIX G – PMHS MODEFRONTIER OPTIMIZATION FOR RECLINED POSTURE

```
#---- Frontier Design DB File info ----------
#modeFRONTIER  (c) ESTECO S.p.A.
#Design DB Table
#----------------------------------------------
#modeFRONTIER Version: modeFRONTIER 2017R5 5.7.1 b2017i017
#Date: Sat Jan 26 08:16:35 IST 2019
#Project Name: PMHS A Opt 2019-01-25 - redline - sensitivity - complete.prj
#Operating System: Windows 10 10.0 amd64
#Java (SDK/JRE) Version: 1.8.0_60
#Java Vendor: Oracle Corporation
#Java Vendor URL: http://java.oracle.com/
#User Name: KBosch
#----------------------------------------------
#Categories
<CATEGORIES clusterPrefix="CLUSTER_" useTableNamePrefix="false">
  <CATEGORY enabled="true" label="" name="SOBOL" symbol="SQUARE,NONE,11,,0"/>
  <CATEGORY enabled="true" label="" name="USRDOE" symbol="SQUARE,NONE,11,,0"/>
  <CATEGORY enabled="true" label="" name="NSGA2" symbol="SQUARE,NONE,11,,0"/>
  <CATEGORY enabled="true" label="" name="TDA" symbol="SQUARE,NONE,11,,0"/>
  <CATEGORY enabled="true" label="" name="DOE_APPROX" symbol="SQUARE,NONE,11,,0"/>
  <CATEGORY enabled="true" label="" name="SIMPLEX" symbol="SQUARE,NONE,11,,0"/>
  <CATEGORY enabled="true" label="" name="USER" symbol="SQUARE,NONE,11,,0"/>
  <CATEGORY enabled="true" label="" name="FULL" symbol="SQUARE,NONE,11,#3C3912,1,#3C3912"/>
  <CATEGORY enabled="true" label="" name="SIMPLEX_DOE" symbol="SQUARE,NONE,11,#3366CC,1,#3366CC"/>
</CATEGORIES>

#----------------------------------------------
```

<ID>	Opt_joint	Opt_joint	Opt_joint	Opt_joint	Combined	Pelvis_Ax	Pelvis_Fx	Pelvis_Fy	T12_Ax	T12_Fx	T12_Fy	no Constraint	Constraint	Constraint	Constraint	Constraint	Constraint	<ERROR>	<VRTUAL>	<TAS DUT	<MARKED>	<CATEGORY>
0	4392.01	0.02	19985.14	0.15	2.09	0.11	0.25	0.84	0.43	0.41	0.06	0.11	0.43	0.25	0.84	0.41	0.05	false	false	true	false	ULH
1	2743.12	0.02	6736.88	0.14	1.31	0.12	0.05	0.51	0.31	0.30	0.03	0.12	0.31	0.05	0.51	0.30	0.03	false	false	true	false	ULH
2	2800.38	0.01	18518.53	0.13	2.11	0.11	0.24	0.84	0.44	0.42	0.05	0.11	0.44	0.24	0.84	0.42	0.05	false	false	true	false	ULH
3	3488.34	0.00	16733.66	0.15	1.93	0.10	0.21	0.78	0.40	0.39	0.06	0.10	0.40	0.21	0.78	0.39	0.06	false	false	true	false	ULH
4	4224.29	0.01	11174.93	0.09	1.98	0.11	0.22	0.79	0.41	0.40	0.05	0.11	0.41	0.22	0.79	0.40	0.05	false	false	true	false	ULH
5	2755.79	0.02	17701.08	0.09	2.45	0.12	0.29	1.07	0.47	0.47	0.08	0.12	0.47	0.29	1.07	0.47	0.08	false	false	false	false	ULH
6	2048.34	0.02	6548.94	0.15	1.28	0.12	0.05	0.47	0.32	0.28	0.03	0.12	0.32	0.05	0.47	0.28	0.03	false	false	true	false	ULH
7	3702.04	0.02	5114.38	0.09	1.66	0.09	0.04	0.74	0.35	0.39	0.04	0.09	0.35	0.04	0.74	0.39	0.04	false	false	true	false	ULH
8	4999.03	0.01	14395.69	0.09	2.26	0.12	0.23	0.93	0.53	0.39	0.06	0.12	0.53	0.23	0.93	0.39	0.06	false	false	true	false	ULH
9	4019.91	0.02	12009.39	0.12	1.92	0.11	0.18	0.76	0.41	0.40	0.04	0.11	0.43	0.18	0.76	0.40	0.04	false	false	true	false	ULH
10	4487.77	0.02	15903.96	0.13	2.04	0.11	0.24	0.79	0.44	0.40	0.06	0.11	0.44	0.24	0.79	0.40	0.06	false	false	true	false	ULH
11	2221.73	0.00	16508.78	0.11	2.05	0.11	0.23	0.80	0.43	0.41	0.06	0.11	0.43	0.23	0.80	0.41	0.06	false	false	true	false	ULH
12	3644.54	0.02	17854.14	0.10	2.38	0.14	0.25	1.02	0.51	0.40	0.06	0.14	0.51	0.25	1.02	0.40	0.06	false	false	false	false	ULH
13	2269.11	0.02	5829.18	0.08	2.34	0.13	0.05	1.11	0.46	0.55	0.04	0.13	0.46	0.05	1.11	0.55	0.04	false	false	false	false	ULH
14	3238.76	0.02	15637.90	0.12	2.10	0.11	0.23	0.84	0.44	0.42	0.05	0.11	0.44	0.23	0.84	0.42	0.05	false	false	true	false	ULH
15	3371.57	0.01	19459.13	0.11	2.16	0.11	0.29	1.01	0.47	0.40	0.07	0.11	0.47	0.29	1.01	0.40	0.07	false	false	false	false	ULH
16	3796.53	0.02	19739.27	0.11	2.38	0.12	0.27	1.02	0.49	0.40	0.07	0.12	0.49	0.27	1.02	0.40	0.07	false	false	false	false	ULH
17	2969.76	0.01	17177.55	0.11	2.24	0.11	0.25	0.97	0.44	0.40	0.07	0.11	0.44	0.25	0.97	0.40	0.07	false	false	true	false	ULH
18	3159.53	0.02	19085.91	0.10	2.39	0.13	0.29	1.00	0.47	0.41	0.07	0.13	0.47	0.29	1.00	0.41	0.07	false	false	false	false	ULH
19	3943.16	0.02	14815.23	0.15	1.90	0.11	0.15	0.76	0.43	0.40	0.04	0.11	0.43	0.15	0.76	0.40	0.04	false	false	true	false	ULH
20	2624.97	0.01	10557.94	0.11	1.69	0.11	0.04	0.72	0.37	0.40	0.04	0.11	0.37	0.04	0.72	0.40	0.04	false	false	true	false	ULH
21	2462.16	0.02	13508.73	0.08	2.37	0.12	0.28	1.01	0.45	0.42	0.07	0.12	0.45	0.28	1.01	0.42	0.07	false	false	false	false	ULH
22	4195.70	0.01	15149.22	0.13	2.00	0.11	0.22	0.82	0.41	0.39	0.06	0.11	0.41	0.22	0.82	0.39	0.06	false	false	true	false	ULH
23	3064.55	0.02	17978.06	0.09	2.52	0.15	0.30	1.04	0.53	0.42	0.08	0.15	0.53	0.30	1.04	0.42	0.08	false	false	false	false	ULH
24	3579.53	0.01	9070.93	0.14	1.62	0.10	0.05	0.62	0.45	0.36	0.03	0.10	0.45	0.05	0.62	0.36	0.03	false	false	true	false	ULH
25	4458.41	0.01	11072.03	0.13	1.84	0.11	0.15	0.72	0.43	0.38	0.04	0.11	0.43	0.15	0.72	0.38	0.04	false	false	true	false	ULH
26	4261.81	0.00	18301.91	0.14	2.06	0.10	0.21	0.89	0.41	0.39	0.06	0.10	0.41	0.21	0.89	0.39	0.06	false	false	true	false	ULH
27	2189.55	0.00	18793.48	0.10	2.31	0.11	0.23	1.03	0.45	0.40	0.07	0.11	0.45	0.23	1.03	0.40	0.07	false	false	false	false	ULH
28	2842.49	0.01	14708.13	0.09	2.27	0.12	0.25	0.96	0.45	0.40	0.07	0.12	0.45	0.25	0.96	0.40	0.07	false	false	true	false	ULH
29	4088.91	0.02	17333.48	0.15	2.04	0.11	0.23	0.79	0.44	0.41	0.06	0.11	0.44	0.23	0.79	0.41	0.06	false	false	true	false	ULH
30	2001.52	0.02	19220.73	0.14	1.90	0.10	0.16	0.83	0.35	0.43	0.03	0.10	0.35	0.16	0.83	0.43	0.03	false	false	true	false	ULH
31	3650.41	0.01	15411.14	0.09	2.27	0.12	0.27	1.00	0.42	0.40	0.07	0.12	0.42	0.27	1.00	0.40	0.07	false	false	false	false	ULH
32	2893.26	0.02	16975.54	0.08	2.64	0.12	0.31	1.14	0.53	0.45	0.09	0.12	0.53	0.31	1.14	0.45	0.09	false	false	false	false	ULH
33	3216.56	0.00	16008.24	0.10	2.14	0.11	0.24	0.93	0.40	0.39	0.06	0.11	0.40	0.24	0.93	0.39	0.06	false	false	true	false	ULH
34	2578.77	0.02	16175.97	0.08	2.55	0.12	0.32	1.10	0.50	0.43	0.09	0.12	0.50	0.32	1.10	0.43	0.09	false	false	false	false	ULH
35	3559.11	0.01	14152.48	0.13	2.03	0.11	0.22	0.80	0.44	0.41	0.05	0.11	0.44	0.22	0.80	0.41	0.05	false	false	true	false	ULH
36	3270.23	0.01	5679.25	0.12	1.29	0.08	0.04	0.49	0.35	0.30	0.03	0.08	0.35	0.04	0.49	0.30	0.03	false	false	true	false	ULH
37	2500.52	0.01	9864.84	0.10	1.87	0.11	0.11	0.73	0.47	0.40	0.04	0.11	0.47	0.11	0.73	0.40	0.04	false	false	true	false	ULH
38	4285.53	0.02	18826.82	0.11	2.29	0.12	0.26	1.01	0.43	0.40	0.07	0.12	0.43	0.26	1.01	0.40	0.07	false	false	false	false	ULH
39	4605.33	0.02	17522.59	0.10	2.36	0.12	0.29	1.03	0.45	0.40	0.08	0.12	0.45	0.29	1.03	0.40	0.08	false	false	false	false	ULH
40	4856.40	0.01	8577.87	0.08	1.87	0.11	0.18	0.77	0.43	0.38	0.05	0.11	0.43	0.19	0.77	0.38	0.05	false	false	true	false	ULH
41	2110.41	0.01	9433.44	0.11	1.54	0.12	0.04	0.66	0.31	0.38	0.03	0.12	0.31	0.04	0.66	0.38	0.03	false	false	true	false	ULH
42	3813.51	0.00	7097.24	0.09	1.56	0.10	0.05	0.63	0.39	0.36	0.04	0.10	0.39	0.05	0.63	0.36	0.04	false	false	true	false	ULH
43	4924.33	0.01	12356.12	0.11	1.99	0.12	0.20	0.83	0.41	0.38	0.05	0.12	0.41	0.20	0.83	0.38	0.05	false	false	true	false	ULH
44	4840.54	0.01	8890.30	0.13	1.66	0.11	0.07	0.66	0.42	0.37	0.04	0.11	0.42	0.07	0.66	0.37	0.04	false	false	true	false	ULH
45	3389.12	0.00	7232.37	0.12	1.43	0.09	0.05	0.57	0.35	0.34	0.03	0.09	0.35	0.05	0.57	0.34	0.03	false	false	true	false	ULH
46	2537.15	0.02	7255.06	0.12	1.48	0.13	0.04	0.58	0.35	0.33	0.03	0.13	0.35	0.04	0.58	0.33	0.03	false	false	true	false	ULH
47	4401.24	0.02	10457.48	0.12	1.72	0.11	0.07	0.70	0.41	0.39	0.04	0.11	0.41	0.07	0.70	0.39	0.04	false	false	true	false	ULH
48	2866.11	0.00	7776.22	0.13	1.44	0.08	0.04	0.56	0.35	0.34	0.03	0.08	0.35	0.04	0.56	0.34	0.03	false	false	true	false	ULH
49	4129.29	0.02	8922.38	0.12	1.62	0.11	0.05	0.64	0.41	0.37	0.04	0.11	0.41	0.05	0.64	0.37	0.04	false	false	true	false	ULH
50	2177.46	0.02	13820.54	0.08	2.26	0.12	0.26	0.93	0.45	0.44	0.06	0.12	0.45	0.26	0.93	0.44	0.06	false	false	true	false	ULH
51	2088.43	0.02	11728.67	0.11	1.71	0.11	0.04	0.74	0.38	0.41	0.03	0.11	0.38	0.04	0.74	0.41	0.03	false	false	true	false	ULH
52	4085.90	0.03	6854.15	0.12	1.55	0.10	0.05	0.58	0.44	0.34	0.04	0.10	0.44	0.05	0.58	0.34	0.04	false	false	true	false	ULH
53	3115.41	0.01	12157.30	0.13	1.94	0.11	0.14	0.73	0.52	0.39	0.04	0.11	0.52	0.14	0.73	0.39	0.04	false	false	true	false	ULH
54	2120.93	0.02	8440.71	0.14	1.48	0.13	0.04	0.59	0.35	0.33	0.03	0.13	0.35	0.04	0.59	0.33	0.03	false	false	true	false	ULH
55	2559.50	0.01	15036.18	0.15	2.82	0.14	0.05	1.22	0.85	0.48	0.08	0.14	0.85	0.05	1.22	0.48	0.08	false	false	false	false	ULH
56	4181.81	0.01	13535.03	0.13	1.95	0.11	0.19	0.78	0.43	0.40	0.04	0.11	0.43	0.19	0.78	0.40	0.04	false	false	true	false	ULH
57	3989.56	0.01	7558.46	0.09	1.71	0.10	0.06	0.67	0.45	0.38	0.04	0.10	0.45	0.06	0.67	0.38	0.04	false	false	true	false	ULH
58	2906.18	0.01	9524.02	0.15	2.77	0.15	0.05	1.19	0.94	0.47	0.08	0.15	0.94	0.05	1.19	0.47	0.08	false	false	false	false	ULH
59	4516.99	0.01	6499.96	0.11	1.49	0.10	0.05	0.58	0.39	0.34	0.04	0.10	0.39	0.05	0.58	0.34	0.04	false	false	true	false	ULH
60	2335.43	0.00	6237.00	0.09	1.65	0.09	0.04	0.71	0.39	0.39	0.03	0.09	0.39	0.04	0.71	0.39	0.03	false	false	true	false	ULH
61	4317.56	0.01	5947.73	0.10	1.43	0.09	0.05	0.56	0.37	0.33	0.04	0.09	0.37	0.05	0.56	0.33	0.04	false	false	true	false	ULH
62	3008.50	0.00	10255.64	0.14	1.69	0.10	0.05	0.65	0.49	0.37	0.04	0.10	0.49	0.05	0.65	0.37	0.04	false	false	true	false	ULH
63	4666.77	0.00	6193.37	0.15	1.43	0.09	0.06	0.54	0.39	0.32	0.04	0.09	0.39	0.06	0.54	0.32	0.04	false	false	true	false	ULH
64	4797.02	0.02	11573.32	0.12	1.92	0.11	0.19	0.75	0.44	0.39	0.04	0.11	0.44	0.19	0.75	0.39	0.04	false	false	true	false	ULH
65	2653.74	0.01	8260.63	0.12	1.47	0.10	0.04	0.60	0.35	0.35	0.03	0.10	0.35	0.04	0.60	0.35	0.03	false	false	true	false	ULH
66	2691.85	0.02	7441.54	0.10	1.46	0.11	0.04	0.63	0.29	0.36	0.03	0.11	0.29	0.04	0.63	0.36	0.03	false	false	true	false	ULH
67	2299.17	0.02	16372.93	0.11	2.09	0.12	0.23	0.82	0.45	0.42	0.05	0.12	0.45	0.23	0.82	0.42	0.05	false	false	true	false	ULH
68	2667.59	0.02	12599.98	0.13	1.78	0.11	0.10	0.75	0.39	0.40	0.04	0.11	0.39	0.10	0.75	0.40	0.04	false	false	true	false	ULH
69	3750.91	0.01	10726.38	0.14	1.78	0.10	0.09	0.68	0.48	0.38	0.04	0.10	0.48	0.09	0.68	0.38	0.04	false	false	true	false	ULH
70	3981.84	0.00	12920.39	0.15	1.92	0.10	0.20	0.75	0.42	0.39	0.05	0.10	0.42	0.20	0.75	0.39	0.05	false	false	true	false	ULH
71	4367.18	0.01	10660.66	0.12	2.27	0.11	0.26	0.99	0.44	0.40	0.07	0.11	0.44	0.26	0.99	0.40	0.07	false	false	true	false	ULH
72	4881.21	0.02	10990.12	0.11	1.86	0.11	0.18	0.72	0.43	0.38	0.04	0.11	0.43	0.18	0.72	0.38	0.04	false	false	true	false	ULH
73	3415.44	0.01	15748.32	0.14	2.03	0.11	0.22	0.80	0.43	0.41	0.06	0.11	0.43	0.22	0.80	0.41	0.06	false	false	true	false	ULH
74	3613.56	0.00	18236.11	0.09	2.48	0.12	0.27	1.05	0.55	0.40	0.08	0.12	0.55	0.27	1.05	0.40	0.08	false	false	false	false	ULH
75	3304.99	0.02	11719.44	0.14	1.65	0.11	0.04	0.69	0.38	0.39	0.04	0.11	0.38	0.04	0.69	0.39	0.04	false	false	true	false	ULH
76	2412.33	0.01	8582.44	0.09	1.74	0.11	0.05	0.69	0.47	0.39	0.04	0.11	0.47	0.05	0.69	0.39	0.04	false	false	true	false	ULH
77	3450.78	0.01	11855.92	0.11	1.99	0.11	0.21	0.79	0.43	0.40	0.05	0.11	0.43	0.21	0.79	0.40	0.05	false	false	true	false	ULH
78	4558.51	0.02	13322.09	0.10	2.05	0.11	0.24	0.81	0.43	0.41	0.05	0.11	0.43	0.24	0.81	0.41	0.05	false	false	true	false	ULH
79	4135.95	0.02	5494.85	0.15	1.32	0.09	0.04	0.48	0.38	0.29	0.03	0.09	0.38	0.04	0.48	0.29	0.03	false	false	true	false	ULH
80	3726.16	0.00	9946.28	0.08	1.91	0.10	0.20	0.76	0.40	0.39	0.05	0.10	0.40	0.20	0.76	0.39	0.05	false	false	true	false	ULH
81	3046.41	0.00	12254.20	0.08	2.11	0.10	0.23	0.91	0.40	0.39	0.06	0.10	0.40	0.23	0.91	0.39	0.06	false	false	true	false	ULH
82	4714.58	0.02	10934.92	0.12	1.87	0.11	0.16	0.74	0.43	0.39	0.04	0.11	0.43	0.16	0.74	0.39	0.04	false	false	true	false	ULH
83	3227.71	0.01	5201.83	0.09	1.42	0.09	0.04	0.55	0.38	0.33	0.03	0.09	0.38	0.04	0.55	0.33	0.03	false	false	true	false	ULH
84	4878.29	0.01	13549.11	0.08	2.21	0.11	0.25	0.92	0.47	0.39	0.07	0.11	0.47	0.25	0.92	0.39	0.07	false	false	true	false	ULH
85	4773.20	0.00	14013.78	0.14	1.95	0.12	0.20	0.80	0.40	0.38	0.05	0.12	0.40	0.20	0.80	0.38	0.05	false	false	true	false	ULH
86	2438.96	0.01	14588.22	0.11	2.13	0.11	0.25	0.84	0.44	0.42	0.06	0.11	0.44	0.25	0.84	0.42	0.05	false	false	true	false	ULH
87	3083.53	0.02	5165.87	0.10	1.17	0.10	0.04	0.48	0.24	0.29	0.02	0.10	0.24	0.04	0.48	0.29	0.02	false	false	true	false	ULH
88	3893.50	0.01	8064.79	0.14	1.50	0.09	0.05	0.59	0.39	0.35	0.04	0.09	0.39	0.05	0.59	0.35	0.04	false	false	true	false	ULH
89	2838.19	0.00	9227.31	0.10	1.86	0.10	0.10	0.70	0.52	0.39	0.04	0.10	0.52	0.10	0.70	0.39	0.04	false	false	true	false	ULH
90	4547.85	0.00	10127.30	0.13	1.79	0.10	0.16	0.70	0.41	0.38	0.04	0.10	0.41	0.16	0.70	0.38	0.04	false	false	true	false	ULH
91	3853.12	0.02	12581.58	0.09	2.13	0.11	0.24	0.84	0.45	0.42	0.06	0.11	0.45	0.24	0.84	0.42	0.05	false	false	true	false	ULH

92	2383.32	0.00	12983.00	0.13	2.05	0.11	0.18	0.76	0.55	0.40	0.04	0.11	0.55	0.18	0.76	0.40	0.04	false	false	true	false	ULH
93	4620.54	0.01	18052.32	0.08	2.77	0.13	0.31	1.17	0.61	0.46	0.10	0.13	0.61	0.31	1.17	0.46	0.10	false	false	false	false	ULH
94	4751.21	0.02	13909.43	0.08	2.24	0.11	0.26	0.99	0.42	0.40	0.07	0.11	0.42	0.26	0.99	0.40	0.07	false	false	true	false	ULH
95	2303.43	0.01	13131.31	0.14	1.89	0.11	0.12	0.73	0.49	0.40	0.04	0.11	0.49	0.12	0.73	0.40	0.04	false	false	true	false	ULH
96	4053.67	0.00	17080.27	0.10	2.38	0.12	0.27	0.98	0.54	0.39	0.07	0.12	0.54	0.27	0.98	0.39	0.07	false	false	true	false	ULH
97	3298.05	0.02	16541.34	0.12	2.11	0.11	0.25	0.83	0.44	0.42	0.06	0.11	0.44	0.25	0.83	0.42	0.06	false	false	true	false	ULH
98	3194.51	0.01	19288.25	0.14	2.15	0.12	0.23	0.92	0.43	0.39	0.06	0.12	0.43	0.23	0.92	0.39	0.06	false	false	true	false	ULH
99	3909.58	0.01	7856.98	0.10	1.69	0.10	0.05	0.65	0.49	0.37	0.04	0.10	0.49	0.05	0.65	0.37	0.04	false	false	true	false	ULH

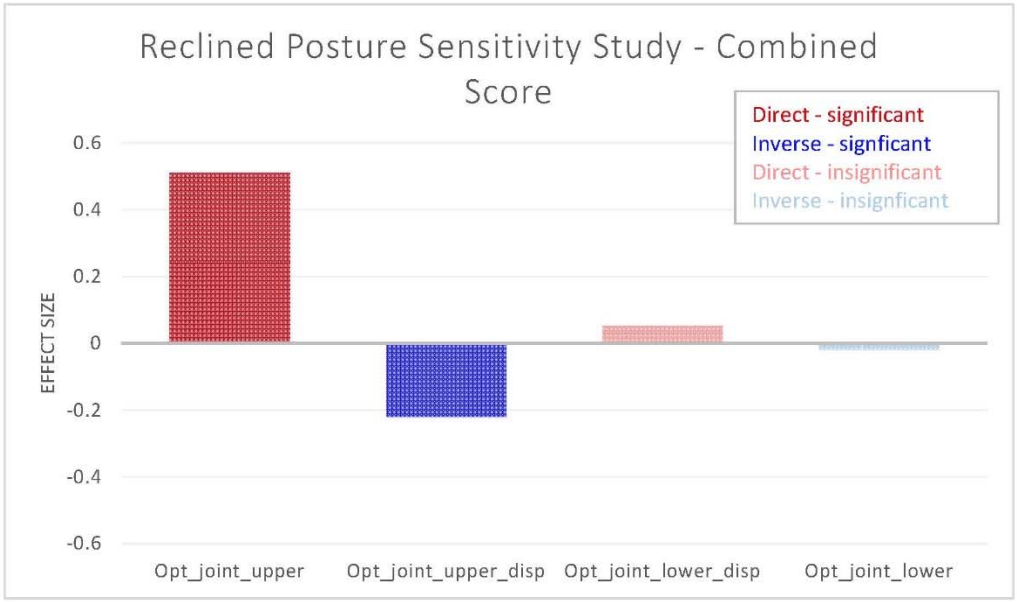
Reclined Posture Sensitivity Study - Combined Score
Direct - significant
Inverse - signficant
Direct - insignificant
Inverse - insignficant
EFFECT SIZE
0.6
0.4
0.2
0
-0.2
-0.4
-0.6
Opt_joint_upper
Opt_joint_upper_disp
Opt_joint_lower_disp
Opt_joint_lower

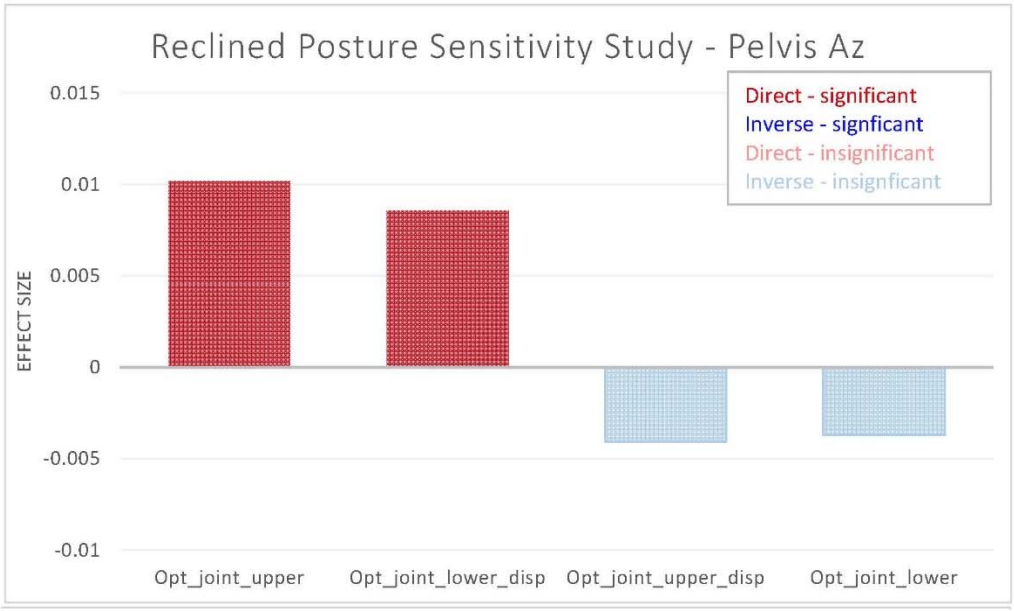
Reclined Posture Sensitivity Study - Pelvis Az
Direct - significant
Inverse - signficant
Direct - insignificant
Inverse - insignficant
EFFECT SIZE
0.015
0.01
0.005
0
-0.005
-0.01
Opt_joint_upper
Opt_joint_lower_disp
Opt_joint_upper_disp
Opt_joint_lower

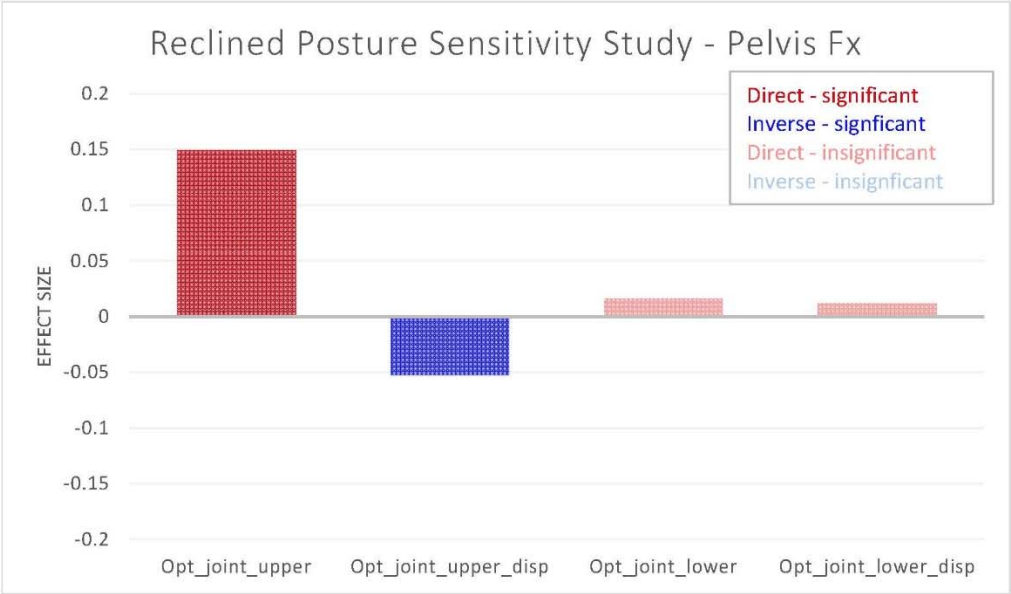
Reclined Posture Sensitivity Study - Pelvis Fx
Direct - significant
Inverse - signficant
Direct - insignificant
Inverse - insignficant
EFFECT SIZE
0.2
0.15
0.1
0.05
0
-0.05
-0.1
-0.15
-0.2
Opt_joint_upper
Opt_joint_upper_disp
Opt_joint_lower
Opt_joint_lower_disp

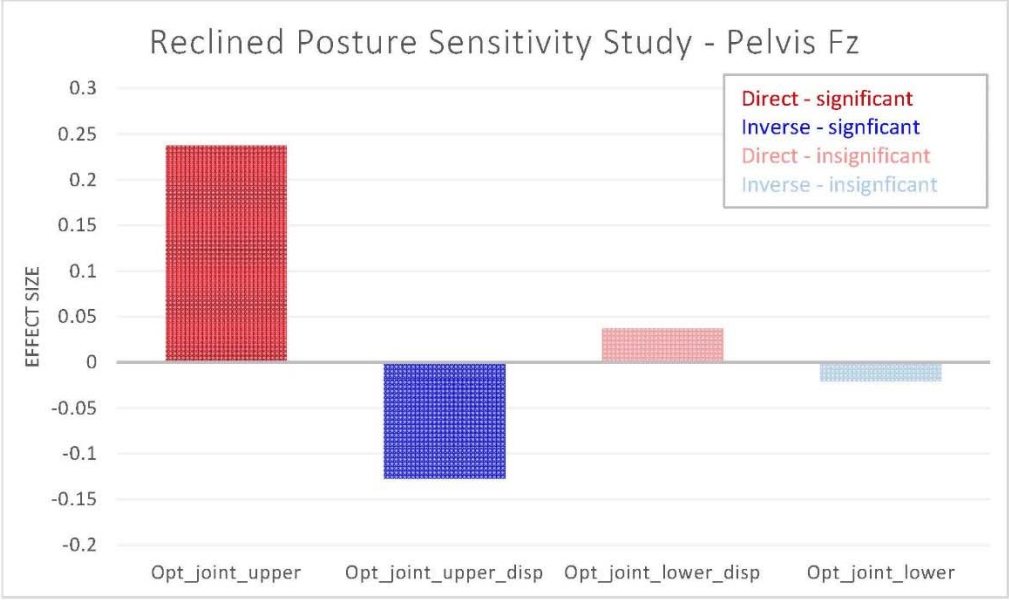
Reclined Posture Sensitivity Study - Pelvis Fz
Direct - significant
Inverse - signficant
Direct - insignificant
Inverse - insignficant
EFFECT SIZE
0.3
0.25
0.2
0.15
0.1
0.05
0
-0.05
-0.1
-0.15
-0.2
Opt_joint_upper
Opt_joint_upper_disp
Opt_joint_lower_disp
Opt_joint_lower

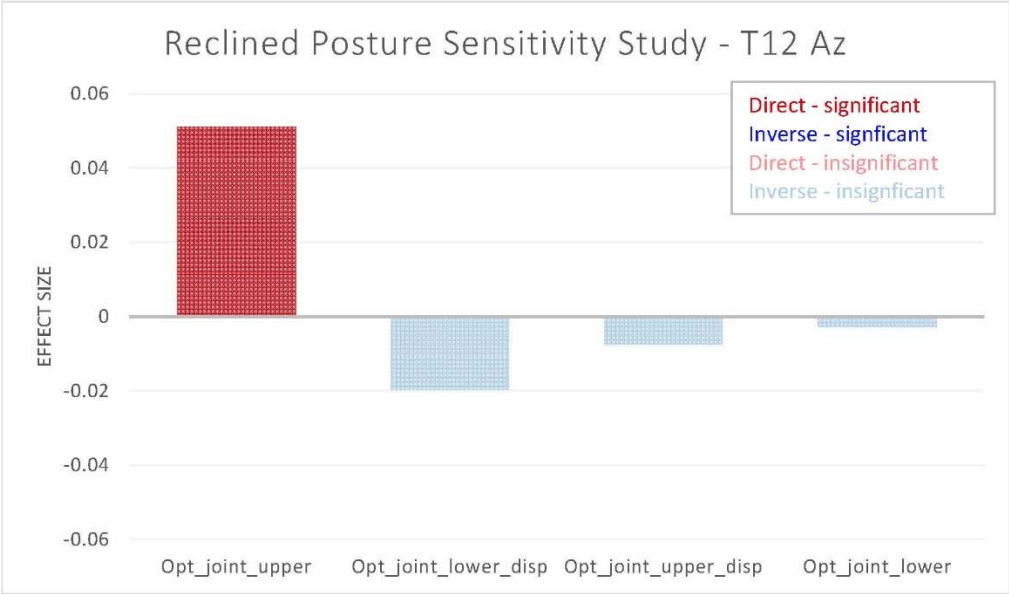
Reclined Posture Sensitivity Study - T12 Az
Direct - significant
Inverse - signficant
Direct - insignificant
Inverse - insignficant
EFFECT SIZE
0.06
0.04
0.02
0
-0.02
-0.04
-0.06
Opt_joint_upper
Opt_joint_lower_disp
Opt_joint_upper_disp
Opt_joint_lower

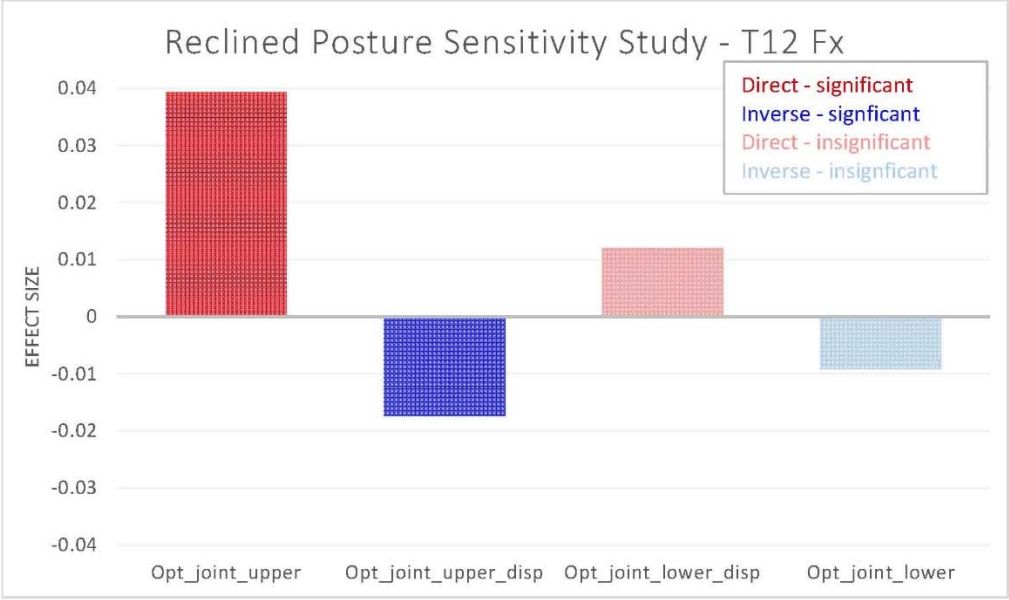
Reclined Posture Sensitivity Study - T12 Fx
Direct - significant
Inverse - signficant
Direct - insignificant
Inverse - insignficant
EFFECT SIZE
0.04
0.03
0.02
0.01
0
-0.01
-0.02
-0.03
-0.04
Opt_joint_upper
Opt_joint_upper_disp
Opt_joint_lower_disp
Opt_joint_lower

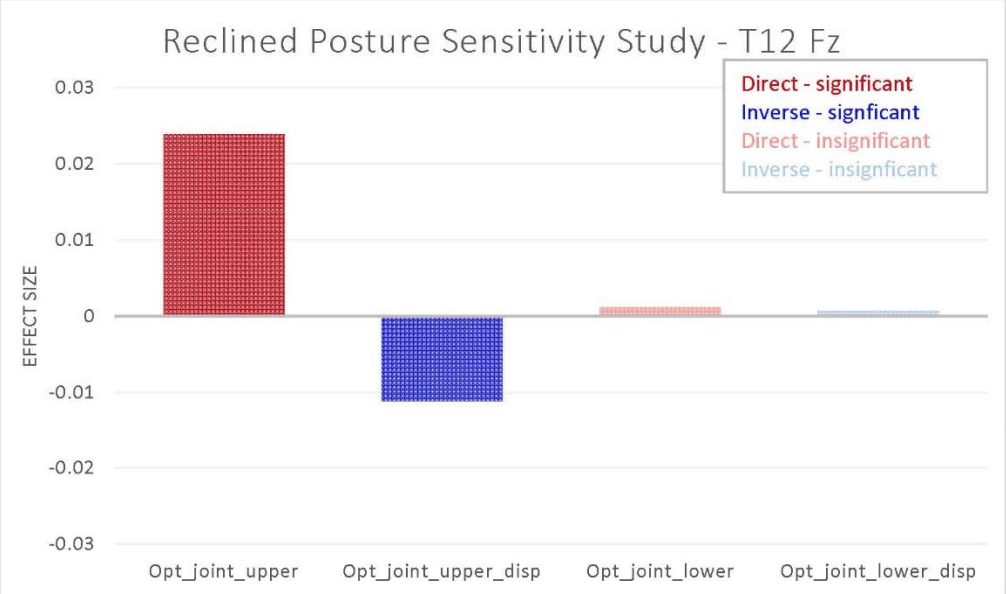
Reclined Posture Sensitivity Study - T12 Fz
Direct - significant
Inverse - signficant
Direct - insignificant
Inverse - insignficant
EFFECT SIZE
0.03
0.02
0.01
0
-0.01
-0.02
-0.03
Opt_joint_upper
Opt_joint_upper_disp
Opt_joint_lower
Opt_joint_lower_disp

```
#--- Frontier Design DB File Info ----------
#modeFRONTIER - (c) ESTECO S.p.A.
#Design 23 Table
#-------------------------------------
#modeFRONTIER Version: modeFRONTIER 2017R5 5.7.1 b20171017
#Date: Sat Jan 26 15:32:03 EST 2019
#Project Name: PMHS A Opt 2019-01-25 - recline - opt 150 - complete.prj
#Operating System: Windows 10 10.0 amd64
#Java (SDK/JRE) Version: 1.8.0_60
#Java Vendor: Oracle Corporation
#Java Vendor URL: http://java.oracle.com/
#User Name: RBosch
#-------------------------------------
#Categories
<CATEGORIES classorPrefix="CLUSTER " useTableNamePrefix="false">
  <CATEGORY enabled="true" label="" name="SOBOL" symbol="SQUARE,NONE,11,,0"/>
  <CATEGORY enabled="true" label="" name="USERDOE" symbol="SQUARE,NONE,11,,0"/>
  <CATEGORY enabled="true" label="" name="NSGA2" symbol="SQUARE,NONE,11,,0" />
  <CATEGORY enabled="true" label="" name="TDA" symbol="SQUARE,NONE,11,,0"/>
  <CATEGORY enabled="true" label="" name="DOE_APPROX" symbol="SQUARE,NONE,11,,0" />
  <CATEGORY enabled="true" label="" name="SIMPLEX" symbol="SQUARE,NONE,11,,0"/>
  <CATEGORY enabled="true" label="" name="UL-H" symbol="SQUARE,NONE,11,,0"/>
  <CATEGORY enabled="true" label="" name="TILLU" symbol="SQUARE,NONE,11,#3DC3912,1,#3DC3912"/>
  <CATEGORY enabled="true" label="" name="SIMPLEX_DOE" symbol="SQUARE,NONE,11,#3366CC,1,#3366CC"/>
  <CATEGORY enabled="true" label="" name="DOE_RANDOM" symbol="SQUARE,NONE,11,#FF9900,1,#FF9900"/>
</CATEGORIES>

#-------------------------------------
```

<ID>	Opt_Join:J_Opt_Join:_	Opt_Join:_	Opt_Join_sq	Opt_Join:_	Combined_	Pelvis_Ac_	Pelvis_Fx_2	Pelvis_Fx_1	T12_Ac_nc	T12_Fx_nc	T12_Fx_no	Objective2	Constraint:	Constraint:	Constraint:	Constraint:	Constraint:	<TRIOS>	<V:RTJA>	<TASIS:_T	<MAACT:>	<CATEGORY>
0	4530.0823	0.0211	11001.6186	0.1481	1.7406	0.1063	0.0567	0.6655	0.4723	0.3797	0.0400	1.7406	1.06E-01	4.72E-01	5.67E-02	6.86E-01	3.80E-01	4.00E-02	false	false	true	false	SIMPLEX_DOE
1	2014.7546	0.0063	6046.7069	0.1259	1.2753	0.1020	0.0407	0.5355	0.2563	0.3152	0.0244	1.2753	1.02E-01	2.56E-01	4.07E-02	5.36E-01	3.15E-01	2.44E-02	false	false	true	false	SIMPLEX_DOE
2	3947.0367	0.0151	14418.9881	0.0873	2.2846	0.1157	0.2647	0.9825	0.4482	0.3886	0.0689	2.2846	1.15E-01	4.49E-01	2.65E-01	9.88E-01	3.99E-01	6.89E-02	false	false	true	false	SIMPLEX_DOE
3	3014.1051	0.0106	10835.4195	0.1169	1.9627	0.1099	0.1067	0.7201	0.4938	0.3940	0.0382	1.9627	1.10E-01	4.94E-01	1.07E-01	7.20E-01	3.94E-01	3.82E-02	false	false	true	false	SIMPLEX_DOE
4	3771.8133	0.0097	10395.3704	0.0994	2.4465	0.1207	0.2820	1.0238	0.5457	0.3855	0.0819	2.4465	1.21E-01	5.46E-01	2.83E-01	1.02E+00	3.90E-01	8.20E-02	false	false	true	false	SIMPLEX_DOE
5	2981.1760	0.0154	5000.0000	0.1397	1.1909	0.1122	0.0511	0.4443	0.2942	0.2513	0.0274	1.1909	1.12E-01	2.94E-01	5.11E-02	4.45E-01	2.51E-01	2.74E-02	true	true	true	false	SIMPLEX
6	2373.0773	0.0160	5000.0000	0.1574	0.8679	0.1430	0.0471	1.2528	0.8101	0.4917	0.0782	0.8679	1.43E-01	8.10E-01	4.71E-02	1.25E+00	4.92E-01	7.82E-02	true	false	true	false	SIMPLEX
7	3541.0331	0.0157	13432.9164	0.1106	1.9372	0.1087	0.1006	0.7633	0.4295	0.4016	0.0412	1.9372	1.09E-01	4.30E-01	1.01E-01	7.66E-01	4.02E-01	4.12E-02	false	true	true	false	SIMPLEX
8	2739.0339	0.0158	5458.9030	0.1574	0.8500	0.1427	0.0480	1.2448	0.8480	0.4885	0.0779	0.8500	1.43E-01	8.48E-01	4.80E-02	1.24E+00	4.88E-01	7.79E-02	true	false	true	false	SIMPLEX
9	3338.0313	0.0158	9998.4006	0.1213	1.6867	0.1098	0.0432	0.6044	0.4206	0.3806	0.0360	1.6867	1.10E-01	4.21E-01	4.32E-02	6.04E-01	3.81E-01	3.60E-02	false	true	true	false	SIMPLEX
10	3417.9170	0.0237	5668.4745	0.1505	1.1393	0.1084	0.0453	0.4624	0.2459	0.2780	0.0241	1.1393	1.08E-01	2.46E-01	4.53E-02	4.62E-01	2.78E-01	2.41E-02	false	false	true	false	SIMPLEX
11	3618.8329	0.0254	5000.0000	0.1524	1.1393	0.1434	0.0989	1.4084	0.8435	0.5554	0.0778	1.1393	1.43E-01	8.43E-01	9.88E-02	1.41E+00	5.55E-01	7.78E-02	true	false	true	false	SIMPLEX
12	2000.0000	0.0145	5000.0000	0.1206	1.2392	0.1158	0.0506	0.4513	0.3148	0.2646	0.0301	1.2392	1.15E-01	3.15E-01	5.06E-02	4.51E-01	2.65E-01	3.01E-02	false	true	true	false	SIMPLEX
13	2000.0000	0.0101	5000.0000	0.1471	1.1262	0.1154	0.0333	0.4313	0.3174	0.2482	0.0203	1.1262	1.15E-01	3.17E-01	3.33E-02	4.31E-01	2.48E-01	2.03E-02	false	false	true	false	SIMPLEX
14	3184.7920	0.0754	5000.0000	0.1574	3.1836	0.1438	0.1277	1.4715	0.8447	0.5734	0.0780	3.1836	1.44E-01	8.44E-01	1.27E-01	1.47E+00	5.73E-01	7.80E-02	false	true	true	false	SIMPLEX
15	2307.2539	0.0135	6948.4127	0.1323	1.2257	0.1083	0.0469	0.4757	0.2809	0.2877	0.0264	1.2257	1.08E-01	2.81E-01	4.69E-02	4.75E-01	2.88E-01	2.64E-02	false	true	true	false	SIMPLEX
16	3358.1785	0.0254	5828.9436	0.1524	3.1846	0.1436	0.1121	1.4184	0.8439	0.5707	0.0779	3.1846	1.44E-01	8.44E-01	1.12E-01	1.42E+00	5.71E-01	7.79E-02	false	false	true	false	SIMPLEX
17	2938.7446	0.0174	5707.7159	0.1313	1.1942	0.1090	0.0504	0.4481	0.2832	0.2544	0.0276	1.1942	1.10E-01	2.83E-01	5.04E-02	4.48E-01	2.54E-01	2.75E-02	false	true	true	false	SIMPLEX
18	3061.4299	0.0254	5000.0000	0.1518	3.1905	0.1440	0.1234	1.4357	0.8445	0.5753	0.0781	3.1905	1.44E-01	8.45E-01	1.23E-01	1.43E+00	5.75E-01	7.81E-02	false	false	true	false	SIMPLEX
19	2405.8034	0.0174	5826.5702	0.1374	1.2004	0.1086	0.0490	0.4585	0.2847	0.2729	0.0267	1.2004	1.09E-01	2.85E-01	4.90E-02	4.59E-01	2.73E-01	2.67E-02	false	true	true	false	SIMPLEX
20	2872.8884	0.0254	5000.0000	0.1470	1.1834	0.1116	0.0315	0.4394	0.2961	0.2572	0.0276	1.1834	1.12E-01	2.96E-01	3.15E-02	4.39E-01	2.57E-01	2.76E-02	false	true	true	false	SIMPLEX
21	3805.1380	0.0254	5407.9532	0.1378	1.1976	0.0933	0.0420	0.4745	0.2726	0.2644	0.0269	1.1976	9.33E-02	2.73E-01	4.20E-02	4.73E-01	2.64E-01	2.69E-02	false	true	true	false	SIMPLEX
22	2451.2845	0.0211	5101.9338	0.1445	1.1947	0.1137	0.0319	0.4392	0.3054	0.2557	0.0288	1.1947	1.14E-01	3.05E-01	3.19E-02	4.39E-01	2.55E-01	2.88E-02	false	true	true	false	SIMPLEX
23	3353.8535	0.0249	5305.8914	0.1398	1.1745	0.1072	0.0469	0.4579	0.2631	0.2741	0.0252	1.1745	1.07E-01	2.63E-01	4.69E-02	4.58E-01	2.74E-01	2.52E-02	false	true	true	false	SIMPLEX
24	3974.6229	0.0254	5249.9471	0.1524	3.1089	0.1430	0.0874	1.3976	0.8428	0.5605	0.0776	3.1089	1.43E-01	8.43E-01	8.74E-02	1.40E+00	5.60E-01	7.76E-02	false	false	true	false	SIMPLEX
25	2747.3767	0.0211	5217.9137	0.1379	1.1858	0.1094	0.0501	0.4491	0.2854	0.2650	0.0267	1.1858	1.09E-01	2.85E-01	5.01E-02	4.49E-01	2.65E-01	2.67E-02	false	true	true	false	SIMPLEX
26	3214.8418	0.0211	5503.1398	0.1479	1.1861	0.1051	0.0466	0.4593	0.2353	0.2752	0.0247	1.1861	1.05E-01	2.35E-01	4.66E-02	4.59E-01	2.75E-01	2.47E-02	false	true	true	false	SIMPLEX
27	3682.3737	0.0254	5522.3392	0.1524	3.1373	0.1433	0.1011	1.4065	0.8433	0.5654	0.0778	3.1373	1.43E-01	8.43E-01	1.01E-01	1.41E+00	5.65E-01	7.78E-02	false	false	true	false	SIMPLEX
28	2981.1239	0.0225	5294.0201	0.1421	1.1827	0.1093	0.0491	0.4517	0.2787	0.2577	0.0262	1.1827	1.09E-01	2.79E-01	4.91E-02	4.52E-01	2.58E-01	2.62E-02	false	true	true	false	SIMPLEX
29	3610.9867	0.0213	5887.2329	0.1432	1.2466	0.0937	0.0405	0.4783	0.3149	0.2921	0.0272	1.2466	9.37E-02	3.15E-01	4.05E-02	4.78E-01	2.92E-01	2.72E-02	false	true	true	false	SIMPLEX
30	3057.4115	0.0244	5211.5127	0.1460	1.1865	0.1109	0.0499	0.4489	0.2850	0.2551	0.0267	1.1865	1.11E-01	2.85E-01	4.99E-02	4.49E-01	2.55E-01	2.67E-02	false	true	true	false	SIMPLEX
31	3199.5215	0.0231	5451.2473	0.1463	1.1743	0.1073	0.0474	0.4585	0.2649	0.2728	0.0252	1.1743	1.07E-01	2.65E-01	4.74E-02	4.57E-01	2.73E-01	2.52E-02	false	true	true	false	SIMPLEX
32	3145.4027	0.0245	5304.2373	0.1488	1.1827	0.1100	0.0492	0.4510	0.2789	0.2573	0.0263	1.1827	1.10E-01	2.79E-01	4.92E-02	4.51E-01	2.57E-01	2.63E-02	false	true	true	false	SIMPLEX
33	3385.8853	0.0243	5457.1830	0.1452	1.1676	0.1055	0.0460	0.4601	0.2551	0.2761	0.0247	1.1676	1.06E-01	2.55E-01	4.60E-02	4.60E-01	2.76E-01	2.47E-02	false	true	true	false	SIMPLEX
34	3316.3794	0.0229	5587.3072	0.1493	1.1831	0.1044	0.0459	0.4568	0.2510	0.2756	0.0244	1.1831	1.04E-01	2.51E-01	4.59E-02	4.61E-01	2.77E-01	2.44E-02	false	true	true	false	SIMPLEX
35	3514.4488	0.0235	5747.8587	0.1489	1.1769	0.0989	0.0439	0.4498	0.2550	0.2748	0.0254	1.1769	9.89E-02	2.55E-01	4.39E-02	4.50E-01	2.85E-01	2.54E-02	false	true	true	false	SIMPLEX
36	3422.1873	0.0230	5636.9609	0.1474	1.1558	0.1021	0.0447	0.4650	0.2400	0.2801	0.0239	1.1558	1.02E-01	2.40E-01	4.47E-02	4.65E-01	2.80E-01	2.39E-02	false	true	true	false	SIMPLEX
37	3571.8330	0.0238	5893.7155	0.1498	1.1736	0.1002	0.0434	0.4678	0.2539	0.2829	0.0253	1.1736	1.00E-01	2.54E-01	4.34E-02	4.68E-01	2.83E-01	2.53E-02	false	true	true	false	SIMPLEX
38	3478.5376	0.0235	5833.0984	0.1490	1.1577	0.1023	0.0445	0.4648	0.2415	0.2802	0.0242	1.1577	1.02E-01	2.42E-01	4.45E-02	4.65E-01	2.80E-01	2.42E-02	false	true	true	false	SIMPLEX
39	3411.6704	0.0223	5775.7375	0.1524	2.9987	0.1444	0.0480	1.3393	0.8304	0.5281	0.0783	2.9987	1.44E-01	8.30E-01	4.81E-02	1.34E+00	5.28E-01	7.83E-02	false	false	true	false	SIMPLEX
40	3397.3315	0.0238	5836.8216	0.1471	1.1623	0.1041	0.0436	0.4617	0.2491	0.2774	0.0243	1.1623	1.04E-01	2.49E-01	4.36E-02	4.62E-01	2.77E-01	2.43E-02	false	true	true	false	SIMPLEX
41	3541.5524	0.0241	5870.1705	0.1477	1.1658	0.1015	0.0440	0.4657	0.2482	0.2813	0.0248	1.1658	1.01E-01	2.48E-01	4.40E-02	4.66E-01	2.81E-01	2.48E-02	false	true	true	false	SIMPLEX
42	3372.6976	0.0232	5595.5790	0.1489	1.1602	0.1026	0.0455	0.4622	0.2470	0.2778	0.0242	1.1602	1.04E-01	2.47E-01	4.55E-02	4.62E-01	2.78E-01	2.42E-02	false	true	true	false	SIMPLEX
43	3448.5892	0.0230	5700.2338	0.1508	1.1682	0.1013	0.0444	0.4653	0.2421	0.2806	0.0242	1.1682	1.02E-01	2.42E-01	4.44E-02	4.65E-01	2.81E-01	2.41E-02	false	true	true	false	SIMPLEX
44	3510.8500	0.0234	5893.8098	0.1500	1.1660	0.1007	0.0439	0.4657	0.2482	0.2817	0.0248	1.1660	1.01E-01	2.48E-01	4.39E-02	4.67E-01	2.82E-01	2.48E-02	true	true	true	false	SIMPLEX
45	3407.2382	0.0233	5620.1822	0.1492	1.1572	0.1028	0.0451	0.4633	0.2434	0.2787	0.0240	1.1572	1.03E-01	2.43E-01	4.51E-02	4.63E-01	2.79E-01	2.40E-02	false	true	true	false	SIMPLEX
46	3486.3012	0.0227	5685.7371	0.1478	1.1636	0.1008	0.0440	0.4670	0.2455	0.2818	0.0245	1.1636	1.01E-01	2.46E-01	4.40E-02	4.67E-01	2.82E-01	2.45E-02	false	true	true	false	SIMPLEX
47	3478.5130	0.0234	5678.0403	0.1498	1.1569	0.1008	0.0430	0.4614	0.2408	0.2788	0.0239	1.1569	1.00E-01	2.43E-01	4.30E-02	4.61E-01	2.79E-01	2.39E-02	false	true	true	false	SIMPLEX
48	3418.8999	0.0237	5558.5540	0.1469	1.1605	0.1036	0.0453	0.4628	0.2463	0.2794	0.0242	1.1605	1.04E-01	2.46E-01	4.53E-02	4.63E-01	2.79E-01	2.41E-02	false	true	true	false	SIMPLEX
49	3441.2524	0.0231	5664.8940	0.1468	1.1555	0.1018	0.0446	0.4648	0.2403	0.2800	0.0241	1.1555	1.02E-01	2.40E-01	4.46E-02	4.65E-01	2.80E-01	2.41E-02	false	true	true	false	SIMPLEX
50	3370.9778	0.0238	5541.9136	0.1491	1.1567	0.1006	0.0431	0.4613	0.2430	0.2787	0.0239	1.1567	1.00E-01	2.43E-01	4.31E-02	4.61E-01	2.78E-01	2.39E-02	false	true	true	false	SIMPLEX
51	3424.2296	0.0229	5665.7796	0.1499	1.1557	0.1021	0.0446	0.4651	0.2397	0.2802	0.0240	1.1557	1.02E-01	2.40E-01	4.46E-02	4.65E-01	2.80E-01	2.40E-02	false	true	true	false	SIMPLEX
52	3406.8130	0.0225	5675.7323	0.1478	1.1554	0.1017	0.0445	0.4655	0.2359	0.2803	0.0240	1.1554	1.02E-01	2.36E-01	4.45E-02	4.66E-01	2.81E-01	2.40E-02	false	true	true	false	SIMPLEX
53	3385.9630	0.0230	5701.0783	0.1467	1.1580	0.1009	0.0443	0.4657	0.2408	0.2814	0.0241	1.1580	1.01E-01	2.41E-01	4.43E-02	4.67E-01	2.81E-01	2.41E-02	false	true	true	false	SIMPLEX
54	3473.2733	0.0230	5680.2552	0.1478	1.1642	0.1010	0.0440	0.4668	0.2460	0.2817	0.0246	1.1642	1.01E-01	2.46E-01	4.40E-02	4.67E-01	2.82E-01	2.46E-02	false	true	true	false	SIMPLEX
55	3396.5480	0.0228	5651.5030	0.1488	1.1540	0.1021	0.0440	0.4642	0.2405	0.2794	0.0238	1.1540	1.02E-01	2.41E-01	4.40E-02	4.64E-01	2.79E-01	2.38E-02	false	true	true	false	SIMPLEX
56	3404.7182	0.0237	5697.4910	0.1501	1.1543	0.1018	0.0447	0.4648	0.2390	0.2800	0.0238	1.1543	1.02E-01	2.39E-01	4.47E-02	4.65E-01	2.80E-01	2.39E-02	false	true	true	false	SIMPLEX
57	3402.7551	0.0226	5720.2561	0.1517	2.9974	0.1443	0.0480	1.3455	0.8305	0.5308	0.0783	2.9974	1.44E-01	8.30E-01	4.80E-02	1.35E+00	5.31E-01	7.83E-02	false	false	true	false	SIMPLEX
58	3399.7017	0.0227	5677.0370	0.1494	1.1549	0.1021	0.0447	0.4647	0.2398	0.2798	0.0238	1.1549	1.02E-01	2.40E-01	4.47E-02	4.65E-01	2.80E-01	2.38E-02	false	true	true	false	SIMPLEX
59	3361.8895	0.0237	5683.8868	0.1483	1.1552	0.1019	0.0448	0.4650	0.2398	0.2798	0.0238	1.1552	1.02E-01	2.40E-01	4.48E-02	4.65E-01	2.80E-01	2.38E-02	false	true	true	false	SIMPLEX
60	3382.9737	0.0227	5675.7766	0.1506	1.1555	0.1023	0.0450	0.4647	0.2415	0.2791	0.0238	1.1555	1.02E-01	2.42E-01	4.50E-02	4.64E-01	2.79E-01	2.38E-02	false	true	true	false	SIMPLEX
61	3395.3287	0.0225	5675.4234	0.1485	1.1534	0.1015	0.0446	0.4651	0.2382	0.2801	0.0239	1.1534	1.02E-01	2.38E-01	4.46E-02	4.65E-01	2.80E-01	2.39E-02	false	true	true	false	SIMPLEX
62	3438.6702	0.0237	5664.7754	0.1502	1.1543	0.1019	0.0446	0.4645	0.2395	0.2798	0.0240	1.1543	1.02E-01	2.40E-01	4.46E-02	4.64E-01	2.80E-01	2.40E-02	false	true	true	false	SIMPLEX
63	3425.5969	0.0227	5703.8934	0.1504	1.1567	0.1015	0.0444	0.4654	0.2408	0.2803	0.0241	1.1567	1.02E-01	2.41E-01	4.44E-02	4.65E-01	2.80E-01	2.41E-02	false	true	true	false	SIMPLEX
64	3403.8102	0.0228	5664.5011	0.1492	1.1551	0.1021	0.0448	0.4645	0.2402	0.2797	0.0238	1.1551	1.02E-01	2.40E-01	4.48E-02	4.65E-01	2.80E-01	2.38E-02	false	true	true	false	SIMPLEX
65	3396.4383	0.0237	5663.9980	0.1487	1.1547	0.1020	0.0447	0.4647	0.2397	0.2798	0.0238	1.1547	1.02E-01	2.40E-01	4.47E-02	4.65E-01	2.80E-01	2.38E-02	false	true	true	false	SIMPLEX
66	3402.7839	0.0226	5684.4922	0.1494	1.1543	0.1017	0.0446	0.4650	0.2389	0.2801	0.0239	1.1543	1.02E-01	2.39E-01	4.46E-02	4.65E-01	2.80E-01	2.39E-02	false	true	true	false	SIMPLEX
67	3417.5744	0.0229	5670.5344	0.1493	1.1551	0.1020	0.0447	0.4648	0.2398	0.2800	0.0239	1.1551	1.02E-01	2.40E-01	4.47E-02	4.65E-01	2.80E-01	2.39E-02	false	true	true	false	SIMPLEX
68	3398.0152	0.0225	5673.7552	0.1489	1.1531	0.1015	0.0446	0.4649	0.2383	0.2800	0.0239	1.1531	1.02E-01	2.38E-01	4.46E-02	4.65E-01	2.80E-01	2.39E-02	false	true	true	false	SIMPLEX
69	3379.1086	0.0224	5680.2401	0.1494	1.1534	0.1017	0.0447	0.4650	0.2390	0.2800	0.0238	1.1543	1.02E-01	2.39E-01	4.47E-02	4.65E-01	2.80E-01	2.38E-02	false	true	true	false	SIMPLEX
70	3391.5799	0.0224	5694.9972	0.1490	1.1539	0.1014	0.0445	0.4653	0.2385	0.2803	0.0239	1.1539	1.01E-01	2.39E-01	4.45E-02	4.65E-01	2.80E-01	2.39E-02	false	true	true	false	SIMPLEX
71	3415.2952	0.0227	5685.1339	0.1495	1.1551	0.1014	0.0445	0.4651	0.2398	0.2802	0.0240	1.1551	1.01E-01	2.40E-01	4.45E-02	4.65E-01	2.80E-01	2.40E-02	false	true	true	false	SIMPLEX
72	3388.1533	0.0224	5681.7135	0.1487	1.1546	0.1019	0.0447	0.4651	0.2391	0.2801	0.0238	1.1546	1.02E-01	2.39E-01	4.47E-02	4.65E-01	2.80E-01	2.38E-02	false	true	true	false	SIMPLEX
73	3394.8475	0.0225	5685.8812	0.1490	1.1536	0.1014	0.0446	0.4651	0.2385	0.2801	0.0239	1.1536	1.01E-01	2.38E-01	4.46E-02	4.65E-01	2.80E-01	2.39E-02	false	true	true	false	SIMPLEX
74	3400.7886	0.0228	5680.5387	0.1493	1.1534	0.1016	0.0446	0.4648	0.2385	0.2800	0.0239	1.1534	1.02E-01	2.38E-01	4.46E-02	4.65E-01	2.80E-01	2.39E-02	false	true	true	false	SIMPLEX
75	3388.5619	0.0225	5678.5026	0.1487	1.1547	0.1019	0.0447	0.4650	0.2394	0.2800	0.0238	1.1547	1.02E-01	2.39E-01	4.47E-02	4.65E-01	2.80E-01	2.38E-02	false	true	true	false	SIMPLEX
76	3397.1719	0.0225	5678.5293	0.1487	1.1534	0.1016	0.0446	0.4650	0.2383	0.2801	0.0239	1.1534	1.02E-01	2.38E-01	4.46E-02	4.65E-01	2.80E-01	2.39E-02	false	true	true	false	SIMPLEX
77	3400.5532	0.0225	5681.4495	0.1497	1.1544	0.1018	0.0446	0.4651	0.2388	0.2801	0.0239	1.1544	1.02E-01	2.39E-01	4.46E-02	4.65E-01	2.80E-01	2.39E-02	false	true	true	false	SIMPLEX
78	3402.1319	0.0225	5680.7128	0.1491	1.1542	0.1017	0.0446	0.4651	0.2388	0.2801	0.0239	1.1542	1.02E-01	2.39E-01	4.46E-02	4.65E-01	2.80E-01	2.39E-02	false	true	true	false	SIMPLEX
79	3393.0852	0.0225	5679.2394	0.1488	1.1548	0.1020	0.0447	0.4649	0.2394	0.2800	0.0238	1.1548	1.02E-01	2.39E-01	4.47E-02	4.65E-01	2.80E-01	2.38E-02	false	true	true	false	SIMPLEX
80	3398.8702	0.0225	5680.3445	0.1490	1.1534	0.1016	0.0446	0.4650	0.2382	0.2801	0.0239	1.1534	1.02E-01	2.38E-01	4.46E-02	4.65E-01	2.80E-01	2.39E-02	false	true	true	false	SIMPLEX
81	3402.5809	0.0227	5671.9026	0.1490	1.1537	0.1017	0.0446	0.4648	0.2388	0.2799	0.0239	1.1537	1.02E-01	2.39E-01	4.46E-02	4.65E-01	2.80E-01	2.39E-02	false	true	true	false	SIMPLEX
82	3390.8539	0.0225	5682.2368	0.1490	1.1534	0.1015	0.0446	0.4650	0.2382	0.2800	0.0239	1.1534	1.02E-01	2.38E-01	4.46E-02	4.65E-01	2.80E-01	2.39E-02	false	true	true	false	SIMPLEX
83	3395.5570	0.0225	5677.3581	0.1487	1.1533	0.1015	0.0446	0.4650	0.2382	0.2801	0.0239	1.1533	1.02E-01	2.38E-01	4.46E-02	4.65E-01	2.80E-01	2.39E-02	false	true	true	false	SIMPLEX
84	3397.9772	0.0225	5681.7293	0.1491	1.1533	0.1016	0.0446	0.4650	0.2382	0.2800	0.0239	1.1533	1.02E-01	2.38E-01	4.46E-02	4.65E-01	2.80E-01	2.39E-02	false	true	true	false	SIMPLEX
85	3394.3325	0.0225	5678.5976	0.1488	1.1532	0.1015	0.0446	0.4649	0.2382	0.2800	0.0239	1.1532	1.02E-01	2.38E-01	4.46E-02	4.65E-01	2.80E-01	2.39E-02	false	true	true	false	SIMPLEX
86	3396.0851	0.0225	5675.0901	0.1488	1.1531	0.1015	0.0446	0.4648	0.2380	0.2800	0.0239	1.1531	1.02E-01	2.38E-01	4.46E-02	4.65E-01	2.80E-01	2.39E-02	false	true	true	false	SIMPLEX
87	3397.5479	0.0225	5676.7521	0.1491	1.1531	0.1016	0.0446	0.4648	0.2382	0.2800	0.0239	1.1531	1.02E-01	2.38E-01	4.46E-02	4.65E-01	2.80E-01	2.39E-02	false	true	true	false	SIMPLEX
88	3398.5734	0.0225	5679.4486	0.1494	1.1548	0.1020	0.0447	0.4648	0.2395	0.2799	0.0238	1.1548	1.02E-01	2.40E-01	4.47E-02	4.65E-01	2.80E-01	2.38E-02	false	true	true	false	SIMPLEX
89	3395.0531	0.0225	5677.9021	0.1488	1.1549	0.1020	0.0447	0.4648	0.2386	0.2800	0.0238	1.1549	1.02E-01	2.40E-01	4.47E-02	4.65E-01	2.80E-01	2.38E-02	false	true	true	false	SIMPLEX
90	3397.2487	0.0225	5679.5180	0.1490	1.1533	0.1016	0.0446	0.4649	0.2383	0.2800	0.0239	1.1533	1.02E-01	2.38E-01	4.46E-02	4.65E-01	2.80E-01	2.39E-02	false	true	true	false	SIMPLEX
91	3395.8565	0.0225	5676.8581	0.1490	1.1531	0.1013	0.0446	0.4648	0.2382	0.2800	0.0239	1.1531	1.02E-01	2.38E-

99	3398.3172	0.0225	5678.1658	0.1491	1.1531	0.1015	0.0446	0.4648	0.2383	0.2800	0.0239	1.1531	1.02E-01	2.38E-01	4.46E-02	4.65E-01	2.80E-01	2.39E-02	false	false	true	false	SIMPLEX
100	3398.9497	0.0225	5679.9424	0.1492	1.1531	0.1015	0.0446	0.4648	0.2383	0.2800	0.0239	1.1531	1.02E-01	2.38E-01	4.46E-02	4.65E-01	2.80E-01	2.39E-02	false	false	true	false	SIMPLEX
101	3397.3873	0.0225	5677.3562	0.1490	1.1531	0.1015	0.0446	0.4648	0.2382	0.2800	0.0239	1.1531	1.02E-01	2.38E-01	4.46E-02	4.65E-01	2.80E-01	2.39E-02	false	false	true	false	SIMPLEX
102	3397.0360	0.0225	5678.5038	0.1490	1.1529	0.1015	0.0446	0.4648	0.2381	0.2800	0.0239	1.1529	1.01E-01	2.38E-01	4.46E-02	4.65E-01	2.80E-01	2.39E-02	false	false	true	false	SIMPLEX
103	3396.8923	0.0225	5678.7038	0.1490	1.1349	0.1021	0.0447	0.4649	0.2396	0.2800	0.0238	1.1549	1.02E-01	2.40E-01	4.47E-02	4.65E-01	2.80E-01	2.38E-02	false	false	true	false	SIMPLEX
104	3397.3963	0.0225	5677.7365	0.1490	1.1531	0.1015	0.0446	0.4649	0.2381	0.2800	0.0239	1.1531	1.02E-01	2.38E-01	4.46E-02	4.65E-01	2.80E-01	2.39E-02	false	false	true	false	SIMPLEX
105	3397.5830	0.0225	5678.4982	0.1491	1.1531	0.1015	0.0446	0.4648	0.2383	0.2800	0.0239	1.1531	1.02E-01	2.38E-01	4.46E-02	4.65E-01	2.80E-01	2.39E-02	false	false	true	false	SIMPLEX
106	3397.2106	0.0225	5678.0810	0.1490	1.1531	0.1015	0.0446	0.4649	0.2382	0.2800	0.0239	1.1531	1.02E-01	2.38E-01	4.46E-02	4.65E-01	2.80E-01	2.39E-02	false	false	true	false	SIMPLEX
107	3397.3409	0.0225	5678.5289	0.1491	1.1530	0.1015	0.0446	0.4648	0.2382	0.2800	0.0239	1.1530	1.02E-01	2.38E-01	4.46E-02	4.65E-01	2.80E-01	2.39E-02	false	false	true	false	SIMPLEX
108	3397.4348	0.0225	5678.7812	0.1491	1.1529	0.1015	0.0446	0.4648	0.2382	0.2800	0.0239	1.1529	1.01E-01	2.38E-01	4.46E-02	4.65E-01	2.80E-01	2.39E-02	false	false	true	false	SIMPLEX
109	3397.4328	0.0225	5678.1322	0.1490	1.1530	0.1015	0.0446	0.4648	0.2382	0.2800	0.0239	1.1530	1.01E-01	2.38E-01	4.46E-02	4.65E-01	2.80E-01	2.39E-02	false	false	true	false	SIMPLEX
110	3397.4106	0.0225	5678.9431	0.1491	1.1530	0.1015	0.0446	0.4648	0.2382	0.2800	0.0239	1.1530	1.02E-01	2.38E-01	4.46E-02	4.65E-01	2.80E-01	2.39E-02	false	false	true	false	SIMPLEX
111	3397.1774	0.0225	5678.2973	0.1491	1.1529	0.1015	0.0446	0.4648	0.2381	0.2800	0.0239	1.1529	1.01E-01	2.38E-01	4.46E-02	4.65E-01	2.80E-01	2.39E-02	false	false	true	false	SIMPLEX
112	3397.0497	0.0225	5679.8798	0.1491	1.1530	0.1015	0.0446	0.4648	0.2381	0.2800	0.0239	1.1530	1.01E-01	2.38E-01	4.46E-02	4.65E-01	2.80E-01	2.39E-02	false	false	true	false	SIMPLEX
113	3397.1875	0.0225	5679.1347	0.1491	1.1534	0.1016	0.0446	0.4649	0.2385	0.2800	0.0239	1.1534	1.02E-01	2.38E-01	4.46E-02	4.65E-01	2.80E-01	2.39E-02	false	false	true	false	SIMPLEX
114	3397.3026	0.0225	5678.7534	0.1491	1.1530	0.1015	0.0446	0.4648	0.2382	0.2800	0.0239	1.1530	1.02E-01	2.38E-01	4.46E-02	4.65E-01	2.80E-01	2.39E-02	false	false	true	false	SIMPLEX
115	3397.2940	0.0225	5679.1202	0.1491	1.1530	0.1015	0.0446	0.4649	0.2382	0.2800	0.0239	1.1530	1.02E-01	2.38E-01	4.46E-02	4.65E-01	2.80E-01	2.39E-02	false	false	true	false	SIMPLEX
116	3397.2592	0.0225	5678.9931	0.1491	1.1530	0.1015	0.0446	0.4648	0.2382	0.2800	0.0239	1.1530	1.02E-01	2.38E-01	4.46E-02	4.65E-01	2.80E-01	2.39E-02	false	false	true	false	SIMPLEX
117	3397.1057	0.0225	5678.9015	0.1491	1.1530	0.1015	0.0446	0.4648	0.2381	0.2800	0.0239	1.1530	1.02E-01	2.38E-01	4.46E-02	4.65E-01	2.80E-01	2.39E-02	false	false	true	false	SIMPLEX
118	3397.3061	0.0225	5679.0392	0.1491	1.1530	0.1015	0.0446	0.4648	0.2381	0.2800	0.0239	1.1530	1.02E-01	2.38E-01	4.46E-02	4.65E-01	2.80E-01	2.39E-02	false	false	true	false	SIMPLEX
119	3397.1824	0.0225	5679.2160	0.1491	1.1529	0.1015	0.0446	0.4648	0.2381	0.2800	0.0239	1.1529	1.01E-01	2.38E-01	4.46E-02	4.65E-01	2.80E-01	2.39E-02	false	false	true	false	SIMPLEX
120	3397.1441	0.0225	5679.3424	0.1491	1.1533	0.1016	0.0446	0.4648	0.2384	0.2800	0.0239	1.1533	1.02E-01	2.38E-01	4.46E-02	4.65E-01	2.80E-01	2.39E-02	false	false	true	false	SIMPLEX
121	3397.0918	0.0225	5679.1068	0.1491	1.1529	0.1015	0.0446	0.4648	0.2381	0.2800	0.0239	1.1529	1.01E-01	2.38E-01	4.46E-02	4.65E-01	2.80E-01	2.39E-02	false	false	true	false	SIMPLEX
122	3396.9726	0.0225	5679.2216	0.1491	1.1530	0.1015	0.0446	0.4648	0.2381	0.2800	0.0239	1.1530	1.01E-01	2.38E-01	4.46E-02	4.65E-01	2.80E-01	2.39E-02	false	false	true	false	SIMPLEX
123	3397.2227	0.0225	5679.0948	0.1491	1.1530	0.1015	0.0446	0.4648	0.2382	0.2800	0.0239	1.1530	1.02E-01	2.38E-01	4.46E-02	4.65E-01	2.80E-01	2.39E-02	false	false	true	false	SIMPLEX
124	3397.1471	0.0225	5679.1534	0.1491	1.1530	0.1015	0.0446	0.4648	0.2382	0.2800	0.0239	1.1530	1.02E-01	2.38E-01	4.46E-02	4.65E-01	2.80E-01	2.39E-02	false	false	true	false	SIMPLEX
125	3397.1441	0.0225	5679.0588	0.1491	1.1530	0.1015	0.0446	0.4648	0.2382	0.2800	0.0239	1.1530	1.01E-01	2.38E-01	4.46E-02	4.65E-01	2.80E-01	2.39E-02	false	false	true	false	SIMPLEX
126	3397.2443	0.0225	5679.1276	0.1491	1.1530	0.1015	0.0446	0.4648	0.2382	0.2800	0.0239	1.1530	1.01E-01	2.38E-01	4.46E-02	4.65E-01	2.80E-01	2.39E-02	false	false	true	false	SIMPLEX
127	3397.1799	0.0225	5679.2566	0.1491	1.1530	0.1015	0.0446	0.4649	0.2381	0.2800	0.0239	1.1530	1.02E-01	2.38E-01	4.46E-02	4.65E-01	2.80E-01	2.39E-02	false	false	true	false	SIMPLEX
128	3397.2382	0.0225	5679.1581	0.1491	1.1529	0.1015	0.0446	0.4648	0.2382	0.2800	0.0239	1.1529	1.01E-01	2.38E-01	4.46E-02	4.65E-01	2.80E-01	2.39E-02	false	false	true	false	SIMPLEX
129	3397.2246	0.0225	5679.0286	0.1491	1.1529	0.1015	0.0446	0.4648	0.2381	0.2800	0.0239	1.1529	1.01E-01	2.38E-01	4.46E-02	4.65E-01	2.80E-01	2.39E-02	false	false	true	false	SIMPLEX
130	3397.3007	0.0225	5679.2114	0.1491	1.1531	0.1015	0.0446	0.4649	0.2382	0.2800	0.0239	1.1531	1.02E-01	2.38E-01	4.46E-02	4.65E-01	2.80E-01	2.39E-02	false	false	true	false	SIMPLEX
131	3397.1832	0.0225	5678.9869	0.1491	1.1530	0.1015	0.0446	0.4648	0.2382	0.2800	0.0239	1.1530	1.02E-01	2.38E-01	4.46E-02	4.65E-01	2.80E-01	2.39E-02	false	false	true	false	SIMPLEX
132	3397.2103	0.0225	5679.1920	0.1491	1.1530	0.1015	0.0446	0.4648	0.2382	0.2800	0.0239	1.1530	1.01E-01	2.38E-01	4.46E-02	4.65E-01	2.80E-01	2.39E-02	false	false	true	false	SIMPLEX
133	3397.1533	0.0225	5679.1374	0.1491	1.1530	0.1015	0.0446	0.4648	0.2382	0.2800	0.0239	1.1530	1.02E-01	2.38E-01	4.46E-02	4.65E-01	2.80E-01	2.39E-02	false	false	true	false	SIMPLEX
134	3397.2134	0.0225	5679.1718	0.1491	1.1529	0.1015	0.0446	0.4648	0.2381	0.2800	0.0239	1.1529	1.01E-01	2.38E-01	4.46E-02	4.65E-01	2.80E-01	2.39E-02	false	false	true	false	SIMPLEX
135	3397.2035	0.0225	5679.1373	0.1491	1.1530	0.1015	0.0446	0.4648	0.2382	0.2800	0.0239	1.1530	1.02E-01	2.38E-01	4.46E-02	4.65E-01	2.80E-01	2.39E-02	false	false	true	false	SIMPLEX
136	3397.1709	0.0225	5679.1317	0.1491	1.1530	0.1015	0.0446	0.4648	0.2382	0.2800	0.0239	1.1530	1.02E-01	2.38E-01	4.46E-02	4.65E-01	2.80E-01	2.39E-02	false	false	true	false	SIMPLEX
137	3397.1908	0.0225	5679.1408	0.1491	1.1530	0.1015	0.0446	0.4648	0.2382	0.2800	0.0239	1.1530	1.02E-01	2.38E-01	4.46E-02	4.65E-01	2.80E-01	2.39E-02	false	false	true	false	SIMPLEX
138	3397.1929	0.0225	5679.1517	0.1491	1.1529	0.1015	0.0446	0.4648	0.2381	0.2800	0.0239	1.1529	1.01E-01	2.38E-01	4.46E-02	4.65E-01	2.80E-01	2.39E-02	false	false	true	false	SIMPLEX
139	3397.1979	0.0225	5679.1939	0.1491	1.1529	0.1015	0.0446	0.4648	0.2381	0.2800	0.0239	1.1529	1.01E-01	2.38E-01	4.46E-02	4.65E-01	2.80E-01	2.39E-02	false	false	true	false	SIMPLEX
140	3397.1883	0.0225	5679.1546	0.1491	1.1529	0.1015	0.0446	0.4648	0.2381	0.2800	0.0239	1.1529	1.01E-01	2.38E-01	4.46E-02	4.65E-01	2.80E-01	2.39E-02	false	false	true	false	SIMPLEX
141	3397.2094	0.0225	5679.1470	0.1491	1.1530	0.1015	0.0446	0.4648	0.2382	0.2800	0.0239	1.1530	1.02E-01	2.38E-01	4.46E-02	4.65E-01	2.80E-01	2.39E-02	false	false	true	false	SIMPLEX
142	3397.1874	0.0225	5679.1830	0.1491	1.1529	0.1015	0.0446	0.4648	0.2381	0.2800	0.0239	1.1529	1.01E-01	2.38E-01	4.46E-02	4.65E-01	2.80E-01	2.39E-02	false	false	true	false	SIMPLEX
143	3397.1709	0.0225	5679.2099	0.1491	1.1530	0.1015	0.0446	0.4648	0.2381	0.2800	0.0239	1.1530	1.02E-01	2.38E-01	4.46E-02	4.65E-01	2.80E-01	2.39E-02	false	false	true	false	SIMPLEX
144	4130.2860	0.0188	19750.7486	0.1388	1.8800	0.1087	0.1674	0.7438	0.4296	0.3946	0.0409	1.8800	1.09E-01	4.30E-01	1.92E-01	7.44E-01	3.95E-01	4.09E-02	false	false	true	false	DOE_RANDOM
145	4560.8515	0.0030	7689.9434	0.1147	1.5854	0.0973	0.0575	0.8273	0.4055	0.3503	0.0363	1.5854	9.73E-02	4.03E-01	5.75E-02	6.27E-01	3.59E-01	3.81E-02	false	false	true	false	DOE_RANDOM
146	4178.7174	0.0045	16784.4817	0.0813	2.4860	0.1190	0.7760	1.0957	0.4867	0.4430	0.0766	2.4860	1.18E-01	4.97E-01	3.70E-01	1.10E+00	4.33E-01	7.65E-02	false	false	true	false	DOE_RANDOM
147	3511.1171	0.0157	7650.6315	0.1352	1.4852	0.0978	0.0424	0.5700	0.4082	0.3352	0.0315	1.4852	9.79E-02	4.08E-01	4.24E-02	5.70E-01	3.35E-01	3.15E-02	false	false	true	false	DOE_RANDOM
148	3539.4864	0.0124	17245.3373	0.1113	2.2518	0.1213	0.2480	0.9618	0.4585	0.3985	0.0637	2.2518	1.21E-01	4.59E-01	2.48E-01	9.62E-01	3.98E-01	6.37E-02	false	false	true	false	DOE_RANDOM
149	3697.1331	0.0004	6383.8507	0.1524	2.8613	0.1408	0.0779	1.1225	0.7988	0.448	0.0718	2.8613	1.41E-01	7.99E-01	7.79E-02	1.12E+00	4.48E-01	7.28E-02	false	false	false	false	SIMPLEX

APPENDIX H – PMHS MODEFRONTIER OPTIMIZATION FOR NOMINAL POSTURE WITH VEST

```
#--- Frontier Design DB File Info ---------------
#modeFRONTIER  - (c) ESTECO S.p.A.
#Design DB Table
#-------------------------------------------------
#modeFRONTIER Version: modeFRONTIER 2017R5 5.7.1 b20171017
#Date: Sun Jan 27 16:39:23 EST 2019
#Project Name: PMHS A Opt 2019-01-26 - vest - sensitivity - complete.prj
#Operating System: Windows 10 10.0 amd64
#Java (SDK/JRE) Version: 1.8.0_60
#Java Vendor: Oracle Corporation
#Java Vendor URL: http://java.oracle.com/
#User Name: KBosch
#-------------------------------------------------
#Categories
<CATEGORIES clusterPrefix="CLUSTER_" useTableNamePrefix="false">
  <CATEGORY enabled="true" label="" name="SOSO1" symbol="SQUARE,NONE,11,,0"/>
  <CATEGORY enabled="true" label="" name="USRDOE" symbol="SQUARE,NONE,11,,0"/>
  <CATEGORY enabled="true" label="" name="NSGA2" symbol="SQUARE,NONE,11,,0"/>
  <CATEGORY enabled="true" label="" name="TOA" symbol="SQUARE,NONE,11,,0"/>
  <CATEGORY enabled="true" label="" name="DOE_APPROX" symbol="SQUARE,NONE,11,,0"/>
  <CATEGORY enabled="true" label="" name="SIMPLEX" symbol="SQUARE,NONE,11,,0"/>
  <CATEGORY enabled="true" label="" name="ULH" symbol="SQUARE,NONE,11,,0"/>
  <CATEGORY enabled="true" label="" name="FULL" symbol="SQUARE,NONE,11,#DC3912,1,#DC3912"/>
  <CATEGORY enabled="true" label="" name="SIMPLEX_DOE" symbol="SQUARE,NONE,11,#3366CC,1,#3366CC"/>
</CATEGORIES>

#-------------------------------------------------
```

<ID>	Opt_join:	Opt_join:	Opt_join:	Opt_join:	Opt_join:	Opt_join:	Combined	Pelvis_Ax_1	Pelvis_Fx_1	Pelvis_Fz_1	T12_Ax	T12_Az	T12_Fx	T12_Fz	no Constraint:	Constraint:	Constraint:	Constraint:	Constraint:	Constraint:	<ERROR>	<VIRTUAL>	<FEASIBLE>	<MARKED>	<CATEGORY>
0	4392.01	0.02	10985.14	0.15	2.69	0.12	0.16	1.21	0.45	0.67	0.08	0.12	0.45	0.16	1.21	0.67	0.08	false	false	false	false	ULH
1	2743.12	0.02	6736.98	0.14	1.67	0.07	0.17	0.63	0.28	0.46	0.05	0.07	0.28	0.17	0.63	0.46	0.05	false	false	true	false	ULH
2	2800.88	0.01	18518.53	0.13	2.66	0.12	0.17	1.17	0.44	0.68	0.08	0.12	0.44	0.17	1.17	0.68	0.08	false	false	false	false	ULH
3	3488.84	0.00	15733.56	0.15	2.47	0.11	0.14	1.09	0.42	0.64	0.08	0.11	0.42	0.14	1.09	0.64	0.08	false	false	false	false	ULH
4	4234.29	0.01	11374.93	0.09	2.57	0.11	0.15	1.16	0.44	0.64	0.08	0.11	0.44	0.15	1.16	0.64	0.08	false	false	false	false	ULH
5	2755.79	0.02	17701.08	0.09	2.59	0.12	0.18	1.16	0.48	0.76	0.09	0.12	0.48	0.18	1.16	0.76	0.09	false	false	false	false	ULH
6	2048.34	0.02	5848.94	0.15	1.60	0.06	0.17	0.61	0.25	0.45	0.05	0.06	0.25	0.17	0.61	0.46	0.05	false	false	true	false	ULH
7	3702.04	0.02	5114.39	0.09	2.57	0.10	0.18	1.17	0.31	0.75	0.06	0.10	0.31	0.18	1.17	0.75	0.06	false	false	false	false	ULH
8	4990.03	0.01	14305.69	0.09	2.94	0.13	0.14	1.34	0.49	0.73	0.12	0.13	0.49	0.14	1.34	0.73	0.12	false	false	false	false	ULH
9	4019.91	0.02	12029.39	0.12	2.25	0.12	0.17	0.96	0.33	0.62	0.06	0.12	0.33	0.17	0.96	0.62	0.06	false	false	true	false	ULH
10	4487.77	0.02	15903.96	0.13	2.55	0.12	0.16	1.12	0.43	0.65	0.08	0.12	0.43	0.16	1.12	0.65	0.08	false	false	false	false	ULH
11	2221.73	0.00	15508.78	0.13	2.54	0.12	0.16	1.11	0.42	0.65	0.08	0.12	0.42	0.16	1.11	0.66	0.08	false	false	false	false	ULH
12	3644.64	0.02	17864.14	0.10	2.86	0.12	0.16	1.29	0.47	0.73	0.09	0.12	0.47	0.16	1.29	0.73	0.09	false	false	false	false	ULH
13	2259.11	0.02	5829.19	0.08	3.08	0.08	0.20	1.51	0.33	0.88	0.07	0.08	0.33	0.20	1.51	0.88	0.07	false	false	false	false	ULH
14	3238.76	0.02	15537.90	0.12	2.55	0.12	0.17	1.11	0.41	0.67	0.08	0.12	0.41	0.17	1.11	0.67	0.08	false	false	false	false	ULH
15	3371.67	0.01	19469.15	0.11	2.97	0.12	0.17	1.36	0.49	0.74	0.10	0.12	0.49	0.17	1.36	0.74	0.10	false	false	false	false	ULH
16	3796.53	0.02	19729.27	0.11	2.86	0.12	0.16	1.29	0.47	0.72	0.09	0.12	0.47	0.16	1.29	0.72	0.09	false	false	false	false	ULH
17	2969.26	0.01	17172.55	0.11	2.78	0.12	0.15	1.26	0.45	0.70	0.09	0.12	0.46	0.15	1.26	0.70	0.09	false	false	false	false	ULH
18	3158.53	0.02	19085.91	0.10	2.90	0.12	0.17	1.29	0.48	0.74	0.09	0.12	0.48	0.17	1.29	0.74	0.09	false	false	false	false	ULH
19	3943.16	0.02	14815.23	0.15	2.24	0.12	0.17	0.95	0.31	0.62	0.06	0.12	0.31	0.17	0.95	0.62	0.06	false	false	true	false	ULH
20	2624.97	0.01	10537.94	0.11	2.15	0.12	0.18	0.86	0.31	0.63	0.06	0.12	0.31	0.18	0.86	0.63	0.06	false	false	true	false	ULH
21	2452.16	0.02	15308.73	0.08	2.96	0.13	0.18	1.32	0.49	0.75	0.10	0.13	0.49	0.18	1.32	0.76	0.10	false	false	false	false	ULH
22	4195.70	0.01	15149.22	0.13	2.59	0.11	0.14	1.17	0.44	0.64	0.08	0.11	0.44	0.14	1.17	0.64	0.08	false	false	false	false	ULH
23	3064.55	0.02	17978.06	0.09	2.94	0.12	0.17	1.31	0.48	0.75	0.09	0.12	0.48	0.17	1.31	0.75	0.09	false	false	false	false	ULH
24	3579.53	0.01	9070.95	0.14	2.01	0.12	0.17	0.78	0.31	0.57	0.06	0.12	0.31	0.17	0.78	0.57	0.06	false	false	true	false	ULH
25	4458.41	0.01	11072.05	0.13	2.20	0.12	0.16	0.94	0.33	0.59	0.06	0.12	0.33	0.16	0.94	0.59	0.06	false	false	true	false	ULH
26	4251.81	0.00	18391.91	0.14	2.72	0.12	0.17	1.24	0.46	0.67	0.10	0.12	0.46	0.17	1.24	0.67	0.10	false	false	false	false	ULH
27	2180.55	0.00	18793.48	0.10	2.97	0.12	0.17	1.36	0.49	0.74	0.10	0.12	0.49	0.17	1.36	0.74	0.10	false	false	false	false	ULH
28	2942.49	0.01	14708.13	0.09	2.76	0.12	0.15	1.24	0.46	0.69	0.09	0.12	0.46	0.15	1.24	0.69	0.09	false	false	false	false	ULH
29	4088.91	0.02	17333.48	0.15	2.52	0.12	0.16	1.10	0.42	0.65	0.08	0.12	0.42	0.16	1.10	0.65	0.08	false	false	false	false	ULH
30	2001.62	0.02	19220.73	0.14	2.40	0.11	0.18	1.03	0.32	0.70	0.07	0.11	0.32	0.18	1.03	0.70	0.07	false	false	false	false	ULH
31	3659.41	0.01	15411.14	0.09	2.85	0.12	0.15	1.30	0.47	0.72	0.09	0.12	0.47	0.15	1.30	0.72	0.09	false	false	false	false	ULH
32	2893.26	0.02	19975.54	0.08	3.20	0.13	0.20	1.45	0.50	0.81	0.11	0.13	0.50	0.20	1.45	0.81	0.11	false	false	false	false	ULH
33	3716.66	0.00	15008.24	0.10	2.72	0.12	0.13	1.24	0.45	0.68	0.10	0.12	0.46	0.13	1.24	0.68	0.10	false	false	false	false	ULH
34	2578.77	0.02	16176.97	0.08	3.09	0.13	0.19	1.41	0.50	0.78	0.10	0.13	0.50	0.19	1.41	0.78	0.10	false	false	false	false	ULH
35	3559.11	0.01	14162.49	0.13	2.38	0.12	0.16	1.02	0.35	0.64	0.07	0.12	0.35	0.16	1.02	0.64	0.07	false	false	false	false	ULH
36	3270.23	0.01	5679.25	0.12	1.74	0.10	0.18	0.63	0.31	0.47	0.06	0.10	0.31	0.18	0.63	0.47	0.06	false	false	true	false	ULH
37	2500.52	0.01	9584.84	0.10	2.15	0.12	0.17	0.88	0.30	0.62	0.06	0.12	0.30	0.17	0.88	0.62	0.06	false	false	true	false	ULH
38	4285.53	0.02	18826.82	0.11	2.86	0.12	0.15	1.30	0.47	0.72	0.09	0.12	0.47	0.15	1.30	0.72	0.09	false	false	false	false	ULH
39	4605.33	0.02	17522.59	0.10	2.90	0.12	0.16	1.32	0.48	0.73	0.09	0.12	0.48	0.16	1.32	0.73	0.09	false	false	false	false	ULH
40	4856.40	0.01	8577.87	0.08	2.30	0.11	0.16	0.98	0.39	0.59	0.07	0.11	0.39	0.16	0.98	0.59	0.07	false	false	true	false	ULH
41	2110.41	0.01	9433.44	0.11	2.09	0.11	0.18	0.82	0.33	0.60	0.06	0.11	0.33	0.18	0.82	0.60	0.06	false	false	true	false	ULH
42	3813.51	0.00	7097.24	0.09	1.98	0.11	0.16	0.78	0.31	0.55	0.06	0.11	0.31	0.16	0.78	0.56	0.06	false	false	true	false	ULH
43	4924.33	0.01	12356.12	0.11	2.38	0.11	0.13	1.17	0.44	0.63	0.08	0.11	0.44	0.13	1.17	0.63	0.08	false	false	false	false	ULH
44	4840.54	0.01	8880.30	0.13	2.06	0.11	0.16	0.86	0.31	0.55	0.05	0.11	0.31	0.16	0.86	0.56	0.05	false	false	true	false	ULH
45	3380.12	0.00	7232.37	0.12	1.89	0.11	0.17	0.71	0.32	0.53	0.06	0.11	0.32	0.17	0.71	0.53	0.06	false	false	true	false	ULH
46	2537.13	0.02	7265.06	0.12	1.80	0.08	0.17	0.70	0.29	0.50	0.06	0.08	0.29	0.17	0.70	0.50	0.06	false	false	true	false	ULH
47	4401.24	0.02	10427.48	0.12	2.12	0.12	0.17	0.87	0.30	0.60	0.06	0.12	0.30	0.17	0.87	0.60	0.06	false	false	true	false	ULH
48	2856.11	0.00	7776.22	0.13	1.87	0.11	0.17	0.68	0.32	0.54	0.05	0.11	0.32	0.17	0.68	0.54	0.05	false	false	true	false	ULH
49	4129.79	0.02	8922.38	0.12	2.05	0.12	0.18	0.81	0.31	0.58	0.06	0.12	0.31	0.18	0.81	0.58	0.06	false	false	true	false	ULH
50	2177.46	0.02	13820.54	0.08	2.82	0.13	0.17	1.24	0.45	0.73	0.09	0.13	0.46	0.17	1.24	0.73	0.09	false	false	false	false	ULH
51	2088.43	0.02	11228.67	0.11	2.18	0.10	0.18	0.84	0.34	0.64	0.06	0.10	0.34	0.18	0.84	0.64	0.06	false	false	true	false	ULH
52	4685.90	0.03	5864.15	0.12	1.96	0.12	0.18	0.77	0.31	0.53	0.06	0.12	0.31	0.18	0.77	0.53	0.06	false	false	true	false	ULH
53	3115.41	0.01	12157.80	0.13	2.13	0.12	0.16	0.88	0.30	0.61	0.06	0.12	0.30	0.16	0.88	0.61	0.06	false	false	true	false	ULH
54	2120.93	0.02	8440.71	0.14	1.80	0.07	0.17	0.71	0.29	0.50	0.05	0.07	0.29	0.17	0.71	0.50	0.05	false	false	true	false	ULH
55	2559.50	0.01	15036.18	0.15	2.67	0.16	0.10	1.07	0.58	0.65	0.10	0.16	0.58	0.10	1.07	0.66	0.10	false	false	false	false	ULH
56	4181.81	0.01	13636.03	0.13	2.39	0.11	0.16	1.03	0.40	0.62	0.07	0.11	0.40	0.16	1.03	0.62	0.07	false	false	false	false	ULH
57	3889.66	0.01	7668.46	0.09	2.03	0.11	0.16	0.83	0.30	0.58	0.05	0.11	0.30	0.16	0.83	0.58	0.05	false	false	true	false	ULH
58	2906.18	0.01	9524.02	0.15	2.62	0.15	0.09	1.05	0.57	0.65	0.10	0.15	0.57	0.09	1.05	0.65	0.10	false	false	false	false	ULH
59	4516.99	0.01	5499.96	0.11	1.94	0.11	0.16	0.76	0.31	0.53	0.06	0.11	0.31	0.16	0.76	0.53	0.06	false	false	true	false	ULH
60	2335.43	0.00	5237.90	0.09	2.56	0.11	0.18	1.15	0.31	0.75	0.06	0.11	0.31	0.18	1.15	0.75	0.06	false	false	false	false	ULH
61	4317.56	0.01	5947.73	0.10	1.90	0.11	0.17	0.74	0.31	0.50	0.06	0.11	0.31	0.17	0.74	0.50	0.06	false	false	true	false	ULH
62	3008.60	0.00	10255.64	0.14	2.01	0.11	0.16	0.78	0.31	0.59	0.06	0.11	0.31	0.16	0.78	0.59	0.06	false	false	true	false	ULH
63	4656.77	0.00	6193.37	0.15	1.86	0.11	0.16	0.72	0.31	0.50	0.06	0.11	0.31	0.16	0.72	0.50	0.06	false	false	true	false	ULH
64	4797.02	0.02	11573.32	0.12	2.28	0.12	0.17	0.98	0.34	0.61	0.07	0.12	0.34	0.17	0.98	0.61	0.07	false	false	true	false	ULH
65	2653.74	0.01	8280.63	0.12	1.94	0.10	0.18	0.74	0.32	0.55	0.06	0.10	0.32	0.18	0.74	0.55	0.06	false	false	true	false	ULH
66	2691.65	0.02	7441.54	0.10	1.98	0.10	0.18	0.76	0.33	0.56	0.06	0.10	0.33	0.18	0.76	0.56	0.06	false	false	true	false	ULH
67	2299.17	0.02	15372.95	0.11	2.65	0.12	0.17	1.15	0.43	0.69	0.08	0.12	0.43	0.17	1.15	0.69	0.08	false	false	false	false	ULH
68	2657.59	0.02	17599.96	0.13	2.19	0.12	0.18	0.89	0.31	0.64	0.06	0.12	0.31	0.18	0.89	0.64	0.06	false	false	true	false	ULH
69	3750.91	0.01	10726.50	0.14	2.05	0.11	0.16	0.84	0.30	0.58	0.05	0.11	0.30	0.16	0.84	0.58	0.05	false	false	true	false	ULH
70	3981.84	0.00	12920.59	0.15	2.26	0.11	0.16	0.96	0.35	0.60	0.07	0.11	0.35	0.16	0.96	0.60	0.07	false	false	true	false	ULH
71	4357.18	0.01	19560.56	0.12	2.91	0.12	0.16	1.32	0.48	0.72	0.10	0.12	0.48	0.16	1.32	0.72	0.10	false	false	false	false	ULH
72	4881.21	0.02	10090.12	0.11	2.24	0.12	0.16	0.96	0.34	0.59	0.06	0.12	0.34	0.16	0.96	0.59	0.06	false	false	true	false	ULH
73	3415.44	0.01	15748.32	0.14	2.40	0.12	0.16	1.03	0.38	0.63	0.07	0.12	0.38	0.16	1.03	0.63	0.07	false	false	false	false	ULH
74	3613.56	0.00	18236.11	0.09	3.18	0.13	0.14	1.46	0.50	0.80	0.15	0.13	0.50	0.14	1.46	0.80	0.15	false	false	false	false	ULH
75	3504.99	0.02	11719.44	0.14	2.09	0.12	0.18	0.83	0.31	0.60	0.06	0.12	0.31	0.18	0.83	0.60	0.06	false	false	true	false	ULH
76	2412.33	0.01	8682.44	0.09	2.09	0.12	0.17	0.83	0.31	0.61	0.06	0.12	0.31	0.17	0.83	0.61	0.06	false	false	true	false	ULH
77	3450.78	0.01	11835.92	0.11	2.35	0.12	0.16	1.01	0.37	0.63	0.07	0.12	0.37	0.16	1.01	0.63	0.07	false	false	false	false	ULH
78	4558.51	0.02	13322.09	0.10	2.63	0.12	0.16	1.17	0.44	0.65	0.08	0.12	0.44	0.16	1.17	0.66	0.08	false	false	false	false	ULH
79	4135.95	0.02	5494.85	0.15	1.81	0.11	0.18	0.69	0.32	0.45	0.06	0.11	0.32	0.18	0.69	0.46	0.06	false	false	true	false	ULH
80	3726.16	0.00	9946.28	0.08	2.43	0.11	0.14	1.07	0.41	0.63	0.07	0.11	0.41	0.14	1.07	0.63	0.07	false	false	false	false	ULH
81	3046.41	0.00	12254.20	0.08	2.68	0.12	0.13	1.22	0.45	0.68	0.09	0.12	0.45	0.13	1.22	0.68	0.09	false	false	false	false	ULH
82	4714.68	0.02	10934.92	0.12	2.24	0.12	0.17	0.95	0.33	0.61	0.06	0.12	0.33	0.17	0.95	0.61	0.06	false	false	true	false	ULH
83	3327.71	0.01	5391.85	0.09	2.32	0.11	0.18	0.98	0.31	0.69	0.06	0.11	0.31	0.18	0.98	0.69	0.06	false	false	true	false	ULH
84	4878.29	0.01	13549.11	0.08	2.86	0.12	0.15	1.30	0.48	0.71	0.11	0.12	0.48	0.15	1.30	0.71	0.11	false	false	false	false	ULH
85	4773.20	0.00	14013.78	0.14	2.52	0.11	0.13	1.13	0.43	0.63	0.08	0.11	0.43	0.13	1.13	0.63	0.08	false	false	false	false	ULH
86	2438.96	0.01	14588.22	0.11	2.56	0.12	0.17	1.11	0.42	0.67	0.08	0.12	0.42	0.17	1.11	0.67	0.08	false	false	false	false	ULH

87	3083.53	0.02	5165.87	0.10	1.66	0.09	0.18	0.60	0.29	0.45	0.05	0.09	0.29	0.18	0.60	0.45	0.05	false	false	true	false	ULH
88	3893.60	0.01	8064.79	0.14	1.95	0.11	0.17	0.76	0.31	0.55	0.06	0.11	0.31	0.17	0.76	0.55	0.06	false	false	true	false	ULH
89	2838.19	0.00	9227.31	0.10	2.07	0.11	0.16	0.84	0.30	0.60	0.06	0.11	0.30	0.16	0.84	0.60	0.06	false	false	true	false	ULH
90	4547.85	0.00	10127.30	0.13	2.18	0.10	0.17	0.91	0.36	0.58	0.06	0.10	0.36	0.17	0.91	0.58	0.06	false	false	true	false	ULH
91	3853.12	0.02	12681.59	0.09	2.54	0.12	0.17	1.10	0.40	0.67	0.08	0.12	0.40	0.17	1.10	0.67	0.08	false	false	false	false	ULH
92	2383.32	0.00	12983.00	0.13	2.17	0.11	0.16	0.91	0.31	0.62	0.06	0.11	0.31	0.16	0.91	0.62	0.06	false	false	true	false	ULH
93	4620.64	0.01	18062.32	0.08	3.51	0.13	0.17	1.64	0.52	0.88	0.17	0.13	0.52	0.17	1.64	0.88	0.17	false	false	false	false	ULH
94	4751.21	0.02	13909.43	0.08	2.87	0.12	0.15	1.31	0.48	0.71	0.09	0.12	0.48	0.15	1.31	0.71	0.09	false	false	false	false	ULH
95	2303.43	0.01	13131.31	0.14	2.15	0.12	0.17	0.88	0.30	0.62	0.06	0.12	0.30	0.17	0.88	0.62	0.06	false	false	true	false	ULH
96	4053.67	0.00	17080.77	0.10	3.03	0.13	0.15	1.38	0.49	0.76	0.12	0.13	0.49	0.15	1.38	0.76	0.12	false	false	false	false	ULH
97	3208.93	0.02	16541.34	0.12	2.65	0.12	0.16	1.17	0.44	0.67	0.08	0.12	0.44	0.16	1.17	0.67	0.08	false	false	false	false	ULH
98	3194.51	0.01	19288.25	0.14	2.69	0.12	0.14	1.21	0.45	0.67	0.09	0.12	0.45	0.14	1.21	0.67	0.09	false	false	false	false	ULH
99	3959.58	0.01	7856.99	0.10	2.03	0.12	0.16	0.81	0.31	0.58	0.06	0.12	0.31	0.16	0.81	0.58	0.06	false	false	true	false	ULH

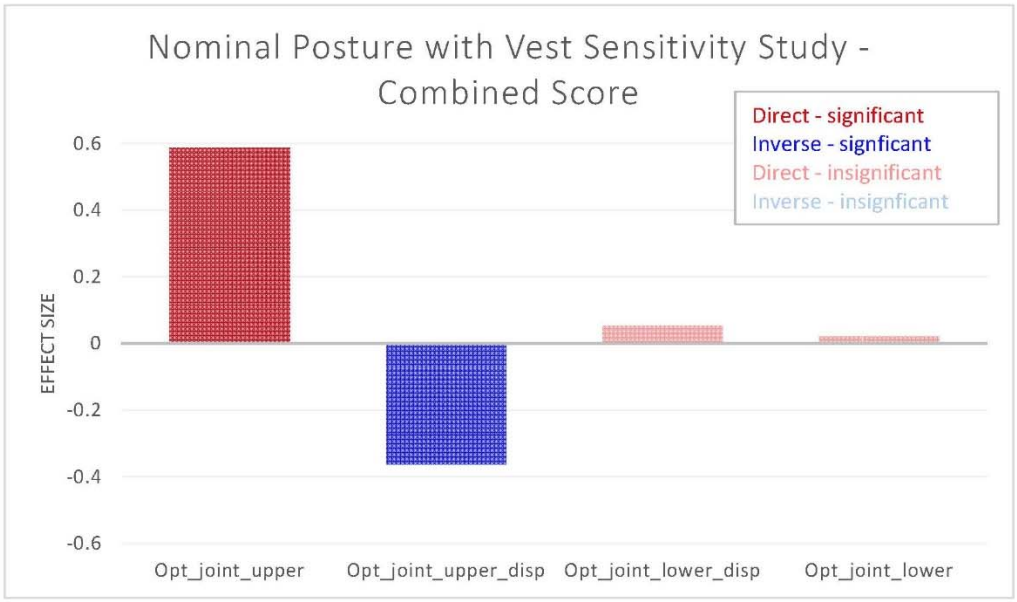
Nominal Posture with Vest Sensitivity Study - Combined Score
Direct - significant
Inverse - signficant
Direct - insignificant
Inverse - insignficant
EFFECT SIZE
0.6
0.4
0.2
0
-0.2
-0.4
-0.6
Opt_joint_upper
Opt_joint_upper_disp
Opt_joint_lower_disp
Opt_joint_lower

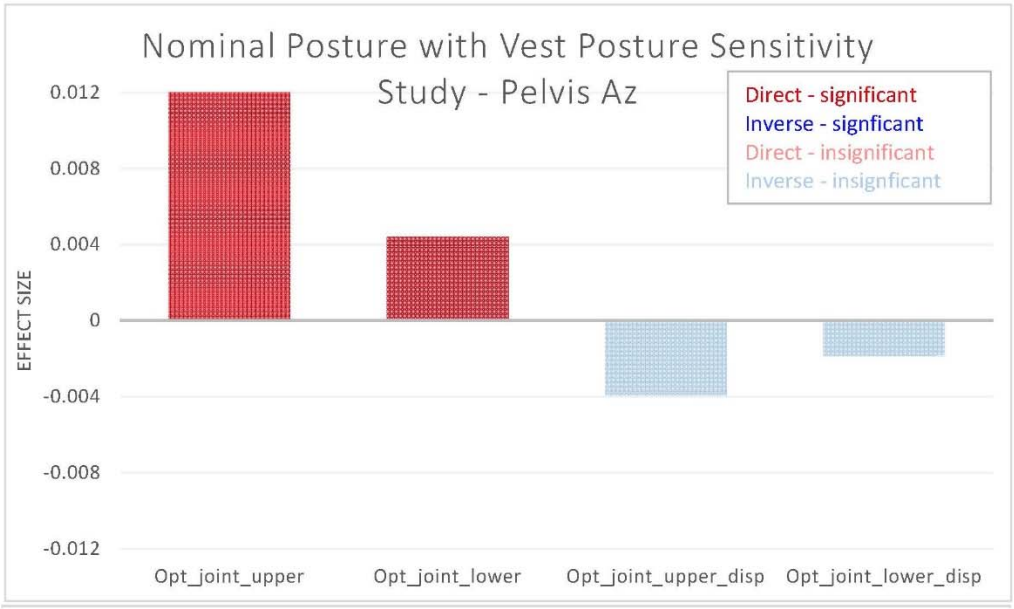
Nominal Posture with Vest Posture Sensitivity Study - Pelvis Az
Direct - significant
Inverse - signficant
Direct - insignificant
Inverse - insignficant
EFFECT SIZE
0.012
0.008
0.004
0
-0.004
-0.008
-0.012
Opt_joint_upper
Opt_joint_lower
Opt_joint_upper_disp
Opt_joint_lower_disp

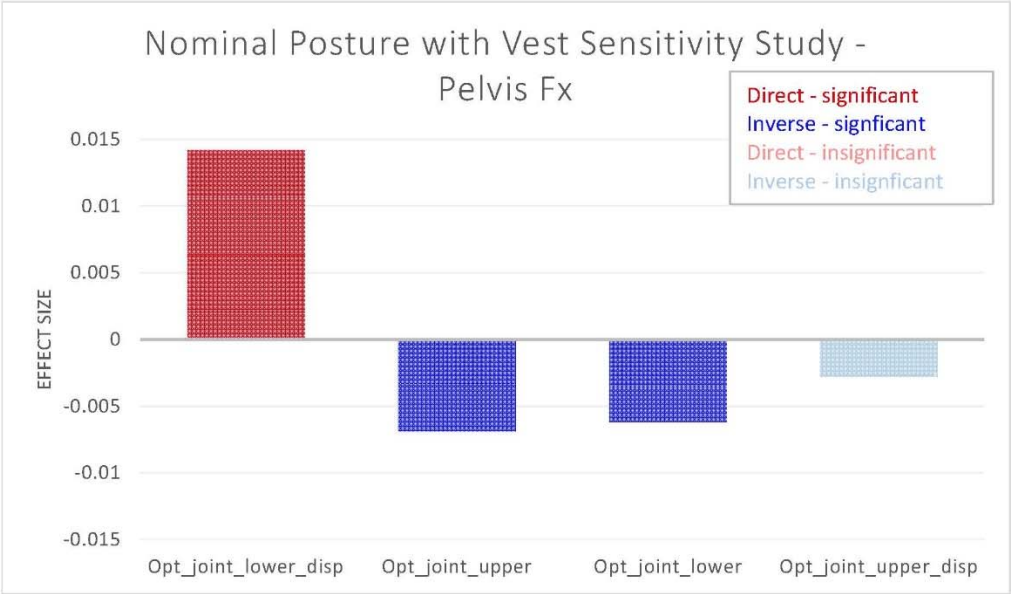
Nominal Posture with Vest Sensitivity Study - Pelvis Fx
Direct - significant
Inverse - signficant
Direct - insignificant
Inverse - insignficant
EFFECT SIZE
0.015
0.01
0.005
0
-0.005
-0.01
-0.015
Opt_joint_lower_disp
Opt_joint_upper
Opt_joint_lower
Opt_joint_upper_disp

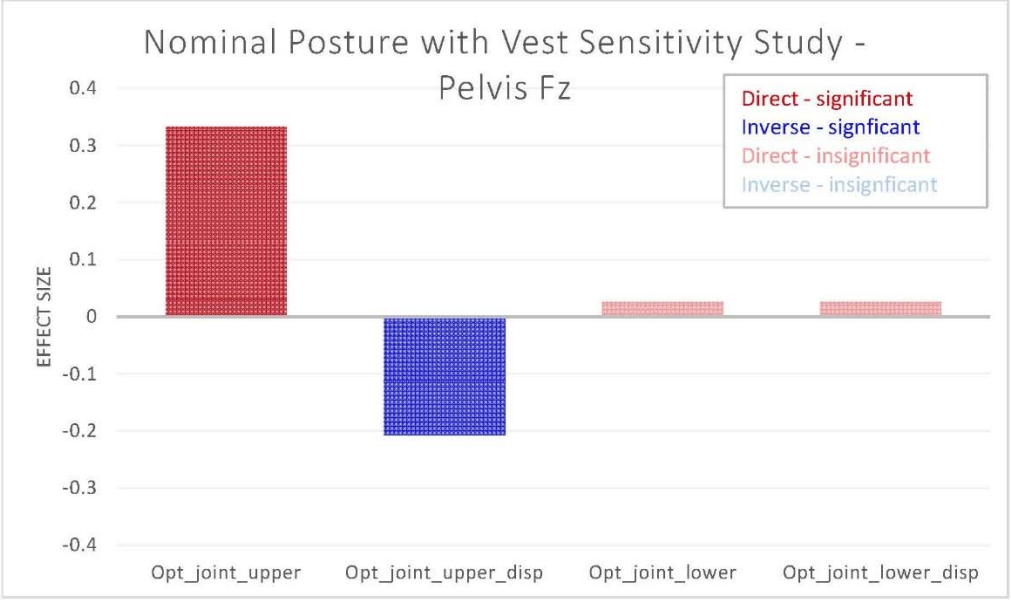
Nominal Posture with Vest Sensitivity Study - Pelvis Fz
Direct - significant
Inverse - signficant
Direct - insignificant
Inverse - insignficant
EFFECT SIZE
0.4
0.3
0.2
0.1
0
-0.1
-0.2
-0.3
-0.4
Opt_joint_upper
Opt_joint_upper_disp
Opt_joint_lower
Opt_joint_lower_disp

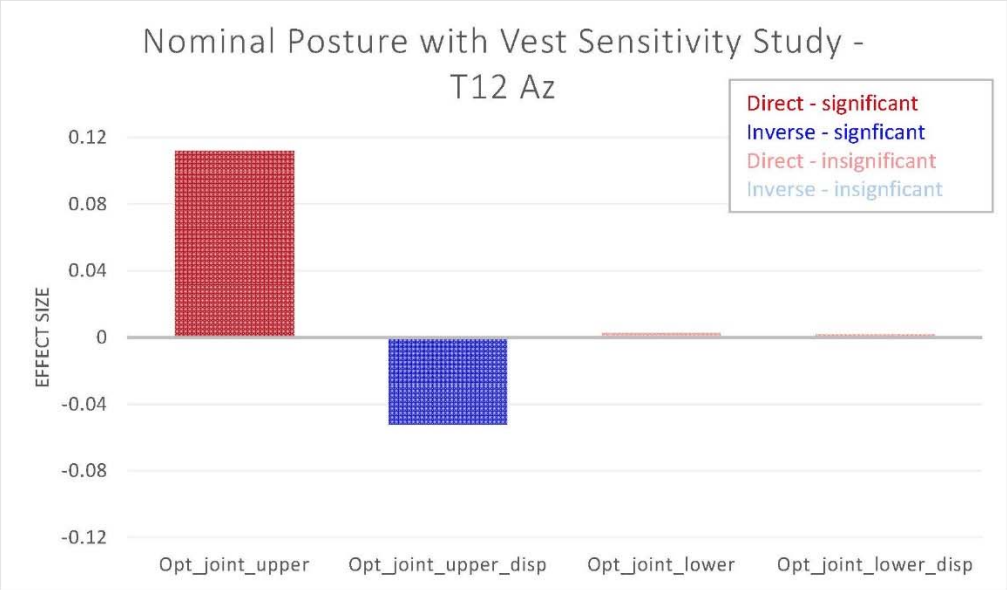
Nominal Posture with Vest Sensitivity Study - T12 Az
Direct - significant
Inverse - signficant
Direct - insignificant
Inverse - insignficant
EFFECT SIZE
0.12
0.08
0.04
0
-0.04
-0.08
-0.12
Opt_joint_upper
Opt_joint_upper_disp
Opt_joint_lower
Opt_joint_lower_disp

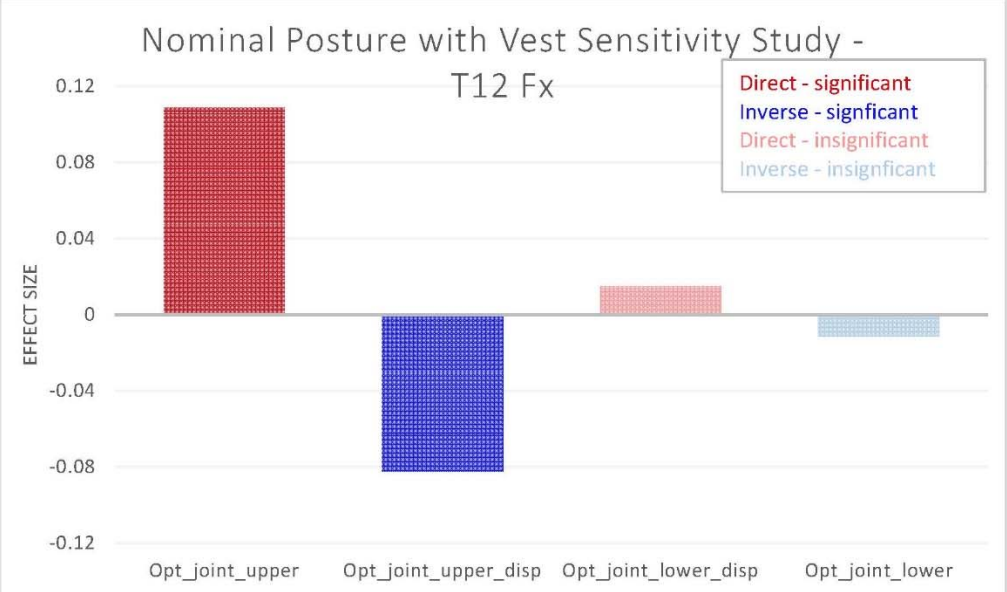
Nominal Posture with Vest Sensitivity Study - T12 Fx
Direct - significant
Inverse - signficant
Direct - insignificant
Inverse - insignficant
EFFECT SIZE
0.12
0.08
0.04
0
-0.04
-0.08
-0.12
Opt_joint_upper
Opt_joint_upper_disp
Opt_joint_lower_disp
Opt_joint_lower

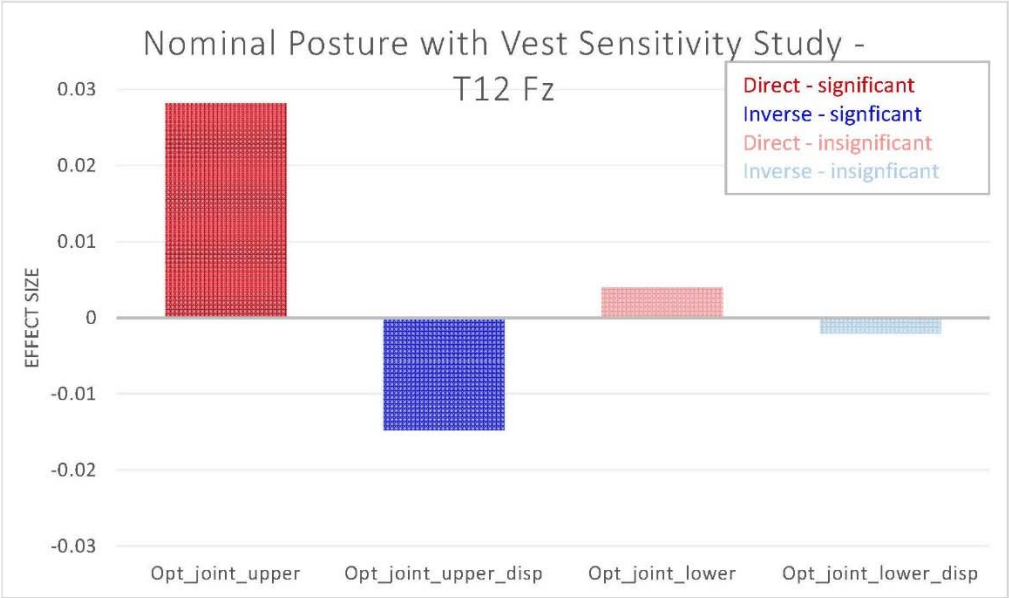
Nominal Posture with Vest Sensitivity Study - T12 Fz
Direct - significant
Inverse - signficant
Direct - insignificant
Inverse - insignficant
EFFECT SIZE
0.03
0.02
0.01
0
-0.01
-0.02
-0.03
Opt_joint_upper
Opt_joint_upper_disp
Opt_joint_lower
Opt_joint_lower_disp

```
#-- Frontier Design DB File Info ----------
#modeFRONTIER  - (c) ESTECO S.p.A.
#Design DB Table
#-----------------------------------------
#modeFRONTIER Version: modeFRONTIER 2017R5 5.7.1 b20171017
#Date: Sun Jan 27 17:10:45 EST 2019
#Project name: PMHS A Opt 2019-01-26 - rest - opt 150.prj
#Operating System: Windows 10 10.0 amd64
#Java (SDK/JRE) Version: 1.8.0_60
#Java Vendor: Oracle Corporation
#Java Vendor URL: http://java.oracle.com/
#User Name: KBosch
#-----------------------------------------
#Categories
<CATEGORIES classorPrefix="CLUSTER " useTableNamePrefix="false">
  <CATEGORY enabled="true" label="" name="SOBOL" symbolic="SQUARE,NONE,11,,0"/>
  <CATEGORY enabled="true" label="" name="USRDOE" symbolic="SQUARE,NONE,11,,0"/>
  <CATEGORY enabled="true" label="" name="NSGA2" symbolic="SQUARE,NONE,11,,0"/>
  <CATEGORY enabled="true" label="" name="TOA" symbolic="SQUARE,NONE,11,,0"/>
  <CATEGORY enabled="true" label="" name="DOT_APPROX" symbolic="SQUARE,NONE,11,,0"/>
  <CATEGORY enabled="true" label="" name="SIMPLEX" symbolic="SQUARE,NONE,11,,0"/>
  <CATEGORY enabled="true" label="" name="ULH" symbolic="SQUARE,NONE,11,,0"/>
  <CATEGORY enabled="true" label="" name="TILLH" symbolic="SQUARE,NONE,11,#DC3912,1,#DC3912"/>
  <CATEGORY enabled="true" label="" name="SIMPLEX_DOE" symbolic="SQUARE,NONE,11,#3366CC,1,#3366CC"/>
</CATEGORIES>

#
```

<ID>	Opt_joint_	Opt_joint_	Opt_joint_	Opt_joint_	Opt_joint_	Combined_	Pelvis_Az_	Pelvis_Fx_	Pelvis_Fz_	T12_Az_rc	T12_Fx_rc	T12_Fz_rc	Objective1	Constraint:	Constraint:	Constraint:	Constraint:	Constraint:	Constraint:	<ERROR>	<VIRTUAL>	<FEASIBLE	<MARKED>	<CATEGORY>
0	4530.08	0.02	11001.67	0.15	2.09	0.12	0.17	0.87	0.30	0.58	0.05	2.09	0.12	0.30	0.17	0.87	0.58	5.48E-03	false	false	true	false	SIMPLEX_DOE
1	2024.75	0.01	6946.71	0.13	1.75	0.08	0.17	0.67	0.23	0.49	0.05	1.75	0.08	0.29	0.17	0.67	0.49	5.21E-02	false	false	true	false	SIMPLEX_DOE
2	3947.04	0.02	14420.00	0.09	2.81	0.12	0.15	1.27	0.47	0.70	0.09	2.81	0.12	0.47	0.15	1.27	0.70	8.50E-02	false	false	false	false	SIMPLEX_DOE
3	3014.11	0.01	10835.41	0.12	2.12	0.12	0.17	0.86	0.30	0.61	0.03	2.12	0.12	0.30	0.17	0.86	0.51	5.56E-03	false	false	true	false	SIMPLEX_DOE
4	9771.81	0.00	18936.38	0.10	3.13	0.19	0.14	1.43	0.49	0.79	0.15	3.13	0.19	0.49	0.14	1.43	0.79	1.46E-01	false	false	false	false	SIMPLEX_DOE
5	2981.16	0.03	9000.00	0.14	1.55	0.07	0.17	0.50	0.25	0.42	0.05	1.55	0.07	0.26	0.17	0.50	0.42	5.00E-02	false	false	true	false	SIMPLEX
6	2323.03	0.02	5000.00	0.15	2.74	0.15	0.17	1.10	0.59	0.68	0.10	2.74	0.15	0.59	0.17	1.10	0.58	1.04E-01	false	false	false	false	SIMPLEX
7	3847.04	0.02	11891.87	0.11	2.32	0.17	0.15	1.00	0.35	0.62	0.07	2.32	0.17	0.35	0.15	1.00	0.62	5.79E-03	false	false	true	false	SIMPLEX
8	3341.03	0.02	10166.90	0.12	2.08	0.12	0.17	0.82	0.30	0.60	0.08	2.08	0.12	0.30	0.17	0.82	0.50	5.93E-02	false	false	true	false	SIMPLEX
9	3328.47	0.02	5733.30	0.15	2.94	0.15	0.17	1.22	0.50	0.76	0.11	2.94	0.15	0.60	0.17	1.22	0.76	1.07E-01	false	false	true	false	SIMPLEX
10	3140.43	0.01	9557.35	0.13	2.04	0.12	0.18	0.79	0.31	0.59	0.06	2.04	0.12	0.31	0.18	0.79	0.59	5.03E-03	false	false	true	false	SIMPLEX
11	2000.00	0.01	5000.00	0.11	1.56	0.06	0.17	0.50	0.24	0.44	0.05	1.56	0.06	0.24	0.17	0.50	0.44	5.03E-02	false	false	true	false	SIMPLEX
12	2000.00	0.01	5000.00	0.13	1.49	0.05	0.17	0.56	0.23	0.43	0.05	1.49	0.05	0.23	0.17	0.55	0.43	4.93E-02	false	false	true	false	SIMPLEX
13	2000.00	0.01	5000.00	0.13	1.50	0.05	0.17	0.56	0.23	0.43	0.05	1.50	0.05	0.23	0.17	0.56	0.43	4.96E-02	false	false	true	false	SIMPLEX
14	2130.02	0.01	5073.35	0.13	1.62	0.07	0.17	0.61	0.25	0.46	0.05	1.62	0.07	0.26	0.17	0.61	0.46	4.85E-02	false	false	true	false	SIMPLEX
15	2187.66	0.01	5486.68	0.13	1.56	0.06	0.17	0.59	0.25	0.44	0.05	1.56	0.06	0.25	0.17	0.59	0.44	4.93E-02	false	false	true	false	SIMPLEX
16	2216.48	0.01	5243.34	0.13	1.54	0.06	0.17	0.58	0.24	0.44	0.05	1.54	0.06	0.24	0.17	0.58	0.44	4.96E-02	false	false	true	false	SIMPLEX
17	2398.83	0.02	5121.67	0.15	1.51	0.06	0.17	0.57	0.24	0.42	0.05	1.51	0.06	0.24	0.17	0.57	0.42	4.80E-02	false	false	true	false	SIMPLEX
18	2000.00	0.00	5182.50	0.12	1.52	0.06	0.17	0.57	0.24	0.43	0.05	1.52	0.06	0.24	0.17	0.57	0.43	4.91E-02	false	false	true	false	SIMPLEX
19	2082.94	0.01	5000.00	0.14	1.47	0.05	0.17	0.56	0.22	0.42	0.05	1.47	0.05	0.22	0.17	0.56	0.42	4.76E-02	false	false	true	false	SIMPLEX
20	2340.88	0.02	5000.00	0.15	1.47	0.05	0.18	0.55	0.23	0.41	0.05	1.47	0.05	0.23	0.18	0.55	0.41	4.85E-02	false	false	true	false	SIMPLEX
21	2352.39	0.02	5050.83	0.14	1.49	0.06	0.18	0.57	0.23	0.42	0.05	1.49	0.06	0.23	0.18	0.57	0.42	4.78E-02	false	true	false	false	SIMPLEX
22	2388.10	0.02	5000.42	0.15	2.89	0.15	0.13	1.18	0.59	0.74	0.11	2.89	0.15	0.59	0.13	1.18	0.74	1.07E-01	false	false	true	false	SIMPLEX
23	2097.03	0.01	5007.80	0.13	1.49	0.05	0.17	0.56	0.23	0.42	0.05	1.49	0.05	0.23	0.17	0.56	0.42	4.86E-02	false	false	true	false	SIMPLEX
24	2000.00	0.01	5000.00	0.13	1.49	0.05	0.17	0.56	0.23	0.43	0.05	1.49	0.05	0.23	0.17	0.56	0.43	4.88E-02	false	false	true	false	SIMPLEX
25	2260.42	0.02	5003.80	0.15	1.47	0.05	0.18	0.56	0.23	0.41	0.05	1.47	0.05	0.23	0.18	0.56	0.41	4.73E-02	false	false	true	false	SIMPLEX
26	2390.63	0.02	5005.79	0.15	3.06	0.15	0.14	1.27	0.60	0.78	0.11	3.06	0.15	0.60	0.14	1.27	0.78	1.09E-01	false	false	true	false	SIMPLEX
27	2245.09	0.02	5000.00	0.15	1.47	0.05	0.18	0.55	0.23	0.41	0.05	1.47	0.05	0.23	0.18	0.55	0.41	4.71E-02	false	true	false	false	SIMPLEX
28	2464.67	0.03	5001.90	0.15	3.11	0.15	0.15	1.30	0.60	0.80	0.11	3.11	0.15	0.60	0.15	1.30	0.80	1.10E-01	false	false	true	false	SIMPLEX
29	2115.17	0.02	5000.48	0.14	1.48	0.05	0.18	0.56	0.23	0.42	0.05	1.48	0.05	0.23	0.18	0.56	0.42	4.78E-02	false	true	false	false	SIMPLEX
30	2348.50	0.02	5001.43	0.15	2.95	0.15	0.12	1.22	0.60	0.76	0.11	2.95	0.15	0.60	0.12	1.22	0.76	1.08E-01	false	false	true	false	SIMPLEX
31	2174.25	0.02	5000.71	0.14	1.48	0.05	0.18	0.56	0.23	0.42	0.05	1.48	0.05	0.23	0.18	0.56	0.42	4.75E-02	false	true	false	false	SIMPLEX
32	2290.42	0.02	5001.19	0.15	1.47	0.05	0.18	0.56	0.23	0.41	0.05	1.47	0.05	0.23	0.18	0.56	0.41	4.73E-02	false	true	false	false	SIMPLEX
33	2098.55	0.01	5002.50	0.14	1.46	0.05	0.17	0.55	0.22	0.41	0.05	1.46	0.05	0.22	0.17	0.55	0.41	4.69E-02	false	true	false	false	SIMPLEX
34	2000.00	0.01	5003.74	0.14	1.45	0.05	0.17	0.55	0.22	0.41	0.05	1.45	0.05	0.22	0.17	0.55	0.41	4.70E-02	false	true	false	false	SIMPLEX
35	2215.03	0.02	5004.27	0.15	2.91	0.13	0.12	1.20	0.59	0.74	0.11	2.91	0.13	0.59	0.12	1.20	0.74	1.07E-01	false	false	true	false	SIMPLEX
36	2140.95	0.01	5001.09	0.14	1.47	0.05	0.17	0.56	0.23	0.42	0.05	1.47	0.05	0.23	0.17	0.55	0.42	4.73E-03	false	true	false	false	SIMPLEX
37	2077.81	0.01	5000.00	0.14	1.46	0.05	0.17	0.55	0.22	0.41	0.05	1.46	0.05	0.22	0.17	0.55	0.41	4.67E-02	false	true	false	false	SIMPLEX
38	2000.00	0.00	5001.23	0.14	1.46	0.06	0.17	0.55	0.22	0.41	0.05	1.46	0.06	0.22	0.17	0.55	0.41	4.73E-02	false	true	false	false	SIMPLEX
39	2020.49	0.01	5001.38	0.15	1.45	0.05	0.17	0.55	0.22	0.41	0.05	1.45	0.05	0.22	0.17	0.55	0.41	4.70E-02	false	true	false	false	SIMPLEX
40	2000.00	0.00	5001.55	0.15	1.44	0.06	0.17	0.53	0.22	0.41	0.05	1.44	0.06	0.22	0.17	0.53	0.41	4.78E-02	false	true	false	false	SIMPLEX
41	2000.00	0.00	5003.25	0.14	NaN	NaN	NaN	NaN	NaN	NaN	NaN	NaN	NaN	NaN	NaN	NaN	NaN	true	false	true	false	false	SIMPLEX
42	2132.27	0.01	5000.81	0.15	1.45	0.05	0.17	0.55	0.22	0.41	0.05	1.46	0.05	0.22	0.17	0.55	0.41	4.67E-03	false	true	false	false	SIMPLEX
43	2000.00	0.00	5002.44	0.14	NaN	NaN	NaN	NaN	NaN	NaN	NaN	NaN	NaN	NaN	NaN	NaN	NaN	NaN	true	false	true	false	SIMPLEX
44	2075.86	0.01	5001.22	0.14	1.45	0.05	0.17	0.55	0.22	0.41	0.05	1.45	0.05	0.22	0.17	0.55	0.41	4.86E-02	false	true	false	false	SIMPLEX
45	2075.84	0.01	5002.03	0.15	1.45	0.05	0.17	0.55	0.22	0.41	0.05	1.45	0.05	0.22	0.17	0.55	0.41	4.85E-03	false	true	false	false	SIMPLEX
46	2000.00	0.00	5004.27	0.15	1.44	0.06	0.17	0.54	0.22	0.41	0.05	1.44	0.06	0.22	0.17	0.54	0.41	4.76E-02	false	true	false	false	SIMPLEX
47	2000.00	0.00	5004.57	0.15	1.43	0.06	0.17	0.52	0.22	0.41	0.05	1.43	0.06	0.22	0.17	0.52	0.41	4.81E-02	false	true	false	false	SIMPLEX
48	2038.47	0.00	5007.45	0.15	2.63	0.14	0.24	1.03	0.49	0.62	0.11	2.63	0.14	0.49	0.24	1.03	0.62	1.06E-01	false	false	true	false	SIMPLEX
49	2009.60	0.00	5003.42	0.14	1.45	0.06	0.17	0.54	0.22	0.41	0.05	1.45	0.06	0.22	0.17	0.54	0.41	4.72E-02	false	true	false	false	SIMPLEX
50	2028.81	0.00	5002.78	0.15	1.44	0.06	0.17	0.54	0.22	0.41	0.05	1.44	0.06	0.22	0.17	0.54	0.41	4.78E-02	false	true	false	false	SIMPLEX
51	2000.00	0.00	5004.55	0.15	NaN	NaN	NaN	NaN	NaN	NaN	NaN	NaN	NaN	NaN	NaN	NaN	NaN	true	false	true	false	false	SIMPLEX
52	2042.02	0.01	5002.65	0.15	1.44	0.06	0.17	0.54	0.22	0.41	0.05	1.44	0.06	0.22	0.17	0.54	0.41	4.71E-02	false	true	false	false	SIMPLEX
53	2000.00	0.00	5002.92	0.15	NaN	NaN	NaN	NaN	NaN	NaN	NaN	NaN	NaN	NaN	NaN	NaN	NaN	true	false	true	false	false	SIMPLEX
54	2024.61	0.00	5002.98	0.15	1.44	0.06	0.17	0.54	0.22	0.41	0.05	1.44	0.06	0.22	0.17	0.54	0.41	4.75E-03	false	true	false	false	SIMPLEX
55	2000.00	0.00	5003.61	0.15	NaN	NaN	NaN	NaN	NaN	NaN	NaN	NaN	NaN	NaN	NaN	NaN	NaN	true	false	true	false	false	SIMPLEX
56	2015.91	0.00	5002.13	0.15	1.44	0.06	0.17	0.54	0.22	0.41	0.05	1.44	0.06	0.22	0.17	0.54	0.41	4.76E-02	false	true	false	false	SIMPLEX
57	2027.35	0.00	5001.75	0.15	1.43	0.06	0.17	0.53	0.22	0.41	0.05	1.43	0.06	0.22	0.17	0.53	0.41	4.80E-03	false	true	false	false	SIMPLEX
58	2033.54	0.00	5000.49	0.15	NaN	NaN	NaN	NaN	NaN	NaN	NaN	NaN	NaN	NaN	NaN	NaN	NaN	true	false	true	false	false	SIMPLEX
59	2009.68	0.00	5002.19	0.15	NaN	NaN	NaN	NaN	NaN	NaN	NaN	NaN	NaN	NaN	NaN	NaN	NaN	true	false	true	false	false	SIMPLEX
60	2014.35	0.00	5002.90	0.15	1.44	0.06	0.17	0.53	0.22	0.41	0.05	1.44	0.06	0.22	0.17	0.53	0.41	4.78E-03	false	true	false	false	SIMPLEX
61	2032.76	0.00	5004.45	0.15	2.63	0.14	0.24	1.03	0.49	0.62	0.11	2.63	0.14	0.49	0.24	1.03	0.62	1.06E-01	false	false	true	false	SIMPLEX
62	2008.10	0.00	5002.27	0.15	1.44	0.06	0.17	0.53	0.22	0.41	0.05	1.44	0.06	0.22	0.17	0.53	0.41	4.70E-02	false	true	false	false	SIMPLEX
63	2015.33	0.00	5002.79	0.15	1.43	0.06	0.17	0.52	0.22	0.41	0.05	1.43	0.06	0.22	0.17	0.52	0.41	4.81E-03	false	true	false	false	SIMPLEX
64	2015.82	0.00	5002.73	0.15	NaN	NaN	NaN	NaN	NaN	NaN	NaN	NaN	NaN	NaN	NaN	NaN	NaN	true	false	true	false	false	SIMPLEX
65	2000.00	0.00	5002.01	0.15	NaN	NaN	NaN	NaN	NaN	NaN	NaN	NaN	NaN	NaN	NaN	NaN	NaN	true	false	true	false	false	SIMPLEX
66	2020.14	0.00	5002.81	0.15	1.43	0.06	0.17	0.53	0.22	0.41	0.05	1.43	0.06	0.22	0.17	0.53	0.41	4.79E-03	false	true	false	false	SIMPLEX
67	2020.73	0.00	5003.69	0.15	1.43	0.07	0.17	0.52	0.22	0.40	0.05	1.43	0.07	0.22	0.17	0.52	0.40	4.83E-02	false	true	false	false	SIMPLEX
68	2017.59	0.00	5003.33	0.15	1.43	0.06	0.17	0.52	0.22	0.41	0.05	1.43	0.06	0.22	0.17	0.52	0.41	4.81E-02	false	true	false	false	SIMPLEX
69	2007.50	0.00	5003.41	0.15	NaN	NaN	NaN	NaN	NaN	NaN	NaN	NaN	NaN	NaN	NaN	NaN	NaN	true	false	true	false	false	SIMPLEX
70	2015.98	0.00	5002.96	0.15	1.43	0.06	0.17	0.53	0.22	0.41	0.05	1.43	0.06	0.22	0.17	0.53	0.41	4.80E-02	false	true	false	false	SIMPLEX
71	2035.13	0.00	5000.85	0.15	2.64	0.14	0.24	1.03	0.50	0.63	0.11	2.64	0.14	0.50	0.24	1.03	0.63	1.06E-01	false	false	true	false	SIMPLEX
72	2009.03	0.00	5003.64	0.15	1.43	0.06	0.17	0.53	0.22	0.41	0.05	1.43	0.06	0.22	0.17	0.53	0.41	4.81E-03	false	true	false	false	SIMPLEX
73	2027.10	0.00	5001.78	0.15	1.43	0.06	0.17	0.53	0.22	0.41	0.05	1.43	0.06	0.22	0.17	0.53	0.41	4.81E-02	false	true	false	false	SIMPLEX
74	2035.13	0.00	5000.85	0.15	2.64	0.14	0.24	1.03	0.50	0.63	0.11	2.64	0.14	0.50	0.24	1.03	0.63	1.06E-01	false	false	true	false	SIMPLEX
75	2015.14	0.00	5003.68	0.15	1.43	0.06	0.17	0.53	0.22	0.41	0.05	1.43	0.06	0.22	0.17	0.53	0.41	4.81E-03	false	true	false	false	SIMPLEX
76	2013.03	0.00	5004.65	0.15	1.43	0.06	0.17	0.52	0.22	0.41	0.05	1.43	0.06	0.22	0.17	0.52	0.41	4.81E-02	false	true	false	false	SIMPLEX
77	2019.55	0.00	5003.31	0.15	1.43	0.07	0.17	0.52	0.22	0.40	0.05	1.43	0.07	0.22	0.17	0.52	0.40	4.83E-02	false	true	false	false	SIMPLEX
78	2017.63	0.00	5003.05	0.15	1.43	0.06	0.17	0.53	0.22	0.41	0.05	1.43	0.06	0.22	0.17	0.53	0.41	4.80E-02	false	true	false	false	SIMPLEX
79	2018.91	0.00	5003.22	0.15	1.43	0.06	0.17	0.52	0.22	0.41	0.05	1.43	0.06	0.22	0.17	0.52	0.41	4.82E-02	false	true	false	false	SIMPLEX
80	2019.59	0.00	5002.80	0.15	1.43	0.06	0.17	0.53	0.22	0.41	0.05	1.43	0.06	0.22	0.17	0.53	0.41	4.81E-02	false	true	false	false	SIMPLEX
81	2018.62	0.00	5002.83	0.15	1.43	0.06	0.17	0.53	0.22	0.41	0.05	1.43	0.06	0.22	0.17	0.53	0.41	4.80E-03	false	true	false	false	SIMPLEX
82	2023.84	0.00	5003.23	0.15	1.43	0.06	0.17	0.53	0.22	0.41	0.05	1.43	0.06	0.22	0.17	0.53	0.41	4.80E-02	false	true	false	false	SIMPLEX
83	2028.10	0.00	5003.53	0.15	2.65	0.14	0.24	1.03	0.50	0.63	0.11	2.65	0.14	0.50	0.24	1.03	0.63	1.06E-01	false	true	false	false	SIMPLEX
84	2023.16	0.00	5003.47	0.15	2.61	0.14	0.23	1.03	0.49	0.62	0.11	2.61	0.14	0.49	0.23	1.03	0.62	1.06E-01	false	false	true	false	SIMPLEX
85	2019.76	0.00	5002.99	0.15	1.43	0.06	0.17	0.53	0.22	0.41	0.05	1.43	0.06	0.22	0.17	0.53	0.41	4.80E-02	false	true	false	false	SIMPLEX
86	2011.01	0.00	5005.13	0.15	1.43	0.06	0.17	0.52	0.22	0.41	0.05	1.43	0.06	0.22	0.17	0.52	0.41	4.81E-02	false	true	false	false	SIMPLEX
87	2007.97	0.00	5005.80	0.15	1.43	0.06	0.17	0.52	0.22	0.41	0.05	1.43	0.06	0.22	0.17	0.52	0.41	4.81E-03	false	true	false	false	SIMPLEX
88	2013.96	0.00	5004.99	0.15	1.43	0.06	0.17	0.52	0.22	0.41	0.05	1.43	0.06	0.22	0.17	0.52	0.41	4.81E-02	false	true	false	false	SIMPLEX
89	2011.10	0.00	5005.08	0.15	1.43	0.06	0.17	0.52	0.22	0.41	0.05	1.43	0.06	0.22	0.17	0.52	0.41	4.82E-02	false	true	false	false	SIMPLEX
90	2011.34	0.00	5006.14	0.15	1.43	0.06	0.17	0.52	0.22	0.41	0.05	1.43	0.06	0.22	0.17	0.52	0.41	4.81E-03	false	true	false	false	SIMPLEX
91	2007.22	0.00	5007.76	0.15	1.43	0.06	0.17	0.52	0.22	0.41	0.05	1.43	0.06	0.22	0.17	0.52	0.41	4.81E-02	false	true	false	false	SIMPLEX
92	2025.00	0.00	5005.93	0.15	2.62	0.14	0.23	1.03	0.49	0.62	0.11	2.62	0.14	0.49	0.23	1.03	0.62	1.06E-01	false	false	true	false	SIMPLEX
93	2013.57	0.00	5004.97	0.15	1.43	0.06	0.17	0.52	0.22	0.41	0.05	1.43	0.06	0.22	0.17	0.52	0.41	4.81E-03	false	true	false	false	SIMPLEX
94	2000.00	0.00	5006.14	0.15	NaN	NaN	NaN	NaN	NaN	NaN	NaN	NaN	NaN	NaN	NaN	NaN	NaN	true	false	true	false	false	SIMPLEX
95	2017.64	0.00	5004.50	0.15	1.43	0.06	0.17	0.53	0.22	0.41	0.05	1.43	0.06	0.22	0.17	0.53	0.41	4.81E-02	false	true	false	false	SIMPLEX
96	2005.73	0.00	5005.90	0.15	1.43	0.07	0.17	0.52	0.22	0.41	0.05	1.43	0.07	0.22	0.17	0.52	0.41	4.81E-03	false	true	false	false	SIMPLEX
97	2014.54	0.00	5005.10	0.15	1.43	0.06	0.17	0.53	0.22	0.41	0.05	1.43	0.06	0.22	0.17	0.53	0.41	4.81E-02	false	true	false	false	SIMPLEX
98	2009.85	0.00	5006.52	0.15	1.43	0.06	0.17	0.52	0.22	0.41	0.05	1.43	0.06	0.22	0.17	0.52	0.41	4.81E-02	false	true	false	false	SIMPLEX
99	2008.02	0.00	5007.29	0.15	1.43	0.06	0.17	0.52	0.22	0.41	0.05	1.43	0.06	0.22	0.17	0.52	0.41	4.81E-02	false	true	false	false	SIMPLEX

100	2010.87	0.00	5007.44	0.15	1.43	0.06	0.17	0.52	0.22	0.41	0.05	1.43	0.06	0.22	0.17	0.52	0.41	4.81E-02	false	true	false	SIMPLEX
101	2005.51	0.00	5008.64	0.15	1.43	0.06	0.17	0.52	0.22	0.41	0.05	1.43	0.06	0.22	0.17	0.52	0.41	4.81E-02	false	true	false	SIMPLEX
102	2001.82	0.00	5010.58	0.15	1.43	0.06	0.17	0.52	0.22	0.41	0.05	1.43	0.06	0.22	0.17	0.52	0.41	4.81E-02	false	true	false	SIMPLEX
103	2000.00	0.00	5013.38	0.15	1.43	0.06	0.17	0.52	0.22	0.41	0.05	1.43	0.06	0.22	0.17	0.52	0.41	4.81E-02	false	true	false	SIMPLEX
104	2004.07	0.00	5010.62	0.15	2.61	0.14	0.23	1.03	0.49	0.61	0.11	2.61	0.14	0.49	0.23	1.03	0.51	1.06E-01	false	false	false	SIMPLEX
105	2005.66	0.00	5008.47	0.15	1.43	0.06	0.17	0.52	0.22	0.41	0.05	1.43	0.06	0.22	0.17	0.52	0.41	4.81E-02	false	true	false	SIMPLEX
106	2007.26	0.00	5009.65	0.15	1.43	0.06	0.17	0.52	0.22	0.41	0.05	1.43	0.06	0.22	0.17	0.52	0.41	4.81E-02	false	true	false	SIMPLEX
107	2005.42	0.00	5010.41	0.15	1.43	0.06	0.17	0.52	0.22	0.41	0.05	1.43	0.06	0.22	0.17	0.52	0.41	4.81E-02	false	true	false	SIMPLEX
108	2000.00	0.00	5012.93	0.15	1.43	0.06	0.17	0.52	0.22	0.41	0.05	1.43	0.06	0.22	0.17	0.52	0.41	4.81E-02	false	true	false	SIMPLEX
109	2000.00	0.00	5012.35	0.15	1.43	0.06	0.17	0.52	0.22	0.41	0.05	1.43	0.06	0.22	0.17	0.52	0.41	4.81E-02	false	true	false	SIMPLEX
110	2000.00	0.00	5017.24	0.15	2.61	0.14	0.23	1.03	0.49	0.61	0.11	2.61	0.14	0.49	0.23	1.03	0.51	1.06E-01	false	false	false	SIMPLEX
111	2004.81	0.00	5009.78	0.15	1.43	0.06	0.17	0.52	0.22	0.41	0.05	1.43	0.06	0.22	0.17	0.52	0.41	4.81E-02	false	true	false	SIMPLEX
112	2000.00	0.00	5014.75	0.15	1.43	0.06	0.17	0.52	0.22	0.41	0.05	1.43	0.06	0.22	0.17	0.52	0.41	4.81E-02	false	true	false	SIMPLEX
113	2003.21	0.00	5011.88	0.15	1.43	0.06	0.17	0.52	0.22	0.41	0.05	1.43	0.06	0.22	0.17	0.52	0.41	4.81E-02	false	true	false	SIMPLEX
114	2001.60	0.00	5012.58	0.15	1.43	0.06	0.17	0.52	0.22	0.41	0.05	1.43	0.06	0.22	0.17	0.52	0.41	4.81E-02	false	true	false	SIMPLEX
115	2000.00	0.00	5014.42	0.15	1.43	0.06	0.17	0.52	0.22	0.41	0.05	1.43	0.06	0.22	0.17	0.52	0.41	4.81E-02	false	true	false	SIMPLEX
116	2000.80	0.00	5013.00	0.15	1.43	0.06	0.17	0.52	0.22	0.41	0.05	1.43	0.06	0.22	0.17	0.52	0.41	4.80E-02	false	true	false	SIMPLEX
117	2000.40	0.00	5014.38	0.15	2.61	0.14	0.23	1.03	0.49	0.61	0.11	2.61	0.14	0.49	0.23	1.03	0.51	1.06E-01	false	false	false	SIMPLEX
118	2000.10	0.00	5013.29	0.15	1.43	0.06	0.17	0.52	0.22	0.41	0.05	1.43	0.06	0.22	0.17	0.52	0.41	4.80E-02	false	true	false	SIMPLEX
119	2000.45	0.00	5011.82	0.15	1.43	0.06	0.17	0.52	0.22	0.41	0.05	1.43	0.06	0.22	0.17	0.52	0.41	4.81E-02	false	true	false	SIMPLEX
120	2000.11	0.00	5014.02	0.15	1.43	0.06	0.17	0.52	0.22	0.41	0.05	1.43	0.06	0.22	0.17	0.52	0.41	4.81E-02	false	true	false	SIMPLEX
121	2000.51	0.00	5015.06	0.15	1.43	0.06	0.17	0.52	0.22	0.41	0.05	1.43	0.06	0.22	0.17	0.52	0.41	4.81E-02	false	true	false	SIMPLEX
122	2000.13	0.00	5013.03	0.15	1.43	0.06	0.17	0.52	0.22	0.41	0.05	1.43	0.06	0.22	0.17	0.52	0.41	4.81E-02	false	true	false	SIMPLEX
123	2000.57	0.00	5012.30	0.15	1.43	0.06	0.17	0.52	0.22	0.41	0.05	1.43	0.06	0.22	0.17	0.52	0.41	4.81E-02	false	true	false	SIMPLEX
124	2000.71	0.00	5012.93	0.15	1.43	0.06	0.17	0.52	0.22	0.41	0.05	1.43	0.06	0.22	0.17	0.52	0.41	4.81E-02	false	true	false	SIMPLEX
125	2000.00	0.00	5013.04	0.15	1.43	0.06	0.17	0.52	0.22	0.41	0.05	1.43	0.06	0.22	0.17	0.52	0.41	4.81E-02	false	true	false	SIMPLEX
126	2000.75	0.00	5013.09	0.15	1.43	0.06	0.17	0.52	0.22	0.41	0.05	1.43	0.06	0.22	0.17	0.52	0.41	4.80E-02	false	true	false	SIMPLEX
127	2000.19	0.00	5013.05	0.15	1.43	0.06	0.17	0.52	0.22	0.41	0.05	1.43	0.06	0.22	0.17	0.52	0.41	4.81E-02	false	true	false	SIMPLEX
128	2000.12	0.00	5013.52	0.15	1.43	0.06	0.17	0.52	0.22	0.41	0.05	1.43	0.06	0.22	0.17	0.52	0.41	4.81E-02	false	true	false	SIMPLEX
129	2000.34	0.00	5013.15	0.15	1.43	0.06	0.17	0.52	0.22	0.41	0.05	1.43	0.06	0.22	0.17	0.52	0.41	4.81E-02	false	true	false	SIMPLEX
130	2000.41	0.00	5013.47	0.15	1.43	0.06	0.17	0.52	0.22	0.41	0.05	1.43	0.06	0.22	0.17	0.52	0.41	4.81E-02	false	true	false	SIMPLEX
131	2000.06	0.00	5013.53	0.15	1.43	0.06	0.17	0.52	0.22	0.41	0.05	1.43	0.06	0.22	0.17	0.52	0.41	4.81E-02	false	true	false	SIMPLEX
132	2000.44	0.00	5013.55	0.15	1.43	0.06	0.17	0.52	0.22	0.41	0.05	1.43	0.06	0.22	0.17	0.52	0.41	4.81E-02	false	true	false	SIMPLEX
133	2000.53	0.00	5013.58	0.15	1.43	0.06	0.17	0.52	0.22	0.41	0.05	1.43	0.06	0.22	0.17	0.52	0.41	4.81E-02	false	true	false	SIMPLEX
134	2000.26	0.00	5013.55	0.15	1.43	0.06	0.17	0.52	0.22	0.41	0.05	1.43	0.06	0.22	0.17	0.52	0.41	4.81E-02	false	true	false	SIMPLEX
135	2000.39	0.00	5013.55	0.15	1.43	0.06	0.17	0.52	0.22	0.41	0.05	1.43	0.06	0.22	0.17	0.52	0.41	4.81E-02	false	true	false	SIMPLEX
136	2000.44	0.00	5013.37	0.15	1.43	0.06	0.17	0.52	0.22	0.41	0.05	1.43	0.06	0.22	0.17	0.52	0.41	4.81E-02	false	true	false	SIMPLEX
137	2000.23	0.00	5013.50	0.15	1.43	0.06	0.17	0.52	0.22	0.41	0.05	1.43	0.06	0.22	0.17	0.52	0.41	4.81E-02	false	true	false	SIMPLEX
138	2000.38	0.00	5013.33	0.15	1.43	0.06	0.17	0.52	0.22	0.41	0.05	1.43	0.06	0.22	0.17	0.52	0.41	4.81E-02	false	true	false	SIMPLEX
139	2000.39	0.00	5013.35	0.15	1.43	0.06	0.17	0.52	0.22	0.41	0.05	1.43	0.06	0.22	0.17	0.52	0.41	4.81E-02	false	true	false	SIMPLEX
140	2000.32	0.00	5013.42	0.15	1.43	0.06	0.17	0.52	0.22	0.41	0.05	1.43	0.06	0.22	0.17	0.52	0.41	4.81E-02	false	true	false	SIMPLEX
141	2000.33	0.00	5013.39	0.15	1.43	0.06	0.17	0.52	0.22	0.41	0.05	1.43	0.06	0.22	0.17	0.52	0.41	4.81E-02	false	true	false	SIMPLEX
142	2000.28	0.00	5013.40	0.15	1.43	0.06	0.17	0.52	0.22	0.41	0.05	1.43	0.06	0.22	0.17	0.52	0.41	4.81E-02	false	true	false	SIMPLEX
143	2000.23	0.00	5013.42	0.15	1.43	0.06	0.17	0.52	0.22	0.41	0.05	1.43	0.06	0.22	0.17	0.52	0.41	4.81E-02	false	true	false	SIMPLEX
144	2000.31	0.00	5013.35	0.15	1.43	0.06	0.17	0.52	0.22	0.41	0.05	1.43	0.06	0.22	0.17	0.52	0.41	4.81E-02	false	true	false	SIMPLEX
145	2000.31	0.00	5013.37	0.15	1.43	0.06	0.17	0.52	0.22	0.41	0.05	1.43	0.06	0.22	0.17	0.52	0.41	4.81E-02	false	true	false	SIMPLEX
146	2000.29	0.00	5013.71	0.15	1.43	0.06	0.17	0.52	0.22	0.41	0.05	1.43	0.06	0.22	0.17	0.52	0.41	4.81E-02	false	true	false	SIMPLEX
147	2000.30	0.00	5013.65	0.15	1.43	0.06	0.17	0.52	0.22	0.41	0.05	1.43	0.06	0.22	0.17	0.52	0.41	4.81E-02	false	true	false	SIMPLEX
148	2000.31	0.00	5013.44	0.15	1.43	0.06	0.17	0.52	0.22	0.41	0.05	1.43	0.06	0.22	0.17	0.52	0.41	4.81E-02	false	true	false	SIMPLEX
149	2000.34	0.0064	5013.19	0.1569	1.4288	0.0622	0.1705	0.5238	0.2199	0.4054	0.0481	1.43	0.06	0.22	0.17	0.52	0.41	4.81E-02	false	true	false	SIMPLEX

APPENDIX I – PMHS MODEFRONTIER OPTIMIZATION FOR RECLINED POSTURE WITH VEST

```
#---- Frontier Design DB File info ----------
#modeFRONTIER  (c) ESTECO S.p.A.
#Design DB Table
#----------------------------------------------
#modeFRONTIER Version: modeFRONTIER 2017R5 5.7.1 b2017i017
#Date: Mon Jan 28 12:10:32 EST 2019
#Project Name: PMHS A Opt 2019-01-27 - redline vest - sensitivity - complete.prj
#Operating System: Windows 10 10.0 amd64
#Java (SDK/JRE) Version: 1.8.0_60
#Java Vendor: Oracle Corporation
#Java Vendor URL: http://java.oracle.com/
#User Name: KBosch
#----------------------------------------------
#Categories
<CATEGORIES clusterPrefix="CLUSTER_" useTableNamePrefix="false">
  <CATEGORY enabled="true" label="" name="SOBOL" symbol="SQUARE,NONE,11,,0"/>
  <CATEGORY enabled="true" label="" name="USRDOE" symbol="SQUARE,NONE,11,,0"/>
  <CATEGORY enabled="true" label="" name="NSGA2" symbol="SQUARE,NONE,11,,0"/>
  <CATEGORY enabled="true" label="" name="TDA" symbol="SQUARE,NONE,11,,0"/>
  <CATEGORY enabled="true" label="" name="DOE_APPROX" symbol="SQUARE,NONE,11,,0"/>
  <CATEGORY enabled="true" label="" name="SIMPLEX" symbol="SQUARE,NONE,11,,0"/>
  <CATEGORY enabled="true" label="" name="USER" symbol="SQUARE,NONE,11,,0"/>
  <CATEGORY enabled="true" label="" name="FULL" symbol="SQUARE,NONE,11,#3C3912,1,#3C3912"/>
  <CATEGORY enabled="true" label="" name="SIMPLEX_DOE" symbol="SQUARE,NONE,11,#3366CC,1,#3366CC"/>
</CATEGORIES>

#----------------------------------------------
```

<ID>	Opt_joint	Opt_joint	Opt_joint	Opt_joint	Combined	Pelvis_Ax	Pelvis_Fx	Pelvis_Fz	T12_Ax	T12_Fx	T12_Fz	no Constraint	Constraint	Constraint	Constraint	Constraint	Constraint	<FEASIBLE>	<VIRTUAL>	<FEASIBLE>	<MARKED>	<CATEGORY>
0	4.39E+03	1.90E-02	2.00E+04	1.49E-01	2.63E+00	1.06E-01	1.30E-01	1.20E+00	3.22E-01	7.58E-01	1.13E-01	1.06E-01	3.22E-01	1.30E-01	1.20E+00	7.58E-01	1.13E-01	false	false	false	false	ULH
1	2743.12	0.02	6736.98	0.14	1.69	0.09	0.16	0.66	0.23	0.48	0.07	0.09	0.23	0.16	0.66	0.48	0.07	false	false	true	false	ULH
2	2800.38	0.01	18518.53	0.13	2.61	0.11	0.14	1.18	0.31	0.76	0.11	0.11	0.31	0.14	1.18	0.76	0.11	false	false	false	false	ULH
3	3488.34	0.00	16733.66	0.15	2.48	0.11	0.12	1.12	0.29	0.72	0.12	0.11	0.29	0.12	1.12	0.72	0.12	false	false	false	false	ULH
4	4224.29	0.01	11174.93	0.09	2.51	0.10	0.12	1.15	0.29	0.72	0.12	0.10	0.29	0.12	1.15	0.72	0.12	false	false	false	false	ULH
5	2755.79	0.02	17701.08	0.09	3.00	0.11	0.14	1.40	0.40	0.85	0.11	0.11	0.40	0.14	1.40	0.85	0.11	false	false	false	false	ULH
6	2048.34	0.02	6548.94	0.15	1.63	0.09	0.15	0.63	0.23	0.46	0.07	0.09	0.23	0.15	0.63	0.45	0.07	false	false	true	false	ULH
7	3702.04	0.02	5114.38	0.09	2.87	0.08	0.16	1.30	0.32	0.86	0.15	0.08	0.32	0.16	1.30	0.85	0.15	false	false	false	false	ULH
8	4999.03	0.01	14395.69	0.09	2.91	0.11	0.15	1.34	0.41	0.78	0.13	0.11	0.41	0.15	1.34	0.78	0.13	false	false	false	false	ULH
9	4019.91	0.02	12009.39	0.12	2.32	0.10	0.15	0.96	0.32	0.69	0.11	0.10	0.32	0.15	0.96	0.69	0.11	false	false	true	false	ULH
10	4487.77	0.02	15903.96	0.13	2.48	0.10	0.14	1.09	0.30	0.72	0.11	0.10	0.30	0.14	1.09	0.72	0.11	false	false	false	false	ULH
11	2221.73	0.00	16508.78	0.11	2.57	0.10	0.15	1.10	0.30	0.75	0.11	0.10	0.30	0.15	1.10	0.75	0.11	false	false	false	false	ULH
12	3644.54	0.02	17854.14	0.10	2.90	0.11	0.14	1.35	0.38	0.82	0.11	0.11	0.38	0.14	1.35	0.82	0.11	false	false	false	false	ULH
13	2269.11	0.02	5829.18	0.08	3.41	0.09	0.19	1.56	0.39	1.02	0.16	0.09	0.39	0.19	1.56	1.02	0.16	false	false	false	false	ULH
14	3238.76	0.02	15637.90	0.12	2.57	0.10	0.16	1.10	0.31	0.77	0.12	0.10	0.31	0.16	1.10	0.77	0.12	false	false	false	false	ULH
15	3371.57	0.01	19459.13	0.11	2.95	0.10	0.14	1.37	0.41	0.81	0.11	0.10	0.41	0.14	1.37	0.81	0.11	false	false	false	false	ULH
16	3796.53	0.02	19739.27	0.11	2.89	0.11	0.14	1.34	0.38	0.82	0.11	0.11	0.38	0.14	1.34	0.82	0.11	false	false	false	false	ULH
17	2969.76	0.01	17177.55	0.11	2.77	0.10	0.13	1.29	0.34	0.78	0.11	0.10	0.34	0.13	1.29	0.78	0.11	false	false	false	false	ULH
18	3159.53	0.02	19085.91	0.10	2.97	0.11	0.14	1.38	0.40	0.84	0.11	0.11	0.40	0.14	1.38	0.84	0.11	false	false	false	false	ULH
19	3943.16	0.02	14815.23	0.15	2.35	0.10	0.15	0.98	0.32	0.70	0.11	0.10	0.32	0.15	0.98	0.70	0.11	false	true	false	false	ULH
20	2624.97	0.01	10557.94	0.11	2.24	0.09	0.14	0.93	0.28	0.68	0.11	0.09	0.28	0.14	0.93	0.68	0.11	false	false	true	false	ULH
21	2462.16	0.02	15308.73	0.08	3.05	0.11	0.15	1.41	0.41	0.86	0.11	0.11	0.41	0.15	1.41	0.85	0.11	false	false	false	false	ULH
22	4195.70	0.01	15149.22	0.13	2.53	0.10	0.12	1.17	0.29	0.72	0.12	0.10	0.29	0.12	1.17	0.72	0.12	false	false	false	false	ULH
23	3064.55	0.02	17978.06	0.09	3.01	0.11	0.14	1.39	0.41	0.85	0.11	0.11	0.41	0.14	1.39	0.85	0.11	false	false	false	false	ULH
24	3579.53	0.01	9070.93	0.14	1.99	0.09	0.15	0.78	0.28	0.59	0.10	0.09	0.28	0.15	0.78	0.59	0.10	false	false	true	false	ULH
25	4458.41	0.01	11072.03	0.13	2.21	0.10	0.14	0.90	0.31	0.65	0.11	0.10	0.31	0.14	0.90	0.65	0.11	false	false	true	false	ULH
26	4261.81	0.00	18301.01	0.14	2.73	0.09	0.14	1.26	0.35	0.75	0.13	0.09	0.35	0.14	1.26	0.75	0.13	false	false	false	false	ULH
27	2189.55	0.00	18793.48	0.10	2.96	0.10	0.14	1.37	0.40	0.83	0.11	0.10	0.40	0.14	1.37	0.83	0.11	false	false	false	false	ULH
28	2842.49	0.01	14708.13	0.09	2.75	0.10	0.13	1.28	0.34	0.78	0.11	0.10	0.34	0.13	1.28	0.78	0.11	false	false	false	false	ULH
29	4088.91	0.02	17333.48	0.15	2.46	0.10	0.15	1.06	0.30	0.73	0.11	0.10	0.30	0.15	1.06	0.73	0.11	false	false	false	false	ULH
30	2001.52	0.02	19220.73	0.14	2.56	0.09	0.15	1.13	0.27	0.80	0.12	0.09	0.27	0.15	1.13	0.80	0.12	false	false	false	false	ULH
31	3650.41	0.01	15411.14	0.09	2.84	0.10	0.14	1.33	0.35	0.80	0.11	0.10	0.35	0.14	1.33	0.80	0.11	false	false	false	false	ULH
32	2893.26	0.02	16975.54	0.08	3.20	0.11	0.18	1.49	0.44	0.88	0.11	0.11	0.44	0.18	1.49	0.88	0.11	false	false	false	false	ULH
33	3216.56	0.00	16008.24	0.10	2.71	0.10	0.13	1.26	0.33	0.77	0.12	0.10	0.33	0.13	1.26	0.77	0.12	false	false	false	false	ULH
34	2578.77	0.02	16175.97	0.08	3.09	0.11	0.15	1.44	0.47	0.86	0.11	0.11	0.47	0.15	1.44	0.85	0.11	false	false	false	false	ULH
35	3559.11	0.01	14152.48	0.13	2.42	0.10	0.16	0.98	0.31	0.74	0.12	0.10	0.31	0.16	0.98	0.74	0.12	false	false	true	false	ULH
36	3270.23	0.01	5679.25	0.12	1.64	0.08	0.16	0.63	0.22	0.48	0.07	0.08	0.22	0.16	0.63	0.48	0.07	false	false	true	false	ULH
37	2500.52	0.01	9864.84	0.10	2.27	0.10	0.15	0.94	0.30	0.68	0.11	0.10	0.30	0.15	0.94	0.68	0.11	false	false	true	false	ULH
38	4285.53	0.02	18826.82	0.11	2.85	0.11	0.14	1.33	0.37	0.80	0.11	0.11	0.37	0.14	1.33	0.80	0.11	false	false	false	false	ULH
39	4605.33	0.02	17522.59	0.10	2.91	0.11	0.14	1.36	0.38	0.82	0.11	0.11	0.38	0.14	1.36	0.82	0.11	false	false	false	false	ULH
40	4856.40	0.01	8577.87	0.08	2.22	0.10	0.14	0.91	0.30	0.66	0.11	0.10	0.30	0.14	0.91	0.65	0.11	false	false	true	false	ULH
41	2110.41	0.01	9433.44	0.11	2.05	0.08	0.15	0.86	0.22	0.63	0.11	0.08	0.22	0.15	0.86	0.63	0.11	false	false	true	false	ULH
42	3813.51	0.00	7097.24	0.09	2.00	0.09	0.15	0.78	0.29	0.59	0.10	0.09	0.29	0.15	0.78	0.59	0.10	false	false	true	false	ULH
43	4924.33	0.01	12356.12	0.11	2.52	0.10	0.12	1.17	0.30	0.71	0.13	0.10	0.30	0.12	1.17	0.71	0.13	false	false	false	false	ULH
44	4840.54	0.01	8890.30	0.13	2.04	0.10	0.13	0.80	0.31	0.60	0.10	0.10	0.31	0.13	0.80	0.60	0.10	false	false	true	false	ULH
45	3389.12	0.00	7232.37	0.12	1.84	0.08	0.16	0.70	0.25	0.54	0.09	0.08	0.25	0.16	0.70	0.54	0.09	false	false	true	false	ULH
46	2537.15	0.02	7255.06	0.12	1.85	0.10	0.15	0.73	0.25	0.53	0.08	0.10	0.25	0.15	0.73	0.53	0.08	false	false	true	false	ULH
47	4401.24	0.02	10457.48	0.12	2.19	0.10	0.14	0.88	0.31	0.65	0.11	0.10	0.31	0.14	0.88	0.65	0.11	false	false	true	false	ULH
48	2866.11	0.00	7776.22	0.13	1.88	0.08	0.16	0.71	0.30	0.54	0.09	0.08	0.30	0.16	0.71	0.54	0.09	false	false	true	false	ULH
49	4129.29	0.02	8922.38	0.12	2.06	0.09	0.13	0.81	0.29	0.61	0.10	0.09	0.29	0.15	0.81	0.61	0.10	false	false	true	false	ULH
50	2177.46	0.02	13820.54	0.08	2.80	0.11	0.15	1.27	0.34	0.82	0.11	0.11	0.34	0.15	1.27	0.82	0.11	false	false	false	false	ULH
51	2088.43	0.02	11728.67	0.11	2.23	0.07	0.14	0.95	0.25	0.70	0.12	0.07	0.25	0.14	0.95	0.70	0.12	false	false	true	false	ULH
52	4085.90	0.03	6854.15	0.12	1.91	0.09	0.16	0.74	0.28	0.54	0.09	0.09	0.28	0.16	0.74	0.54	0.09	false	false	true	false	ULH
53	3115.41	0.01	12157.30	0.13	2.26	0.10	0.15	0.93	0.31	0.67	0.11	0.10	0.31	0.15	0.93	0.67	0.11	false	false	true	false	ULH
54	2120.93	0.02	8440.71	0.14	1.86	0.10	0.15	0.73	0.25	0.54	0.08	0.10	0.25	0.15	0.73	0.54	0.08	false	false	true	false	ULH
55	2559.50	0.01	15036.18	0.15	2.36	0.13	0.14	1.27	0.30	0.69	0.14	0.13	0.30	0.14	1.27	0.69	0.14	false	false	false	false	ULH
56	4181.81	0.01	13535.03	0.13	2.35	0.10	0.15	0.99	0.30	0.70	0.11	0.10	0.30	0.15	0.99	0.70	0.11	false	false	true	false	ULH
57	3989.56	0.01	7558.46	0.09	2.10	0.10	0.14	0.84	0.30	0.62	0.11	0.10	0.30	0.14	0.84	0.62	0.11	false	false	true	false	ULH
58	2906.18	0.01	9524.02	0.15	2.91	0.13	0.15	1.24	0.59	0.66	0.13	0.13	0.59	0.15	1.24	0.66	0.13	false	false	false	false	ULH
59	4516.99	0.01	6499.96	0.11	1.90	0.09	0.16	0.72	0.29	0.54	0.09	0.09	0.29	0.16	0.72	0.54	0.09	false	false	true	false	ULH
60	2335.43	0.00	6237.06	0.09	2.84	0.08	0.16	1.29	0.30	0.87	0.15	0.08	0.30	0.16	1.29	0.87	0.15	false	false	false	false	ULH
61	4317.56	0.01	5947.73	0.10	1.84	0.09	0.16	0.69	0.28	0.52	0.09	0.09	0.28	0.16	0.69	0.52	0.09	false	false	true	false	ULH
62	3008.50	0.00	10255.64	0.14	2.09	0.09	0.15	0.84	0.30	0.62	0.11	0.09	0.30	0.15	0.84	0.62	0.11	false	false	true	false	ULH
63	4666.77	0.00	6193.37	0.15	1.87	0.09	0.16	0.68	0.29	0.52	0.08	0.09	0.29	0.16	0.68	0.52	0.08	false	false	true	false	ULH
64	4797.02	0.02	11573.32	0.12	2.32	0.10	0.15	0.95	0.32	0.70	0.11	0.10	0.32	0.15	0.95	0.70	0.11	false	false	true	false	ULH
65	2653.74	0.01	8260.63	0.12	1.88	0.08	0.16	0.76	0.22	0.57	0.09	0.08	0.22	0.16	0.76	0.57	0.09	false	false	true	false	ULH
66	2691.65	0.02	7441.54	0.10	1.93	0.08	0.15	0.79	0.22	0.59	0.10	0.08	0.22	0.15	0.79	0.59	0.10	false	false	true	false	ULH
67	2299.17	0.02	16372.95	0.11	2.64	0.11	0.16	1.15	0.31	0.80	0.12	0.11	0.31	0.16	1.15	0.80	0.12	false	false	false	false	ULH
68	2667.59	0.02	12599.58	0.13	2.31	0.10	0.15	0.96	0.29	0.69	0.12	0.10	0.29	0.15	0.96	0.69	0.12	false	false	true	false	ULH
69	3750.91	0.01	10726.58	0.14	2.13	0.10	0.14	0.86	0.30	0.63	0.11	0.10	0.30	0.14	0.86	0.63	0.11	false	false	true	false	ULH
70	3981.84	0.00	12920.59	0.15	2.27	0.10	0.14	0.93	0.30	0.68	0.11	0.10	0.30	0.14	0.93	0.68	0.11	false	false	true	false	ULH
71	4367.18	0.01	10660.66	0.12	2.08	0.10	0.14	1.34	0.29	0.80	0.11	0.10	0.29	0.14	1.34	0.80	0.11	false	false	false	false	ULH
72	4881.21	0.02	10090.12	0.11	2.19	0.10	0.14	0.87	0.31	0.66	0.11	0.10	0.31	0.14	0.87	0.66	0.11	false	false	true	false	ULH
73	3415.44	0.01	15748.32	0.14	2.44	0.10	0.16	1.03	0.31	0.73	0.12	0.10	0.31	0.16	1.03	0.73	0.12	false	false	false	false	ULH
74	3613.56	0.00	18236.11	0.09	3.14	0.11	0.16	1.48	0.42	0.85	0.12	0.11	0.42	0.16	1.48	0.85	0.12	false	false	false	false	ULH
75	3304.99	0.02	11719.44	0.14	2.17	0.09	0.14	0.89	0.29	0.65	0.11	0.09	0.29	0.14	0.89	0.65	0.11	false	false	true	false	ULH
76	2412.33	0.01	8582.44	0.09	2.18	0.09	0.14	0.90	0.28	0.65	0.11	0.09	0.28	0.14	0.90	0.65	0.11	false	false	true	false	ULH
77	3450.78	0.01	11835.02	0.11	2.37	0.10	0.16	0.96	0.31	0.72	0.12	0.10	0.31	0.16	0.96	0.72	0.12	false	false	true	false	ULH
78	4558.51	0.02	13322.09	0.10	2.59	0.12	0.13	1.17	0.31	0.75	0.11	0.12	0.31	0.13	1.17	0.75	0.11	false	false	false	false	ULH
79	4135.95	0.02	5494.85	0.15	1.67	0.08	0.16	0.64	0.24	0.47	0.07	0.08	0.24	0.16	0.64	0.47	0.07	false	false	true	false	ULH
80	3726.16	0.00	9946.28	0.08	2.46	0.12	0.12	1.10	0.29	0.70	0.12	0.12	0.29	0.12	1.10	0.70	0.12	false	false	false	false	ULH
81	3046.41	0.00	12254.20	0.08	2.65	0.09	0.13	1.23	0.32	0.76	0.12	0.09	0.32	0.13	1.23	0.76	0.12	false	false	false	false	ULH
82	4714.58	0.02	10934.92	0.12	2.28	0.10	0.14	0.93	0.32	0.67	0.11	0.10	0.32	0.14	0.93	0.67	0.11	false	false	true	false	ULH
83	3227.71	0.01	5201.85	0.09	2.60	0.08	0.14	1.18	0.28	0.79	0.13	0.08	0.28	0.14	1.18	0.79	0.13	false	false	false	false	ULH
84	4878.29	0.01	13549.11	0.08	2.84	0.10	0.14	1.31	0.40	0.77	0.12	0.10	0.40	0.14	1.31	0.77	0.12	false	false	false	false	ULH
85	4773.20	0.00	14013.78	0.14	2.45	0.09	0.12	1.12	0.30	0.70	0.13	0.09	0.30	0.12	1.12	0.70	0.13	false	false	false	false	ULH
86	2438.96	0.01	14588.22	0.11	2.55	0.10	0.16	1.10	0.31	0.76	0.12	0.10	0.31	0.16	1.10	0.76	0.12	false	false	false	false	ULH
87	3083.53	0.02	5165.87	0.10	1.57	0.07	0.16	0.62	0.18	0.47	0.07	0.07	0.18	0.16	0.62	0.47	0.07	false	false	true	false	ULH
88	3893.50	0.01	8064.79	0.14	1.91	0.09	0.16	0.73	0.28	0.56	0.09	0.09	0.28	0.16	0.73	0.56	0.09	false	false	true	false	ULH
89	2838.19	0.00	9227.31	0.10	2.19	0.09	0.14	0.90	0.30	0.65	0.11	0.09	0.30	0.14	0.90	0.65	0.11	false	false	true	false	ULH
90	4547.85	0.00	10127.30	0.13	2.11	0.09	0.13	0.85	0.30	0.63	0.11	0.09	0.30	0.13	0.85	0.63	0.11	false	false	true	false	ULH
91	3853.12	0.02	12581.58	0.09	2.58	0.10	0.16	1.11	0.31	0.77	0.12	0.10	0.31	0.16	1.11	0.77	0.12	false	false	false	false	ULH

92	2383.32	0.00	17983.06	0.13	2.32	0.10	0.14	0.97	0.31	0.69	0.11	0.10	0.31	0.14	0.97	0.69	0.11	false	false	true	false	ULH
93	4620.54	0.01	18052.32	0.08	3.42	0.11	0.17	1.62	0.47	0.91	0.13	0.11	0.47	0.17	1.62	0.91	0.13	false	false	false	false	ULH
94	4751.21	0.02	13909.43	0.08	2.84	0.10	0.14	1.32	0.38	0.79	0.11	0.10	0.38	0.14	1.32	0.79	0.11	false	false	false	false	ULH
95	2303.43	0.01	13131.31	0.14	2.28	0.10	0.15	0.94	0.30	0.68	0.11	0.10	0.30	0.15	0.94	0.68	0.11	false	false	true	false	ULH
96	4053.67	0.00	17080.27	0.10	3.00	0.11	0.15	1.40	0.41	0.82	0.12	0.11	0.41	0.15	1.40	0.82	0.12	false	false	false	false	ULH
97	3298.05	0.02	16541.34	0.12	2.60	0.11	0.14	1.17	0.30	0.76	0.11	0.11	0.30	0.14	1.17	0.76	0.11	false	false	false	false	ULH
98	3194.51	0.01	19288.25	0.14	2.63	0.10	0.12	1.22	0.30	0.76	0.12	0.10	0.30	0.12	1.22	0.76	0.12	false	false	false	false	ULH
99	3909.58	0.01	7856.98	0.10	2.07	0.10	0.14	0.82	0.30	0.61	0.10	0.10	0.30	0.14	0.82	0.61	0.10	false	false	true	false	ULH

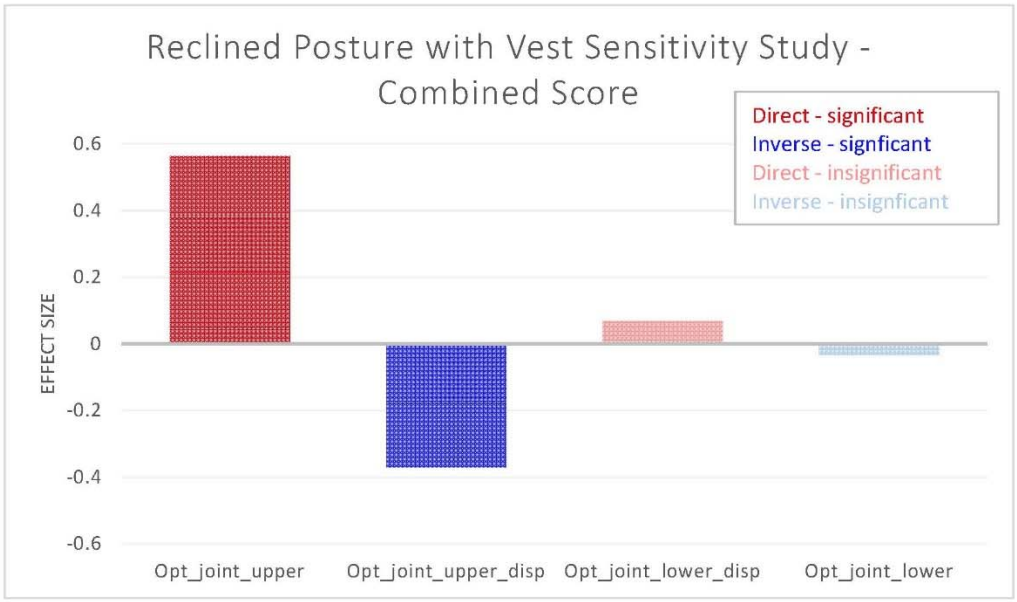
Reclined Posture with Vest Sensitivity Study - Combined Score
Direct - significant
Inverse - signficant
Direct - insignificant
Inverse - insignficant
EFFECT SIZE
0.6
0.4
0.2
0
-0.2
-0.4
-0.6
Opt_joint_upper
Opt_joint_upper_disp
Opt_joint_lower_disp
Opt_joint_lower

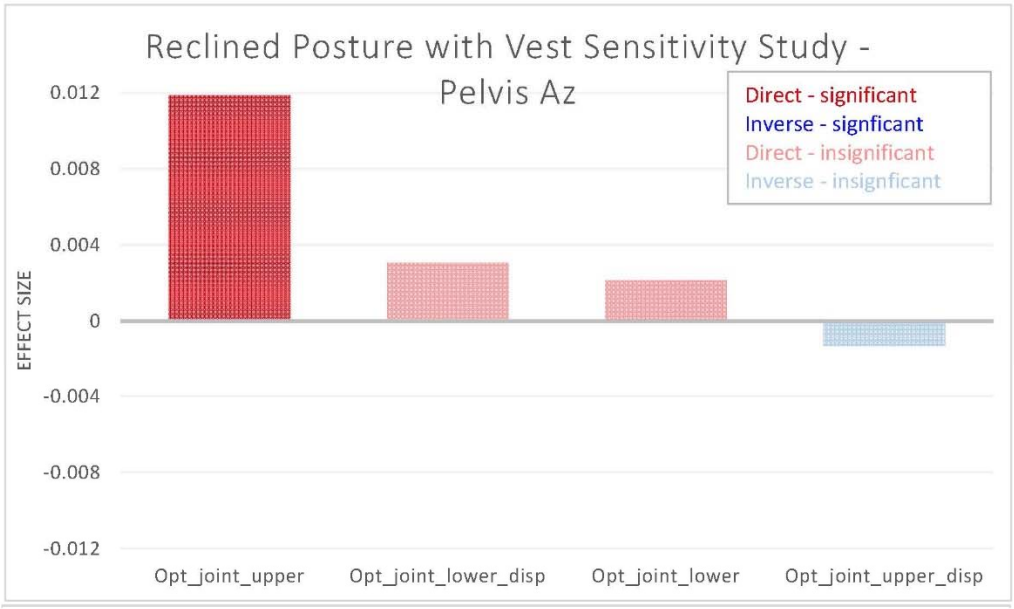
Reclined Posture with Vest Sensitivity Study - Pelvis Az
Direct - significant
Inverse - signficant
Direct - insignificant
Inverse - insignficant
EFFECT SIZE
0.012
0.008
0.004
0
-0.004
-0.008
-0.012
Opt_joint_upper
Opt_joint_lower_disp
Opt_joint_lower
Opt_joint_upper_disp

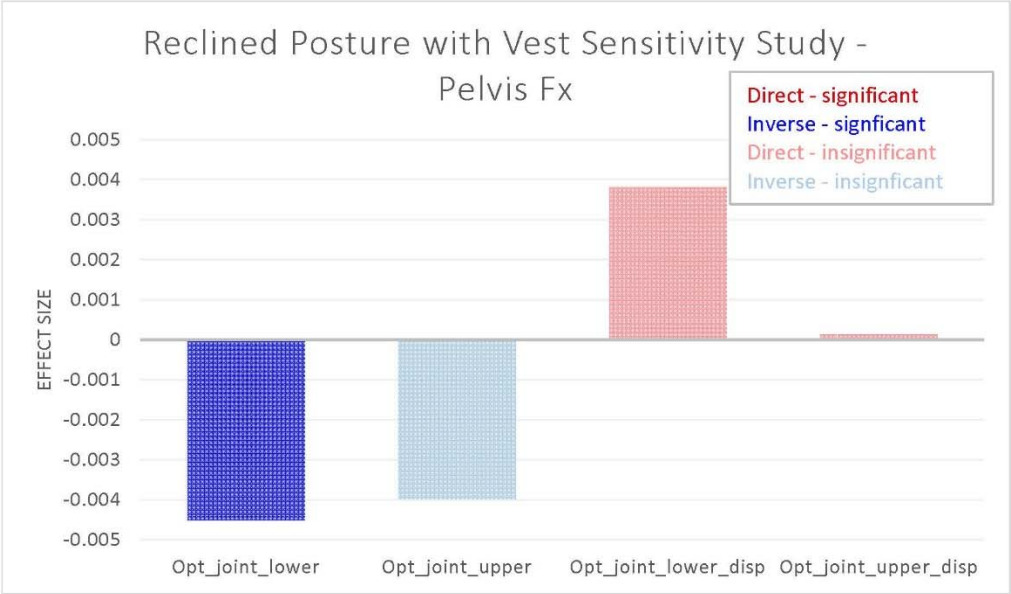
Reclined Posture with Vest Sensitivity Study - Pelvis Fx
Direct - significant
Inverse - signficant
Direct - insignificant
Inverse - insignficant
EFFECT SIZE
0.005
0.004
0.003
0.002
0.001
0
-0.001
-0.002
-0.003
-0.004
-0.005
Opt_joint_lower
Opt_joint_upper
Opt_joint_lower_disp
Opt_joint_upper_disp

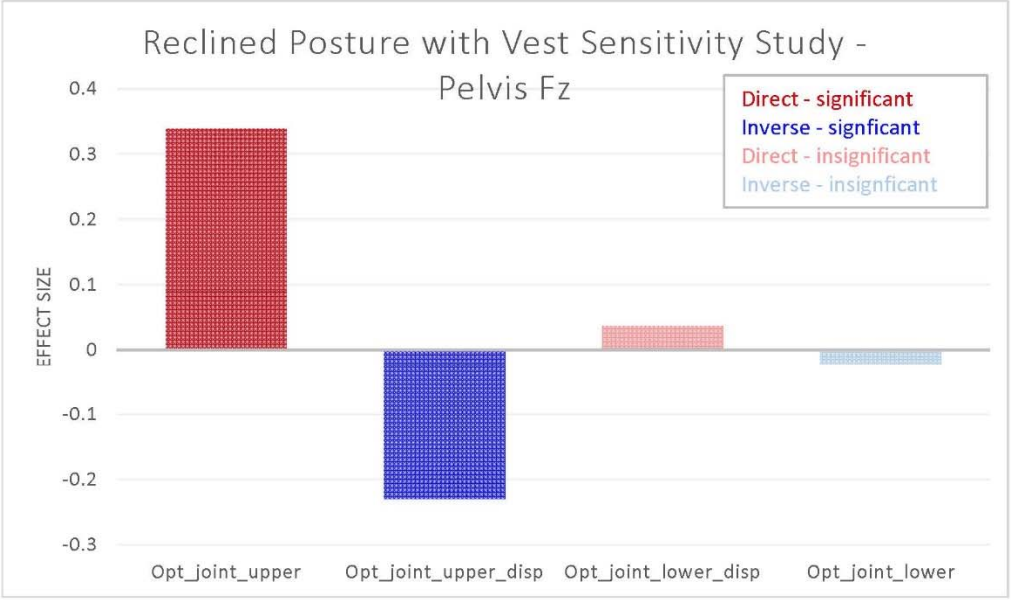
Reclined Posture with Vest Sensitivity Study - Pelvis Fz
Direct - significant
Inverse - signficant
Direct - insignificant
Inverse - insignficant
EFFECT SIZE
0.4
0.3
0.2
0.1
0
-0.1
-0.2
-0.3
Opt_joint_upper
Opt_joint_upper_disp
Opt_joint_lower_disp
Opt_joint_lower

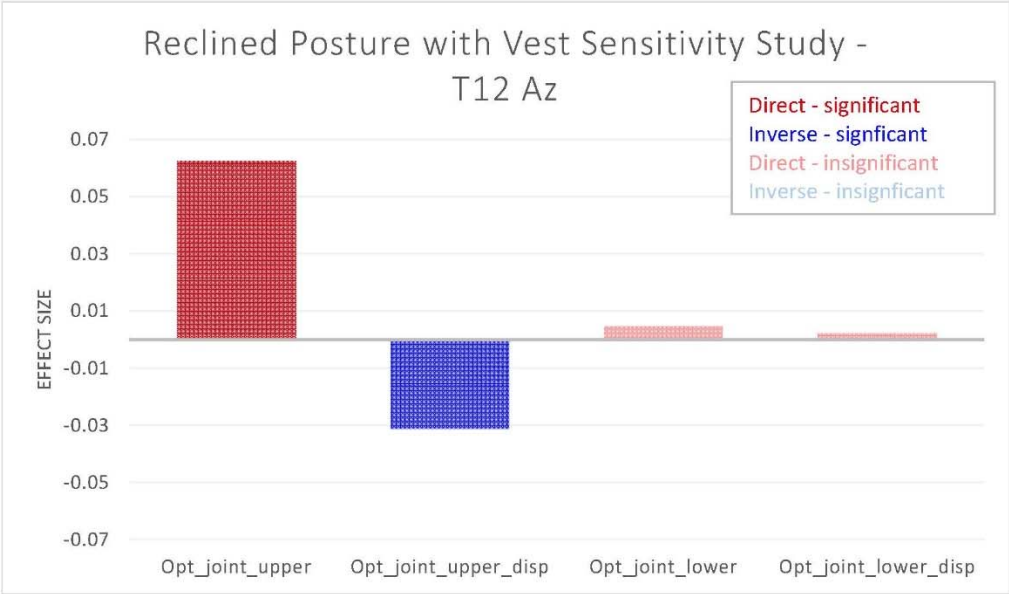
Reclined Posture with Vest Sensitivity Study - T12 Az
Direct - significant
Inverse - signficant
Direct - insignificant
Inverse - insignficant
EFFECT SIZE
0.07
0.05
0.03
0.01
-0.01
-0.03
-0.05
-0.07
Opt_joint_upper
Opt_joint_upper_disp
Opt_joint_lower
Opt_joint_lower_disp

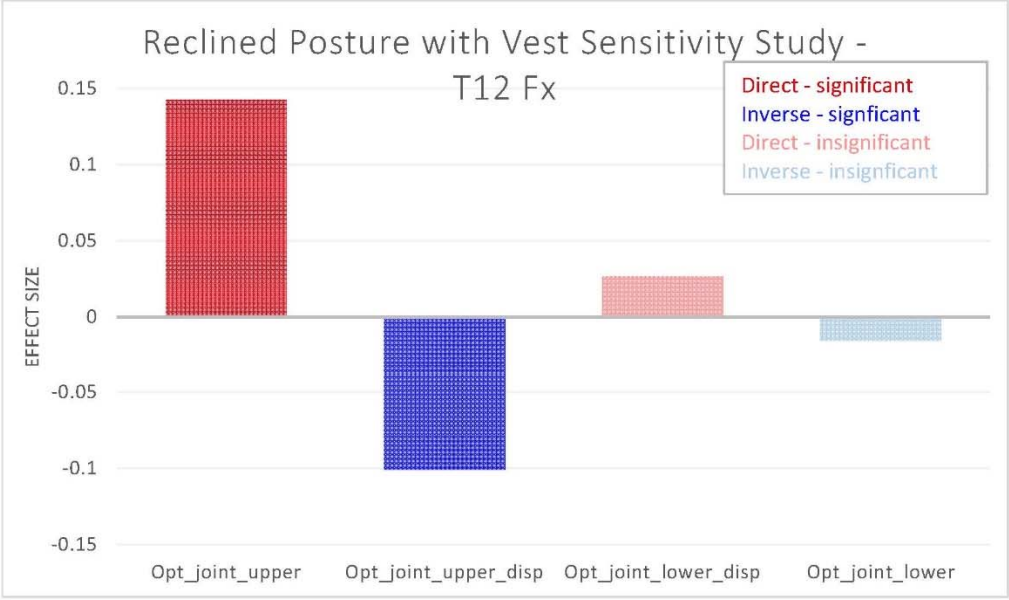
Reclined Posture with Vest Sensitivity Study - T12 Fx
Direct - significant
Inverse - signficant
Direct - insignificant
Inverse - insignficant
EFFECT SIZE
0.15
0.1
0.05
0
-0.05
-0.1
-0.15
Opt_joint_upper
Opt_joint_upper_disp
Opt_joint_lower_disp
Opt_joint_lower

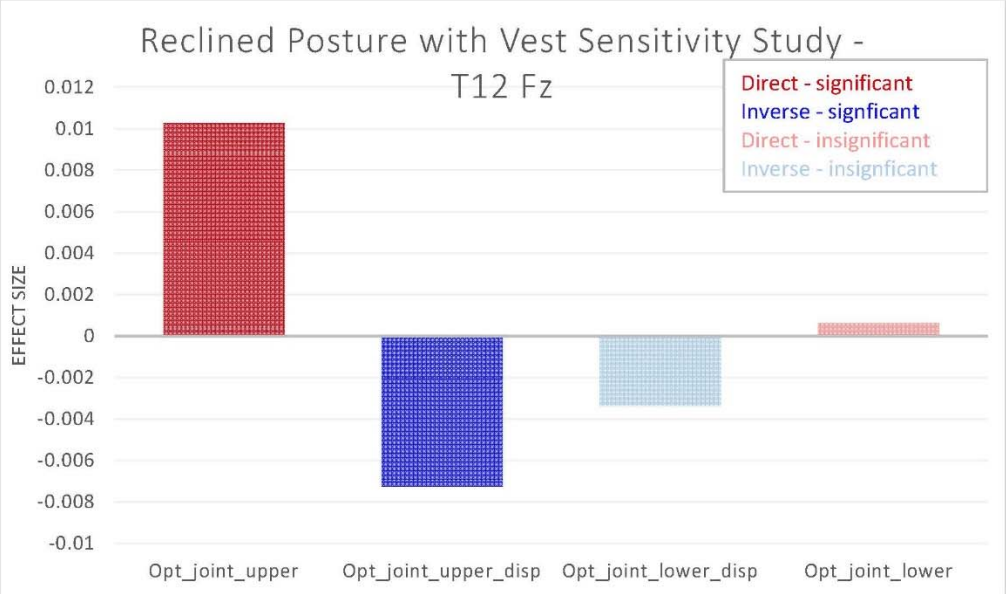
Reclined Posture with Vest Sensitivity Study - T12 Fz
Direct - significant
Inverse - signficant
Direct - insignificant
Inverse - insignficant
EFFECT SIZE
0.012
0.01
0.008
0.006
0.004
0.002
0
-0.002
-0.004
-0.006
-0.008
-0.01
Opt_joint_upper
Opt_joint_upper_disp
Opt_joint_lower_disp
Opt_joint_lower

```
#--- Frontier Design DB File Info ----------
#modeFRONTIER - (c) ESTECO S.p.A.
#Design DB Table
#-------------------------------------------
#modeFRONTIER Version: modeFRONTIER 2017R5 5.7.1 b20171017
#Date: Tue Jan 29 11:45:27 EST 2019
#Project name: PMHS A Opt 2019-01-28 - redline vest - opt 200.prj
#Operating System: Windows 10 10.0 amd64
#Java (SDK/JRE) Version: 1.8.0_60
#Java Vendor: Oracle Corporation
#Java Vendor URL: http://java.oracle.com/
#User Name: KBusch
#-------------------------------------------
#Categories
<CATEGORIES discorPrefix="CLUSTER_" useTableNameInPrefix="false">
  <CATEGORY enabled="true" label="" name="SQRDL" symbol="SQUARE,NONE,11,,0"/>
  <CATEGORY enabled="true" label="" name="USRDOE" symbol="SQUARE,NONE,11,,0"/>
  <CATEGORY enabled="true" label="" name="NSGA2" symbol="SQUARE,NONE,11,,0"/>
  <CATEGORY enabled="true" label="" name="TOA" symbol="SQUARE,NONE,11,,0"/>
  <CATEGORY enabled="true" label="" name="DOE_APPROX" symbol="SQUARE,NONE,11,,0"/>
  <CATEGORY enabled="true" label="" name="SIMPLEX" symbol="SQUARE,NONE,11,,0"/>
  <CATEGORY enabled="true" label="" name="ULP" symbol="SQUARE,NONE,11,,0"/>
  <CATEGORY enabled="true" label="" name="TILLI" symbol="SQUARE,NONE,11,#DC3912,1,#DC3912"/>
  <CATEGORY enabled="true" label="" name="SIMPLEX_DOE" symbol="SQUARE,NONE,11,#3366CC,1,#3366CC"/>
</CATEGORIES>

#-------------------------------------------
```

<ID>	Opt_Joint_T	Opt_Joint_	Opt_Joint_st	Opt_Joint_	Combined_	Pelvis_Az_	Pelvis_Fx_i	Pelvis_Fz_i	T12_Az_nc	T12_Fx_nc	T12_Fz_nc	Objective2	Constraint_	Constraint:	Constraint_	Constraint:	Constraint_	Constraint:	<ERROR>	<VIRTUAL>	<FEASIBLE	<MARKED>	<CATEGORY>
0	4392.0075	0.0196	19985.1386	0.1485	2.8322	0.1057	0.1300	1.2024	0.3221	0.7580	0.1134	2.8322	0.11	0.32	0.13	1.20	0.75	0.11	false	false	false	false	JLH
1	2748.1249	0.0223	6736.9782	0.1433	1.6934	0.0905	0.1254	0.6623	0.2308	0.4529	0.0714	1.6934	0.09	0.23	0.16	0.66	0.48	0.07	false	false	false	false	JLH
2	2800.8307	0.0128	18518.5313	0.1289	2.6135	0.1127	0.1402	1.1805	0.3059	0.7534	0.1108	2.6135	0.11	0.31	0.14	1.18	0.75	0.11	false	false	false	false	JLH
3	3488.8418	0.0091	16733.3575	0.1473	2.4806	0.1137	0.1224	1.1303	0.2867	0.7153	0.1209	2.4806	0.11	0.29	0.12	1.12	0.72	0.12	false	false	false	false	JLH
4	4224.2862	0.0078	11374.9260	0.0879	2.5103	0.0984	0.1219	1.1540	0.2929	0.7235	0.1196	2.5103	0.10	0.29	0.12	1.15	0.72	0.12	false	false	false	false	JLH
5	2238.5503	0.0024	4695.9080	0.1052	1.7928	0.0740	0.1383	0.7308	0.2191	0.5072	0.0873	1.7928	0.07	0.22	0.16	0.71	0.54	0.09	false	false	false	false	SIMPLEX
6	3545.5253	0.0035	5000.0000	0.1128	1.5703	0.0778	0.1382	0.5715	0.2328	0.4581	0.0708	1.5703	0.08	0.23	0.15	0.57	0.45	0.07	false	true	false	false	SIMPLEX
7	2000.0000	0.0064	6708.8438	0.1574	2.8886	0.1273	0.1964	1.2170	0.5854	0.6406	0.1318	2.8886	0.13	0.38	0.26	1.22	0.54	0.13	false	false	false	false	SIMPLEX
8	3613.8995	0.0074	10083.4060	0.1075	2.2410	0.0977	0.1433	0.9148	0.3102	0.6632	0.1099	2.2410	0.10	0.31	0.15	0.91	0.66	0.11	false	false	true	false	SIMPLEX
9	2580.7177	0.0177	5000.0000	0.0873	3.1577	0.0859	0.1633	1.4450	0.3719	0.8420	0.1542	3.1577	0.09	0.37	0.17	1.45	0.84	0.15	false	false	false	false	SIMPLEX
10	3261.8095	0.0045	11931.4803	0.1323	2.2522	0.0968	0.1410	0.9307	0.3081	0.6656	0.1104	2.2522	0.10	0.31	0.14	0.93	0.67	0.11	false	true	false	false	SIMPLEX
11	2807.7430	0.0133	5000.0000	0.1022	1.5408	0.0714	0.1378	0.6103	0.1714	0.4511	0.0680	1.5408	0.07	0.17	0.15	0.61	0.45	0.07	false	true	false	false	SIMPLEX
12	2092.5777	0.0133	5000.0000	0.1243	1.4784	0.0831	0.1436	0.5563	0.2089	0.4356	0.0599	1.4784	0.08	0.21	0.14	0.56	0.43	0.06	false	true	false	false	SIMPLEX
13	3337.9272	0.0038	5000.0000	0.1362	1.5175	0.0781	0.1339	0.5892	0.1823	0.4357	0.0630	1.5175	0.08	0.18	0.15	0.59	0.44	0.06	false	true	false	false	SIMPLEX
14	2839.9343	0.0179	5868.4821	0.1311	1.6607	0.0800	0.1373	0.6282	0.1987	0.4574	0.0692	1.6607	0.08	0.20	0.15	0.63	0.47	0.07	false	true	false	false	SIMPLEX
15	2887.7391	0.0157	5434.7446	0.1250	1.5341	0.0743	0.1366	0.5983	0.1799	0.4558	0.0675	1.5341	0.07	0.18	0.15	0.60	0.45	0.07	false	true	false	false	SIMPLEX
16	2000.0000	0.0254	5217.1373	0.1310	1.5693	0.1066	0.1367	0.5953	0.2709	0.4753	0.0644	1.5693	0.11	0.27	0.14	0.57	0.43	0.06	false	true	false	false	SIMPLEX
17	3542.9545	0.0077	5000.0000	0.1220	1.5625	0.0779	0.1394	0.5729	0.2256	0.4550	0.0705	1.5625	0.08	0.23	0.15	0.57	0.45	0.07	false	true	false	false	SIMPLEX
18	2000.0000	0.0254	5217.1373	0.1310	1.5693	0.1066	0.1367	0.5953	0.2709	0.4753	0.0644	1.5693	0.11	0.27	0.14	0.57	0.43	0.06	false	true	false	false	SIMPLEX
19	3157.2429	0.0121	5054.2806	0.1174	1.5084	0.0691	0.1376	0.5717	0.1926	0.4496	0.0677	1.5084	0.07	0.19	0.15	0.57	0.45	0.07	false	true	false	false	SIMPLEX
20	2000.9999	0.0192	5244.2526	0.1402	1.4700	0.0793	0.1510	0.5564	0.1934	0.4287	0.0612	1.4700	0.08	0.19	0.15	0.56	0.43	0.06	false	true	false	false	SIMPLEX
21	2981.1274	0.0221	5385.3938	0.1524	3.2320	0.1289	0.1409	1.4247	0.6091	0.7805	0.1389	3.2320	0.13	0.61	0.14	1.42	0.79	0.14	false	false	false	false	SIMPLEX
22	2841.1463	0.0185	5000.0000	0.1382	1.4568	0.0792	0.1503	0.5487	0.1933	0.4248	0.0605	1.4568	0.08	0.19	0.15	0.55	0.42	0.06	false	true	false	false	SIMPLEX
23	2142.5527	0.0078	5149.2716	0.1285	1.4305	0.0731	0.1482	0.5590	0.1780	0.4303	0.0619	1.4565	0.07	0.18	0.15	0.56	0.43	0.06	false	true	false	false	SIMPLEX
24	2000.0000	0.0000	5223.9073	0.1247	NaN	NaN	NaN	NaN	NaN	NaN	NaN	NaN	NaN	NaN	NaN	NaN	NaN	NaN	NaN	true	false	true	false	SIMPLEX
25	2000.0000	0.0173	5142.4865	0.1524	3.0871	0.1286	0.1376	1.3389	0.6059	0.7388	0.1378	3.0871	0.13	0.61	0.14	1.34	0.74	0.14	false	false	false	false	SIMPLEX
26	2821.9063	0.0134	5076.3321	0.1283	1.4845	0.0707	0.1335	0.5595	0.1677	0.4387	0.0642	1.4845	0.07	0.17	0.15	0.56	0.44	0.06	false	true	false	false	SIMPLEX
27	3305.2199	0.0161	5234.9331	0.1470	1.4797	0.0673	0.1368	0.5857	0.1845	0.4392	0.0652	1.4797	0.07	0.18	0.15	0.57	0.44	0.07	false	true	false	false	SIMPLEX
28	2365.7383	0.0140	5058.7383	0.1300	1.4644	0.0799	0.1470	0.5518	0.1977	0.4274	0.0606	1.4644	0.08	0.20	0.15	0.55	0.43	0.06	false	true	false	false	SIMPLEX
29	2175.5368	0.0077	5000.0000	0.1125	1.4992	0.0738	0.1509	0.5876	0.1791	0.4431	0.0646	1.4992	0.07	0.18	0.15	0.59	0.44	0.06	false	true	false	false	SIMPLEX
30	2726.4167	0.0163	5157.5734	0.1400	1.4553	0.0780	0.1502	0.5474	0.1898	0.4285	0.0613	1.4553	0.08	0.19	0.15	0.55	0.43	0.06	false	true	false	false	SIMPLEX
31	2900.2577	0.0140	5192.9652	0.1367	1.4378	0.0701	0.1334	0.5520	0.1653	0.4337	0.0634	1.4378	0.07	0.17	0.15	0.55	0.43	0.06	false	true	false	false	SIMPLEX
32	3187.5324	0.0139	5189.9912	0.1401	1.4615	0.0680	0.1362	0.5550	0.1812	0.4379	0.0651	1.4615	0.07	0.18	0.15	0.56	0.44	0.07	false	true	false	false	SIMPLEX
33	2454.4154	0.0072	5258.0911	0.1273	1.4475	0.0651	0.1330	0.5703	0.1533	0.4405	0.0651	1.4475	0.07	0.15	0.15	0.57	0.44	0.07	false	true	false	false	SIMPLEX
34	2433.1644	0.0049	5150.5266	0.1194	1.4591	0.0590	0.1348	0.5790	0.1628	0.4431	0.0664	1.4591	0.06	0.16	0.15	0.57	0.44	0.07	false	false	false	false	SIMPLEX
35	2653.1036	0.0114	5155.9117	0.1349	1.4500	0.0743	0.1308	0.5515	0.1791	0.4318	0.0624	1.4500	0.07	0.18	0.15	0.55	0.43	0.06	false	true	false	false	SIMPLEX
36	2253.2734	0.0078	5271.7578	0.1374	1.4324	0.0708	0.1489	0.5524	0.1705	0.4278	0.0618	1.4324	0.07	0.17	0.15	0.55	0.43	0.06	false	true	false	false	SIMPLEX
37	2000.0000	0.0050	5369.4706	0.1430	1.4103	0.0687	0.1475	0.5447	0.1669	0.4218	0.0607	1.4103	0.07	0.17	0.15	0.54	0.42	0.06	false	true	false	false	SIMPLEX
38	2881.3508	0.0120	5308.9178	0.1424	1.4376	0.0684	0.1342	0.5545	0.1823	0.4330	0.0642	1.4376	0.07	0.16	0.15	0.55	0.44	0.06	false	true	false	false	SIMPLEX
39	2454.9133	0.0056	5378.7807	0.1398	1.4198	0.0660	0.1527	0.5542	0.1553	0.4332	0.0642	1.4198	0.06	0.16	0.15	0.55	0.43	0.06	false	true	false	false	SIMPLEX
40	2653.8434	0.0111	5396.9460	0.1524	2.9103	0.1273	0.1484	1.2436	0.5909	0.6665	0.1316	2.9103	0.13	0.59	0.15	1.24	0.67	0.13	false	false	false	false	SIMPLEX
41	2504.2834	0.0092	5277.8048	0.1339	1.4329	0.0665	0.1523	0.5584	0.1562	0.4356	0.0640	1.4329	0.07	0.16	0.15	0.56	0.44	0.06	false	true	false	false	SIMPLEX
42	2010.0119	0.0014	5534.5817	0.1428	1.3802	0.0570	0.1502	0.5537	0.1388	0.4276	0.0634	1.3802	0.05	0.14	0.15	0.55	0.43	0.06	false	true	false	false	SIMPLEX
43	2000.0000	0.0000	5735.4199	0.1458	NaN	NaN	NaN	NaN	NaN	NaN	NaN	NaN	NaN	NaN	NaN	NaN	NaN	NaN	NaN	true	false	true	false	SIMPLEX
44	2000.0000	0.0000	5471.4012	0.1373	NaN	NaN	NaN	NaN	NaN	NaN	NaN	NaN	NaN	NaN	NaN	NaN	NaN	NaN	NaN	true	false	true	false	SIMPLEX
45	2551.8279	0.0085	5348.5386	0.1411	1.4270	0.0658	0.1522	0.5531	0.1545	0.4328	0.0636	1.4270	0.07	0.15	0.15	0.55	0.43	0.06	false	true	false	false	SIMPLEX
46	2004.0962	0.0021	5538.3810	0.1495	1.3791	0.0600	0.1489	0.5449	0.1415	0.4219	0.0618	1.3791	0.05	0.14	0.15	0.54	0.42	0.06	false	true	false	false	SIMPLEX
47	2000.0000	0.0000	5668.5890	0.1524	NaN	NaN	NaN	NaN	NaN	NaN	NaN	NaN	NaN	NaN	NaN	NaN	NaN	NaN	NaN	true	false	true	false	SIMPLEX
48	2000.0000	0.0000	5501.0384	0.1458	NaN	NaN	NaN	NaN	NaN	NaN	NaN	NaN	NaN	NaN	NaN	NaN	NaN	NaN	NaN	true	false	true	false	SIMPLEX
49	2334.5429	0.0060	5402.4210	0.1424	1.4152	0.0647	0.1509	0.5548	0.1521	0.4297	0.0630	1.4152	0.06	0.15	0.15	0.55	0.43	0.06	false	true	false	false	SIMPLEX
50	2000.0000	0.0016	5543.5465	0.1409	1.3732	0.0581	0.1492	0.5454	0.1363	0.4222	0.0621	1.3732	0.05	0.14	0.15	0.55	0.42	0.06	false	true	false	false	SIMPLEX
51	2000.0000	0.0000	5590.5188	0.1497	NaN	NaN	NaN	NaN	NaN	NaN	NaN	NaN	NaN	NaN	NaN	NaN	NaN	NaN	NaN	true	false	true	false	SIMPLEX
52	2160.0349	0.0048	5449.4705	0.1448	1.4040	0.0669	0.1498	0.5501	0.1509	0.4268	0.0625	1.4040	0.06	0.15	0.15	0.55	0.43	0.06	false	true	false	false	SIMPLEX
53	2051.5715	0.0000	5603.5592	0.1408	NaN	NaN	NaN	NaN	NaN	NaN	NaN	NaN	NaN	NaN	NaN	NaN	NaN	NaN	NaN	true	false	true	false	SIMPLEX
54	2027.8029	0.0035	5447.9933	0.1447	1.4011	0.0653	0.1485	0.5454	0.1560	0.4235	0.0615	1.4011	0.07	0.16	0.15	0.55	0.47	0.06	false	true	false	false	SIMPLEX
55	2000.0000	0.0001	5580.3317	0.1487	1.3832	0.0524	0.1499	0.5464	0.1470	0.4247	0.0629	1.3832	0.05	0.13	0.15	0.55	0.42	0.06	false	true	false	false	SIMPLEX
56	2000.0000	0.0000	5655.4752	0.1503	NaN	NaN	NaN	NaN	NaN	NaN	NaN	NaN	NaN	NaN	NaN	NaN	NaN	NaN	NaN	true	false	true	false	SIMPLEX
57	2013.7100	0.0076	5481.1152	0.1481	1.3897	0.0618	0.1480	0.5458	0.1460	0.4293	0.0620	1.3897	0.06	0.15	0.15	0.55	0.42	0.06	false	true	false	false	SIMPLEX
58	2000.0000	0.0017	5544.9535	0.1524	2.8803	0.1234	0.2310	1.1980	0.5760	0.6228	0.1292	2.8803	0.12	0.58	0.23	1.20	0.62	0.13	false	false	false	false	SIMPLEX
59	2007.1592	0.0015	5537.1002	0.1456	1.3800	0.0573	0.1498	0.5488	0.1364	0.4249	0.0629	1.3800	0.06	0.14	0.15	0.55	0.42	0.06	false	true	false	false	SIMPLEX
60	2000.0000	0.0007	5503.5144	0.1503	1.3788	0.0518	0.1488	0.5458	0.1454	0.4238	0.0628	1.3788	0.05	0.13	0.15	0.55	0.42	0.06	false	true	false	false	SIMPLEX
61	2005.6877	0.0005	5581.0983	0.1494	1.3882	0.0620	0.1488	0.5458	0.1470	0.4228	0.0618	1.3882	0.06	0.15	0.15	0.55	0.42	0.06	false	true	false	false	SIMPLEX
62	2001.4082	0.0007	5568.0086	0.1487	1.3755	0.0530	0.1497	0.5454	0.1402	0.4235	0.0627	1.3755	0.05	0.14	0.15	0.55	0.42	0.06	false	true	false	false	SIMPLEX
63	2000.0000	0.0008	5589.7331	0.1524	2.8756	0.1225	0.2315	1.1972	0.5737	0.6220	0.1286	2.8756	0.12	0.57	0.23	1.20	0.62	0.13	false	false	false	false	SIMPLEX
64	2004.2727	0.0013	5550.2564	0.1475	1.3761	0.0566	0.1486	0.5473	0.1365	0.4235	0.0626	1.3761	0.06	0.14	0.15	0.55	0.42	0.06	false	true	false	false	SIMPLEX
65	2004.8885	0.0017	5495.5318	0.1470	1.3801	0.0615	0.1487	0.5459	0.1484	0.4220	0.0617	1.3801	0.06	0.15	0.15	0.55	0.42	0.06	false	true	false	false	SIMPLEX
66	2001.2771	0.0008	5570.8438	0.1495	1.3742	0.0581	0.1486	0.5450	0.1386	0.4229	0.0626	1.3742	0.05	0.14	0.15	0.55	0.42	0.06	false	true	false	false	SIMPLEX
67	2000.0000	0.0001	5580.9967	0.1478	1.3847	0.0523	0.1500	0.5474	0.1405	0.4255	0.0631	1.3847	0.05	0.15	0.15	0.55	0.43	0.06	false	true	false	false	SIMPLEX
68	2002.9109	0.0016	5549.0349	0.1491	1.3728	0.0578	0.1493	0.5451	0.1358	0.4223	0.0622	1.3728	0.06	0.14	0.15	0.55	0.42	0.06	false	true	false	false	SIMPLEX
69	2000.0000	0.0011	5508.5105	0.1503	1.3689	0.0549	0.1494	0.5445	0.1365	0.4212	0.0622	1.3689	0.05	0.14	0.15	0.54	0.42	0.06	false	true	false	false	SIMPLEX
70	2000.9584	0.0018	5551.0592	0.1505	1.3734	0.0587	0.1490	0.5444	0.1381	0.4213	0.0618	1.3734	0.06	0.14	0.15	0.54	0.42	0.06	false	true	false	false	SIMPLEX
71	2000.5525	0.0012	5529.2568	0.1501	1.3788	0.0607	0.1487	0.5439	0.1432	0.4209	0.0616	1.3788	0.06	0.14	0.15	0.54	0.42	0.06	false	true	false	false	SIMPLEX
72	2001.0572	0.0012	5554.9470	0.1493	1.3714	0.0556	0.1495	0.5455	0.1365	0.4219	0.0624	1.3714	0.06	0.14	0.15	0.55	0.42	0.06	false	true	false	false	SIMPLEX
73	2001.3257	0.0009	5552.0902	0.1497	1.3742	0.0541	0.1496	0.5462	0.1367	0.4230	0.0626	1.3742	0.05	0.14	0.15	0.55	0.42	0.06	false	true	false	false	SIMPLEX
74	2000.8232	0.0016	5553.7720	0.1500	1.3711	0.0579	0.1491	0.5448	0.1357	0.4216	0.0620	1.3711	0.06	0.14	0.15	0.54	0.42	0.06	false	true	false	false	SIMPLEX
75	2002.3967	0.0011	5574.4837	0.1507	1.3699	0.0552	0.1494	0.5448	0.1368	0.4214	0.0623	1.3699	0.05	0.14	0.15	0.54	0.42	0.06	false	true	false	false	SIMPLEX
76	2000.0000	0.0008	5581.9227	0.1514	2.8757	0.1225	0.2315	1.1972	0.5737	0.6221	0.1286	2.8757	0.12	0.57	0.23	1.20	0.62	0.13	false	false	false	false	SIMPLEX
77	2001.9904	0.0014	5557.2318	0.1497	1.3701	0.0567	0.1494	0.5453	0.1349	0.4216	0.0622	1.3701	0.06	0.13	0.15	0.55	0.42	0.06	false	true	false	false	SIMPLEX
78	2001.5489	0.0014	5567.0530	0.1509	1.3674	0.0558	0.1493	0.5443	0.1363	0.4208	0.0620	1.3674	0.06	0.13	0.15	0.54	0.42	0.06	false	true	false	false	SIMPLEX
79	2001.7947	0.0015	5560.9039	0.1515	2.8792	0.1232	0.2311	1.1977	0.5755	0.6226	0.1291	2.8792	0.12	0.58	0.23	1.20	0.62	0.13	false	false	false	false	SIMPLEX
80	2002.1428	0.0009	5577.3385	0.1509	1.3699	0.0539	0.1494	0.5445	0.1381	0.4215	0.0623	1.3699	0.05	0.14	0.15	0.54	0.42	0.06	false	true	false	false	SIMPLEX
81	2001.0538	0.0008	5581.9770	0.1518	2.8756	0.1224	0.2315	1.1972	0.5736	0.6221	0.1286	2.8756	0.12	0.57	0.23	1.20	0.62	0.13	false	false	false	false	SIMPLEX
82	2001.7562	0.0013	5563.9181	0.1502	1.3696	0.0562	0.1494	0.5450	0.1356	0.4213	0.0622	1.3696	0.06	0.14	0.15	0.54	0.42	0.06	false	true	false	false	SIMPLEX
83	2000.1373	0.0012	5561.4394	0.1509	1.3676	0.0559	0.1493	0.5443	0.1353	0.4208	0.0621	1.3676	0.06	0.14	0.15	0.54	0.42	0.06	false	true	false	false	SIMPLEX
84	2000.0000	0.0015	5550.5919	0.1503	1.3698	0.0577	0.1491	0.5444	0.1355	0.4212	0.0620	1.3698	0.06	0.14	0.15	0.54	0.42	0.06	false	true	false	false	SIMPLEX
85	2001.8162	0.0009	5577.3685	0.1509	1.3698	0.0540	0.1494	0.5446	0.1380	0.4215	0.0623	1.3698	0.05	0.14	0.15	0.54	0.42	0.06	false	true	false	false	SIMPLEX
86	2000.4540	0.0014	5557.2861	0.1504	1.3679	0.0569	0.1492	0.5443	0.1343	0.4209	0.0621	1.3679	0.06	0.13	0.15	0.54	0.42	0.06	false	true	false	false	SIMPLEX
87	2000.0000	0.0013	5560.3763	0.1511	2.8777	0.1228	0.2313	1.1974	0.5749	0.6222	0.1289	2.8777	0.12	0.57	0.23	1.20	0.62	0.13	false	false	false	false	SIMPLEX
88	2001.1594	0.0013	5563.1202	0.1504	1.3687	0.0562	0.1493	0.5447	0.1353	0.4211	0.0622	1.3687	0.06	0.14	0.15	0.54	0.42	0.06	false	true	false	false	SIMPLEX
89	2001.7408	0.0016	5553.4388	0.1505	1.3698	0.0578	0.1491	0.5444	0.1356	0.4211	0.0619	1.3698	0.06	0.14	0.15	0.54	0.42	0.06	false	true	false	false	SIMPLEX
90	2000.4375	0.0017	5554.7426	0.1505	1.3686	0.0557	0.1493	0.5445	0.1359	0.4208	0.0622	1.3686	0.06	0.14	0.15	0.54	0.42	0.06	false	true	false	false	SIMPLEX
91	2000.2164	0.0018	5559.5403	0.1509	1.3668	0.0566	0.1492	0.5441	0.1343	0.4206	0.0621	1.3668	0.06	0.14	0.15	0.54	0.42	0.06	false	true	false	false	SIMPLEX
92	2000.0000	0.0014	5557.9004	0.1511	2.8783	0.1230	0.2312	1.1973	0.5751	0.6224	0.1290	2.8783	0.12	0.58	0.23	1.20	0.62	0.13	false	false	false	false	SIMPLEX
93	2000.8349	0.0015	5555.4508	0.1508	1.3676	0.0574	0.1491	0.5441	0.1344	0.4208	0.0620	1.3676	0.06	0.13	0.15	0.54	0.47	0.06	false	true	false	false	SIMPLEX
94	2001.0087	0.0013	5562.0136	0.1511	2.8779	0.1230	0.2313	1.1975	0.5750	0.6223	0.1289	2.8779	0.12	0.57	0.23	1.20	0.62	0.13	false	false	false	false	SIMPLEX
95	2000.5927	0.0014	5558.4380	0.1508	1.3674	0.0589	0.1492	0.5443	0.1341	0.4209	0.0620	1.3674	0.06	0.13	0.15	0.54	0.42	0.06	false	true	false	false	SIMPLEX
96	2001.3382	0.0015	5561.3747	0.1508	1.3687	0.0577	0.1491	0.5441	0.1350	0.4208	0.0619	1.3687	0.06	0.14	0.15	0.54	0.42	0.06	false	true	false	false	SIMPLEX
97	2000.5625	0.0013	5560.1792	0.1507	1.3677	0.0563	0.1492	0.5443	0.1348	0.4208	0.0621	1.3677	0.06	0.13	0.15	0.54	0.42	0.06	false	true	false	false	SIMPLEX
98	2000.4026	0.0014	5559.0541	0.1507	1.3673	0.0567	0.1492	0.5443	0.1344	0.4206	0.0621	1.3673	0.06	0.13	0.15	0.54	0.42	0.06	false	true	false	false	SIMPLEX
99	2000.8817	0.0014	5560.8466	0.1509	1.3671	0.0567	0.1492	0.5442	0.1343	0.4206	0.0621	1.3671	0.06	0.13	0.15	0.54	0.42	0.06	false	true	false	false	SIMPLEX

100	2000.7709	0.0013	5560.5388	0.1508	1.3674	0.0550	0.1493	0.5447	0.1351	0.4207	0.0621	1.3674	0.05	0.14	0.15	0.54	0.42	0.05	false	true	true	false	SIMPLEX
101	2000.5247	0.0014	5557.5536	0.1508	1.3666	0.0568	0.1492	0.5441	0.1339	0.4203	0.0620	1.3666	0.05	0.13	0.15	0.54	0.42	0.05	false	false	true	false	SIMPLEX
102	2000.7413	0.0015	5558.0075	0.1509	1.3673	0.0573	0.1491	0.5440	0.1342	0.4207	0.0620	1.3673	0.05	0.13	0.15	0.54	0.42	0.05	false	false	true	false	SIMPLEX
103	2000.5737	0.0014	5558.5405	0.1508	1.3667	0.0558	0.1492	0.5441	0.1339	0.4205	0.0620	1.3667	0.05	0.13	0.15	0.54	0.42	0.05	false	false	true	false	SIMPLEX
104	2000.7187	0.0014	5559.2864	0.1510	1.3665	0.0568	0.1492	0.5440	0.1340	0.4204	0.0620	1.3665	0.05	0.13	0.15	0.54	0.42	0.05	false	false	true	false	SIMPLEX
105	2000.8762	0.0014	5559.4025	0.1511	2.8788	0.1231	0.2312	1.1975	0.5753	0.6224	0.1290	2.8788	0.12	0.58	0.23	1.20	0.52	0.13	false	false	false	false	SIMPLEX
106	2000.1581	0.0014	5556.7138	0.1508	1.3666	0.0571	0.1491	0.5440	0.1337	0.4206	0.0620	1.3666	0.05	0.13	0.15	0.54	0.42	0.05	false	false	true	false	SIMPLEX
107	2000.7986	0.0015	5556.4968	0.1509	1.3673	0.0573	0.1491	0.5440	0.1342	0.4206	0.0620	1.3673	0.05	0.13	0.15	0.54	0.42	0.05	false	false	true	false	SIMPLEX
108	2000.3305	0.0014	5558.8445	0.1508	1.3666	0.0557	0.1492	0.5441	0.1340	0.4205	0.0620	1.3666	0.05	0.13	0.15	0.54	0.42	0.05	false	false	true	false	SIMPLEX
109	2000.2577	0.0014	5557.5585	0.1508	1.3664	0.0567	0.1492	0.5440	0.1341	0.4204	0.0620	1.3664	0.05	0.13	0.15	0.54	0.42	0.05	false	false	true	false	SIMPLEX
110	2000.0747	0.0014	5557.0175	0.1509	1.3660	0.0588	0.1492	0.5439	0.1338	0.4203	0.0620	1.3660	0.05	0.13	0.15	0.54	0.42	0.05	false	false	true	false	SIMPLEX
111	2000.5802	0.0014	5559.5372	0.1509	1.3667	0.0557	0.1492	0.5441	0.1342	0.4205	0.0620	1.3667	0.05	0.13	0.15	0.54	0.42	0.05	false	false	true	false	SIMPLEX
112	2000.2893	0.0014	5557.4446	0.1508	1.3664	0.0568	0.1492	0.5440	0.1340	0.4204	0.0620	1.3664	0.05	0.13	0.15	0.54	0.42	0.05	false	false	true	false	SIMPLEX
113	2000.4432	0.0014	5559.8066	0.1509	1.3663	0.0588	0.1492	0.5440	0.1340	0.4204	0.0620	1.3663	0.05	0.13	0.15	0.54	0.42	0.05	false	false	true	false	SIMPLEX
114	2000.2383	0.0014	5557.7240	0.1510	2.8785	0.1231	0.2312	1.1975	0.5752	0.6224	0.1290	2.8785	0.12	0.58	0.23	1.20	0.52	0.13	false	false	false	false	SIMPLEX
115	2000.4531	0.0014	5557.5962	0.1508	1.3665	0.0568	0.1492	0.5440	0.1340	0.4205	0.0620	1.3665	0.05	0.13	0.15	0.54	0.42	0.05	false	false	true	false	SIMPLEX
116	2000.0000	0.0014	5555.1460	0.1509	1.3661	0.0557	0.1492	0.5440	0.1339	0.4203	0.0620	1.3661	0.05	0.13	0.15	0.54	0.42	0.05	false	true	true	false	SIMPLEX
117	2000.0000	0.0014	5555.5112	0.1508	1.3660	0.0557	0.1492	0.5439	0.1340	0.4202	0.0620	1.3660	0.05	0.13	0.15	0.54	0.42	0.05	false	true	true	false	SIMPLEX
118	2000.0000	0.0014	5554.9460	0.1510	1.3659	0.0567	0.1492	0.5439	0.1339	0.4202	0.0620	1.3659	0.05	0.13	0.15	0.54	0.42	0.05	false	true	true	false	SIMPLEX
119	2000.0000	0.0014	5554.5038	0.1509	1.3659	0.0586	0.1492	0.5438	0.1340	0.4203	0.0620	1.3659	0.05	0.13	0.15	0.54	0.42	0.05	false	true	true	false	SIMPLEX
120	2000.0374	0.0014	5555.8432	0.1510	2.8783	0.1230	0.2312	1.1975	0.5751	0.6224	0.1290	2.8783	0.12	0.58	0.23	1.20	0.52	0.13	false	false	false	false	SIMPLEX
121	2000.0093	0.0014	5555.3203	0.1508	1.3660	0.0567	0.1492	0.5439	0.1339	0.4203	0.0620	1.3660	0.05	0.13	0.15	0.54	0.42	0.05	false	false	true	false	SIMPLEX
122	2000.0280	0.0014	5555.6589	0.1510	1.3659	0.0570	0.1491	0.5438	0.1337	0.4204	0.0620	1.3659	0.05	0.13	0.15	0.54	0.42	0.05	false	false	true	false	SIMPLEX
123	2000.0000	0.0014	5553.2975	0.1510	1.3657	0.0587	0.1492	0.5438	0.1339	0.4202	0.0620	1.3657	0.05	0.13	0.15	0.54	0.42	0.05	false	true	true	false	SIMPLEX
124	2000.0140	0.0014	5553.5469	0.1510	1.3656	0.0566	0.1492	0.5438	0.1339	0.4202	0.0620	1.3656	0.05	0.13	0.15	0.54	0.42	0.05	false	false	true	false	SIMPLEX
125	2000.0210	0.0014	5552.5148	0.1510	1.3657	0.0563	0.1492	0.5437	0.1342	0.4201	0.0620	1.3657	0.05	0.13	0.15	0.54	0.42	0.05	false	false	true	false	SIMPLEX
126	2000.0000	0.0014	5552.4282	0.1509	1.3657	0.0586	0.1492	0.5438	0.1341	0.4201	0.0620	1.3657	0.05	0.13	0.15	0.54	0.42	0.05	false	true	true	false	SIMPLEX
127	2000.0070	0.0014	5552.5535	0.1510	1.3657	0.0570	0.1491	0.5437	0.1337	0.4202	0.0619	1.3657	0.05	0.13	0.15	0.54	0.42	0.05	false	false	true	false	SIMPLEX
128	2000.0105	0.0014	5551.0680	0.1509	1.3656	0.0570	0.1491	0.5437	0.1337	0.4203	0.0619	1.3656	0.05	0.13	0.15	0.54	0.42	0.05	false	false	true	false	SIMPLEX
129	2000.0138	0.0014	5549.1790	0.1509	1.3653	0.0555	0.1491	0.5435	0.1340	0.4200	0.0619	1.3653	0.05	0.13	0.15	0.54	0.42	0.05	false	false	true	false	SIMPLEX
130	2000.0079	0.0014	5551.6703	0.1509	1.3659	0.0564	0.1492	0.5438	0.1343	0.4202	0.0620	1.3659	0.05	0.13	0.15	0.54	0.42	0.05	false	false	true	false	SIMPLEX
131	2000.0072	0.0014	5552.3342	0.1510	1.3656	0.0567	0.1492	0.5438	0.1339	0.4201	0.0620	1.3656	0.05	0.13	0.15	0.54	0.42	0.05	false	false	true	false	SIMPLEX
132	2000.0185	0.0014	5551.7506	0.1510	1.3655	0.0558	0.1491	0.5437	0.1337	0.4202	0.0619	1.3655	0.05	0.13	0.15	0.54	0.42	0.05	false	false	true	false	SIMPLEX
133	2000.0278	0.0014	5550.1079	0.1510	1.3654	0.0563	0.1492	0.5436	0.1341	0.4200	0.0620	1.3654	0.05	0.13	0.15	0.54	0.42	0.05	false	false	true	false	SIMPLEX
134	2000.0206	0.0014	5548.1200	0.1510	1.3651	0.0569	0.1491	0.5433	0.1336	0.4201	0.0619	1.3651	0.05	0.13	0.15	0.54	0.42	0.05	false	false	true	false	SIMPLEX
135	2000.0739	0.0014	5545.4330	0.1510	1.3647	0.0558	0.1491	0.5434	0.1335	0.4199	0.0619	1.3647	0.05	0.13	0.15	0.54	0.42	0.05	false	true	true	false	SIMPLEX
136	2000.0937	0.0013	5545.9021	0.1510	1.3649	0.0553	0.1492	0.5434	0.1343	0.4198	0.0619	1.3649	0.05	0.13	0.15	0.54	0.42	0.05	false	true	true	false	SIMPLEX
137	2000.0931	0.0014	5548.5614	0.1509	1.3647	0.0583	0.1491	0.5434	0.1342	0.4198	0.0619	1.3647	0.05	0.13	0.15	0.54	0.42	0.05	false	false	true	false	SIMPLEX
138	2000.0705	0.0014	5541.9708	0.1508	1.3645	0.0557	0.1491	0.5433	0.1338	0.4197	0.0619	1.3645	0.05	0.13	0.15	0.54	0.42	0.05	false	true	true	false	SIMPLEX
139	2000.0739	0.0014	5537.8423	0.1509	1.3641	0.0557	0.1491	0.5432	0.1337	0.4196	0.0619	1.3641	0.05	0.13	0.15	0.54	0.42	0.05	false	true	true	false	SIMPLEX
140	2000.0435	0.0014	5537.1913	0.1510	1.3640	0.0566	0.1491	0.5431	0.1339	0.4195	0.0619	1.3640	0.05	0.13	0.15	0.54	0.42	0.05	false	false	true	false	SIMPLEX
141	2000.0574	0.0013	5531.1975	0.1510	1.3633	0.0555	0.1490	0.5428	0.1339	0.4192	0.0618	1.3633	0.05	0.13	0.15	0.54	0.42	0.05	false	true	true	false	SIMPLEX
142	2000.0944	0.0014	5533.1160	0.1508	1.3633	0.0558	0.1490	0.5428	0.1334	0.4194	0.0618	1.3633	0.05	0.13	0.15	0.54	0.42	0.05	false	true	true	false	SIMPLEX
143	2000.0977	0.0014	5530.2340	0.1510	1.3628	0.0588	0.1490	0.5427	0.1332	0.4193	0.0618	1.3628	0.05	0.13	0.15	0.54	0.42	0.05	false	false	true	false	SIMPLEX
144	2000.0400	0.0014	5523.5704	0.1510	1.3622	0.0566	0.1490	0.5425	0.1334	0.4189	0.0617	1.3622	0.05	0.13	0.15	0.54	0.42	0.05	false	true	true	false	SIMPLEX
145	2000.0549	0.0014	5517.4281	0.1508	1.3616	0.0565	0.1489	0.5423	0.1334	0.4187	0.0617	1.3616	0.05	0.13	0.15	0.54	0.42	0.05	false	true	true	false	SIMPLEX
146	2000.0705	0.0013	5503.4286	0.1509	1.3600	0.0553	0.1489	0.5417	0.1334	0.4181	0.0616	1.3600	0.05	0.13	0.15	0.54	0.42	0.05	false	false	true	false	SIMPLEX
147	2000.0733	0.0014	5507.8119	0.1510	1.3604	0.0558	0.1488	0.5418	0.1329	0.4183	0.0616	1.3604	0.05	0.13	0.15	0.54	0.42	0.05	false	true	true	false	SIMPLEX
148	2000.0872	0.0014	5498.8862	0.1510	NaN	NaN	NaN	NaN	NaN	NaN	NaN	NaN	NaN	NaN	NaN	NaN	NaN	NaN	NaN	NaN	true	false	true	false	SIMPLEX
149	2000.0476	0.0014	5524.8085	0.1509	1.3624	0.0586	0.1490	0.5426	0.1334	0.4191	0.0618	1.3624	0.05	0.13	0.15	0.54	0.42	0.05	false	false	true	false	SIMPLEX
150	2000.0593	0.0014	5498.3102	0.1509	1.3593	0.0586	0.1488	0.5415	0.1328	0.4180	0.0616	1.3593	0.05	0.13	0.15	0.54	0.42	0.05	false	false	true	false	SIMPLEX
151	2000.0502	0.0014	5482.3166	0.1508	1.3586	0.0570	0.1487	0.5408	0.1333	0.4173	0.0614	1.3586	0.05	0.13	0.15	0.54	0.42	0.05	false	false	true	false	SIMPLEX
152	2000.0734	0.0014	5483.7532	0.1510	1.3574	0.0563	0.1487	0.5408	0.1325	0.4174	0.0614	1.3574	0.05	0.13	0.15	0.54	0.42	0.05	false	false	true	false	SIMPLEX
153	2000.0893	0.0014	5483.2235	0.1510	1.3561	0.0558	0.1486	0.5406	0.1328	0.4167	0.0613	1.3561	0.05	0.13	0.15	0.54	0.42	0.05	false	false	true	false	SIMPLEX
154	2000.1076	0.0014	5454.9190	0.1509	1.3542	0.0565	0.1485	0.5397	0.1321	0.4162	0.0612	1.3542	0.05	0.13	0.15	0.54	0.42	0.05	false	false	true	false	SIMPLEX
155	2000.1413	0.0014	5420.4823	0.1509	1.3507	0.0563	0.1483	0.5382	0.1310	0.4149	0.0610	1.3507	0.05	0.13	0.15	0.54	0.41	0.05	false	false	true	false	SIMPLEX
156	2000.1053	0.0014	5428.8930	0.1509	1.3520	0.0550	0.1483	0.5385	0.1323	0.4153	0.0610	1.3520	0.05	0.13	0.15	0.54	0.42	0.05	false	false	true	false	SIMPLEX
157	2000.1276	0.0014	5393.0146	0.1509	1.3489	0.0566	0.1481	0.5371	0.1324	0.4138	0.0607	1.3489	0.05	0.13	0.15	0.54	0.41	0.05	false	true	true	false	SIMPLEX
158	2000.1562	0.0015	5337.8096	0.1509	1.3435	0.0586	0.1476	0.5348	0.1327	0.4113	0.0603	1.3435	0.05	0.13	0.15	0.53	0.41	0.05	false	false	true	false	SIMPLEX
159	2000.1839	0.0014	5341.8391	0.1508	1.3428	0.0554	0.1477	0.5350	0.1318	0.4117	0.0604	1.3428	0.05	0.13	0.15	0.53	0.41	0.05	false	false	true	false	SIMPLEX
160	2000.2487	0.0014	5271.5434	0.1508	1.3350	0.0552	0.1470	0.5320	0.1313	0.4086	0.0598	1.3350	0.05	0.13	0.15	0.53	0.41	0.05	false	false	true	false	SIMPLEX
161	2000.2365	0.0014	5265.1701	0.1508	1.3344	0.0551	0.1470	0.5318	0.1312	0.4085	0.0598	1.3344	0.05	0.13	0.15	0.53	0.41	0.05	false	false	true	false	SIMPLEX
162	2000.3102	0.0014	5188.1424	0.1507	1.3237	0.0580	0.1460	0.5278	0.1309	0.4042	0.0590	1.3237	0.05	0.13	0.15	0.53	0.40	0.05	false	false	true	false	SIMPLEX
163	2000.3229	0.0014	5171.1273	0.1508	1.3235	0.0558	0.1460	0.5278	0.1305	0.4042	0.0591	1.3235	0.05	0.13	0.15	0.53	0.40	0.05	false	false	true	false	SIMPLEX
164	2000.4116	0.0015	5043.2444	0.1507	1.3093	0.0556	0.1449	0.5223	0.1302	0.3983	0.0580	1.3093	0.05	0.13	0.14	0.52	0.40	0.05	false	false	true	false	SIMPLEX
165	2000.4320	0.0015	5000.0000	0.1505	1.3061	0.0559	0.1446	0.5205	0.1311	0.3954	0.0576	1.3061	0.05	0.13	0.14	0.52	0.40	0.05	false	true	true	false	SIMPLEX
166	2000.5551	0.0014	5000.0000	0.1505	1.3041	0.0559	0.1446	0.5206	0.1295	0.3963	0.0577	1.3041	0.05	0.13	0.14	0.52	0.40	0.05	false	false	true	false	SIMPLEX
167	2000.5137	0.0015	5000.0000	0.1504	1.3060	0.0557	0.1446	0.5208	0.1307	0.3956	0.0577	1.3060	0.05	0.13	0.14	0.52	0.40	0.05	false	true	true	false	SIMPLEX
168	2000.7071	0.0015	5000.0000	0.1505	1.3056	0.0550	0.1446	0.5206	0.1313	0.3955	0.0576	1.3056	0.05	0.13	0.14	0.52	0.40	0.05	false	true	true	false	SIMPLEX
169	2000.5045	0.0015	5021.5222	0.1508	1.3075	0.0557	0.1447	0.5215	0.1304	0.3974	0.0578	1.3075	0.05	0.13	0.14	0.52	0.40	0.05	false	false	true	false	SIMPLEX
170	2000.5410	0.0015	5010.8111	0.1505	1.3064	0.0556	0.1447	0.5211	0.1303	0.3960	0.0577	1.3064	0.05	0.13	0.14	0.52	0.40	0.05	false	false	true	false	SIMPLEX
171	2000.3548	0.0014	5005.4056	0.1508	1.3046	0.0554	0.1447	0.5208	0.1298	0.3953	0.0577	1.3046	0.05	0.13	0.14	0.52	0.40	0.05	false	true	true	false	SIMPLEX
172	2000.4428	0.0015	5000.0000	0.1505	1.3048	0.0555	0.1446	0.5206	0.1300	0.3964	0.0577	1.3048	0.05	0.13	0.14	0.52	0.40	0.05	false	false	true	false	SIMPLEX
173	2000.5572	0.0014	5002.7028	0.1504	1.3037	0.0550	0.1447	0.5208	0.1289	0.3956	0.0578	1.3037	0.05	0.13	0.14	0.52	0.40	0.05	false	true	true	false	SIMPLEX
174	2000.5198	0.0013	5004.0542	0.1503	1.3030	0.0548	0.1447	0.5209	0.1281	0.3956	0.0578	1.3030	0.05	0.13	0.14	0.52	0.40	0.05	false	true	true	false	SIMPLEX
175	2000.3756	0.0013	5004.7299	0.1505	1.3022	0.0547	0.1447	0.5207	0.1279	0.3964	0.0578	1.3022	0.05	0.13	0.14	0.52	0.40	0.05	false	true	true	false	SIMPLEX
176	2000.2535	0.0012	5007.0948	0.1506	1.2999	0.0541	0.1448	0.5207	0.1263	0.3962	0.0579	1.2999	0.05	0.13	0.14	0.52	0.40	0.05	false	true	true	false	SIMPLEX
177	2000.4568	0.0017	5008.7773	0.1505	1.3007	0.0547	0.1448	0.5208	0.1265	0.3954	0.0579	1.3007	0.05	0.13	0.14	0.52	0.40	0.05	false	true	true	false	SIMPLEX
178	2000.5778	0.0011	5004.3075	0.1504	1.2988	0.0538	0.1448	0.5208	0.1253	0.3962	0.0579	1.2988	0.05	0.13	0.14	0.52	0.40	0.05	false	true	true	false	SIMPLEX
179	2000.5842	0.0009	5003.7585	0.1502	1.2985	0.0527	0.1449	0.5207	0.1260	0.3952	0.0580	1.2985	0.05	0.13	0.14	0.52	0.40	0.05	false	true	true	false	SIMPLEX
180	2000.4521	0.0008	5011.5874	0.1503	1.2993	0.0527	0.1449	0.5208	0.1260	0.3956	0.0581	1.2993	0.05	0.13	0.14	0.52	0.40	0.05	false	true	true	false	SIMPLEX
181	2000.3035	0.0008	5011.3073	0.1503	1.2990	0.0523	0.1449	0.5207	0.1267	0.3954	0.0581	1.2990	0.05	0.13	0.14	0.52	0.40	0.05	false	true	true	false	SIMPLEX
182	2000.3928	0.0007	5008.5956	0.1503	1.2992	0.0513	0.1449	0.5207	0.1274	0.3953	0.0581	1.2992	0.05	0.13	0.14	0.52	0.40	0.05	false	true	true	false	SIMPLEX
183	2000.5508	0.0005	5010.5740	0.1501	1.3005	0.0503	0.1450	0.5209	0.1293	0.3958	0.0582	1.3005	0.05	0.13	0.14	0.52	0.40	0.05	false	true	true	false	SIMPLEX
184	2000.3568	0.0010	5007.9546	0.1505	1.2984	0.0532	0.1448	0.5207	0.1253	0.3952	0.0580	1.2984	0.05	0.13	0.14	0.52	0.40	0.05	false	true	true	false	SIMPLEX
185	2000.4166	0.0008	5004.2175	0.1505	1.2979	0.0522	0.1449	0.5204	0.1265	0.3950	0.0580	1.2979	0.05	0.13	0.14	0.52	0.40	0.05	false	true	true	false	SIMPLEX
186	2000.3986	0.0008	5005.5300	0.1505	1.2970	0.0521	0.1448	0.5206	0.1263	0.3953	0.0580	1.2970	0.05	0.13	0.14	0.52	0.40	0.05	false	true	true	false	SIMPLEX
187	2000.4788	0.0011	5003.1760	0.1505	1.2977	0.0537	0.1448	0.5205	0.1250	0.3958	0.0579	1.2977	0.05	0.13	0.14	0.52	0.40	0.05	false	true	true	false	SIMPLEX
188	2000.5539	0.0011	5000.0000	0.1505	1.2981	0.0538	0.1448	0.5205	0.1253	0.3959	0.0579	1.2981	0.05	0.13	0.14	0.52	0.40	0.05	false	true	true	false	SIMPLEX
189	2000.3510	0.0011	5007.0717	0.1508	1.2968	0.0534	0.1448	0.5207	0.1249	0.3956	0.0578	1.2968	0.05	0.13	0.14	0.52	0.40	0.05	false	true	true	false	SIMPLEX
190	2000.0494	0.0011	5001.2383	0.1511	2.8770	0.1228	0.2314	1.1973	0.5745	0.6222	0.1288	2.8770	0.12	0.57	0.23	1.20	0.52	0.13	false	false	false	false	SIMPLEX
191	2000.5404	0.0010	5000.0000	0.1508	1.2963	0.0531	0.1448	0.5201	0.1250	0.3955	0.0579	1.2963	0.05	0.13	0.14	0.52	0.40	0.05	false	true	true	false	SIMPLEX
192	2000.1837	0.0009	5002.8889	0.1509	1.2966	0.0526	0.1448	0.5198	0.1259	0.3955	0.0579	1.2966	0.05	0.13	0.14	0.52	0.40	0.05	false	true	true	false	SIMPLEX
193	2000.2191	0.0008	5000.0000	0.1510	1.2961	0.0523	0.1448	0.5197	0.1261	0.3954	0.0579	1.2961	0.05	0.13	0.14	0.52	0.40	0.05	false	true	true	false	SIMPLEX
194	2000.2003	0.0011	5003.0903	0.1511	2.8768	0.1228	0.2314	1.1973	0.5744	0.6221	0.1288	2.8768	0.12	0.57	0.23	1.20	0.52	0.13	false	false	false	false	SIMPLEX
195	2000.3482	0.0009	5000.8851	0.1507	1.2968	0.0526	0.1448	0.5200	0.1259	0.3956	0.0579	1.2968	0.05	0.13	0.14	0.52	0.40	0.05	false	true	true	false	SIMPLEX
196	2000.3822	0.0007	5000.0000	0.1509	1.2964	0.0517	0.1448	0.5197	0.1267	0.3954	0.0579	1.2964	0.05	0.13	0.14	0.52	0.40	0.05	false	true	true	false	SIMPLEX
197	2000.3106	0.0009	5006.5893	0.1511	2.8758	0.1223	0.2315	1.1972	0.5738	0.6221	0.1287	2.8758	0.12	0.57	0.23	1.20	0.52	0.13	false	false	false	false	SIMPLEX
198	2000.3395	0.0009	5000.8037	0.1508	1.2967	0.0525	0.1448	0.5199	0.1260	0.3955	0.0579	1.2967	0.05	0.13	0.14	0.52	0.40	0.05	false	true	true	false	SIMPLEX
199	2000.3102	0.0009	5000.5408	0.1510	1.2963	0.0521	0.1449	0.5198	0.1263	0.3954	0.0579	1.2963	0.05	0.13	0.14	0.52	0.40	0.05	false	true	true	false	SIMPLEX

APPENDIX J – CONDITION B HYBRID III CORA OUTPUT FILE

Summary Report Date: Oct 31 2018

Rating of: WIAMan BRC Evaluation

Description: Biomedical Response Corridors

Rating:

No.	Load Case	Rating	Weight
1	Bosch HIII B-1	0.711	1.0
	Total rating	**0.711**	1.0

Load Case Report Date: Oct 31 2018

Rating of: Bosch HIII B-1

Description: Subloadcase

Rating:

No.	Experiment	Rating	Weight
1	HIII_B_Lower_Tibia_Fx	0.780	0.10
2	HIII_B_Lower_Tibia_Fz	0.765	0.10
3	HIII_B_Lower_Tibia_My	0.775	0.10
4	HIII_B_Upper_Tibia_Fz	0.606	0.10
5	HIII_B_Upper_Tibia_Ax	0.773	0.10
6	HIII_B_Upper_Tibia_Az	0.811	0.10
7	HIII_B_Pelvis_Ax	0.606	0.10
8	HIII_B_Pelvis_Az	0.643	0.10
9	HIII_B_T1_Ax	0.742	0.10
10	HIII_B_T1_Az	0.606	0.10
	Total rating of load case 1:	**0.711**	1.0

Experiment Report Date: Oct 31 2018

Report of Experiment: HIII_B_Lower_Tibia_Fx

Description: Lower Tibia Fx

Rating:

No.	Signal	Rating	Weight
1	11TIBILELOH3FOXC	0.780	1.0
	Total rating of experiment 1:	**0.780**	1.0

Signal Report Date: Oct 31 2018

Rating of: HIII_B_Lower_Tibia_Fx

Report of Signal 1 of Experiment 1: 11TIBILELOH3FOXC

Overall Rating: 0.780

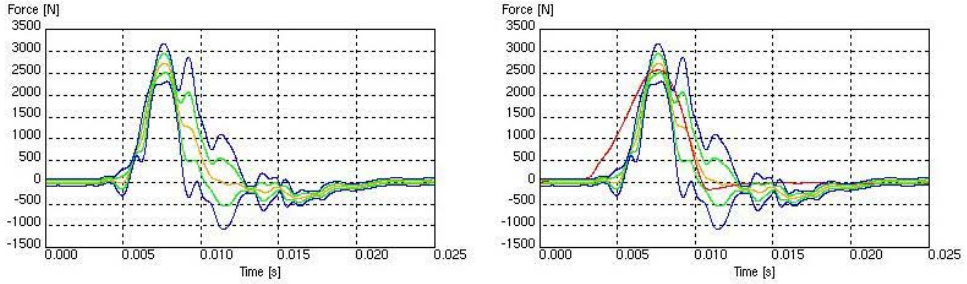

Method	Name				Rating	Weight
1	Corridor Method				0.579	0.357
2	Correlation Method				0.892	0.643
		Value	Rating	Weight		
	Cross correlation function	0.925	0.962	0.333		
	Size	0.714	0.714	0.333		
	Phase shift	0.0000	1.0	0.333		
3	Combination of 1 and 2				**0.780**	-

Parameters:	Evaluation Intervall:	0.0000 - 0.0250
Method 1:	Max. half width of inner corridor:	-
	Max. half width of outer corridor:	-
	Corridor curve file:	Lower_Tibia_Fx_Corridor
	Reference value:	2735.060
	Transition exponent:	1
Method 2:	Limits for phase shift:	0.0003 - 0.0030
	Rating exponents (shape, size, phase):	1, 1, 1

Experiment Report Date: Oct 31 2018

Report of Experiment: HIII_B_Lower_Tibia_Fz

Description: Lower Tibia Fz

Rating:

No.	Signal	Rating	Weight
1	11TIBILELOH3FOZC	0.765	1.0
	Total rating of experiment 2:	**0.765**	1.0

Signal Report Date: Oct 31 2018

Rating of: HIII_B_Lower_Tibia_Fz

Report of Signal 1 of Experiment 2: 11TIBILELOH3FOZC

Overall Rating: 0.765

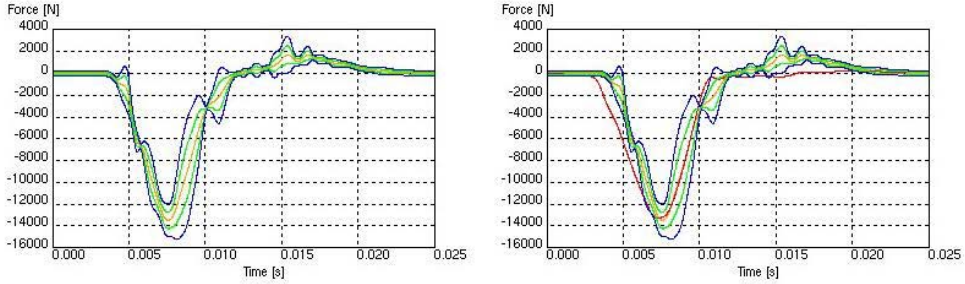

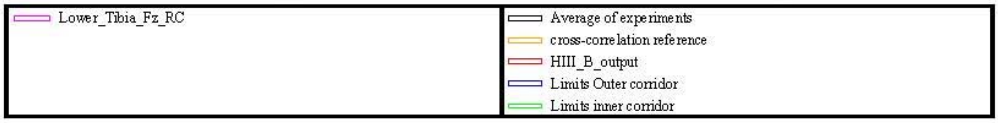

Method	Name				Rating	Weight
1	Corridor Method				0.450	0.357
2	Correlation Method				0.940	0.643
		Value	Rating	Weight		
	Cross correlation function	0.965	0.982	0.333		
	Size	0.838	0.838	0.333		
	Phase shift	0.0000	1.0	0.333		
3	Combination of 1 and 2				**0.765**	-

Parameters:	Evaluation Intervall:	0.0000 - 0.0250
Method 1:	Max. half width of inner corridor:	-
	Max. half width of outer corridor:	-
	Corridor curve file:	Lower_Tibia_Fz_Corridor
	Reference value:	13500.70
	Transition exponent:	1
Method 2:	Limits for phase shift:	0.0003 - 0.0030
	Rating exponents (shape, size, phase):	1, 1, 1

Experiment Report Date: Oct 31 2018

Report of Experiment: HIII_B_Lower_Tibia_My

Description: Lower Tibia My

Rating:

No.	Signal	Rating	Weight
1	11TIBILELOH3MOYB	0.775	1.0
	Total rating of experiment 3:	**0.775**	1.0

Signal Report Date: Oct 31 2018

Rating of: HIII_B_Lower_Tibia_My

Report of Signal 1 of Experiment 3: 11TIBILELOH3MOYB

Overall Rating: 0.775

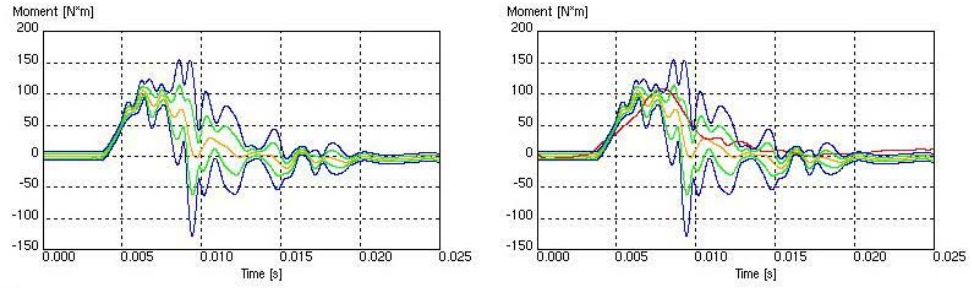

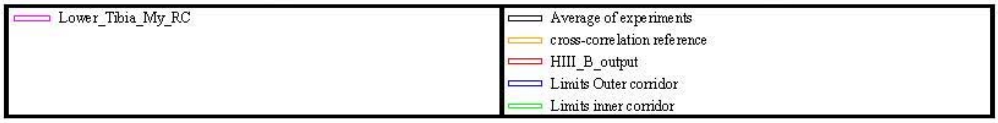

Method	Name	Rating	Weight
1	Corridor Method	0.507	0.357
2	Correlation Method	0.924	0.643
3	Combination of 1 and 2	**0.775**	-

Correlation Method

	Value	Rating	Weight
Cross correlation function	0.890	0.945	0.333
Size	0.826	0.826	0.333
Phase shift	0.0000	1.0	0.333

Parameters:	Evaluation Intervall:	0.0000 - 0.0250
Method 1:	Max. half width of inner corridor:	-
	Max. half width of outer corridor:	-
	Corridor curve file:	Lower_Tibia_My_Corridor
	Reference value:	105.742
	Transition exponent:	1
Method 2:	Limits for phase shift:	0.0003 - 0.0030
	Rating exponents (shape, size, phase):	1, 1, 1

Experiment Report Date: Oct 31 2018

Report of Experiment: HIII_B_Upper_Tibia_Fz

Description: Upper Tibia Fz

Rating:

No.	Signal	Rating	Weight
1	11TIBILEUPH3FOZB	0.606	1.0
	Total rating of experiment 4:	**0.606**	1.0

Signal Report Date: Oct 31 2018

Rating of HIII_B_Upper_Tibia_Fz

Report of Signal 1 of Experiment 4: 11TIBILEUPH3FOZB

Overall Rating: 0.606

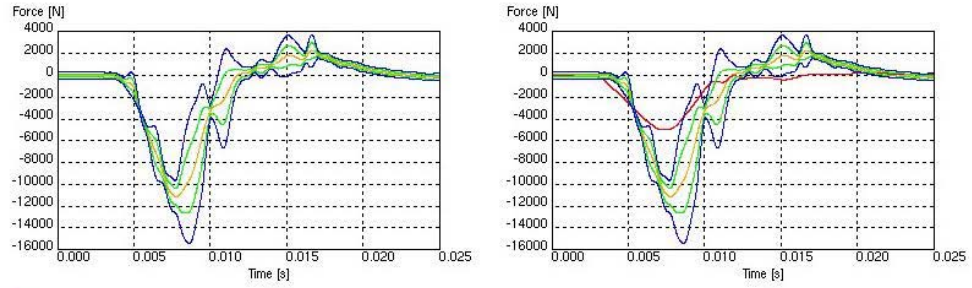

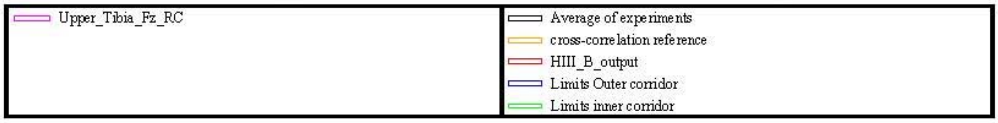

Method	Name				Rating	Weight
1	Corridor Method				0.373	0.357
2	Correlation Method				0.736	0.643
		Value	Rating	Weight		
	Cross correlation function	0.928	0.964	0.333		
	Size	0.243	0.243	0.333		
	Phase shift	0.0000	1.0	0.333		
3	Combination of 1 and 2				**0.606**	-

Parameters:	Evaluation Intervall:	0.0000 - 0.0250
Method 1:	Max. half width of inner corridor:	-
	Max. half width of outer corridor:	-
	Corridor curve file:	Upper_Tibia_Fz_Corridor
	Reference value:	11145.32
	Transition exponent:	1
Method 2:	Limits for phase shift:	0.0003 - 0.0030
	Rating exponents (shape, size, phase):	1, 1, 1

Experiment Report Date: Oct 31 2018

Report of Experiment: HIII_B_Upper_Tibia_Ax

Description: Upper Tibia Ax

Rating:

No.	Signal	Rating	Weight
1	11TIBILEUPH3ACXC	0.773	1.0
	Total rating of experiment 5:	**0.773**	1.0

Signal Report Date: Oct 31 2018

Rating of: HIII_B_Upper_Tibia_Ax

Report of Signal 1 of Experiment 5: 11TIBILEUPH3ACXC

Overall Rating: 0.773

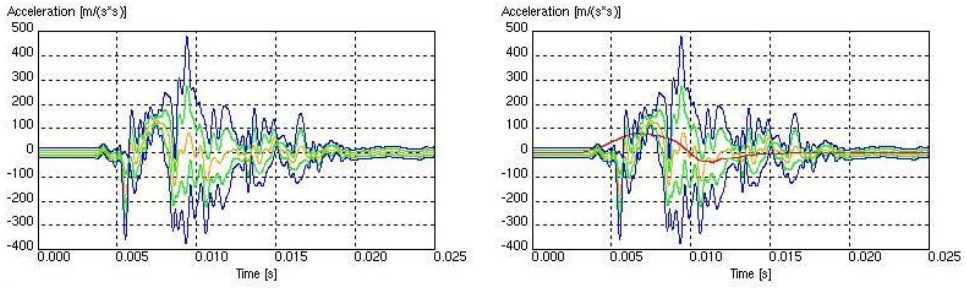

Method	Name				Rating	Weight
1	Corridor Method				0.844	0.357
2	Correlation Method				0.733	0.643
		Value	Rating	Weight		
	Cross correlation function	0.323	0.662	0.333		
	Size	0.537	0.537	0.333		
	Phase shift	0.0000	1.0	0.333		
3	Combination of 1 and 2				**0.773**	-

Parameters:	Evaluation Intervall:	0.0000 - 0.0250
Method 1:	Max. half width of inner corridor:	-
	Max. half width of outer corridor:	-
	Corridor curve file:	Upper_Tibia_Ax_Corridor
	Reference value:	177.999
	Transition exponent:	1
Method 2:	Limits for phase shift:	0.0003 - 0.0030
	Rating exponents (shape, size, phase):	1, 1, 1

Experiment Report Date: Oct 31 2018

Report of Experiment: HIII_B_Upper_Tibia_Az

Description: Upper Tibia Az

Rating:

No.	Signal	Rating	Weight
1	11TIBILEUPH3ACZC	0.811	1.0
	Total rating of experiment 6:	**0.811**	1.0

Signal Report Date: Oct 31 2018

Rating of: HIII_B_Upper_Tibia_Az

Report of Signal 1 of Experiment 6: 11TIBILEUPH3ACZC

Overall Rating: 0.811

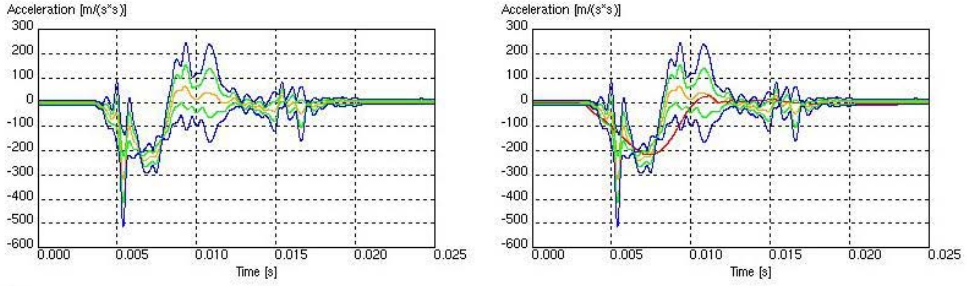

Method	Name				Rating	Weight
1	Corridor Method				0.577	0.357
2	Correlation Method				0.941	0.643
		Value	Rating	Weight		
	Cross correlation function	0.783	0.892	0.333		
	Size	0.931	0.931	0.333		
	Phase shift	0.0000	1.0	0.333		
3	Combination of 1 and 2				**0.811**	-

Parameters:	Evaluation Intervall:	0.0000 - 0.0250
Method 1:	Max. half width of inner corridor:	-
	Max. half width of outer corridor:	-
	Corridor curve file:	Upper_Tibia_Az_Corridor
	Reference value:	317.648
	Transition exponent:	1
Method 2:	Limits for phase shift:	0.0003 - 0.0030
	Rating exponents (shape, size, phase):	1, 1, 1

Experiment Report Date: Oct 31 2018

Report of Experiment: HIII_B_Pelvis_Ax

Description: Pelvis Ax

Rating:

No.	Signal	Rating	Weight
1	11PELV0000H3VAXC	0.606	1.0
	Total rating of experiment 7:	**0.606**	1.0

Signal Report Date: Oct 31 2018

Rating of: HIII_B_Pelvis_Ax

Report of Signal 1 of Experiment 7: 11PELV0000H3VAXC

Overall Rating: 0.606

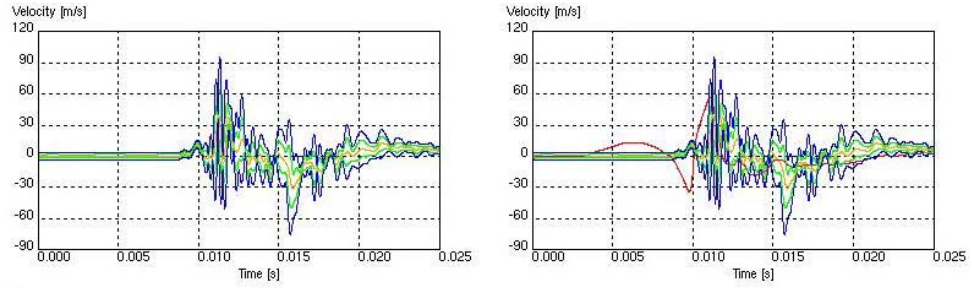

Method	Name				Rating	Weight
1	Corridor Method				0.446	0.357
2	Correlation Method				0.694	0.643
		Value	Rating	Weight		
	Cross correlation function	0.263	0.631	0.333		
	Size	0.452	0.452	0.333		
	Phase shift	0.0000	1.0	0.333		
3	Combination of 1 and 2				**0.606**	-

Parameters:	Evaluation Intervall:	0.0000 - 0.0250
Method 1:	Max. half width of inner corridor:	-
	Max. half width of outer corridor:	-
	Corridor curve file:	Pelvis_Ax_Corridor
	Reference value:	39.898
	Transition exponent:	1
Method 2:	Limits for phase shift:	0.0003 - 0.0030
	Rating exponents (shape, size, phase):	1, 1, 1

Experiment Report Date: Oct 31 2018

Report of Experiment: HIII_B_Pelvis_Az

Description: Pelvis_Az

Rating:

No.	Signal	Rating	Weight
1	11PELV0000H3VAZC	0.643	1.0
	Total rating of experiment 8:	**0.643**	1.0

Signal Report Date: Oct 31 2018

Rating of: HIII_B_Pelvis_Az

Report of Signal 1 of Experiment 8: 11PELV0000H3VAZC

Overall Rating: 0.643

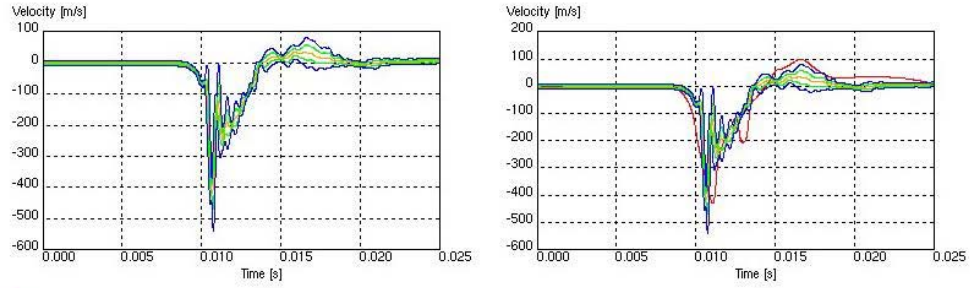

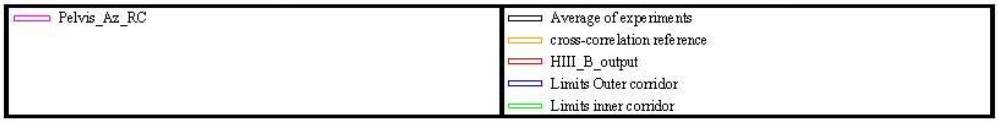

Method	Name	Rating	Weight
1	Corridor Method	0.337	0.357
2	Correlation Method	0.813	0.643
3	Combination of 1 and 2	**0.643**	-

Correlation Method

	Value	Rating	Weight
Cross correlation function	0.891	0.945	0.333
Size	0.495	0.495	0.333
Phase shift	0.0000	1.0	0.333

Parameters:	Evaluation Intervall:	0.0000 - 0.0250
Method 1:	Max. half width of inner corridor:	-
	Max. half width of outer corridor:	-
	Corridor curve file:	Pelvis_Az_Corridor
	Reference value:	416.780
	Transition exponent:	1
Method 2:	Limits for phase shift:	0.0003 - 0.0030
	Rating exponents (shape, size, phase):	1, 1, 1

Experiment Report Date: Oct 31 2018

Report of Experiment: HIII_B_T1_Ax

Description: T1_Ax

Rating:

No.	Signal	Rating	Weight
1	11TS010000H3ACXA	0.742	1.0
	Total rating of experiment 9:	**0.742**	1.0

Signal Report Date: Oct 31 2018

Rating of HIII_B_T1_Ax

Report of Signal 1 of Experiment 9: 11TS010000H3ACXA

Overall Rating: 0.742

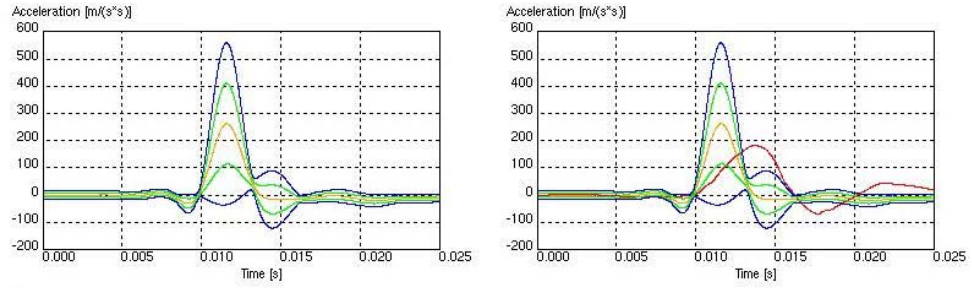

T1_Ax_RC

Average of experiments
cross-correlation reference
HIII_B_output
Limits Outer corridor
Limits inner corridor

Method	Name				Rating	Weight
1	Corridor Method				0.482	0.357
2	Correlation Method				0.887	0.643
		Value	Rating	Weight		
	Cross correlation function	0.421	0.710	0.333		
	Size	0.951	0.951	0.333		
	Phase shift	0.0000	1.0	0.333		
3	Combination of 1 and 2				**0.742**	-

Parameters:	Evaluation Intervall:	0.0000 - 0.0250
Method 1:	Max. half width of inner corridor:	-
	Max. half width of outer corridor:	-
	Corridor curve file:	T1_Ax_Corridor
	Reference value:	262.337
	Transition exponent:	1
Method 2:	Limits for phase shift:	0.0003 - 0.0030
	Rating exponents (shape, size, phase):	1, 1, 1

Experiment Report Date: Oct 31 2018

Report of Experiment: HIII_B_T1_Az

Description: T1_Az

Rating:

No.	Signal	Rating	Weight
1	11TS010000H3ACZA	0.606	1.0
	Total rating of experiment 10:	**0.606**	1.0

Signal Report Date: Oct 31 2018

Rating of: HIII_B_T1_Az

Report of Signal 1 of Experiment 10: 11TS010000H3ACZA

Overall Rating: 0.606

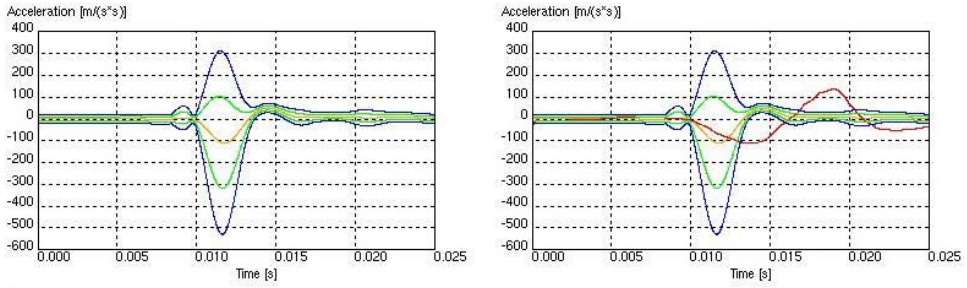

Method	Name				Rating	Weight
1	Corridor Method				0.577	0.357
2	Correlation Method				0.622	0.643
		Value	Rating	Weight		
	Cross correlation function	0.186	0.593	0.333		
	Size	0.273	0.273	0.333		
	Phase shift	0.0000	1.0	0.333		
3	Combination of 1 and 2				**0.606**	-

Parameters:	Evaluation Intervall:	0.0000 - 0.0250
Method 1:	Max. half width of inner corridor:	-
	Max. half width of outer corridor:	-
	Corridor curve file:	T1_Az_Corridor
	Reference value:	111.105
	Transition exponent:	1
Method 2:	Limits for phase shift:	0.0003 - 0.0030
	Rating exponents (shape, size, phase):	1, 1, 1

REFERENCES

1. Alem, N.M., Strawn, G.D. (1996) Evaluation of an Energy Absorbing Truck Seat for Increased Protection from Landmine Blast Seats. US Army Aeromedical Research Laboratory Report No. 96-06. January 1996.
2. Alvarez J. (2011) Epidemiology of Blast Injuries in Current Operations. RTO-MP-HFM-207. Proceedings of RTO Human Factors and Medicine Panel (HFM) Symposium, 2011, Halifax, Canada.
3. Arepally, S., Gorsich, D., Hope, K., Gentner, S., Drotleff, K. (2008) Application of Mathematical Modeling in Potentially Survivable Blast Threats in Military Vehicles. US Army TARDEC-19214RC. 26th Army Science Conference.
4. Atlas, S.W., Regenbogen, V., Rogers, L.F., Kim, K.S. (1986) The Radiographic Characterization of Burst Fractures of the Spine. American Society of Neuroradiology. AJNR 7:675-682.
5. Bailey, A., Christopher, J., Brozoski, F., Salzar, R. (2015) Post Mortem Human Surrogate Injury Response of the Pelvis and Lower Extremities to Simulated Underbody Blast. Annals of Biomedical Engineering, Vol. 43, No. 8, August 2015 pp. 1907–1917.
6. Bailey, A., Christopher, J., Henderson, K., Brozoski, F., Salzar, R. (2013) Comparison of Hybrid-III and PMHS Response to Simulated Underbody Blast Loading Conditions. IRCOBI Conference 2013. IRC-13-25.
7. Begeman, P.C., Visarius, H., Nolte, L.P., Prasad, P. (1994) Viscoelastic Shear Responses of the Cadaver and Hybrid III Lumbar Response. 38th Stapp Car Crash Conference (Ft. Lauderdale, FL). 14 pp.

8. Belmont, P.J. (2010) Epidemiology of combat wounds in Operation Iraqi Freedom and Operation Enduring Freedom: orthopaedic burden of disease. Journal of surgical Orthopaedic Advances (1548-825X), 19 (1), p. 2.
9. Benesch, B. (2011) Utilizing Vehicle Response Data from Under-Body Blast Tests. Ballistics 2011: 26th International Symposium. DEStech Publications, 2011, pp. 2047-2054.
10. Bosch, K., Harris, K., Clark, D., Scherer, R., Melotik, J. (2014) Blast Mitigation Seat Analysis – Drop Tower Data Review. 2014 NDIA Ground Vehicle Systems Engineering and Technology Symposium Modeling & Simulation, Testing and Validation (MSTV) Technical Session. August 12-14, 2014.
11. Bosch, K., Harris, K., Clark, D., Scherer, R., Melotik, J. (2015) Blast Mitigation Seat Analysis - Assessment of the Effect of Personal Protective Equipment on the 5th Percentile Female Anthropomorphic Test Device Performance in Drop Tower Evaluations. DETC2015-46342. Proceedings of the ASME 2015 International Design Engineering Technical Conferences & Computers and Information in Engineering Conference IDETC/CIE 2015. August 2-5, 2015.
12. Bosch, K. (2016) Blast Mitigation Seat Analysis – Evaluation of Lumbar Compression Data Trends in 5th Percentile Female Anthropomorphic Test Device Performance Compared to 50th Percentile Male Anthropomorphic Test Device in Drop Tower Testing. DETC2016-59094. Proceedings of the ASME 2016 International Design Engineering Technical Conferences & Computers and Information in Engineering Conference IDETC/CIE 2016. August 21-24, 2016.

13. Carter, James A., MacLeod, D., Callahan, P. Blast Mitigating Seat. U.S. Patent 8,091,964 B2 issued January 10, 2012.
14. Champion, H., Holcomb, J., Young, L.A. (2009) Injuries from Explosions: Physics, Biophysics, Pathology, and Required Research Focus. The Journal of TRAUMA Injury, Infection, and Critical Care 66:1468-1477.
15. Chandler, R.F. (1985) Human Injury Criteria Relative to Civil Aircraft Seat and Restraint Systems. SAE 851847. October 1985.
16. Danelson, K.A., Kemper, A.R., Mason, M.J., Tegtmeyer, M., Swiatkowski, S.A., Bolte IV, J.H., Hardy, W.N. (2015) Comparison of ATD to PMHS Response in the Under-Body Blast Environment. Stapp Car Crash Journal, Vol. 59, November 2015. P. 445-520.
17. Danelson, K., Watkins, L., Hendricks, J., Frounfelker, P., Pizzolato-Heine, K., Valentine, R., Loftis, K. (2018) Analysis of the Frequency and Mechanism of Injury to Warfighters in the Under-body Blast Environment. Stapp Car Crash Journal, Vol. 62, November 2018. P. 489-513.
18. Davis, J., Stinner, D., Bailey, J., Aden, J., Hsu, J. (2012) Factors Associated with Mortality in Combat-related Pelvic Fractures. Skeletal Trauma Research Consortium. J Am Acad Orthop Surg 2012; 20(suppl 1):S7-S12.
19. Denis, F. (1983) The Three Column Spine and its Significance in the Classification of Acute Thoracolumbar Spinal Injuries. Spine. Philadelphia, PA. 1983 Nov-Dec; 8(8): 817-31.

20. Desjardins, S. (2003) The Evolution of Energy Absorption Systems for Crashworthy Helicopter Seats. American Helicopter Society 59th Annual Forum, Phoenix, Arizona, May 6-8, 2003.
21. Dooge, D., Dwarampudi, R., Schaffner, G., Miller, A., Thyagarajan, R., Vunnam, M., Babu, V. (2011) Evolution of Occupant Survivability Simulation Framework using FEM-SPH Coupling. US Army TARDEC-22044.
22. Evans, F.G., Lissiner, H.R., Patrick, L.M. (1962) Acceleration-induced Strains in the Intact Vertebral Column. J Appl Physiol. 1962 May; 17: 405-9.
23. Gray, H. (1918) Anatomy of the Human Body. 20th Edition. Philadelphia: Lea & Febiger, accessed on Bartleby.com on 27 December 2016.
24. Greenhalgh P.G., Panzer M.D., Spratley E.M., Salzar R.S. (2018) Analysis of Forces through the Seated Pelvis during Under Body Blasts; 13th World Congress on Computational Mechanics. WCCM2018-1017.
25. Imaging of the Cervical Spine: Wedge Fracture. (2013) University of Virginia. http://www.med-ed.virginia.edu/courses/rad/cspine/fracture16.html. Accessed 31 January 2016.
26. Jankel Blastech Seating A-Series (2013). http://old.jankelts.com/products/product-details.cfm@pID=18. Accessed 27 December 2016.
27. Joint Publication 1-02 (2010). Department of Defense Dictionary of Military and Associated Terms. 8 November 2010. pp 124.

28. Kang, D.G., Lehman, R.A. Jr., Carragee, E.J. (2015) Wartime Spine Injuries: Understanding the Improvised Explosive Device and Biophysics of Blast Trauma. The Spine Journal 12: 849-857.
29. King, A. (2014) BME 7995 Biomechanics in Blast. Lecture on Spinal Injuries. Wayne State University. Fall 2014.
30. King, A. (2016) BME 7100 Mathematical Modeling in Bioengineering. Lecture on Biomechanics of the Thoracolumbar Spine: Anatomy, Response, and Tolerance. Wayne State University.
31. Kulkarni, K.B., Ramalingam, J., Thyagarajan, R. (2013) Evaluating the effectiveness of various blast loading descriptors as occupant injury predictors for underbody blast events. ESI US INC TROY MI.
32. Kulkarni, K.B., Ramalingam, J., Thyagarajan, R. (2014) Assessment of the accuracy of certain reduced order models used in the prediction of occupant injury during under-body blast events. US Army TARDEC-24274.
33. Labun, L.C., Rapaport, M. (1994) A Third Generation Energy Absorber for Crash Attenuating Helicopter Seating. American Helicopter Society 50th Annual Forum, Washington DC, May 11-13, 1994.
34. Loftis, K.L., Mazuchowski II, Lt Col E.L, Clouser, M.C., Gillich, P.J. (2019) Prominent Injury Types in Vehicle Underbody Blast. Military Medicine, 184, 3/4:261, 2019.
35. MADYMO. (2015) Human Body Models Manual Release 7.6. TASS International.
36. MADYMO. (2015) Model Manual Release 7.6. TASS International.

37. MADYMO. (2015) Reference Manual Version 7.6. Design, Simulation, and Virtual Testing. TASS International.
38. Magerl, F.F. (1994) A Comprehensive Classification of Thoracic and Lumbar Injuries. European Spine Journal (0940-6719), 3 (4), pp. 184.
39. McDermott, M. (2014) New Vehicle Seats Improve Troop Survivability in Blast Events. National Defense NDIA Viewpoint.
40. ModeFRONTIER (2017) User Guide Release 2017R5. ESTECO SpA.
41. Moore, K.L., Agur, A.M.R., Dalley, A.F (2010) Essential Clinical Anatomy 4th Edition. Lippincott Williams & Wilkins. Dallas, TX. pp. 205-217
42. Myklebust, J., Sances, Jr., A, Maiman, D., Pintar, F., Chilbert, M., Rauschning, W., Larson, S., Cusick, J., Ewing, C., Thomas, D., and Saitzberg, B. (1983) Experimental Spinal Trauma Studies in the Human and Monkey Cadaver. SAE International, Warrendale, PA. SAE Paper No. 831614.
43. Nance, S. (2014) Blast-Attenuating Seats. Science and Technology Save Lives from Hidden Threats. Ground Combat & Tactical USR Annual AUSA Issue. October 2014 Volume 5, Issue 5.
44. NATO (2007) Test Methodology for Protection of Vehicle Occupants against Anti-Vehicular Landmine Effects, Final Report of HFM-090 Task Group 25.
45. Olivares, Gerardo. High G Energy Absorbing Seat Mechanism for Vertical Loading Conditions. Idenfitication Number: 11IP008. Wichita State University.
46. Owens, B.D., Kragh, J.F., Wenke, J.C., Macaitis, J., Wade, C.E., Holcomb, JB. (2008) Combat Wounds in Operation Iraqi Freedom and Operation Enduring

Freedom. The Journal of Trauma: Injury, Infection, and Critical Care Issue: Volume 64(2), February 2008, pp 295-299.

47. Oxland T.R. (1992) Burst fractures of the human thoracolumbar spine: a biomechanical investigation. Ph D Dissertation, Yale University, New Haven
48. Perry, B.J., Henderson, K.A., Spratley, E.M., Zhang, J.Y., Merkle, A.C., Salzar, R.S. (2016) Effects of Seated Soldier Posture on Pelvic Force Transmissibility. NATO HFM-271. Injury assessment methods for vehicle occupants in blast-related events.
49. Pietsch, H.A., Bosch, K.E., Weyland, D.R., Spratley, E.M., Henderson, K.A., Salzar, R.S., Smith, T.A., Sagara, B.M., Demetropoulous, C.K., Dooley, C.J., Merkle, A.C. (2016). Evaluation of WIAMan Technology Demonstrator - Biofidelity relative to Sub-Injurious PMHS Response in Simulated Under-body Blast Events. Stapp Car Crash Journal, Vol. 60. November 2016. P.199-246.
50. Poles, S. (2003). The SIMPLEX Method. ESTECO Technical Report 2003-005.
51. Qinetic BlastRide Seat (2016). https://www.qinetiq-na.com/products/militaryprotection/blast-seat/. Accessed 27 December 2016.
52. Ragel B.T., Allred C.D., Brevard S., Davis R.T., Frank E.H. (2009) Fractures of the thoracolumbar spine sustained by soldiers in vehicles attacked by improvised explosive devices. Spine 2009;34:2400–5.
53. Ramalingam, J., Chandra, S., Thyagarajan, R. (2013) Reduced Order Modeling for Rapid Simulations of Blast and Rollover Events of a Ground Vehicle and its Occupants Using Rigid Body Dynamic Models. US Army TARDEC-23785.

54. Ramasamy, A., Hill, A.M., Hepper, A.E., Bull, A.M.J., Clasper J.C. (2009) Blast Mines: Physics, Injury Mechanisms And Vehicle Protection. Department of Bioengineering, Royal School of Mines, Imperial College, London, SW7 2AZ. JR Army Med Corps 155(4). pp. 258-264.
55. Royal, J. (2008) Casualty Wounding Patterns in Special Operations Forces in Operation Iraqi Freedom. Journal of Special Operations Medicine. Volume 8, Edition 2 / Spring 08. pp. 55-60.
56. Rupp, J.D., Flannagan, C.A.C., Kuppa, S.M. (2010) An Injury Risk Curve for the Hip for Use in Frontal Impact Crash Testing. Journal of Biomechanics 43. pp. 527-531.
57. SAE Aerospace Standard (2015), “Performance Standard for Seats in Civil Rotorcraft, Transport Aircraft, and General Aviation Aircraft,” SAE Standard AS8049, Rev. August 2015.
58. Society of Automotive Engineers (1995) “Surface Vehicle Recommended Practice J211-1: Instrumentation for Impact Test. Part 1: Electronic Instrumentation,” Warrendale, PA.
59. Shukla, N. (2013) Analysis of the Articulated Total Body (ATB) and Mathematical Dynamics Model (MADYMO) Software Suites for Modeling Anthropomorphic Test Devices (ATDs) in Blast Environments. Army Research Laboratory ARL-TR-6458. May 2013.
60. Singer, P.W. (2012) The Evolution of Improvised Explosive Devices (IEDs). Armed Forces Journal. February 2012.

61. Singh, A. P. (2017) Lumbar Spine Anatomy. https://boneandspine.com/lumbar-spine-anatomy/ Accessed 27 February 2019.
62. Spratley E.M, Rawska K., Demetropoulus C.K., Merkle A.C., Salzar R.S. (2016) Local vs. Global Motion in Whole-Body UBB Testing. NATO HFM-271. Injury assessment methods for vehicle occupants in blast-related events.
63. Spratley, E.M., Henderson, K.A., Merkle, A.C., Salzar, R.S. (2016) Repeatability and Matched-Pair Response between PMHS and Hybrid-III using the UVA Odyssey Underbody Blast Simulator. Proceedings of the 2016 International IRCOBI Conference on the Biomechanics of Injury.
64. Spratley, E.M., Rawska, K., Kim, T., Salzar, R.S. (2015) Fidelity of the MADYMO Facet Pedestrian Model for Simulation of Underbody Blast Events. 53rd Annual SAFE Symposium. November 2-4, 2015.
65. Stemper, B.D., Baisden, J.L., Yoganandan, N., Pintar, F.A., DeRosia, J., Whitley, P., Paskoff, G.R., Shender, B.S. (2012) Effect of loading rate on injury patterns during high rate vertical acceleration. Proceedings of the 2012 International IRCOBI Conference on the Biomechanics of Injury.
66. Tabiei, A., Nilakantan, G. (2007) Reduction of Acceleration Induced Injuries from Mine Blasts under Infantry Vehicles. Department of Aerospace Engineering and Engineering Mechanics, University of Cincinnati, OH.
67. Tank Automotive Research Development Engineering Center (2015) TARDEC 30-Year Strategy, 29AUG15, DIST A.
68. Tegtmeyer, M. (2012) The WIAMan Development Program: Objectives and Rationale, Army Research Lab, http://usarmy.vo.llnwd.net, 2012.

69. Thyagarajan, R., Ramalingam, J., Kulkarni, K. (2014) Occupant-Centric Platform (OCP) Technology-Enabled Capabilities Demonstration (TECD) Comparing the Use of Dynamic Response Index (DRI) and Lumbar Load as Relevant Spinal Injury Metrics. U.S. Army Tank Automotive Research, Development, and Engineering Center Technical Report. Registration No. 24373. 09 January 2014.
70. Tile, M. (1996) Acute Pelvic Fractures: I. Causation and Classification. J Am Acad Orthop Surg 1996; 4:143-151.
71. USSC Group ASP Crew (2016). http://www.usscgroup.com/seating/asp-crew/?useimg= Accessed 27 December 2016.
72. Weaver, Caitlin M.; Stitzel, Joel D. Pelvic response of a total human body finite element model during simulated under body blast impacts. Proceedings of the 2015 International IRCOBI Conference on the Biomechanics of Injury
73. Willen, J., Lindahl, S., Irstam, L., Aldman, B., Nordwall, A. (1984) The thoracolumbar crush fracture (an experimental study on instant axial dynamic loading: the resulting fracture type and its stability). Spine. 1984;9:624–631.
74. Yoganandan, B.D. Stemper, J.L. Baisden, F.A. Pintar, G.R. Paskoff, B.S. Shender. (2015) Effects of acceleration level on lumbar spine injuries in military populations. Spine J, 15 (2015), pp. 1318–1324
75. Yoganandan, N. (2014) Dynamic Responses of Intact Post Mortem Human Surrogates from Inferior-to-Superior Loading at the Pelvis. Stapp Car Crash Journal 58: 123.

76. Yoganandan, N. Ray, G. Pintar, F.A. Myklebust, J.B. Sances Jr., A (1989) Stiffness and Strain Energy Criteria to Evaluate the Threshold of Injury to an Intervertebral Joint. J. Biomechanics Vol 22, No. 2, pp. 135-142.

ABSTRACT

OPTIMIZATION OF UNDERBODY BLAST ENERGY-ATTENUATING SEAT MECHANISMS USING MODIFIED MADYMO HYBRID III AND HUMAN BODY MODELS

by

KELLY E. B. BOSCH, PE

August 2019

Advisors: Dr. John M. Cavanaugh; Dr. Paul C. Begeman

Major: Biomedical Engineering

Degree: Doctor of Philosophy

Energy attenuating (EA) blast seats, although not new to the market, have not been fully characterized with respect to energy attenuation capability and the resulting effects on occupant protection. EA seats utilize stroking mechanisms to absorb energy and reduce the vertical forces imparted on the occupant's pelvis and lower spine complex. Although a variety of EA seats are available on the market, the fundamental question behind how to optimize the force and deflection rates of the EA mechanisms to effectively reduce occupant injury has not yet been answered. Using modeling and simulation techniques, this research developed a tool to determine optimal force and deflection profiles to reduce pelvis and lower spine injuries experienced by Warfighters in underbody blast events using a generic seat model with MAthematical DYnamic MOdels (MADYMO, TASS International, Inc.) software. This optimizing tool can be shared with EA seat manufacturers and applied to military seat development efforts for EA mechanisms for a given occupant and designated blast severity.

Using Hybrid III anthropomorphic test device (ATD) and post-mortem human surrogate (PMHS) data from the University of Virginia in a sub-injurious Condition A (4

m/s seat velocity) and injurious Condition B (10 m/s seat velocity), this research is summarized in the following specific aims:

1. **Hybrid III Rigid Seat Validation:** Validate Hybrid III ATD model response in rigid seat in sub-injurious Condition A.
2. **Human Body Model Rigid Seat Validation:**
    a. **Condition A:** Validate human body model response with PMHS in rigid seat for sub-injurious Condition A.
    b. **Condition B:** Validate human body model response in rigid seat with injurious Condition B.
3. **Seat Optimization with Human Body Model:** Vary force-deflection properties of EA seat mechanism and run parametric sensitivity study with human body model to reduce acceleration in pelvis and forces in lumbar region for injurious Condition B.
4. **Hybrid III Output from Optimized Seat:** Verify Hybrid III response with injurious Condition B in rigid seat, then apply optimal EA properties to the seat and determine acceleration in pelvis and lower spine forces for Hybrid III ATD model for Condition B as target injury criteria for seat manufacturers.

AUTOBIOGRAPHICAL STATEMENT
KELLY E. B. BOSCH, PE

EDUCATION:

2019	PhD	Biomedical Engineering	Wayne State University
2009	ME	Automotive Engineering	University of Michigan-Ann Arbor
2008	BSE	Mechanical Engineering	University of Michigan-Ann Arbor

PROFESSIONAL EXPERIENCE:

2016 to Date	Karma Automotive	Manager - Safety Systems Integration
2013 to 2016	TARDEC/Booz Allen Hamilton	Engineer - Blast Mitigation, WIAMan Team
2012 to 2013	Tesla Motors	Vehicle Test Engineer - Crash Safety
2009 to 2012	Exponent	Associate - Vehicle Engineering
2004 to 2008	Ford Motor Company	Intern - Dummy Lab, Crash Safety, Materials

NOTABLE PUBLICATIONS:

Bosch, K. (2016) Blast Mitigation Seat Analysis – Evaluation of Lumbar Compression Data Trends in 5th Percentile Female Anthropomorphic Test Device Performance Compared to 50th Percentile Male Anthropomorphic Test Device in Drop Tower Testing. DETC2016-59094. Proceedings of the ASME 2016 International Design Engineering Technical Conferences & Computers and Information in Engineering Conference. August 21-24, 2016.

Pietsch, H.A., **Bosch, K.E**., Weyland, D.R., Spratley, E.M., Henderson, K.A., Salzar, R.S., Smith, T.A., Sagara, B.M., Demetropoulous, C.K., Dooley, C.J., Merkle, A.C. (2016) Evaluation of WIAMan Technology Demonstrator -Biofidelity relative to Sub-Injurious PMHS Response in Simulated Under-body Blast Events. Stapp Car Crash Journal, Vol. 60. November 2016. P.199-246.

Bosch, K., Harris, K., Clark, D., Scherer, R., Melotik, J. (2015) Blast Mitigation Seat Analysis - Assessment of the Effect of Personal Protective Equipment on the 5th Percentile Female Anthropomorphic Test Device Performance in Drop Tower Evaluations. DETC2015-46342. Proceedings of the ASME 2015 International Design Engineering Technical Conferences & Computers and Information in Engineering Conference IDETC/CIE 2015. August 2-5, 2015.

Bosch, K., Harris, K., Clark, D., Scherer, R., Melotik, J. (2014) Blast Mitigation Seat Analysis – Drop Tower Data Review. 2014 NDIA Ground Vehicle Systems Engineering and Technology Symposium Modeling & Simulation, Testing and Validation (MSTV) Technical Session. August 12-14, 2014.

NOTABLE ACHIEVEMENTS:

2017 – Karma Automotive CEO Achievement Award for planning and execution of developmental crash testing
2014 – Booz Allen Hamilton Performance and Team Award for drop tower data analysis
2012 – Professional Engineer (PE) – Mechanical Engineering. Arizona State Board of Technical Registration, License #54301
2008 – Graduated Summa Cum Laude from University of Michigan-Ann Arbor with BSE-ME